



CARDIFF UNIVERSITY

Cardiff University School of Engineering

**Auto Rickshaw Impacts with Pedestrians -
A Computational Analysis of Post-
Collision Kinematics and Injury
Mechanics**

A Thesis Submitted to Cardiff University for the
Degree of Doctor of Philosophy

By

Ahmed Jabbar Rahi AL-Graitti

September 2019

ABSTRACT

Motor vehicle-related pedestrian road traffic collisions are a major road safety challenge and a leading public health issue, since they are a primary cause of death and serious injury worldwide. In many developing countries, the auto-rickshaw—a three-wheeled vehicle with a canvas roof and side curtains – poses a significant risk to pedestrian safety due to the poor impact energy absorption of its structures and materials.

This study presents a parametric and comparative analysis of auto-rickshaw-related pedestrian impacts and pedestrian-ground impacts by computational simulation, using a Finite Element model of an auto-rickshaw and LS-DYNA, 50th percentile adult male and six-year-old child Hybrid III Anthropometric Test Devices (dummies). The comparative study explored the kinematic responses and injury metrics associated with both adults and children impacted by an auto-rickshaw, as well as the most commonly impacted areas of an auto-rickshaw and the injury metrics for the adult pedestrian produced by primary and secondary impacts.

The output data of the impact simulation was correlated against reported injury metrics, Head Injury Criterion, Neck Injury Criterion, Combined Thoracic Index, Injury Abbreviated Injury Scale and reported risk level. The results suggest that adult pedestrians are subjected to a relatively high risk of head, neck and chest injuries during primary impacts at 10, 20 and 35km/h, respectively, and some of the impact simulations suggest a risk of fatality. The 6YO-child pedestrians are at risk of serious head and neck injury at 10 and 15km/h, respectively.

During secondary impacts, defined as impacts with a floor surface, head and neck injuries produced from ground contact are significant, including fatal injury, at 10km/h and greater, while insignificant chest injuries were observed at 40km/h. Vehicle impact response was investigated and Aluminium-6016-T4 and magnesium-AZ31B windscreen frame materials and a polycarbonate windscreen were found to produce the lowest injury risk of all the materials investigated whilst offering the greatest safety at the lowest cost.

The present study provides valuable evidence for informing a series of recommendations and guidelines to make the auto-rickshaw safer during impacts with pedestrians.

Overall, it has found that impact velocity, vehicle contact region, impact position and pedestrian size significantly influence the post-kinematic response of a pedestrian impacted by an auto-rickshaw and injury risk during primary and secondary impacts. Moreover, child pedestrians are subject to a relatively higher risk, compared to adults, during primary impacts. Secondary impacts were associated with a greater risk of head and neck injuries compared to primary impacts, even at low-impact velocities. Secondary impacts, however, produced much lower chest injury risk compared to primary impacts. Thus, even at relatively low impact velocities, the auto-rickshaw cannot be considered a ‘pedestrian friendly’ vehicle for use in urban areas.

Future suggestions to reduce the injury risk level and increase the safety of the auto-rickshaw should be the implementation of strict safety regulations and, or, consideration of engineering solutions, such as retrofitting injury mitigation technologies to those auto-rickshaw contact regions which pose the greatest risk of producing pedestrian injury. In addition, modification of the frontal end geometry of the vehicle is recommended to ensure that injury risk is minimised during primary and secondary impacts.

ACKNOWLEDGEMENTS

The work in this thesis was achieved with the support of many people that I would like to thank

I would like to thank my sponsor who provided me an opportunity to join the Higher Committee of Education Development in Iraq (HCED) scholarship program. Without their and Cardiff University support it would not be possible to conduct this research.

I would like to thank my supervisors, Dr. Michael Jones and Dr. Allan Masson Jones, for their motivation, encouragement, advice, continuous support of my Ph.D. study, and immense knowledge. Their guidance help me in my research and writing of this thesis.

Besides my supervisors, I would like to thank the School of Engineering research office staff for their support through all the duration of my Ph.D.

Every step of my academic progress and personal achievements would not be possible without out the support, prayers, and faith of my parents.

This work would never be complete without the patience, constant encouragement, sacrifices and support of my beloved wife and soul mate Nufooth and my daughters and son to you I dedicate every accomplishment in my life.

TABLE OF CONTENTS

ABSTRACT.....II

ACKNOWLEDGEMENTS..... IV

TABLE OF CONTENTS.....V

LIST OF FIGURES.....XV

LIST OF TABLES.....XXI

LIST OF ABBREVIATIONS.....XXIII

1. INTRODUCTION & LITERATURE REVIEW.....1

1.1 Introduction.....1

1.2 Published outcomes.....3

1.3 Road accident data.....4

1.3.1 Pedestrian injury patterns and injury severity according to body regions during primary and secondary impacts.....8

1.4 Anatomy and injury risk.....12

1.4.1 Head anatomy and injury risk.....12

1.4.2 Neck anatomy and injury risk.....15

1.4.3 Chest anatomy and injury risk.....17

1.5 Injury criteria and thresholds.....18

1.5.1 Head injury criteria and thresholds.....18

1.5.2 Neck injury criteria and thresholds.....21

1.5.3 Chest injury criteria and thresholds.....23

1.6 The major factors influencing pedestrian kinematic response, injury patterns and injury risk during primary and secondary impacts.....24

1.6.1 Vehicle factors.....25

1.6.1.1 Vehicle frontal geometry.....25

1.6.1.2 Vehicle impact velocity.....28

1.6.1.3 Vehicle impact region.....31

1.6.2	Pedestrian factors.....	32
1.6.2.1	Pedestrian age and size.....	33
1.6.2.2	Pedestrian impact position and posture.....	35
1.7	Passive and active safety approaches.....	37
1.7.1	Active safety.....	37
1.7.2	Passive safety.....	37
1.7.2.1	Aluminium.....	39
1.7.2.2	Magnesium.....	40
1.7.2.3	Polycarbonate.....	41
1.8	Cost-Benefit-Analysis (CBA) and road traffic accidents costs.....	42
1.9	Finite Element Analysis (FEA).....	43
1.9.1	Impact test dummies.....	45
1.10	Thesis structure.....	48
2.	METHODS.....	50
2.1	Introduction.....	50
2.2	Modelling.....	52
2.2.1	Mathematical model.....	52
2.2.2	Physical model.....	54
2.2.3	Code description.....	54
2.2.4	Computational vehicle model.....	54
2.2.4.1	Mesh quality.....	55
2.2.4.2	Mesh generation.....	55
2.2.4.3	Material properties and thicknesses of the vehicle components.....	62
2.2.4.4	Vehicle model simplification.....	62
2.2.4.5	Vehicle components constrain.....	64
2.2.5	Pedestrian models.....	65
2.2.5.1	Converting position of the 6YO-child dummy.....	66

2.3	Impact simulation environment.....	69
2.3.1	Pedestrian impact positions and vehicle contact regions.....	69
2.3.2	Contact types and friction coefficients.....	70
2.3.3	Ground types.....	73
2.3.4	Impact velocity and gravity.....	73
2.3.5	Solution control.....	74
2.3.6	Database definition for results collections.....	74
2.3.7	Results filter and frequency.....	75
2.4	Expected results.....	75
2.4.1	Post kinematic response in the primary and secondary impacts.....	75
2.4.1.1	Head contact location.....	75
2.4.1.2	Head contact angles.....	75
2.4.1.3	Head contact time.....	75
2.4.1.4	Throw distance.....	76
2.4.2	Selected injury parameters in the primary and secondary impacts.....	76
2.4.2.1	Head injury and risk level.....	76
2.4.2.2	Upper neck injury and risk level.....	77
2.4.2.3	Chest injury and risk level.....	80
2.5	Auto rickshaw engineering modifications for adult pedestrian safety enhancement.....	81
2.6	Brief Cost-Benefit-Analysis (CBA).....	83
3.	RESULTS	85
3.1	Introduction.....	85
3.2	Primary impacts.....	86
3.2.1	Kinematic response during primary impacts.....	86
3.2.1.1	Kinematic response during impacts at the vehicle's centreline.....	89

3.2.1.2 Kinematic response at impacts 42cm offset from the vehicle's centreline.....	91
3.2.2 Head contact locations and angles during primary impacts.....	94
3.2.3 Head contact time duration during primary impacts	96
3.2.3.1 Head contact time duration during impacts at the vehicle's centreline.....	96
3.2.3.2 Head contact time duration at 42cm offset from the vehicle's centreline.....	96
3.2.4 Head injury criterion and injury risk level during primary impacts.....	96
3.2.4.1 Head injury criterion and risk level during primary impacts at the vehicle's centreline.....	97
3.2.4.2 Head injury criterion and risk level at primary impacts 42cm offset from the vehicle's centreline.....	99
3.2.5 Upper neck injury criteria and injury risk level during primary impacts.....	102
3.2.5.1 Upper neck injury criteria and risk level during primary impacts at the vehicle's centreline.....	102
3.2.5.2 Upper neck injury criteria and risk level at primary impacts 42cm offset from of the vehicle's centreline.....	104
3.2.6 Chest contact locations during primary impacts.....	105
3.2.7 Chest contact time duration during primary impacts.....	105
3.2.8 Chest injury criteria and injury risk level during primary impacts.....	106
3.3 Secondary impacts.....	107
3.3.1 Kinematic response during secondary impacts.....	107
3.3.1.1 Kinematic response during secondary impacts at the vehicle's centreline.....	107
3.3.1.2 Kinematic response during secondary impacts at 42cm offset from the vehicle's centreline.....	108
3.3.2 Throw distance.....	113

3.3.2.1	Throw distance at the vehicle’s centreline.....	113
3.3.2.2	Throw distance at 42cm offset from the vehicle’s centreline.....	114
3.3.3	Comparison of the kinematic response of an adult pedestrian during impact a Real-World accident with simulations.....	114
3.3.4	Head injury criterion and injury risk level during secondary impacts.....	115
3.3.4.1	Head injury criterion and injury risk level during secondary impacts at the vehicle’s centreline.....	116
3.3.4.2	Head injury criterion and injury risk level during secondary impacts at 42cm offset from the vehicle’s centreline.....	117
3.3.5	Upper neck injury criteria and injury risk level during secondary.....	118
3.3.5.1	Upper neck injury criteria and injury risk level during secondary at the vehicle’s centreline.....	118
3.3.5.2	Upper neck injury criteria and injury risk level during secondary at 42cm offset from the vehicle’s centreline.....	119
3.3.6	Chest injury criterion and injury risk level during secondary impacts.....	122
3.3.6.1	Chest injury criterion and injury risk level during secondary impacts at the vehicle’s centreline.....	122
3.3.6.2	Chest injury criterion and injury risk level during secondary impacts at 42cm offset from the vehicle’s centreline.....	123
3.4	The sensitivity of the model contact parameters.....	125
3.4.1	Primary impacts.....	125
3.4.1.1	Kinematic response.....	125
3.4.1.2	Head injury.....	125
3.4.2	Secondary impacts.....	126
3.4.2.1	Kinematic response	126
3.4.2.1.1	Original case scenario.....	126
3.4.2.1.2	First case scenario.....	126
3.4.2.1.3	Second case scenario.....	127
3.4.2.1.4	Third case scenario.....	127

3.4.2.1.5 Fourth case scenario.....	127
3.4.2.1.6 Fifth case scenario.....	127
3.4.2.1.7 Sixth case scenario.....	127
3.4.2.2 Head injury.....	129
3.5 Comparison between primary and secondary impacts for adult pedestrian....	129
3.5.1 Head injury criterion and injury risk level during primary and secondary impacts.....	130
3.5.1.1 Head injury criterion and injury risk level during primary and secondary impacts at the vehicle's centreline.....	130
3.5.1.2 Head injury criterion and injury risk level during primary and secondary impacts at 42cm offset from the vehicle's centreline.....	132
3.5.2 Upper neck injury criteria and injury risk level during primary and secondary impacts.....	135
3.5.2.1 Upper neck injury criteria and injury risk level during primary and secondary impacts at the vehicle's centreline.....	135
3.5.2.2 Upper neck injury criteria and injury risk level during primary and secondary impacts at 42cm offset from the vehicle's centreline.....	137
3.5.3 Chest injury criterion and injury risk level during primary and secondary impacts.....	140
3.5.3.1 Chest injury criterion and injury risk level during primary and secondary impacts at the vehicle's centreline.....	140
3.5.3.2 Chest injury criterion and injury risk level during primary and secondary impacts at 42cm offset from the vehicle's centreline.....	142
3.6 Auto rickshaw engineering modification for adult pedestrian safety enhancement.....	145
3.6.1 Head injury and injury risk level during primary impacts after vehicle modifications.....	145
3.6.1.1 Head injury and injury risk level during primary impacts after vehicle modifications at the vehicle's centreline.....	145
3.6.1.2 Head injury and injury risk level during primary impacts after vehicle modifications at 42cm from the vehicle's centreline.....	147

3.6.2 Upper neck injury and injury risk level during primary impacts after vehicle modifications.....	149
3.6.2.1 Upper neck injury and injury risk level during primary impacts after vehicle modifications at the vehicle’s centreline.....	149
3.6.2.2 Upper neck injury and injury risk level during primary impacts after vehicle modifications at 42cm from the vehicle’s centreline.....	151
3.6.3 Chest injury and injury risk level during primary impacts after vehicle modifications.....	153
3.6.3.1 Chest injury and injury risk level during primary impacts after vehicle modifications at the vehicle’s centreline.....	153
3.6.3.2 Chest injury and injury risk level during primary impacts after vehicle modifications at 42cm from the vehicle’s centreline.....	154
4. DISCUSSION.....	156
4.1 Introduction.....	156
4.2 Primary impacts.....	157
4.2.1 Kinematic response during primary impacts.....	157
4.2.1.1 Kinematic response during impacts at the vehicle’s centreline.....	158
4.2.1.2 Kinematic response at impacts 42cm offset from the vehicle’s centreline.....	159
4.2.2 Head contact locations and angles during primary impacts	160
4.2.3 Head contact time duration during primary impacts.....	162
4.2.3.1 Head contact duration during impacts at the vehicle’s centreline.....	162
4.2.3.2 Head contact time duration at 42cm offset from the vehicle’s centreline.....	164
4.2.4 Head injury criterion and injury risk level during primary impacts.....	166
4.2.4.1 Head injury criterion and risk level during primary impacts at the vehicle’s centreline.....	167
4.2.4.2 Head injury and risk level at primary impacts 42cm offset from the vehicle’s centreline.....	168
4.2.5 Upper neck injury and injury risk level during primary impacts.....	170

4.2.5.1 Upper neck injury and risk level during primary impacts at the vehicle's centreline.....	171
4.2.5.2 Upper neck injury and risk level at primary impacts 42cm offset from of the vehicle's centreline.....	173
4.2.6 Chest contact locations during primary impacts.....	177
4.2.7 Chest contact duration during primary impacts.....	178
4.2.8 Chest injury and injury risk level during primary impacts.....	178
4.3 Secondary impacts.....	180
4.3.1 Kinematic response during secondary impacts.....	180
4.3.1.1 Kinematic response during secondary impacts at the vehicle's centreline.....	180
4.3.1.2 Kinematic response during secondary impacts at 42cm offset from the vehicle's centreline.....	182
4.3.2 Throw distance.....	184
4.3.2.1 Throw distance at the vehicle's centreline.....	184
4.3.2.2 Throw distance at 42cm offset from the vehicle's centreline.....	185
4.3.3 Comparison of the kinematic response of an adult pedestrian during impact a Real-World accident with simulations.....	186
4.3.4 Head injury and injury risk level during secondary impacts.....	187
4.3.4.1 Head injury and injury risk level during secondary impacts at the vehicle's centreline.....	187
4.3.4.2 Head injury and injury risk level during secondary impacts at 42cm offset from the vehicle's centreline.....	188
4.3.5 Upper neck injury and injury risk level during secondary impacts.....	189
4.3.5.1 Upper neck injury and injury risk level during secondary impacts at the vehicle's centreline.....	190
4.3.5.2 Upper neck injury and injury risk level during secondary impacts at 42cm offset from the vehicle's centreline.....	191
4.3.6 Chest injury and injury risk level during secondary impacts.....	192
4.3.6.1 Chest injury and injury risk level during secondary impacts at the vehicle's centreline.....	193

4.3.6.2 Chest injury and injury risk level during secondary impacts at 42cm offset from the vehicle's centreline.....	194
4.4 The sensitivity of the model contact parameters.....	195
4.4.1 Primary impacts.....	195
4.4.1.1 Kinematic response.....	195
4.4.1.2 Head injury.....	195
4.4.2 Secondary impacts.....	196
4.4.2.1 Kinematic response.....	196
4.4.2.2 Head injury.....	196
4.5 Comparison between primary and secondary impacts for adult pedestrian.....	197
4.5.1 Head injury and injury risk level during primary and secondary impacts.....	197
4.5.1.1 Head injury and injury risk level during primary and secondary impacts at the vehicle's centreline.....	197
4.5.1.2 Head injury and injury risk level during primary and secondary impacts at 42cm offset from the vehicle's centreline.....	199
4.5.2 Upper neck injury and injury risk level during primary and secondary impacts.....	203
4.5.2.1 Upper neck injury and injury risk level during primary and secondary impacts at the vehicle's centreline.....	203
4.5.2.2 Upper neck injury and injury risk level during primary and secondary impacts at 42cm offset from the vehicle's centreline.....	205
4.5.3 Chest injury and injury risk level during primary and secondary impacts.....	208
4.5.3.1 Chest injury and injury risk level during primary and secondary impacts at the vehicle's centreline.....	208
4.5.3.2 Chest injury and injury risk level during primary and secondary impacts at 42cm offset from the vehicle's centreline.....	209
4.6 Auto rickshaw engineering modifications for adult pedestrian safety enhancement.....	211

4.6.1	Head injury and injury risk level during primary impacts after vehicle modifications.....	211
4.6.1.1	Head injury and injury risk level during primary impacts after vehicle modifications at the vehicle’s centreline.....	212
4.6.1.2	Head injury and injury risk level during primary impacts after vehicle modifications at 42cm offset from the vehicle’s centreline.....	214
4.6.2	Upper neck injury and injury risk level during primary impacts after vehicle modifications.....	215
4.6.2.1	Upper neck injury and injury risk level during primary impacts after vehicle modifications at the vehicle’s centreline.....	216
4.6.2.2	Upper neck injury and injury risk level during primary impacts after vehicle modifications at 42cm offset from the vehicle’s centreline.....	217
4.6.3	Chest injury and injury risk level during primary impacts after vehicle modifications.....	218
4.6.3.1	Chest injury and injury risk level during primary impacts after vehicle modifications at the vehicle’s centreline.....	218
4.6.3.2	Chest injury and injury risk level during primary impacts after vehicle modifications at 42cm offset from the vehicle’s centreline.....	218
4.7	Limitations.....	220
5.	CONCLUSION.....	222
5.1	Research conclusions.....	222
5.1.1	Primary impacts for the 50 th percentile adult and 6YO-child pedestrians...	222
5.1.2	Secondary impacts for the 50 th percentile adult pedestrian.....	223
5.1.3	Auto rickshaw engineering modifications for adult pedestrian safety enhancement.....	225
5.2	Future work.....	226
6.	REFERENCES.....	227
7.	APPENDICES.....	248

LIST OF FIGURES

Figure 1-1. Design of the exterior of an auto rickshaw; (a) Bajaj passenger vehicle; (b) Atul passenger vehicle; (c) Piaggio goods vehicle; (d) Applications police vehicle.....6

Figure 1-2. AIS and Risk level.....7

Figure 1-3. Distribution of all pedestrian injury patterns by body region and injury severity level.....9

Figure 1-4. Pedestrian injury pattern and injury severity during impacts with multi-purpose vehicles (MPVs) in France between 1996 and 2007.....9

Figure 1-5. Injury body regions and injury details of pedestrian impacted by an auto-rickshaw; (a) Injury body regions; (b) injury details..... 11

Figure 1-6. Head section.....13

Figure 1-7. Skull fractures; (a) Different stages of skull fracture injuries; (b) Linear and depressed skull fractures..... 14

Figure 1-8. Neck bone structure.....15

Figure 1-9. The triangles of the neck.....16

Figure 1-10. Compression injury.....17

Figure 1-11. Anatomy of the rib cage from lateral and anterior views..... 18

Figure 1-12. Wayne State Tolerance Curve (WSTC)..... 19

Figure 1-13. Setup of child pedestrian-passenger vehicle impacts and vehicle control parameters.....26

Figure 1-14. Spring-mass model.....38

Figure 2- 1. Methodology diagram of the study.....51

Figure 2- 2. Auto rickshaw dimensions.....54

Figure 2- 3. Auto rickshaw model; (a) rear view; (a) side view; (c) front view.....55

Figure 2- 4. FE Model of the auto rickshaw.....61

Figure 2- 5. Auto rickshaw model simplification steps; (a) FEM of auto rickshaw including driver dummy mass; (b) Calculation of rear vehicle components masses by removing frontal vehicle components; (c) Simplified auto rickshaw model.....63

Figure 2-6. Simplified auto rickshaw model.....64

Figure 2- 7. Constrained translational and revolute joints.....65

Figure 2- 8. 50th Percentile Hybrid III adult pedestrian dummy.....66

Figure 2- 9. 6YO- Hybrid III child dummy in sitting position.....66

Figure 2- 10. 6YO-child dummy converting process (sitting to standing).....68

Figure 2- 11. Auto rickshaw–adult pedestrian impact simulations at different positions; (a) Front centre (b) Front offset; (c) Rear centre; (d) Rear offset; (e) Side centre; (f) Side offset.....71

Figure 2- 12. Auto rickshaw–child pedestrian impact simulations at different positions; (a) Front centre (b) Front offset; (c) Rear centre; (d) Rear offset; (e) Side centre; (f) Side offset.....72

Figure 2- 13. Vehicle-pedestrian impact simulation setup.....73

Figure 2- 14. Axial and shear forces of the upper neck.....78

Figure 2- 15. Head-Neck motion phases during impacts ;(a) rear impacts;(b) front impacts.....78

Figure 2- 16. Acceleration and deflection points location of Hybrid III adult male dummy for the chest injury calculation (a) The measurement acceleration point location of the spinal cord; (b) The central measurement deflection point location of the dummy chest.....80

Figure 3- 1. The kinematic response of adult pedestrian dummy impacted at different vehicle regions and impact positions (a) pedestrian impacted at the vehicle’s centre in front, rear and side position; (b) pedestrian impacted at 42 cm offset of the vehicle’s centre in front, rear and side position at 30 km/h.....87

Figure 3- 2. The kinematic response of 6YO-child pedestrian dummy impacted at different vehicle regions and impact positions (a) pedestrian impacted at the vehicle’s centre in front, rear and side position; (b) pedestrian impacted at 42 cm offset of the vehicle’s centre in front, rear and side position at 30 km/h.....88

Figure 3- 3. Head contact locations for adult pedestrian of the auto rickshaw.....	95
Figure 3- 4. HIC values in the frontal impacts at the vehicle’s centreline for adult and 6YO-child pedestrians	98
Figure 3- 5. HIC values in the rear impacts at the vehicle’s centreline for adult and 6YO-child pedestrians	98
Figure 3- 6. HIC values in the side impacts at the vehicle’s centreline for adult and 6YO-child pedestrians	99
Figure 3- 7. HIC values in the frontal impacts at 42 cm offset from the vehicle’s centreline for adult and 6YO-child pedestrians.....	100
Figure 3- 8. HIC values in the rear impacts at 42 cm offset from the vehicle’s centreline for adult and 6YO-child pedestrians	101
Figure 3- 9. HIC values in the side impacts at 42 cm offset from the vehicle’s centreline for adult and 6YO-child pedestrians	101
Figure 3- 10. Upper neck injury values for adult and 6YO-child pedestrians impacted at the vehicle’s centreline	103
Figure 3- 11 Upper neck injury values for adult and 6YO-child pedestrians impacted at 42cm offset from the vehicle’s centreline	105
Figure 3- 12. CTI values for adult pedestrian in the frontal impacts at two vehicle contact regions (centreline and 42cm offset).....	106
Figure 3- 13. The full kinematic response of adult pedestrian dummy impacted at the vehicle’s centreline in different impact positions (front, rear and side) during the primary and secondary impacts.....	110
Figure 3- 14. The full kinematic response of adult pedestrian dummy impacted at 42cm offset from the vehicle’s centreline in different impact positions (front, rear and side) during the primary and secondary impacts.....	111
Figure 3- 15. Landing patterns of adult pedestrian dummy impacted at different impact velocities and different vehicle regions (a) pedestrian impacted at the vehicle’s centre in front, rear and side position; (b) pedestrian impacted at a 42cm offset of the vehicle’s centre in front, rear and side position.....	112

Figure 3- 16. Throw distance and impact velocity at different pedestrian positions, front, rear and side at centreline of the vehicle.....113

Figure 3- 17. Throw distance and impact velocity at different pedestrian positions, front, rear and side at 42cm offset from the vehicle’s centreline.....114

Figure 3- 18. Comparison of post impact kinematic response between a Real-World pedestrian-auto-rickshaw rear impact accident with simulations. Pedestrian offset from vehicle centreline at (a) 15km/h; (b) 25km/h; (c) 30km/h and (d) CCTV-Real-World accident115

Figure 3- 19. Adult pedestrian head-ground directions at different impact velocities at initial front, rear and side impact positions at the vehicle’s centreline.....116

Figure 3- 20. Adult pedestrian head-ground directions at different impact velocities at initial front, rear and side impact positions at 42cm offset from the vehicle’s centreline.....118

Figure 3-21. The full kinematic response of adult pedestrian dummy impacted in the rear offset scenario at 30km/h including the effect of different friction coefficients; (a) original, (b) first scenario, (c) second scenario, (d) third scenario, (e) fourth scenario, (f) fifth scenario, (g) sixth scenario.....128

Figure 3- 22. HIC for primary and secondary front impacts at the vehicle’s centreline.....131

Figure 3- 23. HIC for primary and secondary rear impacts at the vehicle’s centreline.....131

Figure 3- 24. HIC for primary and secondary side impacts at the vehicle’s centreline.....132

Figure 3- 25. HIC for primary and secondary front impacts at offset 42cm offset from the vehicle’s centreline.....133

Figure 3- 26. HIC for primary and secondary rear impacts at offset 42cm offset from the vehicle’s centreline.....134

Figure 3- 27. HIC for primary and secondary side impacts at offset 42cm offset from the vehicle’s centreline.....134

Figure 3- 28. Upper neck injury values for primary and secondary front impacts at the vehicle’s centreline.....136

Figure 3- 29. Upper neck injury values for primary and secondary rear impacts at the vehicle’s centreline136

Figure 3- 30. Upper neck injury values for primary and secondary side impacts at the vehicle’s centreline137

Figure 3- 31. Upper neck injury values for primary and secondary front impacts at 42cm offset from the vehicle’s centreline138

Figure 3- 32. Upper neck injury values for primary and secondary rear impacts at 42cm offset from the vehicle’s centreline139

Figure 3- 33. Upper neck injury values for primary and secondary side impacts at 42cm offset from the vehicle’s centreline139

Figure 3- 34. CTI for primary and secondary frontal impacts at the vehicle’s centreline.....141

Figure 3- 35. CTI for primary and secondary rear impacts at the vehicle’s centreline.....141

Figure 3- 36. CTI for primary and secondary side impacts at the vehicle’s centreline.....142

Figure 3- 37. CTI for primary and secondary frontal impacts at 42cm offset from the vehicle’s centreline143

Figure 3- 38. CTI for primary and secondary rear impacts at 42cm offset from the vehicle’s centreline144

Figure 3- 39. CTI for primary and secondary side impacts at 42cm offset from the vehicle’s centreline144

Figure 3- 40. HIC values for adult pedestrian impacts at the vehicle’s centreline for all simulations run in frontal impact with a polycarbonate windscreen and modified windscreen frame materials..... 146

Figure 3- 41. HIC values for adult pedestrian impacts at the vehicle’s centreline for all simulations run in rear impact with a polycarbonate windscreen and modified windscreen frame materials.....146

Figure 3- 42. HIC values for adult pedestrian impacts at the vehicle’s centreline for all simulations run in side impact with a polycarbonate windscreen and modified windscreen frame materials.....147

Figure 3- 43. HIC values for adult pedestrian impacts at 42cm offset from the vehicle’s centreline for all simulations run in frontal impact with a polycarbonate windscreen and modified windscreen frame materials..... 148

Figure 3- 44. HIC values for adult pedestrian impacts at 42cm offset from the vehicle’s centreline for all simulations run in rear impact with a polycarbonate windscreen and modified windscreen frame materials..... 149

Figure 3- 45. Upper neck injury values at the vehicle’s centreline for all simulations run in frontal impact with a polycarbonate windscreen and modified windscreen frame materials.....150

Figure 3- 46. Upper neck injury values at the vehicle’s centreline for all simulations run in rear impact with a polycarbonate windscreen and modified windscreen frame materials.....151

Figure 3- 47. Upper neck injury values at 42cm offset from the vehicle’s centreline for all simulations run in frontal impact with a polycarbonate windscreen and modified windscreen frame materials.....152

Figure 3- 48. Upper neck injury values at 42cm from the vehicle’s centreline for all simulations run in rear impact with a polycarbonate windscreen and modified windscreen frame materials.....153

Figure 3- 49. Chest injury values at the vehicle’s centreline for all simulations run in frontal impact with a polycarbonate windscreen and modified windscreen frame materials.....154

Figure 3- 50. Chest injury values at 42cm offset from the vehicle’s centreline for all simulations run in frontal impact with a polycarbonate windscreen and modified windscreen frame materials.....155

LIST OF TABLES

Table 2- 1. Element quality control parameters.....56

Table 2- 2. Meshed vehicle components characteristics.....57

Table 2- 3. Material mechanical properties of the model vehicle components.....63

Table 2- 4. Thicknesses of the vehicle components.....63

Table 2- 5. Contact friction coefficients.....70

Table 2-6. Intercept load values of upper neck injury for the 50th percentile Hybrid III adult male and 6YO-child dummies for front Impacts.....79

Table 2- 7. Intercept load values of upper neck injury for the 50th percentile Hybrid III male dummy for rear impacts.....79

Table 2- 8. The intercept load values of chest injury for the 50th percentile Hybrid III male dummy for front impacts.....81

Table 2- 9. Material modification for pedestrian safety improvement.....83

Table 3- 1. The sequence of adult pedestrian-vehicle interaction and contact time at the vehicle’s centreline.....90

Table 3- 2. The sequence of 6YO-child pedestrian-vehicle interaction and contact time at the vehicle’s centreline.....91

Table 3- 3. The sequence of adult pedestrian-vehicle interaction and contact time at 42cm offset from the vehicle’s centreline.....93

Table 3- 4. The sequence of 6YO-child pedestrian -vehicle interaction and contact time at 42cm offset from the vehicle’s centreline.....94

Table 3- 5. Head contact angles for adult and child pedestrians during various impact positions and two vehicle contact regions (Centreline and offset).....95

Table 3- 6. Upper neck injury values for adult pedestrian in the secondary impacts at the vehicle’s centreline in different impact positions (front, rear and side positions).....121

Table 3- 7. Upper neck injury values for adult pedestrian in the secondary impacts at 42cm offset from the vehicle’s centreline in different impact positions (rear and side positions).....121

Table 3- 8. Chest injury values for adult pedestrian in the secondary impacts at the vehicle’s centreline in different impact positions (front, rear and side positions)... 124

Table 3- 9. Chest injury values for adult pedestrian in the secondary impacts at 42cm offset from the vehicle’s centreline in different impact positions (front, rear and side positions).....124

Table 3-10. HIC values vs friction coefficients during primary impacts..... 126

Table 3-11. HIC values Vs friction coefficients during secondary impacts.....129

LIST OF ABBREVIATIONS

Symbol	Definition
6YO	Six-Year-Old
SUVs	Sport Utility Vehicles
MUV	Multi Utility Vehicle
LTVs	Light Truck Vehicles
NCAP	New Car Safety Assessment Programme
GTRs	Global Technical Regulations
AIS	The Abbreviated Injury Score
MPV	Multi-Purpose Vehicle
AAAM	Association for the Advancement of Automotive Medicine
ICH	IntraCerebral Haematomas
HIC	Head Injury Criterion
N_{ij}	Upper neck injury criterion for front impacts
N_{km}	Upper neck injury criterion for rear impacts
CTI	Combined Thoracic Index
ATDs	Anthropomorphic Testing Devices
WSTC	Wayne State Tolerance Curve
GSI	Gadd Severity Index
NHTSA	National Highway Traffic Safety Administration
AAMA	American Automobile Manufacturers Association
AAM	Alliance of Automobile Manufacturers
FMVSS	Federal Motor Vehicle Safety Standards
M_y	Moment for the upper neck at the occipital condyles
PHMSs	Post Mortem Human Subjects
MANIC	Multi-Axial Neck Injury Criterion
A_{max}	Spinal Acceleration Criterion
VC	Viscous Criterion
BLE	Bonnet Leading Edge
BCH	Bumper Centre Height
BD	Bumper Depth
BL	Bumper Lead
GA	Grill Angle
PCDS	Pedestrian Crash Data Study
ABS	Autonomous Braking Systems
VRUs	Vulnerable Road Users
PC	Polycarbonate

List of abbreviations

Mg	Magnesium
Si	Silicon
Zn	Zinc
RTI	Road Traffic Injury
CBA	Cost-Benefit-Analysis
FEA	Finite Element Analysis
FE	Finite Element
FEM	Finite Element Model
MADYMO	Mathematical Dynamical Models
LSTC	Livermore Software Technology Corporation
GM	General Motors
ECE	Economic Commission for Europe
D_{\max}	The mid-sternum chest deflection
int	The critical intercept index
F	Force
M	Momentum
KE	Kinetic Energy
E	Energy
VA	Vehicle velocity
P	Impact Force
M	Vehicle mass
d	Maximum plastic deformation
CAD	Computer Aided Design
IGES	Initial Graphic Exchange Specification
CNRD	Constrained Nodal Rigid Body
NCAC	National Crash Analysis Center
ENDTIM	Termination Time
TSLIMIT	The shell element time step assignment
DT2MS	Time step size for mass scaled solution
ASCII	American Standard Code Information Interchange
CG	Centre of Gravity

1. INTRODUCTION & LITERATURE REVIEW

1.1 Introduction

Nearly 1.2 million people are killed and up to 50 million injured in traffic accidents worldwide annually [1]. This number is predicted to increase to 3.6 million by the end of 2030, making traffic accidents the third leading cause of death globally [2]. Transport-related injuries are particularly high in cities in low - and middle-income countries. It is estimated that approximately one million people are killed annually in road accidents in such places, which represents almost 85% of the worldwide total [3]. While much work has been carried out on the impact of collisions between pedestrians and four-wheeled vehicles, significantly less research has been dedicated to three-wheeled vehicles, in particular auto-rickshaws. Given that they represent one of the most common modes of transport in developing countries, it is important that such vehicles are investigated, to improve safety and reduce the amount of injuries and fatalities.

With these factors in mind, this research aims to assess the safety of both adult and child pedestrians impacted by auto-rickshaws in urban areas in developing countries. It will do so by means of a parametric and comparative analysis of auto-rickshaw - related pedestrian impacts and pedestrian - ground impacts by computational simulation, using a Finite Element model of an auto-rickshaw and an LS-DYNA 50th percentile adult male and six-year-old (6YO) child Hybrid III Anthropometric Test Device (dummies). More specifically, the study will develop a set of injury risk data for the most frequent body regions injured for pedestrians impacted by auto-rickshaws. It will characterise the kinematic response for adult and child pedestrians, injury metrics and injury risk for the head, upper neck and chest produced in the primary impacts (pedestrian-vehicle interactions) and compare all results to identify which of them could become highly injured. In addition, this study will investigate the effect of auto-rickshaws on ground contact and compare the injury risk produced in primary and secondary impacts.

Overall, it is the intention to use the data to establish a logical database to judge whether the auto-rickshaw is safe to use in urban areas. Consequently, suitable

engineering modifications can be suggested to reduce the negative effects of any injury risk. This study has the potential to provide a wealth of important predictive accident data for researchers, bioengineers, auto-rickshaw manufacturers and local governments. This may enable them to make decisions and develop regulations, which can reduce the number of fatalities and severity of injuries, thus reducing the vehicle production cost compared to injury costs.

The following objectives have been identified to achieve these aims:

- To investigate the influence of impact velocity, vehicle contact region, impact position and pedestrian size on the kinematic response, injury metrics and injury risk of adult and child pedestrians head, neck and chest during primary impacts.
- To investigate the influence of impact velocity, vehicle contact region and impact position on the kinematic response and injury risk of the adult pedestrian head, neck and chest during secondary impacts.
- To identify which impact could cause greater injury risk (primary or secondary impacts) relevant to the head, neck and chest for the adult pedestrian.
- To investigate the influence of different material properties and thicknesses of the vehicle components on injury risk reduction for the adult pedestrian head, neck and chest during primary impacts.
- Finally, to investigate the economic effect of the vehicle engineering modifications and the medical saving costs associated with severe head injuries (AIS4+) and serious upper neck and chest injuries (AIS3+).

As a means of contextualising the study, this chapter will provide important background information and information on previous relevant research that has been carried out. More specifically, it provides a summary of accident data, injury criteria and injury risk thresholds with a particular focus on the head, upper neck and chest. It will also discuss the primary and secondary impacts of road traffic accidents and the main factors that can lead to different injury patterns and injury risks.

1.2 Published outcomes

Refereed journal articles

A. J. AL-Graitti, G. A. Khalid, P. Berthelson, A. Mason-Jones, R. Prabhu, M. D Jones. ‘Auto Rickshaw Impacts with Pedestrians: A Computational Analysis of Post-Collision Kinematics and Injury Mechanics’. *International Journal of Biomedical and Biological Engineering*. Vol: 11, No, 11, pp.612-631, 2017.

P.Berthelsona,, P. Ghassemi, J.W. Wood, G.G. Stubblefield, **A. J. Al-Graitti**, M.D. Jones, M.F. Horstemeyer, S. Chowdhury, R.K. Prabhu. ‘A Coupled Finite Element-Mathematical Surrogate Modeling Approach to Assess Occupant Head Injury Risk Due to Vehicular Impacts’. *International Journal for Numerical Methods in Biomedical Engineering*, under consideration.

Peer-reviewed conference papers

A. J. AL-Graitti, G. A. Khalid, P. Berthelson, A. Mason-Jones, R. Prabhu, M. D Jones. ‘Auto Rickshaw Impacts with Pedestrians: A Computational Analysis of Post-Collision Kinematics and Injury Mechanics’. *Proceedings of the 19th international Conference on Mathematical and Computational Biomedical Engineering*, Italy, Venice, 2017.

A. J. Al-Graitti, G. A. Khalid, P. Berthelson, R. Prabhu, M. D Jones. ‘A Comparative Study of the Kinematic Response and Injury Metrics Associated with Adults and Children Impacted by an Auto Rickshaw’. *Intelligent Computing -Proceedings of the Computing Conference*, London, Springer, Cham, pp. 424-443, 2019, **Best student paper award**.

A. J. Al-Graitti, T. Smith, R. Prabhu, M. D Jones. ‘Auto rickshaw – pedestrian head and neck impact injury mitigation- an analysis of impact material alternatives, their costs and their benefits’. *Proceedings of the international Conference on Computational and Experimental Engineering and Sciences*, Japan, Tokyo University, 2019. Submitted to Springer.

Workshops

A. J. Al-Graitti, M. D Jones. ‘Tuk Tuks are coming to Cardiff –despite safety fears!': *Auto Rickshaw -Pedestrians Impacts: A Computational Analysis of Post-Collision Kinematics and Injury Risk*. *Sustainable Transport Workshop – Landscape, Opportunities and Capabilities*, Catapult, Cardiff University, **Best poster award**.

1.3 Road accident data

Motor vehicle-related pedestrian road traffic collisions are a major road safety challenge. According to the World Health Organization they produce almost a quarter of all road traffic-related deaths [2]. Accidents in developing countries are 70 times more likely to occur than in developed countries. Furthermore, the vast majority of road accident fatalities are vulnerable road users, such as pedestrians [4]. The annual traffic statistics in Saudi Arabia in 1999 showed that road accidents caused almost 6,000 serious pedestrian injuries and 1,000 deaths [5]. In Africa, pedestrian fatality is also a major issue, with road traffic accidents accounting for an estimated 39% of all deaths in Tanzania, 75% in Cote d'Ivoire [6] and 85% in Ethiopia [7]. In Bangladesh, pedestrian accidents with auto-rickshaws, buses, trucks and tractors have a higher fatality risk than impacts with cars [8].

Children are particularly vulnerable road users as passengers, cyclists and pedestrians. As pedestrians, they may walk, play or even work on roads in close proximity to vehicles. All these interactions, together with a variety of other risk factors associated with childhood, increase their vulnerability to road traffic injury [9]. Trauma is a major cause of paediatric injury [10] and statistically, child pedestrians are the group most likely to be involved in vehicle-pedestrian impacts. Males aged between 5 and 14 years and females between 10 and 19 years have the highest fatality rates amongst all pedestrians. In developed countries, between 5% and 10% of children suffering road traffic injuries are pedestrians. However, in developing countries, the proportion ranges between 30% and 40% [11]. Roads have always been unsafe places for children. Nonetheless, the rapid increase in traffic and a shift towards transportation on roads makes the issue particularly pressing today [12].

These road traffic accidents, which cause pedestrian injuries and fatalities have devastating impacts on families, human pain and suffering, loss of productivity and pressure on the emergency services and insurance resources. The noticeable increase in road accidents in developing countries, compared to developed countries, could be the result of many factors, such as road infrastructures [13], road design and pavements [14, 15], human behaviour (both drivers [16-18] and pedestrians [19, 20]), traffic mix, traffic lights [21], speed cameras [22], vehicle model and technology [23, 24] and the common transport mode. It has been reported that passenger cars, sport utility vehicles

(SUVs) and vans are the most common registered vehicles in developed countries [25, 26], 46% of passenger cars were involved in fatal pedestrian accidents in the US [26], while 74% of passenger cars were involved in fatal pedestrian accidents in France [27]. However, in Japan, pedestrian accidents are more commonly associated with light trucks and vans than passenger cars [28].

In contrast, developing countries have unique common vehicles that comprise a much wider range of modes than those in developed countries. These vehicles can be classified into two main types: non - motorised and motorised transport. The non - motorised mode includes bicycles, rickshaws and animals, such as camels and horses. In contrast, the motorised mode includes motorcycles, auto-rickshaws and cars. All these modes of transport can be observed to share the same road.

Auto-rickshaws, which are the focus of this study, require consideration in more detail. These vehicles are one of the chief modes of transport in developing countries, such as India, Pakistan, Nepal, Bangladesh, Cambodia, Laos, Philippines, Sri Lanka, Thailand, Guatemala, Ethiopia, Sudan and Egypt [29]. Many people consider auto-rickshaws to be one of the best solutions for their urgent and special needs at early morning and night times, when there are few public transport services [30]. Auto-rickshaws have the ability to negotiate narrow roads, better manoeuvrability in small-turn radii roads and consume less fuel than cars. This means that they provide greater access to urban areas and are easier to drive [31 - 33]. The total number of auto rickshaws varies between 2% and 11% in the eight of the major Indian cities; 10% to 20 % of daily trips are in fact, made on motorised road transport modes [34]. Due to population increases, in many developing countries such as India, the production of motorised three - wheelers has doubled between 2003 and 2010 [34]. The problem is, however, that auto-rickshaws are responsible for a large number of road accidents. In India, they are only second to motorized two - wheelers in terms of accident risk [35]. In the city of Hyderabad, for example, it was noted that 17% of pedestrians were killed in car/jeep/multi utility vehicle (MUV)/auto-rickshaw accidents [36]. In contrast, in Sudan, 19% of auto-rickshaw accidents involved in auto rickshaw-pedestrian collisions [37]. Thus, it is apparent that there is an urgent need to explore what can be done to reduce such accidents, which is one of the key aims of this study.

It is noteworthy that there are several popular auto rickshaw designs, including those used for passengers or goods that might affect the kinematic response and injury risk for a pedestrian impacted by the vehicle in urban areas, see Figure 1-1. This study will be focused on Bajaj design, since it is the most common design in many developing countries, as shown in Figure 1-1 (a).



Figure 1-1. Design of the exterior of an auto rickshaw; (a) Bajaj passenger vehicle; (b) passenger vehicle; (c) Piaggio goods vehicle; (d) Applications police vehicle [38].

With the engineering successes associated with driver and passenger safety, pedestrian protection is now becoming the most crucial road traffic safety priority, not only in low-income countries but also in many other countries. Consequently, it has become an increasingly important focus for automotive safety research. However, most engineering research has focused on the most common vehicles involving pedestrians in developing countries, such as passenger cars, light truck vehicles (LTVs) and vans. In addition, the most common safety programmes tend to focus on the impacts of pedestrian four-wheeled vehicles, such as the European New Car Assessment Program (NCAP) and Global Technical Regulations (GTRs), even though there is a lack of real accident data relevant to the impacts of pedestrian auto-rickshaw impacts. Engineering reconstructions relevant to pedestrian-vehicle-based impacts using experimental and computational modelling are increasingly applied to understand the main parameters which might significantly influence injury risk.

They enable the simulation of different initial and boundary conditions and they can lead to new engineering proposals. However, less efforts have been focused on the impacts of auto-rickshaw - pedestrian impacts in urban areas and their safety for the environment in which they operate remains unknown [32, 39, 40].

Numerous studies have pointed out that the majority of pedestrians are impacted by the front end of the vehicle during primary impacts [41-43]. Therefore, most studies on pedestrian-vehicle impacts locate a pedestrian at the front of the vehicle when investigating different parameters on the kinematic response, injury metrics and injury risk. Thus, it is significantly important for automotive engineers to understand the concepts of injury mechanism and injury which are used for road accident reconstructions and injury risk classifications [44]. The injury mechanism is the mechanical and physiological change and deformation of the anatomical structures. The severity of a resulting injury [37] can be measured by different scoring systems for injury assessment in clinical practice: the anatomical scales, the physiological scales and a combination of the two (anatomic and physiologic reactions) [37, 45-48]. The Abbreviated Injury Scale (AIS) is one of the most commonly used anatomic scales to classify the injury risk level for different regions of the body. AIS is an anatomic method which classifies the individual injury body region according to a 6-point scale of severity (1=minor, 2=moderate, 3=serious, 4=severe, 5=critical and 6=fatal), which predicts the threat to life [49, 50], as shown in Figure 1-2. While the importance of exploring the impact of front-end vehicle impacts is increasingly recognised by researchers, it continues to be investigated within the context of four-wheeled vehicles. Thus, this study aims to break new ground by carrying out similar studies on a three-wheeled vehicle: the auto-rickshaw.

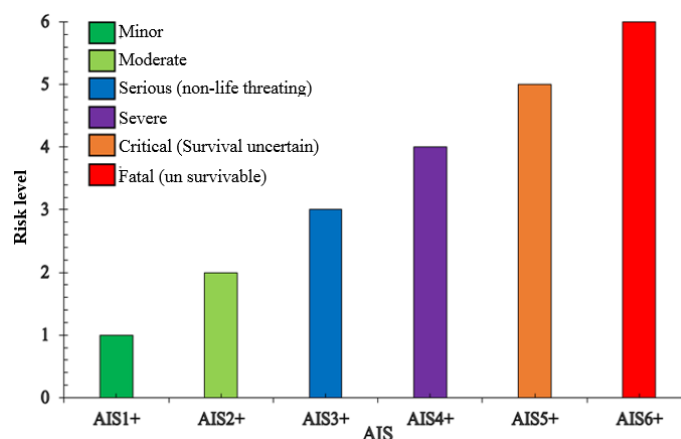


Figure 1-2. AIS and risk level; data obtained from [51, 52].

1.3.1 Pedestrian injury patterns and injury severity according to body regions during primary and secondary impacts

Pedestrian - vehicle impact scenarios can be called “primary impacts” which describe the interactions between pedestrian body regions and vehicle components [53-55]. During these impacts, momentum transfers from the vehicle to the pedestrian. However, primary impacts terminate when the pedestrian is totally separated from contact with the vehicle [56]. This means that a flying phase starts, followed by a subsequent falling phase terminated by ground interactions between the pedestrian’s body regions and the ground. This is known as a “secondary impact” [54, 55]. In addition, the pedestrian body slides on the ground until the whole body comes to rest [56]. The travelling distance of the pedestrian is measured at the pedestrian’s centre of gravity from the initial impact position to the point of rest, which includes flying, falling and sliding, all of which can also be called the “throw distance” [53, 56, 57].

Many statistical studies have reported the injury patterns and injury severity during primary impacts in developed and developing countries to identify the most frequently injured body region and the injury severity. This can help to establish a useful database for all researchers and engineers who are interested in improving pedestrian safety [58-61].

An analytical study, including 521 pedestrian-vehicle impact cases between 1994 and 1999 in the USA, shows that the lower extremities and head are the most frequently injured body regions [58]. Head injuries are the most serious injuries and can often lead to death [58]. Nonetheless, lower limb injuries are also important and can lead to disability and result in high social costs. The same study cited above found significant differences in injury severity. For example, the risk of lower limb injury was between moderate (AIS2+) and serious (AIS3+), while the risk of head injury was considerably high and could result in fatal injuries [59], see Figure 1-3 for more details.

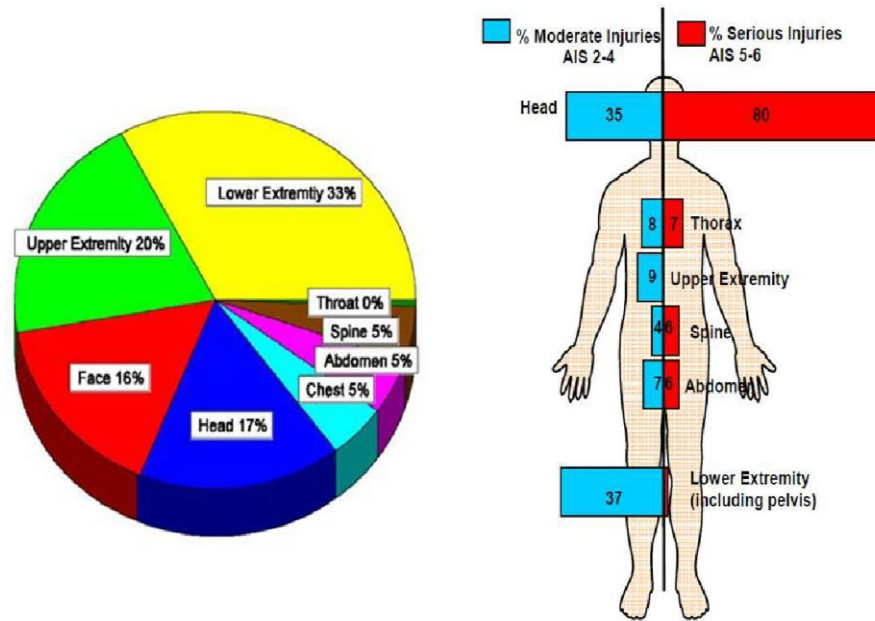


Figure 1-3. Distribution of all pedestrian injury patterns by body region and injury severity level [58].

A French study analysed road accident data for 10,703 pedestrians who were injured or killed in an accident involving a multi-purpose vehicle (MPV) between 1996 and 2007. It found that the most frequently injured body regions were the lower extremities (50%), the head/face/neck (38%) and the upper extremities (27%). Severe injury (AIS4+) was significantly the most common in pedestrian head injuries, followed by thorax, abdomen, spine, pelvis and lower extremities. In contrast, serious (AIS3+) injury mostly involved the lower and upper extremities, followed by head, chest and pelvis [60], as shown in Figure 1-4.

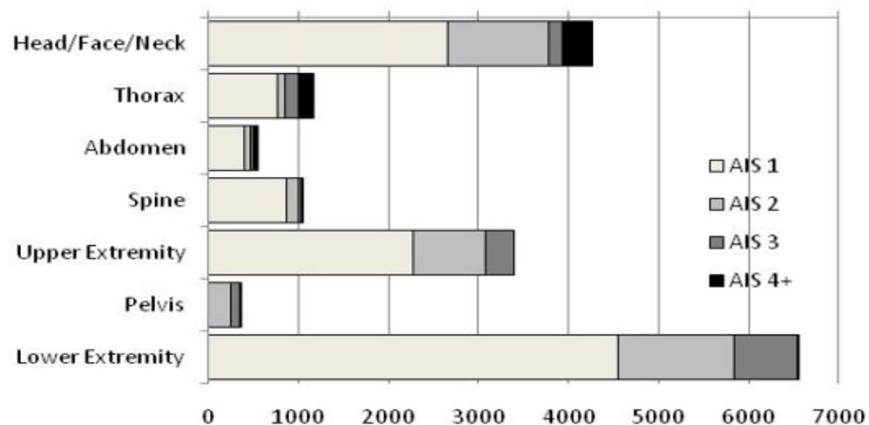


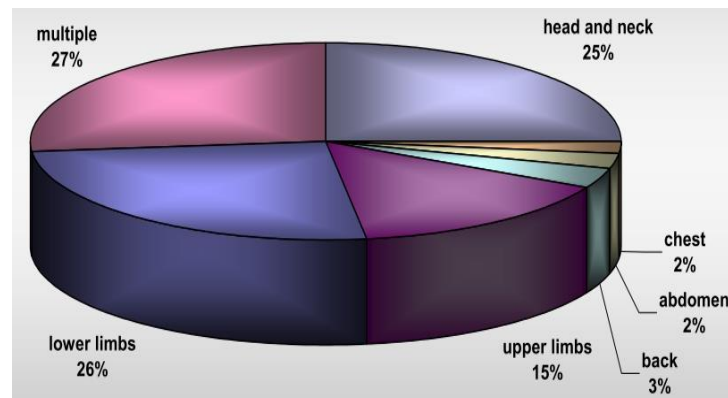
Figure 1-4. Pedestrian injury pattern and injury severity during impacts with multi-purpose vehicles (MPVs) in France between 1996 and 2007 [60].

The distribution of pedestrian injuries between moderate (AIS2+) and fatal (AIS6+) injuries in the USA, Europe and Japan shows that the head, neck and chest are the most frequently injured body regions and can cause fatal or significant severe injuries more than any other body regions [61]. This occurs when a pedestrian is impacted by the front of a vehicle, whether it has a one-box design, an SUV or a passenger vehicle [61]. An investigation of pedestrian - passenger car road traffic accident data in three Chinese cities (Beijing, Shanxi and Chongqing) between 2006 and 2008 determined that the majority of pedestrians were male. Furthermore, the most commonly injured body region was the head, followed by thorax and extremities with serious (AIS3+) and severe (AIS4+) injuries [62].

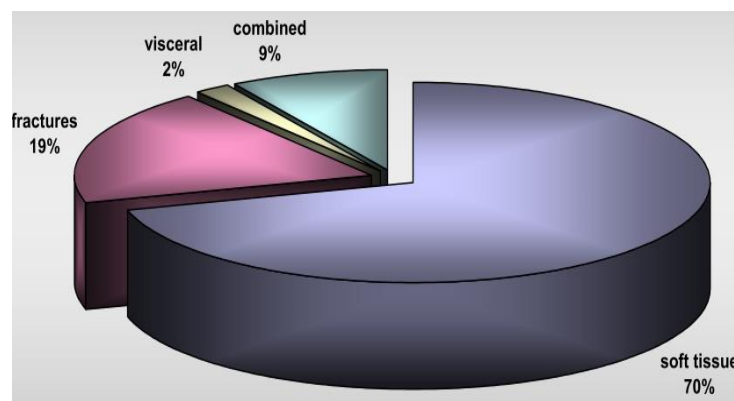
It can, therefore, be concluded that injury patterns and injury severity vary according to the front end geometry of a vehicle. However, in all cases the head, neck and chest are the most frequently fatally injured body regions during pedestrian-four-wheeled vehicles impacts. These vehicles are most commonly involved in primary pedestrian impacts in developed countries, whereas auto-rickshaws are the most common vehicle in developing countries. Auto rickshaws possess a unique front - end geometry typically with only one front wheel and tyre, headlamp and mudguard rather than a bumper (fender). The complex geometry has the potential to produce more varied and complex injury patterns and injury risks during pedestrian-auto-rickshaw impacts. With this in mind, it is essential to study these types of vehicles in more detail to ascertain whether similar injury patterns and risks exist. An analytical study of real-world accidents, in the Sudan, has suggested that head, neck and chest injuries are significant, while soft tissue and fractures are the most frequent injuries for pedestrians impacted by auto-rickshaws [63], as shown in Figure 1-5. However, many more studies, such as the current one, that are grounded in empirical evidence need to be carried out.

An Indian study collected road traffic accident data between November 2005 and June 2006 from hospitals in Hyderabad for a total of 781 cases. Of these cases, 139 subjects were injured in 114 auto-rickshaw impact scenarios. There was no significant difference between passengers and pedestrians injured by the auto-rickshaw impacts. In addition, head, neck and lower limbs were found to be the most frequent minor injuries (AIS1+), followed by moderate (AIS2+) and fatal (AIS6+) injuries [64].

Similarly, it was pointed out that most of the pedestrians who impacted with an auto-rickshaw were adults (95% of cases). Just 5% were children under the age of 10 years old. In addition, soft tissue injuries were the most common injury, while 14% had a neurological deficit when analysing the accident data for 100 patients in Sri Lanka [65].



(a)



(b)

Figure 1-5. Injury body regions and injury details of pedestrian impacted by an auto-rickshaw; (a) injury body regions; (b) injury details [63].

Although injury patterns and injury risks vary according to vehicle type, it can be seen that the head, neck and chest are the most frequently injured body regions during primary impacts and can lead to severe injuries, disability or even death. However, pedestrians will eventually interact with the ground during the most common vehicle-pedestrian impact scenarios producing further pedestrian injury patterns and injury risks.

A German study reported that secondary impacts cause 65% of all injuries [54] and similarly, accident data from Birmingham (UK) showed that ground interactions are responsible for 56% of all injuries [66]. Thus, there are wide variations in post-impact kinematics during the free-flight impact of a pedestrian's motion when they are initially impacted by a four-wheeled vehicle. Most statistical and numerical studies have focused on head injuries produced during ground contact as the most frequently injured body region [55, 67-72].

No statistical or computational analysis has reported the secondary impacts for a pedestrian who has initially been impacted by an auto-rickshaw. In addition, head injuries including neck and chest injuries have been suggested as the most frequent fatal injuries compared to other body regions. Nonetheless, it is unknown whether this will be the same within the context of a three-wheeled vehicle and the developing world. Thus, this is the principal of the study. Before moving on to consider injury criteria and thresholds, it is important to gain an understanding of the anatomy of the three most commonly injured body regions: head, neck and chest. This will help to gain a better understanding of the importance of collecting and analysing robust data to reduce such injuries with auto-rickshaws in developing countries.

1.4 Anatomy and injury risk

The word 'anatomy' derives from the ancient Greek and Latin words "ana" and "tome" meaning "cut up". It is the study of the structures that make up the body and how these structures are related to each other. Understanding anatomy is very useful in injury mechanisms, healing wounds and caring for the sick [73]. It includes many subspecialties, such as gross anatomy, microscopic anatomy, developmental anatomy and embryology [74]. The following section briefly reviews the regional anatomy of the head, neck and chest and the probable injury severity of each one, to better appreciate the complex nature of injuries in these body regions.

1.4.1 Head anatomy and injury risk

A brief explanation of head anatomy and head injury severity can help to better understand the head injury mechanism and injury risk classification. The head is defined as the body region consisting of skin, scalp, skull, meninges and brain [75].

The skin is the outer surface of the human head and the first protective layer [75], see Figure 1-6. Skin injuries can be categorised as superficial or deep. They also include contusions (bruises), lacerations (cuts) and abrasions (scrapes) [76]. The scalp is a 5 to 7mm thick layer, consisting of hair, skin and facial muscles, as shown in Figure 1-6.

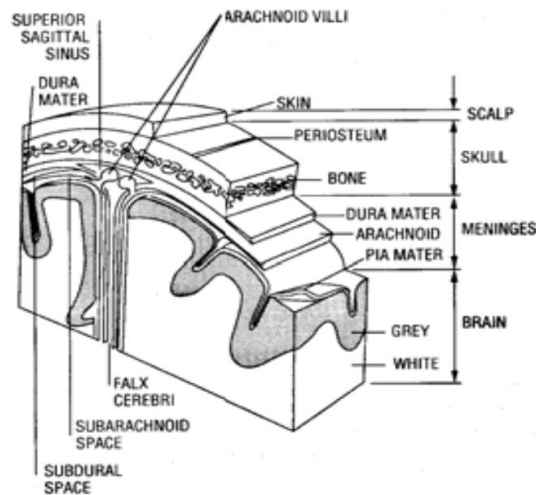
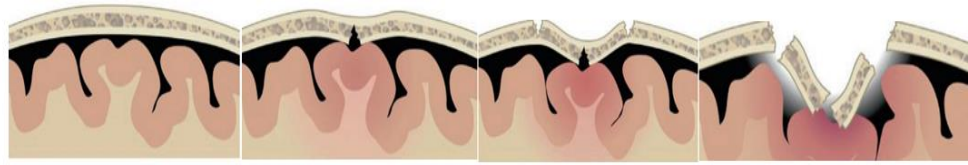
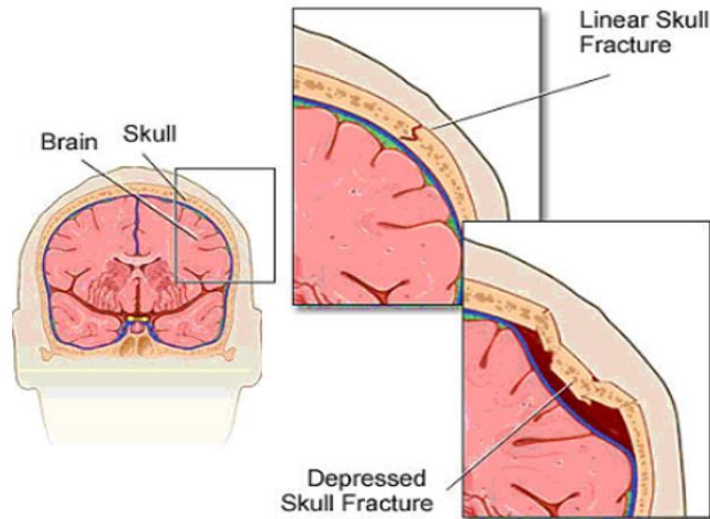


Figure 1-6. Head section [76].

Scalp swellings and lacerations are commonly sustained injuries during pedestrian accidents when the pedestrian's head impacts directly with the vehicle structure. According to Association for the Advancement of Automotive Medicine (AAAM), this type of injury can be classified as a minor injury (AIS1+) [77]. The skull is a "sturdy box", which contains and protects the brain. It consists of eight different bones: the unpaired frontal, occipital, sphenoid and ethmoid bones and the paired temporal and parietal bones [77]. Each one has three distinct layers: inner, outer and diploe. A skull fracture can occur with or without brain damage and therefore, it can be divided into two types: linear or depressed, as shown in Figure 1-7. A linear skull fracture is a cracked single line, while a depressed fracture is defined as the depression of a bone fragment greater than the thickness of the skull, which is depressed into the cranial cavity and can damage brain tissue and blood vessels [78]. This is often caused by translational and/or rotational forces as a result of acceleration or deceleration of the brain. In many cases, skull fractures are not life-threatening.



(a)



(b)

Figure 1-7. Skull fractures; (a) different stages of skull fracture injuries; (b) linear and depressed skull fractures [79].

Brain injury can occur by a direct force applied to the head or a force applied to the head via the neck as in whiplash injuries. These can result in deformation of the brain tissue according to the magnitude of the deformation [80].

Moderate head injuries (AIS2+) include a vault fracture, consisting of a cerebral concussion with the likelihood of haemorrhage; intracerebral haematomas (ICH), both petechial and subcortical; and subarachnoid haemorrhage of more than 6 hours, not associated with a coma [81]. Other examples include a basilar fracture, including cerebral concussion or a subdural haemorrhage, both of which can be classified as serious injuries (AIS3+) [81]. Lesions of soft tissue, skull fractures, brain bleeding, brain contusions and lacerations and bone structure deformations can also be classified as severe injuries (AIS4+) [81-84]. Cerebral injury, including ischaemic brain damage, can be directly related to head trauma, associated with more than six hours of coma can be classified as a critical injury (AIS5+) [49]. A fatal head injury indicates

death as a result of a brain stem injury, which typically involves laceration, crushing, penetrating or transection [85]

1.4.2 Neck anatomy and injury risk

The neck is the cylindrical connection between the head and the body. Its role is supporting the head and serving as a conduit for vessels and nerves passing between the head and body as well as a passageway for materials entering the digestive system and a passageway for the respiratory system [73]. It has many vasculatures, including arteries and veins, which carry oxygenated blood to the brain and carry deoxygenated blood away from the brain to the heart [86]. Moreover, the cervical spine is a complex structure consisting of 7 cervical vertebrae, which protect the spinal cord [86], as shown in Figure 1-8.

The first two vertebrae are called atlas and axis, which provides support for the human head [87]. The bones are linked together by facet joints, which are small joints between the vertebrae, that together with the neck muscles, allow the head to move in any direction [87].

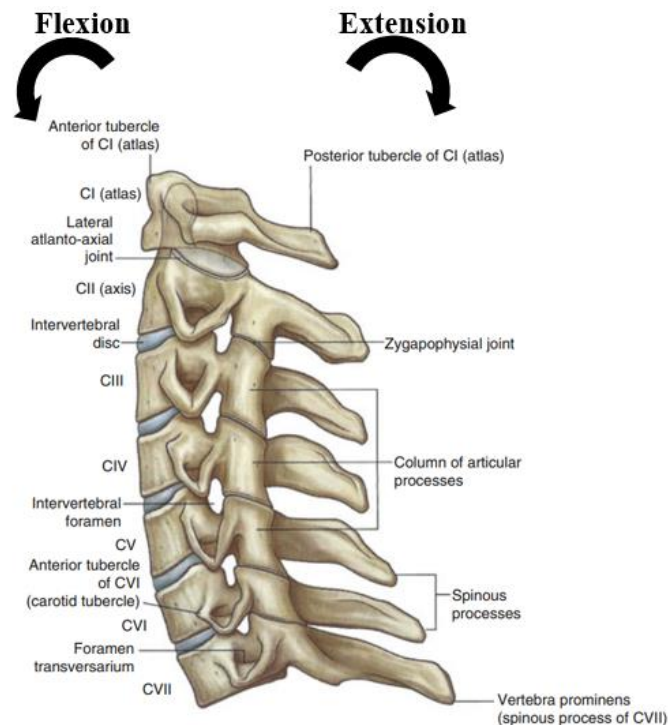


Figure 1-8. Neck bone structure [88].

It can be divided into four regions: the anterior, posterior, posterior cervical and sternocleidomastoid regions, as shown in Figure 1-9. The posterior region is behind the lateral border of the trapezius muscle and is the nape or nucha. In contrast, the lateral region is behind the sternocleidomastoid muscle and is bounded in front by this muscle, below by the clavicle and behind by the trapezius muscle. The sternocleidomastoid region corresponds to the projection of this muscle [89].

The anterior region is in front of the sternocleidomastoid muscle and is bounded posteriorly by this muscle, in front by the midline of the neck and above by the border of the mandible. A small area behind the mandibular angle and in front of the mastoid process is called the fossa retromandibularis. It lodges the posterior part of the parotid gland, nerves and vessels. The anterior and lateral regions are divided into a number of triangles by the omohyoid muscle descending obliquely from front to back and crossing the sternocleidomastoid muscle [89].

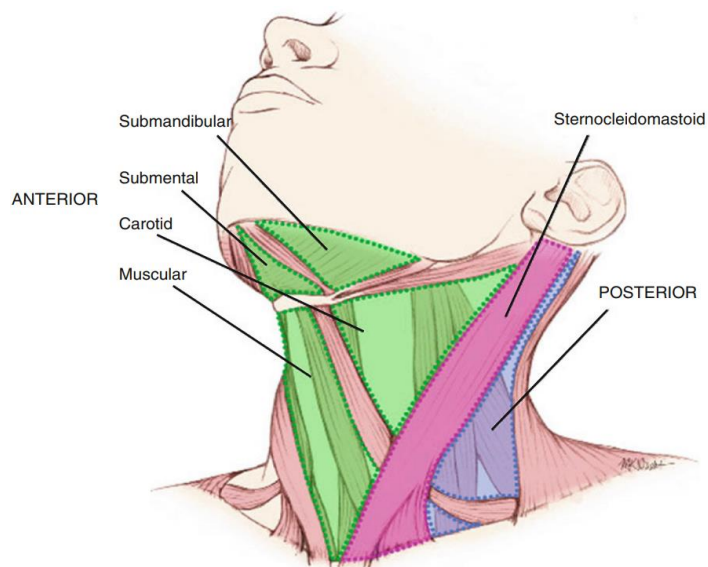


Figure 1-9. The triangles of the neck [90].

These regions would cause neck soft tissue injury and ligament rupture with symptoms, such as neck pain and stiffness, shoulder weakness, dizziness, headache and memory loss [91]. In addition, this region can suffer cervical vertebral fractures, which may result in irreversible spinal cord injury resulting from cervical vertebrae compression [86], as shown in Figure 1-10.

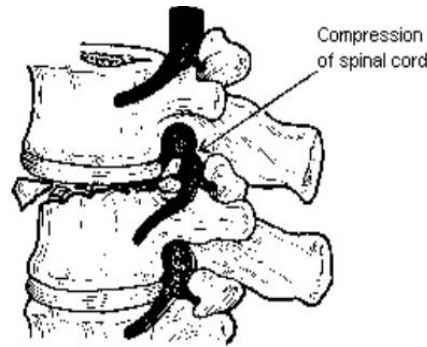


Figure 1-10. Compression injury [86].

Injuries to the neck and spinal cord during vehicle impact scenarios normally result from a combination of forces and bending at occipital condyles [92]. Moderate (AIS2+) neck injuries are associated with neurological deficit and vocal cord involvement, while serious neck injuries (AIS3+) are related to the rupture of small blood vessels of the occipital condylar joints, alar ligament rupture, damage to the spinal cord (disc rupture and nerve root damage) and brainstem, and even death [93-96].

Severe (AIS4+) neck injuries include phrenic nerve injury. Critical upper neck injuries (AIS5+) are linked to subcutaneous tissue abrasion and contusion hematoma, vascular injury (neurological deficit), carotid artery and jugular vein laceration, oesophagus, larynx, pharynx, salivary gland, thyroid gland, trachea and vocal cord injuries [81].

1.4.3 Chest anatomy and injury risk

The thorax is located in the superior part of the torso above the abdomen. It consists of skin, subcutaneous fat and some superficial musculature, such as the pectoral muscles and paraspinous muscles. The thoracic wall includes the spine, the ribcage and intercostal musculature. The thoracic cavity includes the pulmonary cavity and contains vital organs, such as the heart, lungs and major blood vessels, see Figure 1-11.

Chest injuries can cause different injury risks and severities. Moderate chest injuries (AIS2+) includes fracture of at least two ribs or the sternum, a partial thickness of soft tissue injury or bronchus tear distal to main stem [81]. Serious chest injuries (AIS3+) consist a fracture of at least three to five separate ribs on one side of the body, lung contusion and minor heart contusion [81, 97-99]. Severe injuries (AIS4+) include

fracture of at least five ribs (or three bilaterally), including a “flail” rib, having two fracture locations. The flail ribs involve a free-floating rib segment between fractures, causing a particularly unstable chest wall, which may also be associated with severe breathing difficulties, bilateral lung laceration, minor aortic laceration and major heart contusion [81, 96, 98, 100]. Critical chest injuries (AIS5+) include bilateral flail chest, major aortic laceration and lung laceration with pneumothorax tension [100].

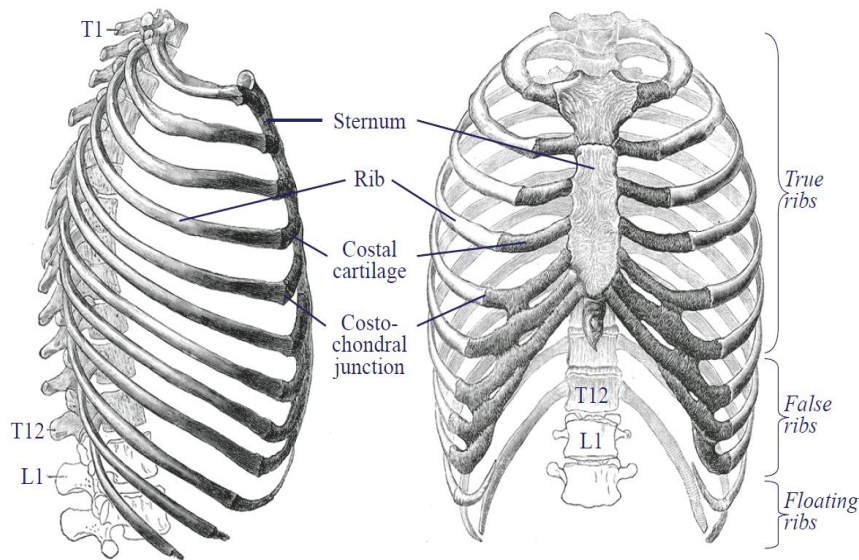


Figure 1-11. Anatomy of the rib cage from lateral and anterior views [101].

1.5 Injury criteria and thresholds

Previous literature has shown that the head, neck and chest are the most frequently injured body regions (section 1.3.1), injuries which are potentially life-threatening and cause a high risk of disability or even death. Explaining the proposed injury criteria and injury thresholds for these three body regions is important. This section will explain the Head Injury Criterion (HIC) for head injury risk, the criterion for upper neck injuries and risk (N_{ij} and N_{km}) and the Combined Thoracic Index (CTI) for chest injury risk.

1.5.1 Head injury criteria and thresholds

Head injury risk produced during impacts can be measured by a range of variables, such as the body's kinetic energy, transmitted force, the stress and strain of the structure and the head acceleration [102]. Each of these variables, either alone or in

combination may be produced during primary and secondary impacts. Head acceleration measurements are used as a key correlation for head injury and are applied to predict head injury risk. Head injury thresholds have been developed by subjecting human volunteers, adult cadavers or primates and other animal surrogates to translational and or rotational accelerations and evaluating any significant corresponding injuries [103]. Observed head injury risk correlates with head accelerations to produce head injury threshold values. These thresholds have been further investigated through the use of computational modelling and anthropomorphic testing devices (ATDs) in threshold testing and accident reconstruction. The thresholds have generally been expressed in terms of kinematic variables to provide an indicator with which incidents can be assessed. Head injury thresholds will be discussed generally in terms of translational accelerations, particularly those relating to adults and children in different impact positions.

The Wayne State Tolerance Curve (WSTC), founded by Wayne State University in the 1950s, was the first suggested tolerance for a head injury to evaluate head injury risk. It established a correlation between the magnitude of acceleration and the pulse duration required to produce a skull fracture, see Figure 1-12. Generally, impulses with high acceleration can cause injuries and lower accelerations require longer pulses to cause injuries [103]. A combination of magnitude and duration, which lies above the WSTC, can indicate a risk of severe head injury (AIS4+). The WSTC data provides the foundation for several currently widely used injury metrics, such as the Gadd Severity Index (GSI), which was developed by Charles Gadd of the General Motors Corporation in 1966 to account for the shape of the acceleration pulse [104, 105].

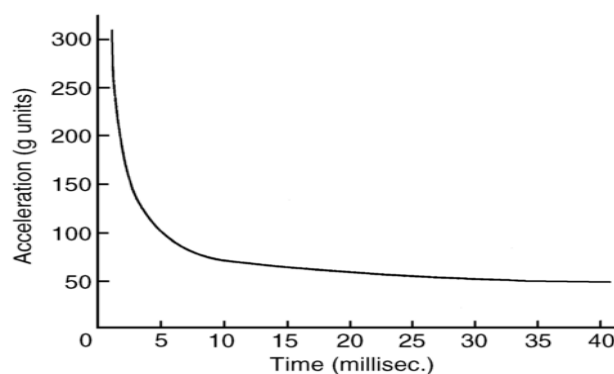


Figure 1-12. Wayne State Tolerance Curve (WSTC) [80].

Gadd reasoned that some measure of the area under the acceleration/time curve for a given impact could form the basis for such an index. However, it was apparent that a low level of acceleration lasting for a long time was not injurious, whereas a higher level of acceleration acting for a shorter time was much more likely to be so, even though the area under the acceleration/time curve could be the same. It was suggested that if GSI exceeded a value of 1000, there would be a threat to life. Gadd weighted the area measurement in favour of the acceleration component by raising the acceleration value to the power of 2.5. This is because the absolute slope of the WSTC is plotted on a logarithmic axis [80]. The mathematical expression for the GSI is:

$$\text{Gadd Severity Index (GSI)} = \int_{t_1}^{t_2} a(t)^{2.5} dt \quad (1.1).$$

Where a is the linear acceleration pulse measured in terms of acceleration in units of gravity (g), and (t) is the time duration of the impact in milliseconds. GSI has been highly criticised because it deviates considerably from the WSTC. Therefore, a new Head Injury Criterion (HIC), was developed, which considers only that part of the acceleration-time curve, which can be associated with injury, irrespective of the waveform shape. This new criterion was suggested by the National Highway Traffic Safety Administration (NHTSA) based on the work of Versace in 1971, to quantitatively assess the head injury risk [106]. The HIC is the most commonly adopted severity coefficient [102, 107]. Prasad and Mertz [82] and Mertz et al. [108] have reported skull fracture and brain injury curves based on data analysis for many previous experimental studies (including cadavers, human volunteers and live animals) [109-112].

An HIC value of 1000 corresponds to a 16% and 18% risk of severe head injuries during frontal and rear impacts [82, 113, 114], when the impact time duration is 15ms or lower [82, 113]. Kikuchi et al. [115] concluded that the frontal and lateral impacts to the head have different tolerances, with the lateral impact tolerance for skull fracture being about 80% lower than for frontal; stating that this difference must be included in any risk function for side impact head injury. Similarly, Hertz [84] and McIntosh et al [116] concluded that a HIC of 800 is associated with a skull fracture risk during a side impact to the head. These curves represent an estimate of the injury risks for the adult population, since adult cadavers were used to obtain the biomechanical data and this data was not normalised for size, mass and tissue tolerance effects. A child's

head has different morphometrics (size and shape) and anatomical structures than an adult, which influence the head impact response and structural integrity. Klinich et al [117] commented that the major difference between children and adults is the proportion of total mass in the head and skull structure and tissue strength. Whilst a child's skull can easily deform, it is less susceptible to fracture. These differences logically would result in a variation in head injury thresholds.

The American Automobile Manufacturers Association (AAMA), which is now known as the Alliance of Automobile Manufacturers (AAM), therefore, used a scaling method to estimate the limit values of head injury for children of different ages [93]. It proposed a HIC of 700 for a six-year-old (6YO) child and a HIC of 570 and 390 was suggested for a three-year-old child and a one-year-old child, respectively. The NHTSA has adopted these thresholds and suggested to the Federal Motor Vehicle Safety Standards (FMVSS) that these limits should be set at a 5% of severe head injury risk (AIS4+) [93] or a 23% risk of serious head injury (AIS3+) [117]. These values correspond with brain injury or skull fracture [118]. They are also associated with head injuries, such as injuries occurring at the base of the skull or compound, comminuted or depressed skull fractures [81, 117]. Therefore, the Head Injury Criterion (HIC) will be used in the current study to measure injury risk. The mathematical expression will be explained in Chapter 2, section, 2.4.2.1.

1.5.2 Neck injury criteria and thresholds

There are currently no widely accepted criteria established for neck injuries due to their geometrical and structural complexities. However, the NHTSA and FMVSS have both defined the allowable neck forces to avoid neck injuries, based on a select number of volunteers, cadavers and test dummies to provide criteria for predicting injury risk to people with varying anthropometric characteristics based on various automotive impacts and restraint systems [87, 119-121]. The current injury criteria for the neck contains individual tolerance limits for compression (neck compression), tension (force stretching the neck), shear (force perpendicular to the neck column), flexion moment (forward bending of the neck) and extension moment (rearward bending of the neck) [87, 122, 123].

The NHTSA established a neck injury criterion with four neck loading mechanisms and critical limits in the front impacts called ' N_{ij} '. In 1984, Prasad and Daniel [124]

developed the concept of a composite neck injury indicator based on a linear combination of axial tension loads and extension (rearward) bending moments as a result of experimental results on porcine subjects. Axial force and moment for the upper neck were measured at the occipital condyles (M_y) using a methodology initially developed by Klinich et al. [117] and Kleinberger et al [119]. They applied earlier biomechanical experimental research using human volunteers, porcine and human subjects and post mortem human subjects (PHMSs) and established critical intercept values for N_{ij} calculation [87, 122-126]. The established intercept values are designed to be used for adults, however, a scaling method was used for different dummy sizes and various critical intercept values were proposed for infants (12-month-old), (3 and 6YO) children, small females and midsize adult males to assess vehicle safety in frontal impacts [93].

Rear impacts are a significant measure for rear impact related neck injuries. A neck injury criterion called ' N_{km} ' was suggested for such impacts. This approach is similar to the frontal impact criterion ' N_{ij} ' [127]. However, with respect to possible upper neck injury mechanisms during rear impacts, shear force loads rather than axial force loads are regarded as the critical load. Previously, it was assumed that shear force loads were significantly harmful to the facet joints, particularly in the upper neck region [128, 129]. Shear forces and bending moment (flexion/extension), therefore, were suggested for upper neck injury criterion (N_{km}) calculation during rear impacts. Mertz and Patrick [87] applied a series of experimental tests based on human volunteers and suggested critical intercept values, up to which no injury is expected. These values are designed to fit a midsize adult-male, however, no up-to-date scaling method was proposed to establish the critical intercept values during rear impacts for other sizes. Regarding upper neck injury threshold, it was proposed that an upper neck injury criteria (N_{ij} and N_{km}) of 1 corresponded to a 22% probability of sustaining serious upper neck injuries [93], which are associated with a risk of alar ligament rupture, damage to the spinal cord and brainstem and death [93, 94, 130].

Currently, there are no upper neck injury criterion and injury tolerance limits approved for side impacts. However, one proposed solution is the multi-axial neck injury criteria (MANIC), which also includes the effects of side acceleration on the neck [131]. Upper neck injury criterion (N_{ij}) for frontal impacts, therefore, will be used in the

present study to assess the risk of upper neck injury in adults and children. In addition, N_{km} will only be used to assess the upper neck injury risk for adults. All critical intercept values and upper neck injury criteria (N_{ij} and N_{km}) expressions will be explained in chapter 2, section 2.4.2.2.

1.5.3 Chest injury criteria and thresholds

Many studies have shown that chest tolerance to blunt impact is highly dependent on overall bone strength [132, 133]. It is essential, therefore, to explain various chest injury criteria to assess suitable chest injury risk predictors, which can be used to measure and predict chest injury risk accurately in the real world.

The spinal acceleration criterion (A_{max}) was the first criterion used to evaluate human thoracic response to dynamic loads. It is based on experiments by Mertz and Gadd between 1968 and 1970 [134] and observed that the level of acceleration that humans withstand decreases with exposure length. The FMVSS states that peak spinal accelerations, measured with a Hybrid III ATD, should not exceed 60g for more than 3ms to avoid severe thoracic injuries and serious thoracic soft tissue injuries [135]. However, subsequently it was found that spinal acceleration is not a suitable criterion for chest injuries for a number of reasons; the criterion was determined as load-dependent and the criteria do not identify any local areas of high stress to the ribcage [135]. Chest deformation or deflection for blunt frontal loading was more appropriate than the spinal acceleration criterion [136]. A deformation of 63mm indicates a 33% risk of sustaining a serious chest injury [137] and a 4% risk of a severe chest injury, such as heart/aortic injury [99, 108, 119].

Lau and Viano approved the Viscous Criterion (VC) for the evaluation of soft tissue injuries [137]. The VC is the maximum current product of thoracic compression (C), which represents instantaneous compression, $C(t)$ and thoracic compression rate (V), which represents the velocity of chest deformation $V(t)$. Both values are determined by measuring the sternum deflection [138]. In addition, sixteen lateral thoracic impact tests of whole-body cadavers were conducted. They found that maximum viscous response and maximum chest compression were significantly better predictors of thoracic injury than spinal accelerations. Logistic regression of this data showed a VC of 1 m/sec, which indicated that a 33% chest deflection produced a 50% risk of serious

thoracic injury. Moreover, it was proposed that a Hybrid III ATD threshold VC be less or equal to 1.0 m/s. The VC for chest injury is not used widely [139].

In 1998, the currently applied criterion the Combined Thoracic Index (CTI) was introduced for thoracic injury by the NHTSA. Considered a suitable tool for predicting a chest injury it has proved a better injury frequency predictor of real-world chest injuries than chest deflection or acceleration alone [93, 140]. This is due to the fact that in some cases, the maximum deflection of the Hybrid III dummy chest can be overlooked as a result of the fact that only one chest deflection gauge is available at the centre of the chest [93, 141, 142]. Therefore, a linear combination model was developed for injury criteria to assess thoracic trauma and predict serious chest injury. As it combined two independent chest injury criteria, deflection and acceleration, it was therefore deemed more appropriate than two independent criteria [127]. The model measures the change in the distance between the breastbone and the spine, a reaction to pressure on the chest [143]. Therefore, CTI will be used in this study to assess the risk of chest injury in adults from frontal impacts. The mathematical expression will be explained in chapter 2, section 2.4.2.3.

Although the main factors, which can cause a considerable increase in pedestrian-vehicle impacts in developing countries have been identified, there are many parameters relevant to pedestrian and vehicle, which significantly influence injury patterns and injury risk and need to be identified.

1.6 The major factors influencing pedestrian kinematic response, injury patterns and injury risk during primary and secondary impacts

This section will briefly focus on the most important parameters that influence the pedestrian kinematic response, injury patterns and injury risk during primary and secondary impacts. These can be divided into two types: factors relevant to vehicles and factors associated with pedestrians. Vehicle factors consist of different parameters, such as frontal geometry, impact velocity and vehicle contact region, while pedestrian parameters entail pedestrian age and size and impact position (orientation), including posture.

1.6.1 Vehicle factors

Vehicle characteristics and engineering facilities significantly influence the safety of all vulnerable road users, including pedestrians. These factors include frontal vehicle geometry, impact velocity and vehicle contact regions.

1.6.1.1 Vehicle frontal geometry

Several studies have indicated that the majority of pedestrians are impacted by the vehicle frontal geometry during primary impacts [41-43]. Therefore, the frontal geometry and stiffness significantly influences pedestrian kinematic response, injury patterns and injury risk [57, 67, 88, 144-151]. During pedestrian-vehicle impacts, the four-wheel vehicle bumper (fender) impacts the lower legs, causing both feet to leave the ground. In addition, the bonnet (hood) leading edge (BLE) impacts with the upper legs and torso, after which the pedestrian's body rotates towards the vehicle bonnet [71]. In contrast, when pedestrian-auto-rickshaw impacts occur at the vehicle centreline, the mudguard impacts the lower extremities. When impacts occurred at the vehicle offset, a significant pedestrian rotation was produced about the side of the vehicle, resulting from asymmetric contact with the vehicle side. Therefore, three-wheeled vehicle-pedestrian impacts produce a different kinematic response compared to four-wheeled vehicles [40]. This is worthy of investigation to ensure that specific guidelines can be applied to auto-rickshaws as opposed to general vehicle criteria that may or may not be relevant.

Many studies have investigated pedestrian-vehicle impacts and reported that the windscreen [66, 67, 152, 153], windscreen frame [153, 154], A-pillars, front panel [153] and bonnet [67] are the most frequently head injurious vehicle components and can cause life-threatening or fatal head injuries for adults and children [66]. However, fewer attempts have been made to investigate pedestrian-auto-rickshaw impacts. Nonetheless, some studies have suggested that the windscreen and windscreen frame are the most frequently impacted regions to the head of the adult pedestrian during primary impacts [40]. However, the location of adult head impacts have not been reported. Moreover, to date, the primary impacts of auto-rickshaw components on the heads of child pedestrians has still not been investigated. Therefore, there is a clear shortcoming in current research in this area, which this study aims to address through

its exploration of injury risk and thresholds with auto-rickshaws during adult and child pedestrian impacts.

Injury patterns and injury risks are sensitive and can be influenced by many parameters, such as the stiffness of vehicle components and the front-end geometry of a vehicle during primary impacts. Zhang et al. [148] investigated the influence of the front-end of an SUV on pedestrian head injury, concluding that the stiffness of the front end of the vehicle significantly affects head acceleration, producing high HIC values, which correspond to a high head injury risk. This was a consequence of less energy being absorbed by a stiffer structure and less deformation/displacement occurring during pedestrian-vehicle impacts. Similarly, King [88] commented that the acceleration response to head impact depends on the stiffness and geometry of the surface. Yao et al. [57] used the MADYMO programme to reconstruct 23 child pedestrian-vehicle impacts using the front end of a passenger car, including windshield, bonnet, grill, bumper, lower bumper and spoiler. These structures were controlled by a set of parameters, such as bumper centre height (BCH), bumper depth (BD), bumper lead (BL) and grill angle (GA), as shown in Figure 1-13. In addition, three different stiffnesses were used: the high, medium and low impact position to investigate the influence of front-end geometry and stiffness on the head injury risk of a child pedestrian. The study found that the head impact injury risk to the child was significantly influenced by the vehicle shape and stiffness of the front end.

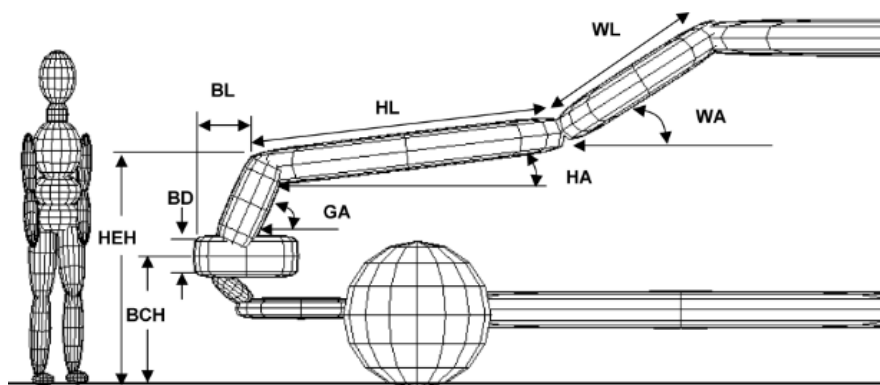


Figure 1-13. Setup of child pedestrian-passenger vehicle impacts and vehicle control parameters [57].

A cross-sectional study by Henary et al. [149] analysed the U.S. Pedestrian Crash Data Study (PCDS) database, from 1994-1998, concluding that adult pedestrians impacted

by light truck vehicles (LTVs) had a greater risk of injury and mortality than passenger vehicles. Similarly, Tanno et al. [145] concluded that pedestrians who were impacted by flat-front vehicles sustain severe injuries at a lower impact velocity, compared with bonnet-front vehicles when analysing 101 pedestrian-vehicle impact scenarios that occurred in southern Japan between 1993 and 1998.

The previous results were emphasised by Roudsari et al. [146] who established that pedestrians impacted by LTVs sustained a three times greater severe injury risk compared with passenger vehicles. Moreover, the mortality rate was two times greater for pedestrians struck by LTVs than passenger vehicles when the study analysed the Pedestrian Crash Data between 1994 and 1998 in six U.S. cities. Similar findings were reported by the study of Ballesteros et al. [150], which concluded that pedestrians impacted by sport utility vehicles (SUVs), pick-up trucks and vans were twice as likely to sustain brain, chest and abdominal injuries, even at low impact velocities, compared with passenger vehicles. This study was based on accident data for pedestrians injured in the U.S. state of Maryland between 1995 and 1999.

During the initial pedestrian-vehicle impacts, the kinematic response of the impacted pedestrian will continue until a pedestrian eventually loses contact with the vehicle and falls to the ground. The throw distance of a pedestrian is significantly influenced by many factors, including vehicle front-end geometry. Bhalla et al. [53] found that throw distance for an adult pedestrian was 45% influenced by vehicle geometry. They investigated different vehicle geometries, including, SUVs, mid-size and small-size vehicles and found that a high bonnet leading edge (BLE) produces a high throw distance, this was confirmed by Hamacher et al. [72]. In addition, Simms et al. [155] reported that forward projection occurs when a high-fronted vehicle geometry impacts a pedestrian. Moreover, a study by Crocetta et al. [70] found that the most common sequence of landing patterns for adult pedestrians impacted by a van vehicle were ground impacts at the pelvis or legs, followed by torso and head. In contrast, the head of adult pedestrians first impacted the ground when they were initially impacted by a large SUV. These findings were reported when the study investigated the influence of different vehicle front-ends on pedestrian landing mechanisms with the ground using three low-fronted vehicles represented by a sports car, compact car and big car and two high-fronted vehicles, represented by an SUV and van.

Regarding pedestrian injuries caused by the ground, the front-end geometry of a vehicle considerably influences the injury patterns and injury risk. Simms et al. [156] used the MADYMO programme to investigate the influence of vehicle shape on pedestrian head injury risk during secondary impacts. The study used two pedestrian sizes (midsize and small female) impacted by a passenger vehicle and SUV and concluded that the head injuries and HIC values produced by the ground impacts are significantly correlated with the bonnet leading edge (BLE). Similar findings were reported by Hamacher et al. [72] who stated that a high BLE increases the head injury risk during contact with the ground. However, comparison between a passenger vehicle and the auto-rickshaw, which has a front-end geometry almost similar to an LTV and van with a high frontal end, has not yet been investigated.

Given the fact that the auto-rickshaw is so widely used by people in developing countries, it is clear that more needs to be done to ensure that such vehicles meet safety needs and that their potentially damaging effect on pedestrians during an impact can be reduced. It is important to establish how the front end of such vehicles will affect pedestrian throw distance, landing orders and injury risk. This study explores these aspects.

1.6.1.2 Vehicle impact velocity

Impact velocity is the key factor, which significantly influences the kinematic response of a pedestrian impacted by a vehicle during primary and secondary impacts [68, 151]. Head impact time duration is the most common aspect during primary impacts, which can be used by engineers and road accident investigators to reconstruct the accident and improve the pedestrian safety of vehicles. Understanding and identifying the head impact time can be used by automotive designers to enhance active safety, such as pop up, autonomous braking systems (ABS) and airbag technologies, considering the activation time protection with different pedestrian detection sensors [151, 157-159].

Head impact time duration can be defined as the duration of contact between the first pedestrian body region with a vehicle, until pedestrian head contact occurs [160]. Numerous studies have indicated that the head contact time decreases with increasing impact velocity for both child [57, 160-162] and adult pedestrians [55, 159-164]. However, most of the previous studies investigated pedestrians impacted by four-wheeled vehicles. No previous attempts have been made to report head contact time

for pedestrians impacted by auto-rickshaws. Therefore, head contact time duration for adult and children pedestrians impacted by three-wheeled vehicles at different impact velocities is uncertain. As auto-rickshaws are used so frequently in developing countries, it is essential that head impact time durations are explored, specifically within this context, to aid pedestrian safety and reduce any potential consequences of an impact. This is a further important aspect that this study wishes to explore.

Impact velocity is a crucial factor that can affect injury severity, for both vehicle occupants and vulnerable road users (VRUs), including pedestrians. Many previous studies have concluded that impact velocity is a key determinant of injury severity and fatality during primary impacts for both adults and children [161, 165-167]. Pedestrian road accident investigations have reported that the vast majority of pedestrian impact injuries are associated with impact velocities of between 25 and 55km/h [168, 169]. Therefore, many regulations have been established worldwide to control vehicle-driving velocity in urban areas. In the UK, for example, it was legislated that 20 and 30 mph limits be applied in urban environments, which is equal to 32 and 48km/h, respectively [170, 171]. Road accident databases in Europe show that the most frequent impact velocity is up to 40 km/h in urban areas, which has been taken as a base factor when designing the New Car Safety Assessment Programme (Euro-NCAP) impact test procedure [172] and 35km/h for the Global Technical Regulations (GTR) [173].

Under the concept of road traffic injury (RTI), vehicle mass and vehicle impact velocity are properties of all the energy that can be transferred during an impact. Impact velocity significantly influences the transfer energy, compared with vehicle mass. Khorasani-Zavareh et al. [165] commented that increasing vehicle impact velocity increases the transfer of energy during impacts and produces harmful or fatal injuries. Similarly, Watanabe et al. [166] concluded that the injury risk became greater with the impact velocity when investigating the risk of head and chest injury. The study used three different pedestrian Finite Element (FE) models, including a mid-size adult male (50thpercentile), a large-size adult male (95thpercentile), and a female (5thpercentile), impacted by three FE vehicle models (Sedan, SUV, Mini-Van) at two vehicle contact regions (centre and the corner of the bumper) at impact velocities between 20 and 50km/h. Similar findings were reported by Hyeok Park et al. [167],

who concluded that the Combined Thoracic Index (CTI) increased with impact velocity, which indicated an increase in chest injury risk. The study investigated chest injury during unconstrained frontal impacts between human and mobile robots using the MADYMO programme. McNally and Rosenberg [174] concluded that the probability of a serious thoracic injury, based on CTI, linearly increased significantly with impact velocity and increased the probability of sustaining a serious chest injury when evaluating the safety of a 6YO-child cyclist impacted by vehicles.

In addition, many studies have concluded that there is a significant correlation between HIC criterion and impact velocity for both adult [68, 149, 160, 163, 164, 175, 177-181] and child pedestrians [57, 149, 161], during primary impacts. This indicates that an increase in impact velocity leads to an increase in head injury risk. However, many previous studies have also concluded that there is no obvious correlation between pedestrian HIC ground interactions and vehicle impact velocity [68, 156, 176, 182]. Shi et al. [176], nonetheless, concluded that head injury risk was influenced by pedestrian body landing order. In addition, landing head first may produce a greater head injury risk. The authors collected these results from an investigation of pedestrian-vehicle impacts for four different pedestrian sizes (50th and 95th males, 5th female 10YO-child pedestrians), six initial gait percentages (10%, 25%, 40%, 60%, 75% and 90%) and five distinct vehicle types at impact velocities of between 20 and 60km/h. Furthermore, many other studies have concluded that head injury risk, caused by a secondary impact, is higher than the head injury risk from a primary impact, even at low impact velocities, such as at 20km/h [70-72, 176]. Simms and Wood [55], confirmed that the HIC produced by secondary impacts results in far more unpredictable injuries than primary impacts.

During pedestrian-vehicle impacts, throw distance increases according to impact velocity. Many previous studies have found that there is a noticeable correlation between the throw distance and impact velocity [53, 72, 160, 183-186]. In addition, Fugger et al. [183] and Wood et al. [186], when exploring the pedestrian projection distance, used a numerical model to estimate vehicle impact velocity, proposing that the forward throw distance of the impacted pedestrian would be in the range of 3–11m at an impact velocity of 25km/h. Tammua and Duma [71] and Simms et al. [155], on the other hand, reported that velocities of 25km/h might cause forward projection

distances of almost 5m. The variation in impact velocity leads to different landing orders. Crocetta et al. [70] concluded that the changes in impact velocity influences pedestrians' dynamic response, which leads to different ground contacts and landing mechanisms. Similarly, Kendall et al. [68] reported that vehicle impact velocity influences kinematic response and ground impact mechanisms. Moreover, Shi et al. [176] found that increasing vehicle impact velocity increased the rotational angle of the pedestrian body and was highly correlated with the pedestrian ground landing mechanisms. Otte and Pohlemann [54] reported that the body flew at close to the vehicle velocity before impacting with the ground with the left knee first when impacting a real-world pedestrian dummy with a car at 79km/h.

It is apparent from the literature that most researchers have tended to focus on adult and child pedestrian-four-wheeled vehicle impacts. However, less attention has been paid to report the injury outcomes produced by adult pedestrian-auto-rickshaw impacts [32, 40]. Although some studies have concluded, when investigating primary impacts with auto-rickshaws, that head injury risk for adult pedestrians is significant at impact velocities between 10 and 30km/h, primary impacts for child pedestrians have not been reported. In addition, no previous studies have reported the throw distance, landing orders and injury metrics produced by secondary impacts, when a pedestrian is initially impacted by an auto-rickshaw. This very apparent research gap makes it clear that much more needs to be done to ensure pedestrian safety in developing countries. The findings of this study will address such concerns and provide manufacturers and engineers with important data that can be used to improve models and designs with safety in mind.

1.6.1.3 Vehicle impact region

Even though impact velocity is the key parameter that significantly influences kinematic response and injury risk of a pedestrian during primary impacts, head impact location and head impact angle during pedestrian-vehicle impacts represent a significant aspect of the dynamic response. The head impact angle refers to the angle between the direction of the head impact velocity and the ground reference level during pedestrian-vehicle impacts [53]. In contrast, the head contact location is the position of a pedestrian head impact with the vehicle components. Okamoto et al. [187]

concluded that the head impact location and impact angle are influenced by the initial vehicle-pedestrian contact location.

Regarding injury risk, it has been reported that vehicle contact region affects the injury risk, particularly in head and chest body regions [166]. Similarly, McNally and Rosenbeng [174] concluded that the thoracic injury of a 6YO-child on a bicycle varied with vehicle contact region when investigating the influence of the vehicle centreline and bumper corner on injury risk. Gupta and Yang [182] concluded that the variation in vehicle contact region leads to a significant variation in landing injuries when investigating the influence of different vehicle front-end profiles (mid-size vehicle and a SUV vehicle), pedestrian sizes (50th, 5th and 6YO-child) and vehicle impact regions (centreline and bumper corner) at impact velocities of 30 and 40km/h.

The previous studies investigated the influence of the vehicle contact region of four-wheeled vehicles on pedestrian kinematic response, including head impact location and head impact angle. In addition, they explored injury risk during primary impacts and landing injuries. Three-wheeled vehicles have been investigated to some extent by Chawla et al. [40], who concluded that the dynamic response of an adult pedestrian changes significantly with vehicle contact region, with a vehicle offset producing a rotational movement to the vehicle side. However, head impact time, location, angles and landing injuries were not reported. In addition, the dynamic response and injury outcomes of a child pedestrian impacted by an auto rickshaw at different front impact regions, or landing injuries of an adult pedestrian initially impacted by an auto rickshaw at both vehicle contact regions (centreline and offset) have also, not been reported. Therefore, this study is the first to attempt the exploration of such factors within the context of auto-rickshaws.

1.6.2 Pedestrian factors

Pedestrian size is significantly associated with pedestrian gender and age, which influences the dynamic response and injury outcomes during pedestrian-vehicle impacts. In addition, pedestrian impact position is noticeably associated with pedestrian behaviour and pedestrian culture, which can lead to different kinematic responses and injury metrics during pedestrian-vehicle impacts.

1.6.2.1 Pedestrian age and size

Pedestrian age is significantly associated with pedestrian size. Huelke [188] and Brun-Cassan et al. [189] reported that children differ from adults in many respects, due to the large variability of body size, mass distribution, characteristics of the developing body structures and injury tolerance. Similarly, Klinich et al. [117] and Okamoto et al. [187] reported that there were significant differences in size, mass, height and anatomical features between adults and children. Many previous studies have concluded that these differences lead to a significant variation in kinematic response, severity and injury patterns for different pedestrian sizes [69, 123, 149, 151, 162, 166, 187, 190, 191] and make the head of the child less resistant to impact trauma [192, 193].

Head impact location and head impact time are the most commonly studied elements of the dynamic response of a pedestrian impacted by a vehicle. Okamoto et al. [187] reported that the head impact location varied with pedestrian height, which is associated with pedestrian size and age. Similarly, Peng et al. [151] commented that the head impact location varied with pedestrian size, while Liu and Yang [161] concluded that the head impact time observed during pedestrian-vehicle impacts for adults and 15YO-child pedestrians is significantly influenced by pedestrian size. More specifically, they found that the head contact time duration for a 6YO-child is less than for a 15YO-child. The study investigated a range of impact velocities between 30 and 50km/h and the front-end shape of a mid-size passenger car impacting the side of a pedestrian body. Similar findings were reported by Ito et al. [194], who concluded that the head contact time occurred later during the primary impact, in accordance with age when investigating the kinematic response and head injury mechanisms of vehicle impacts with three children (3YO, 6YO and 10YO) and an adult interacting with three different vehicles during side impacts at 10 and 40km/h.

The European Enhanced Vehicle Safety Committee (EEVC) established subsystem head safety tests using two different head forms (for adults and children). They reported that there is a significant difference in head impact angle between adults and children: at 40km/h, corresponding to 65 and 50 degrees, respectively [195]. Peng et al. [151] also emphasised the results of EEVC, concluding in their study, that the head impact angle varied with size. Similarly, Watanabe et al. [166] found that variation in

pedestrian size influences injury risk variation when investigating head and chest injuries. Venkatason et al. [192] found that variation in pedestrian size leads to a significant difference between the HIC and injury risk.

During pedestrian-vehicle impacts, the neck region is the most stressed body part due to the relative motion between the head and the torso [196]. Previous studies by Lapner et al. [197] and McGeehan et al. [198] reported that the child's neck is easily injured and Eppinger et al. [93] commented that a variation between the neck ligament stress, neck circumferences and neck length for adult and child might affect injury severity. A similar finding was made by Parr et al. [94] who commented that the variation in gender, neck strength, head size, neck length and body mass all influence the upper neck injury criterion (N_{ij}). Elias et al. [199] found that although the head, neck and chest are connected to each other, a neck injury might occur even when there are no head or chest injuries. Therefore, a neck injury is significantly sensitive to pedestrian size and age.

These results were based on the analyses of crash test data from front and side impacts with a school bus, to assess the protective capability and injury mitigation for occupants during impacts at velocities between 48 and 72km/h. Most of those previous studies focused on the neck injury criterion during frontal vehicle impacts. Shear force is the most common force in rear impacts and may be more harmful. Panjabi et al. [91], for example, concluded that shear force has a significant influence on spinal cord injuries and is associated with soft tissue injuries to the cervical spine intervertebral joints [128, 129].

It is clear from the above that all previous studies have reported the impact sequence for adult and child pedestrians during primary impacts when impacted by a four-wheeled vehicle, including the dynamic sequence, head impact location, head impact time and head impact angles. In addition, injury patterns for both adults and children, including different body regions, such as head, neck and chest have been explored. There are, however, few studies on adult pedestrian-auto-rickshaw impacts, particularly in terms of the kinematic response, injury metric and injury risk. Child pedestrians-auto rickshaw impacts have not been investigated. In addition, head impact location, head impact time, head impact angle and neck injury for both adult and child pedestrians have not yet been reported [32, 40]. This gap in current research

makes it apparent that there is an urgent need to address such issues to improve the safety of pedestrians in developing countries where auto-rickshaw use is particularly common.

1.6.2.2 Pedestrian impact position and posture

Pedestrian impact position and posture during primary and secondary impacts are significant factors that influence the dynamic response, injury patterns and injury risk during pedestrian-vehicle impacts. Yao et al. [57] concluded that the dynamic response and injury outcome for a child pedestrian, during primary impacts are significantly influenced by the initial posture and the orientation of the pedestrian. The kinematic response includes the post interactions between the pedestrian's body regions and vehicle components. Head contact time, location and angles are significantly influenced by pedestrian impact position and posture. Simms and Wood [200] conclude that the pedestrian impact position significantly influences the dynamic response of pedestrians during primary impacts. The study noted that the front and rear facing impact positions led to earlier head impacts, due to a lower effective radius of rotation about the bonnet leading edge compared to side positions. These results were based on investigations of pedestrian head contact forces with the vehicle and ground using two impact positions, including front and side at impact velocities of 18, 36 and 72km/h, respectively. However, head impact location and head impact angles were not investigated in Simms and Wood's study [200]. Peng et al. [151] concluded that leg posture has a significant influence on the dynamic response of adult and child pedestrians, resulting from a change in position of the centre of gravity and resulting head impact locations and impact angle variation. The change in a pedestrian's gait can result in the absence of head-vehicle impacts at low vehicle impact velocities. The study used two pedestrian sizes (50th adult and 6YO-child) during seven gait percentages (0%, 20%, 40%, 60%, 80%, front and rear) with five different vehicle frontal profiles including super mini car (SMC), small family car (SFC), large family car (LFC), multi-purpose vehicle (MPV) and sport utility vehicle (SUV).

The changes in pedestrian impact orientation and gait during an impact could influence the injury risk. Simms and Wood [55], therefore, investigated the influence of impact position on impact load during pedestrian-vehicle impacts including front, rear and side position, reporting that side impacts produce low impact loads, compared to

frontal and rear impacts. This might be a result of the lower effective radius of rotation about the vehicle front during pedestrian front and rear impact positions compared to the side position. Similarly, Liu et al. [175] concluded that the risk of skull and brain injury was greater for an adult impacted to the rear impact position, compared to the front and side impact positions. They tested pedestrian-passenger vehicle impacts at different impact positions, including front, rear and side using a Finite Element Method (FEM), changing the gait of a pedestrian during primary impacts was found to significantly influence pedestrian injury risk. Previously, Peng et al. [151] concluded that a change in pedestrian gait resulted in a change in the centre of gravity, which produced different stress points on the pedestrian head and different linear and angular accelerations, which are associated with different injury risk.

Moreover, Bhalla et al. [53] concluded that impact position significantly influences the pedestrian throw distance, by up to 28% when investigating two impact positions, front and side, impacted by various vehicle geometries, such as SUVs, mid and small sizes. Hamacher et al. [72] concluded that the leg and arm posture of a pedestrian, during pedestrian-vehicle impacts, significantly influenced a pedestrian's rotation during the secondary impacts. This study used four different pedestrian sizes (5th percentile female, 50th percentile, 95th percentile male and 6-year-old child) located at the front of a vehicle in the side position with different stances impacted by six vehicle models (compact car, sedan, van, SUV, one box, sports car) at impact velocities between 20 and 40km/h. The study of Crocetta et al. [70] concluded that the changes in pedestrian posture, during the side impact position, influences pedestrian dynamic response, which leads to different ground contacts and landing mechanisms. Similarly, Kendall et al. [68] found that the change in pedestrian stances and impact orientation significantly influences kinematic response and ground impact mechanisms.

This section has indicated that all previous studies have investigated the influence of pedestrian impact position, during pedestrian-four-wheeled vehicle impacts, including three impact orientations (front, rear and side). Less emphasis has been given to investigate the influence of adult pedestrian impact position, during pedestrian-auto-rickshaw impacts, including rear and side impacts. Furthermore, rear and side impact positions have not been investigated for child pedestrians. Given the growing importance that is being given to improving child safety, it is clear that more efforts

must be made to protect child pedestrians, particularly in developing countries where such a large proportion of fatal accidents occur. In addition, frontal impacts and pedestrian posture have not been investigated, during primary and secondary impacts within the context of auto-rickshaws. Moreover, no previous studies have investigated the influence of different initial impact position on the throw distance, landing orders, injury metric and injury risk when a pedestrian is initially impacted by an auto-rickshaw. Again, this highlights an urgency for this study such that it provides clear, empirical evidence that can help manufacturers and engineers to improve safety standards.

1.7 Active and passive safety approaches

Typically, pedestrian-vehicle safety can be split into two types: active and passive safety. The essential purpose of these two approaches is to prevent road traffic accidents or reduce injury risk during collision accidents.

1.7.1 Active safety

The active approach is focused on a system of warnings, that attempt to avoid road accident scenarios occurring in the first instance by reducing the vehicle velocity automatically prior to impacting an object, such as using anti-lock braking systems (ABS) and detective radars [201, 202].

1.7.2 Passive safety

Passive safety features are systems that are passive until required. They activate during an impact to minimise the harm or damage and protect all road users, including occupants and pedestrians. Seat belts, airbags and interior and exterior vehicle structure impact mitigation designs are examples of such safety features [201]. Engineering enhancements to the vehicle front-end geometry, materials and component thicknesses could increase a vehicle's ability to absorb and dissipate impact energy during pedestrian-vehicle impacts [203] and could significantly lead to a reduction in injury risk and fatality. Jakobsson et al. [204] noted a trend towards increasing risk of injury if a higher acceleration impulse was estimated to have occurred in a real-world crash. In particular, a high acceleration impulse was estimated when stiff structures were engaged during impact. In addition, Muser et al. [205]

suggested that cars produced in the late-1990s had a stiffer structure than previous vehicles and therefore produce an impulse with higher acceleration levels. As shown in Figure 1-14, a basic spring-mass model provides a reasonable approximation of the stiffness response. The application of a spring that has a nonlinear force-deflection characteristic leads to a considerable improvement in vehicle crash tests.

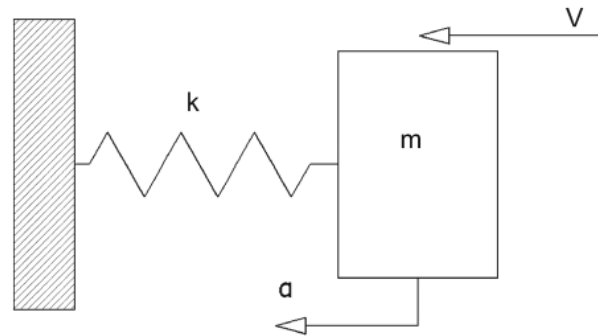


Figure 1-14 Spring-mass model [206].

Where k is the spring stiffness (N/m), m is the object mass (kg), v is the initial impact velocity (m/s) and a is the model's displacement (m). The basic concept is, that during impact, as shown in Figure 1-4, when the stiffness of a spring is high it produces less displacement and a higher acceleration. If the stiffness of the spring was low it would produce a greater displacement and a lower acceleration. Similarly, Linder et al [206] concluded that the vehicles which perform well in damageability (very stiff structure) impart a higher acceleration. While vehicles with less stiff structures can be significantly deformed and produce low accelerations. Therefore, the stiffness is the key factor during pedestrian-vehicle impacts and vehicle-vehicle impacts, which produce variation in the mean accelerations, pulse shape and peak accelerations.

Traditionally, automobile bodies have been made of low carbon steels, mainly due to their low cost and malleable nature, making them the most common form of steel, the average price for steel is currently approximately \$0.93/kg [207]. Recently, there has been a change from low carbon steels to a combination of steels, light alloys and polymer matrix composites [208]. One of the reasons the automobile industry has been targeting these new materials is for their reduced weight, which allows for an improved fuel economy and more importantly, reduced environmental pollution [208]. Furthermore, these materials have not been selected solely on their weight reduction potential, but also for factors including safety, durability and cost.

The two materials that stand out as the best alternatives to steel are aluminium and magnesium, especially for use in automotive manufacture. Although the two materials are both more expensive than carbon steel, they are far cheaper alternatives than composite materials, which are mostly used in high performance vehicles. Aluminium is far more popular and widely used than magnesium in the automotive industry, but there are still many examples of magnesium being used in structural applications within some of the leading vehicle brands [209]. Whilst it is desirable for the safety of pedestrians that the vehicle deforms under impact, it is also important for the structure to remain rigid when in normal use so that the body of the vehicle keeps its shape to protect occupants. The body of a vehicle deforms during acceleration and deceleration when load transfer occurs [210], such that a stiff structure will minimise the amount of bending taking place. However, the structural parts of material in the vehicle must be redesigned to achieve the same stiffness [211]. There are also some alternative materials to glass that can be used for the windscreen of a vehicle. Polycarbonate (PC) sheet is one of the transparent thermoplastics that is often used in the windscreens of automobiles and aircraft. The material weighs significantly less than glass and better absorbs energy during impact. Polycarbonate is used widely throughout the car industry as a windscreen and is implemented into high performance cars for its weight reduction and high-impact resistance [212, 213].

1.7.2.1 Aluminium

It is expected that the growth of aluminium in the automotive industry will mainly be in the body structures and body panels of a vehicle, such as a car's front bumper and bonnet, which are the areas associated with crashworthiness during an accident [208]. Aluminium has a density of 2700 kg/m^3 , which is much lower than that of steel (approximately 7890 kg/m^3). Coupled with the fact that aluminium has a higher crash energy absorption per unit weight, the use of aluminium over steel means great weight saving can be achieved by automobile manufacturers, whilst also improving the crashworthiness of the structure [208]. Many studies [214-216] have pointed out that energy absorption is a significant design factor for pedestrian safety and aluminium alloys have excellent energy absorption properties. Energy absorption can lead to a reduction in the transferred kinetic energy during pedestrian-vehicle impacts and thus, can prevent or reduce the peak reaction force transfer to the pedestrian and decrease

the injury risk [217]. The average prices of aluminium and magnesium are higher than steel with an approximate price of \$2.29/kg and \$5.36/kg, respectively [207].

Each aluminium alloy is given a four-digit number, where the first digit indicates the major alloying element, the second-if different from 0-indicates a variation of the alloy and the third and fourth digits identify the specific alloy in the series. The alloys that are most widely used for these applications are the 5xxx series Al-Mg alloys, which are non-heat treatable, and the 6xxx series Al-Mg-Si alloys, which are heat treatable and can therefore be strengthened through heat treatment [209]. In contrast, alloys with a higher yield strength tend to be more expensive and suit structural applications within aircraft, such as the 7xxx series aluminium-zinc alloys.

1.7.2.2 Magnesium

Although magnesium is the third most commonly used metal in automobiles, after steel and aluminium, it has limited structural applications in today's vehicles, but may experience significant growth in the future, should certain challenges be overcome. Magnesium has many advantages over both steel and aluminium. Firstly, it is the lightest structural metal with a density of about 1780 kg/m³ and has a specific strength similar to cast iron. Hence, it can provide an even greater mass reduction than aluminium [208]. In addition, magnesium has a high specific stiffness, great cast ability and many alloys even have a better crashworthiness rating than aluminium. Magnesium also has many disadvantages, with one of the main problems being its poor galvanic corrosion resistance. Pure magnesium has the highest standard reduction potential of the structural automotive metals, making it vulnerable to galvanic corrosion. For this reason, magnesium is always alloyed with other metals, mainly aluminium and zinc, to provide adequate corrosion resistance as well as sufficient strength and formability [208]. AZ91 is one of the most commonly used types of magnesium and has made significant inroads to replacing aluminium in many non-structural and low-temperature applications [209]. AZ91 is, however, not suitable for external structural applications, due to its poor formability and is mostly limited to applications inside the car.

The number of commercially available magnesium sheet alloys for external automobile body panels is very limited, with the most popular being the AZ31B Mg-Al-Zn alloy. One issue with magnesium sheet is that the properties are usually

anisotropic so the strength and ductility may vary with direction on the sheet due to an irregular grain structure [208]. Another issue that surrounds magnesium sheet is the limited formability at room temperature, which makes assembly processes for outer body panels difficult [208, 218]. There are far more examples of magnesium sheet being used for inner panels, which form the structure of the vehicle but cannot be seen from the outside, such as the space frame and inner door panels of cars [208, 219]. Despite this, there are still a few applications of magnesium sheet to the external structural elements of automobiles, mostly through prototype models. For example, Volkswagen made a prototype car bonnet for their Lupo model using AZ31 sheet [208] and General Motors have made several structural panels in their cars, including bonnets, out of similar magnesium sheet materials [215, 218]. In addition, the study of Savic et al. (2014) [220] concluded that the Mg AZ31-O produced the most favourable HIC score relative to other automotive materials, such as AZ61-O, ZEK100, 6111-T4 and 5182-O, when considering pedestrian safety improvements by a series of experimental and numerical tests.

1.7.2.3 Polycarbonate

Glass has long been used as the “go-to material” for windscreens in the automotive industry, albeit in the modern day, it has been in the form of laminated glass (two sheets of glass with a polymer interlayer) [221]. Whilst glass does have excellent transparency and scratch resistance, it is a brittle material and has a lower impact resistance than many competing windscreen materials [222]. It has an average price of \$1.70 [223]. Polycarbonate (PC) is a very durable material with excellent impact resistance and is often used in the windscreens of race cars, motorcycles, fighter jets and is even used in bullet-resistant glass (the polycarbonate is sandwiched between layers of glass) [213, 222]. PC can easily be worked and moulded, hence why it has such a range of applications. It is a highly transparent polymer in visible light and even has superior light transmission characteristics than many types of glass. Nonetheless, the material has a low scratch resistance, so marks much more easily [222]. However, thin sheets of clear film are often used as a cost-effective way to protect the PC from damage [213]. The price of PC is almost double that of glass per kg, with an approximate cost of \$3.08/kg [224].

1.8 Cost-Benefit-Analysis (CBA) and road traffic accidents costs

As will be explored in more detail in the subsequent chapter, this study will use a cost-benefit analysis to investigate how auto-rickshaws can have the greatest safety at the lowest cost. Therefore, it is important to understand exactly what is meant by a cost-benefit analysis, given that it can have different meanings depending on the field in which it is employed. The main aim of a cost-benefit analysis is to maximise the present value of all benefits less that of all costs [225]. Maximising the present value of the benefits varies according to the project. For example, the benefits could be environmental, political or medical. Therefore, it is a useful analytical tool for planners, manufacturers and engineers to simplify the decision-making process. Automobile engineers, who are interested in creating safe vehicles, tend to focus on injury mitigation, which is related to passive safety, or accident prevention which is related to active safety.

Road traffic accidents have an estimated total cost of US\$65 billion for low- and middle-income countries, which exceeds the total annual amount of money that these countries receive for developmental assistance [1]. A study in Bangladesh showed that the average treatment cost during a hospitalisation for a road traffic injury in 2001 was US\$86. However, the per capita annual income was less than US\$500 [226]. In addition, estimations in Thailand found the average total cost incurred per patient who suffered a road traffic injury in 2004 to be US\$2596, which exceeded the per capita annual income of US\$2513 [227]. Thus, mitigating potential road traffic injuries is paramount in not only improving public health, but also allowing for a reduction to these extortionately high costs that hinder growth in developing countries. Therefore, estimating the increased cost of these suggested materials must be balanced against the potential costs saved by attaining a lower severity injury.

Several studies have shown that mean costs incurred during road traffic accidents increase with injury severity [228-231]. Costs associated with road traffic injuries differ between countries, especially when comparing costs within developing countries to that of higher-income countries, where the healthcare is more advanced and far more expensive. One study of road traffic injuries in Indonesia estimated that average total costs for minor injuries are around US\$464 per crash, for serious injuries are around US\$1,400 and for fatal injuries are approximately US\$37,168 [229]. A

similar study in India found minor injuries in 2013 cost approximately US\$628, while major injuries cost US\$6,047 and fatal injuries were predicted at US\$114,487 [232]. These studies highlight the economic disparity between the road traffic injury costs of two Asian countries, where different transport modes are used including auto-rickshaws. However, they do not differentiate between the costs of injuries to different areas of the body or the actual AIS level of those injuries. The study of Nguyen et al. [231] provided a more in-depth analysis of how costs differ between AIS level injuries and body region for pedestrian road traffic injuries in the Thai Binh province, Vietnam. Pedestrians injured in the study had the highest direct medical costs, higher than cyclists, motorcyclists and car occupants. The study estimated the mean costs to pedestrians for three different body regions: head, neck and chest and classified the cost of injury according to AIS between moderate (AIS2+) and critical (AIS5+) injury. The average cost for severe head injuries were estimated to be \$2700, while neck and chest injuries were estimated to cost as high as \$1520 for serious injuries. No significant cost differences were reported for both body regions [231].

1.9 Finite Element Analysis (FEA)

In addition to the cost-benefit analysis, this study will also make use of a finite element model (FEM) to better understand the specific mechanics of an auto-rickshaw - pedestrian impact interaction. FEMs enable researchers and engineers to gain a clearer understanding of an impact scenario in the simulation environment [233]. There are many types of software that can be used according to the desired simulation. However, MADYMO and LS-DYNA are the most common and widely used in vehicle-vehicle and vehicle-pedestrian impact tests.

MADYMO (Mathematical Dynamical Models) is a general-purpose software package, which can be used to simulate the dynamic behaviour of mechanical schemes. It is used widely in industrial engineering, research laboratories and technical universities. It has a unique combination of fully integrated multibody and finite element techniques. MADYMO software has been used for many pedestrian models [153, 234, 235]. The software code is appropriate for running numerous models, as it simplifies structures into a series of ellipsoids, connected by joints with the suitable mass and inertia properties. A vehicle and a dummy can be modelled with ellipsoids, which

approximate their exact geometry and their stiffness values can be modelled as single force-deflection load curves [236].

LS-DYNA, on the other hand, is an explicit 3D non-linear finite element code developed by John Hallquist at Lawrence Livermore National Laboratories in 1976 [236, 237]. Its completely automated contact analysis capability and error-checking features have allowed users worldwide to solve effectively many impact problems, such as vehicle-vehicle impacts and vehicle-cyclist and pedestrian-vehicle impacts [233]. This finite element (FE) approach has permitted the input of different materials, based on real-world data and experimental investigations. LS-DYNA's strength lies in its ability to deal with large structure deformations and to closely simulate interactions between different material types and complex geometries enabling pedestrian-vehicle interactions. For this reason, a decision was made to use LS-DYNA in this study.

Livermore Software Technology Corporation (LSTC) distributes a commercial version of LS-DYNA, which is widely used by global automotive companies, such as General Motor (GM), Chrysler, Ford, Jaguar, Volvo, Peugeot, Citroen, Opel and Renault [238]. An explicit time integration scheme offers advantages over the implicit methods found in many FEA codes. A solution is advanced without forming a stiffness matrix (therefore, saving storage requirements). Complex geometries may be simulated with many elements that undergo large deformations. For a given time step, an explicit code needs fewer computations per time step than an implicit one. This advantage is particularly strong in solid and shell structures. In extensive vehicle impact crash analyses, the explicit method has been shown to be quicker, more accurate and more versatile than implicit methods [239]. The fully automated contact analysis capability in LS-DYNA is easy to use, robust and validated. It uses constraint and penalty methods to satisfy contact conditions. These techniques have worked extremely well over the past twenty years in numerous applications, such as full-car crashworthiness studies, systems/component analyses and occupant safety analyses. Many impact dummies have been developed to use in road traffic accident reconstructions.

1.9.1 Impact test dummies

Originally in 1949, an impact test dummy named Sierra Sam was introduced by Samuel Alderson, which was designed based on cadaver and animal testing information to look like a human. This launched a 95th percentile male, which became the prototype and was the model for later more anthropomorphic dummy constructions. Muscles, joints and other parts of the human body were specifically modelled and simulated in dummies [240, 241]. The main features of the dummy were durability and serviceability. However, it had poor repeatability and was limited to its human-like exterior shape, body weight and the stiffnesses and ranges of motion of its articulated limb joints.

In 1971, the first automotive crash test dummy (Hybrid I–50th percentile male dummy) was introduced by General Motors (GM), Alderson Research and Sierra Engineering. It was more durable and brought about more consistent results. However, the data acquired did not give enough insight into how to reduce injury and only the effectiveness of restraint could be tested [242, 243]. In 1972, the Hybrid II dummy was produced with respectable knee, spine and shoulder response as a result of the shape and joint stiffness improvements. Furthermore, it was the first dummy to meet the Federal Motor Vehicle Safety Standard (FMVSS) requirements for frontal impact testing, to fulfil regulations governing restraint systems. However, it was not enough to replicate the human response.

After 1972, many material and biomechanical engineering studies continued by testing different materials, to obtain the ideal stiffness properties to increase the accuracy and reliability of the crash dummies [242, 243]. In 1976, General Motors launched a new adult dummy with a new neck and thorax called Hybrid III dummy. It had more transducers, better data collection and became the industry standard [242]. The Hybrid III dummies, (anthropomorphic test devices (ATDs)) include the 95th percentile male, 5th percentile female, 50th, three and six years old (6YO) child dummies in life-size dummies, equipped with sensors that recorded accelerations, forces, moments and displacements. This recorded data can be used to assess the injury risk levels for many body regions that a human would experience during a collision. In an ideal world, ATDs should behave like real human beings, while being robust enough to produce

consistent results across several impacts. There is a wide variety of ATDs available to represent different human sizes and shapes [244].

One decade later, the FMVSS 208/ New Car Safety Assessment Programme (NCAP) became accepted as an alternative test methodology for government compliance. In 1998, it was used by Economic Commission for Europe (ECE)-R94 and came into effect. Several sensors were fixed to the head, chest and neck to record all loads during the impacts, such as the head area of the dummies used in impact tests, which record the absolute value of the acceleration and deceleration with time [243, 245].

Howard et al. [246] created and developed a series of human pedestrian models (6yr old child, 5th, 50th and 95th) for use in LS-DYNA. These models were validated against cadaver tests conducted by the study of Ishikawa et al. [247]. Generally, model trajectories and head velocities were found to correlate well with the test results. Head and pelvis acceleration correlation was reasonable and some differences for chest acceleration were noted. It was noted that differences in arm contact may have accounted for the lack of correlation for chest acceleration. Iwamoto et al. [248] developed a 50th percentile male occupant finite element whole-body human model, designed to be used in the softwares PAM-CRASH and LS-DYNA. The base model had approximately 83,500 elements, of which 30,000 were solids, 51,000 were shell/membrane and 2,500 were beam elements. More detailed sections of the head/face, shoulder and internal organs were also developed, which took the element total to over 216,000. The computational time required, when using the more detailed model was found to be considerable. Cadaver test corridors were used for validation and injury prediction when reconstructing accidents and was considered promising. Ruan et al. [249] also developed an LS-DYNA human model, namely a 50th finite element whole-body model. It was validated against individual cadaver tests instead of test corridors, as the authors considered the corridors too broad for meaningful validation. The study noted that validation against cadavers is less than ideal, as muscle tone and circulatory systems are ignored. Their model consisted of approximately 119,000 elements.

In addition, McLeod and Hubbard [250] described the concept, design, and development of a crash test dummy head, concluding that the dummy head is probably undamaged during normal use and produces higher acceleration. Corresponding to

more severe conditions than a human could tolerate thus invalidating using the dummy head at the margins of human tolerance. Similarly, Mertz [251] reported that the Hybrid III curve lies within the range of the low-velocity, non-fracture cadaver data and within the range of the low-velocity fracture data. Since it is a durable head, the Hybrid III response will not duplicate the high-velocity fracture data but will indicate an increasing level of acceleration within increasing impact velocity.

As a result of regulatory and ethical concerns, human cadavers are infrequently used for biomechanical experiments. Therefore, numerical techniques, especially the use of finite element (FE) models, are applied to understand the response and injury mechanisms of adults and children in road traffic accidents and can provide a detailed biomechanical response and improve injury prediction. Finite element (FE) analysis has become an effective method for investigating and reconstructing pedestrian-vehicle impacts.

With respect to pedestrian-auto-rickshaw impacts, there are relatively few studies that have reported the kinematic response and injury metrics for an adult pedestrian [32, 40]. Unfortunately, to date, there is no comprehensive computational or experimental data available that quantitatively describes the dynamic response and injury metrics for adult and child pedestrians initially impacted by an auto-rickshaw. In addition, pedestrian-ground impacts caused by auto-rickshaws have not yet been investigated. Moreover, no previous attempts have been made to investigate the effect of secondary impacts on pedestrian injury patterns and injury risk. The data is also valuable for estimating the main injurious vehicle components and to suggest effective engineering modifications, which can lead to injury and pedestrian safety mitigation. Consequently, this shortage of relevant data currently limits the value of pedestrian safety and prevents a better understanding of the underlying pedestrian fatality and injury severity risk in developing countries and potentially, the identification of new engineering suggestions for better safety and injury mitigation. These are all problems that this study hopes to address.

1.10 Thesis structure

This thesis consists of five chapters. This chapter has explained the proposed study and outlines the literature review, which offers a review of the accident data and the fundamental theory of injury criteria and injury risk thresholds, in particular, of the head, upper neck and chest. It also explains a brief anatomy of these body regions. In addition, it has discussed the main concepts of primary and secondary impacts and the main factors that lead to different injury patterns and injury risks.

Chapter 2 describes the modelling of an auto-rickshaw FE model and the environment of pedestrian-vehicle impacts. It also explains the calculation of injury metrics of the head, neck and chest, as well as injury risk levels for an adult and 6YO-child pedestrians during primary impacts. In addition, the injury metrics and injury risk for an adult pedestrian, during secondary impacts, are considered. Moreover, it suggests a different alternative material for the front vehicle components, to enhance adult pedestrian safety. Finally, it explains the cost-benefit analysis for suggesting modifications and injury mitigations.

Chapter 3 describes the computational results for both adult and child pedestrians, including post kinematic response, the most frequently impacted, stiffest and most injurious vehicle components, injury metrics and injury risk during primary impacts. In addition, this data is used to assess the influence of pedestrian size on kinematic response and injury risk. Furthermore, injury metrics and injury risk for adult pedestrians, during secondary impacts, are investigated and the results are compared with primary impacts, to assess which impacts could produce a greater injury risk. Finally, the results of the modified materials and thicknesses of the auto-rickshaw components are explained, as well as their influence on injury mitigations relevant to the head, upper neck and chest.

Chapter 4 discusses the key findings of this research, including the interaction between adult and child pedestrians and the auto-rickshaw, injury matrices and injury risk. This chapter also describes pedestrian-ground impacts, including the landing orders, throw distance, pedestrian ground impact directions, injury metrics and injury risk. In addition, suggested modifications associated with injury risk reduction are discussed. Moreover, the costs of the modified vehicle components will be estimated and

compared with the original costs. Furthermore, injury costs relevant to the head and neck produced by the modified material will be compared to the original injury costs, to assess the engineering modifications economically. The limitations of this research study will also be discussed.

Finally, Chapter 5 summarises the principal findings of this research and suggests directions for future research in pedestrian-vehicle impact investigations.

2. METHODS

2.1 Introduction

Finite element analysis is a discrete event modelling method that involves the reduction of structures, bodies and/or liquids to discrete elements. The physical characteristics of these elements are determined by a relatively simple mathematical equations set. Any change in state, imposed on a given element by an external source (e.g. physical, gravitational or dynamic load), can be easily calculated. Not only can one determine the changes within the element but also an influence on the surrounding environment, including neighbouring elements and other bodies can be calculated by the application of interface properties. This method allows analysis of complex problems by disassembling the problem into solvable parts [252].

- This chapter explains the FE method of building an auto rickshaw model by ANSA and LS-DYNA software.
- Defining a pedestrian-vehicle impact simulation environment by LS-DYNA code.
- Calculation of injury metrics of head, neck, chest and injury risk level for adult pedestrian in the primary impacts.
- Calculation of injury metrics of head, neck and injury risk level for a six-year old-child pedestrian during primary impacts.
- Calculation of injury metrics of head, neck, chest and injury risk level for an adult pedestrian during secondary impacts.
- Suggestion of safety enhancement using different alternative materials for the frontal vehicle components (windscreen and windscreen frame).
- Cost-Benefit-Analysis (CBA) for suggested modifications, see Figure 2- 1.

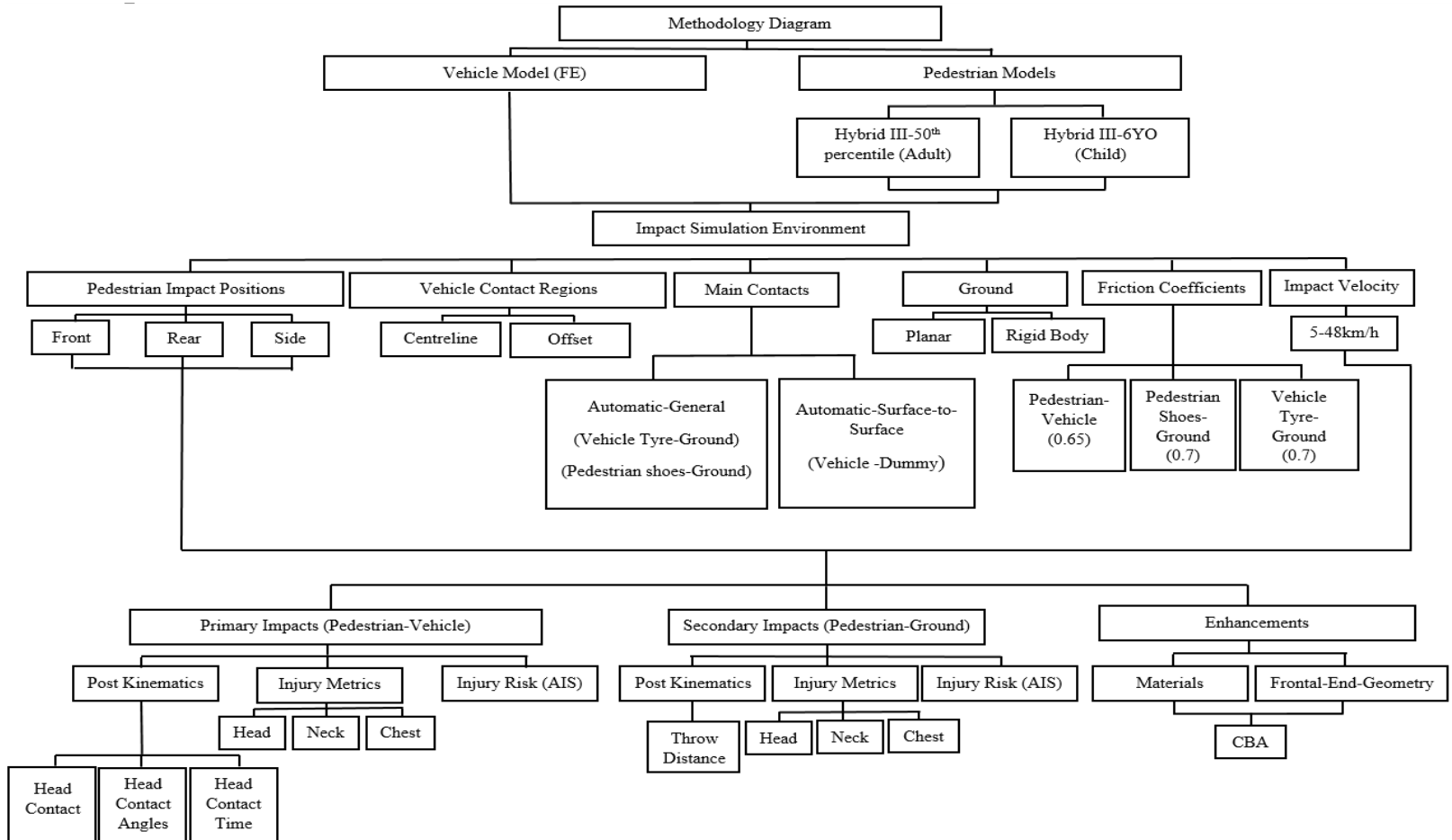


Figure 2- 1. Methodology diagram for the study.

2.2 Modelling

2.2.1 Mathematical model

The second law of motion, formulated by Sir Isaac Newton between (1642 and 1727), is the fundamental law for most vehicle dynamic analyses, as shown in (2. 1) [252]. Vehicle manufacturers intentionally impact vehicles with dummies inside the vehicle or outside, to assess the effectiveness of various safety characteristics. The concept behind injury severity is investigation of the force applied to a pedestrian during a vehicle impact. To reduce injury incidence, the applied force needs to be decreased by reducing the acceleration (or deceleration) by vehicle velocity reduction according to the following formula:-

$$\text{Force (F)} = m \cdot a \quad (2. 1)$$

Where F is the applied vehicle force; a is the resulting acceleration of the vehicle and m is the vehicle mass. In most impact cases high momentum is generated by the vehicle in the travelling direction, which can be defined as the extent to which it is difficult to stop a moving object, such as a vehicle according to the following formula:-

$$\text{Momentum (M)} = m \cdot v \quad (2. 2)$$

Where m is the vehicle mass and v is the vehicle travelling velocity. In addition, the applied vehicle motion converts the potential energy (PE) to kinetic energy (KE), and depends exclusively on the vehicle mass and velocity, as shown in the following formula:-

$$\text{Kinetic Energy (KE)} = \frac{1}{2} m \cdot v^2 \quad (2. 3)$$

Where m is the vehicle mass associated with vehicle type and size and v is the vehicle travelling velocity, which is significantly important, as the velocity is incorporated in the energy formula by a square power.

Both the momentum and kinetic energy of the vehicle, during the pedestrian-vehicle impact are transferred to the impacted pedestrian, which causes the motion response (kinematic) and injury risk level for different injury criteria. Moreover, the structure of a vehicle will absorb energy by undergoing deformation, however, it must do so in a controlled manner to also protect the occupants of the vehicle [253]. During impact the material will undergo initial elastic deformation before beginning to deform

plastically [254]. Automotive structures primarily rely on plastic deformation for absorption of kinetic energy [253-255]. It is important that the materials do not require significant impact forces to plastically deform. As the vehicle impacts a pedestrian, some of its kinetic energy is absorbed as internal energy in the vehicles deforming structure, with the remaining energy being the sum of the kinetic energies of the vehicle and pedestrian [256]. Using conservation of energy, (2. 4) and (2. 5) express a simplified relationship between the total energy of the system before and after impact, respectively.

$$E_1 = \frac{1}{2} m_{A1} V_{A1}^2 + \frac{1}{2} m_{B1} V_{B1}^2 \quad (2. 4)$$

$$E_2 = \frac{1}{2} m_{A2} V_{A2}^2 + \frac{1}{2} m_{B2} V_{B2}^2 + E_{\text{absorbed}} \quad (2. 5)$$

Where E is the total energy of the system, m_A is the mass of the vehicle, m_B is the mass of the pedestrian, V_A is the velocity of the vehicle, V_B is the velocity of the pedestrian and E_{absorbed} is the kinetic energy, which is absorbed by the vehicle structure after impact.

Subscripts (2. 4) and (2. 5) denote the system before and after impact, respectively. For simulations in this study the pedestrian is stationary with no velocity, therefore, the total energy before impact is solely the kinetic energy of the vehicle, i.e.

$$E_1 = \frac{1}{2} m_{A1} V_{A1}^2$$

As E_1 and E_2 are equal, it can be clearly seen that to reduce the kinetic energy transferred to the pedestrian and hence mitigate potential injuries, the energy absorbed via deformation of the vehicle structure should be maximised. Studies of car-pedestrian impacts have agreed with this and show that when the head impacts with the car bonnet, Head Injury Criterion (HIC) values are inversely proportional to the deformation of the bonnet [256]. A simple expression can be used for the energy absorbed by a structure under impact, given in (2. 6) [208].

$$E_{\text{absorbed}} = P \times d = (Ma) \times d \quad (2. 6)$$

Where P is the impact force, M is the mass of the vehicle, a is the average deceleration of the vehicle and d is the maximum plastic deformation. Equation (2. 6) shows that the energy absorbed is proportional to the maximum plastic deformation of its structure. If the materials experience large amounts of plastic deformation, then the

resultant acceleration of the pedestrian will be lower than it is for stiff materials, that absorb little kinetic energy, thus, leading to a reduced likelihood of producing severe injuries.

2.2.2 Physical model

An auto-rickshaw typically has three wheels and a frontal geometry consisting of a mudguard with an attached headlamp, an upright body and windscreen, a canvas roof and small cabin, with a maximum velocity of 55km/h. In addition, the total vehicle mass is almost 295 kg and almost 373 kg including the vehicle driver [257, 258]. The main material of the vehicle structure is steel. The whole vehicle dimensions are shown in Figure 2- 2.

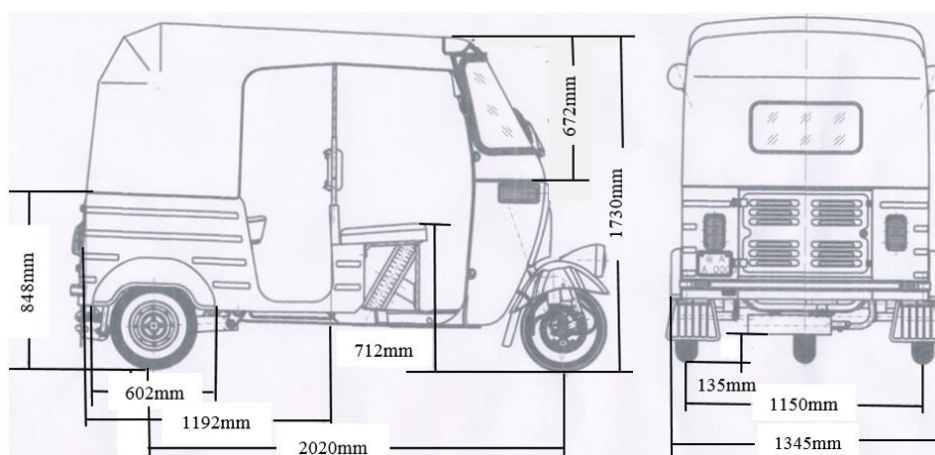


Figure 2- 2. Auto rickshaw dimensions.

2.2.3 Code description

LS-DYNA is a finite element (FE) system generally used for “transient dynamic analysis of highly nonlinear problems”. The program uses an explicit time integration scheme, which determines the solutions to the simulations [259]. Internal and external forces are summed at each node point and a nodal acceleration is computed by dividing by nodal mass. The solution is advanced by integrating this acceleration in time [260].

2.2.4 Computational vehicle model

Computer Aided Design (CAD) of an auto rickshaw model was converted by ANSYS software to an Initial Graphics Exchange Specification (IGES) model, see Figure 2- 3. Then, an FE model was created by ANSA software using dimensions from the real

vehicle, as shown in Figure 2- 2. The accuracy and efficiency of finite element simulations are highly reliant on mesh quality [261, 262].

Therefore, a fine mesh of acceptable quality was required to produce accurate results and furthermore, avoid error terminations, such as a negative volume in the solid element during the simulation process.

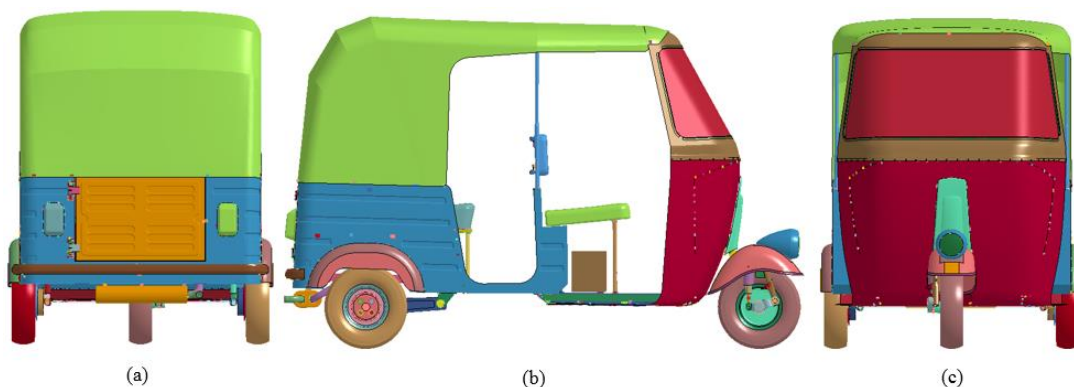


Figure 2- 3. Auto rickshaw model; (a) rear view; (a) side view; (c) front view.

2.2.4.1 Mesh quality

Mesh quality is “The characteristics of a mesh that permit a particular numerical partial differential equation simulation to be efficiently performed with fidelity to the underlying physics and with the accuracy required for the problem” [261, 262]. Therefore, mesh quality is very important and plays a crucial role in the numerical calculation accuracy and stability; mesh quality control was the first step before the mesh generation process. The overall vehicle mesh quality was controlled in the modelling process, shown in Table 2- 1.

2.2.4.2 Mesh generation

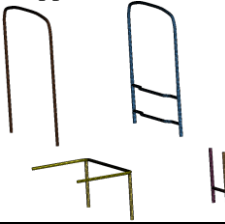
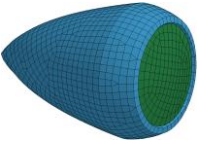
Mesh generation includes mesh type, size and geometrical attributes. There are three different mesh types, 1D, 2D and 3D, relevant to element dimension [263]. Mostly, auto rickshaw components were shell plates, which means that the length and width of the structure is considerably larger than its thickness. Therefore, 2D mesh type was used.

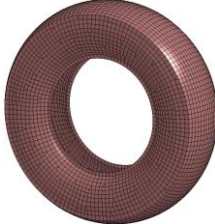
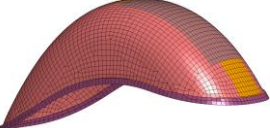
Mixed elements of linear quadrilateral and triangular elements were used, with average element size for the whole model between 6.5 and 8mm and minimum length for the whole model between 3.8 and 5mm, see Table 2- 2. The total number of elements for the whole meshed model were 843911. So, the whole meshed model is very complex and computationally “expensive”, see Figure 2- 4. However, frontal vehicle profile plays an effective role in pedestrian injury and the probability of injury severity. Therefore, this study focused on the front-end vehicle geometry.

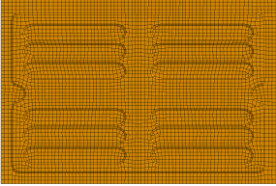
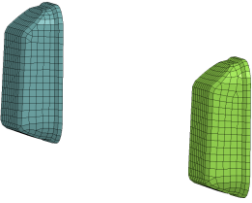
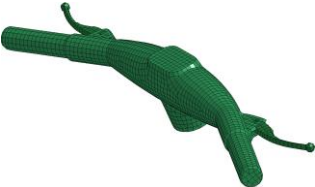
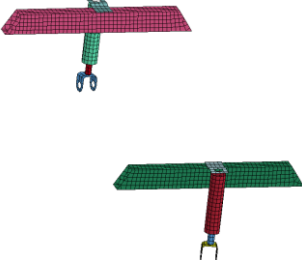
Table 2- 1. Element quality control parameters [264, 265].

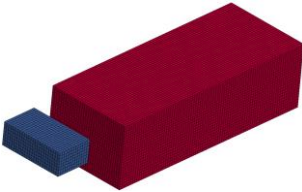
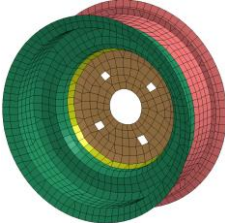
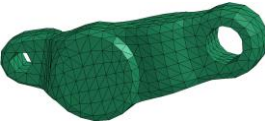
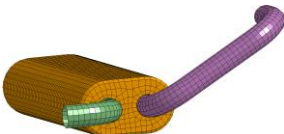
Quality parameters	Allowable min/max
Aspect ratio	5
Warping	15
Jacobian	0.6
Minimum side length	5
Maximum side length	12
Minimum quadrilateral internal angle	45
Maximum quadrilateral internal angle	145
Minimum triangular internal angle	15
Maximum triangular internal angle	120
Triangles %	5

Table 2- 2. Meshed vehicle components characteristics.

Vehicle components	Average element size (mm)	Minimum element length (mm)	Element type	Vehicle components	Average element size (mm)	Minimum element length (mm)	Element type
Frontal sheet plate 	8	5	Linear quadrilateral & triangular	Supported columns 	6.5	5	Linear quadrilateral & triangular
Roof 	8	5	Linear quadrilateral & triangular	Cushions 	7	3.8	Linear quadrilateral & triangular
Rear chassis 	8	5	Linear quadrilateral & triangular	Head-lamp 	8	5	Linear quadrilateral & triangular

<p>Floor support plates</p> 	<p>8</p>	<p>4</p>	<p>Linear quadrilateral & triangular</p>	<p>Frontal leading edge</p> 	<p>8</p>	<p>5</p>	<p>Linear quadrilateral & triangular</p>
<p>Tyre</p> 	<p>8</p>	<p>5</p>	<p>Linear quadrilateral & triangular</p>	<p>Front mudguard</p> 	<p>8</p>	<p>5</p>	<p>Linear quadrilateral & triangular</p>
<p>Windscreen</p> 	<p>8</p>	<p>5</p>	<p>Linear quadrilateral & triangular</p>	<p>Dashboard panel</p> 	<p>8</p>	<p>5</p>	<p>Linear quadrilateral & triangular</p>

<p>Windscreen frame</p> 	8	5	Linear quadrilateral & triangular	<p>Rear door</p> 	8	5	Linear quadrilateral & triangular
<p>Connected bar between front tyre and handbar</p> 	8	5	Linear quadrilateral & triangular	<p>Rear lights</p> 	8	4.9	Linear quadrilateral & triangular
<p>Handbar</p> 	8	5	Linear quadrilateral & triangular	<p>Rear suspension link</p> 	8	4	Linear quadrilateral & triangular
<p>Rear Suspension</p> 	8	5	Linear quadrilateral & triangular	<p>Front suspension</p> 	8	5	Linear quadrilateral & triangular

<p>Rear bumper</p> 	8	5	Linear quadrilateral & triangular	<p>Floor plates</p> 	8	5	Linear quadrilateral & triangular
<p>Engine and fuel tank</p> 	8	5	Linear quadrilateral & triangular	<p>Wheel</p> 	8	5	Linear quadrilateral & triangular
<p>Battery</p> 	8	5	Linear quadrilateral & triangular	<p>Frontal knuckle</p> 	8	5	Linear quadrilateral & triangular
<p>Exhaust</p> 	8	5	Linear quadrilateral & triangular				

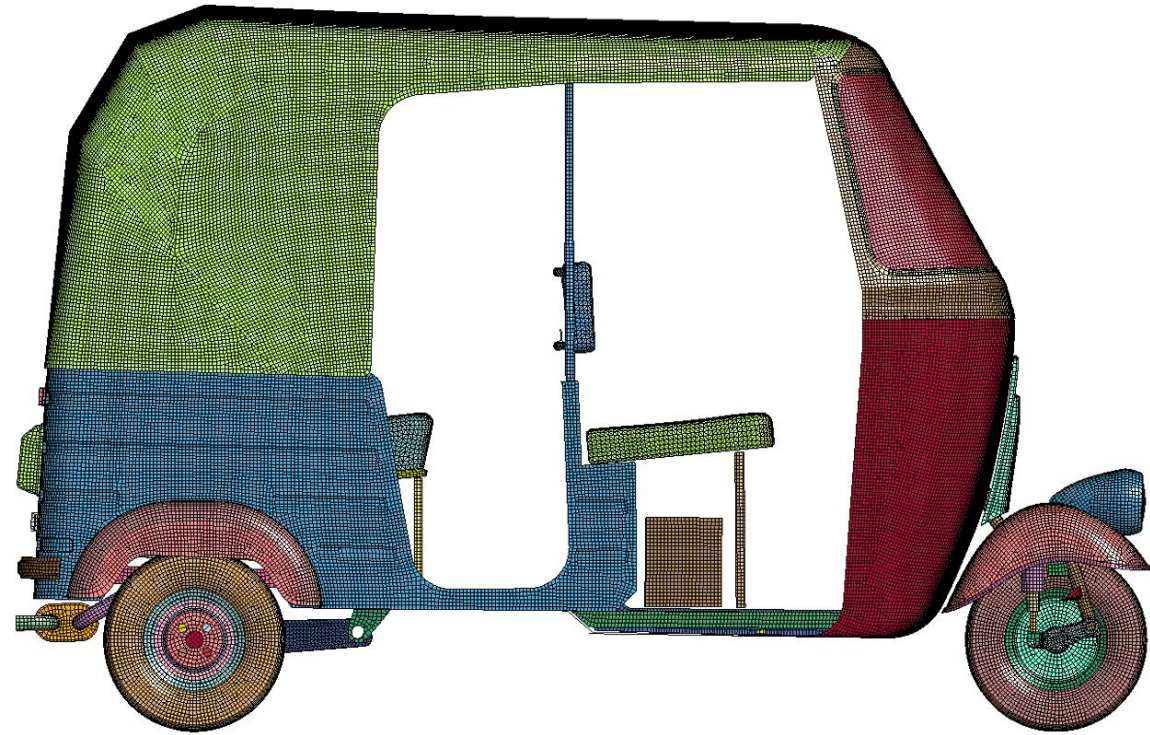


Figure 2- 4. FE Model of the auto rickshaw.

2.2.4.3 Material properties and thicknesses of the vehicle components

Vehicle material types and properties are the most important factors, which effect significantly the accuracy of the impact simulation. Moreover, material types and properties should fulfil the automotive criteria, such as safety, environment, lightweight, fuel consumption, cost and design. Mostly, the vehicle model consists of shells, which need to identify thicknesses for every single shell besides mechanical material properties. However, it has nine solid parts, so it was only a requirement that the material properties of structures such as, suspensions, cushions, engine, fuel tank, battery, knuckle and rims be assigned. The vehicle components materials were selected by the LS-DYNA material library.

The tyre was modelled by MAT_ELASTIC. While, the windscreen and vehicle structures were modelled by MAT_PIECEWISE_LINEAR_PLASTICITY. Cushions were modelled by MAT_FOAM_LOW_DENSITY and the roof was modelled by MAT_FABRIC. All vehicle components thicknesses were defined by SECTION_SHELL. The material mechanical properties and shell thicknesses of the vehicle components are shown in Table 2- 3 and Table 2- 4.

2.2.4.4 Vehicle model simplification

To minimise the computational run time, vehicle simplification was required thus, only the front-end vehicle geometry of the auto-rickshaw was considered. However, to meet the total real mass (373 kg) of the auto rickshaw including driver mass a Hybrid III dummy was positioned inside the vehicle, see Figure 2- 5 (a).

All the frontal components of the auto rickshaw were removed to measure the mass, centre of gravity and the moment of inertia of the rear vehicle parts, including the driver by LS-DYNA software (LS-Pre-Post), as shown in Figure 2- 5 (b). The vehicle rear components were simplified, such that only one element was generated to represent the same mass, centre of gravity and moment of inertia of the simplified parts, to make the model masses the same as the original simplified ones, see Figure 2- 5 (C).

Table 2- 3. Material mechanical properties of the model vehicle components.

Vehicle item	Mass density (kg/mm ³)	Young's modulus (Gpa)	Poisson's ratio	Yield stress (GPa)	Shear modulus (Gpa)	Tangent modulus	Ref
Tyre	1.700e-006	24.61	0.32	-			[265, 267]
Windscreen	2.500e-006	76	0.30	0.138		1	[220, 267, 268]
Vehicle structure	7.890e-006	210	0.30	0.25		1	[269]
Cushion (Latex)	1.010e-007	0.00416	0.35				[270]
Roof	6.800e-006	135	0.35		5		[271]

Table 2- 4. Thicknesses of the vehicle components.

Vehicle components	Thicknesses (mm)
Tyre	3
Windscreen	5.8
Vehicle structure	1.2-2
Roof	2

The simplified vehicle model, therefore, has less components than the full model. The front of the auto rickshaw model consists of a mudguard, headlamp, frontal sheet plate, sheet plate edge (cladding), windscreen, windscreen frame, front wheel, steering column, handle bar steering, inner dashboard plate, frontal knuckle, chassis members, one tyre and front damper spring suspension, as shown in Figure 2- 6. The total number of elements for the simplified meshed model are 207684.

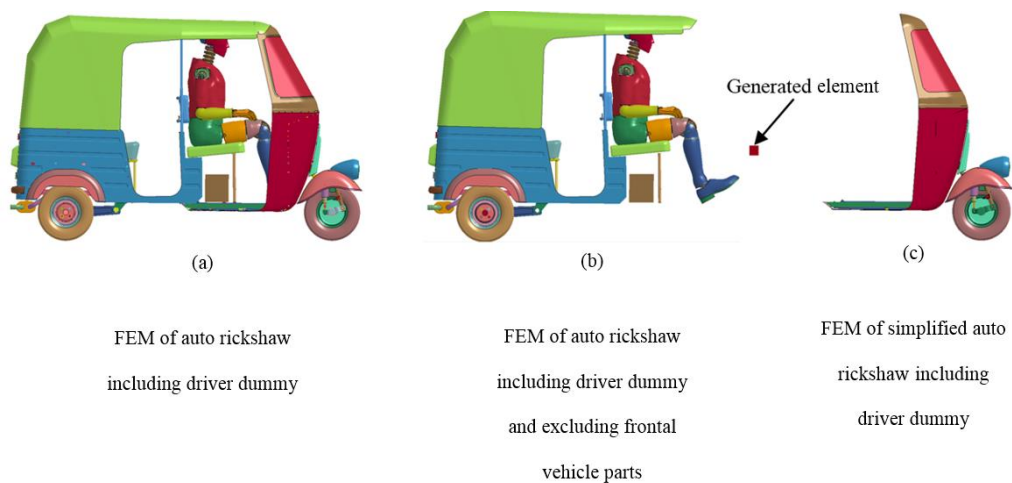


Figure 2- 5. Auto rickshaw model simplification steps; (a) FEM of auto rickshaw including driver dummy mass; (b) calculation of rear vehicle components masses by removing frontal vehicle components; (c) simplified auto rickshaw model.

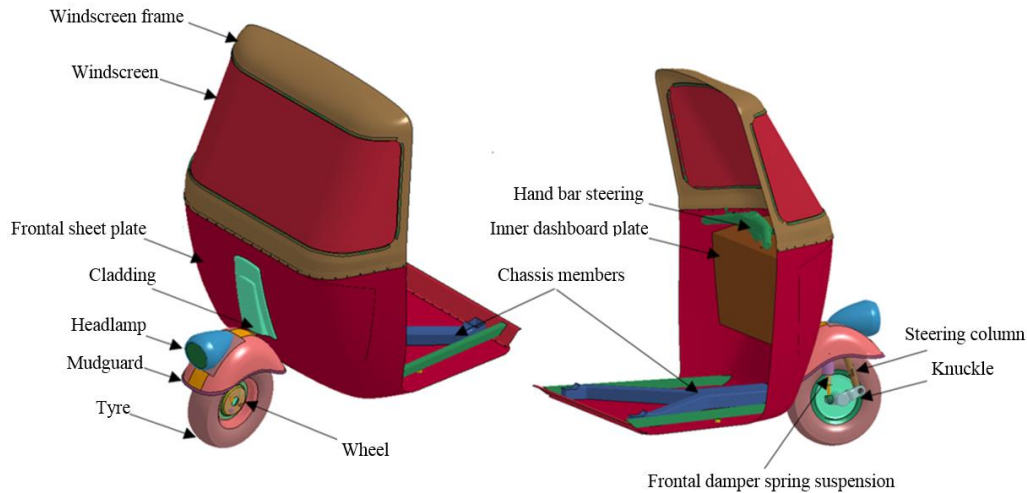


Figure 2- 6. Simplified auto rickshaw model.

2.2.4.5 Vehicle components constrain

All of the vehicle components of the simplified model were jointed together by using different constraint types within the FE software, LS-DYNA (LS-Pre-Post), to decrease the motion space. It was mentioned that the extra nodes that were needed to be added to a rigid body may be located anywhere in the model, even outside the body since they are part of the rigid body [273].

Therefore, a `CONSTRAINED_EXTRA_NODES_SET` was used to connect the generated element of the removed vehicle components to the frontal vehicle model as the first constrain type, while, `NODAL_RIGID_BODY` connects two opposite nodes [274]. Rigid bodies can be defined without elements by providing a list of nodal points that are included in the rigid body definition [275]. Therefore, Constrained Nodal Rigid Body (CNRB) was the second constraint type used to connect the vehicle components to each other. In addition, one `JOINT_TRANSLATIONAL` was used to constrain frontal suspension damper with the vehicle components and five `JOINT_REVOLUTE` were used, see Figure 2- 7.

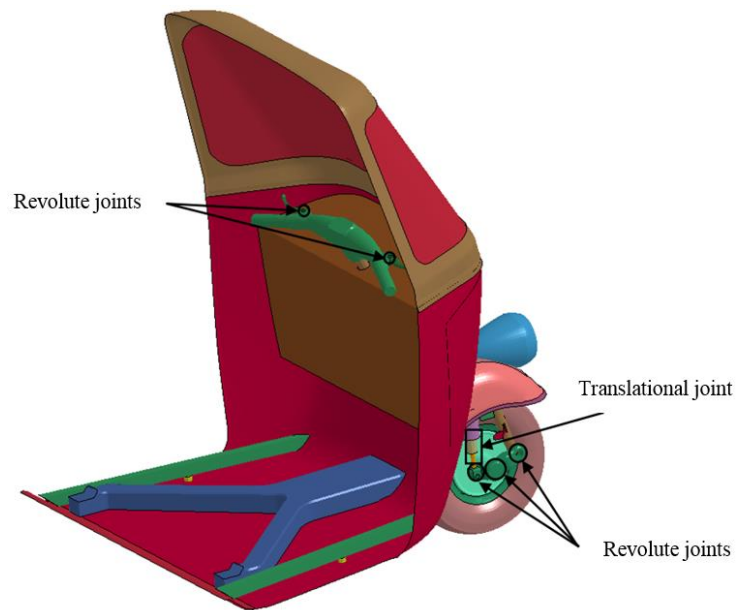


Figure 2- 7. Constrained translational and revolute joints.

2.2.5 Pedestrian models

Currently, the Livermore Software Technology Corporation (LSTC) only has a Hybrid III 50th percentile adult standing dummy, with a height of 168mm and weight of 78.6Kg, for pedestrian impact tests (see Figure 2-8). This dummy is based on Hybrid III 50th percentile male Rigid-FEM. This model was selected because it is the most generic impact test dummy to record injury criteria [276]. However, the LSTC and the National Crash Analysis Centre (NCAC) have developed a six-year-old (6YO)-child dummy, with a height of 1140 mm and weight of 23Kg, in a sitting position (as shown in Figure 2-9). Therefore, in this study, only two pedestrian dummies were used for pedestrian safety assessments: a standing adult dummy and a child dummy in a sitting position. However, converting from sitting to standing will be considered for the child dummy.

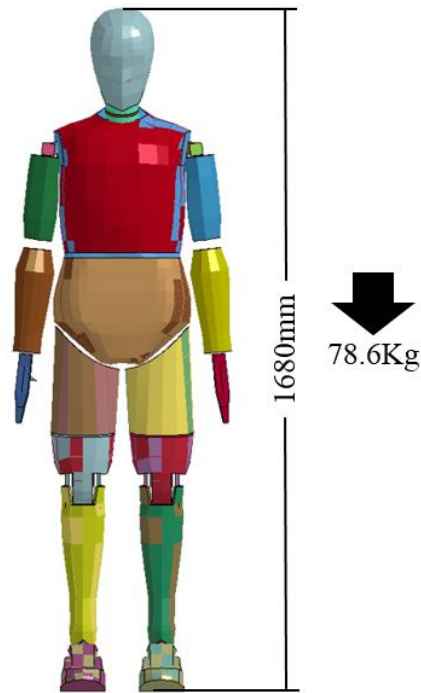


Figure 2- 8. 50th Percentile Hybrid III adult pedestrian dummy.



Figure 2- 9 6YO- Hybrid III child dummy in sitting position.

2.2.5.1 Converting position of the 6YO-child dummy

A positional change, from sitting to standing was made using LS-PrePost and ANSA software. The changes did not disturb the integrity of any of the dummy joints. In addition, no material properties were changed, or dummy model components renumbered.

The first step was to import the 6YO-child dummy into LS-PrePost and rotate the left and right feet by 30 degrees counter clockwise, see Figure 2- 10 (a). Secondly, the dummy file was imported into ANSA software to rotate the dummy feet and leg angle from 60 degrees to zero counter clockwise at the knee's rotational axis. Then, the feet, legs and thighs were rotated 90 degrees clockwise to position the dummy in vertical-standing position. The Entities-function-rotate option was used to rotate the feet and leg angles from 60 degrees to zero counter clockwise at the knee's rotational axis. Then, the feet, legs and thigh were rotated 90 degree clockwise to position the dummy in vertical-standing position, as shown in Figure 2- 10 (b).

However, the pelvis needed to be modified to ensure a biofidelic post kinematic dummy response to create accurate injury values, as demonstrated in Figure 2- 10 (c).

Therefore, the deformed pelvis elements were deleted which produced a pelvis gap. Thus, it was essential to fill the gap with a mixed element shell mesh of 6 mm as reported by Mohan et al., 2007 and 2009 [277, 278]. Still, however, there was another gap between the thighs and the pelvis which required construction. Consequently, a shell mesh was used by selecting edges to bridge the gap between the thighs and the pelvis, see Figure 2- 10 (c). Then finally, the 6YO-child dummy was converted from a sitting to a standing position that can be used in impact simulations, as shown in Figure 2- 10 (d).

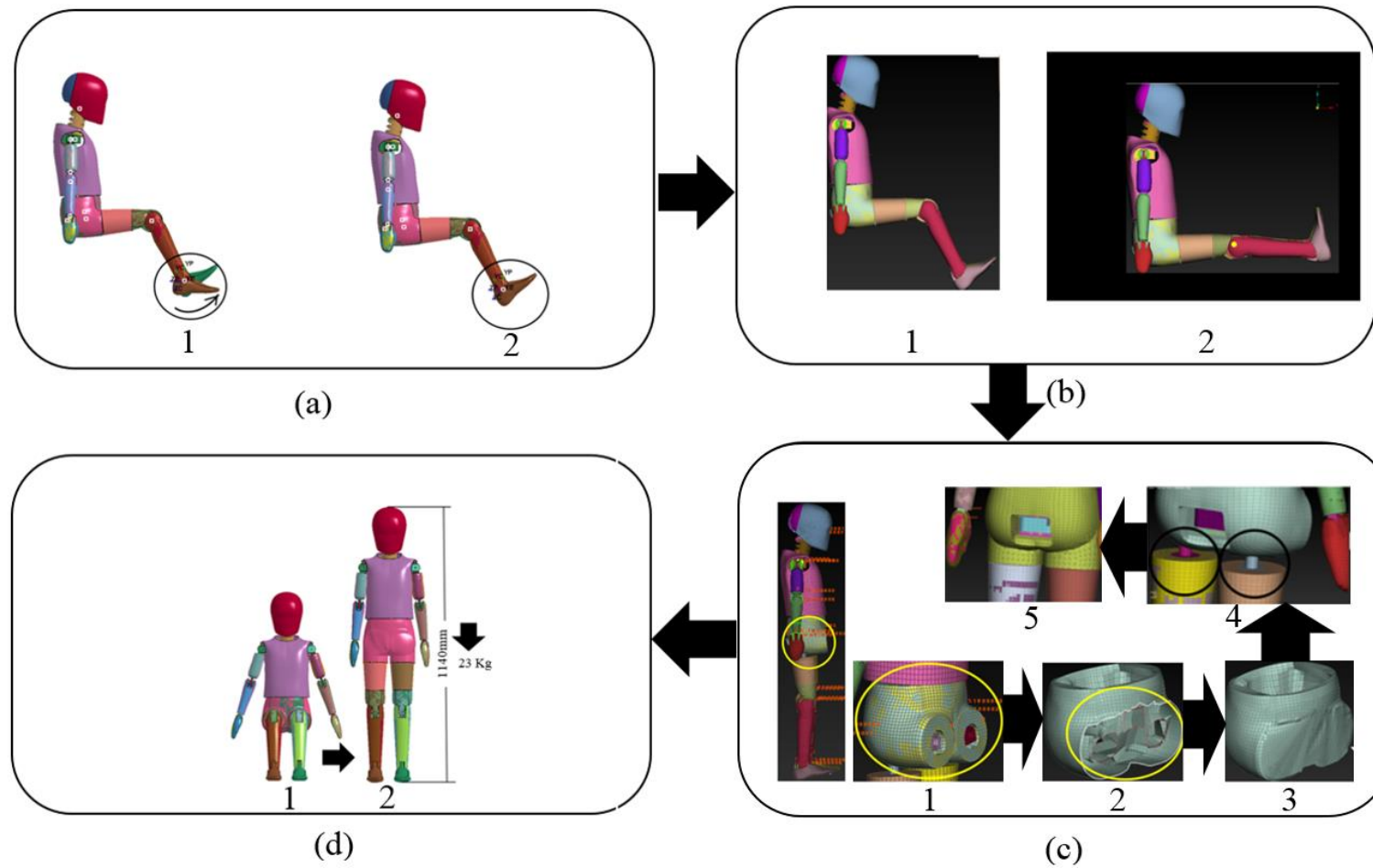


Figure 2- 10 6YO-child dummy converting process (sitting to standing).

2.3 Impact simulation environment

Simulation setup includes the final impact conditions in the LS-DYNA environment.

The following parameters identify the impact simulations:-

- Pedestrian impact positions (front, rear and side in walking position).
- Vehicle contact regions (at the vehicle centreline and at 42cm offset from the vehicle centreline).
- Contact types and friction coefficients.
- Ground types.
- Gravity and vehicle impact velocities.
- Solution control.
- Database definition for results collection.
- Results filter and frequency.

2.3.1 Pedestrian impact positions and vehicle contact regions

Different vehicle contact regions and impact positions could provide a varied data of post kinematic response, injury metrics and injury risk. However, pedestrian sizes and impact velocity variations could cover a greater range of pedestrian-auto rickshaw accident data. Therefore, two dummies were used in this study (adult and child pedestrian).

Pedestrian models were positioned in contact with two main vehicle regions, at the centreline and 42cm offset from the vehicle centreline. Three major impact positions, were simulated front (face-to-face with the vehicle), rear (back-to-face) and in a walking posture facing laterally with the right leg forward (without walking speed), and left arm positioned backward to cover the whole possible impact scenarios, as mentioned in the literature, see Figures 2- 11 and 2- 12. However, it is well known that in cases where the pedestrian has a transverse velocity, subsequent movement can be significantly altered [200].

2.3.2 Contact types and friction coefficients

Accurate modelling of contact interfaces between bodies is critical for predictive finite element simulations. In this research, different contacts were used, TIED_SHELL_EDGE_TO_SURFACE_OFFSET_CONTACT is a contact interface, which uses either a kinematic or penalty type constraint method to tie offset slave nodes to the master segment and it was the first contact type used to define the contact between the vehicle windscreen and the adhesive solid part [279]. CONTACT_GENERAL is simple, fast, robust and widely used [280], therefore, it was used to define the contact between the auto rickshaw tyre and the ground along the moving path [281]. To simulate pedestrian-auto rickshaw impacts with a logical post kinematic response of the crash dummies and to avoid penetration issues, which could cause numerical instability, selecting a robust and efficient contact method to define the interaction between pedestrian dummies and vehicle components was of great importance. Consequently, AUTOMATIC_SURFACE_TO_SURFACE was used [175, 280]. The contact friction coefficient between the pedestrian dummy parts and rickshaw was 0.65, while, it was 0.7 between the dummies shoes and the ground and between the tyre and the ground [164, 175, 281], shown in Figure 2- 13. However, contact parameters might influence the kinematic response and injury metrics. The coefficient of friction is one of the most significant contact parameters, thus, the influence of various friction coefficients, between the dummy and the vehicle, the dummy and the ground and the vehicle tyre and the ground were investigated, see Table 2-5

Table 2- 5. Contact friction coefficients.

Pedestrian-vehicle	Pedestrian-ground and vehicle tyre-ground
0.30 [181]	0.70 [164, 175, 281]
0.75 [181]	0.70 [164, 175, 281]
0.65 [164, 175, 281]	0.30 [181]
0.65 [164, 175, 281]	0.75 [181]
0.30 [181]	0.75 [181]
0.75 [181]	0.30 [181]

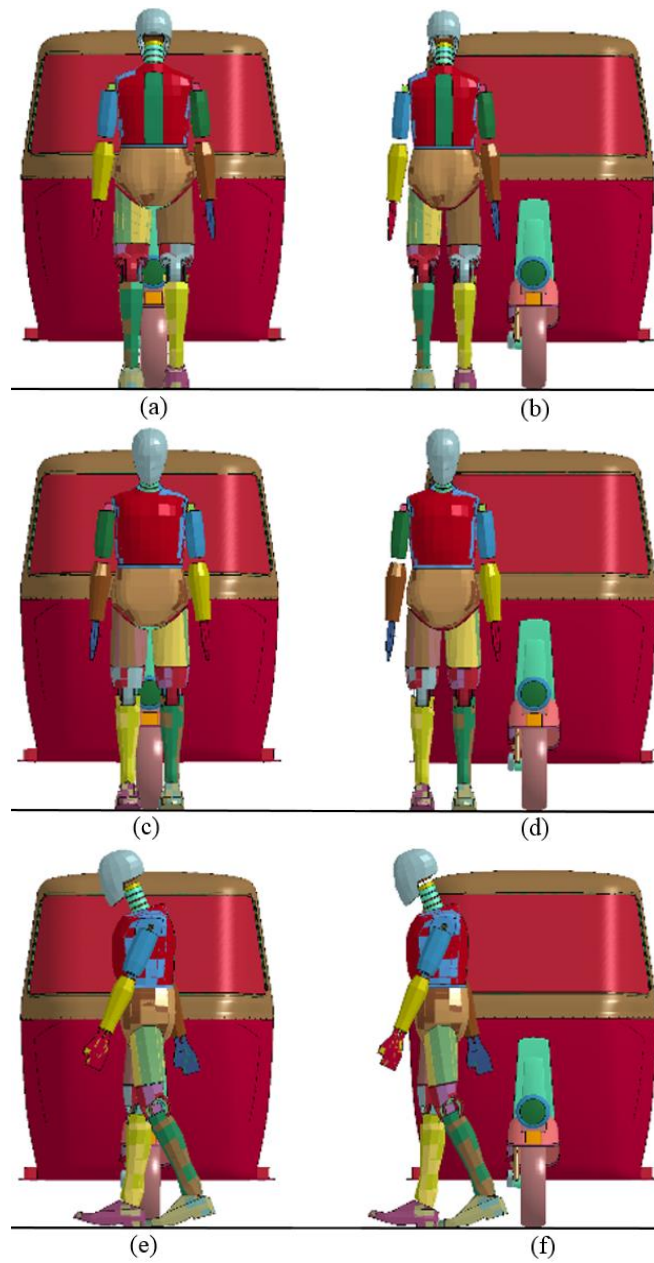


Figure 2- 11. Auto rickshaw–adult pedestrian impact simulations at different positions; (a) front centre (b) front offset; (c) rear centre; (d) rear offset; (e) side centre; (f) side offset.

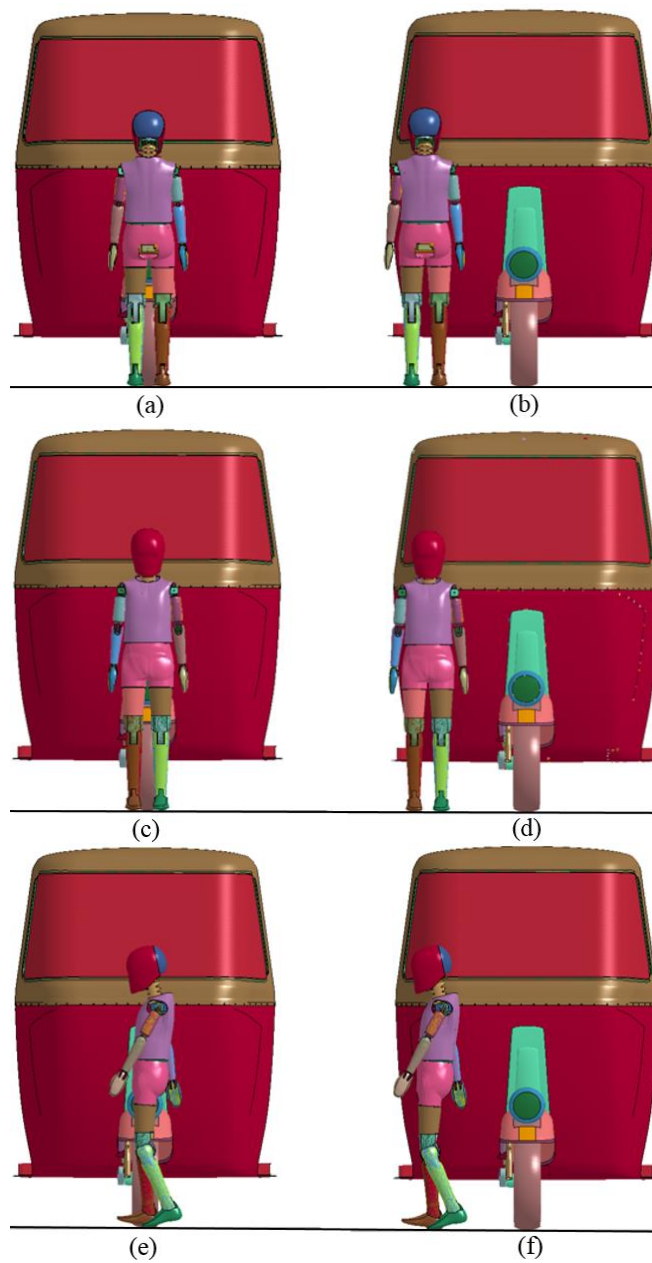


Figure 2- 12. Auto rickshaw–child pedestrian impact simulations at different positions; (a) front centre (b) front offset; (c) rear centre; (d) rear offset; (e) side centre; (f) side offset.

2.3.3 Ground types

A planar ground was used for the primary impacts (pedestrian-vehicle-contact). While, the road surface, on which the pedestrian finally landed, was modelled as a concrete for the secondary impacts (pedestrian-ground-contact) [176].

2.3.4 Impact velocity and gravity

INITIAL_VELOCITY was used to define varied vehicle impact velocity between 5km/h and 48km/h for adult pedestrian-auto rickshaw impact scenarios during the primary impacts and 5km/h to 40km/h for the 6YO-child pedestrian-auto rickshaw impacts in the primary impacts. For the adult secondary impacts, velocities between 10km/h and 40km/h were used for the secondary impacts.

For the modified material impact tests, velocities between 10km/h and 40km/h were used for the adult pedestrian to assess injury mitigation. In addition, the same impact velocities were assigned to the translational mass, using PART_INERTIA to ensure that the whole dynamic system, including the frontal vehicle components and the removed rear vehicle parts represented by one generated element, moved to impact with the pedestrians at the same impact velocity. In addition, LOAD_BODY_Z was used to define the gravity of $9.806e-003ms^{-2}$, as shown in Figure 2- 13.

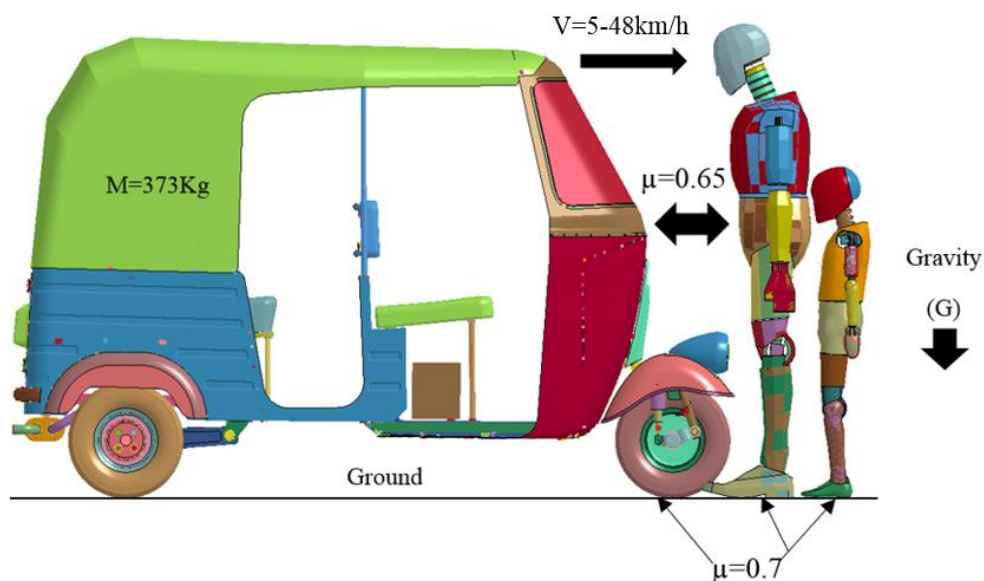


Figure 2- 13. Vehicle-pedestrian impact simulation setup.

2.3.5 Solution control

Solution control has a significant influence on simulation stability and accuracy. CONTROL_TERMINATION was used to define the simulation termination time. Wood et al (2005) noted that the impact duration during which the momentum was completely transferred to the pedestrian during the pedestrian-vehicle impact [186]. Bunketorp et al (1980) pointed out that impact duration for leg to bumper interaction only was in the range of between 56 and 140 ms and furthermore, that vehicle-pedestrian impact, such as bonnet or windscreen impact, extends the total duration of contact significantly [279]. While, Chawla et al (2003), concluded that the contact duration between the adult pedestrian and auto rickshaw was 175ms [40]. Therefore, the termination time (ENDTIM) was defined as 220ms for the primary impacts to an adult pedestrian. While, 100ms was defined for the primary impacts to the 6YO-child pedestrian, because the contact time of child pedestrian-vehicle was expected to be less than adult, as a result of child dummy centre of gravity being lower than the adult and the child dummy size and mass is less than adult.

Furthermore, although increasing the simulation time of an impact scenario could be considered computationally expensive, it was necessary to increase the simulation time of the secondary impact for the adult pedestrian to ensure that pedestrian body contacts the ground. Therefore, it was defined between 550 and 830ms. As recommended by LS-DYNA manual, using MAT_PIECEWISE_LINEAR_PLASTICITY, the shell element minimum time step assignment (TSLIMIT) was applied as 1.000e+020 and time step size for mass scaled solution (DT2MS) was defined as 8.000e-004.

2.3.6 Database definition for results collections

It was essential to define all the output results, which needed to be calculated and collected before running all the pedestrian-vehicle impact simulations. Therefore, DATABASE was used to define the expected results using American Standard Code for Information Interchange (ASCII) to define specific functions such as NODOUT, JNFORC, JSTIFR and DEFORC.

The NODOUT function has specific nodes for a dummy head and chest accelerations. While, JNFORC has specific nodes of upper neck forces, including axial and shear forces, JSTIFR for specific joints at occipital condyle of moment stiffness and DEFORC for specific chest compression springs for deflection [283].

2.3.7 Results filter and frequency

To reduce the uncertainty of time shifts when comparing the electronic data films, a Butterworth pre-filter with a frequency of 180 of c/s (HZ) was used to collect the head, neck and chest loading and criteria for adult pedestrian, as recommended by the NHTSA [119, 283].

Butterworth pre-filters with a frequency of 1000 and 60 Hz were used to collect the head and neck loads respectively for the 6YO-child pedestrian, as calibrated by (LSTC) and (NCAC) [284].

2.4 Expected results

2.4.1 Post kinematic response in the primary and secondary impacts

Kinematic response can be defined as the behaviour of a pedestrian after being impacted by a vehicle producing primary and secondary impacts. The post kinematic responses are to be obtained from different impact simulations, including different impact positions (front, rear and side), with two vehicle impact regions (at the vehicle centreline and at 42cm offset from the vehicle centreline) and different impact velocities, studying the following parameters of head contact location, head contact angles, head contact time, throw distance and injury metrics.

2.4.1.1 Head contact location

Head contact location, is the location of the pedestrian head impacted by vehicle components obtained from the interaction between pedestrian head and vehicle components.

2.4.1.2 Head contact angles

The head contact angle refers to the angle between the direction of the head impact velocity and the ground reference level during pedestrian-vehicle impacts [53].

2.4.1.3 Head contact time

Head contact time can be defined as the pedestrian head contact time with the vehicle components in milliseconds.

2.4.1.4 Throw distance

Throw distance is defined as the distance between the position of the initial impact and the body's final resting position or pedestrians travel distance from the initial impact position to the final position of the pedestrian on the ground [186], based on the pedestrian's centre of gravity (CG). It is a very effective tool for estimating impact speed in road accident investigation [53, 56, 57].

2.4.2 Selected injury parameters in the primary and secondary impacts

The pedestrian injury risk was evaluated in terms of selected injury parameters and tolerance levels. The Head Injury Criterion (HIC₁₅), the Upper neck Injury Criterion (N_{ij} and N_{km}) and Combined Thorax Index (CTI) will be used to assess the risk of pedestrian head, upper neck and chest injury.

2.4.2.1 Head injury and risk level

Head injury criterion is calculated by HIC the following equation:-

$$\text{HIC} = \max \left[\frac{1}{t_2 - t_1} \int_{t_1}^{t_2} a(t) dt \right]^{2.5} (t_2 - t_1) \quad (2.7)$$

Where a is the resultant linear acceleration, measured at the head centre of gravity in units of gravity; t_1 and t_2 are the two time instants during the impact, describing an interval between the starting and the end of the injurious time - period, identifying the maximum value of HIC, i.e. ($t_2 - t_1 \leq 15$ ms) [41, 113]. HIC values, calculated from the impact simulations, will be compared with two head injury thresholds for the adult pedestrian, HIC₁₅=1000 for front and rear impacts, which indicates a probability of severe head injury (AIS4+) of between 16 and 18% [113-115] and HIC=800 for side impacts [84, 115, 116]. HIC encompasses bone structure deformation, soft tissue damage, skull fracture, brain contusions and laceration and/or brain bleeding [113, 115, 116].

For the 6YO-child pedestrian, HIC values will be compared with head injury thresholds, HIC₁₅=700 for the front, rear and side impacts, indicates a 23% risk of serious head injury AIS3+ [117] or a 5% probability of severe head injury AIS4+, corresponding with brain injury or skull fracture [118]. It is also associated with head injuries such as comminuted or depressed skull fractures [81, 117].

The risk level of the head injury for both adult and child pedestrians will be assessed and classified based on AIS codes. Moderate AIS2+ to fatal head injury AIS6+ using NHTSA categorisation is based on two different sets of, HIC against injury curves, Prasad/Mertz curves and the lognormal curves, as shown in following formulae [114,117, 285].

$$\text{(Moderate), AIS} \geq 2 = \frac{1}{(1+e^{2.49+\frac{200}{\text{HIC}}-0.00483*\text{HIC}})} \quad (2.8)$$

$$\text{(Serious), AIS} \geq 3 = \frac{1}{(1+e^{3.39+\frac{200}{\text{HIC}}-0.00372*\text{HIC}})} \quad (2.9)$$

$$\text{(Severe), AIS} \geq 4 = \frac{1}{(1+e^{5.02-0.00351*\text{HIC}})} \quad (2.2)$$

$$\text{(Critical), AIS} \geq 5 = \frac{1}{(1+e^{7.82+\frac{200}{\text{HIC}}-0.00429*\text{HIC}})} \quad (2.3)$$

$$\text{(Fatal), AIS} \geq 6 = \frac{1}{(1+e^{12.24+\frac{200}{\text{HIC}}-0.00565*\text{HIC}})} \quad (2.4)$$

2.4.2.2 Upper neck injury and risk level

Upper neck injury criteria for the front and rear impacts will be calculated by N_{ij} and N_{km} , based on the following equations:-

$$\text{Upper neck injury for frontal impact (Nij)} = \frac{F_z}{F_{int}} + \frac{M_y}{M_{int}} \quad (2.5)$$

$$\text{Upper neck injury for rear impact (Nkm)} = \frac{F_x}{F_{int}} + \frac{M_y}{M_{int}} \quad (2.6)$$

F_z represents the maximum axial force (tension/compression) and M_y represents the maximum flexion (forward) /extension (rearward) bending moment [286], see Figure 2- 14 and Figure 2-15. Four different load cases are associated with the neck injury criterion, which are referred to as N_{ij} , where “ij” represents indices for the four injury mechanisms; namely, (N_{te}), (N_{tf}), (N_{ce}) and (N_{cf}), where (N_{te}) represents tension-extension, (N_{tf}) represents tension-flexion, (N_{ce}) represents compression-extension and (N_{cf}) represents compression-flexion for both load and moment.

The index "int" gives a critical intercept value for both the load and moment of the hybrid III adult male and 6YO-child dummies, as shown in Table 2- . The intercept values of the Hybrid III dummies are calculated from the output wave signal of both the load and moment during an impact. While, F_x represents the maximum shear force

(anterior/posterior) and M_y represents the maximum flexion (forward) /extension (rearward) bending moment, see Figure 2- and Figure 2-15. There are four possible load cases associated with N_{km} : the (N_{fa}) , (N_{ep}) , (N_{fp}) , and (N_{ea}) . (N_{fa}) represents flexion-anterior, (N_{ep}) represents extension-posterior, (N_{fp}) represents flexion-posterior and (N_{ea}) represents extension-anterior [95].

N_{km} values represent the maximum value between the four load cases, the index "int" gives a critical intercept value for both the load and moment, as shown in Table 2- . The intercept values for the Hybrid III is calculated from the output wave signal of both the load and moment. However, no N_{km} or intercepts values were proposed for child dummies. Therefore, in this study only N_{ij} values were calculated for both adult and child dummies. N_{km} values for rear impacts were calculated only for adult dummy.

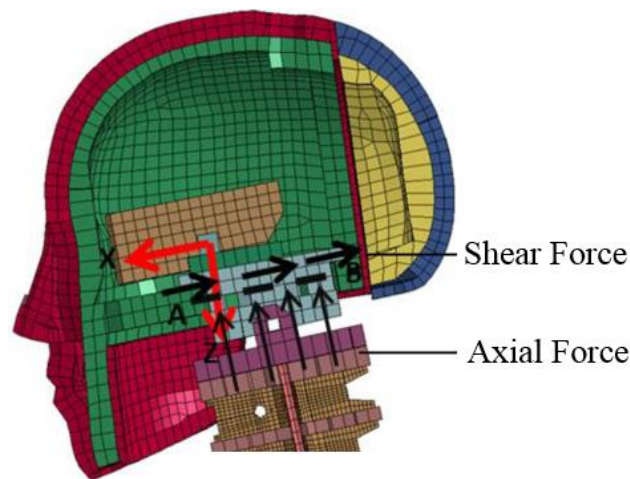


Figure 2- 14. Axial and shear forces of the upper neck.

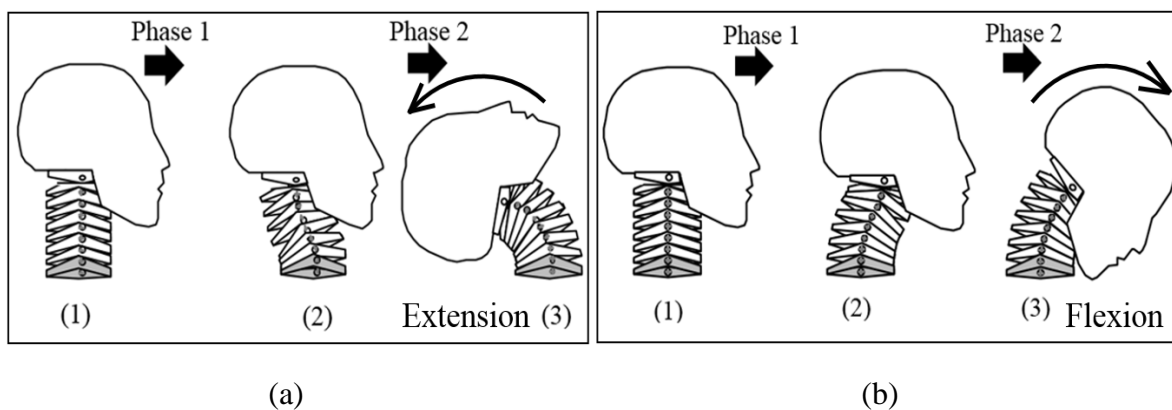


Figure 2- 15. Head-Neck motion phases during impacts; (a) extension ;(b) flexion [119].

Table 2- 6. Intercept load values of upper neck injury for the 50th percentile Hybrid III adult male and 6YO-child dummies for front Impacts.

Load case	Adult values [90]	6YO-child [119]
Extension	-135 N. m	-37 N.m
Flexion	+310 N. m	+93 N.m
Tension force	+6806 N	+2800 N
Compression force	-6160 N	-2800 N

Table 2- 7. Intercept load values of upper neck injury for the 50th percentile Hybrid III male dummy for rear impacts.

Load case	Values [127, 287]
Extension	47.5 N.m
Flexion	+88.1 N.m
Shear force	±845 N

Both N_{ij} and N_{km} values calculated from the impact simulations will be compared with upper injury thresholds of adult and 6YO-child pedestrians, N_{ij} and $N_{km}=1$ for front and rear impacts, which indicates 22% probability of serious upper neck injury AIS3+ [93].

They are associated with a risk of rupture of small blood vessels of the occipital condylar joints, alar ligament rupture with symptoms of neck pain and stiffness, shoulder weakness, dizziness, headache, memory loss and damage to the spinal cord, resulting from cervical vertebrae compression, disc rupture and nerve root damage, damage to the brainstem and even death. An increasing N_{ij} and N_{km} are associated with ligament rupture, damage to the spinal cord, brainstem and death [91-94, 117, 130].

The risk level of the upper neck injury for both adult and child pedestrians will be assessed and classified based on (AIS) codes. Moderate AIS2+ to critical neck injury AIS5+ using the following NHTSA categorisation formulae [93]:-

$$\text{(Moderate), AIS} \geq 2 = \frac{1}{1+e^{2.054-1.195*N_{ij}}} \quad (2. 15)$$

$$\text{(Serious), AIS} \geq 3 = \frac{1}{1+e^{3.227-1.969*N_{ij}}} \quad (2. 16)$$

$$\text{(Severe), AIS} \geq 4 = \frac{1}{1+e^{2.693-1.965*N_{ij}}} \quad (2.17)$$

$$\text{(Critical), AIS} \geq 5 = \frac{1}{1+e^{3.817-1.195*N_{ij}}} \quad (2.18)$$

There is currently no supported injury criteria that specifically considers neck injuries sustained during lateral impacts. One proposed solution to this issue is the multi-axial neck injury criteria (MANIC), which also includes the effects of side acceleration on the neck [131], however, this injury criterion is not yet approved and so has no injury tolerance limits. In addition, the Hybrid III dummies, used in this study, do not support the measurement of side neck response. Therefore, only upper neck injury and injury risk for front and rear impact were calculated.

2.4.2.3 Chest injury and risk level

Chest injury criterion for the frontal impact will be calculated by the Combined Thoracic Index (CTI) based on the following equation:-

$$\text{Combined Thoracic Index (CTI)} = \frac{A_{\max}}{A_{\text{int}}} + \frac{D_{\max}}{D_{\text{int}}} \quad (2.19)$$

Where, A_{\max} is the 3 ms clip value (single peak) of the resultant spinal cord linear acceleration in units of gravity, see Figure 2- 16 (a) [93]. D_{\max} is the mid-sternum chest deflection value at the central point of the chest dummy in millimetres, calculated from the output wave signal of crash dummies, as shown in Figure 2- 16 (b) [93]. The index "int" gives a critical intercept value for both the acceleration and deflection of the hybrid III male dummy, as shown in Table 2- .

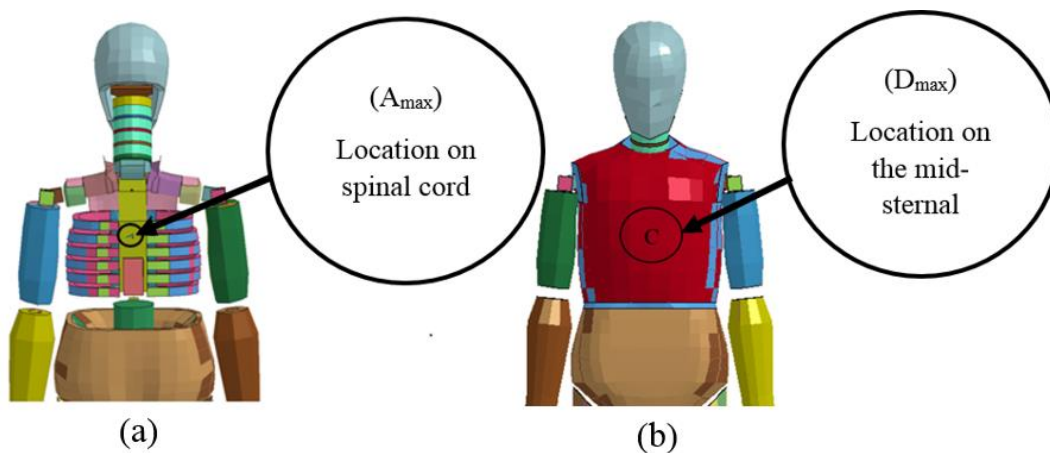


Figure 2-16. Acceleration and deflection points location of Hybrid III adult male dummy for the chest injury calculation (a) the measurement acceleration point location of the spinal cord; (b) the central measurement deflection point location of the dummy chest.

Table 2- 8. The intercept load values of chest injury for the 50th percentile Hybrid III male dummy for front impacts.

Load case	Adult values [119]
Aint (g)	90
Dint (mm)	103

CTI values, calculated from the impact simulations, will be compared with chest injury thresholds for adult pedestrians, CTI=1 for frontal impacts, which indicates a 25% probability of serious chest injury AIS3+ [93]. It corresponds with fracture of at least three to five separate ribs on one side of the body, lung contusion and minor heart contusion [81, 97]. However, the 6YO-child used in this study does not support CTI calculations. Thus, CTI for frontal impacts will only calculate for the adult pedestrian dummy.

The risk level of the chest injury for adult pedestrians was assessed and classified based on (AIS) codes. Moderate (AIS2+) to critical neck injury (AIS5+) using the following NHTSA categorization formulae [93]:-

$$\text{(Moderate), AIS} \geq 2 = \frac{1}{1+e^{4.874-6.036*CTI}} \quad (2. 20)$$

$$\text{(Serious), AIS} \geq 3 = \frac{1}{1+e^{8.224-7.125*CTI}} \quad (2. 7)$$

$$\text{(Severe), AIS} \geq 4 = \frac{1}{1+e^{9.872-7.125*CTI}} \quad (2. 8)$$

$$\text{(Critical), AIS} \geq 5 = \frac{1}{1+e^{14.242-6.589*CTI}} \quad (2. 9)$$

2.5 Auto rickshaw engineering modifications for adult pedestrian safety enhancement

Pedestrian-vehicle impacts are difficult to control and can occur as a result of many factors, such as pedestrian and driver behaviour, road design and networks and traffic mix, etc. Therefore, passive safety could be more relevant to pedestrian safety. Injury severity mitigation in passive safety can be achieved by changing the frontal vehicle-end geometry and/or changing the material properties and thicknesses of the frontal vehicle components.

When assessing the viability of the auto rickshaw design changes outlined in this study, a number of factors must be accounted for. First and foremost, the design changes must provide good potential to reduce pedestrian injuries in the unfortunate occurrence of an impact with an auto rickshaw. Secondly, the economic feasibility of these design changes must be deliberated, to assess whether they are practical within their environment.

This section focusses on improving the passive safety of the auto rickshaw by altering the material composition of the vehicle to “reduce the crash severity by allowing controlled energy dissipation through structure deformation” [288]. The main criteria for pedestrian safety is to control the acceleration pulse of the impact to below the upper limit of human tolerance [270], therefore it is desirable to design the auto rickshaw with materials that have high impact energy absorption, so that the deceleration of the vehicle is sufficiently low.

Aluminium and magnesium stand out as the best alternatives to steel structures. In addition, Polycarbonate (PC) has a significant influence on pedestrian protection as an alternative to glass windscreen materials. Therefore, these materials were used in the frontal components of the auto rickshaw. The materials and their properties that have been selected to replace steel and glass in the structure of the auto rickshaw will be the subject to computational analyses in this study.

Materials with a range of strength and stiffness were selected to assess the material that is best suited to mitigate injuries to the pedestrian. Multiple grades of aluminium were selected for analysis. Material properties were used to improve pedestrian safety as apart of passive safety approach, see Table 2- .

The materials were chosen because of their availability, high resistance to corrosion low mass (weight) and that they are easily formable [211]. However, improving the stiffness of aluminium alloy by increasing the part thickness should be specified by a certain factor so that it has the same stiffness as steel. The factor by which the thickness has to be increased for equal stiffness can be calculated using the following formula [211].

$$\frac{t_B}{t_A} = \sqrt[3]{\frac{E_A}{E_B}} \quad (2.10)$$

Where t_A is the thickness for the original material (i.e. steel part) and t_B is the thickness of the new material (i.e. aluminium/magnesium part). E_A and E_B are the Young's modulus for the original and new materials, respectively.

For body-structure sheets, the thickness of aluminium alloys should be increased by a factor of approximately 1.45 to have the same stiffness as the original steel panel [211]. While, to develop the magnesium alloy stiffness is to increase the part thickness by a certain factor so that it has the same stiffness as steel. For body-structure sheets, the thickness of magnesium alloys should be increased by a factor of approximately 1.67 [209]. All injury criteria such as HIC, N_{ij} , N_{km} , CTI and the risk level for the adult pedestrian impacted by the modified auto-rickshaw will be compared with the original value to assess the pedestrian safety improvement.

Table 2- 9. Material modification for pedestrian safety improvement.

Material	Density (kg/mm ³)	Young's modulus (GPa)	Poisson's ratio	Yield stress (GPa)	Thicknesses (mm)	References
Al 6016-T4	2.700e-006	70	0.33	0.147	3	[289]
Al 6061-T6	2.700e-006	71.1	0.33	0.250	3	[289]
Al 6111-T4	2.700e-006	70	0.33	0.160	3	[208, 211]
Al 5182-O	2.710e-006	70	0.33	0.119	3	[208, 290]
Al 5754-O	2.710e-006	70	0.33	0.102	3	[208, 291]
AZ31B	1.780e-006	45	0.35	0.165	3.34	[209, 292]
PC	1.200e-006	1.5	0.37	0.62	5	[293]

2.6 Brief Cost-Benefit-Analysis (CBA)

A cost-benefit analysis was conducted to determine which modified material has lowest cost, compared to the original and replacement materials. The average price for steel, which is currently used in structural elements, is approximately \$ 0.93 / kg [207]. The current glass windscreen has an average price of \$ 1.70 [223]. While, modified materials such as, aluminium and magnesium are more expensive than steel,

with aluminium having an average price of \$ 2.29 / kg and magnesium higher again at an average price of \$ 5.36 [207], whereas polycarbonate has a price nearly double that of glass per kg, with approximate cost of \$ 3.08 / kg [224]. Also, which material can contribute to saving the costs associated with injury. Therefore, the costs of severe head injury AIS4+ and neck injury AIS3+ caused by the original material of the vehicle components will be assumed to be similar to that reported by the study of Nguyen et al. 2013 in the Thai Binh province, Vietnam [231].

This study estimated the mean costs of pedestrian hospitalisation could be as high as \$ 2700 for AIS4+ head injuries. In addition, it was noted that injuries to the spine, which includes the neck and chest, had no significant cost difference and often had the lowest costs of all body regions, being approximately 38% lower than head injuries. Neck and chest injuries were estimated to cost as high as \$ 1520 for serious injuries AIS3+, the average annual income in the Thai Binh province is just \$ 695 [294]. The costs only represent those incurred during the patient's stay at one particular hospital, so does not consider transfer of the patient to a higher level hospital or loss of work due to injuries, thus, the actual costs are likely to far exceed these estimates [231]. In addition, the cost of the original and modified vehicle components will be considered in this study.

3. RESULTS

3.1 Introduction

This chapter presents the following results:-

- The influence of impact velocity, impact position (including front, rear and side), vehicle contact region (centreline and 42cm offset from the vehicle centreline) and pedestrian size (including two pedestrian sizes: adult and 6YO-child) on the post-kinematic response, head, and upper neck injury risk during primary impacts. In addition, chest injury risk during primary impacts for adult pedestrians impacted by an auto rickshaw will be reported.
- The full kinematic response will be given, including primary and ground interactions of the head, upper neck, and chest injury risk during primary and secondary impacts for an adult pedestrian impacted by an auto rickshaw at two vehicle impact regions (centreline and 42cm from the vehicle centreline) in three impact positions (i.e. front, rear and side). These scenarios were simulated at impact velocities ranging between 10 and 40km/h.
- Various materials were investigated to assess pedestrian safety in terms of head, upper neck, and chest injury risk mitigation using Abbreviated Injury Scale (AIS) coding. In addition, a cost benefit analysis was conducted for the modified vehicle and for medical cost saving.

3.2 Primary impacts

This section considers the post-kinematic response of a pedestrian's head contact location, head contact time and injury criteria. The injuries to the head, upper neck and chest are influenced by parameters such as, impact velocity, impact position, vehicle contact region and pedestrian size. Furthermore, the injury risk level produced from primary impacts was classified, based on AIS Coding.

3.2.1 Kinematic response during primary impacts.

The kinematic response for adult and child pedestrians during a primary impact is defined as the dynamic response after the impact, including the pedestrian body regions impacted with vehicle components at different times, head contact time, head contact locations and head impact angles.

Generally, the impact contact time between the impacted pedestrian body regions and vehicle components decreases with increasing impact velocity during all of the impact simulations. Dummy kinematics were captured for all of the impact simulations. Examples of 30km/h impact related kinematic responses for adult pedestrian are provided for three different impact positions against two vehicle contact regions (centreline and offset), see Figure 3-1. Meanwhile, the impact related kinematic responses for a 6YO-child pedestrian is presented in Figure 3-2.

Tables 3-1 to 3-4 show all of the sequences of adult and child pedestrians-vehicle interaction and contact time during the impact simulations at 30km/h. In addition, it was observed that the vehicle components deformed the pedestrian's body regions during primary impacts.

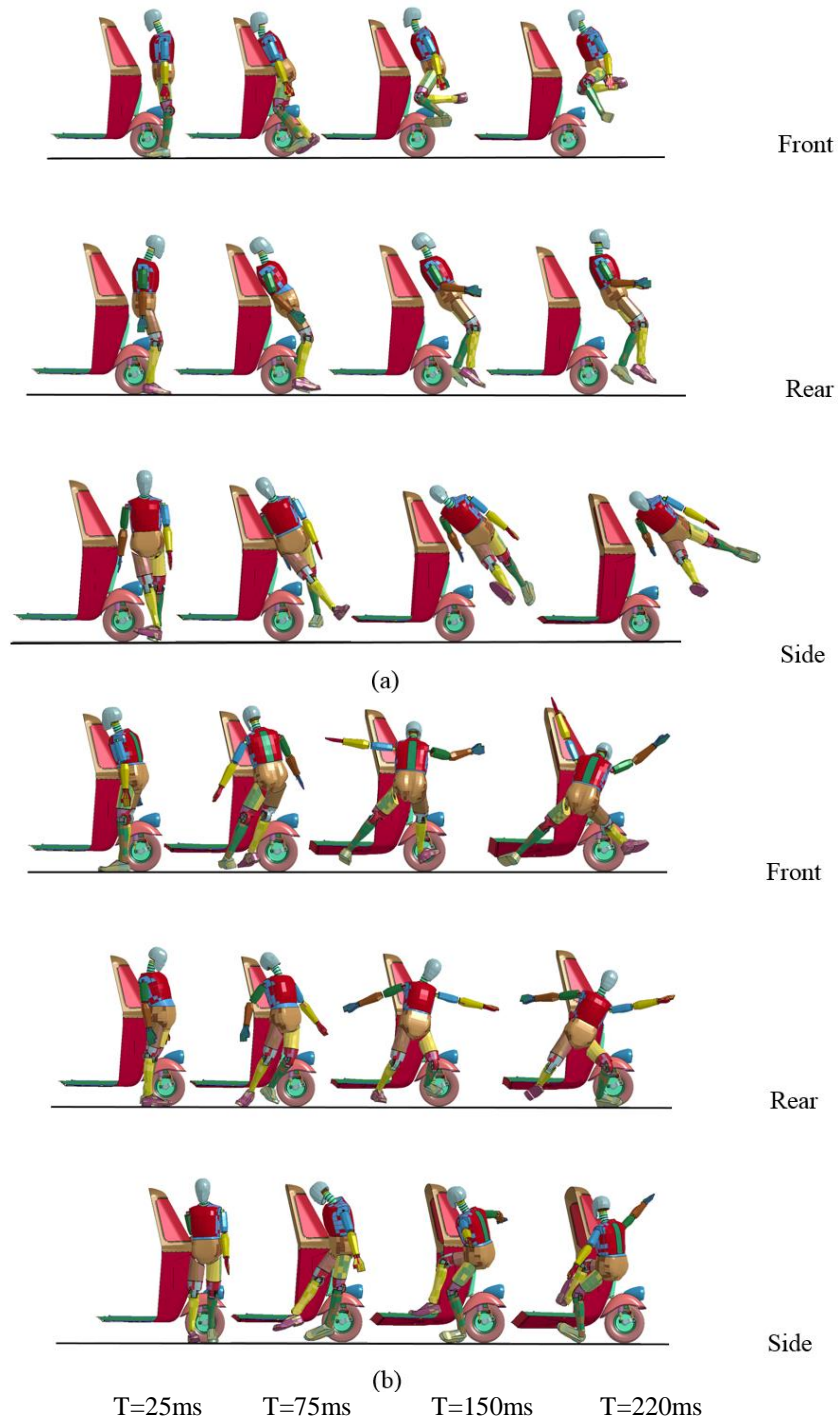


Figure 3- 1. The kinematic response of adult pedestrian dummy impacted at different vehicle regions and impact positions (a) pedestrian impacted at the vehicle's centre in front, rear and side position; (b) pedestrian impacted at 42 cm offset from the vehicle's centre in front, rear and side position at 30 km/h.

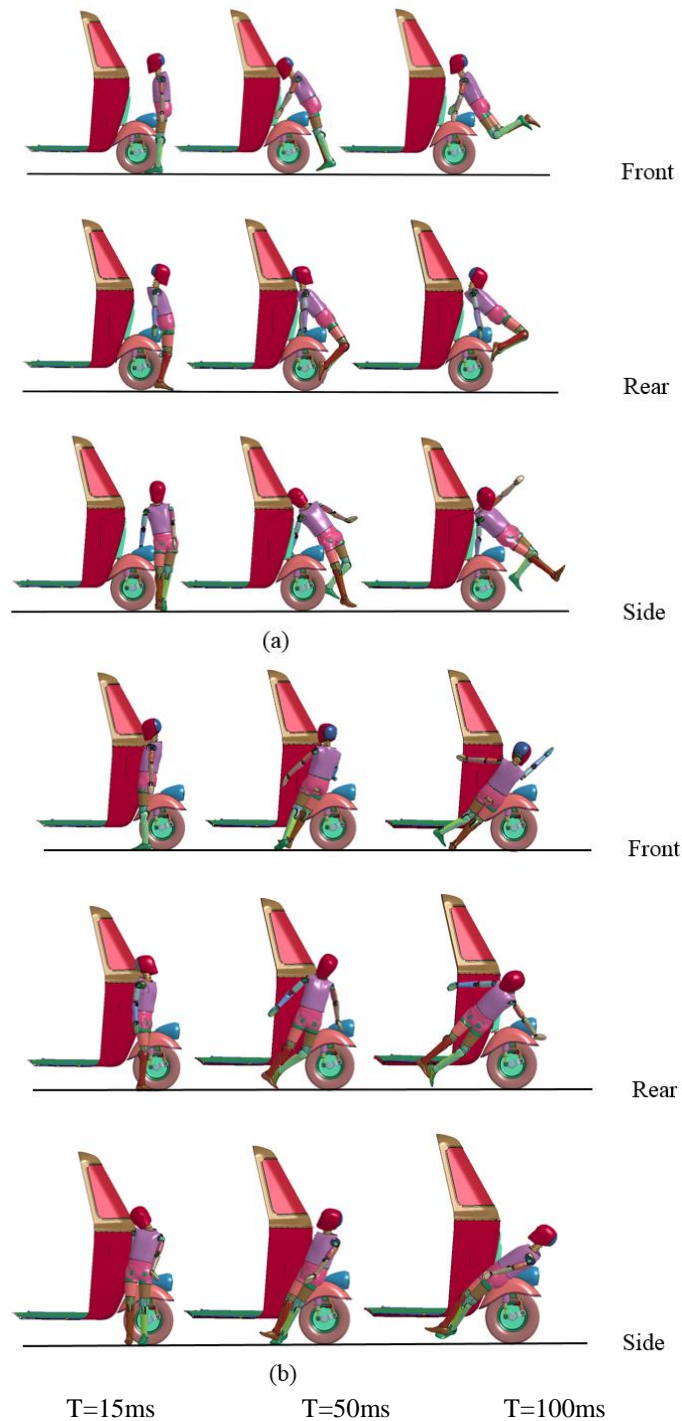


Figure 3- 2. The kinematic response of 6Y0-child pedestrian dummy impacted at different vehicle regions and impact positions (a) pedestrian impacted at the vehicle's centre in front, rear and side position; (b) pedestrian impacted at 42 cm offset from the vehicle's centre in front, rear and side position at 30 km/h.

3.2.1.1 Kinematic response during impacts at the vehicle's centreline

Figures 3- 1 (a) and 3-2 (a) show the kinematic response of impacts at the vehicle's centerline for front, rear and side-impact orientations for adult and 6YO-child pedestrians, respectively.

For adult pedestrians, the frontal impact occurred between the pedestrian's knees and the front head lamp of the vehicle. Tibial interactions occurred with the mudguard, which was followed by the lower torso impacting the frontal vehicle edge (the windscreen frame) and the upper torso (specifically the chest) contacting with the windscreen. The head was accelerated in both the forward and vertical directions, and impacted with the upper windscreen and upper part of the windscreen frame at the same time, as illustrated in Table 3-1. Finally, the adult pedestrian moved in a backward direction with simple rotation towards the left side of the vehicle. For the 6YO-child pedestrian, the first interaction in a frontal impact was between the lower region of the femur and the mudguard. Then, the femur and lower torso contacted with the headlamp. The tibia impacted with the front tyre and the head impacted the lower region of the windscreen frame, as shown in Figure 3-2 (a) and Table 3-2.

For the adult pedestrian, a rear impact occurred between both knees and the head lamp. Tibial contact occurred with the mudguard and the lower torso contacted the frontal vehicle edge, which produced a high impact force. The right and left hands produced a glancing impact with the lower frontal sheet plate, and then the upper torso struck the windscreen. The head interacted with the upper vehicle windscreen frame, and then the adult pedestrian moved in a forward direction, although they were not rotated, see Table 3-1. For the child pedestrian, the lower torso impacted the headlamp in a rear impact. The knees then collided with the mudguard and at the same time the tibia impacted with the auto rickshaw's front tyre, the upper femurs contacted with the headlamp, the upper torso impacted with the lower front sheet plate and the head interacted with the lower part of windscreen and windscreen frame components, as shown in Figure 3-2 (a).

For the adult pedestrian, a side impact occurred between the right knee and head lamp, which produced pedestrian ankle pro and supination. It also produced a high force that concentrated at the right hand and arm as a result of contact with the lower frontal sheet plate and frontal leading edge. Furthermore, the right arm was pushed behind the

pedestrian's upper torso and the femur rotated in accordance with auto rickshaw's frontal vehicle geometry. Then, the upper right arm interacted with the windscreen. The dummy was then observed to vault over the auto rickshaw, such that the head struck the upper side of the windscreen frame, before rotating to the vehicle's right-hand side. For the child pedestrian, the initial contact occurred between the child's right femur and the vehicle mudguard. Then, the upper part of the right femur and the lower torso contacted with the headlamp. At the same time, the right tibia was struck by the front tyre. The right arm was then pushed behind the pedestrian's upper torso and impacted with the front sheet plate. Finally, the child pedestrian's head collided with the lower part of the windscreen and windscreen frame, see Figure 3-2 (a).

Table 3- 1. The sequence of adult pedestrian-vehicle interaction and contact time at the vehicle's centreline.

Impact position	Vehicle contact region	Pedestrian contact region	Contact time duration (ms)
Front	Front head lamp	Knees	0-20
	Mudguard	Tibia	0-35
	Front vehicle edge (windscreen frame)	Lower torso	30-75
	Windscreen	Upper torso, specifically the chest	35-75
	Upper windscreen and upper frame	Head	50-65
Rear	Front head lamp	Knees	0-17
	Mudguard	Tibia	2-47
	Frontal vehicle edge (windscreen frame)	Lower torso	27-54
	Windscreen	Upper torso	62-72
	Upper windscreen frame	Head	82-92
Side	Headlamp	Right knee	0-49
	Lower front sheet plate and front leading edge	Right hand and arm	22-27
	Windscreen	Upper right arm	52-85
	Upper side of the windscreen frame	Head	100-105

Table 3- 2. The sequence of 6YO-child pedestrian-vehicle interaction and contact time at the vehicle's centreline.

Impact position	Vehicle contact region	Pedestrian contact region	Contact time duration (ms)
Front	Mudguard	The lower part of the femur	0-47.5
	Front headlamp	The upper part of the femur	5-40
	Front headlamp	Lower torso	5-100
	Front tyre	Tibia	7.5-27.5
	Lower front sheet plate	Right and left hands	45-55
	The lower part of the windscreen frame	Head	42.5-55
Rear	Front head lamp	Lower torso	0-75
	Mudguard	Knees	7.5-32.5
	Front tyre	Tibia	7.5-35
	Headlamp	Femur	15-32.5
	Lower front sheet plate	Upper torso	40-95
	The lower part of the windscreen / frame	Head	40-50
Side	Mudguard	Right femur	0-20
	Headlamp	The upper part of the right femur	2.5-27.5
	Headlamp	Lower torso	5-95
	Front tyre	Right tibia	5-15
	The lower part of the windscreen / frame	Head	45-60

3.2.1.2 Kinematic response at impacts 42cm offset from the vehicle's centreline

Figure 3- 1 (b) and 3-2 (b) demonstrates the kinematic response of impacts at 42cm offset from the vehicle's centreline for front, rear and side-impact orientations for adult and 6YO-child pedestrians, respectively.

For the adult pedestrian, a frontal offset impact occurred between the lower torso and the frontal offset vehicle edge, which produced a high force. The right femur struck at the frontal lower sheet plate, and the right hand and arm were impacted by the frontal vehicle edge and the frontal lower sheet plate. Subsequently, the upper torso

(specifically the chest) interacted with the windscreen, the right knee contacted with the frontal lower sheet plate and the head contacted with the upper side of the windscreen region. Finally, the pedestrian rotated, and the left femur interacted with the frontal lower sheet plate and the right-hand side of the vehicle. For the 6YO-child pedestrian, the first contact was between head and the lower windscreen/frame. Their chest then interacted with the front offset edge. The right-hand body regions (including the femur, patella and tibia) and the left-hand body regions (including the arm, patella and tibia) struck the lower front sheet plate. Finally, the child pedestrian rotated to the vehicle's right-hand side, as shown in Figure 3-2 (b)

For adult pedestrian, initial offset rear impact occurred between the lower torso and the front leading edge. The left hand impacted the lower vehicle sheet plate and the left arm impacted the frontal leading edge. The left knee impacted the lower frontal sheet plate and the left tibia impacted the lower sheet plate. The pedestrian was subsequently rotated to the right of the vehicle, the head simultaneously contacted with the upper side corner of the windscreen and windscreen frame. No impacts occurred at the upper torso. While for 6YO-child pedestrian, the initial interaction was between the upper torso and the lower offset windscreen frame, then the left arm and the left hand impacted by the lower front sheet plate. The child pedestrian head collided both the lower windscreen and windscreen frame. Then, left tibia, right arm, right tibia and right hand contacted with the lower front sheet plate. Lastly, the child pedestrian rotated to the vehicle's right-hand side, see Figure 3-2 (b)

For the adult pedestrian, the initial offset side impact occurred between the right arm and the right-hand leading edge, and the right hand impacted with the lower front sheet plate. Subsequently, the right hand twisted behind the upper torso and the whole body rotated to the right-hand side of the vehicle, such that the right femur struck the lower sheet plate. The pedestrian subsequently turned to face the vehicle. Nonetheless, no torso or head contact occurred. Lastly, the pedestrian rotated further to the right-hand side of the vehicle. Thus, for all impact positions, the first interaction occurred between the frontal leading edge and the lower torso and upper limbs. The impact then occurred with the other pedestrian body regions, as shown in Table 3-3. The rotational dynamic for the pedestrian was the significant kinematic response in all impact positions. There was only a simple rotation about the longitudinal axis during the side impact. While for the 6YO-child pedestrian, the first interaction was between the right arm/hand and

lower torso with the lower front sheet plate. The child's head then impacted both the vehicle windscreen and windscreen frame, see Table 3-4. Then, the right tibia and knee contacted the lower front sheet plate. Finally, the child pedestrian rotated to the right-hand side of the vehicle, see Figure 3-2 (b).

Table 3- 3. The sequence of adult pedestrian-vehicle interaction and contact time at 42cm offset from the vehicle's centreline.

Impact position	Vehicle contact region	Pedestrian contact region	Contact time duration (ms)
Front	Front offset edge	Lower torso	0-43
	Front offset edge	Right femur	5-32
	Front edge and lower sheet plate	Right hand and arm	11-15
	Windscreen	Upper torso, specifically chest	12-47
	Front lower sheet plate	Right knee	17-32
	Upper side windscreen	Head	24-27
Rear	Front leading edge	Lower torso	0-27
	Front leading edge	Left arm	7-12
	Lower front sheet plate	Left knee	14-27
	Lower sheet plate	Left tibia	32-37
	Upper side corner of windscreen and frame	Head	60-65
Side	Right leading edge	Right arm	0-60
	Lower front sheet plate	Right hand	2-5
	Lower sheet plate	Right femur	47
	-	No head and torso contacts	-

Table 3- 4. The sequence of 6YO-child pedestrian -vehicle interaction and contact time at 42cm offset from the vehicle's centreline.

Impact position	Vehicle contact region	Pedestrian contact region	Contact time duration (ms)
Front	The lower part of windscreen	Head	0-22.5
	Front offset edge	Chest	7.5-30
	Front offset edge	Right arm	17.5-20
	Lower front sheet plate	Right femur	17.5-27.5
	Lower front sheet plate	Right knee	22.5-25
	Lower front sheet plate	Left knee	30-64.5
	Lower front sheet plate	Right tibia	42.5-50
	Lower front sheet plate	Left arm	47.5-100
	Lower front sheet plate	Left tibia	67.5-100
Rear	Front offset edge	Upper torso	0-25
	Lower Front Sheet Plate	Left arm	5-12.5
	Lower front sheet plate	Left hand	10-12.5
	Lower Windscreen / Frame	Head	15-17.5
	Lower front sheet plate	Left tibia	40-50
	Lower front sheet plate	Right arm	42.5-62.5
	Lower front sheet plate	Right tibia	50-52
	Lower front sheet plate	Right hand	60-62
Side	Lower front sheet plate	Right arm	0-40
	Lower front sheet plate	Right hand	2-5
	Lower front sheet plate	Right lower torso	15-37.5
	Lower Windscreen / Frame	Head	17.5-20
	Lower front sheet plate	Right tibia and knee	35-45

3.2.2 Head contact locations and angles during primary impacts

Notably, it is established that the head contact locations vary with impact position, vehicle contact region and pedestrian size. The upper and lower parts of the windscreen and the windscreen frame are the most frequently impacted, stiffest and the most injurious vehicle components. However, the adult pedestrian's head interacted with

the upper regions of the windscreen and windscreen frame, while the child impacted with the lower parts of auto rickshaw components, see Figure 3-3. In terms of head contact angles, it varied with impact position, vehicle impact region and pedestrian size. However, mostly, head contact angles of the 6YO-child were less than adult. In addition, no head contact angle was observed for the adult pedestrian during the side offset, which is a result of no head-vehicle interactions occurring at impact velocities between 5 and 40km/h, see Table 3-5.

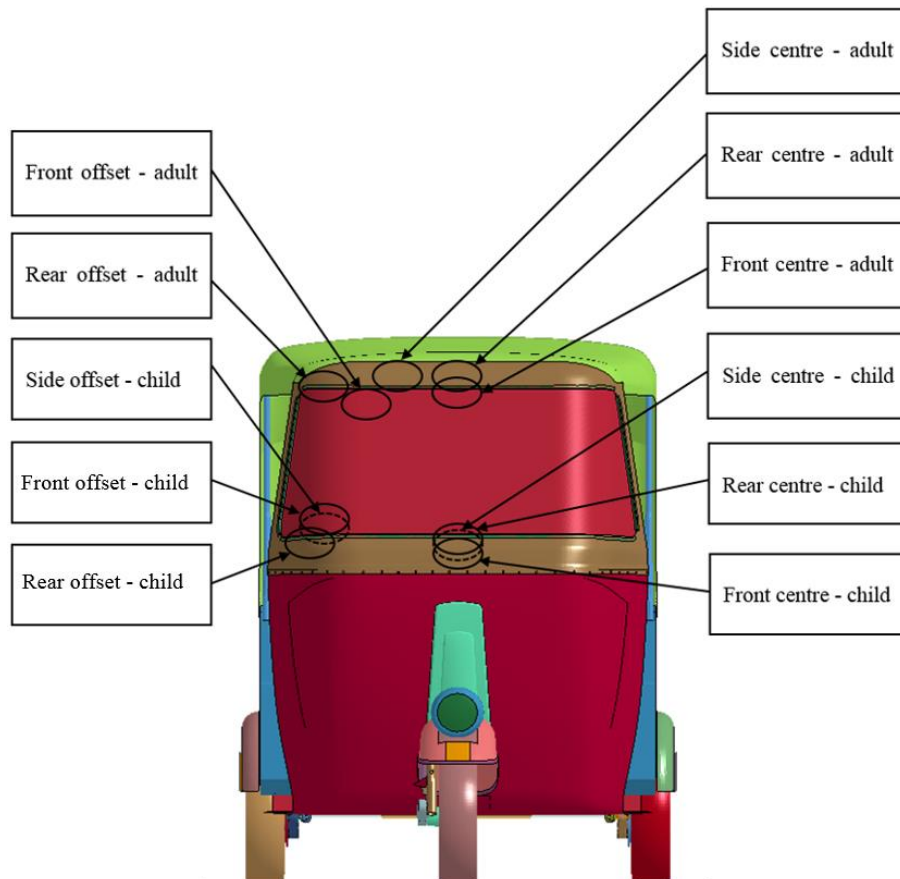


Figure 3- 3. Head contact locations for adult pedestrian of the auto rickshaw.

Table 3- 5. Head contact angles for adult and child pedestrians during various impact positions and two vehicle contact regions (centreline and offset).

Impact position	Adult (degrees)	6YO-child (degrees)
Front-centre	31	20
Front-offset	24	17
Rear-centre	18	19
Rear-offset	47	19
Side-centre	45	20
Side-offset	No head contact	39

3.2.3 Head contact time duration during primary impacts

Head contact time is defined as the time duration between the first contact of the human body and the head contact against the vehicle's components [160]. The head contact time for a pedestrian was explored at two-vehicle contact regions (vehicle's centreline and 42cm offset from the vehicle's centreline) at different impact positions (front, rear and side) and two pedestrian sizes (adult and 6YO-child).

3.2.3.1 Head contact time duration during impacts at the vehicle's centreline

During all of the primary impact simulations, the head contact time was different for various impact positions and the high velocity of impact resulted in short head contact times for both the adult and child pedestrians, see Figures A-1 and B-1. However, in most cases, the head contact time for the child was less than that of the adult. In addition, during all of the impact simulations, no contacts occurred between the head and vehicle components for the adult and child at 5 km/h, see Figures C-1 to C-3. Moreover, the effective rotational angle for both adult and child pedestrian about the frontal sheet plate of the auto rickshaw varied with the impact position, see Figure A-2 and B-2.

3.2.3.2 Head contact time duration at 42cm offset from the vehicle's centreline

Generally, the head contact time for both adult and child decreased with impact velocity at all impact positions. However, no head contact time was observed during the adult pedestrian-vehicle impacts in the side-offset scenario, see Figures A-3 and C-6. In addition, the child's head contact time was less than the adult's. Moreover, the head contact time for both pedestrian sizes impacted at 42cm offset from the vehicle's centreline was less than that produced at the vehicle's centreline, see Figures C-4 to C-6.

3.2.4 Head injury criterion and injury risk level during primary impacts

Head injury severity for both pedestrian size (adult and child) was examined using the Head Injury Criterion (HIC₁₅) and the head injury risk level was investigated using the AIS at different locations (front, rear and side) at two-vehicle contact regions (centerline of the vehicle and 42cm offset from the vehicle's centreline).

3.2.4.1 Head injury criterion and risk level during primary impacts at the vehicle's centreline

In general, all HIC values, for both pedestrian sizes (adult and paediatric), at the vehicle's centreline increased considerably with vehicle impact velocity at all impact positions (front, rear and side), see Figures A-4, A-5, B-4 and B-5.

Figure 3-4 demonstrates HIC values and impact velocities during the frontal impact position at the vehicle's centreline for the adult and 6YO-child pedestrians. It can be observed that the HIC values of the 6YO-child pedestrians are generally higher than the adults at impact velocities between 5 and 40km/h. In addition, the HIC values of the adult pedestrian exceeded the threshold, $HIC_{15}=1000$ at 30km/h, while the HIC values for the child pedestrian exceeded the threshold, $HIC_{15}=700$ at 20km/h.

Figure 3-5 shows HIC values and impact velocities during rear impact positions at the vehicle's centreline for adult and child pedestrians. It can be seen that the child pedestrian's HIC values are higher than the adults. Moreover, the HIC values of the adult pedestrian exceeded the threshold, $HIC_{15}=1000$ at 25km/h. Whereas, the HIC values of the child pedestrian exceeded the threshold, $HIC_{15}=700$ at 20km/h.

Figure 3-6 illustrates HIC values and impact velocities during side-impact positions at the vehicle's centreline for adult and child pedestrians. It can be seen that the HIC values of child pedestrian are higher than adults. Furthermore, the HIC values of the adult pedestrian do not exceed the threshold, $HIC=800$ at impact velocities between 5 and 40km/h. However, HIC of adults exceeded the threshold, $HIC=800$ at 48km/h (see Figure A-4), while the HIC values of child pedestrian exceeded the threshold, $HIC_{15}=700$ at 20km/h, see Figure B-4.

Figures A-6 to A-8 and B-6 to B-8 show that the head injury risk for adult and 6YO-child pedestrians, respectively, in the front and rear impact positions was significantly higher than that produced in the side-impact position. However, it was also observed that the head injury risk level between moderate AIS2+ and fatal AIS6+ for the child pedestrian is higher than that for the adult in most cases, see Tables C-1 to C-3.

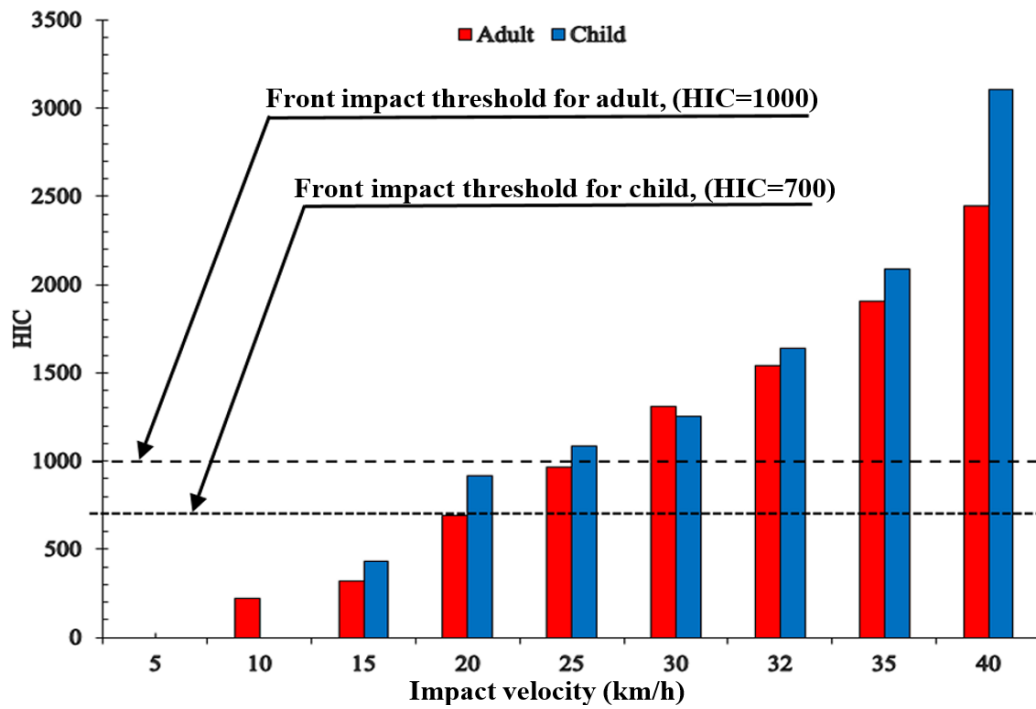


Figure 3- 4. HIC values in the frontal impacts at the vehicle’s centreline for adult and 6YO-child pedestrians.

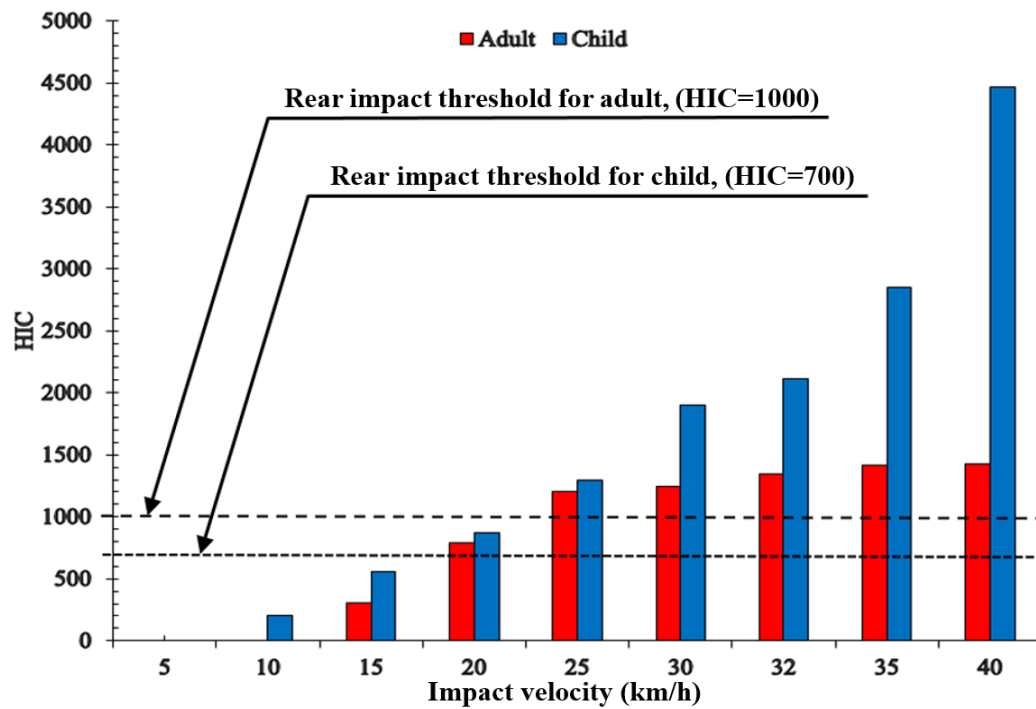


Figure 3- 5. HIC values in the rear impacts at the vehicle’s centreline for adult and 6YO-child pedestrians.

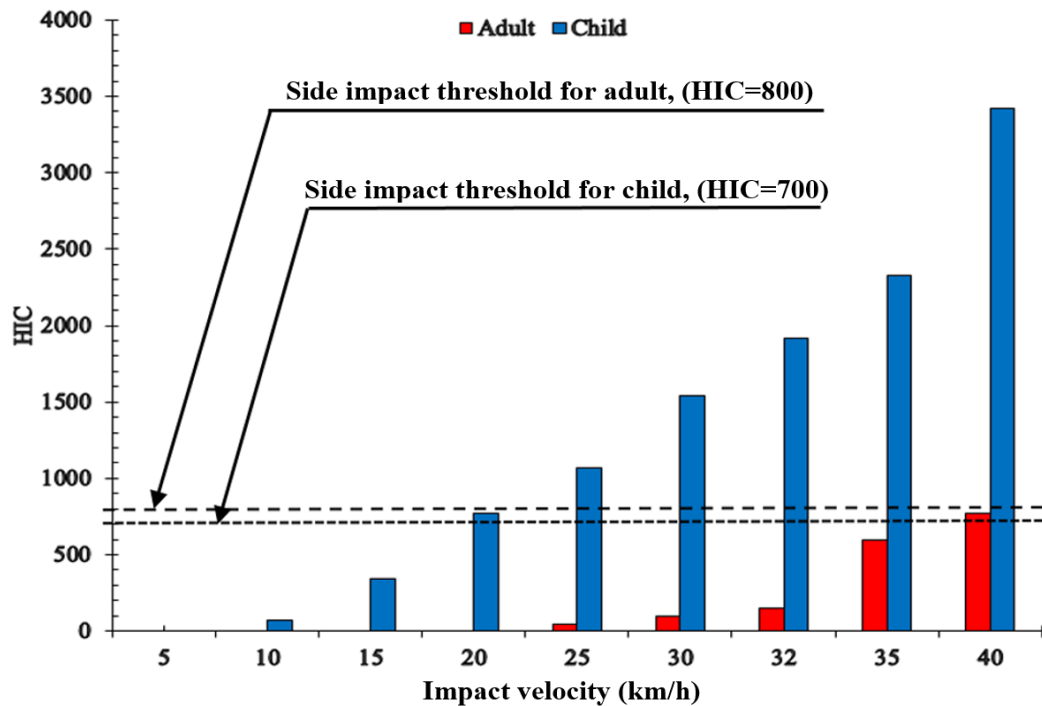


Figure 3- 6. HIC values in the side impacts at the vehicle's centreline for adult and 6YO-child pedestrians.

3.2.4.2 Head injury criterion and risk level at primary impacts 42cm offset from the vehicle's centreline

In most impact positions, the HIC values for both adult and paediatric pedestrians increased considerably with vehicle impact velocity.

Error! Reference source not found. illustrates HIC values and impact velocities during the frontal impact position at 42cm offset from the vehicle centreline for the adult and 6YO-child pedestrians. It is observed that the HIC values for the 6YO-child pedestrians are generally higher than those for the adults during all impact velocities from 5 to 40km/h. In addition, the HIC values of adult pedestrian exceeded the threshold, $HIC_{15}=1000$ at 25km/h, while the HIC values for the child pedestrian exceeded the threshold, $HIC_{15}=700$ at 10km/h.

Figure 3-8 shows HIC against impact velocity at the rear impact position at 42cm offset from the vehicle's centreline for the adult and child pedestrians. All HIC of the values for both pedestrian sizes are increased significantly with impact velocity. However, no head-vehicle contact occurred for the adult pedestrian until 15km/h. It has been seen that the HIC values for the 6YO-child pedestrians are higher than adults. Furthermore,

the HIC values for the adult pedestrian exceeded the threshold, $HIC_{15}=1000$ at 20km/h. HIC values of child pedestrian exceeded the threshold, $HIC_{15}=700$ at 10km/h.

Figure 3-9 demonstrates HIC values and impact velocities during the side-impact position at 42cm offset from the vehicle's centreline for adult and 6YO-child pedestrians. It is observed that no HIC values were produced for the adult pedestrian at impact velocities between 5 and 48km/h as a result of no head-vehicle interactions being produced, see Figure A-5. No child pedestrian head contacts occurred until 15km/h. In addition, HIC values increase noticeably with impact velocity and exceeded the threshold, $HIC_{15}=700$ at 15km/h, see Figure B-5.

Figures A-9, A-10 and B-9 to B-11 show that the head injury risk produced in the rear impact position for adult and child pedestrians, respectively, is higher than that produced in the front impact position. However, head injury risk, between moderate AIS2+ and fatal AIS6+ for the child is in most cases higher than those in the adult, see Tables C-4 to C-6.

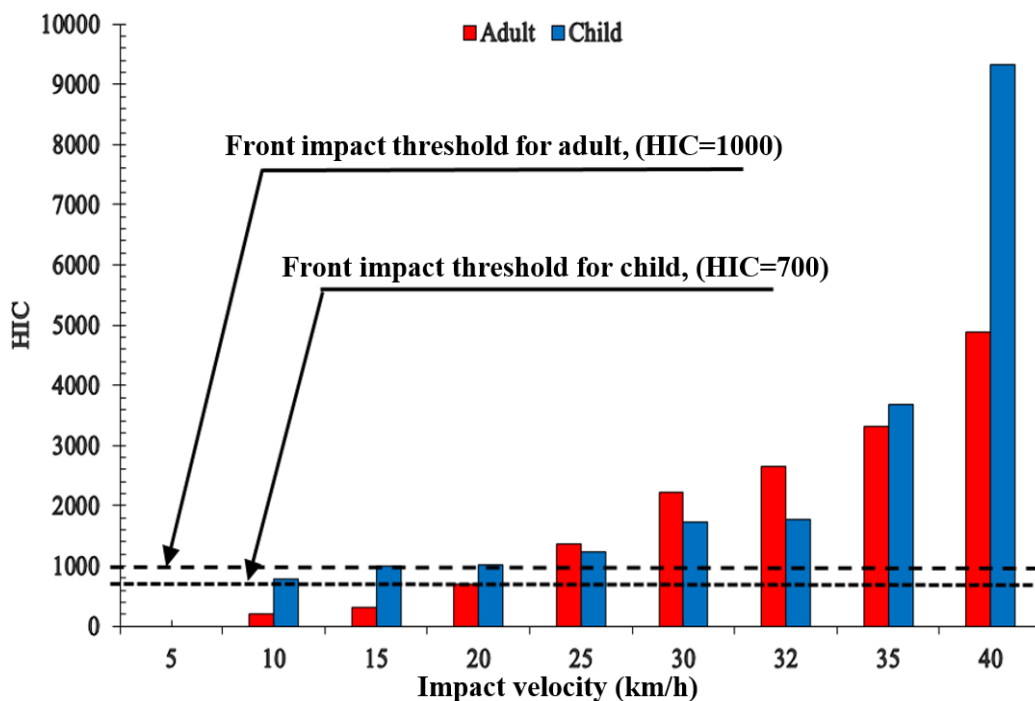


Figure 3- 7. HIC values in the frontal impacts at 42 cm offset from the vehicle's centreline for adult and 6YO-child pedestrians.

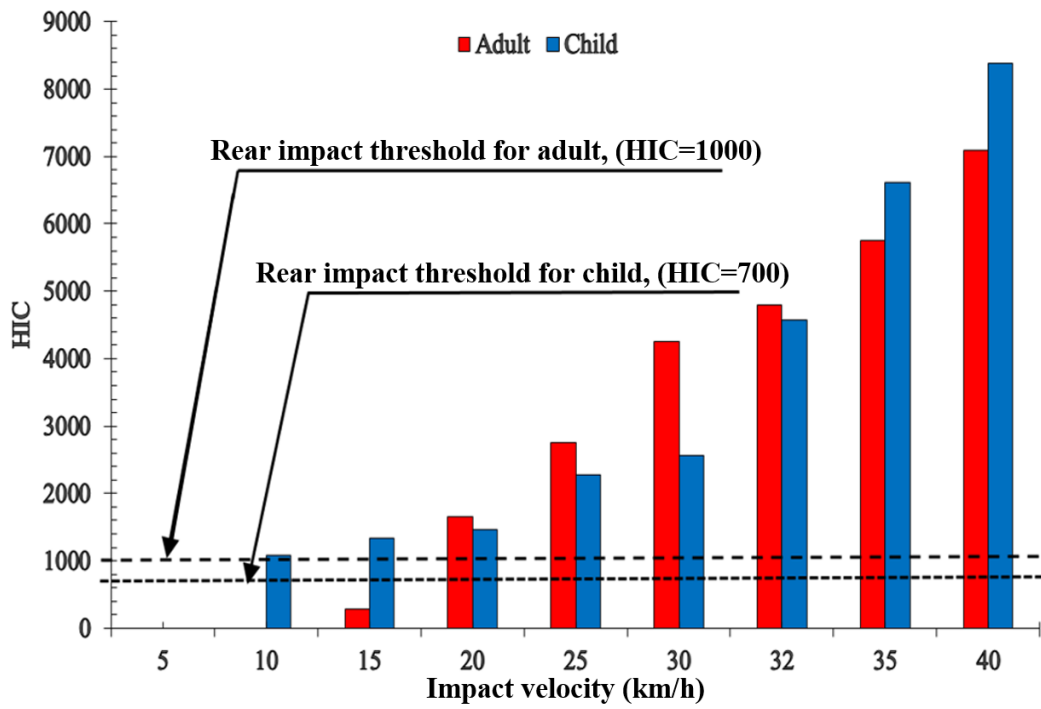


Figure 3- 8. HIC values in the rear impacts at 42 cm offset from the vehicle’s centreline for adult and 6YO-child pedestrians.

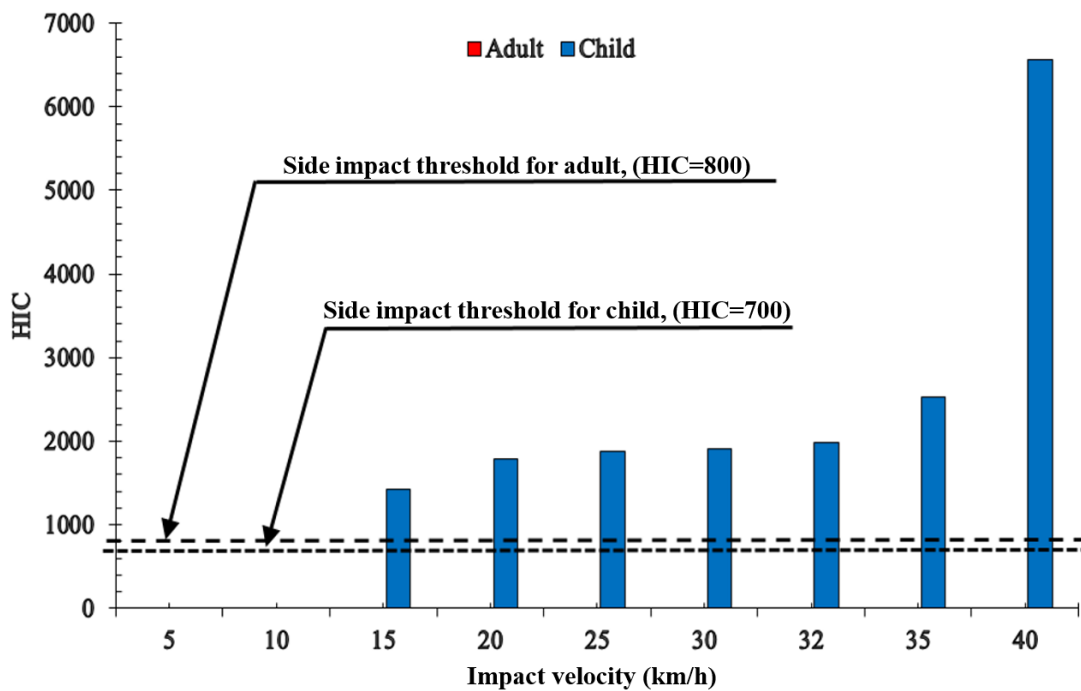


Figure 3- 9. HIC values in the side impacts at 42 cm offset from the vehicle’s centreline for adult and 6YO-child pedestrians.

3.2.5 Upper neck injury criteria and injury risk level during primary impacts

Although, there is no upper neck injury assessment for 6YO-child in the rear impacts. Upper neck injury for adult and child pedestrians during the front impacts was assessed based on N_{ij} criterion. While, N_{km} criterion only was used to examine upper neck injury for adult pedestrian in the rear impacts. In addition, upper neck injury risk level was investigated using the AIS at two-vehicle contact regions, centerline of the vehicle and 42cm offset from the vehicle centreline for both adult and child pedestrians.

3.2.5.1 Upper neck injury criteria and risk level during frontal primary impacts at the vehicle's centreline

The neck injury risk for both adult and child is represented by the Neck Injury Criteria N_{ij} for frontal impacts. In addition, upper neck load cases varied with pedestrian size, impact velocity and vehicle contact regions. Compression-extension (N_{ce}) was the maximum load case for the adult pedestrian at 5 and 10km/h. While, it was tension-extension (N_{te}) at 15 to 40km/h, as shown in Figure A-11.

However, compression-extension (N_{ce}) was the maximum load case for the 6YO-child pedestrian at 5km/h, see Figure B-12. While, it was tension-extension (N_{te}) at impact velocity between 10 to 40km/h. The N_{ij} values were determined by selecting the worst load conditions, from each of the different impact velocities, see Figure B-12.

The maximum load conditions for frontal impacts for the adult and child were chosen to signify the worst-case upper neck load situations and they represent N_{ij} values, as shown in Figure 3- 10. The N_{ij} values for both adult and child pedestrians were observed to increase noticeably with vehicle impact velocity. The N_{ij} values for 6YO-child pedestrians are higher than the adults. Moreover, the N_{ij} values for adults exceeded the threshold, $N_{ij}=1$ at 25 km/h. Despite the fact, the N_{ij} for the child exceeded the threshold, $N_{ij}=1$ at 15km/h, this indicates a significantly higher upper neck injury vulnerability to the child pedestrian than an adult in a front impact, see Figure 3- 10.

Table C-7 shows the upper neck injury risk for adult and 6YO-child pedestrians at the vehicle's centreline during frontal impacts. It can be seen from this table that the upper neck injury risk between moderate AIS2+ and critical AIS5+ in the frontal impacts for the child is higher than for the adult at impact velocities between 5 and 40km/h.

For rear impacts, the N_{km} values were only identified for the adult pedestrian by selecting the worst-case load condition during each of the different impact velocities. The results show that flexion-anterior (N_{fa}) was the worst-case at 5 km/h and extension-posterior (N_{ep}) at 10 km/h. Meanwhile, at 15 km/h, 20 km/h and 25 km/h, the flexion-posterior (N_{fp}) load case was the maximum peak between all of the upper neck load conditions and the flexion-anterior (N_{fa}) value was selected at 30 km/h as the worst-case. Extension-anterior (N_{ea}) was the worst upper neck load case at 32 km/h and extension-posterior N_{ep} was the maximum load between 35 and 48 km/h, see Figure A-12.

The maximum load conditions for the front and rear impacts (shown in Figures A-11 and A-12) were selected to represent the worst-case upper neck load situations of both N_{ij} and N_{km} , see Figure A-13. In addition, N_{km} exceeded the rear impact threshold, $N_{km}=1$ at 10 km/h, which indicates a significantly greater upper neck injury vulnerability to rear impacts. In addition, the upper neck injury risk produced in the rear impacts was greater than that produced in the frontal impacts, see Figures A-14 and A-15.

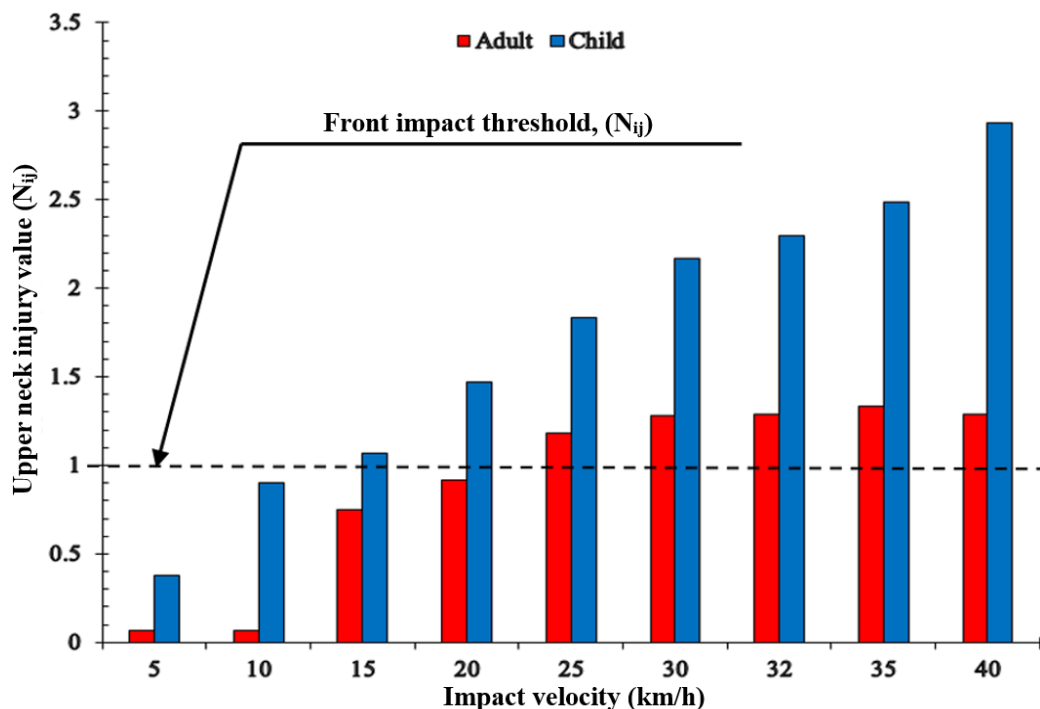


Figure 3- 2. Upper neck injury values for adult and 6YO-child pedestrians impacted at the vehicle's centreline.

3.2.5.2 Upper neck injury criteria and risk level at primary impacts 42cm offset from of the vehicle's centreline

The neck injury risk for both adult and 6YO-child pedestrians is represented by the Neck Injury Criteria N_{ij} for frontal impacts. The upper neck load cases varied with pedestrian size, vehicle contact regions and impact velocity. Compression-extension (N_{ce}) was the worst-case at 5 km/h. Tension-extension (N_{te}) was selected as the worst load case at impact velocities between 10 km/h and 25km/h. When the impact velocity increased from 30 to 40km/h, tension-flexion (N_{tf}) was the maximum load, see Figure A-16. Meanwhile, for the 6YO-child, the tension-flexion (N_{tf}) was the worst-case at impact velocities between 5 and 40km/h, see Figure B-13.

The maximum load conditions at 42cm offset from the vehicle's centreline for the frontal impact for the adult and child pedestrian were chosen to signify the worst-case upper neck load situations and represents N_{ij} values, as shown in Figure 3- 11.

N_{ij} values for both adult and child pedestrians were observed to increase noticeably with vehicle impact velocity. N_{ij} values for 6YO-child pedestrians are higher than the adults. Moreover, the N_{ij} values for the adults exceeded the threshold, $N_{ij}=1$ at 25 km/h. The N_{ij} for the child exceeded the threshold, $N_{ij}=1$ at 15km/h, which indicates that the child pedestrian has a significantly higher upper neck injury vulnerability than an adult in the front impacts, see Figure 3- 11.

In addition, it can be seen that upper neck injury risk between moderate AIS2+ and critical AIS5+ in the frontal impacts for child is higher than adult at impact velocities between 5 and 40km/h, see Table C-8.

For the rear impacts N_{km} values were only identified for the adult pedestrian by selecting the worst-load cases during different impact velocities. Flexion - posterior (N_{fp}) was the worst load at 5 km/h, flexion - anterior (N_{fa}) at 10 km/h, flexion - posterior (N_{fp}) between 15 km/h and 20 km/h and extension - posterior (N_{ep}) at 25 km/h to 48 km/h, see Figure A-17.

The worst load conditions for N_{ij} and N_{km} were chosen from Figures A-16 and A-17, to represent the neck injury value and to evaluate the risk of an upper neck injury. Figure A-18 shows that N_{km} increased significantly with impact velocity. For frontal impacts, N_{ij} exceeded the threshold, $N_{ij}=1$ at 25 km/h; while for rear impacts, N_{km}

exceeded the threshold, $N_{km}=1$ at 15 km/h, see Figure A-18. Therefore, the rear impact position is considered to be the worst-case and has a high risk of severe neck injury, regardless of vehicle contact region (i.e., centreline or offset), see Figures A-19 and A-20.

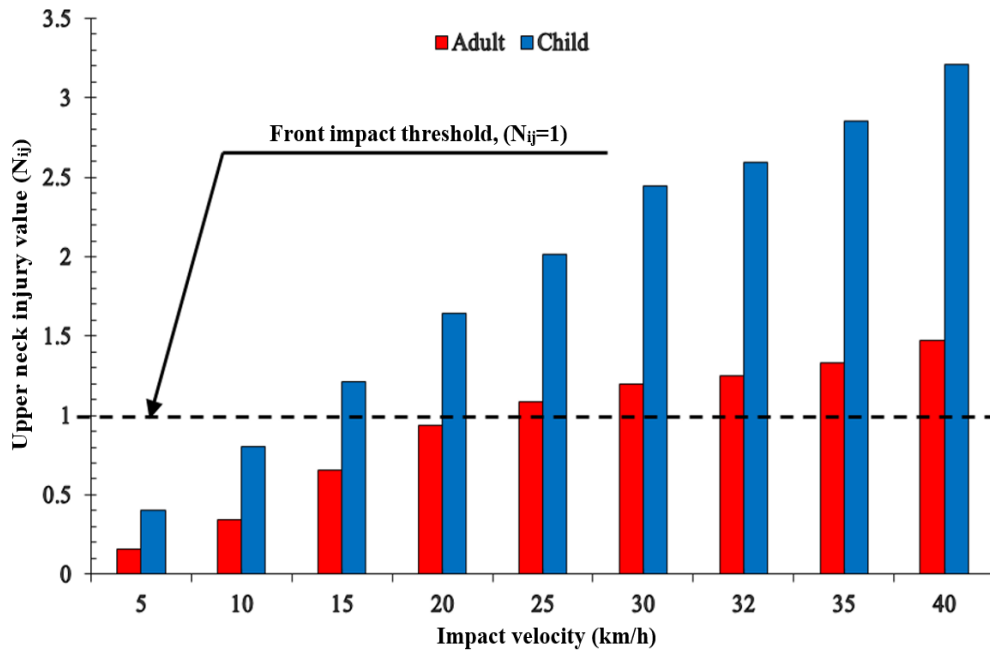


Figure 3- 11. Upper neck injury values for adult and 6YO-child pedestrians impacted at 42cm offset from the vehicle's centreline.

3.2.6 Chest contact locations during primary impacts

In this section, chest contact locations will only report for the adult pedestrian. From impact simulations, it was established that the chest contact locations vary depending on vehicle contact region. The windscreen is the most frequently impacted, stiffest and most injurious vehicle component, as shown in Figure A-21.

3.2.7 Chest contact time duration during primary impacts

Chest contact time is the duration between the first interaction between the pedestrian's chest and the vehicle components.

Chest contact time was investigated at two-vehicle contact regions (vehicle's centreline and 42cm offset from the vehicle's centreline) in the front impact position with various impact velocities. During all of the impact simulations, the chest interaction time was decreased with impact velocity. In the front impact at the vehicle

centreline, no contacts occurred between the chest and the windscreen at 5km/h. In addition, it is higher than that produced at front-offset. Therefore, chest contact time was varied with vehicle contact region, see Figure A-22.

3.2.8 Chest injury criteria and injury risk level during primary impacts

Chest injury was only examined for the adult pedestrian using the Combined Thoracic Index CTI, for frontal impacts. While, chest injury risk was investigated based on AIS coding at two-vehicle contact regions (centreline of the vehicle and offset). All CTI values increased significantly with vehicle impact velocity at both vehicle-contact regions. In addition, CTI values produced in the vehicle centreline were exceeded the threshold, CTI=1 at 35Km/h or greater. While, CTI values produced in the offset exceeded the threshold, CTI=1 at 40km/h, see Figure 3- 12.

The risk of chest injury was assessed by relating CTI values to the AIS at a various risk levels from moderate AIS2+ to critical AIS5+. In addition, it was found that the front-centre impact is higher than that produced at offset, see Figures A-23 and A-24.

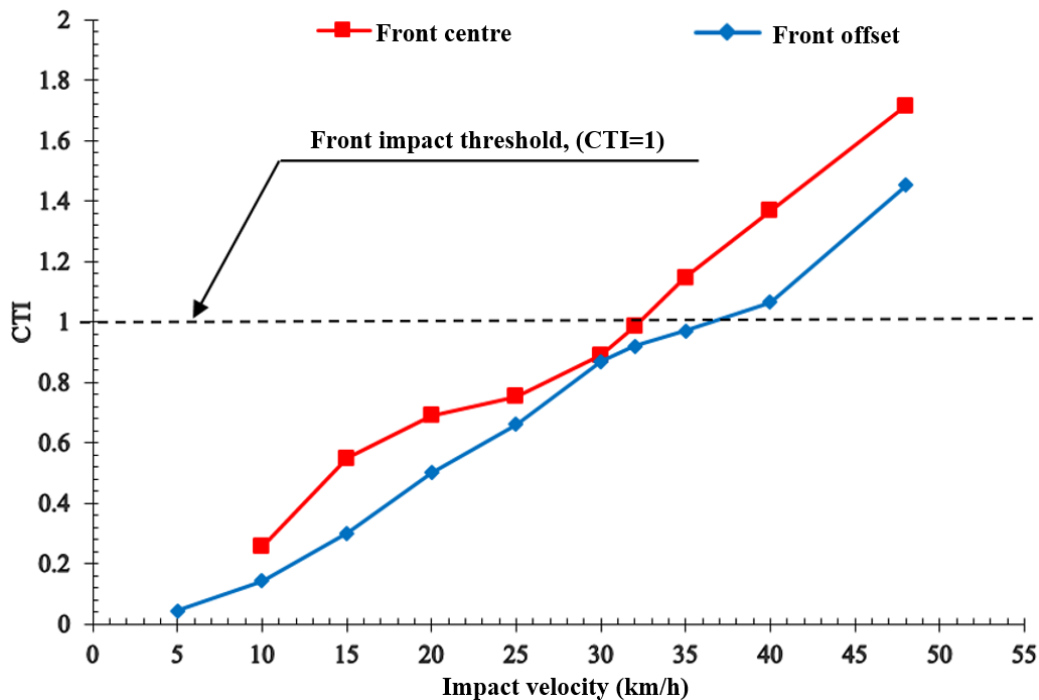


Figure 3- 12. CTI values for adult pedestrian in the frontal impacts at two vehicle contact regions (centreline and 42cm offset).

3.3 Secondary impacts

The majority of this section is focused on the interaction between the adult pedestrian and the ground, resulting from auto rickshaw impacts at two vehicle regions (centreline and 42cm offset from the vehicle centreline) at three different impact positions (front, rear and side) with various selected impact velocities for each position. This section covers the full post kinematic response of the adult pedestrian, throw distance, injury criteria; for the head, upper neck and chest. In addition, injury risk level was classified based on AIS coding.

3.3.1 Kinematic response during secondary impacts

Full post kinematic responses includes the pedestrian-vehicle interaction, flying, falling and sliding responses. The primary impact represent only the interaction between pedestrian body regions and the vehicle components and the secondary impacts, represent the pedestrian, flying, falling and contacting with the ground and sliding subsequent to projection from the impacting vehicle.

3.3.1.1 Kinematic response during secondary impacts at the vehicle's centreline

Figure 3- 13 shows the full kinematic response for the adult pedestrian impacted at the vehicle centerline at front, rear and side impact orientations, including primary and secondary impacts at 30km/h.

During the primary impacts, the first frontal impact occurred between the pedestrian's knees and the front headlamp and the final impact was between the head and the upper windscreen and upper section of the windscreen frame, which both occurred at 50ms. The flying phase started when both feet left the ground at 105ms and moved in a rearward path with high momentum and a simple rotation towards the vehicle's left-hand side. In addition, rotational movement was produced during a right sided impact with the ground resulting in a face-to-face ground contact and an almost 180 degree relative leg rotation.

Throughout the rear primary impact scenario, both knees were impacted by the headlamp, followed by the head impacting the upper vehicle windscreen frame at 82ms. When contact was lost, forward motion was produced and no significant rotation was observed. A secondary impact occurred during the falling phase,

producing contact between the left foot and the ground with a noticeable rotation, while the right foot impacted the ground twice. Significant flexion was observed to the left tibia, producing two left knee-ground and right tibia contacts.

Finally, the whole body became unbalanced, rotating forward in the direction of impact, producing a face-to-face ground interaction.

In the side primary impact scenario, the interaction started between the vehicle headlamp and the right knee and both feet completely leaving the ground at 30ms. Only during this scenario was the pedestrian observed to vault over the auto-rickshaw with a significant rotation around the Y-axis, such that the head struck the upper side of the windscreen frame at 100ms. Subsequently a significant rotation to the right-hand side of the vehicle was observed. At 107ms, the pedestrian completely lost contact with the vehicle and a falling phase started at 593ms. The right foot contacted with the ground, which produced ankle rotation. The head impacted at the face with the ground three times, between 652 and 658ms, followed by a significant neck bending between 658 to 695ms. The second head impact was between 697 and 712ms and the third impact was between 720 to 778ms. Then, the right-hand side contacted with the ground and the left leg dropped producing a rotation, which changed the motion to a slide which caused a chest-ground impact.

3.3.1.2 Kinematic response during secondary impacts at 42cm offset from the vehicle's centreline

Figure 3- 14 shows the full kinematic sequence of impacts at a 42cm offset from the vehicle centreline for the front, rear and side pedestrian impact orientations.

The front offset primary impacts produced a significant transfer of momentum between the lower torso and the frontal offset vehicle edge. The head impacted the windscreen at 24ms and the left foot left the ground at 44ms before the pedestrian lost contact with the vehicle at 55ms.

Both feet totally left the ground and a flying phase began at 60ms. Finally, the pedestrian rotated and the left femur contacted with the frontal lower sheet plate and the right-hand side of the vehicle before falling to the ground. The left foot contacted with the ground at 315ms and the right foot at 365ms. No head-ground contact

occurred due to the pedestrian falling on their lower torso. The tibia and right femur collided with the legs at angle of almost 180 degrees.

During the rear-offset primary impact, contact occurred between the lower torso and the vehicle front leading edge. The head simultaneously impacted with the upper side corner of the windscreen and windscreen frame at 60ms. Both feet left the ground at 85ms for a period of almost 75ms. The secondary impact occurred at 160ms and impact occurred between the right foot and the ground for a period of 25ms and the left foot impacting at 210ms for a period of 12ms. Foot contact was lost at the right foot at 222ms and the left foot between 312 and 485ms. A noticeable flexion was observed in both left and right legs, producing left knee contact at 370ms. Body rotation was produced and the left hand and arm impacted the ground for nearly 27ms. The left side of the torso contacted the ground at almost 575ms. Head-ground-contact occurred at the face at 580ms and the whole body was observed to slide and rotate, until it was face down with the ground at 700ms. Finally, a significant rotational movement was produced after 760ms, when the whole body contacted the ground at its back.

The side-offset primary impacts occurred between the right arm and the right leading vehicle edge. No head impact occurred during this scenario. A flying phase began when the feet left the ground at 50ms and then an impact occurred between the left foot and the ground, for approximately 100ms. The whole pedestrian body lost contact with the vehicle at 145ms, subsequently turning to face the vehicle. No torso or head contact occurred. The pedestrian rotated to the right-hand side of the vehicle before entering a falling phase at 417ms. The left foot interacted the ground, followed by the right foot contact prior to the lower torso impacting the ground and rotating such that the back of the head contacted the ground at 542ms. The whole pedestrian body significantly rotated to its back on the ground at 570ms and continued sliding on the ground until it came to rest. The kinematic response of each position varied with the impact velocity resulting in different body region contacts and ground contact orders, see Figure 3- 15.

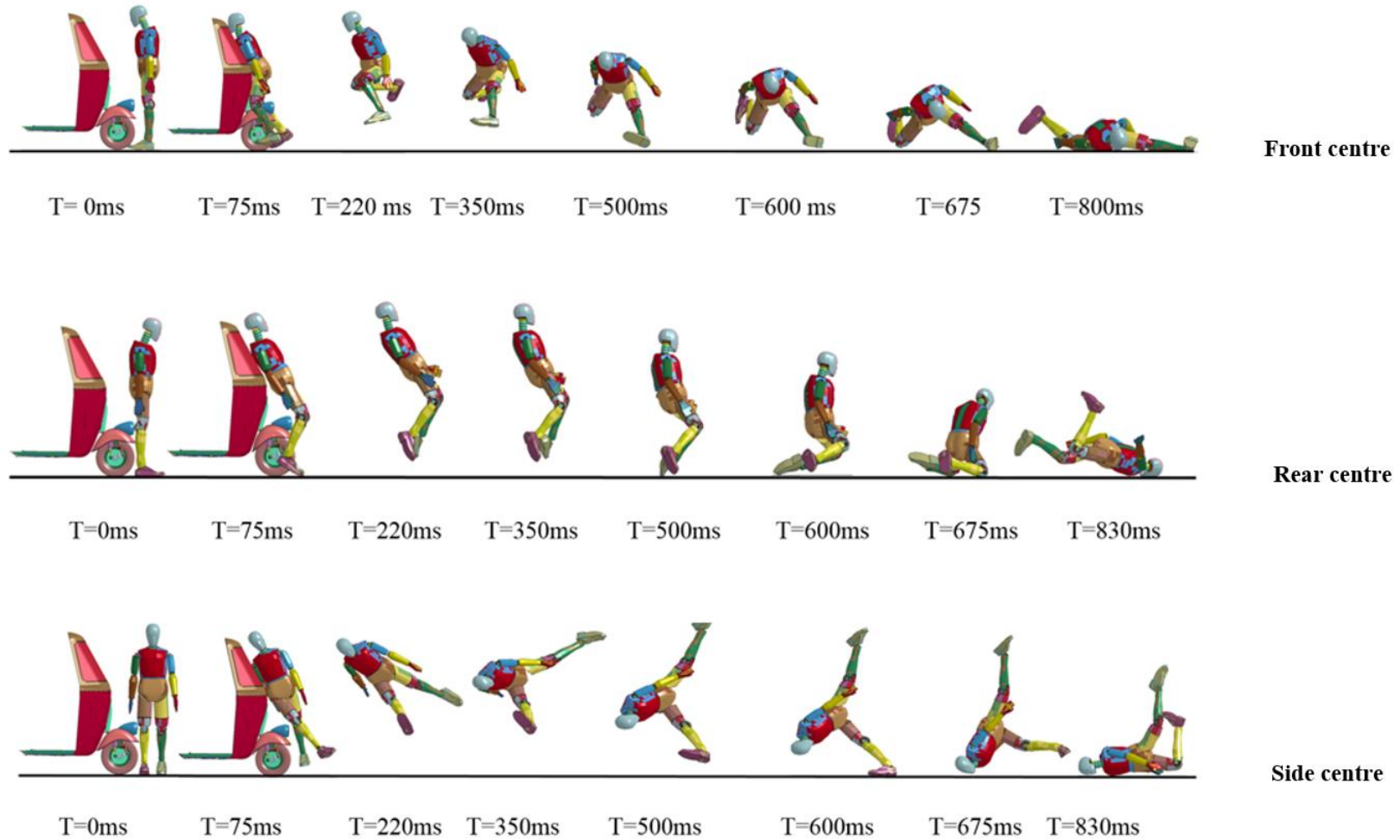


Figure 3- 3. The full kinematic response of adult pedestrian dummy impacted at the vehicle's centreline in different impact positions (front, rear and side) during the primary and secondary impacts.

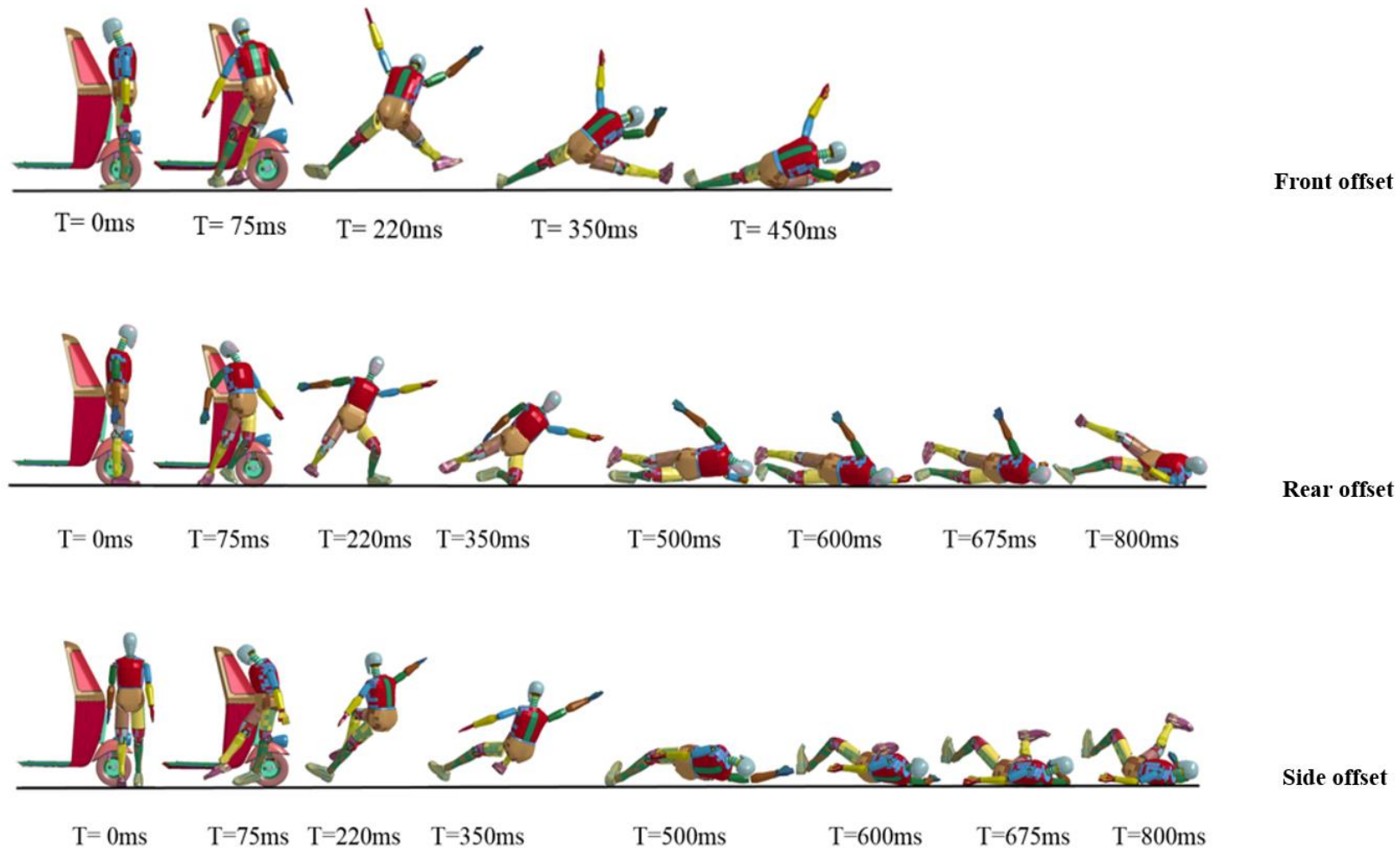


Figure 3- 14. The full kinematic response of adult pedestrian dummy impacted at 42cm offset from the vehicle's centreline in different impact positions (front, rear and side) during the primary and secondary impacts.

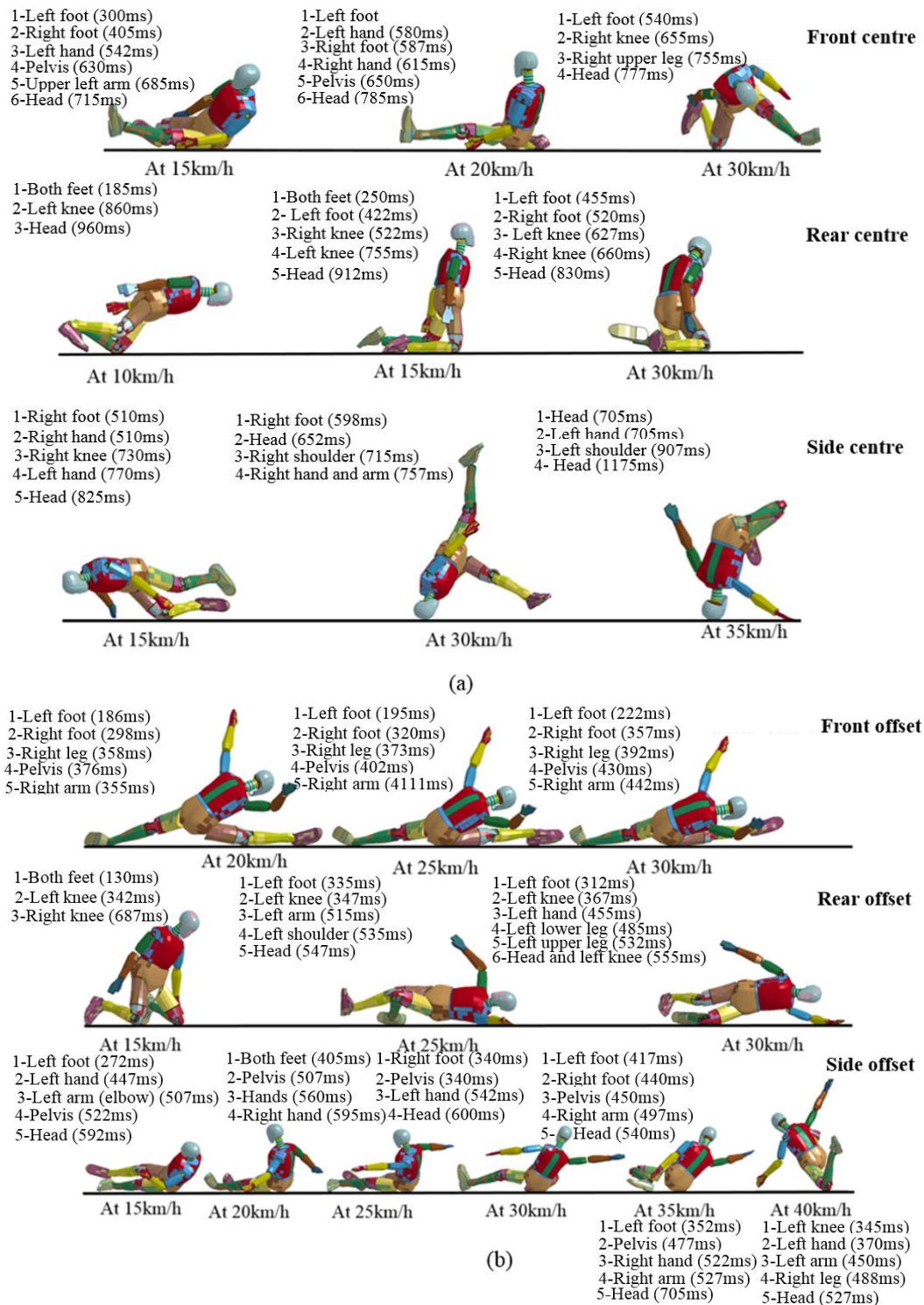


Figure 3- 15. Landing patterns of adult pedestrian dummy impacted at different impact velocities and different vehicle regions (a) pedestrian impacted at the vehicle’s centre in front, rear and side position; (b) pedestrian impacted at a 42cm offset from the vehicle’s centre in front, rear and side position.

3.3.2 Throw distance

Establishing a correlation between the throw distance, during a vehicle-pedestrian road accident and vehicle impact velocity is a valuable tool in road traffic accident investigations. A correlation can be established between the kinematic response of the adult pedestrian ATD, during accident reconstruction of different impact scenarios, including different positions, vehicle velocities and two vehicle contact regions (i.e. centreline and offset). Generally, throw distance increased with the vehicle's impact velocity, as shown in Figures 3-16 and 3-17.

3.3.2.1 Throw distance at the vehicle's centreline

Figure 3- 16 shows the throw distance for adult pedestrian impacted at the vehicle centreline. During all impact positions, throw distance increased significantly with impact velocity. In addition, the throw distances produced during rear impacts were greater than those produced during the frontal and side impacts.

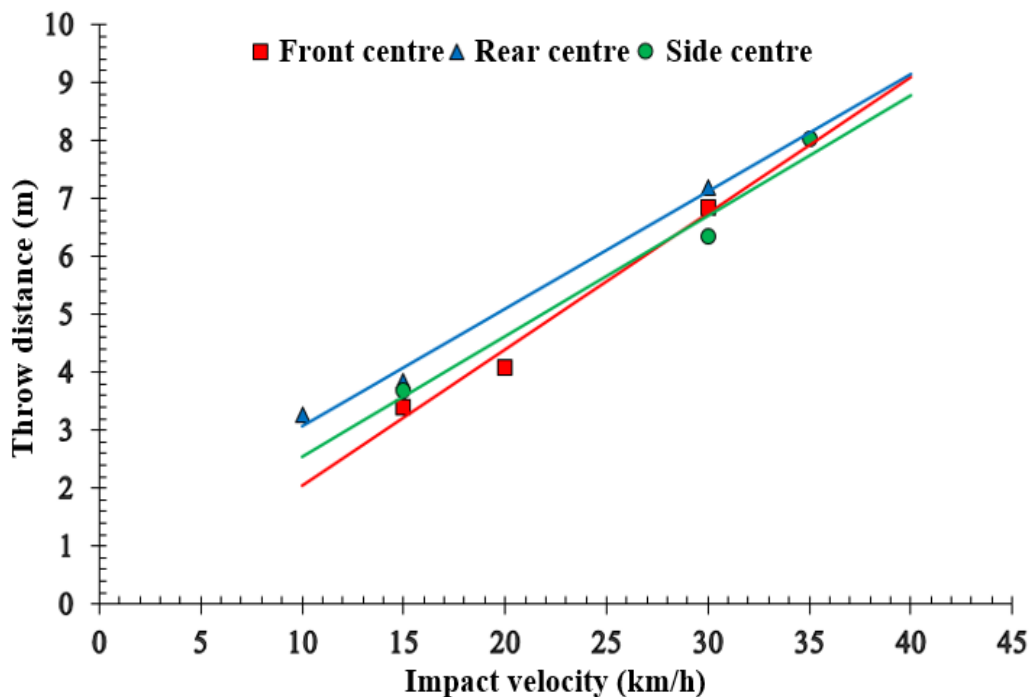


Figure 3- 16. Throw distance and impact velocity at different pedestrian positions, front, rear and side at centreline of the vehicle.

3.3.2.2 Throw distance at 42cm offset from the vehicle's centreline

Figure 3- 17 illustrates the throw distance for an adult pedestrian impacted at 42cm from the vehicle centreline. Throw distance increased with impact velocity. Moreover, the throw distances produced during the rear impacts were greater than those produced during the frontal and side impacts. However, the impact at the vehicle centreline produced a greater throw distance than that provided at the 42cm offset.

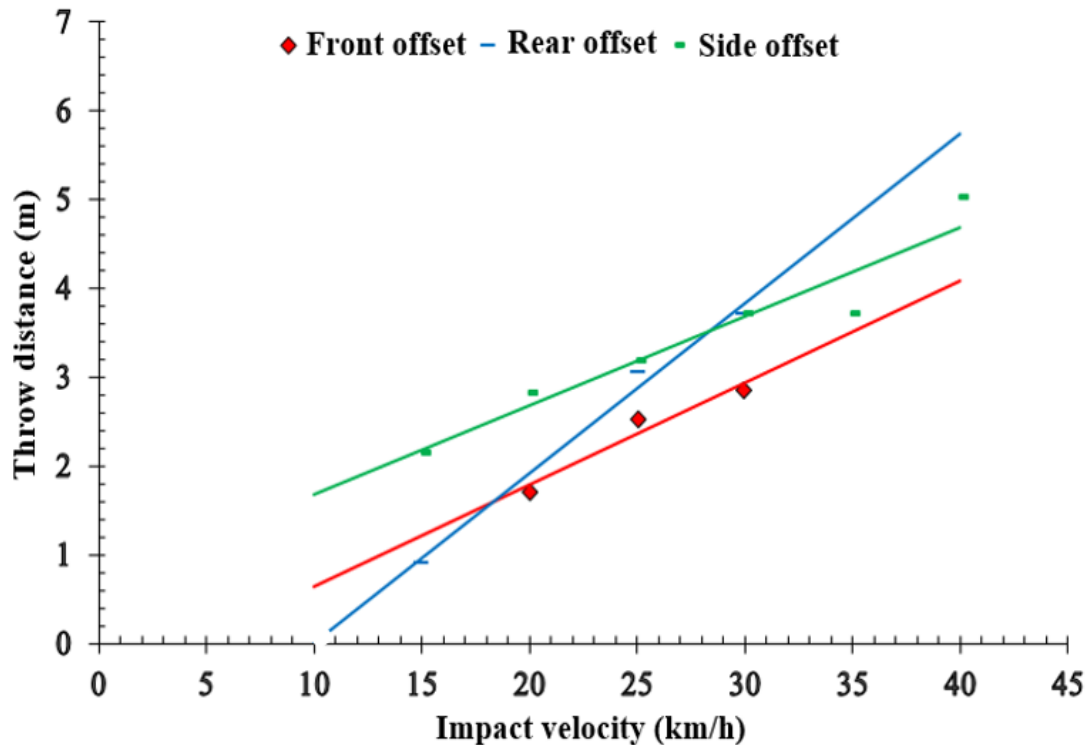


Figure 3- 17. Throw distance and impact velocity at different pedestrian positions, front, rear and side at 42cm offset from the vehicle's centreline.

3.3.3 Comparison of the kinematic response of an adult pedestrian during impact a Real-World accident with simulations

A real-world pedestrian-auto-rickshaw rear-offset accident, captured by CCTV in India, was investigated by simulated impacts at a range of velocities between 15, 25 and 30km/h in an attempt to “best match” the kinematic response of the adult pedestrian against impact velocity. A velocity of 25 km/h was considered the best match, see Figure 3- 18.

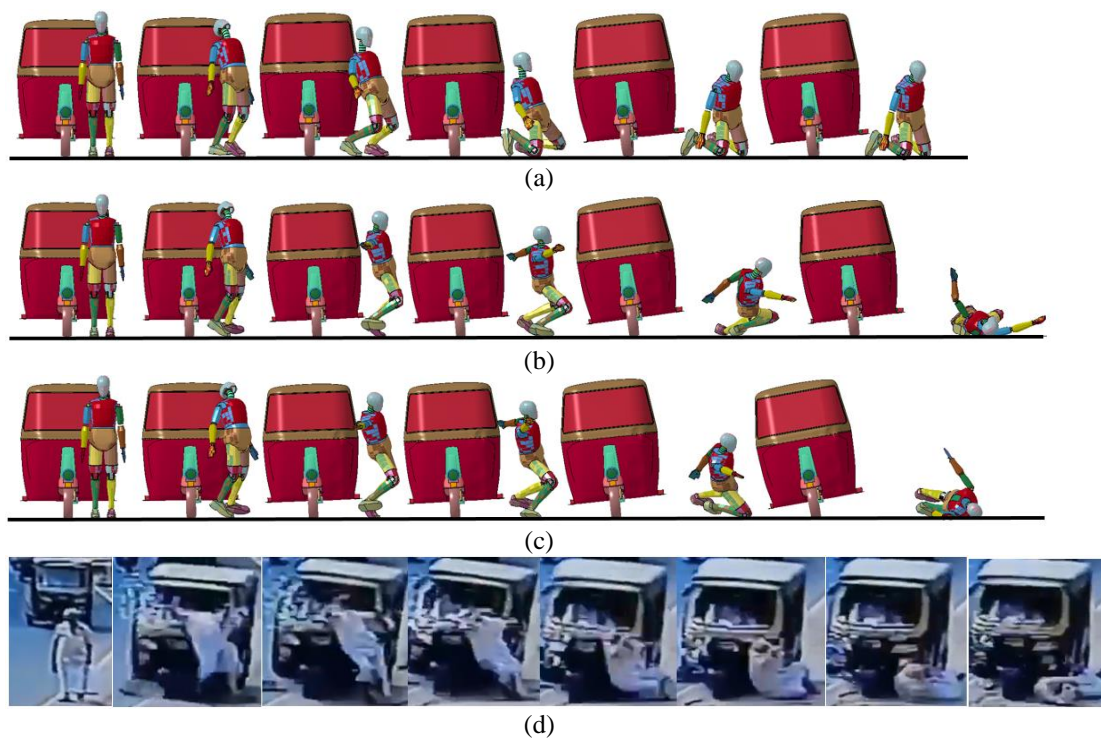


Figure 3- 18. Comparison of post impact kinematic response between a Real-World pedestrian-auto-rickshaw rear impact accident with simulations. Pedestrian offset from vehicle's centreline at (a) 15km/h; (b) 25km/h; (c) 30km/h and (d) CCTV-Real-World accident [292].

The lower torso of the simulated pedestrian was observed to impact with the leading frontal edge of the vehicle. Both feet then left the ground and the head impacted the upper corner of the windscreen and windscreen frame. The body rotated to the side of the vehicle and entered the falling phase until the feet impacted the ground. The lower torso and head impacted with the ground and the whole body then slid and rotated to contact the ground. The legs, lower torso and head sequentially contacted the ground.

3.3.4 Head injury criterion and injury risk level during secondary impacts

Head injuries were evaluated during secondary impacts by using the head injury criterion HIC_{15} values, which were converted to Abbreviated Injury Scale (AIS) values to assess head injury severity risk.

This section describes the investigation of the injury potential at three impact positions (front, rear and side) at selected impact velocities from 10 to 40km/h and two vehicle contact regions, the vehicle centreline and 42cm offset.

3.3.4.1 Head injury criterion and injury risk level during secondary impacts at the vehicle's centreline

During pedestrian-vehicle impacts between the vehicle centreline and pedestrian front, rear and side impact positions, it can be observed that the variation in impact velocity leads to different pedestrian head-ground contact directions, see Figure 3- 19. Impact direction of the head with the ground and the HIC head injury threshold values produced during the secondary impacts were observed.

Generally, HIC values fluctuated with vehicle impact velocity and exceeded the head injury thresholds, $HIC_{15}=1000$ at all impact positions (front, rear and side) at impact velocity between 10 and 35km/h, see Figure D-1.

Head injury risk levels against HIC values for adult pedestrians at the vehicle centreline in front, rear and side impacts are demonstrated in Table D-1. In general, injury risk levels, including moderate AIS2+ to fatal AIS6+, are significant and produced a 100% risk even at the low impact velocity at 10km/h.

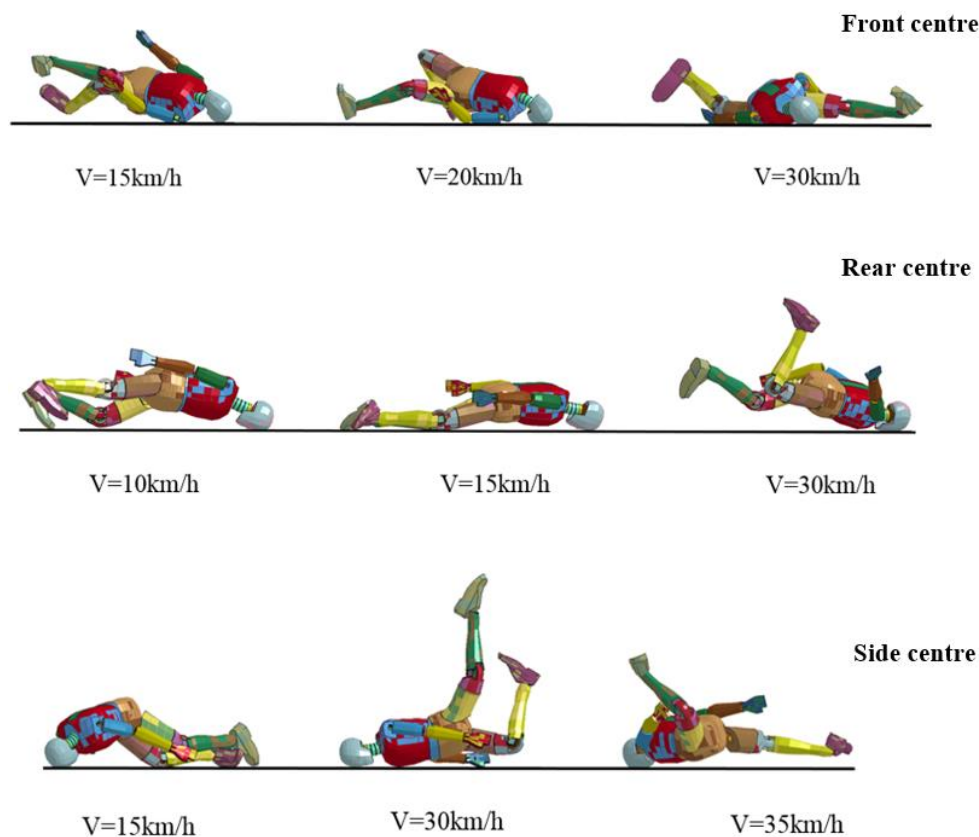


Figure 3- 19. Adult pedestrian head-ground directions at different impact velocities at initial front, rear and side impact positions at the vehicle's centreline.

3.3.4.2 Head injury criterion and injury risk level during secondary impacts at 42cm offset from the vehicle's centreline

For pedestrian-vehicle impacts at 42cm offset from the vehicle centreline at front, rear and side impact positions, it can be seen that impact velocity variation leads to different pedestrian head-ground contact directions, as shown in Figure 3- 20.

Following the direction of the impact between the adult pedestrian head and the ground, all HIC values produced during the secondary impacts were evaluated based on head injury threshold, $HIC_{15}=1000$.

Generally, the HIC values were observed to fluctuate with impact velocity. No HIC values were produced during the front offset impact scenarios as a result of no head contact occurring with the ground. During the rear impacts, no head-ground interaction was observed at 15km/h. The HIC value exceeded the HIC threshold, $HIC_{15}=1000$ at 25km/h, however, the HIC value produced at 30km/h was below the threshold. Side impacts were tested at impact velocities between 15km/h and 40km/h, HIC values only exceeded the threshold, $HIC_{15}=1000$ at 15, 25, 30 and 40km/h, as shown in Figure D-2. Therefore, no dependency was observed between all HIC values produced from the ground contacts and impact velocity.

Head injury risk levels against HIC values for adult pedestrian at 42cm from the vehicle centreline in front, rear and side impacts are illustrated in Table D-2. In addition, no head injury risks were produced during the frontal impacts. Side impact produced significant head injury risk levels at 15km/h, 25km/h, 30km/h and 40km/h, with almost 100% fatal head injury risk.

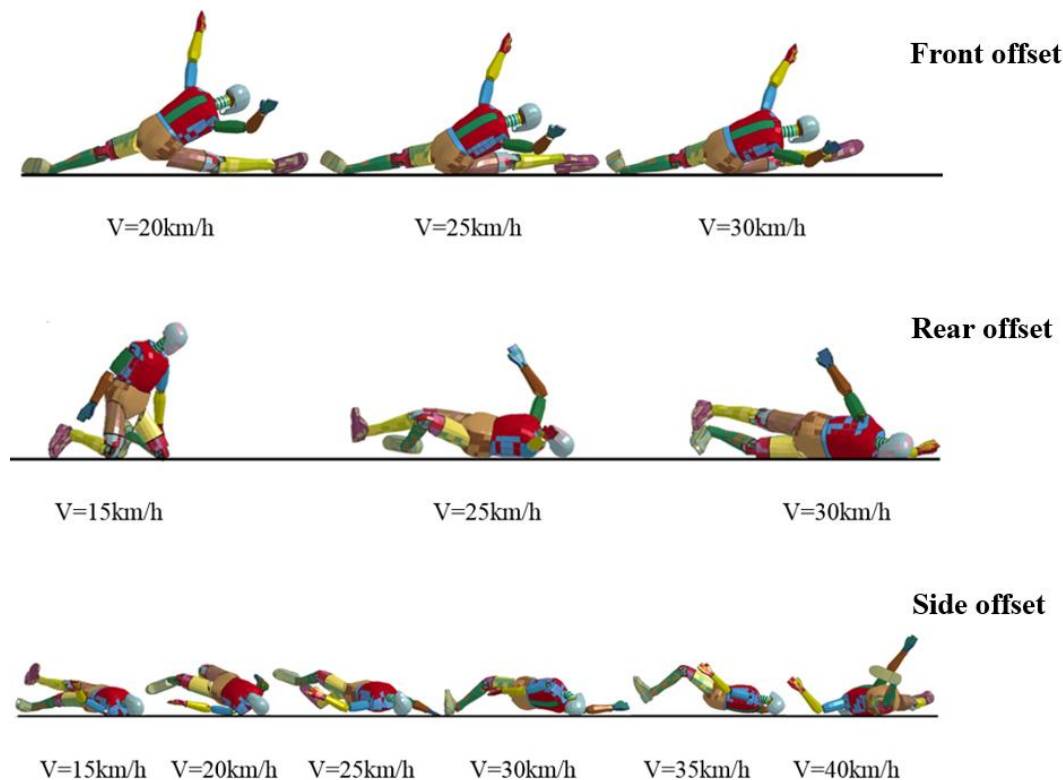


Figure 3- 4. Adult pedestrian head-ground directions at different impact velocities at initial front, rear and side impact positions at 42cm offset from the vehicle's centreline.

3.3.5 Upper neck injury criteria and injury risk level during secondary impacts

The neck injury criterion N_{ij} and N_{km} (for frontal and rear impact exposures, respectively), were applied to the simulation data and subsequently converted into an AIS score, to assess the associated upper neck injury severity risk.

3.3.5.1 Upper neck injury criteria and injury risk level during secondary impacts at the vehicle's centreline

Frontal impacts, following the impact direction with the ground at different impact velocities are shown in Figure 3- 19. Upper neck load cases and injury criterion N_{ij} and N_{km} are varied. Extension-posterior (N_{ep}) was the maximum load case, N_{km} at 15km/h and 20km/h. While, compression-flexion (N_{cf}) was the worst load case produced at 30km/h, which represents the N_{ij} , see Figure D-3.

In addition, N_{km} values produced at 15km/h and 20km/h, exceeded the upper neck injury threshold, $N_{km}=1$. While, the N_{ij} value produced at 30km/h was below the upper neck injury threshold, $N_{ij}=1$, see Table 3- 6.

Rear impacts, following the impact direction with the ground at different impact velocities are shown in Figure 3- 19. Compression-extension (N_{ce}) was the maximum load case, which present the N_{ij} at 10km/h, 15km/h and 30km/h, as illustrated in Figure D-4. Furthermore, N_{ij} values produced at all impact velocities between 10km/h and 30km/h exceeded the upper neck injury threshold, $N_{ij}=1$, see Table 3- 6.

Side impacts, following the impact direction with the ground at different impact velocities shown in Figure 3- 19. Compression-extension (N_{ce}) is the worst load case N_{ij} at 15km/h, 30km/h and 35km/h, demonstrated in Figure D-5. Moreover, N_{ij} values produced at all impact velocities from 15km/h to 35km/h exceeded the upper neck injury threshold, $N_{ij}=1$, see Table 3- 6. Therefore, upper neck load cases, upper neck injury criterion and upper neck injury values N_{ij} and N_{km} varied with impact velocity. In addition, upper neck injury values N_{ij} and N_{km} fluctuated with impact velocity at the vehicle centreline during the secondary impacts.

Upper neck injury risk against N_{ij} and N_{km} values for adult pedestrian at the vehicle centreline in front, rear and side impacts are shown in Figures D-6 to D-8. Generally, during frontal impact, upper injury risk produced by N_{km} values, was higher than that produced by N_{ij} . While, upper neck injury risk, produced during the rear and side impacts are associated with high injury risks.

3.3.5.2 Upper neck injury criteria and injury risk level during secondary impacts at 42cm offset from the vehicle's centreline

During frontal impacts, no head-ground contacts were observed, thus, no head injury values were produced. However, the head tended to move to the side, and might cause neck injury, see Figure 3- 20. Due to modelling limitations, no N_{ij} values and risk levels calculations were possible for primary side impacts. For the rear and the side impacts, upper neck load conditions and injury criterion, N_{ij} and N_{km} are varied.

Rear impacts, following the impact direction with the ground at different impact velocities are shown in Figure 3- 20. Upper neck load cases and injury criterion N_{ij} and N_{km} are varied. Flexion-posterior (N_{fp}) was the maximum load condition at 15km/h. While, extension-anterior (N_{ea}) was the worst load case produced at 25km/h, see Figure D-9. When the impact velocity changed to 30km/h, compression-flexion (N_{cf}) was produced as the worst load case, and represents the N_{ij} value, Figure D-9.

Furthermore, N_{km} values produced at impact velocities between 15km/h and 25km/h exceeded the upper neck injury threshold, $N_{km}=1$, see Table 3- 7. While, N_{ij} value produced at 30km/h was below the injury threshold, $N_{ij}=1$, Table 3- 7.

Side impacts, following the impact direction with the ground at different impact velocities are shown in Figure 3- 20. Upper neck load conditions and injury criterion N_{ij} and N_{km} are varied. Extension-posterior (N_{ep}) was the maximum load case, which represents the N_{km} at impact velocities of 15km/h, 20km/h, 25km/h and 35km/h, see Figure D-10. While, extension-anterior (N_{ea}) was the worst load case at 30km/h, as shown in Figure D-10.

When the impact velocity increased to 40km/h, tension-extension (N_{te}) was produced as the maximum upper neck load and present N_{ij} , as illustrated in Figure D-10. Additionally, all N_{km} values produced at impact velocities between 15km/h and 35km/h exceeded the upper neck injury threshold, $N_{km}=1$. While, N_{ij} values produced at 40km/h were below the threshold, $N_{ij}=1$, as shown in Table 3- 7. Thus, upper neck load cases, upper neck injury criterion and upper neck injury values N_{ij} and N_{km} varied with impact velocity. Moreover, upper neck injury values N_{ij} and N_{km} fluctuated with impact velocity at 42cm from the vehicle centreline in the secondary impacts.

Upper neck injury risks against N_{ij} and N_{km} values for adult pedestrian at 42cm from the vehicle centreline in the rear and side impacts are illustrated in Figure D-11 and D-12. Mostly, upper injury risks produced by N_{km} values were higher than those produced by N_{ij} .

Table 3- 6. Upper neck injury values for adult pedestrian in the secondary impacts at the vehicle's centreline in different impact positions (front, rear and side positions).

Front			
Impact velocity (km/h)	15	20	30
Upper neck injury values	N_{km}	N_{km}	N_{ij}
	1.78	4.49	0.71
Rear			
Impact velocity (km/h)	10	15	30
Upper neck injury values	N_{ij}	N_{ij}	N_{ij}
	1.98	1.77	1.23
Side			
Impact velocity (km/h)	15	30	35
Upper neck injury values	N_{ij}	N_{ij}	N_{ij}
	1.26	3.02	2.47

Table 3- 7. Upper neck injury values for adult pedestrian in the secondary impacts at 42cm offset from the vehicle's centreline in different impact positions (rear and side positions).

Rear						
Impact velocity (km/h)	15	25	30			
Upper neck injury values	N_{km}	N_{km}	N_{ij}			
	1.10	2.02	0.50			
Side						
Impact velocity (km/h)	15	20	25	30	35	40
Upper neck injury values	N_{km}	N_{km}	N_{km}	N_{km}	N_{km}	N_{ij}
	3.48	2.06	4.5	4.08	3.21	0.71

3.3.6 Chest injury criterion and injury risk level during secondary impacts

Chest injury risk as a result of frontal impacts is assessed by using the Combined Thoracic Index (CTI) for adult pedestrians caused by the ground contact when the initial impact occurred at the vehicle centreline and offset in three initial impact positions (front, rear and side).

3.3.6.1 Chest injury criterion and injury risk level during secondary impacts at the vehicle's centreline

From pedestrian-vehicle impacts at the centreline of the vehicle during front, rear and side impact positions, it can be observed that the variation in impact velocity leads to different pedestrian chest-ground contact directions, see Figure 3- 19.

The frontal chest impact direction with the ground and chest injury risk, during the secondary impacts, will assess based on the CTI values from frontal chest impacts with ground.

Frontal impacts, following the impact direction with the ground at different impact velocities are shown in Figure 3- 19. No frontal chest-ground contacts were observed at 15km/h and 20km/h, however, frontal chest-ground interactions occurred at 30km/h and produced CTI values below the chest injury threshold, CTI=1, see Table 3- 8.

Rear impacts, following the ground impact direction at various impact velocities are illustrated in Figure 3- 19. Frontal chest impacts occurred at 10km/h, 15km/h and 30km/h and produced CTI values at all impact velocities. All CTI values fluctuated with impact velocity. In addition, CTI values were below the injury threshold, CTI=1, as shown in Table 3- 8.

Following the ground impact direction at the side impact position, frontal chest impacts occurred at 15km/h, 30km/h and 35km/h. CTI values fluctuated with impact velocity, furthermore, all CTI values were below the injury threshold, CTI=1 at all impact velocities, as shown in Table 3- 8.

Therefore, CTI values fluctuated with impact velocity during the secondary impacts. Chest injury risk during the secondary impacts for adult pedestrian at the vehicle centreline is correlated with CTI values, see Figures D-13 to D-15.

3.3.6.2 Chest injury criterion and injury risk level during secondary impacts at 42cm offset from the vehicle's centreline

Pedestrian-vehicle impacts at 42cm from the vehicle centreline at front, rear and side impact positions showed that the variation in impact velocity leads to different pedestrian chest-ground contact directions, see Figure 3- 20. Frontal chest impact direction with the ground and chest injury during secondary impacts will be assessed, based on the CTI when frontal chest impacts with ground.

For the front impacts, no chest-ground contact occurred at any of the impact velocities of 20km/h, 25km/h and 30km/h.

During the rear impacts, following the ground impact direction, no chest-ground interactions were observed at 15km/h and 25km/h, see Figure 3- 20. While, frontal chest-ground impacts occurred at 30km/h and produced CTI value below the chest injury threshold, $CTI=1$, as shown in see Figure 3- 20 and Table 3- 9.

For the side impacts, following the ground impact direction, no chest-ground contacts occurred at 15km/h, 20km/h, 25km/h, 30km/h and 35km/h, see Figure 3- 20.

While, impact at 40km/h produced CTI values below the injury threshold, $CTI=1$, see Figure 3- 20 and Table 3- 9.

Chest injury risk during the secondary impacts for adult pedestrian, at 42cm from the vehicle centerline, is associated with CTI values, see Figures D-16 and D-17.

Table 3- 8. Chest injury values for adult pedestrian in the secondary impacts at the vehicle’s centreline in different impact positions (front, rear and side positions).

Front			
Impact velocity (km/h)	15	20	30
Chest injury values	CTI	CTI	CTI
	-	-	0.70
Rear			
Impact velocity (km/h)	10	15	30
Chest injury values	CTI	CTI	CTI
	0.46	0.74	0.41
Side			
Impact velocity (km/h)	15	30	35
Chest injury values	CTI	CTI	CTI
	0.46	0.57	0.25

Table 3- 9. Chest injury values for adult pedestrian in the secondary impacts at 42cm offset from the vehicle’s centreline in different impact positions (front, rear and side positions).

Front						
Impact velocity (km/h)	20	25	30			
Chest injury values	CTI	CTI	CTI			
	-	-	-			
Rear						
Impact velocity (km/h)	15	25	30			
Chest injury values	CTI	CTI	CTI			
	-	-	0.18			
Side						
Impact velocity (km/h)	15	20	25	30	35	40
Chest injury values	CTI	CTI	CTI	CTI	CTI	CTI
	-	-	-	-	-	0.18

3.4 The sensitivity of the model contact parameters.

The coefficient of friction has a significant influence on the pedestrian-vehicle impact simulations in terms of the kinematic response and injury risk. The original simulations of the current study used two friction coefficients; 0.65, for the contact between the pedestrian dummy and the vehicle and 0.7 for the interaction between the pedestrian dummy feet and the ground and the vehicle tyre and the ground. This section explains the sensitivity associated with variation in the frictional coefficients on the kinematic response and head injury risk during primary and secondary impacts.

3.4.1 Primary impacts

Rear offset impacts scenario were analysed because they produced the most injurious primary impact scenarios.

3.4.1.1 Kinematic response

During all the impact scenarios shown in Figure 3-21, the initial interactions at the offset rear occurred between the lower torso and the front leading edge. The left hand collided the lower vehicle sheet plate and the left arm impacted the frontal leading edge. The left knee interacted with the lower frontal sheet plate and the left tibia impacted the lower sheet plate. The pedestrian was subsequently rotated to the right of the vehicle with no upper torso contacts observed during all the impact scenarios, shown in Figure 3-21. Finally, the pedestrian head contacted with the upper corner of the windscreen and windscreen frame. It was observed that the variation in friction coefficients during primary impacts had no significant influence on the kinematic response.

3.4.1.2 Head injury

Head injury was examined for the rear offset subject to different frictional coefficients, relevant to pedestrian-vehicle and pedestrian feet-ground/vehicle tyre-ground contacts using HIC15 during primary and secondary impacts.

Table 3-10 shows HIC values for adult pedestrian impacted in the rear impact position at 42cm offset from the vehicle centreline at 30km/h during primary impacts. It was observed that all HIC values exceeded the threshold (HIC=1000) during all impact scenarios. Moreover, no significant changes occurred during all impact scenarios.

Table 3-10. HIC values vs friction coefficients during primary impacts

Impact scenarios	Friction coefficient (pedestrian-vehicle)	Friction coefficient (pedestrian shoes-ground)	Friction coefficient (vehicle's tyre-ground))	HIC
Original case	0.65	0.70	0.70	4259
First case	0.30	0.70	0.70	4227
Second case	0.75	0.70	0.70	3918
Third case	0.65	0.30	0.30	4308
Fourth case	0.65	0.75	0.75	3919
Fifth case	0.30	0.75	0.75	4308
Sixth case	0.75	0.30	0.30	4026

3.4.2 Secondary impacts

3.4.2.1 Kinematic response

All rear offset impact scenarios were simulated at 30km/h. During all rear-offset impact scenarios, both feet left the ground at 85ms for a period of almost 75ms. However, the variation in the friction coefficient has a significant influence on the kinematic response during secondary impacts, see Figure 3-21.

3.4.2.1.1 Original case scenario

During the rear-offset original secondary impact, the secondary impact occurred at 160ms and impact occurred between the right foot and the ground for a period of 25ms and the left foot impacting at 210ms for a period of 12ms. Foot contact was lost at the right foot at 222ms and the left foot between 312 and 485ms. A noticeable flexion was observed in both left and right legs, producing left knee contact at 370ms. Body rotation was produced and the left hand and arm impacted the ground for nearly 27ms. The left side of the torso contacted the ground at almost 575ms. Head-ground-contact occurred at the face at 580ms and the whole body was observed to slide and rotate, until it was face down with the ground at 700ms. Finally, a significant rotational movement was produced after 760ms, when the whole body contacted the ground at its back, see Figure 3-21 (a).

3.4.2.1.2 First case scenario

Figure 3-21 (b) shows the rear-offset first secondary impact scenario, the secondary impact occurred at 202ms and impact occurred between the right foot and the ground for a period of 23ms and the left foot impacting at 282ms for a period of 12ms. Then

the pedestrian impacted the ground on his right knee at 332ms for 28ms. In addition, no head-ground interaction was observed.

3.4.2.1.3 Second case scenario

Figure 3-21 (c) shows the rear-offset second secondary impact scenario. The secondary impact occurred at 175ms and impact occurred between the right foot and the ground for a period of 47ms, then again, the right foot comes to contact with the ground at 205ms for a period of 62ms and the left foot impacting at 275ms for a period of 32ms. A noticeable flexion was observed in both left and right legs, producing left knee contact at 360ms. Body rotation was produced and the left hand impacted the ground at 405ms for nearly 25ms. The left side of the torso contacted the ground at almost 570ms. In addition, no head contact was observed.

3.4.2.1.4 Third case scenario

Figure 3-21 (d) shows the rear-offset third secondary impact scenario. This impact scenario produced kinematic response similar to that produced in the original case scenario, see Figure 3-21 (a).

3.4.2.1.5 Fourth case scenario

Figure 3-21 (e) shows the rear-offset fourth secondary impact scenario. This impact scenario produced kinematic response similar to that produced in the original and the third impact case scenarios, see Figure 3-21 (a) and (d).

3.4.2.1.6 Fifth case scenario

Figure 3-21 (f) shows the rear-offset fifth secondary impact scenario. This impact scenario produced kinematic response similar to that produced in the first impact scenario, see Figure 3-21 (b).

3.4.2.1.7 Sixth case scenario

Figure 3-21 (g) shows the rear-offset fifth secondary impact scenario. This impact scenario produced kinematic response similar to that produced in the second impact scenario, see Figure 3-21 (c).

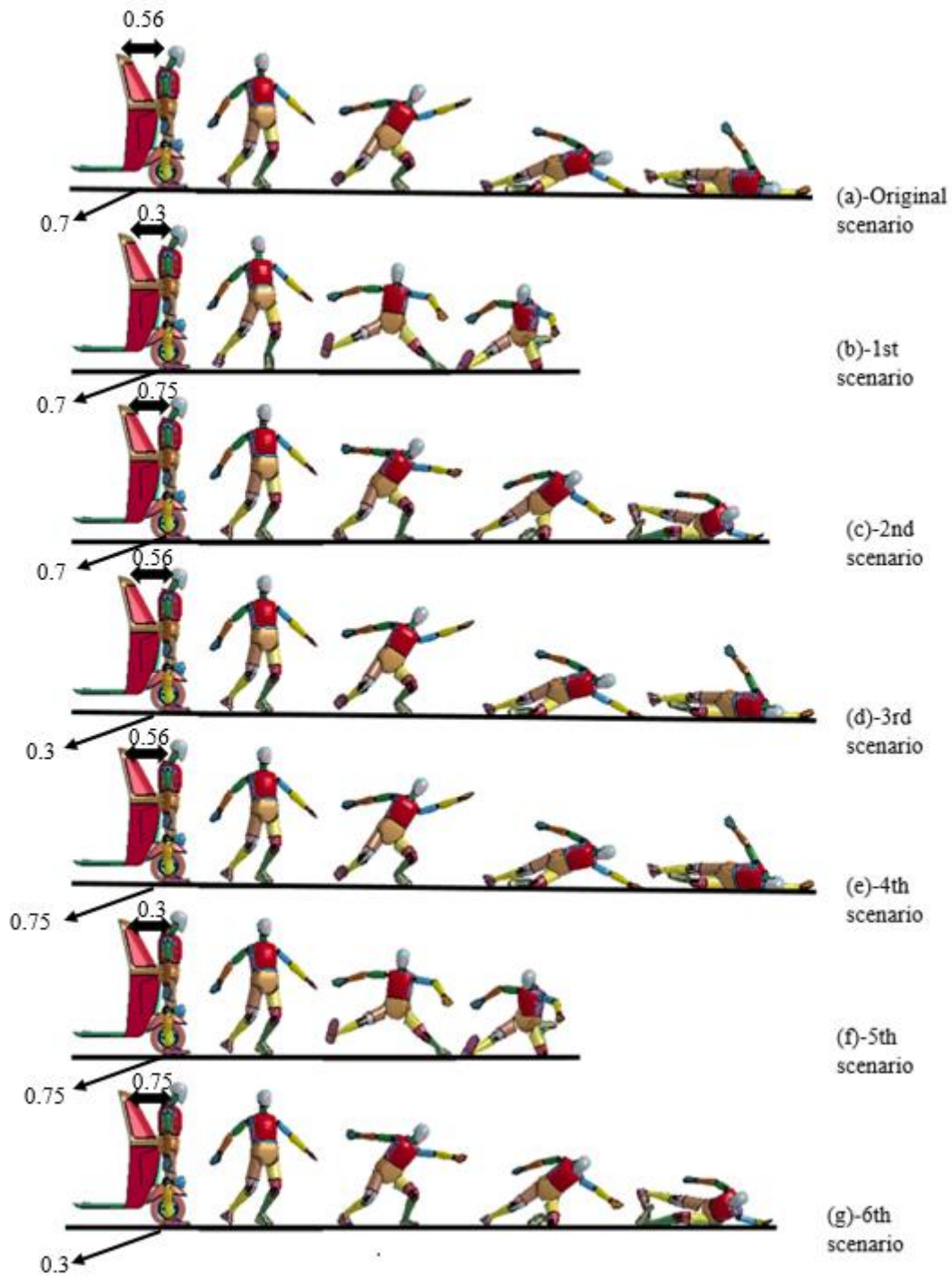


Figure 3-21. The full kinematic response of adult pedestrian dummy impacted in the rear offset scenario at 30km/h including the effect of different friction coefficients; (a) original, (b) first scenario, (c) second scenario, (d) third scenario, (e) fourth scenario, (f) fifth scenario, (g) sixth scenario.

3.4.2.2 Head injury

Table 3-11 shows HIC values for adult pedestrians impacted in the rear impact position at 42cm offset from the vehicle centreline at 30km/h during secondary impacts. It was observed that all HIC values produced in the original, third and fourth impact scenarios did not exceed the threshold (HIC=1000) during all impact scenarios. Moreover, even though the variation in frictional coefficient produced a significant kinematic response variation, there was no significant change in HIC during all impact scenarios when the pedestrian head contacted with the ground, see Table 3-11.

Table 3-11. HIC values Vs friction coefficients during secondary impacts

Impact scenarios	Friction coefficient (pedestrian-vehicle)	Friction coefficient (pedestrian shoes-ground)	Friction coefficient (vehicle's tyre-ground)	HIC
Original case	0.65	0.70	0.70	580
First case	0.30	0.70	0.70	No head contact
Second case	0.75	0.70	0.70	No head contact
Third case	0.65	0.30	0.30	580
Fourth case	0.65	0.75	0.75	580
Fifth case	0.30	0.75	0.75	No head contact
Sixth case	0.75	0.30	0.30	No head contact

3.5 Comparison between primary and secondary impacts for adult pedestrian

This section presents an investigation of head, upper neck and chest injuries and injury risk level for adult pedestrian in the primary and secondary impacts to assess their relative impact risks, considering both vehicle contact regions (centreline and offset) and three different impact positions (front, rear and side).

3.5.1 Head injury and injury risk level during primary and secondary impacts

3.5.1.1 Head injury criterion and injury risk level during primary and secondary impacts at the vehicle's centreline

During frontal primary impacts, HIC values increased significantly with impact velocity and exceeded the threshold $HIC_{15}=1000$ at 30km/h, see Figure 3- 21.

Secondary impact HIC values fluctuated and were often higher than those produced during primary impacts and exceeded the threshold $HIC_{15}=1000$ at all impact velocities, even with low impact velocity at 15 and 20km/h, as shown in Figure 3- 21.

Rear primary impacts, showed a similar trend, producing higher HIC values at increasing impact velocities, exceeding the threshold $HIC_{15}=1000$ at 25km/h, however, no head impact was produced at 10km/h, as shown in Figure 3- 22. Secondary impacts again followed a similar trend, with HIC values fluctuating with impact velocity, although values were significantly higher than that produced during primary impacts, which exceeded the threshold $HIC_{15}=1000$ during all impact velocities, as demonstrated in Figure 3- 22.

Side primary impacts produced no head-vehicle contact at 15km/h, see Figure 3- 23. All HIC values increased with impact velocity at 30 and 35km/h, though did not exceed the threshold $HIC=800$, as shown in Figure 3- 23. Secondary side impacts, followed the impact direction of the head with the ground, HIC values fluctuated and were often higher than those produced during primary impacts. The HIC values also exceeded the head injury thresholds $HIC_{15}=1000$, as illustrated in Figure 3- 23.

Head injury risk for adult pedestrians at the vehicle centreline at front, rear and side impact positions produced during the secondary impacts is higher than primary impacts. In addition, even at the low impact velocity of 10km/h a 100% fatal head injury risk was produced, see Figures E-1 to E-3.

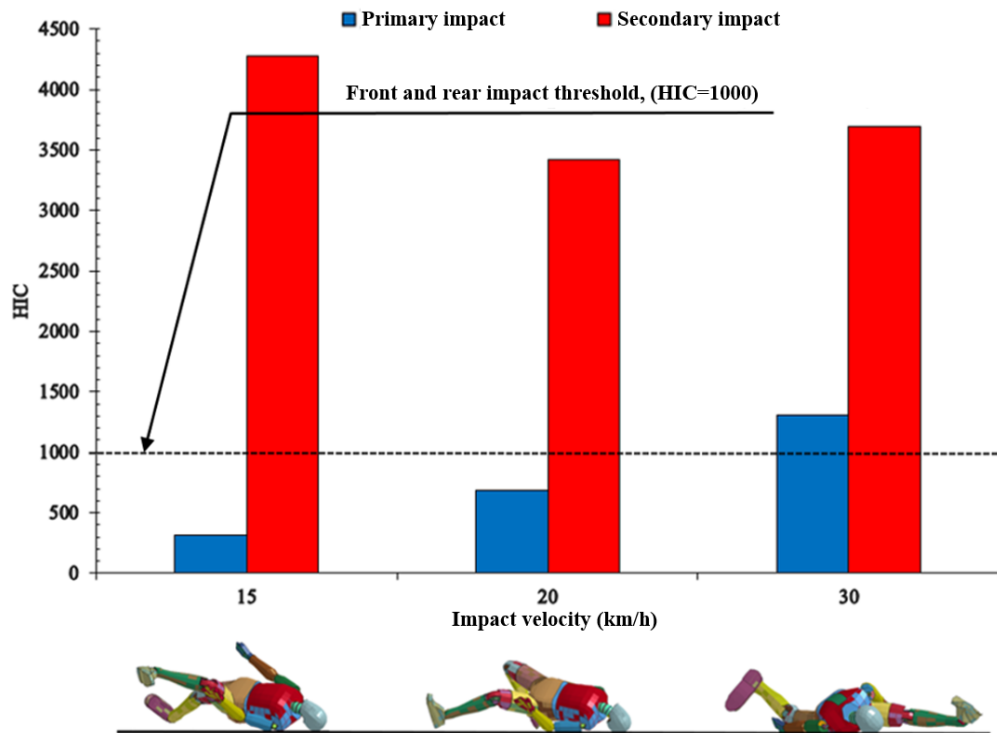


Figure 3- 22. HIC for primary and secondary front impacts at the vehicle's centreline.

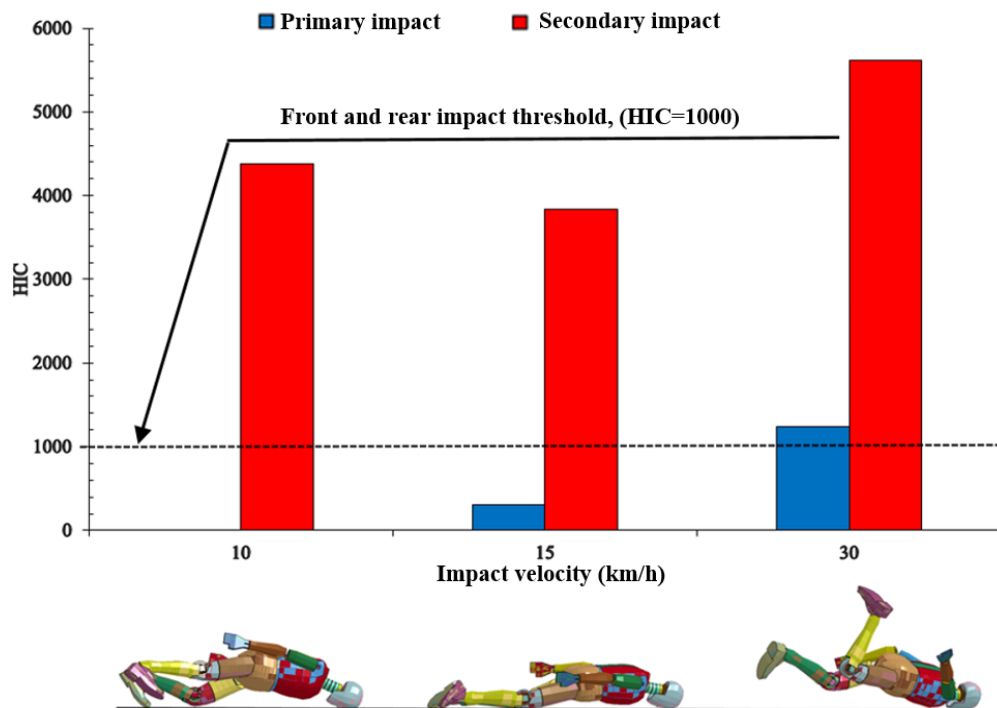


Figure 3- 23. HIC for primary and secondary rear impacts at the vehicle's centreline.

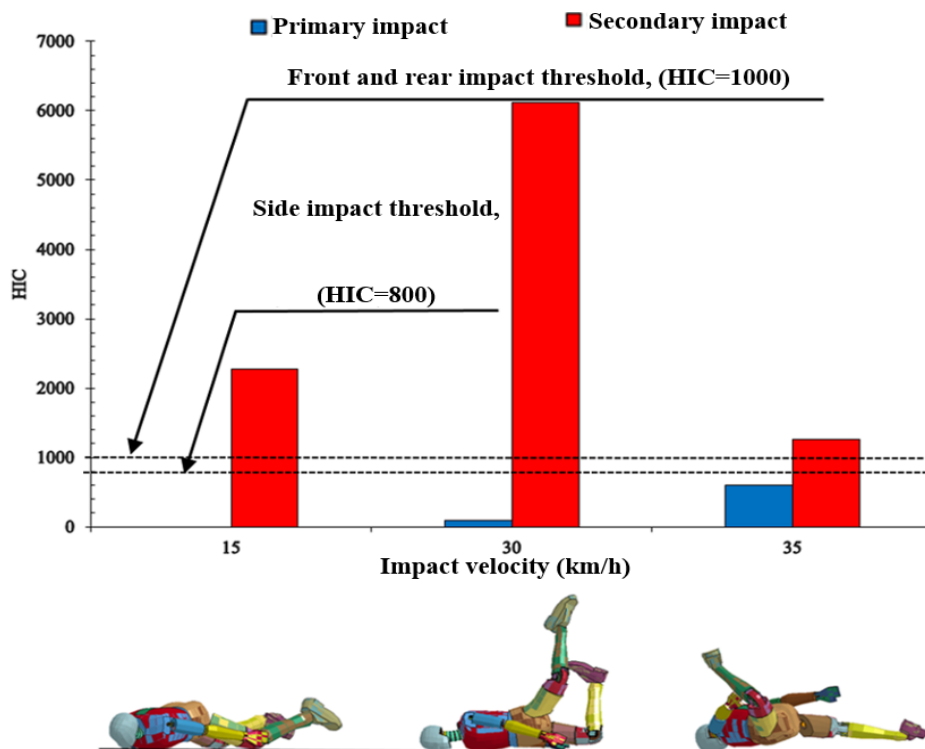


Figure 3- 24. HIC for primary and secondary side impacts at the vehicle's centreline.

3.5.1.2 Head injury criterion and injury risk level during primary and secondary impacts at 42cm offset from the vehicle's centreline

During frontal primary impacts, HIC values increased significantly with increasing impact velocity, exceeding the $HIC_{15}=1000$ threshold at 25km/h, see Figure 3- 24. Secondary impacts produced no head contacts with the ground at all impact velocities, as presented in Figure 3- 24.

For rear primary impact, the HIC values significantly increased with impact velocity and exceeded the threshold HIC_{15} at 20km/h, as shown in Figure 3- 25. HIC values during secondary impacts, fluctuated and were potentially lower than those produced during primary impacts, no head-ground contact was observed at 15km/h, see Figure 3- 34. The HIC value exceeded the HIC threshold at 25km/h, however, the HIC value produced at 30km/h was below the threshold, as demonstrated in Figure 3- 25.

Primary side impacts produced no head-vehicle interactions between 15 and 40km/h and thus, no HIC values were produced, see Figure 3- 26. Secondary impact HIC values fluctuated with impact velocity, only exceeding the HIC_{15} threshold at 15, 25, 30 and 40km/h, see Figure 3- 26.

Head injury risk, for adult pedestrian at 42cm offset from the vehicle centreline at front, rear and side impact positions produced during the secondary impacts is quite high and produced almost 100% fatal head injury risk in most cases, see Figures E-4 to E-6.

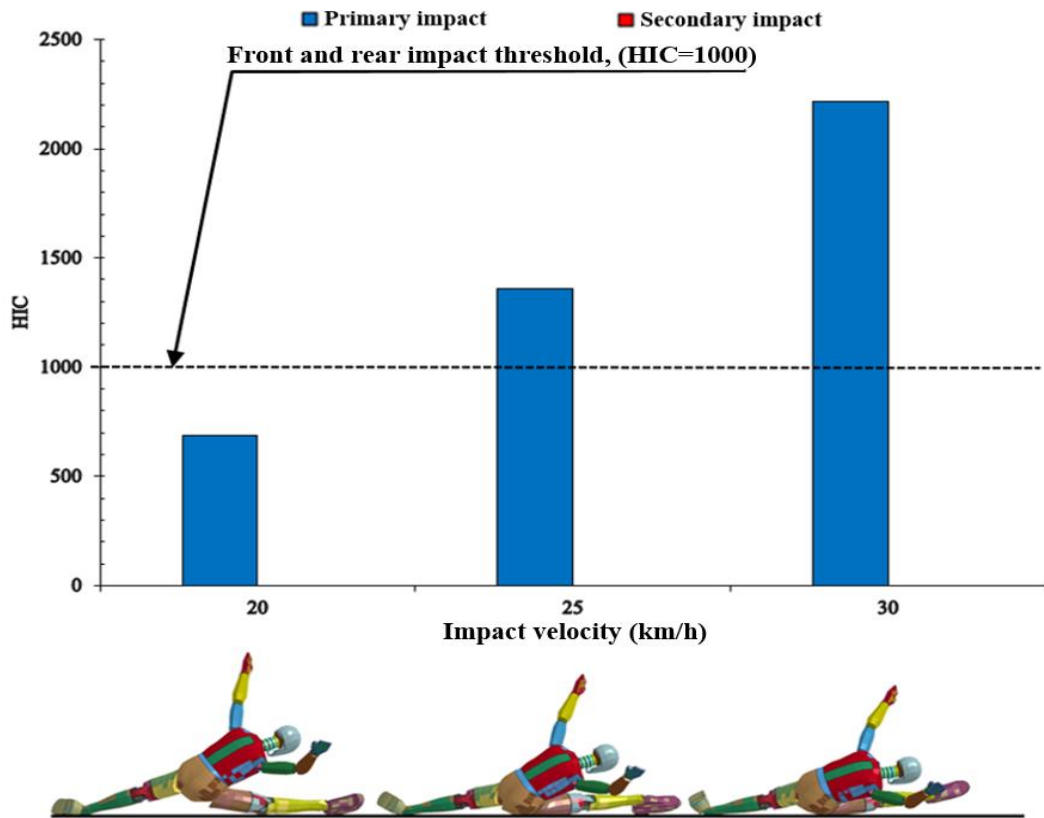


Figure 3- 25. HIC for primary and secondary front impacts at offset 42cm offset from the vehicle's centreline.

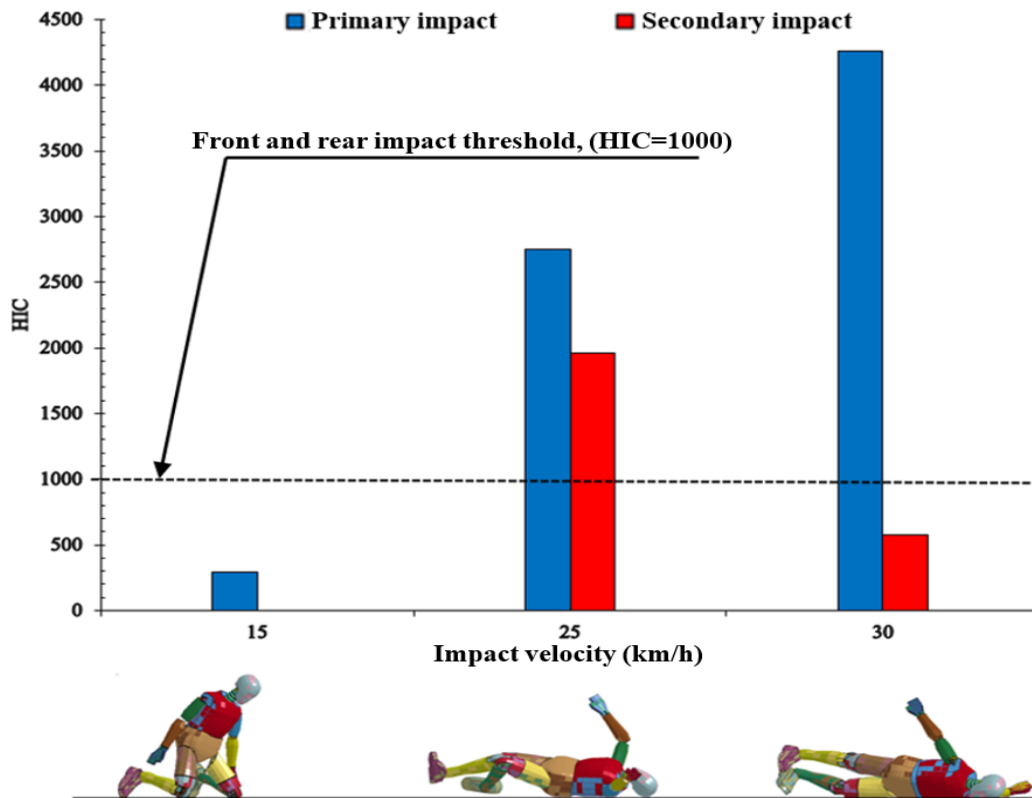


Figure 3- 26. HIC for primary and secondary rear impacts at offset 42cm offset from the vehicle's centreline.

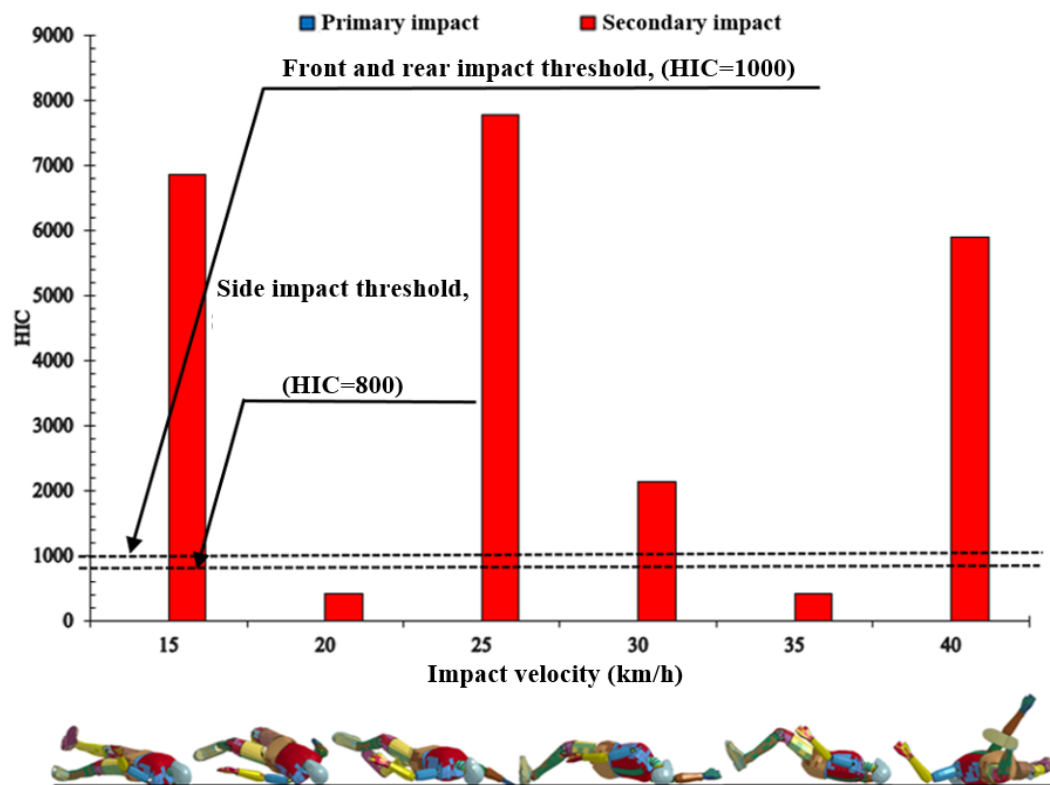


Figure 3- 27. HIC for primary and secondary side impacts at offset 42cm offset from the vehicle's centreline.

3.5.2 Upper neck injury criteria and injury risk level during primary and secondary impacts

3.5.2.1 Upper neck injury criteria and injury risk level during primary and secondary impacts at the vehicle's centreline

Upper neck loads for adult pedestrian impacts at the vehicle centreline at all impact positions are varied during primary and secondary impacts, see Figures E-7 to E-9.

For frontal primary impacts at the vehicle centreline the pedestrian upper neck injury values increased significantly with impact velocity; N_{ij} values exceeded the threshold $N_{ij}=1$ at 30km/h, as illustrated in Figure 3- 27. For secondary impacts, N_{km} values exceeded the threshold $N_{km}=1$ at 15 and 20km/h. Meanwhile, at 30km/h, the N_{ij} value was below the threshold (1), see Figure 3- 27.

Rear primary impacts produced significantly greater upper neck injury values with increasing impact velocity, with N_{km} exceeding the N_{km} threshold at 10km/h, as demonstrated in Figure 3- 28. Secondary impacts produced fluctuating upper neck injury values; N_{ij} values exceeded the threshold at 10km/h and above, see Figure 3- 28.

Due to modelling limitations, no N_{ij} values and risk level calculations were possible for primary side impacts, however, secondary impacts, produced upper neck injury values, which fluctuated with impact velocity. N_{ij} values exceeded the threshold at 15km/h and above, see Figure 3- 29.

Upper neck injury risk for adult pedestrians at the vehicle centreline at front, rear and side impact positions relevant to N_{km} values produced during both primary and secondary impacts are associated with high upper neck injury risk than N_{ij} values, see Figures E-10 to E-12.

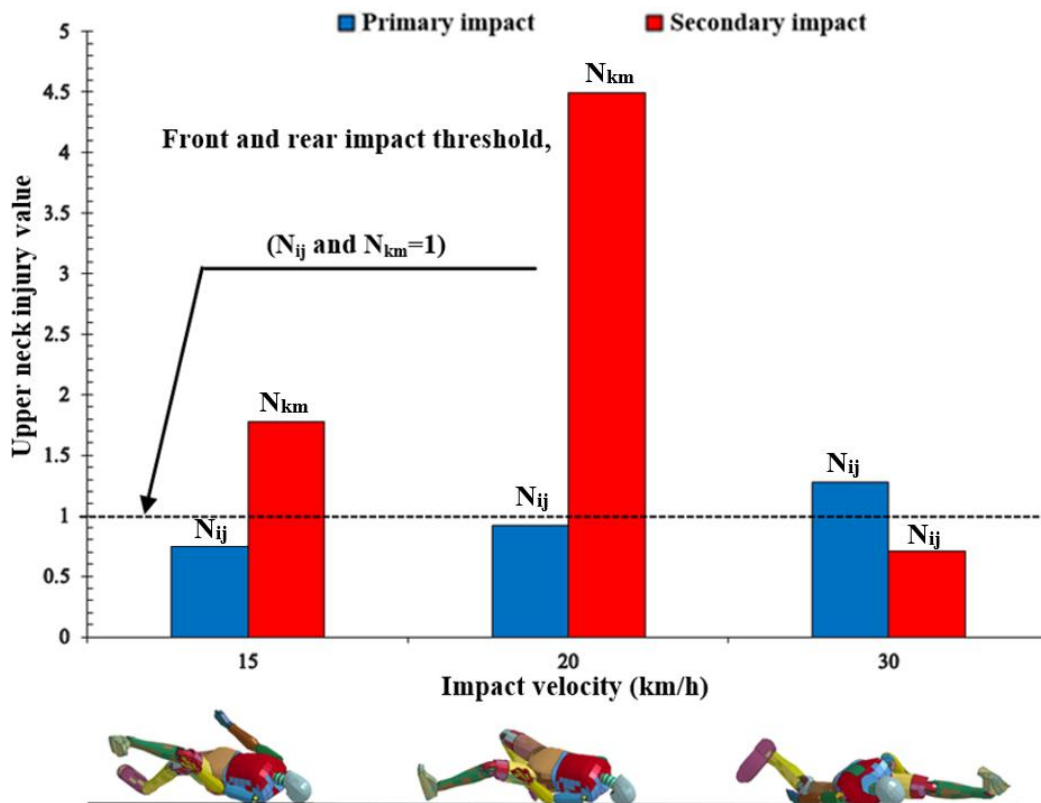


Figure 3- 28. Upper neck injury values for primary and secondary front impacts at the vehicle's centreline.

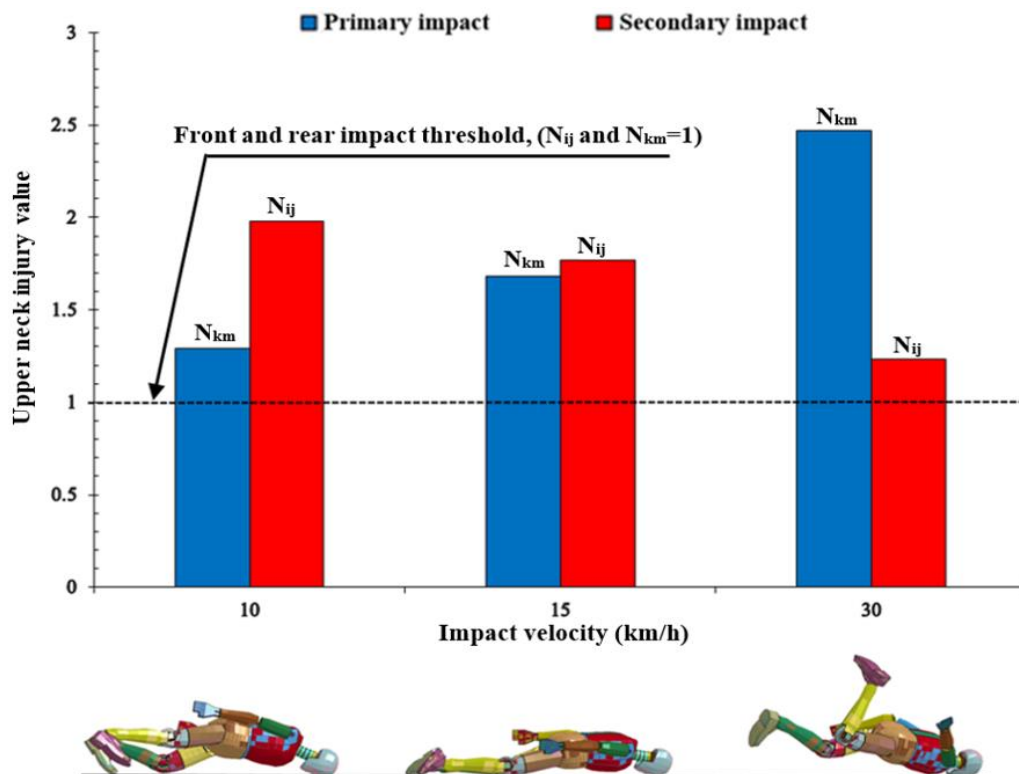


Figure 3- 29. Upper neck injury values for primary and secondary rear impacts at the vehicle's centreline.

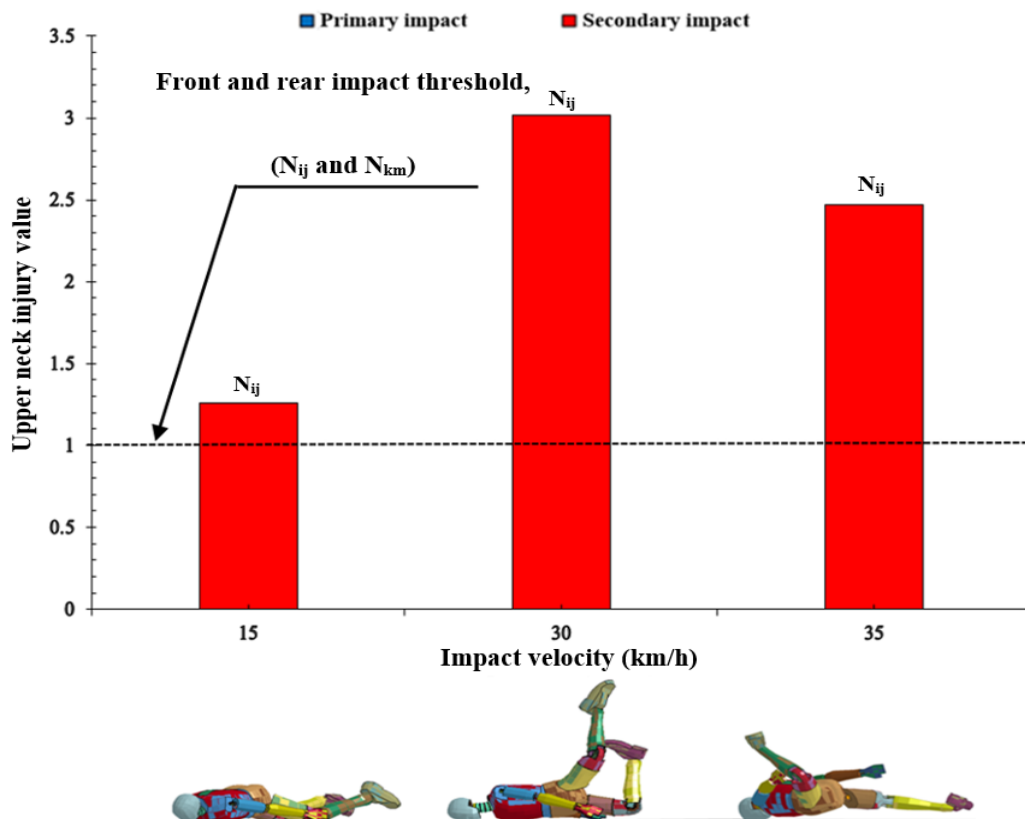


Figure 3- 30. Upper neck injury values for primary and secondary side impacts at the vehicle's centreline.

3.5.2.2 Upper neck injury criteria and injury risk level during primary and secondary impacts at 42cm offset from the vehicle's centreline

Upper neck loads for adult pedestrian impacts at 42cm from the vehicle centreline, in all impact positions are varied during primary and secondary impacts, see Figures E-13 to E-15.

Frontal primary impacts, offset at the vehicle centreline, produced pedestrian upper neck injury values, which increased significantly with impact velocity. N_{ij} values exceeded the threshold at 25km/h and above, see **Error! Reference source not found..** Secondary impacts produced no head contact with the ground and thus, no head or neck injury values N_{ij} or N_{km} were produced in this position.

In addition, head-neck movement tends to move in the side direction, due to side neck injury limitations, no upper neck injury values were calculated in this position in the secondary impacts, as illustrated in **Error! Reference source not found..**

For rear primary impacts, upper neck injury values increased with the vehicle impact velocity; N_{km} values exceeded the threshold at 15km/h and above, as shown in **Error! Reference source not found.** For secondary impacts, N_{km} values exceeded the threshold at 15 and 25km/h. No significant N_{ij} value was produced until 30km/h, though this was below the threshold (1), see **Error! Reference source not found.**

No primary side impacts N_{ij} values were calculated in this study. Secondary impacts produced upper neck injury values, which fluctuated with impact velocity; N_{km} exceeded the threshold between 15 and 35km/h. Again, no significant N_{ij} value was produced until 40km/h, see **Error! Reference source not found.**

Upper neck injury risk for adult pedestrian at 42cm offset from the vehicle centreline in front, rear and side impact positions relevant to N_{km} values produced during both primary and secondary impacts are associated with higher upper neck injury risk than N_{ij} values, see Figures E-16 to E-18.

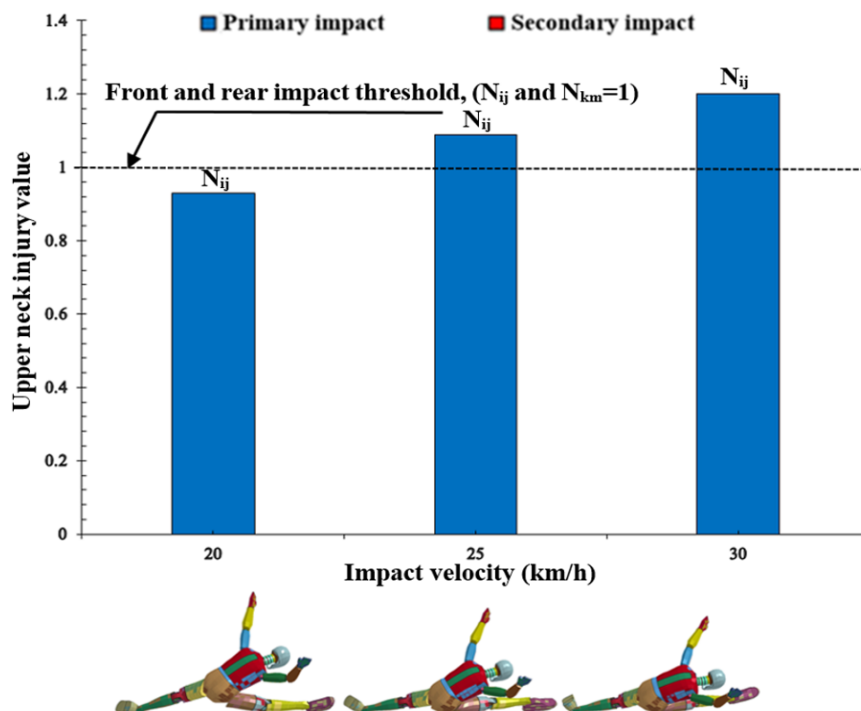


Figure 3- 5. Upper neck injury values for primary and secondary front impacts at 42cm offset from the vehicle's centreline.

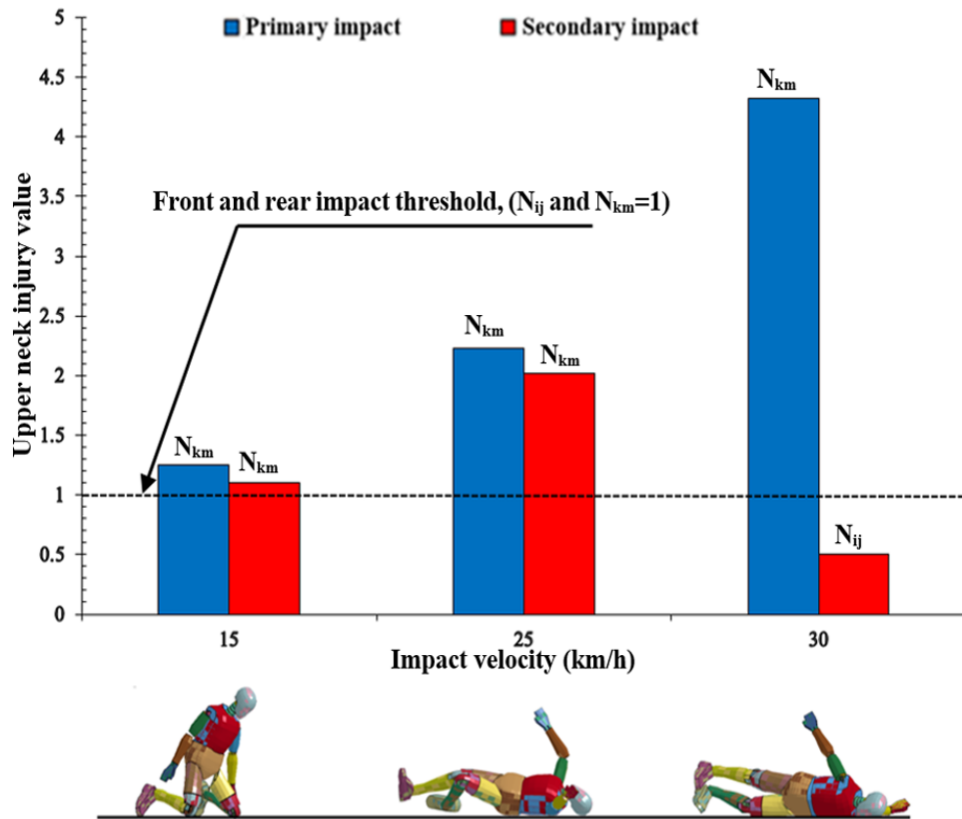


Figure 3- 32. Upper neck injury values for primary and secondary rear impacts at 42cm offset from the vehicle's centreline.

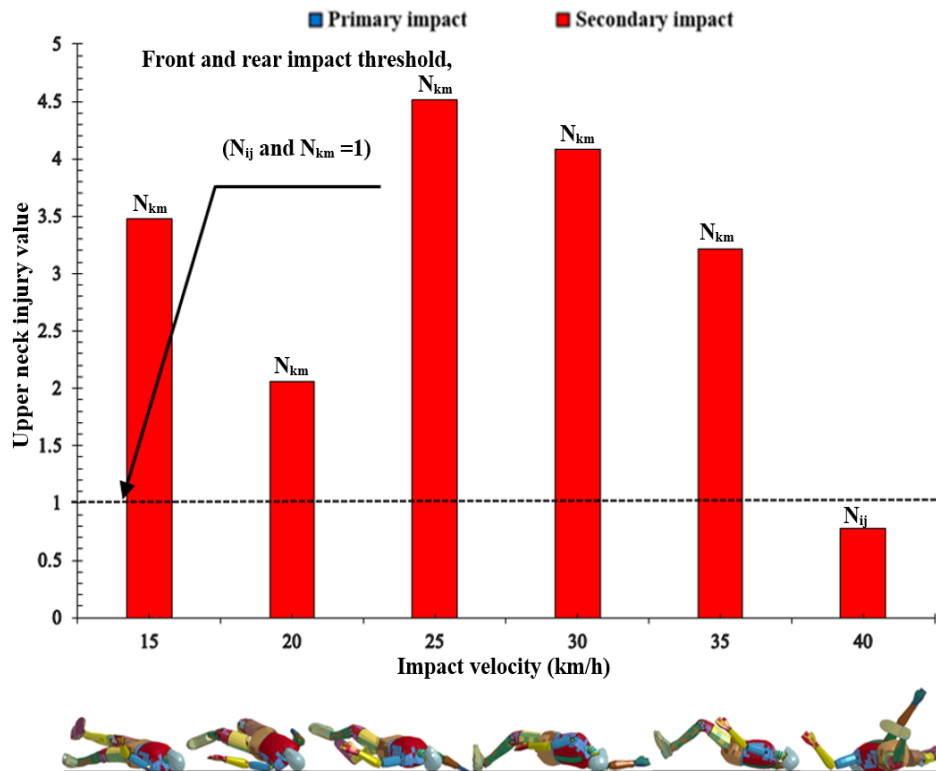


Figure 3- 33. Upper neck injury values for primary and secondary side impacts at 42cm offset from the vehicle's centreline.

3.5.3 Chest injury criterion and risk level during primary and secondary impacts

3.5.3.1 Chest injury criterion and risk level during primary and secondary impacts at the vehicle's centreline

During frontal primary pedestrian impacts, CTI values were observed to increase significantly with impact velocity, however, all CTI values were below the threshold for injury CTI=1 at impact velocities between 15 and 30km/h. Secondary impacts produced no significant CTI values at impacts velocities of 20km/h or below and CTI values were less than those produced during primary impacts at 30km/h, see Figure 3-33.

Rear primary impacts produced no frontal chest impacts. During secondary impacts, all CTI values fluctuated with impact velocity, all CTI values were below the threshold, see Figure 3-34.

For primary side impacts, again no front chest impacts occurred. For secondary impacts, all CTI values fluctuated with impact velocity and all values were below the threshold (1) at impact velocities between 15 and 35km/h, see Figure 3-35.

Chest injury risk, for adult pedestrians at the vehicle centreline at front, rear and side impact positions produced during the primary impacts is higher than those produced during the secondary impacts, see Figures E-19 to E-21.

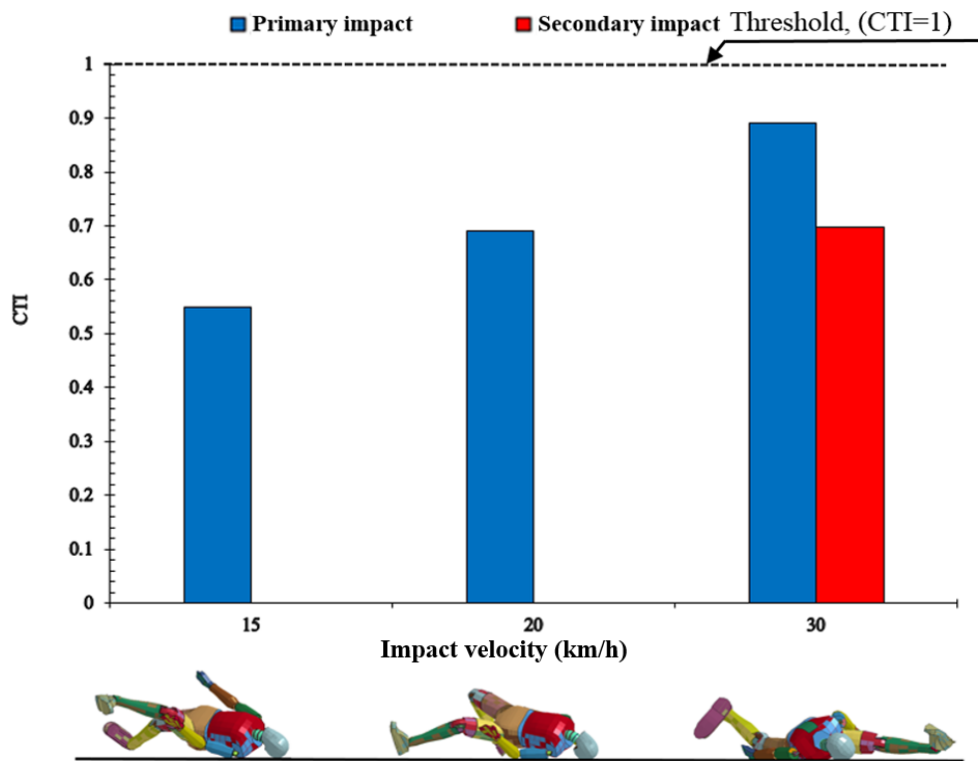


Figure 3- 34. CTI for primary and secondary frontal impacts at the vehicle's centreline.

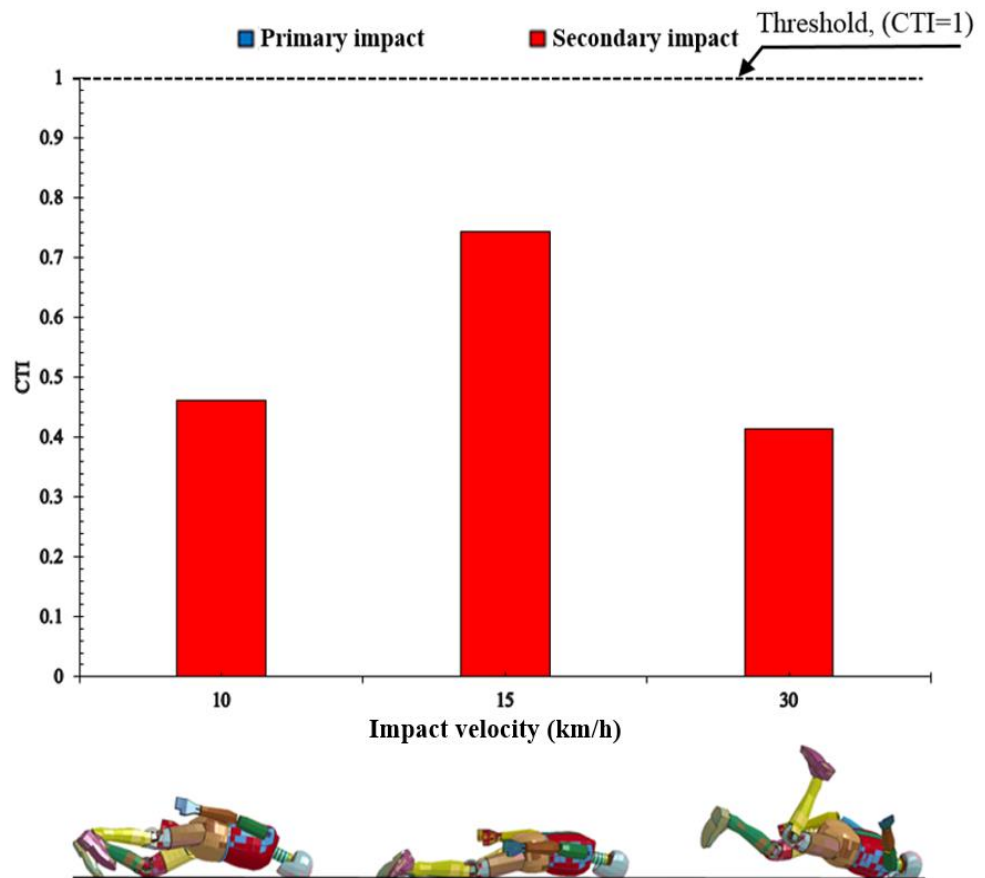


Figure 3- 35. CTI for primary and secondary rear impacts at the vehicle's centreline.

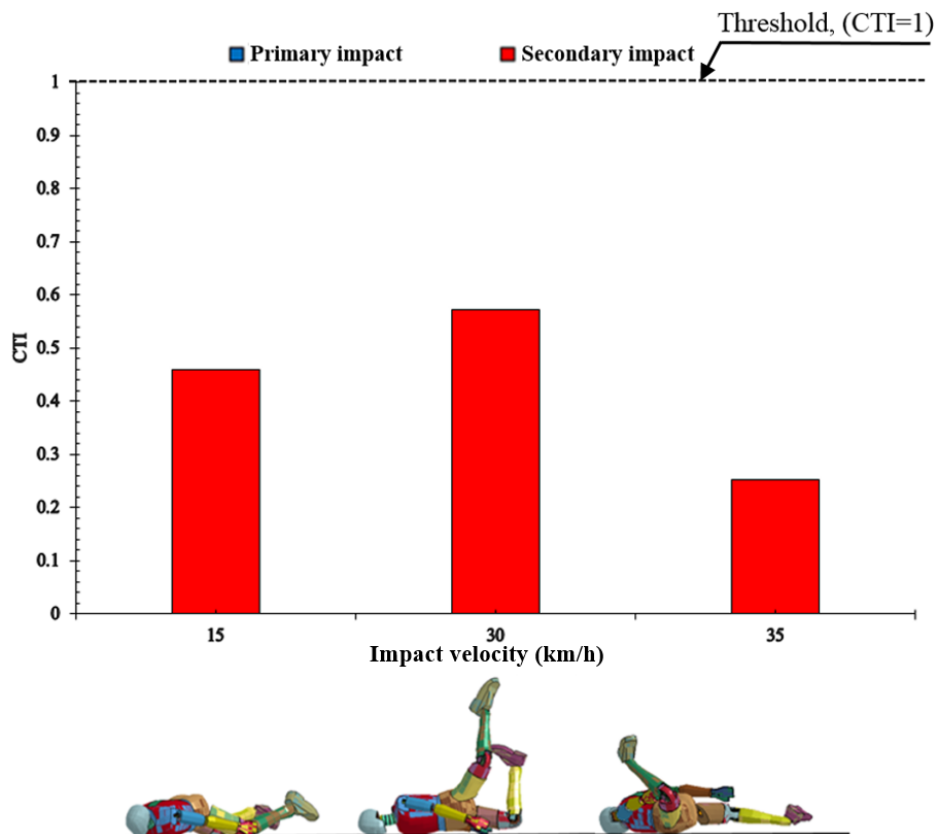


Figure 3- 36. CTI for primary and secondary side impacts at the vehicle's centreline.

3.5.3.2 Chest injury criterion and risk level during primary and secondary impacts at 42cm offset from the vehicle's centreline

For front primary impacts offset 42cm from the vehicle centreline, CTI values increased significantly with impact velocities between 20 and 30km/h, however, all CTI values were below the threshold. For secondary impacts, no chest-ground contact occurred at any of the impact velocities, see Figure 3- 36.

Rear primary impacts produced no frontal chest impacts. Secondary impacts produced no front chest-ground contact at 15 and 25km/h. Meanwhile, when the impact velocity increased to 30km/h, chest-ground contact was observed, though the CTI values were below the threshold, as shown in Figure 3- 37.

During primary side impacts, no frontal chest impacts occurred. Secondary impacts produced no chest-ground contacts between 15 and 35km/h. However, at 40km/h, chest-ground contact was observed, which produced CTI values below the threshold, as demonstrated in Figure 3- 38.

Chest injury risk for adult pedestrians at 42cm offset from the vehicle centreline at front, rear and side impact positions produced during the secondary impacts are significantly lower, see Figures E-22 to E-24.

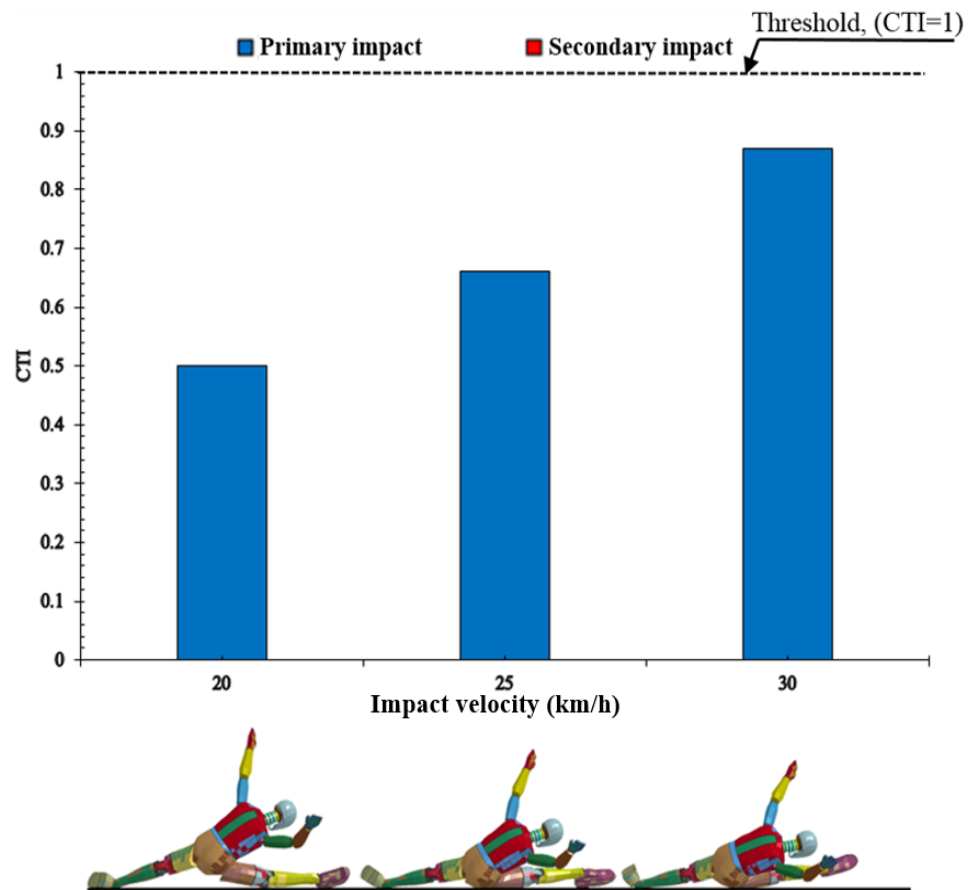


Figure 3- 37. CTI for primary and secondary frontal impacts at 42cm offset from the vehicle's centreline.

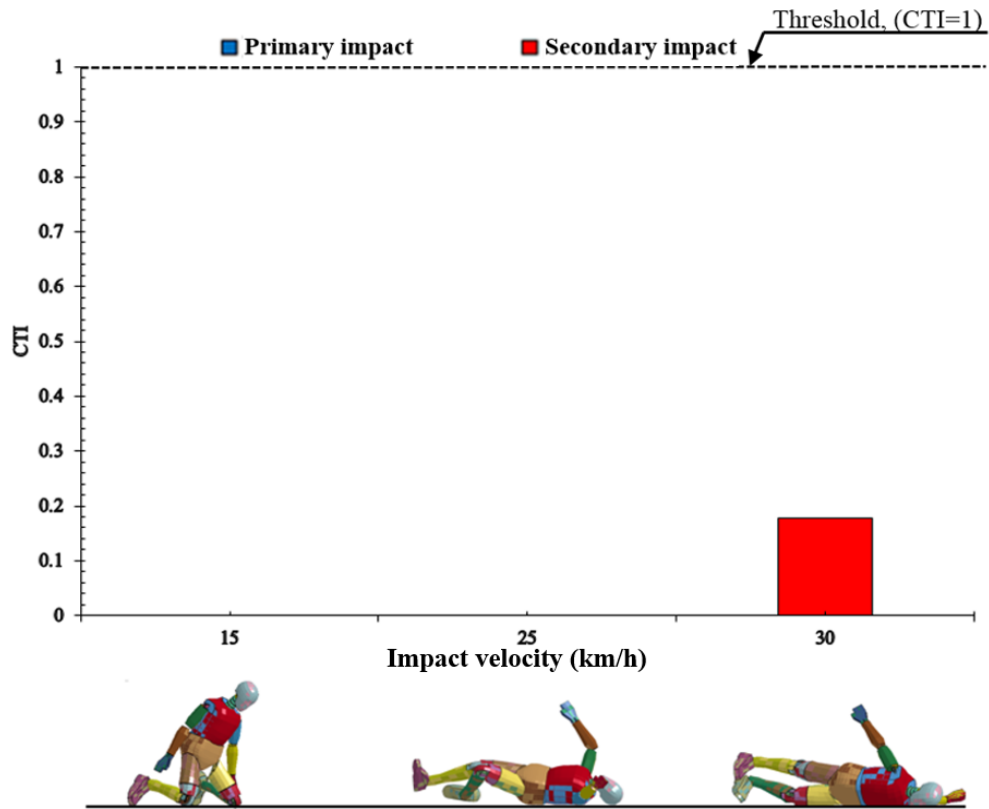


Figure 3- 38. CTI for primary and secondary rear impacts at 42cm offset from the vehicle's centreline.

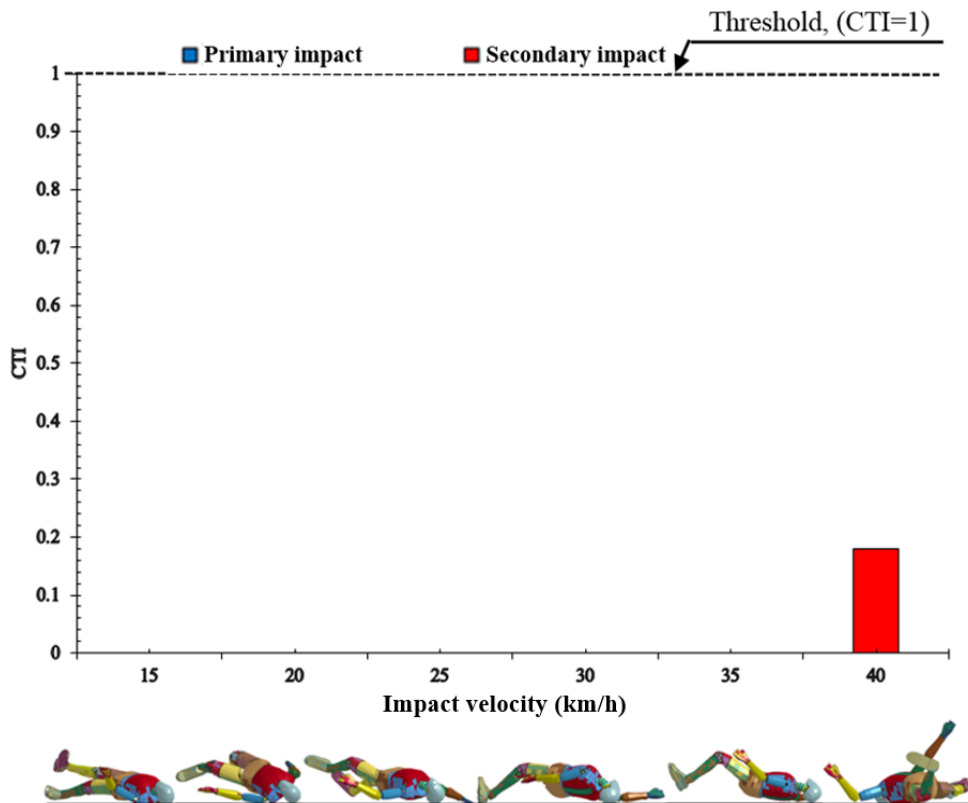


Figure 3- 39. CTI for primary and secondary side impacts at 42cm offset from the vehicle's centreline.

3.6 Auto rickshaw engineering modification for adult pedestrian safety enhancement

This section presents an investigation of the effects of material and material thicknesses modifications for the most frequently impacted, stiffest and most injurious vehicle components (windscreen and windscreen frame) on the injury risk for an adult pedestrian during primary impacts. Different materials and thicknesses are investigated to assess injury risk, based on HIC_{15} , N_{ij} , N_{km} and CTI and associated AIS.

3.6.1 Head injury and injury risk level during primary impacts after vehicle modifications

3.6.1.1 Head injury and injury risk level during primary impacts after vehicle modifications at the vehicle's centreline

The HIC values were investigated for an adult male pedestrian impacted by the auto rickshaw at the vehicle centreline at front, rear and side impact positions at impact velocities between 10 and 40km/h, for the original vehicle materials and the modified materials are shown in Figures 3- 39 to 3- 41. Iterations of the modified auto rickshaw include a polycarbonate windscreen with differing windscreen frame material. While, head injury risk, specifically severe head injury (AIS4+) for the adult pedestrian at the vehicle centreline in all impact positions (front, rear and side) for the original vehicle materials and the modified materials, are presented in Figures F-1 to F-3.

Comparing HIC values for the original materials of the windscreen and windscreen frame, to the modified materials shows a significant improvement can be made to HIC values and head injury risk for frontal and rear impacts at the vehicle centreline for all windscreen frame materials with PC windscreen. However, Aluminium 6016-T4 and Magnesium AZ31B show a remarkable decrease in HIC values and injury risk level at all impact velocities, see Figures 3- 39, 3- 41, F-1 and F-2. Despite this, the HIC values and head injury risk during the side impact positions produce by far the worst results, with large increases in HIC at all velocities through implementation of the PC windscreen and modified windscreen frame materials, as demonstrated in Figures 3- 41 and F-3.

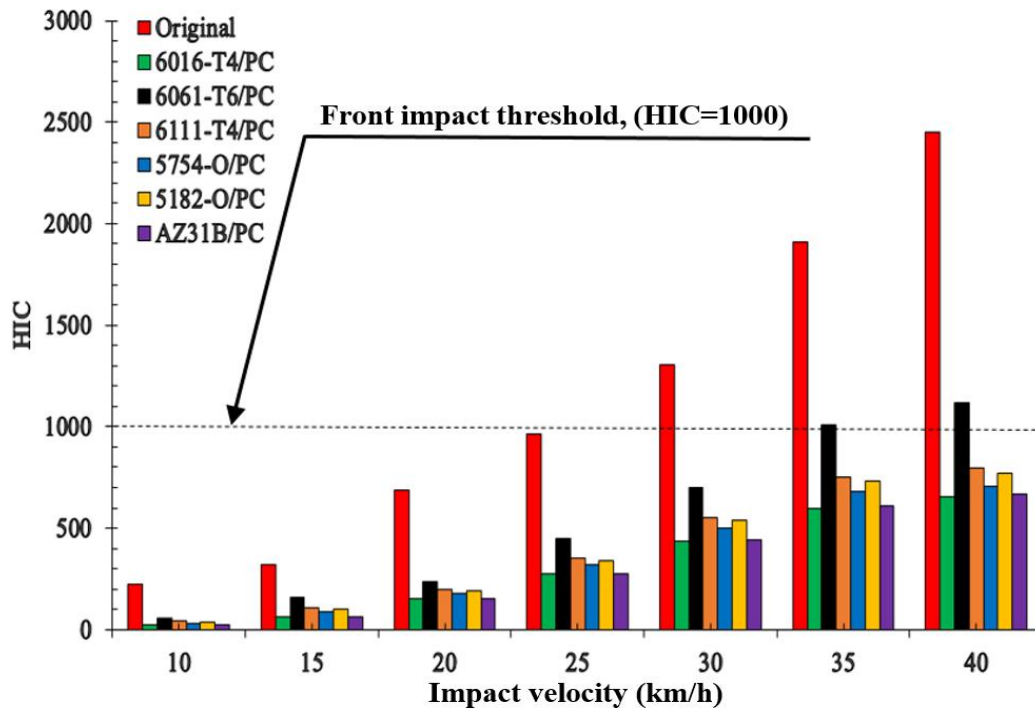


Figure 3- 40. HIC values for adult pedestrian impacts at the vehicle’s centreline for all simulations run in frontal impact with a polycarbonate windscreen and modified windscreen frame materials.

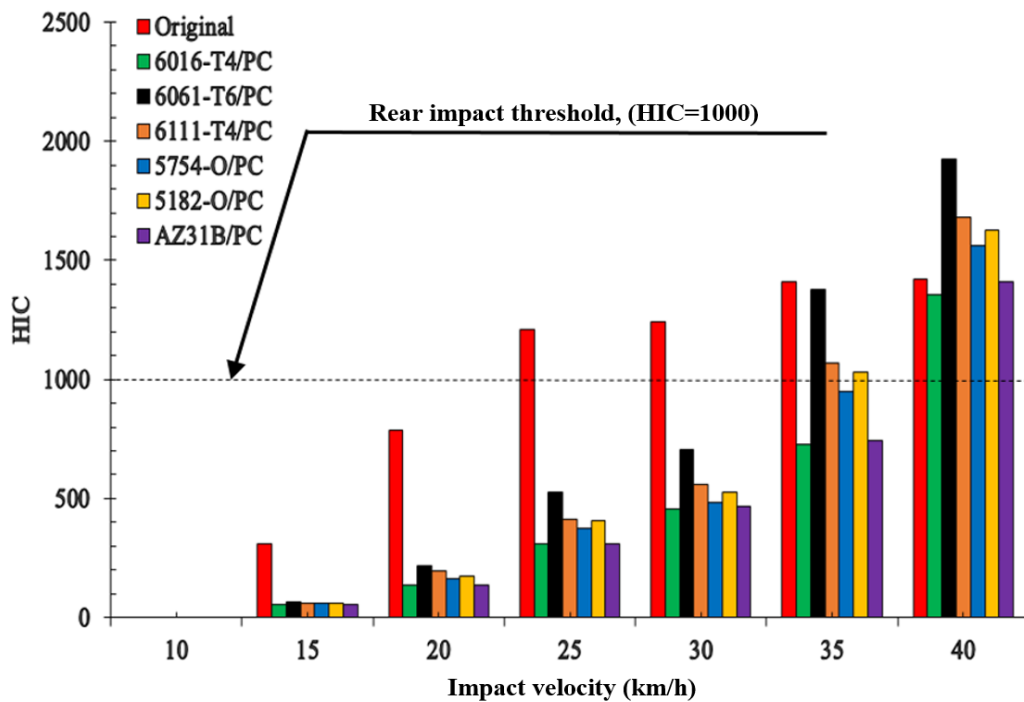


Figure 3- 41. HIC values for adult pedestrian impacts at the vehicle’s centreline for all simulations run in rear impact with a polycarbonate windscreen and modified windscreen frame materials.

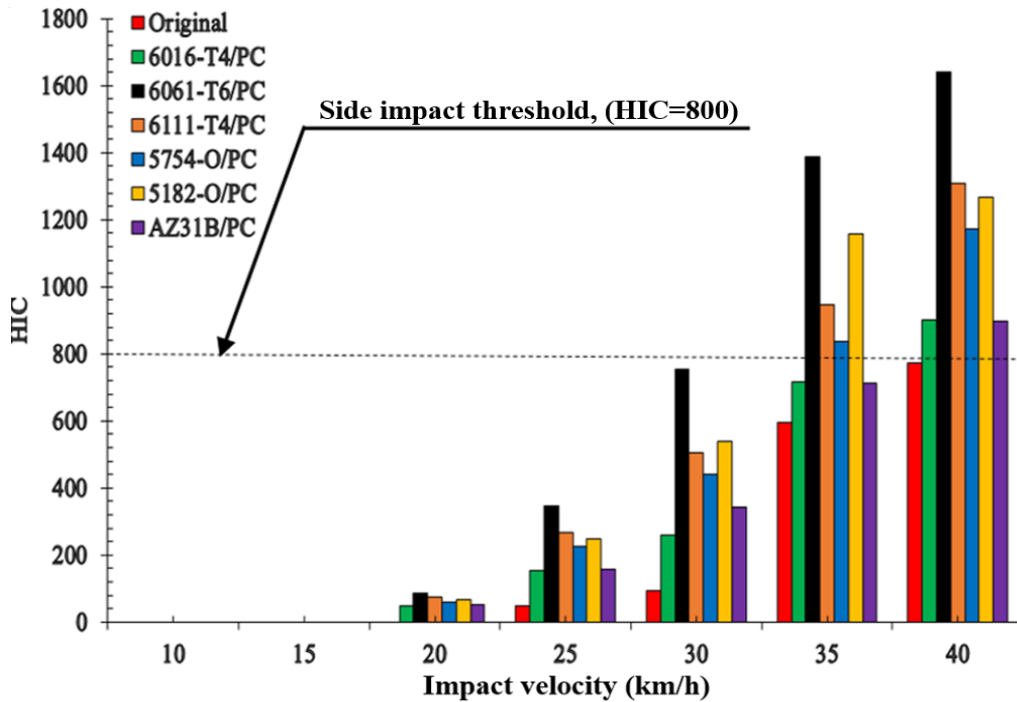


Figure 3- 42. HIC values for adult pedestrian impacts at the vehicle's centreline for all simulations run in side impact with a polycarbonate windscreen and modified windscreen frame materials.

3.6.1.2 Head injury and injury risk level during primary impacts after vehicle modifications at 42cm from the vehicle's centreline

The HIC values for an adult male pedestrian impacted by the auto rickshaw at 42cm offset from the vehicle centreline in front and rear impact positions at impact velocities between 10 and 40km/h, for the original vehicle materials and modified materials are shown in Figures 3- 42 and 3- 43. The iterations of the modified auto rickshaw all include a polycarbonate windscreen with differing windscreen frame material.

Head injury risk, specifically severe head injury AIS4+, for the adult pedestrian at 42cm from the vehicle centreline in all impact positions (front, rear and side) for the original vehicle materials and the modified materials are presented in Figures F-4 and F-5.

It can be observed that pedestrian safety improved significantly as the HIC values and head injury risk reduced at all impact velocities for the front and rear impact positions at the 42cm offset, as illustrated in Figures 3- 42, 3- 43, F-4 and F-5. Although the modified materials show a greater reduction in head injury risk for the offset positions, the HIC values and head injury risk produced in offset positions are significantly greater than those at the vehicle centreline.

In addition, side offset impacts are not included in this study, since there was no adult pedestrian head contact with the vehicle at impact velocities of between 10 and 40km/h.

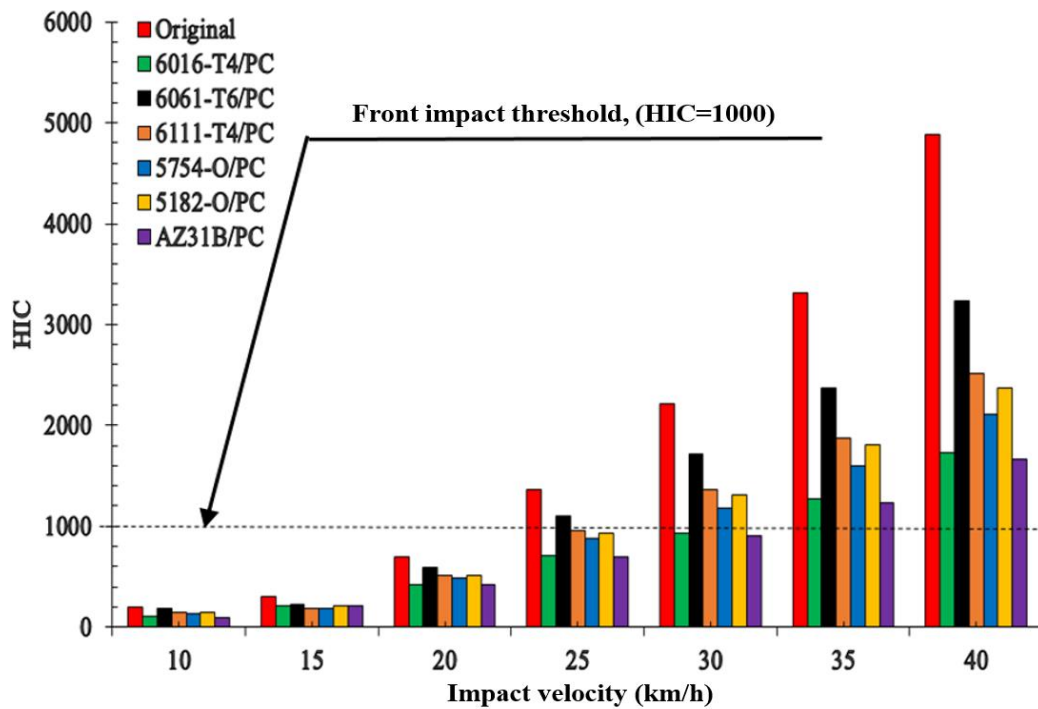


Figure 3-43. HIC values for adult pedestrian impacts at 42cm offset from the vehicle's centreline for all simulations run in frontal impact with a polycarbonate windscreen and modified windscreen frame materials.

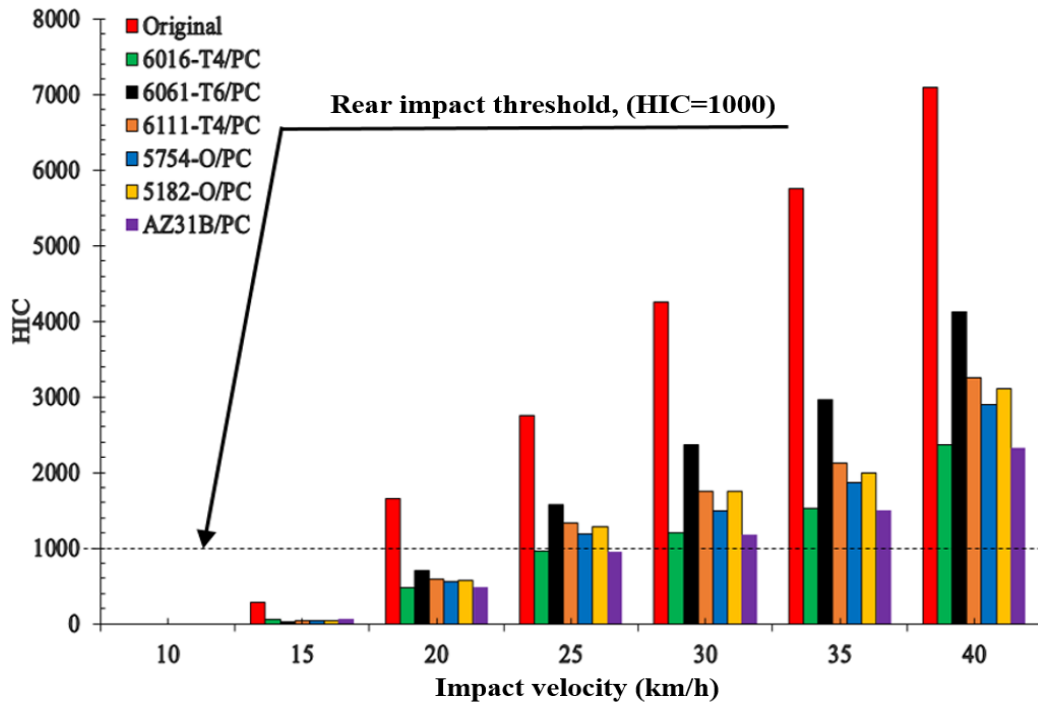


Figure 3- 44. HIC values for adult pedestrian impacts at 42cm offset from the vehicle's centreline for all simulations run in rear impact with a polycarbonate windscreen and modified windscreen frame materials.

3.6.2 Upper neck injury and injury risk level during primary impacts after vehicle modifications

3.6.2.1 Upper neck injury and injury risk level during primary impacts after vehicle modifications at the vehicle's centreline

The upper neck injury values at the vehicle centreline in frontal N_{ij} and rear N_{km} impact positions at velocities between 10 and 40km/h, for the original auto rickshaw materials and the modified materials are shown in Figures 3- 44 and 3- 45. As above, the modified auto rickshaw iterations all include a polycarbonate windscreen with differing windscreen frame material.

Upper neck injury risk, specifically serious neck injury AIS3+, for the adult pedestrian at the vehicle centreline at front and rear impact positions for the original vehicle materials and the modified materials are presented in Figures F-6 and F-7.

Comparing upper neck injury values for the original materials of the windscreen and windscreen frame, with the modified materials, indicates that remarkable reductions

to upper neck injury risk were attained for all simulations in frontal impacts to the vehicle centreline.

Overall, the greatest improvements were observed for the simulations with a PC windscreen and either Aluminium 6016-T4 or Magnesium AZ31B windscreen frame materials, which exhibited notable decreases in N_{ij} values at all impact velocities, as shown in Figures 3- 44 and F-6. Alternatively, the material modifications only show slight improvements for rear impacts and still have high N_{km} values, which would produce great upper neck injury risk, see Figures 3- 45 and F-7.

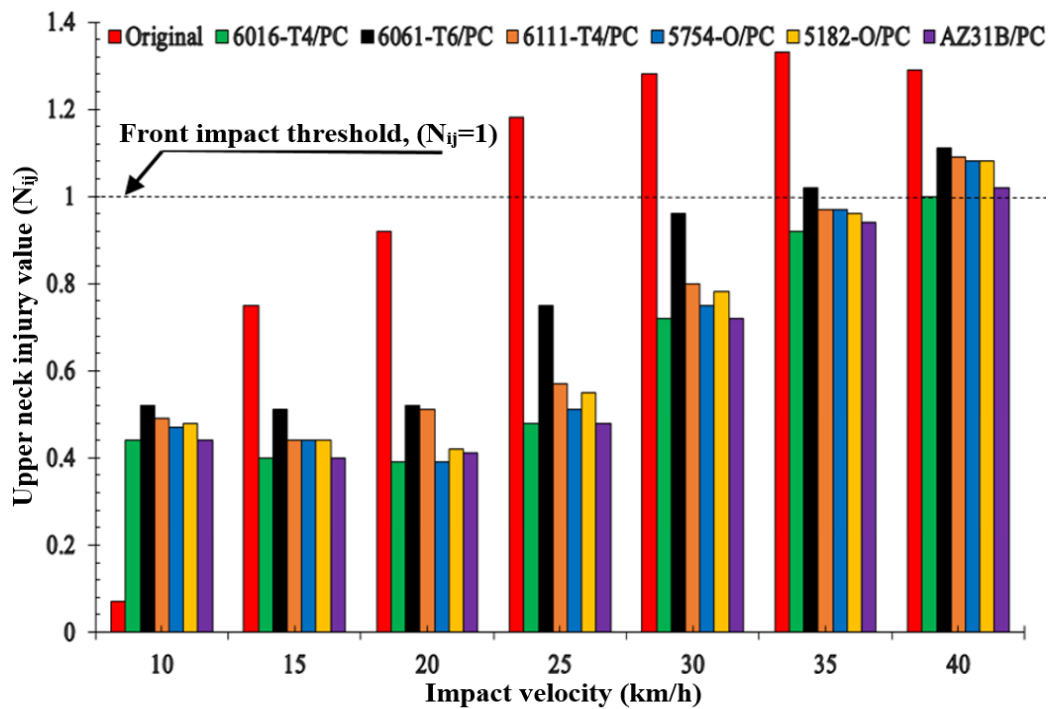


Figure 3- 45. Upper neck injury values at the vehicle's centreline for all simulations run in frontal impact with a polycarbonate windscreen and modified windscreen frame materials.

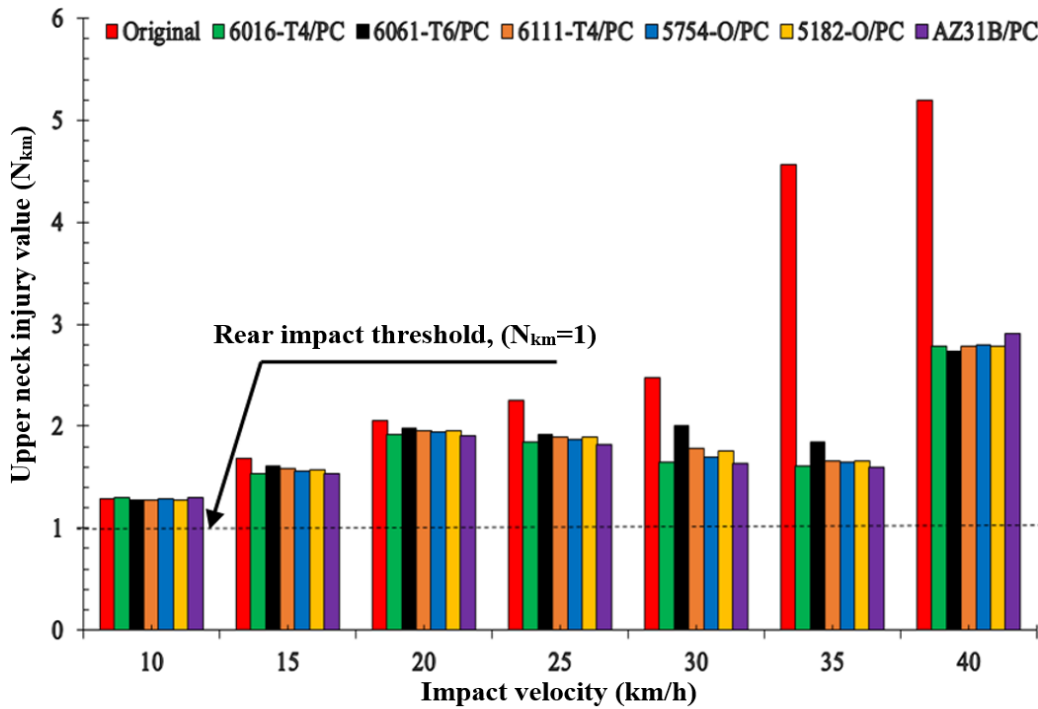


Figure 3- 46. Upper neck injury values at the vehicle's centreline for all simulations run in rear impact with a polycarbonate windscreen and modified windscreen frame materials.

3.6.2.2 Upper neck injury and injury risk level during primary impacts after vehicle modifications at 42cm from the vehicle's centreline

The upper neck injury values for an adult male pedestrian impacted by the auto rickshaw at 42cm offset from the vehicle centreline in frontal N_{ij} and rear N_{km} impact positions and impact velocities between 10 and 40km/h, for the original auto rickshaw materials and the modified materials are shown in Figures 3- 46 and 3- 47. The modified auto rickshaw iterations all include a polycarbonate windscreen with differing windscreen frame material.

Upper neck injury risk, specifically serious neck injury AIS3+, for the adult pedestrian at 42cm offset from the vehicle centreline in front and rear impact positions for the original vehicle materials and the modified materials are presented in Figures F-8 and F-9.

Comparing upper neck injury values, for the original materials of the windscreen and windscreen frame, with the modified materials shows that adult pedestrian safety associated with upper neck injury risk was improved significantly for frontal impacts in all simulations, see Figure F-8.

Once again, the simulations run with a PC windscreen and either Aluminium 6016-T4 or Magnesium AZ31B showed the most notable decrease in N_{ij} values at all impact velocities, as presented in Figure 3- 46. Similar to rear impacts at the vehicle centreline, rear impacts at a 42cm offset show the material modifications provided only minor safety improvements, with N_{km} values still producing a high upper neck injury risk, see Figures 3- 47 and F-9. There was also little difference between the N_{km} values of the modified materials for all impact velocities.

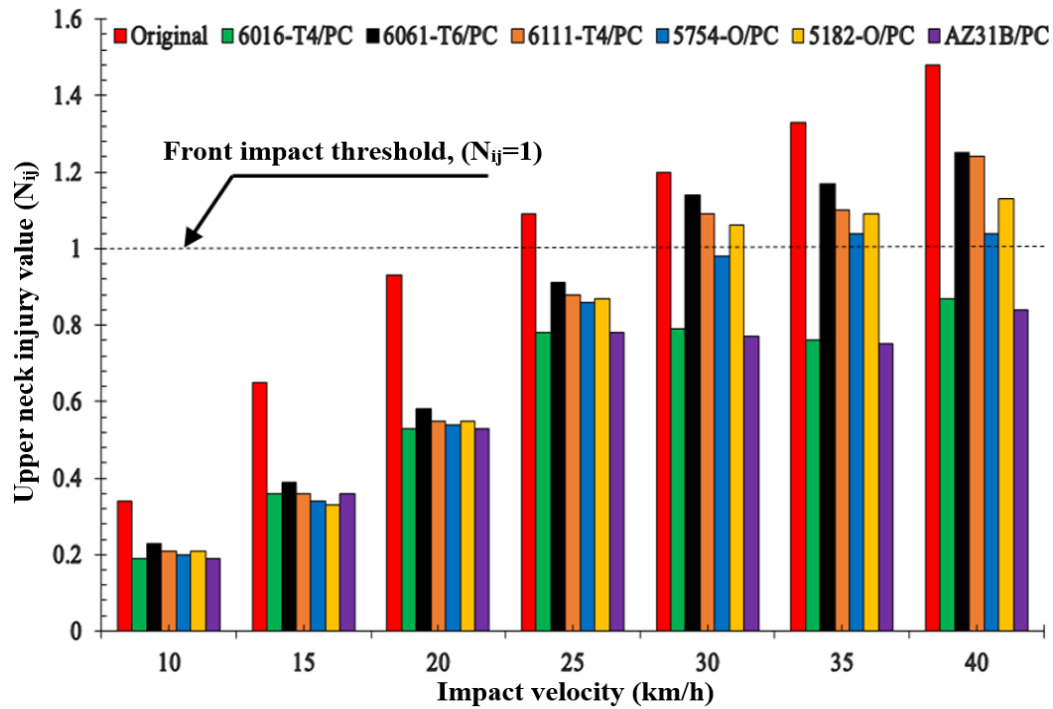


Figure 3-47. Upper neck injury values at 42cm offset from the vehicle's centreline for all simulations run in frontal impact with a polycarbonate windscreen and modified windscreen frame materials.

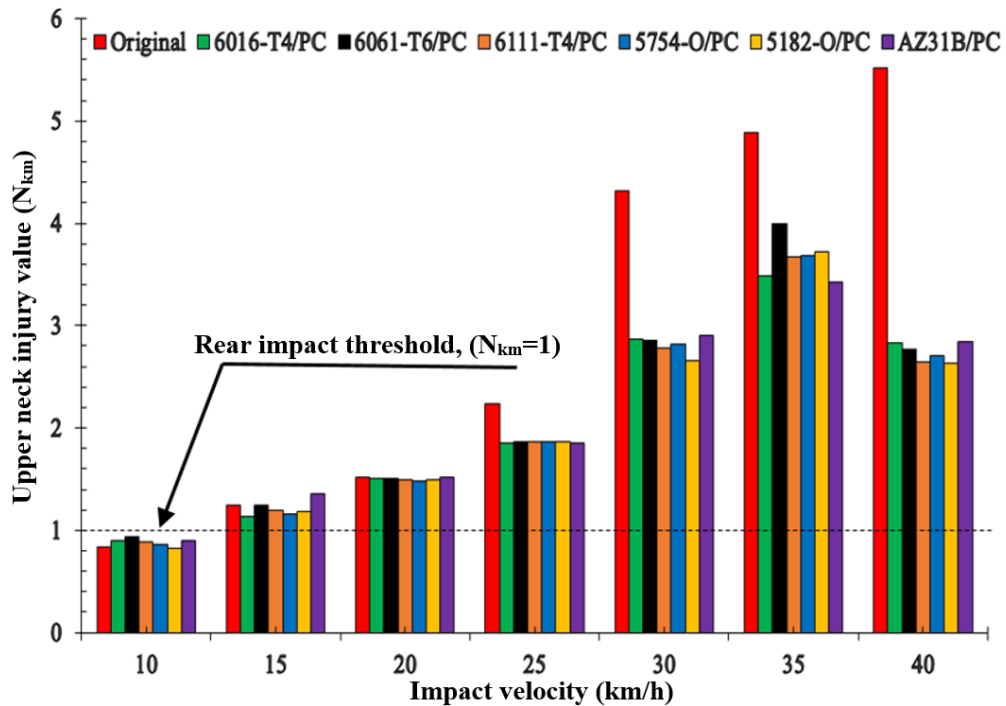


Figure 3-48. Upper neck injury values at 42cm from the vehicle's centreline for all simulations run in rear impact with a polycarbonate windscreen and modified windscreen frame materials.

3.6.3 Chest injury and injury risk level during primary impacts after vehicle modifications

3.6.3.1 Chest injury and injury risk level during primary impacts after vehicle modifications at the vehicle's centreline

The chest injury CTI values at the vehicle centreline at the frontal impact position at velocities between 10 and 40km/h, for the original auto rickshaw materials and the modified materials are shown in Figure 3- 48. As above, the modified auto rickshaw iterations all include a polycarbonate windscreen with differing windscreen frame material.

Chest injury risk, specifically serious chest injury AIS3+, for the adult pedestrian at the vehicle centreline at the frontal impact position for the original vehicle materials and the modified materials are presented in Figure F-10.

Comparing chest injury values CTI for the original materials of the windscreen and windscreen frame, with the modified materials shows that adult pedestrian safety, associated with chest injury risk, was improved significantly for frontal impacts during all simulations, see Figure F-10. Once again, the simulations were run with a PC windscreen and either Aluminium 6016-T4 or Magnesium AZ31B showed the most

significant decrease in CTI values at all impact velocities, as demonstrated in Figure 3- 48.

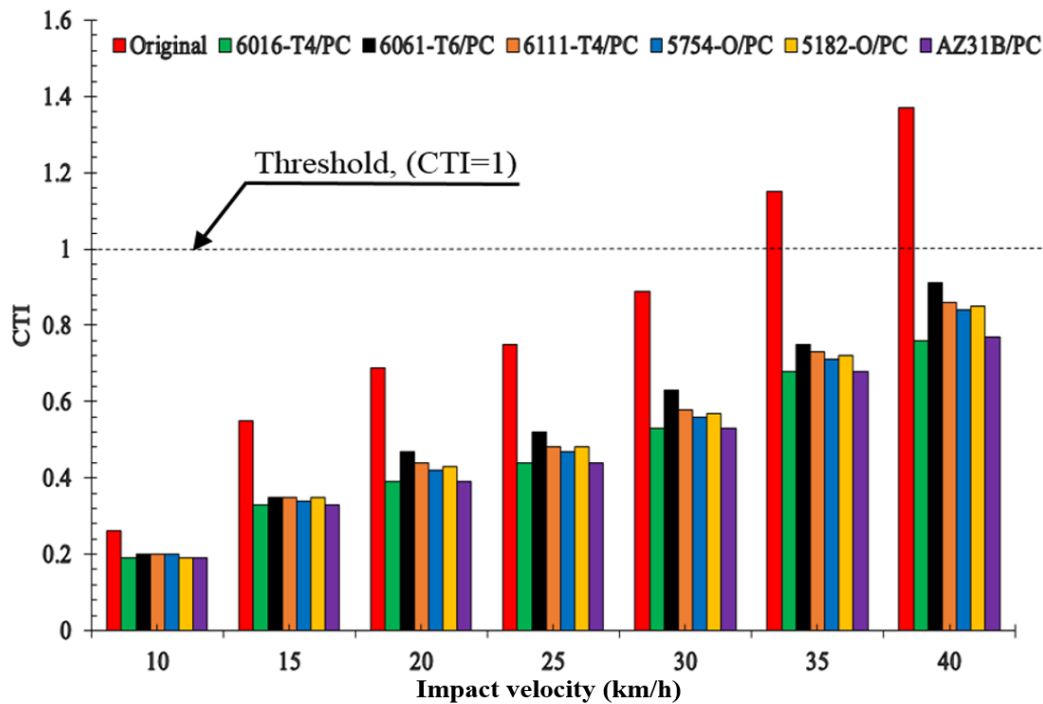


Figure 3-49. Chest injury values at the vehicle's centreline for all simulations run in frontal impact with a polycarbonate windscreen and modified windscreen frame materials.

3.6.3.2 Chest injury and injury risk level during primary impacts after vehicle modifications at 42cm from the vehicle's centreline

The chest injury values at 42cm offset from the vehicle centreline at the frontal impact position CTI at impact velocities between 10km/h and 40km/h, for the original auto rickshaw materials and the modified materials, are shown in Figure 3- 49. As above, the modified auto rickshaw iterations all include a polycarbonate windscreen with differing windscreen frame material.

Chest injury risk, specifically serious chest injury AIS3+, for the adult pedestrian at the vehicle centreline and frontal impact position for the original vehicle materials and the modified materials are presented in Figure F-11.

Associating chest injury values CTI, for the original materials of the windscreen and windscreen frame, with the modified materials illustrates that adult pedestrian safety, related to chest injury risk, was improved considerably for frontal impacts in all simulations, as shown in Figure F-11. Once again, the simulations run with a PC

windscreen and either Aluminium 6016-T4 or Magnesium AZ31B showing the most notable reduction in CTI values at all impact velocities, see Figure 3- 49.

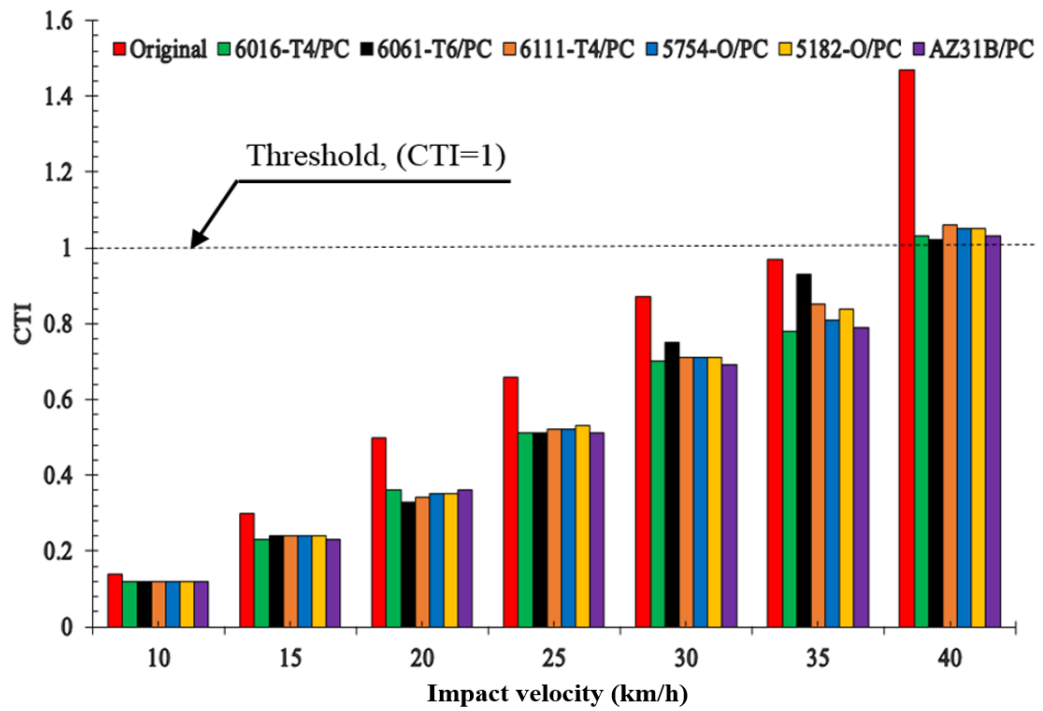


Figure 3-50. Chest injury values at 42cm offset from the vehicle's centreline for all simulations run in frontal impact with a polycarbonate windscreen and modified windscreen frame materials.

4. DISCUSSION

4.1 Introduction

This chapter discusses four main study investigations:-

- The primary vehicle impact for adult and child pedestrians.
- A secondary ground impact for an adult pedestrian.
- The influence of different vehicle “point of impact” material properties and thicknesses of the windscreen and windscreen frame on adult pedestrian head, neck and chest injury mitigation and their associated costs and benefits.

The impact scenarios will be discussed, based on pedestrian-vehicle impact at various impact velocities, at two contact regions, at the centreline of the vehicle and at 42cm offset from the vehicle centreline in three impact positions (front, rear and side) using two pedestrian dummy sizes, adult and 6YO-child. Moreover, the study will describe vehicle impact response characteristics, including the kinematic response, throw distance, injury parameters and injury risk level, associated with impact at three body regions, head, neck and chest.

4.2 Primary impacts

Real-World pedestrian impacts occur with highly variable initial pedestrian kinematics and kinetics conditions. In addition, small postural perturbations significantly influence pedestrian impact kinematics and kinetics. This study investigated the kinematic response of pedestrians who are impacted by an auto rickshaw, and who are subject to a narrow range of particular initial conditions, because its objective was to computationally simulate the relatively unfamiliar impact biomechanics of the auto rickshaw in comparison to more common four-wheeled vehicles. The influence of the impact velocity, impact position including three orientations (front, rear and side), pedestrian size (using two crash dummies: 50th percentile male and 6YO-child Hybrid III) and vehicle contact region (at the vehicle's centreline and 42cm offset from the vehicle's centreline) were investigated. Pedestrian kinematics and injury risks were assessed and compared across all simulations. .

4.2.1 Kinematic response during primary impacts

Previously, efforts have been reported of the analysis of the kinematic response of an adult pedestrian impacted by an auto rickshaw in the rear and side-impact standing positions. The analysis was, however, relatively superficial and further research is needed. Analyses of the front and walking side impacts for the adult pedestrian at the vehicle's centreline and offset were notably absent. In addition, the kinematic response for 6YO-child pedestrian has not yet been reported. Consequently, this section reports all of the variations of the impact positions for the adult pedestrian impacted by the auto rickshaw (including front, rear and side impact in the walking position) at both of the vehicle contact regions (centreline and 42cm offset from the vehicle's centreline). Moreover, the kinematic response of a 6YO-child pedestrians impacted by an auto rickshaw was examined for the first time at the same three impact positions and both vehicle contact regions (centreline and 42cm offset from the vehicle's centreline) at a range of impact velocities, between 5 and 40km/h.

Generally, all of the initial contacts occurred most frequently below the pedestrian's centre of gravity and the lower frontal vehicle parts for both adult and child pedestrians. Furthermore, the kinematic response for an adult impacted at both vehicle contact regions (centreline and offset) is similar to that for a child. The dynamic response during the impact at the vehicle's centreline produced a forward trajectory,

for both adult and child pedestrians in the travelling direction of the vehicle. While, a significant rotational response was observed for the adult and child to the vehicle's right-hand-side, due to impact asymmetry, as shown in Figures 3-1 and 3-2.

4.2.1.1 Kinematic response during impacts at the vehicle's centreline

The first interaction with the pedestrian generally occurred between the lower limbs and the lower frontal vehicle components (head-lamp, frontal sheet plate and mudguard), nevertheless, size still had a significant influence on the dynamic response and injury mechanics [149, 151].

The results show that the sequence of the adult pedestrian-vehicle impacts occurred between the knees-headlamp, tibia-mudguard, lower torso-windscreen frame, chest-windscreen/frame, upper extremities-windscreen/front sheet plate and head-upper region of the windscreen/frame in all impact positions (front, rear and side), as shown in Figures 3-1 (a) and Table 3-1. While, the sequence of the 6YO-child -vehicle impacts occurred between the lower extremities-mudguard/tyre/front sheet plate/headlamp, lower torso-headlamp, upper torso-front sheet plate and head-lower region of the windscreen/frame in all impact positions (front, rear and side), as shown in Figures 3-2 (a) and Tables 3-2. In addition, this study found that the frontal impact kinematic response was similar to the rear impacts, in that little or no rotation was produced. However, side impact to a walking posture for both adult and child pedestrians produced rotation around the pedestrian's longitudinal axis, dependent on the forward or rearward position of the ipsilateral leg, since this created a lever arm and change in the orientation of the pelvis prior to impact, as shown in Figures 3-1 (a) and, 3-2 (a), and Tables 3-1 and 3-2. This might result from the effect of changing the pedestrian's posture, which led to changes in the centre of gravity, as previously mentioned by Peng et al (2012) [151].

Therefore, the significant differences are the head impact locations of the adult impacts with the upper regions of the windscreen/frame, while the head of the 6YO-child impacted with the lower regions of the windscreen/frame. No chest-vehicle impacts occurred for the 6YO-child, while the adult's chest impacted the vehicle windscreen. This might be a result of the centre of gravity differences, specifically that the centre of gravity of the 6YO-child is lower than the adults.

Moreover, differences between the mass and height of the adult and the 6YO-child (78.6 compared to 23kg and 1680 compared to 1140mm, respectively) and anatomical features [117] might produce numerous kinematic perturbations at the vehicle contact regions. Similarly, the response is consistent with Peng et al. (2012), who concluded that variations in size led to variations in kinematic response, body region-vehicle contact order and injury risk [151].

In summary, impact velocity, impact position, posture and vehicle contact regions are influenced by kinematic response during pedestrian-vehicle impacts. Therefore, the pedestrian's size has a significant influence on the contact body region of pedestrian-vehicle components and impact time duration, see Figures 3-1 (a) and 3-8 (a) and Tables 3-1 and 3-4. When impacted symmetrically, both adults and children are moved forward in the travelling direction of the vehicle. These results were obtained during pedestrian-vehicle impacts when pedestrian's velocity was defined as stationary. In cases where the pedestrian had a transverse velocity, subsequent movement could be significantly changed, thus, influencing the head impact locations [200].

4.2.1.2 Kinematic response at impacts 42cm offset from the vehicle's centreline

The responses show that the sequence of the adult pedestrian-vehicle impacts occurred between the lower torso and the front offset sheet plate, the lower extremities/knees and the front offset edge/lower offset sheet plate, the upper extremities and the front offset edge/lower offset sheet plate and the chest-windscreen and head-upper right corner of the windscreen/frame, in all impact positions (i.e. front, rear and side). However, no head impacts occurred with the vehicle components in the side offset impact scenario, due to impact asymmetry at the vehicle's right-hand-side, which resulted in a significant rotation about the vehicle's right-hand-side; as shown in Figure 3-1 (b) and Table 3-3. The sequence of the 6YO-child's -vehicle impacts occurred between the head and the lower corner of the windscreen and or windscreen frame, the upper torso/chest and the front offset edge, the upper extremities and the front offset edge/lower front offset sheet plate and the lower extremities and the lower front offset sheet plate/front offset edge in all impact positions (i.e. front, rear and side), as shown in Figure 3-2 (b) and Table 3-4. Therefore, the significant differences are the head impact location of the adult's impacts with the upper curved sharp regions of the

windscreen/windscreen frame, while the head of the 6YO-child impacts with the lower regions of the windscreen/windscreen frame. No adult head-vehicle impacts occurred during the side offset scenario at all impact velocities (i.e. between 5 and 48km/h), due to significant rotation about the right-hand-side of the vehicle as a result of asymmetrical impacts; see Table 3-3. Whilst the child similarly rotated to the right side of the vehicle, head impacts did occur during the side offset scenario; see Table 3-4. This might be a result of variation in the position of the centre of gravity or mass, size differences and or anatomical features [117].

These results are in good agreement with Chawla et al. (2003), who concluded that the kinematics of an adult pedestrian impacted by an auto rickshaw changed when the impact orientation changed and vehicle offset was significant, because of the rotational behaviour of the pedestrian body caused by asymmetric contacts [40].

Similarly, this response is consistent with Peng et al. (2012), who concluded that leg posture has a significant influence on the dynamic response of the adult pedestrian, as a result of a changing position of the centre of gravity. In addition, the variation in pedestrian size produced variations in kinematic response, body region-vehicle contact orders and injury risk [151]. Furthermore, the responses are consistent with Yao et al.'s (2007) study of 23 real accident cases involving child pedestrian-passenger vehicle impacts, reconstructed by MADYMO, collected from German In-Depth Accident Study (GIDAS), which stated that kinematic response is significantly affected by impact position and initial impact posture [57].

Impact velocity, impact position, posture, vehicle contact regions and pedestrian size were recognised as affecting the dynamic response during pedestrian-vehicle impacts, see Figures 3-1 (b) and 3-2 (b) and Tables 3-3 and 3-4. However, both adult and child responded to the asymmetric impacts by rotating about the side of the vehicle.

In summary, pedestrian body region impact patterns and impact time durations produced a range of kinematic response sequences, with respect to vehicle contact region, impact position, impact velocity and size, which can inform improved auto rickshaw design.

4.2.2 Head contact locations and angles during primary impacts

With respect to head impact, across all the vehicle-pedestrian impact simulations, the most frequently impacted vehicle regions were the upper regions of the windscreen

and windscreen frame, as shown in Figure 3-3. These findings show agreement with Chawla et al's (2003) study, which reported that the windscreen and windscreen frame are the most frequently impacted components relevant to the head of the adult pedestrian impacted with an auto rickshaw [40]. The study did not, however, report head impact location and head impact angle, such that injury metrics could not be determined. Therefore, this section discusses for the first time the head impact location and head contact angles for adult and child pedestrians impacted by an auto rickshaw during primary impacts.

The adult's head impacts occurred against the upper region of the windscreen and windscreen frame, as shown in Figure 3-3. However, the child, impacted the lower regions of auto rickshaw components, see Figure 3-3 and in the majority of impact scenarios, produced head contact angles that were lower than the adults, resulting in a centre of gravity, mass and length variation, as shown in Table 3-5. The responses show a good agreement with the European Enhanced Vehicle Safety Committee (EEVC) child and adult head-form subsystem head safety tests, which established that the head impact angles for the adult and child at 40km/h are 65 and 50 degrees, respectively [195].

Variation in vehicle contact region, pedestrian size, impact position and posture influenced head contact location and angle, as demonstrated in Figure 3-3 and Table 3-5. These findings are in good agreement with Peng et al. (2012), who concluded that the pedestrian gait and size influenced the kinematic response and injury risk resulting due to a change in the centre of gravity [151]. Similarly, these responses again show a good agreement with Okamoto et al. (2017), who concluded, when investigating the influence of the frontal end of the vehicle, pedestrian size, the vehicle contact region and impact velocity on the head injury, that the head impact location and impact angle was influenced by the vehicle contact location and pedestrian height [187]. The study used two different vehicle front-ends (a passenger car and a utility vehicle) and four dummy sizes (large, medium and small sized adults and a 6YO-child). In addition, the impacts were simulated at the vehicle's centreline and at the side of the vehicle during impact velocities of 20, 40 and 60km/h in side impact positions.

This study produced head contact locations and angles that were influenced by the impact position, vehicle contact region and pedestrian size, as shown in Figure 3-3 and Table 3-5. There was, however, no significant influence of impact velocity on impact

angle observed in this study, possibly as a result of the unique frontal end of the auto rickshaw, which is almost flat (“van-like”).

The importance of the head impact locations and angles are that they enable us to identify subsystem test procedures at different impact positions and vehicle contact regions to assist injury mitigation. This could be achieved by using the current study data, relevant to the head impact locations and angles, to simulate head impact by dropping a head-form onto a prescribed impact surface. However, experimental data might be needed to increase the reliability of the head impact locations and angles for a pedestrian impacted by an auto rickshaw. To conclude, changes in pedestrian impact position and vehicle contact region produced variations in head contact location and head contact angle as a result of kinematic response variation.

4.2.3 Head contact time duration during primary impacts

This section discusses, for the first time, head contact duration during pedestrian-auto rickshaw impacts considering the following factors, impact velocity, impact positions, vehicle contact regions and pedestrian size; as demonstrated in Figures A-1, A-3 and B-1, B-3, and Figures 3-4 to 3-9.

4.2.3.1 Head contact duration during impacts at the vehicle’s centreline

Head contact duration was investigated at different impact velocities and different impact positions with the adult and 6YO-child at the vehicle centreline. Three pedestrian orientations (i.e. front, rear and side) were investigated for both adult and child. No head impacts were produced at 5 km/h for either adult or child in all impact positions as a result of a low momentum transfer to the pedestrian at low impact velocities during the impact.

During frontal impacts, the adult head impacts occurred at velocities between 10 and 40 km/h. The adult head impact durations were between 177 and 50 ms, as shown in Figure C-1. No child head impact occurred at 10km/h, due to the impacts occurring between the lower/upper regions of the femur with the mudguard/headlamp and the lower torso with the head lamp. These impacts dissipated most of the transferred kinetic energy during the impacts. Therefore, the child's head was not accelerated sufficiently to impact with the vehicle components. Child head impacts occurred at velocities between 15 and 40 km/h, which caused high momentum transfer to the child

during the impact, which accelerated the head to impact with the lower region of the windscreen frame to produce impact durations of between 87 and 30 ms, as shown in Figure C-1.

During rear impacts, no adult head impact occurred at 10km/h, due to low momentum transfer to the adult. Head impacts occurred at velocities between 15 and 40 km/h and produced impact durations between 153 and 70ms, as shown in Figure C-2. Child head impacts occurred at impact velocities between 10 and 40km/h and produced head impact durations between 123 and 30ms, see Figure C-2.

During side impacts, no adult head impacts occurred at impact velocities between 10 and 20km/h, due to the posture of the adult, which was in a walking position. Interactions between the vehicle components and the body regions occurred at the lower and upper body regions with vehicle components, which indicates that most of the kinetic energy was dissipated by the lower and upper extremities; thus, potentially limiting the acceleration of the head to impact with the vehicle. This may be a result of variations in the position of the legs, which influence the centre of gravity in the side position. These results are in agreement with Peng et al. (2012), who stated that a change in gait led to a change in the centre of gravity [151] that can result in an absence of head-vehicle impacts at low vehicle impact velocities. Adult head impacts occurred at impact velocities between 25 and 40km/h and produced head impact durations between 118 and 75ms, see Figure C-3. Child head impacts occurred at impact velocities between 10 and 40km/h and produced head impact durations between 123 and 30ms, see Figure C-3.

These responses indicate that the head impact durations, produced at the side impact positions, are greater than those produced during frontal and rear impacts. This indicates that the head of the adult and child pedestrians contacted with the vehicle components at the front impact position earlier than rear and side impacts, which is a result of significant torso bending towards the front-end of the vehicle and the effect of the contact orders of others body regions with the vehicle components. In addition, this might be happen because of the effective angles of rotation for adult frontal and rear impacts are lower about the frontal edge of the auto rickshaw sheet plate than the side impacts, being 4, 7 and 10 degrees, respectively, see Figure A-2. Meanwhile, for the child pedestrian, the lower effective angles of rotation were about the headlamp

during the front, rear and side impacts, and were 18, 19 and 21 degrees, respectively, see Figure B-2.

Although the front-end of the auto rickshaw is quite different to that of a typical passenger car, (i.e. possessing no front bumper across the width of the vehicle, no bonnet or bonnet leading edge and only one wheel, as shown in Figures A-2 and B-2), similar observations were made by Simms and Wood (2005), who noted that the front and rear facing impact positions led to earlier head impacts, due to a lower effective radius of rotation about the bonnet leading edge, compared to side positions. These results were concluded based on investigations of the adult pedestrian head contact forces with the vehicle and ground using two impact positions, including front and side at impact velocities of 18, 36 and 72km/h [200]. These data can be very useful for activation time protection for automotive engineering safety countermeasures.

Even though head impact duration varied with impact position, for both the adult and child during impact at the vehicle's centreline, these results establish that the head impact duration at the vehicle centreline for the child is less than that for the adult. Thus, the child's head impacts with the vehicle's components earlier than the adult's head, which is a result of the differences in size, mass, height, anatomical features [117] and the variation in the effective angles of the rotation in frontal, rear and side impacts about the front end of the auto rickshaw.

Although, the size of the adult, specifically the height, is different from the 15-YO-child pedestrian, these responses are in good agreement with Liu and Yang (2003), who found that the head contact time duration for 6YO-child is less than the 15YO-child. Their study investigated a range of impact velocities between 30 and 50km/h and the front-end geometry of a mid-size passenger car impacting the side [161]. Similar findings were reported by Ito et al. (2017), who concluded, when investigating the kinematic response and head injury mechanisms of vehicle impacts with three child (3YO, 6YO and 10YO) and an adult interacting with three different vehicles during side impacts at 10 and 40km/h, that the head contact time became later in accordance with age [194].

4.2.3.2 Head contact time duration at 42cm offset from the vehicle's centreline

Head impact time duration was examined at different impact velocities and different impact positions with adult and child pedestrians, 42cm offset from the vehicle's

centreline. The three impact positions were investigated. No head impacts were produced at 5 km/h for either adult or child in all impact positions as a result of low momentum transfer to the pedestrians at low impact velocities during the impact.

During frontal impacts, adult head impacts did occur at velocities between 10 and 40 km/h, the higher impact velocity producing high momentum and kinetic energy transfer to the adult during the impact. The adult head impact durations occurred between 78 and 23 ms, as shown in Figure C-4. The child's head impacts occurred at the same impact velocities producing impact duration between 15 and 5ms, see Figure C-4.

During rear impacts, no adult head impacts occurred at 10km/h, as a result of most of the kinetic energy being transferred to the lower torso and the upper and lower extremities. In addition, low impact velocities produced low momentum transfer, which was not sufficient to accelerate the adult head to impact with the vehicle components. Increasing the impact velocities between 15 and 40km/h produced head contact durations between 118 and 48ms, as shown in Figure C-5. The child's head impacts occurred at impact velocities between 15 and 40km/h, producing head impact durations between 28 and 10ms.

During side impacts, no adult head impacts occurred at impact velocities between 10 and 40km/h, due to significant rotations to the vehicle side, a result of asymmetric impacts, as shown in Figure C-6. No child head impacts occurred at 10km/h, since the relatively low momentum and kinetic energy was absorbed by the impacting upper extremities. This might cause deceleration to the child's head and cause it to interact with the vehicle's components at low impact velocities. Impact velocities between 15 and 40km/h produced head impact durations of between 35 and 13ms, as shown in Figure C-6.

These results emphasise that the head impact duration, during impacts at the 42cm offset from the vehicle's centreline for adult and child pedestrians was less than at the vehicle's centreline, see Figures A-1, A-3, B-1 and B-3. An explanation for this difference is that the body's rotation to the vehicle's side at the offset is a result of the frontal vehicle geometry and asymmetrical impact to the pedestrian and movement to the vehicle's right-hand-side, which affects the pedestrian body-region-vehicle-component impact order. However, head contact time for the child, is less than that of the adult. This response indicates that the child's head impacts with the vehicle

components earlier than the adult's, which is a consequence of the differences in size, mass, centre of gravity, height and anatomical features [117, 187]. In addition, these results are in good agreement with Peng et al. (2012) [163] and Yang et al. (2005), based on a Real-World accidents investigations [69].

In summary, head contact time duration for both the adult and child decreased with impact velocity in all impact positions at both vehicle contact regions. The responses are consistent with those of previous studies, which concluded that the head impact time duration decreased with impact velocity [159, 161-163].

Thus, the contact duration of head impacts with the front of the auto rickshaw was observed to vary widely as a result of the vehicle's impact velocity, impact position, contact region and the pedestrian's size, which will assist automotive designers to improve safety [157, 159]. In particular, these findings can be used by automotive designers to enhance safety by retro engineering/engineering safety mitigation strategies.

4.2.4 Head injury criterion and injury risk level during primary impacts

While investigations have previously been conducted into head injury for a standing adult pedestrian who is impacted by an auto rickshaw to the rear and side at the centreline and offset at impact velocities between 10, 20 and 30km/h, the front and side walking positions have not been investigated. In addition, the influence of a wide range of the impact velocities has not been investigated. Moreover, head injury and injury risk for a 6YO-child pedestrian impacted by an auto rickshaw during primary impacts have not yet been investigated.

This section discusses the head injury and injury risk during pedestrian-vehicle impacts considering the following main factors: impact velocity, impact position, vehicle contact region and pedestrian size. The importance of this study is its potential application by researchers and engineers who wish to modify the front-end of the vehicle and to establish regulatory frameworks that are relevant to pedestrian safety. To date, most vehicle-safety regulations have been focused on four-wheeled vehicles, such as the Global Technical Regulations (GTRs) and European New Car Safety Assessment Programme (Euro-NCAP), while no regulations have been established for an auto rickshaw or other three-wheel vehicles.

4.2.4.1 Head injury criterion and risk level during primary impacts at the vehicle's centreline

During frontal impacts, the results emphasise, that the HIC exceeded the head injury thresholds, $HIC_{15} = 1000$ and 700 for adult and child, at 30 and 20km/h respectively, see Figure 3-4. These findings are in good agreement with the study of Chawla et al. (2003), which concluded that the head injury risks for the adult pedestrian were “quite high” during impact with an auto rickshaw at 30km/h [40]. In addition, the results indicate that the HIC for the child is higher than the adult by an average of 17% at impact velocities between 15 and 40km/h . In addition, the head injury risk to the child is greater than the adult by an average increase of 10% , 5% , 4% , 3% and 6% , for moderate, serious, severe, critical and fatal head injuries, respectively; as shown in Table C-1.

During rear impacts, the results emphasise that the HIC exceed the head injury threshold $HIC_{15} = 1000$ and 700 for the adult and child at 25 and 20km/h , respectively, see Figure 3-5. Again the HIC for the child is greater than the adult by an average increase of 75% , at impact velocities between 15 and 40km/h , corresponding to an average child head injury risk increase of 7% , 13% , 30% , 42% and 36% for moderate, serious, severe, critical and fatal head injuries, respectively; as shown in Table C-2.

Most HIC and head injury risk values were higher than those produced during frontal impacts for both adult and child pedestrians, as shown in Figures A-4, A-6, A-7, B-4, B-6 and B-7. This maybe a consequence of the interaction between the head and the lower region of the windscreen and windscreen frame, which have different stiffnesses, thicknesses and geometries, as shown in Figure 3-3. The responses show agreement with the study by King (2018), which reported that the acceleration response to impact depends on the stiffness and geometry of the head impact surface [88]. They are also consistent with the study by Zhang et al. (2018), which, concluded that the stiffness of the front-end structure directly influences the head' acceleration during the vehicle-pedestrian impacts and the HIC is higher when the structure's is higher [148].

During side impacts, the results emphasise that the HIC for the adult did not exceed the head $HIC = 800$ injury threshold between 5 and 40km/h . However, it exceeded the injury threshold at 48km/h . While, the child exceeded the $HIC = 700$ threshold at

impact velocities between 20 and 40km/h, as illustrated in Figure 3-6. These results show that the HIC for the child is higher than the adult by an average increase of 100%. In addition, the head injury risks to the child are greater than the adult by an average 72%, 82%, 70, 54% and 38% for moderate, serious, severe, critical and fatal head injuries, respectively; as shown in Table C-3.

Therefore, the HIC and head injury risk for both adult and child pedestrians, produced at the side impact position at the vehicle centreline were relatively low compared with frontal and rear impacts, as shown in Figures 3-4 to 3-6, A-6 to A-8 and B-6 to B-8. This is probably a result of the effective angles of rotation about the frontal edge of the auto rickshaw, during frontal and rear impacts being lower than the side impacts, as shown in Figures A-2 and B-2. This may produce head-vehicle contact force variation during the variation in the pedestrian impact position. Even though, the front-end of the auto rickshaw is different than four wheel passenger vehicles, the results show a good agreement with the previous study by Simms and Wood (2005) [200], which reported that the side impacts produced low impact loads when compared to the frontal impacts at impact velocities of 18, 36 and 72km/h. This happens because of the lower effective radius of rotation about the frontal vehicle-end in the front and rear impact positions compared to the side position [200].

4.2.4.2 Head injury and risk level at primary impacts 42cm offset from the vehicle's centreline

During frontal impacts, the results show that the HIC exceeded the head injury thresholds $HIC_{15}=1000$ and 700 for the adult and child at 25 and 10km/h respectively, see Figure 3-7. Emphasising that the HIC for the child is greater than the adult by an average of 77 % at impact velocities between 10 and 40km/h. In addition, the head injury risks for the child is higher than the adult, as shown in Table C-4.

During rear impacts the adult head contacts occurred at 15-40 km/h, as presented in Figure 3-8 emphasising that the HIC exceeded the threshold $HIC_{15}=1000$ at 20 km/h or higher, as illustrated in Figure 3-8. Child head contacts exceeded the $HIC_{15}=700$ threshold between 10 and 40km/h, see Figure 3-8. These results emphasise that the HIC of the child is higher than the adult by an average 46 %, at impact velocities between 10 and 40km/h. Moreover, head injury risk for the child is greater than the adult, see Table C-5.

For the adult during side impacts, no HIC and head injury risks were produced at impact velocities between 5km/h and 40km/h, due to no head contacts was produced, see Figure 3-9. Child head impacts occurred at impact velocities between 15 to 40km/h, as shown in Figure 3-9. The results indicate that the HIC for the child exceeded the threshold $HIC_{15}=700$ at 15 km/h, as presented in Figure 3-9. Additionally, child head injury risk is greater than the adult, as shown in Table C-6. Although, side offset impacts are the safest scenario for adults, since no head impacts occurred with vehicle components, they are unsafe for children.

Thus, the HIC and head injury risk for both adult and child pedestrians, produced at the rear offset were relatively high compared with frontal and side impacts, as shown in Figures 3-7 to 3-9, A-9, A-10 and B-9 to B-11. These results emphasising that rear impacts at 42cm offset from the vehicle centreline are the most injurious scenarios, because they produced the highest head accelerations. This is a consequence of the interaction between adult and child pedestrian head contacting with the upper and lower curved sharp corner of both windscreen and windscreen frame respectively, having different stiffnesses, thicknesses and shape, as shown in Figure 3-3. The findings are in good agreement with the study of King (2018), which commented that the acceleration response to impact depends on the stiffness and the geometry of the surface impacted by the head [88]. In addition, these results are in good agreement with the previous studies of Jakobsson et al. [204], Muser et al. [205] and Linder et al. [206], all of whom concluded that the stiff structures of cars are responsible for high acceleration impulses and increasing risks of injury during primary impacts. Similarly, the study by Zhang et al. (2018), concluded that the stiffness of the front-end structure directly influences the head's acceleration during the vehicle-pedestrian impacts. When testing two head-forms for adult and child pedestrian impacts with a vehicle bonnet (hood), greater the stiffness of the structure, the higher the HIC [148].

In summary, impact velocity is a key factor in head injury and injury risk for both adults and children. These findings are in good agreement with many previous studies, which conclude that the head injury risk during primary impacts increases with impact velocity [57, 68, 149, 160-164, 175-180]. Therefore, HIC for both sizes increased remarkably with the vehicle impact velocity at both vehicle contact regions and all impact positions. Similarly, these responses show a good agreement with the study by Khorasani-Zavareh et al. (2015), that the transferred energy, during impacts, can be

increased with the vehicle impact velocity and produce harmful or fatal injuries [165]. Furthermore, a 6YO-child may sustain a serious or severe head injury at impact velocities that are lower than an adult. These results in a good agreement with previous studies, which concluded that size influences the injury risk [68, 69, 149, 166, 190, 191]. However, variation in the impact position and vehicle contact region showed significant HIC and head injury risk variation when the results showed that the HIC and head injury risk, produced during the rear offset scenario, are higher than other impact scenarios for both sizes. These outcomes, are in agreement with the study by Yao et al. (2007), demonstrate that the dynamic responses and injury outcomes, during primary impact, are significantly influenced by the initial posture and the orientation of a pedestrian. In addition, head impact injury risk to the child was influenced by the vehicle shape and stiffness of the frontal end of the vehicle [57].

There is, however, a significant difference between the HIC and injury risk between the 6YO-child and the adult. These findings are in agreement with the study of Venkatasan et al. (2014) [192]. This difference may arise because of the significant differences between the material properties of the viscoelastic materials used to define the skin material of the head for both adult and child dummies, as well as the bulk modulus of the adult, which is 21 times greater than the child, 0.5 and 0.0236, respectively. In addition, the rigid material that is used to define the skull material of the adult head has a Young's modulus that is three times greater than the child, 205 and 70, respectively. These differences mean that the adult's head is stiffer than the child's, which might result in less kinetic energy being transferred during impact to the adult head than child and could, in part, be associated with a lower predicted injury risk compared to the child. Furthermore, the disproportionality between relative aspects in terms of head mass, size, skin softness, elastic skull bones and neck support structures may form the basis for the higher incidence of head injury [192, 193]. Compared to the adult's head, these features make the head of the child less resistant to impact trauma [192, 193].

4.2.5 Upper neck injury and injury risk level during primary impacts

This section discusses for the first time the upper neck injury and injury risk for pedestrians impacted by the auto rickshaw considering the following parameters: impact velocity, impact position, vehicle contact region and pedestrian size. In

addition, (N_{ij}) was used to assess the upper neck injury risk for adult and pedestrians during frontal impacts. While (N_{km}) was only used for the adults in the rear impacts.

4.2.5.1 Upper neck injury and risk level during primary impacts at the vehicle's centreline

Pedestrian impacts at the centreline of the vehicle were assessed for frontal impacts by the Neck Injury Criterion, N_{ij} based on four different upper neck load cases, as shown in Figures A-11 and B-12, calculated from the combination of axial force and bending moment at the occipital condyle. N_{ij} is typically expressed in terms of the “worst-case” axial force and bending moment produced during an impact.

For the adult pedestrian a relative motion occurred between the head and torso towards the vehicle, which is due to frontal contacts between the headlamp and knees and the mudguard and tibia at impact velocities between 5km/h and 10km/h. No head or chest-vehicle impacts occurred. This pedestrian behaviour produced high compression and extension loads of 0.13KN and 6.31KN.mm, respectively. Compression-extension load case (N_{ce}), therefore, represented the worst load case of N_{ij} with values 0.16 and 0.2 respectively, see Figure A-11. Increasing the impact velocity between 15 and 40km/h produced a high momentum transfer, which led to a significant head and torso movement and chest and head contacts with the auto rickshaw components, as shown in Figure 3-1 (a).

This behaviour influenced the upper neck loads, which produced high tension loads between 1.5 and 4.37KN. The tension-extension load case (N_{te}), therefore, denotes the maximum neck load, which represent the N_{ij} at impact velocities between 15 and 40 km/h, as demonstrated in Figure A-11. The impact velocity exceeded the upper neck injury threshold $N_{ij}=1$ at 25 km/h and greater, see Figures 3-10 and A-13. The 6YO-child demonstrated a relative motion between the head and torso towards the vehicle, which is due to frontal impacts between the mudguard and lower leg and the headlamp and upper leg at 5km/h. No head or chest-vehicle impacts occurred, however, a high compression-extension load case (N_{ce}) was produced, which represented the worst N_{ij} load case, as demonstrated in Figure B-12. N_{ce} , corresponding to a value of 0.38 with an associated 17%, 8%, 13% and 4% risk of moderate AIS2+, serious AIS3+, severe AIS4+ and critical AIS5+ upper neck injury risks, respectively, see Figure B-14.

Increasing the vehicle impact velocities between 10 and 40km/h, produced a high momentum and kinetic energy transfer, which significantly accelerated the child's body to contact with the vehicle. In this case, the sequence of the contacts, included contact between the lower torso and the frontal headlamp and produced significant head and torso movement towards the vehicle components, resulting in child head-vehicle contacts, as shown in Figure 3-2 (a). This behaviour produced high tension loads, of between 0.6 and 1.6KN, compared to compressions, which were between 0.16 and 0.6KN at impact velocities between 10 and 40km/h. The tension-extension load case (N_{te}), therefore, represents the worst neck load, with N_{ij} between 10 and 40 km/h producing values between 0.90 and 2.93, see Figure B-12. The velocity at impact exceeded the injury threshold $N_{ij}=1$ between 15 and 40km/h, as shown in Figures 3-10 and A-13. In addition, the responses indicate that the N_{ij} for the child is higher than the adult by an average 100 % at impact velocities between 10 and 40km/h.

Rear impact related neck injury risk for adult pedestrians at the vehicle centreline was assessed by the Neck Injury Criterion, N_{km} based on four different load conditions, as shown in Figure A-12, calculated based on the combination of shear force and bending moment at the occipital condyle. Mostly, the upper neck injury loads during the rear impact at the centreline of the vehicle varied with impact velocity, as a result of head-neck movement. Flexion-anterior (N_{fa}) denotes the maximum load value of N_{km} at 5 km/h of 0.35, which indicated a forward motion. Extension-posterior (N_{ep}), indicated a rearward motion at 10km/h, with a value of 1.29. However, the flexion-posterior (N_{fp}) condition, indicates the forward motion was maximal at impact velocities between 15 and 25 km/h, corresponding with values between 1.68 and 2.25. The flexion-anterior (N_{fa}) load condition indicated a forward motion at 30km/h, corresponding to 2.47. Extension-posterior (N_{ep}) load conditions produced the highest risk upper neck load case, with a rearward motion at 32 km/h, corresponding to a value of 2.99. Extension-posterior (N_{ep}), was a rearward motion at impact velocities between 35 to 48 km/h, producing values from 4.65 to 5.94. Extension-anterior (N_{ea}) was excluded from the upper neck injury evaluation, since, it was lower than the other maximum load cases. Velocities between 10 km/h and 48 km/h exceeded the upper neck injury threshold $N_{km}=1$, as shown in Figure A-13, corresponding to an upper neck injury risk including serious neck injury corresponding to an AIS3+, shown in Figure A-15. However, the probability of moderate AIS2+ was 100% when an N_{km} of 5.94

was produced at 48km/h. While, the probability for sustaining serious AIS3+ and severe AIS4+ were almost 100% at an N_{km} of 4.88 at 35km/h, as shown in Figure A-15. A velocity of 5 km/h produced an N_{km} of 0.35, which is less than the neck injury threshold, but still represents a serious neck injury risk of 7.5%, as shown in Figures A-13 and A-15. These responses could be established as a useful database for use by vehicle designers in establishing a regulatory framework for the auto rickshaw.

4.2.5.2 Upper neck injury and risk level during primary impacts at 42cm from the vehicle's centreline

For the adult pedestrian, the simulations show that the pelvis impacted the frontal offset edge of the auto rickshaw windscreen frame, during the frontal impacts at the vehicle offset, at 5km/h, producing a relative head and torso movement towards the vehicle. In addition, as a result of low momentum transfer with the adult pedestrian at 5km/h, the torso inclined slightly towards the vehicle windscreen and this resulted in a superficial chest contact.

This behaviour produced a compression-extension load case (N_{ce}) representing the worst load case of N_{ij} , corresponding to a value of 0.16 at 5 km/h, see Figure A-16. High momentum and kinetic energy transfer was produced during adult pedestrian primary impacts at velocities between 10 and 25km/h, compared to 5km/h, producing N_{ij} values between 0.34 and 1.09. This can significantly influence the dynamic response of an adult pedestrian impacted by the auto rickshaw and result in a potential variation in the contact times for the adult-vehicle impacts. For example, the chest contact time reduced from 66 to 16ms at impact velocities between 10 and 25km/h, compared to 143ms at 5km/h, as shown in Figure A-22. This indicates that the adult chest contacted the vehicle windscreen earlier when the impact velocity increased, which means the adult torso and head accelerated more quickly towards the vehicle, resulting in noticeable head-windscreen impacts, as shown in Figure 3-3.

In addition, this kinematic response significantly influenced the head and torso motion and produced tension-extension loads (N_{te}) as the maximum neck load (N_{ij} values) at impact velocities between 10 and 25 km/h, as demonstrated in Figure A-16. Increasing the vehicle impact velocities from 30 to 40km/h led to a change in the body region contact sequence. For example, the first contact occurred between the pelvis and the front offset edge of the windscreen frame, then the upper right leg and the right hand

and arm impacted the front sheet plate. In addition, the chest impacted the windscreen and the right knee impacted the front sheet plate. Finally, the head impacted the windscreen, as shown in Figure 3-1 (b) and Table 3-3.

This kinematic response significantly influenced the upper neck load variation and produced tension loads between 2.8 and 3.7 times greater than the compression loads, at impact velocities between 30 and 40km/h, respectively. In addition, the flexion bending moments were between 2.8 and 4.0 times greater than the extension bending moments at impact velocities between 30 and 40km/h respectively. The tension-flexion (N_{tf}), therefore, was the maximum upper neck load at impact velocities between 30km/h and 40km/h, producing an N_{ij} of between 1.20 and 1.44, as shown in Figure A-16. The impact velocity exceeded the upper neck injury threshold $N_{ij}=1$ at impact velocities between 25km/h and 40km/h, see Figure 3-11. Whilst for the 6YO-child, asymmetrical impacts at 42cm offset from the vehicle centreline produced a significant body kinematic response, with a significant rotational movement about the right-hand-side of the vehicle. In addition, the contact order was the head with the windscreen and then chest and the right arm with the frontal offset edge, see Figure 3-2 (b).

This behaviour significantly influenced the head and torso motion and therefore, produced tension loads between 5.8 and 8.6 times greater than the compression loads at impact velocities between 5 and 40km/h, respectively. In addition, flexion bending moments were produced which were between 9.0 and 3.5 times greater than extension bending moments at impact velocities between 5 and 40km/h, respectively. Thus, the tension-flexion load case (N_{tf}) represents the worst load case of N_{ij} at impact velocities between 5km/h and 40km/h, corresponding to values of 0.40 to 3.21, see Figure B-13. The velocity of impact exceeds the injury threshold $N_{ij}=1$ at 15km/h and higher, as shown in Figures 3-11 and A-18. These results correspond to different injury risks of upper neck injury from 17-86%, 8-96%, 13-98% and 4-51% of moderate AIS2+, serious AIS3+, severe AIS4+ and critical AIS5+ injury risks, as shown in Figures B-15. In addition, most N_{ij} and upper neck injury risks for adults and children, produced during the impact at 42cm offset from the vehicle centreline, are higher, compared to those produced during the impact at the vehicle centreline, as shown in Figures A-14 and A-19. This might be a consequence of head impacts at the upper and lower curved sharp region of the windscreen and other body regions contacting with the vehicle

components, resulting in significant neck twisting during translation to the side of the vehicle, see Figure 3-3. However, the results show that the N_{ij} of the child is higher than the adult by an average 100 % at impact velocities between 10 and 40km/h.

Offset rear impacts were assessed by N_{km} , calculated based on the combination of shear force and bending moments at the occipital condyle. In general, the upper neck injury loads in the rear impact position at the vehicle offset varied with impact velocity because of head-neck movement. The forward motion produced the greatest risk of injury during impacts at velocities between 5 km/h and 20 km/h, with flexion-posterior (N_{fp}) representing the worst risk of N_{km} at 5 km/h, corresponding with a value of 0.4. Flexion-anterior (N_{fa}) at 10 km/h produced an N_{km} of 0.84 and flexion-posterior (N_{fp}) was the maximum upper neck load, when the impact occurred at velocities between 15 and 20 km/h, corresponding with 1.25 and 1.52, respectively. However, the extension-posterior (N_{ep}) provided the greatest risk of neck injury from a rearward motion at impact velocities between 25 and 48 km/h, corresponding with values from 2.23 to 5.60. Extension-anterior (N_{ea}) was excluded from the neck injury assessment, since, it was mainly lower than other upper neck load cases, as shown in Figure A-14. So, these responses exceeded the upper neck injury threshold $N_{km}=1$ between 15 km/h and 48 km/h, as shown in Figure 3-6, producing different injury risk levels, including serious neck injury AIS3+, as shown in Figure A-16.

In addition, the probability of moderate AIS2+ was 100% with an N_{km} of 5.6 at 48km/h. The probability of sustaining serious AIS3+ and severe AIS4+ injuries were 100% when the N_{km} was 4.32 at 30km/h, as shown in Figure A-16. The other neck injury values at 5 and 10 km/h were less than the neck injury threshold, though still represented injury risk, as shown in Figure A-16. Even when no head contact occurred with the auto rickshaw at 5 and 10km/h, such as rear-centre impacts, high neck loading occurred producing an N_{km} of 0.35 at 5km/h, which is associated with a 17%, 8%, 12% and 4% risk of moderate, serious, severe and critical upper neck injuries, respectively. While, 1.29 at 10km/h corresponded with a 38%, 34%, 46% and 10% risk, respectively, as shown in Figures 3-6 and A-16.

In summary, the, N_{ij} and N_{km} values for frontal impacts are considerable and increase with impact velocity. In terms of injury risk, the risks of head and upper neck injury for the 6YO-child are greater than the adult, thus a child may be seriously injured at impact velocities below those expected to produce injury in the adult, see Tables C-7

and C-8. These results are in good agreement with Liu and Yang (2003), who concluded that size significantly influences the injury risk at each body region [161] and Parr et al (2012), who commented that the variation in gender, neck strength, head size, neck length and body mass all influence N_{ij} [94]. Eppinger et al. (1999) [93] also commented that a variation in neck ligament stress, neck circumferences and neck length for adult and child might affect the injury severity. In addition, N_{km} and injury risk, during rear impacts, were higher than N_{ij} and injury risk during frontal impacts at both vehicle contact regions. The reasons for these responses is that N_{km} calculations depend on the instantaneous shear force, which is produced by the motion of the pedestrian's spine pushing the head forward and then pulling the head backwards, as shown Figure 3-1. The shear force, F_x , produces a high upper neck injury risk when compared to the axial force, F_z , acting during frontal impacts. Shear force is also associated with soft tissue injury to the intervertebral joints of the cervical spine, as specified in previous studies [145, 181]. Therefore, front and rear impact positions have a significant influence on upper neck injury and injury risk, while the vehicle contact region does not have a significant influence on the N_{ij} , exceeding the injury threshold at 25 km/h during frontal impacts (centreline and offset), as shown in Figures A-13 and A-18. A possible explanation is that tension-extension (N_{te}) load cases may have less of an effect when compared to other load cases on upper neck injury at low impact velocities between 15 and 25km/h, as shown in Figures A-11 and A-16. The vehicle contact region did effect rear impact N_{km} , when it exceeded the threshold at 10 km/h and 15 km/h for the rear-centre and rear-offset impacts, respectively, as shown in Figures A-13 and A-18, because they have different combination loads, which is extension-posterior (N_{ep}) and flexion-posterior (N_{fp}), as shown in Figures A-12 and A-17. In addition, the present study found that the upper neck injury risks, produced at the vehicle offset, are greater than those at the vehicle centreline. This might be a result of asymmetric impacts resulting in significant rotational movements for both the adult and child about the side of the vehicle.

Thus, the upper neck load cases and upper neck injury risk vary with impact velocity, impact position, vehicle contact region and pedestrian size a result of variations in the kinematic response, including the relative motion between the head and the torso. These results are consistent with Barbani et al. (2014), who concluded that during pedestrian impacts with motor vehicles that the neck is the most stressed body part

(severe or moderate level), due to the relative motion between the head and the torso [196]. In addition, even in the absence of head impact, upper neck injury can occur as a consequence of the kinematic response of adult and child pedestrians, resulting in head and neck accelerations. Moreover, upper neck injury N_{ij} and N_{km} risk will be more prevalent than head injury. What constitutes a low risk (harmless) impact velocity for upper neck injury will not be the same as a head injury, which means that head injury is typically assessed for pedestrian -vehicle impacts rather than inertia. However, neck injury is associated with head-neck movement, produced during the kinematic response to an impact. These findings are in good agreement with Lapner et al. (2003) [197] and McGeehan et al. (2006) [198], who concluded that the child's neck is easily injured.

Similarly, the results are in a good agreement with Elias et al. (2001) [199], who found that even though during child impacts, dummy head and chest impact loads did not exceed injury thresholds, neck injury N_{ij} could exceed the injury threshold in the majority of cases. These conclusions were established based on the analyses of the crash tests data during the front and side impacts for a school bus to assess the protective capability and injury mitigation for occupants during impact velocities between 48 and 72km/h.

There is currently no supported injury criteria that specifically considers neck injuries sustained during lateral impacts. One proposed solution to this issue is the multi-axial neck injury criteria (MANIC), which also includes the effects of side acceleration on the neck [131]. However, this injury criterion has not yet been approved so has no injury tolerance limits. In addition, the crash dummies used in the current study do not support the side neck injury calculations. Side impact related upper neck injury has not been investigated and is, therefore, recommended for future study.

4.2.6 Chest contact locations during primary impacts

With regard to chest impact, throughout the vehicle-adult pedestrian impact simulations in the frontal position, the most commonly impacted vehicle region was the windscreen. Changes in vehicle contact region produced variation in the chest impact contact location, see Figure A-21.

4.2.7 Chest contact duration during primary impacts

This section discusses the chest contact duration for the adult pedestrian impacted by the auto rickshaw in the frontal impact position at the vehicle centreline and 42cm offset at impact velocities between 5 and 48km/h for the first time. Chest contact duration, during frontal impacts, was investigated at different impact velocities at two vehicle contact regions (centreline and offset), see Figure A-22. For front-centre impacts, no chest-vehicle contact occurred at 5 km/h, a result of low momentum and kinetic energy transfer at the low impact velocity. All interactions occurred between the lower extremities and headlamp and mudguard. Chest contacts occurred when the impact velocity increased, a consequence of high momentum transfer in the vehicle direction and contact durations between 180ms and 30ms at impact velocities of 10km/h and 48km/h.

Front offset impacts produced chest contact durations between 143ms and 8ms at impact velocities between 5 and 48km/h. Therefore, chest contact time decreased with impact velocity, at both vehicle contact regions (centreline and offset). However, chest contact durations, offset from the vehicle centreline were less than centreline impacts, occurring earlier than the centreline impacts. An explanation is that the first impacts occurred with the frontal edge of the vehicle. While the first impact at the vehicle centreline was with the headlamp and the mudguard, this caused a delay to the chest impact with the windscreen, due to variation in the contact orders of the body regions, as shown in Table 3-1 and 3-3.

4.2.8 Chest injury and injury risk level during primary impacts

Chest injury risk during frontal impacts is represented by the Combined Thoracic Index (CTI), which is produced by considering the combination of the resultant spinal cord linear acceleration and the mid-sternum chest deflection at the central point of the chest. CTI is applied using the chest injury threshold, which is $CTI = 1$, reported in [93]. This represents a 25% risk of serious chest injury [92]. Impact velocity significantly affects chest injury [167]. In addition, the stiffness of the frontal vehicle structure has an influence on energy absorption and affects chest response (deformation). This section discusses the chest injury and injury risk for the adult pedestrian impacted by the auto rickshaw in the front impacts at impact velocities

between 5 and 48km/h at two vehicle contact regions (centreline and offset) using CTI for the first time.

For front-centre impacts, no chest contacts occurred at 5 km/h, however, contacts were produced at 10 km/h. CTI increased from 0.26 at 10km/h to 1.72 at 48 km/h. The response emphasises that CTI exceeded the chest injury threshold, $CTI=1$, at 35km/h and greater, see Figure 3-12. Chest injury risk, including serious chest injury, at 35km/h increased and exceeded the serious injury risk threshold AIS3+ (25% of serious injury AIS3+) by 24% with a CTI of 1.15, as shown in Figures A-23 and 3-12. In addition, the chance of moderate AIS2+ and serious AIS3+ chest injuries were 100% and 98%, respectively, when CTI was 1.72 at 48km/h, as shown in Figure A-23.

For the front-offset impacts, impact velocities between 5 and 48 km/h produced CTI values between 0.04 and 1.45. Thus, indicating that CTI exceeds the threshold, $CTI=1$ at 40km/h and greater, as shown in Figure 3-12 and chest injury risk, including serious chest injury AIS3+, increased and exceeded the serious injury risk threshold (25% of AIS3+) by 10% at 40km/h, producing a CTI of 1.07, as shown in Figure A-24. Increasing the impact velocity resulted in an increase in the resultant accelerations of the spinal cord and significantly influences the CTI and chest injury risk. Hence, it can be concluded that the CTI, produced during frontal impacts, increased with impact velocity at both vehicle contact regions (centreline and offset), providing a robust correlation between impact velocity and CTI during the primary impacts at both vehicle contact regions.

These findings are in some agreement with the only current available study by McNally and Rosenberg (2013), which investigated the risk of a 6YO-child during a cycle accident in three impact positions (at the vehicle centreline and both vehicle bumper corners) at impact velocities of 20, 30 and 40km/h. It was concluded that the probability of a serious thoracic injury, based on CTI, significantly linearly increased with impact velocity and increased the probability of sustaining a serious chest injury [174]. In addition, the responses are consistent with the study by Hyeok Park et al. (2016) [167], when investigating chest injury during unconstrained frontal impacts between human and mobile robots using MADYMO, which concluded that the CTI increased linearly with impact velocity at impact velocities between 1 and 5m/s. However, vehicle contact region did effect CTI and chest injury risk, when the injury

exceeded the threshold, CTI=1 at 35 km/h and 40 km/h for the front-centre and front-offset impacts, see Figure 3-12.

The spinal cord accelerations, which ranged between 22 and 155g and the mid-sternum chest deflection between 7 and 54mm, produced at the vehicle centreline, are higher than those produced during the offset impact, which produced spinal cord accelerations between 7 and 83g and mid-sternum chest deflections between 7 and 54mm.

4.3 Secondary impacts

Many variables of a pedestrian's initial position and posture influence the post-kinematic response and injury mechanics of real-world pedestrian-vehicle accidents. The unique geometry of the auto-rickshaw induced many varied post impact postural perturbations prior to secondary pedestrian - ground interactions. This section describes, for the first time, the sequences of those post impact kinematic responses for the adult pedestrian during the secondary impacts. The aim of this study is to enhance the safety of pedestrians in urban areas by providing kinematic, injury and injury risk data for subsequent application to the development of safety countermeasures. Therefore, it was essential to understand the influence of the front of the auto-rickshaw geometry on the pedestrian post-kinematic response during secondary impacts. In this study a 50th percentile male Hybrid III model was integrated with an auto-rickshaw finite element model and impact simulations run to produce secondary pedestrian - ground contacts at a selected range of pre-impact velocities between 10 and 40 km/h. The influence of the pedestrian's impact position (front, rear and side), during impact, was investigated at two vehicle contact regions (centreline and offset), producing six simulated impact mechanisms.

4.3.1 Kinematic response during secondary impacts

4.3.1.1 Kinematic response during secondary impacts at the vehicle's centreline

'Secondary impacts' describe a phase of a pedestrian – vehicle impact scenario when the pedestrian is judged to pass from the primary impact phase to a 'flying' and or 'falling phase'.

Related to front impact, the phase of secondary impact occurred between 162 and 105ms after the primary impact (post impact), at impact velocities between 15 and

30km/h, which indicated that the flying phase had begun; that the adult pedestrian had lost contact completely with the auto rickshaw and that both feet had left the ground. Variation in the impact velocities produced a variation in momentum transfer, such that the pedestrian was rotated about the vehicle side (left), see Figure 3-13. The falling phase began between 300 and 540ms post impact at impact velocities between 15 and 30km/h and was observed to produce a rear head to ground impact between 15 and 20km/h. While, impact velocity at 30km/h produced a face to ground impact, as shown in Figures 3-15 (a) and D-2.

For the rear impacts, a flying phase occurred when both feet left the ground between 280 and 100ms post impact at impact velocities between 10 and 30km/h. The falling phase began at between 185 and 455ms at impact velocities between 10 and 30km/h and produced face to ground impacts, as shown in Figures 3-13, 3-15 (a) and D-2.

During side impacts, the flying phase began between 185 and 90ms post impact at impact velocities between 15 and 35km/h, which indicates that the increasing impact velocity reduced the flying time, due to an increased momentum and kinetic energy transfer during the primary impact. The landing phase began between 510 and 705ms at impact velocities between 15 and 35km/h and produced a face to ground contact at all impact velocities, as shown in Figures 3-13, 3-15 (a) and D-2. This behaviour may be a result of the unique frontal design of the auto rickshaw and the associated impact position and posture, which significantly influences the pedestrian kinematic response as a result of changes to the position of the centre of gravity.

The responses show good agreement with Peng et al (2012), who investigated the effects of pedestrian gait, vehicle-frontal geometry and impact velocity on the kinematics of the adult and child pedestrian head. The study concluded that leg posture had a significant influence on the dynamic response of the adult, resulting from a change in position of the centre of gravity [151]. In addition, leg posture caused a significant rotational movement to the adult pedestrian head, through more than 110, 135 and 180 degrees at impact velocities of 15, 30 and 35km/h, respectively, before impacting the ground, see Figure 3-15 (a).

These findings are in good agreement with the study of Hamacher et al (2012), which concluded that the pedestrian's rotation is highly influenced by leg and arm posture during the impacts between a pedestrian and a vehicle [72]. Thus, it can be concluded that an increasing vehicle impact velocity increases the rotational angle of a pedestrian

body and may significantly influence the pedestrian contact landing order. These findings are in agreement with the study of Shi et al. (2018), which found that increasing vehicle impact velocity increased the rotational angle of the pedestrian body and was highly correlated with the pedestrian-ground landing mechanisms [176].

In addition, in most impact positions at the vehicle centreline, the landing patterns and contact orders, between the adult body regions and the ground, varied with impact velocity, see Figure D-2. Moreover, at most impact positions at the vehicle centreline, the right and the left feet contacted with the ground, which produced a potential ankle rotation. This might be as a result of the body mass being concentrated at the ankle joints during the landing phase and might generate high contact forces because of the effect of pedestrian posture. Therefore, the pedestrian might have a high potential for severe right ankle injury.

4.3.1.2 Kinematic response during secondary impacts at 42cm offset from the vehicle's centreline

During frontal impacts, the phase of secondary impact occurred between 92 and 82ms post impact at impact velocities between 20 and 30km/h, which indicated that the flying phase had begun, that is, when both feet left the ground and the adult pedestrian lost contact completely with the auto rickshaw. In addition, a significant body rotation, about the vehicle side, occurred as a result of the asymmetric impacts, see Figure 3-14. The falling phase began between 182 and 222ms post impact, at impact velocities between 20 and 30km/h and was observed to produce no head to ground impacts, as shown in Figures 3-15 (b) and D-4.

For the rear impacts, a flying phase began when both feet left the ground at between 33 and 22ms post impact at impact velocities between 15 and 30km/h. The falling phase began between 130 and 312ms at impact velocities between 15 and 30km/h and was observed to produce no head impacts at 15km/h. In addition, a rear head to ground impact and face to ground contact was observed at 25 and 30km/h, as shown in Figure D-4.

During the side-offset impact scenario, the flying phase began between 75 and 47ms post impact at impact velocities between 15 and 40km/h. The falling phase occurred between 272 and 345ms, producing rear head-ground impacts at impact velocities between 15 and 35km/h. When the impact velocity increased to 40km/h, a significant

adult pedestrian dynamic face to ground impact response was produced. During this impact scenario, the sequence of landing patterns was similar to that produced by van vehicles reported in the study of Crocetta et al. (2015) [70], which reported that the most common impact mechanism for an adult pedestrian impacted by a van, firstly produced pelvis or legs-ground impacts, followed by torso and the head impacts, see Figures 3-14 and 3-15 (b).

In addition, for the impacts at 42cm offset from the vehicle's centerline, the landing patterns and contact orders between the adult body regions and the ground varied with impact velocity, see Figure 3-15 (b). Moreover, in most cases, the sequence of pedestrian-ground-contact was feet, knees, upper legs and pelvis. This occurred because the rotation of the pedestrian's body was inadequate to raise the pelvis and torso above the head, before ground interactions occurred. The pelvis impacted with the ground first, followed by the feet, knees and legs. The results are in a good agreement with Otte and Pohlemann (2001) [54], who used a real pedestrian dummy and impacted it with a car at 79km/h and reported that the body flew nearly at the vehicle velocity, before colliding with the ground with the left knee first. However, in the present study, direct head-ground contact only occurred in the side position at the vehicle's centerline, resulting from the significant rotational behaviour, which is influenced by the walking position posture, as shown in Figure 3-13. This could be as a result of increasing vehicle impact velocity, which leads to a post impact kinematic response and pedestrian landing sequence change, see Figure 3-14.

Although the front-end of the auto rickshaw is different to the Sedan, Minicar, SUV, MPV and One-box vehicle, the findings are in good agreement with the study of Shi et al. (2018), which reported that increasing vehicle impact velocity increases the pedestrian body rotational angle and is highly correlated with the pedestrian-ground landing mechanisms [176]. It was previously established that the four-wheel vehicle bumper impacts the lower legs, causing both feet to leave the ground. Additionally, the leading edge strikes the upper legs and torso, after which the pedestrian's body rotates towards the bonnet (hood) (Tamura and Duma, 2011) [71]. The simulation responses indicate that the frontal shape geometry of the three-wheeled vehicle result in a very different post impact -kinematic response than that produced by four-wheeled vehicles.

A notable correlation was found between the initial conditions, such as impact orientations, vehicle contact regions and vehicle impact velocity, pedestrian body movement and rotation, which could lead to a significant change in pedestrian kinematic movement. These findings are in good agreement with the study by Crocetta et al. (2015) [70], which concluded that the changes in pedestrian posture during the side impact position and changes in impact velocity influence pedestrian dynamic response, which leads to different-ground contacts and landing mechanisms. In addition, these findings are consistent with Kendall et al. (2006) [68], who concluded that the vehicle impact velocity, pedestrian stances and impact orientation all influence kinematic response and ground impact mechanisms.

4.3.2 Throw distance

Forward projection occurs when a relatively high-fronted vehicle geometry impacts a pedestrian [155]. An auto rickshaw has a relatively high front-end geometry, thus, in some cases, a significant throw distance can be expected. The throw distance can be calculated from the kinematic response of the adult pedestrian during reconstruction of different impact scenarios. Bhalla et al (2002) [53] reported that throw distance, a combination of flying, falling and sliding distance, was directly affected by vehicle-pedestrian geometry by almost 45%, when investigating three different vehicle types (SUV, Mid and small size vehicles) impacted with different pedestrian sizes (50th and 95th adults male, 5th adult female and 6 and 9YO-children) at impact velocities between 20 and 60km/h. The influence of the auto rickshaw frontal geometry has not been previously investigated. In this present study, therefore, throw distance was investigated at two auto-rickshaw contact regions (centreline and offset) in three different impact positions for the adult male pedestrian 50th (front, rear, and side) at a range of impact velocities between 10 and 40km/h.

4.3.2.1 Throw distance at the vehicle's centreline

For frontal impacts at the vehicle centreline, the range of the throw distances was between 3.4 and 6.8m at an impact velocity of between 15 and 30km/h, the rear position was produced 3.3 and 7.1m at between 10 and 30km/h and the side impact between 3.7 and 8.0m at between 15 and 35km/h, see Figure 3-16. The throw distances produced during side impacts was potentially higher than those produced at the other positions, considering the total weight of the auto-rickshaw vehicle and the mass of

the driver. Even though frontal geometry and mass are different for four-wheeled vehicles, these results are consistent with other studies, which predict that velocities of 25km/h might produce forward projection distances of almost 5m [71, 155]. This is also in agreement with Fugger et al. (2002) [183] and Wood et al. (2005) [186], who related the pedestrian projection distance estimated by numerical model to vehicle impact velocity, proposing that the forward throw distance of the impacted pedestrian would be in the range of 3–11m, at impact velocities of 25km/h. This may be as a result of the vehicle's unique frontal geometry, similar to box and van vehicles, which cause high momentum transfer at the vehicle's centerline. Consequently, the pedestrian's body was projected forward in the vehicle's impact direction. These results in good agreement with Hamacher et al. (2012), who reported high bonnet leading edge (BLE) vehicles such as, one box produced a high throw distance [72] as a result of high momentum transfer with high (BLE) vehicles compared to other vehicles.

4.3.2.2 Throw distance at 42cm offset from the vehicle's centreline

During impacts at 42cm offset from the vehicle centerline, for frontal impacts, the throw distances between 1.7 and 2.9m, at 20 to 30km/h and rear impacts a range of throw distances between 0.9 and 3.7m at impact velocities between 15 and 30km/h. The side impact position throw distance range was between 2.1 and 5.0m at 15 to 40km/h. These results indicate that the throw distance produced at the vehicle's centerline was greater than that produced at the vehicle offset in all impact positions (front, rear and side), as shown in Figure 3-17; as a result of high momentum and energy transfer in the forward travel, with less body rotation to the vehicle side. Impact at the vehicle offset, however, caused a significant rotation to the left-hand side of the vehicle, due to impact asymmetry about the right and left hand side. Moreover, offset impact orientations caused the pedestrian's body to imbalance, producing a subsequent rotation around the longitudinal axis because of the unique frontal design of the auto-rickshaw.

To conclude, throw distance significantly increased with impact velocity at all impact positions and both vehicle contact regions. These findings are in good agreement with previous studies, which found that the throw distance increases with impact velocity [53, 72, 160, 183-186]. However, throw distance produced at the vehicle centreline

was greater than that produced at the offset, because no significant rotational movement about the vehicle's side was produced. Therefore, a robust relationship between vehicle impact velocity and throw distance was established for all impact cases. However, with respect to impact position, the vehicle contact region and contact period had a significant influence on throw distance, which is consistent with the study by Bhalla et al (2002), who concluded that a robust relationship can be seen between the vehicle impact velocity and total throw distance. In addition, it was concluded that pedestrian impact position influences throw distance by up to 28% [53]. Throw distance is, however, also sensitive to other impact parameters, such as relative pedestrian vehicle geometry and vehicle contact regions.

4.3.3 Comparison of the kinematic response of an adult pedestrian during impact a Real-World accident with simulations

Accident reconstruction is a method for simulating the road accident environment and conducting in-depth biomechanical engineering analyses for identifying the cause and effect relationships of injurious scenarios. It is significantly useful in developing recommendations for making roads and vehicles safer by resulting in improvements to safety for all road users, including the vulnerable road users (VRUs).

In terms of pedestrian post-kinematic response, a real CCTV video of pedestrian-auto-rickshaw impact to the rear-offset position was captured and a simulation conducted of computational impacts at three different velocities; 15, 25 and 30km/h, considering the vehicle's impact velocity, total mass including (vehicle mass and passengers) and exact vehicle impact region.

The post-kinematic response results show that during the primary impacts, the sequence of the main interactions occurred between the lower torso and the front leading edge and the head-windscreen/frame, as shown in Figure 3-1. The contact time varied with impact velocity; increasing the impact velocity led to a significant rotation to the vehicle side, as a result of a high momentum transfer produced during the increasing impact velocities. During the secondary impacts, which began when the pedestrian body loses contact with the vehicle, the adult pedestrian impacted the ground with both feet, then landed on his knees at 15km/h, with no torso and head-ground impacts occurring as a result of a low momentum transfer to the pedestrian body, as shown in Figures 3-15 (b) and 3-18 (a). When the impact was simulated at

25km/h, the pedestrian fall sequence with the ground was tibia, knee, arm, torso and finally the head. In addition, sliding with a rotational movement to the body was observed during the impact as a result of high momentum transfer during the impact period, as a result of the influence of the impact at 42cm offset from the vehicle centreline and the asymmetrical impacts, as shown in Figures 3-15 (b) and 3-18 (b).

During the impact at 30km/h, the sequence of landing was feet, knees, hand, legs and finally head-ground contact, see Figure 3-18 (c). Therefore, the simulation results at an impact velocity of 25km/h shows the greatest agreement with the Real-Accident scenario, during both the primary and secondary phases, see Figure 3-18 (b) and (d). As a result of an absence of real-accident relevant to pedestrian-auto rickshaw impacts. The simulations can, therefore, be considered as a validation of the pedestrian-auto rickshaw impact model, which is used in this study. In addition, the computational results are very useful for predicting the likely impact velocity during a road accident, for reconstructing the kinematics of road accident scenarios and to analyse the accident factors and impact environment accurately to improve the safety in urban areas.

4.3.4 Head injury and injury risk level during secondary impacts

Head injury risk was evaluated during secondary impacts by using the head injury criterion HIC_{15} . All HIC produced during different impact scenarios were converted to Abbreviated Injury Scale (AIS) coding to assess the head injury severity risk. The three impact positions were simulated at impact velocities at between 10 and 40km/h at the vehicle centerline and offset.

4.3.4.1 Head injury and injury risk level during secondary impacts at the vehicle's centreline

For frontal impacts, following the impact direction of the pedestrian head with the ground, rear-head-ground impacts occurred at 15 and 20km/h. While, the front-head-ground impacts occurred at 30km/h, see Figure 3-19. HIC and injury risk levels were significantly higher and fluctuated with impact, producing HIC values of 4277, 3426 and 3696 at 15, 20 and 30km/h, respectively. The results indicate that the HIC exceeded the threshold $HIC_{15}=1000$ at all impact velocities, even at the relatively low impact velocities of 15 and 20km/h, see Figure D-1, and generated a 100% fatal head injury risk, as shown in Table D-1.

For rear impacts, following the impact direction of the pedestrian head with the ground, front-head-ground impacts occurred at impact velocities of 10, 15 and 30km/h, see Figure 3-19. HIC values and injury risk levels were potentially high and fluctuated with impact velocity, producing HIC values of 4382, 3839 and 5617 at 10, 15 and 30km/h, respectively. The results emphasise that the HIC exceeded the threshold $HIC_{15}=1000$ during all impact velocities, including a low impact velocity of 10km/h, see Figure D-1, and generated 100% fatal head injury risk, as presented in Table D-1.

For side primary impacts, following the impact direction of the pedestrian head with the ground, front-head-ground impacts occurred at impact velocities of 15, 30 and 35km/h, as shown in Figure 3-19. Therefore, the frontal head injury threshold of 1000 was applied, rather than the side impact threshold (800) during the secondary impacts. HIC and injury risk levels were significantly greater and fluctuated with impact velocity, producing HIC values of 227, 6126 and 1260 at 15, 25 and 35km/h, respectively. The simulations show that the HIC exceeded the threshold $HIC_{15}=1000$ with a significant injury risk level for all impact velocities, even at a low impact velocity of 15km/h; see Figure D-1 and Table D-1.

4.3.4.2 Head injury and injury risk level during secondary impacts at 42cm offset from the vehicle's centreline

Frontal impacts, follow the impact direction of the pedestrian's head with the ground shown in Figure 3-20, no head contact occurred with the ground at impact velocities of 20, 25 and 30km/h. A logical explanation is that significant body rotation to the vehicle side as a result of asymmetry, produced a landing sequence of left foot, right foot, right leg, pelvis and right elbow, see Figure 3-15 (b).

During impacts to the rear, following the impact direction of the pedestrian head with the ground, no head-ground contact was observed at 15km/h, the adult pedestrian fell on the ground on the knees, as demonstrated in Figure 3-20. When the impact velocity increased to 25 and 30km/h, rear-head-ground and front-head-ground impacts occurred, as demonstrated in Figure 3-20, producing HIC values of 1957 and 580, respectively, as shown in Figure D-2. The results indicate that the HIC produced at 25km/h exceeded the threshold $HIC_{15}=1000$ at 25km/h with a high head injury risk probability, see Figure D-2 and Table D-2. However, the HIC produced at 30km/h was below the threshold $HIC_{15}=1000$, as shown in Figure D-2.

For side impacts, following the impact direction of the pedestrian head with the ground, front-head-ground impacts occurred at impact velocities of 15, 20, 25, 30 and 35km/h, as shown in Figure 3-20, producing HIC values of 6861, 419, 7780, 2130 and 418, respectively, as shown in Figure D-2. While, the rear-head-ground impact occurred at 40km/h, as illustrated in Figure 3-20, producing a HIC value of 5894, see Figure D-2. Therefore, the head injury threshold of 1000, for front and rear impacts, was applied instead of the 800 for the side impacts. The simulations emphasise that the HIC and injury risks fluctuate with impact velocity and exceed the threshold $HIC_{15}=1000$ at 15, 25, 35 and 40km/h, as shown in Figure D-2, with almost a 100% fatal head injury risk at impact velocities of 15, 25 and 40km/h, see Table D-2.

To summarise, HIC produced at all impact positions and both vehicle-contact regions fluctuated with impact velocity. Head injury risk was associated with HIC and produced high injury risk. Variation in the vehicle contact area, impact position and impact velocity significantly influenced pedestrian landing patterns. These outcomes are in a good agreement with Gupta and Yang (2013), who concluded that the landing injuries are significantly varied with vehicle contact location during front of vehicle impacts at the vehicle centreline and at the bumper corner. The study examined three pedestrian sizes, 5th, 50th adults and 6YO-child, impacted by two frontal vehicle geometries, mid-size vehicle and SUV, at impact velocities of 30 and 40km/h [182]. The current study determined that HIC and injury risk varied with impact velocity, vehicle contact region and impact position. In addition, there was no robust correlation between HIC and impact velocity, which is in good agreement with previous studies [68, 156, 176, 182], which concluded that there was no obvious correlation observed between pedestrian HIC-ground and impact velocity. Moreover, the present study concluded that the HIC was influenced by landing patterns, which is in a good agreement with Shi et al (2018), who concluded that the head injury risk was influenced by pedestrian body landing order [176]. The study was investigating four pedestrian sizes, 50th, 95th of adult male pedestrians, 5th adult female 10YO-child pedestrian impacted by five different frontal vehicle ends, Sedan, minicar, SUV, MPV and one box at impact velocity of 30 and 40km/h in the side impact position.

4.3.5 Upper neck injury and injury risk level during secondary impacts

Upper neck injury values and risk levels were investigated for the front, rear and side impacts at both vehicle contact regions (centreline and offset).

4.3.5.1 Upper neck injury and injury risk level during secondary impacts at the vehicle's centreline

The front, secondary impact related neck injury, following the impact direction of the pedestrian head with the ground, resulted from the kinematic response and body rotation during different impact velocities. No significant N_{ij} value was produced at an impact velocity of 15 and 20km/h, because the pedestrian impacted the ground via back-face-contact, see Figure 3-19. However, the extension-posterior (N_{ep}) load with rearward motion produced N_{km} values corresponding to 1.78 and 4.49 at 15 and 20km/h, respectively, as shown in Figure D-3 and Table 3-6. In the neck injury load cases, flexion-anterior (N_{fa}), flexion-posterior (N_{fp}) and extension-anterior (N_{ea}) were excluded from the upper neck injury assessment. Since, their values were lower than the maximum load (N_{ep}), see Figure D-3. This indicates that the upper neck injury values exceeded the threshold $N_{km}=1$ at 15km/h, as shown in Table 3-6 and were associated with a 52% risk of AIS2+, 57% of AIS3+ and approximately 70% of AIS4+ and 16% of AIS5+, see Figure D-4. However, the upper neck injury risks were significantly greater at 20km/h, producing a 97% risk of AIS2+, nearly 100% of AIS3+ and AIS4+ and 83% of AIS5+, as shown in Figure D-6. When the impact velocity increased to 30km/h, the kinematic response changed, producing face-to-ground contact as shown in Figure 3-19, and compression-flexion (N_{cf}) load producing an N_{ij} value corresponding to 0.7.

Compression-extension (N_{ce}), tension-extension (N_{te}) and tension-flexion (N_{tf}) upper neck loads were excluded from the upper neck injury valuation, since their values were lower than the worst load case (N_{cf}), as demonstrated in Figure D-3. The upper neck injury value was below the threshold $N_{ij}=1$ and produced upper neck injury risks lower than those produced by N_{km} at 15 and 20km/h, see Table 3-6 and Figure D-6.

Rear secondary impacts, following the impact direction of the pedestrian head with the ground, resulted from different landing patterns caused by an increasing impact velocity. No N_{km} values were produced at impact velocities between 10 and 30km/h, because the pedestrian impacted the ground with the face, as illustrated in Figure 3-19. Therefore, compression-extension (N_{ce}) load case of N_{ij} between 1.98 and 1.23 were produced at impact velocities between 10 and 30km/h, respectively, as demonstrated in Figure D-4 and Table 3-6. Upper neck injury loads for tension-

extension (N_{te}), tension-flexion (N_{tf}) and compression-flexion (N_{cf}) were excluded, see Figure D-4. These values, indicate that N_{ij} values exceeded the threshold $N_{ij}=1$ at 10 km/h and greater, as presented in Table 3-6, equivalent to 58% risk of AIS2+, 66% of AIS3+, 77% of AIS4+ and 19% of AIS5+, see Figure D-7.

During side impacts, following the impact direction of the pedestrian head with the ground, secondary impacts produced compression-extension (N_{ce}) values, categorised as a worst load case N_{ij} values of 1.26 and 2.47 at impact velocities between 15 and 35 km/h, as shown in Figure D-5 and Table 3-6. For the upper neck loads, compression-flexion (N_{cf}), tension-extension (N_{te}) and tension-flexion (N_{tf}) were excluded, as illustrated in Figure D-5. These values indicate that N_{ij} exceeded the threshold $N_{ij}=1$ at 15 km/h, as shown in Table 3-6 and correspond to a 37% risk of AIS2+, 32% of AIS3+, 45% of AIS4+ and 9% of AIS5+, see Figure D-8.

4.3.5.2 Upper neck injury and injury risk level during secondary impacts at 42cm offset from the vehicle's centreline

During the front secondary impacts, no N_{ij} and injury risk to the front and rear of the neck, N_{ij} and N_{km} , were produced at all impact velocities between 20 and 30km/h, since, the neck movement tended to move in to the side, as shown in Figure 3-20.

During rear offset secondary impacts, no head-ground impact occurred at 15km/h due to the pedestrian's knees first contacting with the ground, see Figure 3-20. However, even though no head-ground contacts occurred at 15km/h, flexion-posterior (N_{fp}) load characterised the worst-case risk (N_{km}) of 1.10 at 15km/h, a consequence of the pedestrian body forward motion, which corresponds to a 32% risk of AIS2+, 26% of AIS3+, 37% of AIS4+ and 8% of AIS5+, see Figure D-11. Meanwhile, the extension-anterior load was the maximum load condition (N_{ea}) at 25 km/h with a value of 2.02, which is associated with a rearward motion, as shown in Figure D-9 and Table 3-7. Moreover, both (N_{fp}) and (N_{ea}) produced at 15 and 25km/h exceeded the threshold $N_{km}=1$ even with no head-ground contact at the low impact velocity of 15km/h, see Figure D-11 and Table 3-7. When the impact velocity increased to 30km/h, the kinematic response changed, resulting in an increased whole pedestrian body acceleration, producing different body-ground contact orders and times, as presented in Figure 3-15 (b). A significant head-ground impact direction changed the orientation to face to ground, see Figure 3-20. A compression-flexion (N_{cf}) load was produced,

which signifies that the N_{ij} produced with a value of 0.5, was below the threshold $N_{ij}=1$; as demonstrated in Figure D-9 and Table 3-7.

The side secondary impact, following the impact direction of the pedestrian head with the ground, presented in Figure 3-20, resulted from a rear-ground impact. Extension-posterior (N_{ep}), with a rearward motion, was produced during most impact velocities, with values of 3.5, 2.0, 4.5 and 3.2 at 15, 20, 25 and 35km/h, respectively, as illustrated in Figure D-10 and Table 3-7. Nevertheless, extension-anterior (N_{ea}) with forward motion produced an N_{km} value of 4.08 at 30km/h. Two upper neck loads were omitted from the upper neck injury assessment, flexion-anterior (N_{fa}) and flexion-posterior (N_{fp}), see Figure D-10 and Table 3-7. A face to ground impact occurred at 40km/h, producing a N_{ij} of 0.78, which represents tension-extension (N_{te}), as shown in Figure D-10 and Table 3-7. Even with a high impact velocity the N_{ij} was below the threshold $N_{ij}=1$, as shown in Table 3-7 and was associated with low upper neck injury risk, see Figure D-12. Meanwhile, N_{km} exceeded the threshold $N_{km}=1$ at 15 km/h and produced an 89% risk of AIS2+, 97% serious injury AIS3+, 98% of AIS4+ and 59% of AIS5+, as shown in Figure D-12.

Although, this study shows that the upper neck injury risk is correlated with N_{ij} and N_{km} , there was no robust correlation between the upper neck injury values and vehicle impact velocity. During secondary impact, both N_{ij} and N_{km} depends on the head-ground direction and head-neck movement. Secondary impact was influenced by the post-kinematic response, specifically the landing patterns, which were influenced by factors such as impact velocity, impact position and vehicle contact region, which led to upper neck load variations. In addition, the upper neck injury risk, produced from the ground contacts, was significant even at the low impact velocity of 10km/h, indicating that upper neck injury values including N_{ij} and N_{km} were quite sensitive.

4.3.6 Chest injury and injury risk level during secondary impacts

Combined Thoracic Index (CTI) was used to assess chest injury and risk level during frontal impacts at both vehicle contact regions (centreline and offset) during secondary impacts.

4.3.6.1 Chest injury and injury risk level during secondary impacts at the vehicle's centreline

During frontal secondary impacts, following the impact direction of the pedestrian frontal chest with the ground, no front chest-ground contacts were observed at 15 and 20km/h. This may be a result of the significant rotation of the pedestrian body about the frontal geometry of the auto rickshaw, the adult pedestrian body impacting the ground at the pelvis, left shoulder and torso, see Figures 3-15 (a) and 3-20. When the impact velocity increased to 30km/h, the pedestrian's body accelerated with high forward velocity in the vehicle impact direction. The adult pedestrian impacted the ground with the left foot and right knee between 500 and 675ms post impact, see Figures 3-13 and 3-20, corresponding to a CTI of 0.7, which is below the CTI=1 threshold, see Table 3-8, which predicates a 34% risk of AIS2+, 3.8% of AIS3+, 0.75% of AIS4+ and 0.01% of AIS5+, as illustrated in Figure D-13.

For rear secondary impacts, following the impact direction of the pedestrian frontal chest with the ground, front chest-ground contacts were observed at all impact velocities, as a result of a change in the impact direction, as demonstrated in see Figure 3-19. The CTI fluctuated between 0.46 and 0.41 at impact velocities between 10 and 30km/h, as shown in Table 3-8. All CTI values were below the threshold CTI=1, see Table 3-8 and indicate different injury risk levels. However, the maximum CTI of 0.74 at 15km/h corresponds to a 40% risk of AIS2+, 5% of AIS3+, 1% of AIS4+ and 0.01% of AIS5+, as illustrated in Figure D-14.

For secondary side impacts, following the impact direction of the pedestrian frontal chest with the ground, even though the initial impact position was to the side, front chest-ground contacts were produced at all impact velocities, as shown in Figure 3-19. Variation in the landing patterns, were observed at different impact velocities, as presented in Figure 3-15(a). The CTI varied from 0.46 to 0.25 at impact velocities between 15 and 35km/h, as shown in Table 3-8. None of the CTI exceeded the chest injury threshold CTI=1, see Table 3-8. However, the maximum CTI of 0.57 at 30km/h indicates 19% risk of AIS2+, 1.5% of AIS3+, 0.3% of AIS4+ and 0% of AIS5+, as shown in Figure D-15.

4.3.6.2 Chest injury and injury risk level during secondary impacts at 42cm offset from the vehicle's centreline

Front secondary impacts follow the impact direction of the pedestrian frontal chest with the ground. No front chest-ground contacts occurred, as shown in Figure 3-20, as a result of the asymmetric impact at the vehicle offset, which produced a significant kinematic response and body rotation to the left side of the vehicle. Moreover, it also introduced a clear imbalance in the post-kinematic response, compared to that at the vehicle's centerline. The torso, femur and tibia contacted with the ground, rather than the head and chest, at all impact velocities between 20 and 30km/h, as shown Figure 3-15 (b).

Rear secondary impacts follow the impact direction of the pedestrian frontal chest with the ground. No chest-ground contacts occurred at 15 and 25km/h, see Figure 3-15, thus, no CTI, as shown in Table 3-9. Therefore, there was no chest injury risk associated with the different body-ground contact orders, as shown in Figure 3-15 (b). When the impact velocity increased to 30km/h, a significant impact force was generated, which accelerated the whole body and changed the impact direction, producing front chest-ground contact, see Figure 3-20. The measured CTI was 0.18 at 30km/h, which is below the threshold $CTI=1$, as shown in Table 3-9. The results indicate a 2% risk of AIS2+, 0.09% of AIS3+, 0.02% of AIS4+ and 0% of AIS5+, see Figure D-16.

Side secondary impacts follow the impact direction of the pedestrian's frontal chest with the ground. No chest-ground contacts occurred at impact velocities between 15 and 35km/h, with no CTI resulting from the different kinematic response and landing patterns, see Figures 3-20 and 3-15 (b). When the impact velocity increased to 40km/h, a significant impact force was generated. This accelerated and unbalanced the whole body, changing the kinematic response and impact direction and producing a front chest-ground contact, as illustrated in Figure 3-20, with a CTI of 0.18, which is below the threshold $CTI=1$, as demonstrated in Table 3-9. The results indicate a 2% risk of AIS2+, 0.09% of AIS3+, 0.02% of AIS4+ and 0% of AIS5, as shown in Figure D-17.

Therefore, all CTI produced during the secondary impacts varied with impact velocity and depended on the pedestrian's landing patterns and impact direction with the

ground. No robust relationship could be established between CTI and impact velocity during the secondary impacts, CTI and chest injury risk during the secondary impacts are sensitive.

4.4 The sensitivity of the model contact parameters.

The results of the sensitivity analysis for the contact parameters have been reported, based on the friction coefficient variation between the adult pedestrian-vehicle and the pedestrian feet-ground/ the vehicle's tyre-ground. The analysis includes the kinematic response and associated head injury risk during primary and secondary impacts.

4.4.1 Primary impacts

In general, results for the original impact scenario show that offset impact scenarios produced a significant rotation to the vehicle right side, when the friction coefficient between the vehicle's tyre-ground/pedestrian shoes-ground was 0.7 and the friction coefficient between the pedestrian-vehicle was 0.65, see Figure 3-21 (a). In addition, the results show that the rear offset impact scenario is the worst case scenario, producing the most injurious impact scenario during primary impacts. This section will discuss the kinematic response and head injury risk during primary impacts considering the variation in friction coefficients.

4.4.1.1 Kinematic response

Noticeably, rear offset impact scenarios produced a significant body rotation, owing to the interaction between the frontal leading edge of the vehicle and the lower torso during all impact scenarios, as shown in Figure 3-21 and, therefore, no significant kinematic response change was observed during the variation in friction coefficients during primary impacts.

4.4.1.2 Head injury

The results show that variation only in the friction coefficient is relevant to contact between pedestrian and vehicle 0.30 and 0.75, for the first and second impact scenarios instead of 0.65 for the original impact scenario could cause a slight HIC value reduction, see Table 3-10. Whilst, the variations in other friction coefficients relevant to the contact between pedestrian shoes and ground and vehicle tyre and ground could result in HIC fluctuation, see Table 3-10. Thus, the variation in friction coefficients

for the current study contact model has no significant influence on a head injury during primary impacts.

4.4.2 Secondary impacts

4.4.2.1 Kinematic response

In general, the results show that the variation in friction coefficients still produces a significant pedestrian body rotation to the right side of the vehicle. In addition, similar frictional coefficients for contacts between the pedestrian and the vehicle result in a similar kinematic response, see Figure 3-21 (a, d and e); (b and f) and (c and g). Moreover, using the same frictional coefficient value (0.65), for contacts between the pedestrian and vehicle produce similar kinematic responses to the original impact simulation with head-ground contacts, see Figure 3-21 (a), (d) and (e). Even though the variation in both frictional coefficients relevant to the vehicle and ground results in no head-ground contacts., these impact scenarios produced variation in the kinematic response, body-ground contact orders and the interaction time, see Figure 3-21.

4.4.2.2 Head injury

During rear offset impacts, the head-ground impacts occurred only in three different impact scenarios, the original, the third and the fourth scenarios only when the friction coefficient was defined as 0.65 and produced face to ground contacts with HIC value of 580, which is below the threshold, (HIC=1000), see Figure 3-21 (a), (d), (e) and Table 3-11. Therefore, there was no influence on HIC during all impact scenarios when the pedestrian's head contacted the ground, see Table 3-11.

To conclude, the sensitivity analysis for the friction coefficient relevant to the contacts shows that a variation in frictional coefficient has no significant influence on the kinematic response and head injury risk for the adult pedestrian during primary impacts. Whilst, it is only has a significant influence on the kinematic response, body-ground contact orders and contact time during secondary impacts.

4.5 Comparison between primary and secondary impacts for adult pedestrian.

This section compares the injury criteria and injury risk of the adult pedestrian subjected to both primary vehicle impacts and secondary ground contacts and associated head, upper neck and chest injuries and risks, using HIC, N_{ij} , N_{km} and CTI at both vehicle contact regions (centreline and offset) in three impact position, front, rear and side. The main purpose of this comparison was to investigate which impacts have a potential influence on the injury risk severity and could cause a fatal injury. In addition, comparing the influence of the impact velocity on the injury risk produced by primary and secondary impacts during all impact position and vehicle contact regions. This will assist in the preparation of, for the first time, a database for engineering, local governments, manufacturers and decision makers to establish effective strategies or regulations for reducing the driving speed in the urban areas or recommendations for successful active or passive safety countermeasures.

4.5.1 Head injury and injury risk level during primary and secondary impacts

Head injury criterion and injury risk level for the adult pedestrian caused by primary and secondary impacts were compared to assess injury severity and risk.

4.5.1.1 Head injury and injury risk level during primary and secondary impacts at the vehicle's centreline

During front primary impacts, there was a significant increase in HIC between 318 and 1307 at impact velocities from 15 to 30km/h. The responses show that HIC increased significantly with impact velocity and exceeded the threshold $HIC_{15}=1000$ at 30 km/h, as demonstrated in Figure 3-21, which corresponds with 98% risk of AIS2+, 88 % of AIS3+, 40% of AIS4+, 9% of AIS5 and 2% of fatal head injury AIS6+, see Figure E-1. Front secondary impacts produced HIC between 4277 and 3696 at impact velocities between 15 and 30 km/h. HIC fluctuated with impact velocity and exceeded the threshold $HIC_{15} =1000$ at 15 km/h and greater, see Figure 3-21 and indicates almost a 100% risk of fatal head injury, as demonstrated in Figure E-1. Therefore, all HIC and injury risk, produced by the secondary impacts in the front impact position, were higher than during primary impacts.

During rear primary impact scenarios, no head contact was observed at 10km/h, which resulted from the pedestrian's body sliding on the frontal shape of the vehicle with a body-back contact with the vehicle's components. When the vehicle impact velocity increased, the measured HIC were between 309 and 1244 at impact velocities of 15 and 30 km/h, respectively. The HIC increased very significantly with impact velocity and exceeded the threshold $HIC_{15}=1000$ at 30km/h, as shown in Figure 3-22, and produced 97% risk of AIS2+, 75% of AIS3+, 34% of AIS4+, 7% of AIS5+ and 0.5% of fatal head injury AIS6+, as presented in Figure E-2. During rear secondary impacts, the HIC fluctuated between 4382 and 5617 at impact velocities between 10 and 30 km/h, indicating that HIC exceeded the threshold $HIC_{15}=1000$ at 10 km/h and greater, see Figure 3-22 and a 100% fatal head injury, as illustrated in Figure E-2. Thus, all HIC and injury risk produced by the secondary impacts during rear impacts were greater than the primary impacts.

The side primary impacts were simulated between 15 and 35km/h. No head-vehicle interaction occurred at a low impact velocity of 15km/h, however, HIC increased from 95 to 597 at 30km/h and 35km/h, respectively, which indicates a significant increase with impact velocity. HIC, however, did not exceed the threshold $HIC =800$, see Figure 3-23. HIC at 35km/h indicates a different injury risk level of 52 % of AIS2+, 18% of AIS3+, 5% of AIS4+, 0.37% of AIS5+ and 0.01% of fatal head injury, as shown in Figure E-3. In addition, HIC and head injury risk were significantly less than those produced during the front and rear primary impacts at 30km/h.

This might be a consequence of the fact that the majority of the kinetic energy and momentum was transferred during contact with the vehicle's components at the knees, hands, arms and then finally the head. In addition, the posture of the legs and hands, during the impacts, have a significant influence on changing the centre of gravity and affecting the kinematic response. The simulations are consistent with Peng et al (2012) [151], who stated that the change in gait changed the position of the centre of gravity. In addition, the effective angle of rotation about the frontal edge of the auto rickshaw sheet plate in the side impact was greater than for frontal and rear impacts, which might significantly influence impact loads, as shown in Figure A-2. Even though, the frontal geometry of the auto rickshaw is different to passenger vehicles, the results show a good agreement with the study of Simms and Wood (2006), which found that side impacts produce low impact loads compared to the frontal and rear impacts. This

might be a result of the lower effective radius of rotation about the vehicle front, during front and rear impact positions compared to the side position [55].

For the side secondary impacts, the measured HIC fluctuated between 2274 and 1260 at impact velocities between 15 and 35 km/h, which indicates no robust correlation between HIC and impact velocity. The influence of body rotation between 90 to 180 degrees about the Y-axis resulted in the pedestrian's face impacting with the ground. Two injury thresholds were used to assess the head injury risk, $HIC=800$ for the side impacts and $HIC_{15}=1000$ for front impacts, as shown in Figure 3-23. HIC exceeded the thresholds at 15 km/h and greater and indicate a 100 % risk of AIS2 and AIS3+, 95% of AIS4+, 86% of AIS5+ and 63 % of AIS6+ fatal injury, see Figure E-3. In addition, all HIC and injury risk, produced by the secondary impacts in the side impact position, were higher than that produced during primary impacts. This might be a consequence of the fact that a concentrating direct impact force was produced at the pedestrian's head during the side impacts and moreover, the frequency of head-ground impact order being less than the front and rear impacts and the head moving downward toward the ground with less body region-ground contacts, as shown in Figures 3-13 and 3-15 (a). The simulations are in good agreement with Shi et al (2018), who concluded that a head-first landing may produce a greater head injury risk [176].

Therefore, HIC and head injury risk, produced by the secondary impacts, were greater than those produced during primary impacts when adult pedestrian-auto rickshaw impacts occurred at the vehicle's centerline.

4.5.1.2 Head injury and injury risk level during primary and secondary impacts at 42cm offset from the vehicle's centreline

In relation to the front primary impacts, the measured HIC increased significantly between 690 and 2215, at impact velocities between 20 and 30km/h. These responses indicate that HIC increased with impact velocity and exceeded the threshold $HIC_{15}=1000$ at 25 km/h and higher, as presented in Figure 3-24 and produced an 98% risk of AIS2+, 82% of AIS3+, 44% of AIS4+, 11% AIS5+ and 1% of fatal head injury probability, see Figure E-4. For front secondary impacts, no head-ground contact was observed during the secondary impacts at all velocities between 20 and 30km/h, as shown in Figure 3-24. This is a result of significant pedestrian rotation about the vehicle's right-hand side, which produced unbalanced movement and lower torso and

leg contacts with the ground, without head contact. Therefore, no HIC and head injury risks were observed during the secondary impacts associated with this impact position.

In relation to the rear primary impacts, the HIC increased noticeably between 289 and 4259 at impact velocities between 15 and 30km/h. The simulations show that HIC increased with impact velocity and exceeded the threshold $HIC_{15}=1000$ at 25 km/h and greater, as shown in Figure 3-25, which is associated with a 100% risk of AIS2+, AIS3+ and AIS4+, and 98% of AIS5+ and 96% corresponding to fatal head injury, see Figure E-5. In addition, they indicate that the HIC and head injury risk produced at front and rear primary impact positions at the vehicle offset, were significantly greater than those at the vehicle's centerline during primary impacts. This is caused by the impact with the vehicle windscreen and windscreen frame, which could be considered to be the stiffest and most injurious vehicle components (Roudsari et al., 2005) [67]. For the rear secondary impact, no head-ground contact occurred at 15km/h, because the pedestrian contacted the ground with the knees. Therefore, there were no HIC values or head injury risks produced, as shown in Figures 3-25 and E-5. Impact velocities of 25 and 30km/h produced HIC values of 1957 and 580, respectively. Indicating that no robust correlation could be established between HIC and impact velocity during the secondary impact. Moreover, that HIC exceeded the threshold $HIC_{15}=1000$ only at 25 km/h, as shown in Figure 3-25 and is associated with a 100% risk of AIS2+, 98% of AIS3+, 86% of AIS4+, 61% of AIS5+ and 22 % of fatal head injury, see Figure E-5. However, HIC and head injury risk were less than those measured during primary impacts, perhaps as a consequence of different landing orders at different impact velocities, which led to different body regions contacting with the ground, absorbing the impact force and decelerating the head.

Side primary impact were simulated between 10 and 40km/h and no head contact occurred, due to asymmetry about the right and the left-hand side of the dummy. This produced a significant post-kinematic rotation for the adult pedestrian. For the side secondary impacts, HIC changed from 6861 and 5894 at impact velocities of 15 and 40 km/h, see Figure 3-26. The simulations establish no robust correlation between HIC and impact velocity. Body rotation produced a loss of pedestrian balance and contact with the right-hand side of the vehicle, resulting from the impact at the vehicle offset. The pedestrian's head impacted with the ground in different directions as a result of variation in vehicle impact velocity, such as back-face-ground contacts were

produced between 15 and 35km/h and face-ground contacts at 40km/h. Therefore, two head injury thresholds were used to analyse the secondary impacts $HIC=800$ for the side impacts and $HIC_{15}=1000$ for frontal and rear impacts. These values indicate that HIC exceeded the thresholds at 15 km/h and greater, except at 20 and 35km/h, as shown in Figure 3-26, which specifies a 100% risk of fatal head injury, see Figure E-6. This impact position could be the safest impact scenario compared with other positions at both the vehicle's centerline and offset during the primary impacts. However, it produces a 100% risk of fatal head injury during secondary impacts.

In summary, during primary impacts, HIC dependably increased with vehicle impact velocity, suggesting that the HIC was linearly associated with vehicle impact velocity and high linear accelerations and energy and momentum transfer. This finding is consistent with previous studies, which concluded that the HIC increased with impact velocity during primary impacts [68, 149, 160, 163, 164, 175-181]. It can be concluded that impact at 42cm offset from the vehicle's centerline, such as the rear-offset impact position, could cause high head injury severity, due to contact with the corner of both the windscreen and windscreen frame. The side-offset position was the safest impact scenario, since no head impact occurred with the vehicle components. Even a low impact velocity at 10km/h caused high injury severity and exceeded the head injury threshold $HIC_{15}=1000$, which predicts that depressed skull fracture might occur [78]. In addition, during the primary impacts, the safest impact scenario could change to a fatal and injurious impact scenario during the secondary impacts with 100% risk of a fatal head injury. There was no robust relationship established between HIC and impact velocity during secondary impacts, which is consistent with previous studies [68, 156, 176, 182], which concluded that there was no obvious correlation observed between pedestrian HIC-ground and impact velocity. However, different landing patterns and significant body rotation, caused by impact velocity variation, led to a remarkable change in the direction of the contact with the ground and caused noticeable HIC and head injury risk variations. These reasons led to head deceleration caused by lower extremities and torso landing cushioning the head-to-ground interactions. And is in good agreement with Shi et al (2018), who concluded that no obvious correlation existed between the HIC and impact velocity during secondary impacts. These results were collected from an investigation of pedestrian-vehicle impacts for four different pedestrian sizes (50th and 95th males, 5th female 10YO-child

pedestrians), six gait percentages (from 10 to 9%) and five distinct vehicle types at impact velocities between (20 and 60km/h) [176]. Additionally, in the present study, most cases, produced HIC values from ground contacts which were significantly higher than those produced during primary impacts, even at the low impact velocity of 10km/h. The reason for this is that the ground contact is very stiff compared to the vehicle contact, resulting in very high accelerations of short duration for the ground contact. These results are in good agreement with the studies of Jakobsson et al. [204], Muser et al. [205] and Linder et al. [206], who concluded that stiffness is significantly correlated with high acceleration impulses and increasing injury risks of injury. Moreover, it might also be a result of the auto rickshaw front-end geometry, which is similar to high-fronted vehicle type, producing head accelerations due to the lower extremities and torso contacts buffering the head-to-ground interaction. These findings are in good agreement with previous studies, which concluded that the pedestrian head injury risk, caused by the secondary impacts, was higher than those resulting from the primary impacts, even at low impact velocities at 20km/h [70-72, 176].

Regarding the reliability for HIC values produced during secondary impacts, this study believes that most of HIC values are high. The use of Hybrid III crash dummies during impact tests instead of using cadavers might explain the higher HIC values because of the durability of the Hybrid III dummy's head compared to the cadaver's head. This might be the reason for the increasing head acceleration during secondary impacts, while the cadaver's head might be damaged during the same test conditions. These findings are consistent with previous studies, which concluded that the head of the Hybrid III dummy is more durable than the cadaver's head during impact tests, which lead to a significant increase in the dummy head acceleration when cadaver head damage probably could occur under the same test conditions [250, 251].

Therefore, during secondary impacts, HIC and head injury risk are sensitive, unpredictable and influenced by many factors, which is consistent with Simms and Wood (2006), who concluded that the HIC produced by secondary impacts results in far less injury risk predictability than primary impacts [55].

4.5.2 Upper neck injury and injury risk level during primary and secondary impacts

In this section, the upper neck injury criteria and injury risk level of the adult pedestrian, produced by primary and secondary impacts, were compared to assess which has significant injury severity and risk.

4.5.2.1 Upper neck injury and injury risk level during primary and secondary impacts at the vehicle's centreline

Front primary impact is related to neck injury by N_{ij} . It appears that the tension-extension (N_{te}) load, representing the N_{ij} , were between 15 and 30km/h, as shown in Figure E-7, which corresponds to an N_{ij} of 0.75 and 1.28, respectively, see Figure 3-27. Compression-flexion (N_{cf}), compression-extension (N_{ce}) and tension-flexion (N_{tf}) have been excluded from the upper neck injury assessment of the frontal impact, since their values were lower than the worst injury case (N_{te}), as shown in Figure E-7. These values indicate that N_{ij} exceeded the threshold $N_{ij}=1$ at 30 km/h as presented in Figure 3-27, and were associated with 37% risk of AIS2+, 33% of AIS3+, 46% of AIS4+ and 9 % of AIS5+, as demonstrated in Figure E-10. Therefore, the upper neck injury values and injury risk increased with impact velocity during the primary impacts.

With respect to the front, secondary impact related neck injury, no N_{ij} values were produced at an impact velocity of 15 and 20km/h, because the pedestrian impacted the ground via back of head- ground contact, see Figure 3-19. Thus, the N_{km} was applied to measure the upper neck injury risk, because of head-neck movement. The extension-posterior (N_{ep}) load with rearward motion, signifies the N_{km} were 1.78 and 4.49 at 15 and 20km/h, respectively, see Figures E-7 and 3-27. The flexion-anterior (N_{fa}), flexion-posterior (N_{fp}) and extension-anterior (N_{ea}) were omitted from the upper neck injury valuation. In the meantime, their values were lower than the maximum load (N_{ep}), as shown in Figure E-7. The upper neck injury values exceeded the threshold $N_{km}=1$ at 15km/h, as presented in Figure 3-27 and corresponded with a 52% risk of AIS2+, 57% of AIS3+, almost 70% of AIS4+ and 16% of AIS5+. While, N_{km} , associated with 4.49 at 20km/h, represents 97% risk of AIS2+, approximately 100% of AIS3+ and AIS4+ and 83% of AIS5+, as shown in Figure E-10. At 30km/h, the impact direction with the ground changed, producing face-to-ground contact, as seen

in Figure 3-19. Thus, N_{ij} was used to measure the upper neck injury, because of head-neck movement, which produced compression-flexion (N_{cf}) corresponding with 0.7, as illustrated in Figures E-7 and 3-27. Compression-extension (N_{ce}), tension-extension (N_{te}) and tension-flexion (N_{tf}) upper neck loads were omitted from the upper neck injury evaluation. Subsequently, their values were lower than the worst load case (N_{cf}), see Figure E-7. The upper neck injury value was below the threshold $N_{ij}=1$, as demonstrated in Figure 3-27.

In addition, N_{km} values were higher, compared to the N_{ij} of the primary and secondary impacts and the upper neck injury risk produced by the ground impact at 15 and 20km/h, which was higher than those produced during the primary impacts. No robust correlation could be established, between upper neck values and impact velocity, during the secondary impacts, since it depends on head-ground impact direction, which determines the specific upper neck injury criterion N_{ij} or N_{km} .

During rear primary impacts, extension-posterior (N_{ep}) load with rearward motion signifies the worst N_{km} load case at 10km/h (1.29). Flexion-posterior (N_{fp}) represents the maximum load of N_{km} at 15km/h (1.68) and flexion-anterior (N_{fa}) with the forward motion of N_{km} at 30km/h (2.47), as shown in Figures E-8 and 3-28. Extension-anterior (N_{ea}) was excluded from the upper neck injury assessment, because it was lower than the worst-case injury cases, see Figure E-8. These values indicate that N_{km} exceeded the threshold $N_{km}=1$ at 10 km/h and greater, see Figure 3-28 and corresponded to 37% risk of AIS2+, 33% of AIS3+, 46% of AIS4+ and 9% of AIS5+, as illustrated in Figure E-11.

Rear secondary impacts, following the impact direction of the pedestrian head with the ground, resulted from different landing patterns, caused by the increasing impact velocity. No N_{km} values were produced at impact velocities between 10 and 30km/h, because the pedestrian impacted the ground with the face, see Figure 3-28. Therefore, a compression-extension (N_{ce}) load case of N_{ij} between 1.98 and 1.23 was produced at impact velocities between 10 and 30km/h, as illustrated in Figures E-8 and 3-28. Again, upper neck injury loads of tension-extension (N_{te}), tension-flexion (N_{tf}) and compression-flexion (N_{cf}) were excluded from the neck injury evaluation, because their values were lower than the worst load cases, see Figure E-8. These values, demonstrate that N_{ij} exceeded the threshold $N_{ij}=1$ at 10 km/h and greater, as presented in Figure 3-28. These results are equivalent to a 58% risk of AIS2+, 66% of AIS3+,

77% of AIS4+ and 19% of AIS5+, as shown in Figure E-11. In addition, N_{ij} and injury risk level, produced during the secondary impacts, were higher than those produced during primary impacts at 10 and 15km/h.

During side primary impacts, no N_{ij} , relevant to side impact, were calculated in this study as a result of the head and neck moving to the side direction. However, following the impact direction of the pedestrian head with the ground during a secondary impact, compression-extension (N_{ce}) denoted a worst load case N_{ij} of between 1.26 and 2.47 at impact velocities between 15 and 35 km/h, see Figures E-9 and 3-29. For the upper neck loads, compression-flexion (N_{cf}), tension-extension (N_{te}) and tension-flexion (N_{tf}) were excluded from the upper neck injury assessment, since their values were not the maximum loads, as shown in Figure E-9. These values indicate that N_{ij} exceeded the threshold $N_{ij}=1$ at 15 km/h, see Figure 3-29 and correspond to a 37% risk of AIS2+, 32% of AIS3+, 45% of AIS4+ and 9% of AIS5+, as shown in Figure E-12. In addition, upper neck values and injury risk, produced from primary impacts, increased with impact velocity. The upper neck values and injury risk produced from secondary impacts varied with impact velocity.

4.5.2.2 Upper neck injury and injury risk level during primary and secondary impacts at 42cm offset from the vehicle's centreline

During a front primary impact, tension-extension (N_{te}) represents the worst N_{ij} risk at 20 and 25 km/h, corresponding with 0.93 and 1.09, as illustrated in Figure E-13 and Figure 3-30. Meanwhile, tension-flexion load (N_{tf}) signifies the maximum load of N_{ij} at 30km/h, consistent with 1.20, see Figures E-13 and 3-30. Compression-extension (N_{ce}) and compression-flexion (N_{cf}) have been excluded from the upper neck injury calculation because their values were not the worst loads, as shown in Figure E-13. These values indicate that N_{ij} exceeded the threshold $N_{ij}=1$ at 25 km/h and higher, as demonstrated in Figure 3-30 and sustained an almost 32% risk of AIS2+, 25 % of AIS3+, 36% of AIS4+ and 7 % of AIS5+, as shown in Figure E-16.

For frontal secondary impacts, no neck injury values, relevant to the front and rear criteria N_{ij} and N_{km} , were produced during the secondary impacts at all impact velocities between 20 and 30km/h. Consequently, neck movement tended to be in the side direction, see Figure 3-30.

In a rear primary impact, flexion-posterior (N_{fp}) represents the maximum upper neck injury risk of N_{km} at 15, equivalent to 1.25, as shown in Figures E-14 and 3-31. Meanwhile, extension-posterior (N_{ep}) load cases were associated with an N_{km} of 2.23 and 4.32 at 25 and 30 km/h, respectively, see Figures E-14 and 3-31. Both loads represent a rearward motion, upper neck loads flexion-anterior (N_{fa}) and extension-anterior (N_{ea}) were excluded from the upper neck injury assessment because their values were not the highest injurious loads, as demonstrated in see Figure E-14. N_{km} exceeded the threshold $N_{km}=1$ at 15 km/h and higher, as shown in Figure 3-31 and are associated with a 36% risk of AIS2+, 32% of AIS3+, 44% of AIS4+ and 9% of AIS5+, as presented in Figure E-17.

The rear secondary impact, following the impact direction of the pedestrian's head with the ground, resulted from the kinematic response, body rotation and different landing orders during impact velocity variation, as shown in Figure 3-20. Flexion-posterior (N_{fp}) load characterises the worst risk of N_{km} , producing 1.10 at 15km/h corresponding to a forwarding motion, see Figures E-14 and 3-31. Meanwhile, the extension-anterior load was the maximum load condition (N_{ea}) at 25 km/h with a value of 2.02 for rearward motion, as demonstrated in Figures E-14 and 3-31. Two different loads of the upper neck were excluded, resulting from lower values, such as flexion-anterior (N_{fa}) and extension-posterior (N_{ep}) excluded from the upper neck injury assessment, because their values were not the highest injurious loads, see Figure E-14. These values have exceeded the threshold $N_{km}=1$ even with no head-ground contact at a low impact velocity of 15km/h, as shown in Figure 3-31. The results are associated with a 32% risk of AIS2+, 26% of AIS3+, 37% of AIS4+ and 8% of AIS5+, see Figure E-17. When the impact velocity increased to 30km/h, the kinematic response changed, a result of increasing the whole pedestrian body acceleration, which caused different body-ground contact orders and time durations, see Figure 3-15(b). A significant head-ground impact direction change occurred, producing a face-ground contact, see Figure 3-31. Therefore, a compression-flexion (N_{cf}) load signifies that the N_{ij} was produced with a value of 0.5, which is below the threshold $N_{ij}=1$, as shown in Figures E-14 and 3-31.

For the side primary impact, no N_{ij} values, relevant to side impact, were calculated in this study as a result of head and neck movement tending to move to the side direction. However, following the impact direction of the pedestrian head with the ground in a

secondary impact, resulting from a rear-ground impact, an extension-posterior (N_{ep}) load with rearward motion produced values of 3.45, 2.06, 4.51 and 3.21 at impact velocities of 15, 20, 25 and 35km/h respectively, see Figures E-15 and 3-32. Nevertheless, extension-anterior (N_{ea}) load with forward motion represents an N_{km} of 4.08 at 30km/h, as presented in Figures E-15 and 3-32. Two upper neck loads were omitted from the upper neck injury assessment, since their values were not the highest injurious loads, flexion-anterior (N_{fa}) and flexion-posterior (N_{fp}), as shown in Figure E-15. Meanwhile, a face-to-ground impact occurred at 40km/h, producing an N_{ij} of 0.78, which represent tension-extension (N_{te}) load. N_{km} represents extension-posterior (N_{ep}) load cases at most impact velocities between 15 and 35km/h, except at an impact velocity of 30 km/h, which produced an extension-anterior (N_{ea}) load. Even with a high impact velocity at 40km/h, the N_{ij} was below the threshold $N_{ij}=1$, see Figures E-15 and 3-32. Meanwhile, N_{km} exceeded the threshold $N_{km}=1$ at 15 km/h and produced an 89% risk of AIS2+, 97% serious injury AIS3+, 98% of AIS4+ and 59% of AIS5+, as shown in Figure E-18.

In summary, during primary impacts, upper neck injury criteria N_{ij} and N_{km} and injury risk increased with vehicle impact velocity. In addition, N_{km} during primary and secondary impacts produced higher injury risks than those produced by N_{ij} . This could be a result of the influence of shear forces, which were previously specified as being associated with soft tissue injuries to the cervical spine intervertebral joints [128, 129]. Furthermore, it could cause pain in the neck, almost twice as frequently as frontal impacts N_{ij} . This is caused by the shear forces, which could cause potential harm to the spinal cord. These findings in good agreement with Panjabi et al (1998), which concluded that the shear force has a significant influence on spinal cord injuries [91]. However, there was no robust correlation between the upper neck injury values, injury risk level and vehicle impact velocity during the secondary impacts. Also, using N_{ij} or N_{km} , during the secondary impacts, depends on the head-ground direction and head-neck movement. These results indicate that the secondary impact was influenced by the post-kinematic response, specifically the landing patterns caused by factors such as impact velocity, impact position, the vehicle contact region and ground-impact direction. In addition, the upper neck injury risk produced from the ground contacts is significantly higher than those produced during primary impacts, even at the low

impact velocity of 10km/h. Therefore, upper neck injury criteria including N_{ij} and N_{km} are sensitive.

4.5.3 Chest injury and injury risk level during primary and secondary impacts

Combined Thoracic Index (CTI) was used to assess chest injury and risk level during primary and secondary impacts.

4.5.3.1 Chest injury and injury risk level during primary and secondary impacts at the vehicle's centreline

For the frontal primary impacts, Combined Thoracic Index (CTI) increased marginally between 0.55 and 0.89 at impact velocities from 15 to 30 km/h. CTI did not exceed the threshold $CTI=1$, see Figure 3-33. The CTI at 30km/h was associated with a 62% risk of AIS2+, 13% of AIS3+, 3% of AIS4+ and 0.02% of AIS5+, as shown in Figure E-19.

During frontal secondary impacts, following the impact direction of the pedestrian front chest with the ground, no front chest-ground contacts were observed at 15 and 20km/h, as shown in Figure 3-33. Though could result from a pedestrian impact to the back-torso, which is caused by the different dynamic response as a result of change in impact velocity and leads to different landing patterns with the ground (back-ground contact), as shown in Figure 3-15 (a). When the impact velocity increased to 30km/h, the pedestrian's body accelerated in the impact direction, producing a CTI of 0.7, which is less than that produced during primary impacts and below the threshold $CTI=1$, see Figure 3-33. The results predict a 34% risk of AIS2+, 3.8% of AIS3+, 0.75% of AIS4+ and 0.01% of AIS5+, see Figure E-19.

Since, the CTI criterion was only designed for frontal impacts, no CTI chest injury risk was produced during rear primary impacts. For rear secondary impacts, front chest-ground contacts were seen at all impact velocities, resulting from changing the impact direction, as shown in Figure 3-34. The CTI fluctuated between 0.46 and 0.41, at impact velocities between 10 and 30km/h. All CTI were below the threshold $CTI=1$, as shown in Figure 3-34 and indicate different injury risk levels. The maximum CTI of 0.74 at 15km/h corresponds to a 40% risk of AIS2+, 5% of AIS3+, 1% of AIS4+ and 0.01% of AIS5+, see Figure E-20.

Since, the CTI criterion was only proposed for frontal impacts, no CTI chest injury risk level was measurable during side primary impacts. For secondary side impacts, following the impact direction of the pedestrian front chest with the ground, even though initial impact position was side position, front chest-ground contacts occurred at all tested impact velocities, as shown in Figure 3-35, due to landing pattern variation, caused by different impact velocities, see Figure 3-15 (a). The CTI varied from 0.46 to 0.25 at impact velocities between 15 and 35km/h. None of the CTI exceeded the chest injury threshold $CTI=1$, as shown in Figure 3-35, however, a maximum CTI of 0.57 was produced at 30km/h, indicating a 19% risk of AIS2+, 1.5% of AIS3+, 0.3% of AIS4+ and 0% of AIS5+, see Figure E-21.

4.5.3.2 Chest injury and injury risk level during primary and secondary impacts at 42cm offset from the vehicle's centreline

For the frontal primary impacts, there was a slight increase in the CTI between 0.5 and 0.87, with impact velocities from 20 km/h to 30 km/h, which indicates that CTI were below the threshold $CTI = 1$ at all impact velocities; see Figure 3-36. The maximum CTI was 0.87, as shown in Figure 3-36, which is associated with a 59% risk of AIS2+, 12% of AIS3+, 2% of AIS4+ and 0.02% of AIS5+, see Figure E-22. In addition, all CTI and chest injury risks were lower than those produced during the front primary impact at the vehicle's centerline.

The frontal secondary impacts follow the impact direction of the pedestrian frontal chest with the ground. No front chest-ground contacts occurred, due to the asymmetric impact at the vehicle offset, see Figure 3-15 (b). The offset caused a significant kinematic response and body rotation about the side of the vehicle. Moreover, it also caused a clear imbalance in the post-kinematic response, compared to that at the vehicle's centerline. Therefore, torso, femur and tibias come into contact with the ground rather than the head and chest contacts.

For rear primary impacts, no CTI were measured in rear primary impacts, due to the aforementioned limitation of CTI. The secondary impacts follow the impact direction of the pedestrian frontal chest with the ground. No chest-ground contacts occurred at 15 and 25km/h, as shown in Figure 3-37 and therefore, no CTI and injury risk as a result of different body-ground contact orders, see Figure 3-15 (b). When the impact velocity increased to 30km/h, a significant impact force was generated, which

accelerated the whole body and changed the impact direction, producing front chest-ground contacts, see Figure 3-37. The measured CTI was 0.18 at 30km/h, which is below the threshold $CTI=1$, shown in Figure 3-37 and indicates a 2% risk of AIS2+, 0.09% of AIS3+, 0.02% of AIS4+ and 0% of AIS5+, see Figure E-23.

As discussed previously, CTI could not be produced during primary side impacts. The secondary impacts follow the impact direction of the pedestrian frontal chest with the ground. No chest-ground contacts occurred at impact velocities between 15 and 35km/h and no CTI resulted from the different kinematic responses, see Figure 3-38. When the impact velocity increased to 40km/h, a significant impact force was generated. This accelerated the whole body and it totally lost balance and changed kinematic response and impact direction, producing a front chest-ground contact with a CTI of 0.18, which is below the threshold $CTI=1$, as shown in Figure 3-38. The results indicate a 2% risk of AIS2+, 0.09% of AIS3+, 0.02% of AIS4+ and 0% of AIS5+, see Figure E-24.

In summary, CTI criterion of chest injury risk in front primary impacts indicates that the pedestrian could sustain a greater chest injury severity when impacted at the vehicle's centerline than when impacted at 42cm offset from the vehicle's centerline. This could result from high energy transfers to the centre of the pedestrian chest, momentum and concentrated force to the pedestrian's chest in the vehicle forward impact direction, with less rotation and a longer chest-vehicle windscreen interaction time than that at the offset. However, all of the CTI were below the injury threshold $CTI=1$. Additionally, CTI and chest injury risk during the primary impacts increased with impact velocity and a strong relationship could be observed. For the secondary impacts, all CTI varied with impact velocity and depended on the pedestrian's landing patterns relative to the ground and frontal chest-ground contact direction. In addition, the CTI and chest injury risks were less than those produced during the primary impacts, with no robust relationship between CTI and impact velocity established. Therefore, CTI and chest injury risk level are sensitive and influenced by many factors during primary and secondary impacts, varying noticeably with the impact position, vehicle contact region, vehicle velocity and body contact order.

4.6 Auto rickshaw engineering modifications for adult pedestrian safety enhancement

The data derived from the adult pedestrian-vehicle primary impacts studies provides an opportunity for the development of injury mitigation analyses within the context of the study of the auto rickshaw, in relation to many cost-benefit related issues with respect to injury cost saving, vehicle mass reduction and engineering modification cost. This section discusses the effects of material selection and thickness modifications of the most frequently impacted, stiffest and most injurious vehicle components (windscreen and windscreen frame) on the head, upper neck and chest injury risk for an adult pedestrian during the primary impacts with brief economic considerations.

4.6.1 Head injury and injury risk level during primary impacts after vehicle modifications

The study by Nguyen et al. 2013 [231], provides an in-depth consideration of how costs differ between AIS level injuries and body region for pedestrian road traffic injuries in Thai Binh province, Vietnam. Estimating that the mean costs associated with pedestrians, whilst hospitalised, could be as high as \$ 2700 for AIS4+ head injuries. These are very considerable costs given that the average annual income in the Thai Binh province is just \$ 695 [294]. These costs account for only those incurred during the patient's stay at hospital and do not consider the transfer of the patient to a higher -level hospital or loss of work, due to injuries. Thus, the actual costs are likely to far exceed these estimates [231]. Regardless of the country in question, it is clear that if the severity of an injury was to be reduced then so would the associated medical expenses and thus, the effects of injury mitigation strategies may have a beneficial impact on developing countries. Therefore, the results of this study will concentrate on comparing the likelihood of an adult male pedestrian suffering severe head injuries AIS4+ during an impact with an auto rickshaw constructed with the original materials and an auto rickshaw constructed with different materials.

4.6.1.1 Head injury and injury risk level during primary impacts after vehicle modifications at the vehicle's centreline

The frontal impact HIC for an adult pedestrian impacted by the original auto rickshaw (steel windscreen frame and glass windscreen) exceeded the threshold $HIC_{15}=1000$ at 30km/h, as shown in Figure 3-37. Different aluminiums were simulated for the windscreen frame (Types 6016-T4, 6061-T6, 6111-T4, 5754-O and 5182-O) and one magnesium (AZ31B). Polycarbonate (PC) was used for the windscreen. All modified auto rickshaw designs (aluminium and magnesium windscreen frame and polycarbonate windscreen) produced significantly lower HIC values, with almost all not exceeding the head injury threshold at all impact velocities (10-40km/h). The exception was aluminium 6016-T6, whose associated HIC values exceeded the threshold $HIC_{15}=1000$ at 35km/h and above; however, it still confirmed that significant improvements were feasible, since the threshold was exceeded at an impact velocity 5km/h higher than the original material, see Figure 3-37. The responses indicate an average AIS4+ reduction, at impact velocities between 10 and 40km/h of 33%, 32%, 32%, 32% and 33% for 6016-T4, 6111-T4, 5754-O, 5182-O and AZ31B materials, respectively, as shown in Figure F-1. This was considerably lower for the 6061-T6 material, which produced an average AIS4+ reduction of 27%. Due to the reduction in severe head injury, these results estimate that the modified materials might provide an average medical cost saving for a pedestrian impacted by an auto rickshaw in Vietnam of \$882, 847, 868, 853 and 881 for 6016-T4, 6111-T4, 5754-O, 5182-O and AZ31B, respectively [231]. Whilst, for the 6061-T6 material, this average cost saving was estimated to be \$732 [231].

For rear impacts, HIC values for the adult impacted by the original auto rickshaw exceeded the threshold $HIC_{15}=1000$ at 25km/h, as presented in Figure 3-38. All auto rickshaw simulations possessing the modified materials produced considerably lower HIC values than the original vehicle design. Aluminium 6061-T6, 6111-T4 and 5182-O only produced HIC that exceeded the threshold at 35km/h and aluminium 6016-T4 and 5754-O and magnesium AZ31B at 40km/h. This indicates that excellent improvements to pedestrian safety may be produced, as the modified materials increased the HIC threshold by at least 10km/h or 15km/h greater than the original auto rickshaw. In addition, these results indicate an average AIS4+ reduction at impact

velocities between 10 and 40km/h of 19%, 5%, 12%, 15%, 13% and 19% for 6016-T4, 6061-T6, 6111-T4, 5754-O, 5182-O and AZ31B, respectively, see Figure F-2. Due to the reduction in severe head injury observed for rear impacts, these results estimate that the modified materials may provide an average medical cost saving of between \$139 and \$524 [231].

For side impacts, HIC for the adult pedestrian impacted by the original auto rickshaw did not exceed the threshold $HIC=800$ at all impact velocities between 10 and 40km/h, as demonstrated in Figure 3-39. However, all simulations for the modified auto rickshaw design showed a large increase in HIC compared to that of the original materials for all impact velocities. Thus, side impacts to the centreline of the auto rickshaw exhibited by far the most injurious HIC results, as no improvement was made after altering the windscreen and windscreen frame materials. The simulations also surpassed the HIC threshold at 35 km/h for aluminium 6061-T6, 6111-T4, 5754-O and 5182-O with an average AIS4+ increase of 27%, 11%, 7% and 13%, respectively, see Figure F-3.

Moreover, aluminium 6016-T4 and AZ31B exceeded the HIC threshold at 40km/h with an average AIS4+ increase of 2%, as shown in Figure F-3. Due to an increase in severe head injury observed for side impacts, these responses estimate that the modified materials provide an average medical cost increase, rather than medical cost saving of between \$54 and \$735 [231]. Contact between the auto rickshaw and torso may be the reason for this rise in HIC for the PC windscreen, particularly at higher velocities, since more of the torso makes contact with the PC windscreen than at lower velocities, where the torso also contacts with the stiffer lower windscreen frame. When the torso impacts with the 'stiff' glass windscreen or the lower section of the metal windscreen frame, less energy is absorbed by the material than a material that exhibits large amounts of deformation. More kinetic energy is transferred to the torso, potentially pushing the pedestrian's body away from the vehicle after impact. Although this would result in a high risk of injury to the upper torso (chest), it may push the body away enough such that the head contact is actually minimised as it accelerates back towards the vehicle during neck extension. When the polycarbonate windscreen impacts with the torso it deforms very significantly, such that less energy is transferred to the torso and the body is not pushed away as much as it was by the

stiffer materials. This may lead to the head of the pedestrian having a more significant impact with the vehicle and producing a higher HIC value than the glass windscreen.

4.6.1.2 Head injury and injury risk level during primary impacts after vehicle modifications at 42cm offset from the vehicle's centreline

For frontal impacts, HIC values for the adult pedestrian, impacted by the original auto rickshaw, exceeded the threshold $HIC_{15}=1000$ at 25km/h, as illustrated in Figure 3-40. Similar to that produced by the original materials, the HIC produced by aluminium 6061-T6 also exceeded the head injury threshold at 25km/h. The modified vehicle designs, that include the aluminium 6111-T4, 5754-O and 5182-O windscreen frame materials, produced HIC values that were considerably reduced, exceeding the threshold at 30km/h. Aluminium 6016-T4 and Magnesium AZ31B produced the most promising results, with HIC values that exceeded the threshold only at 35km/h, indicating that pedestrian safety was improved by the modified designs, since the HIC threshold was exceeded at impact velocities at least 5km/h to 10km/h higher than the original materials.

In addition, the results indicate an average AIS4+ reduction, at impact velocities between 10 and 40km/h of 30%, 7%, 14%, 21%, 16% and 31% for 6016-T4, 6061-T6, 6111-T4, 5754-O, 5182-O and AZ31B, respectively, see in Figure F-4. Due to the reduction observed in severe head injury, the results estimate that the modified materials may equate to an average medical cost saving of between \$179 and \$845 [231].

For rear impacts, HIC values for the adult pedestrian impacted by the original auto rickshaw exceeded the threshold $HIC_{15}=1000$ at 20km/h, as shown in Figure 3-41. The HIC values produced by the modified vehicle designs, that included aluminium 6061-T6, 6111-T4, 5754-O and 5182-O, exceeded the head injury threshold at 25km/h. For the modified designs, that included aluminium 6016-T4 and magnesium AZ31B, HIC considerably reduced and exceeded the threshold only at 30km/h, as illustrated in Figure 3-41. These results indicate that good improvements were made to pedestrian safety, since the HIC threshold value was exceeded at impact velocities at least 5km/h or 10km/h higher than the original materials. Furthermore, the results indicate an average AIS4+ reduction at impact velocities between 10 and 40km/h of 44%, 17%, 26%, 33%, 27% and 45% for 6016-T4, 6061-T6, 6111-T4, 5754-O, 5182-O and

AZ31B, respectively, see Figure F-5. Due to these reductions in severe head injuries, the results produced an estimated average medical cost saving of between \$461 and \$1208.

No head contact occurred at the side offset impact position for both the original vehicle materials or the modified materials. Therefore, it can be concluded that the two stand out performers that provide the greatest HIC reduction in an auto rickshaw-pedestrian impact are aluminium 6016-T4 and magnesium AZ31B for the windscreen frame material and PC for the windscreen. These materials produced the largest amounts of deformation for all velocities, hence, they absorbed the most energy during impact and produced the lowest pedestrian HIC values. These results show a good agreement with Savic et al. (2014) [220], who concluded that the Mg AZ31-O had the lowest and, hence, most favourable HIC score relative to other automotive materials, such as AZ61-O, ZEK100, 6111-T4 and 5182-O, when considering pedestrian safety improvements by a series of experimental and numerical tests.

In addition, this conforms with the study by Nikolaevich et al (2014) [214], which stated that energy absorption is a significant design factor for pedestrian safety and stated that aluminium alloys have excellent energy absorption. Consequently, if greater amounts of energy are absorbed by vehicle components, then the kinetic energy of the vehicle is controlled during the impact, while preventing or reducing the peak reaction force transfer to the pedestrian [217].

As a consequence, the HIC values produced during impacts at the vehicle offset are significantly higher than those produced at the vehicle centreline, which produced a greater injury risk. Reasons for centreline impacts generally having lower HIC than offset impacts may be that the initial contact is made by the front mudguard to the lower extremities of the pedestrian, which pushes the legs away from the vehicle. Offset impacts produce initial impacts at the frontal leading edge of the windscreen frame with the torso area of the pedestrian, which arches the pedestrian's body around the vehicle and appears to lead to more energetic head contacts.

4.6.2 Upper neck injury and injury risk level during primary impacts after vehicle modifications

Nguyen et al. 2013 [231], commented that the injuries to the spine, which includes the neck and chest, had no significant cost difference and often had the lowest costs of all

body regions, being approximately 38% lower than head injuries. Neck and chest injuries were estimated to cost as much as \$1520 for serious injuries (AIS3+) [231].

4.6.2.1 Upper neck injury and injury risk level during primary impacts after vehicle modifications at the vehicle's centreline

Pedestrian impacts at the centreline of the vehicle were assessed for frontal and rear impacts by the N_{ij} and N_{km} . For frontal impacts, the N_{ij} for the adult pedestrian impacted by the original auto rickshaw exceeded the threshold $N_{ij}=1$ at 25km/h, as shown in Figure 3-42. It also indicates that N_{ij} values considerably reduced for all modified materials. In addition, aluminium 6061-T6 produced the greatest N_{ij} and exceeded the threshold at velocities of 35km/h, while aluminium 6111-T4, 5754-O and 5182-O, and Magnesium AZ31B, produced N_{ij} values that exceeded the threshold at 40km/h, see Figure 3-42. Furthermore, aluminium 6016-T4 produced remarkable N_{ij} values, that did not exceed the threshold $N_{ij}=1$ at all impact velocities between 10 and 40km/h, see Figure 3-42. The results indicate that pedestrian upper neck safety was improved even when the threshold was exceeded at impact velocities 10km/h to 15km/h greater than the original materials. In the case of aluminium 6016-T4, the auto rickshaw would have exceeded the threshold at an impact velocity over 15km/h higher than the original auto rickshaw design. Additionally, the results indicate an average AIS3+ reduction at impact velocities between 10 and 40km/h of 11%, 8%, 10%, 10% and 10% and 11% for 6016-T4, 6061-T6, 6111-T4, 5754-O, 5182-O and AZ31B, respectively, see Figure F-6. Due to the reductions in serious upper neck injury risk, the results for the modified materials are estimated to provide an average medical cost saving of between \$120 and \$179 [231].

For rear impacts, N_{km} of the original auto rickshaw design exceeded the upper neck injury threshold $N_{km}=1$ at 10km/h, shown in Figure 3-43. N_{km} , for the modified materials, reduced only marginally compared to that seen for frontal impacts. However, all N_{km} values still exceeded the upper neck injury threshold at 10km/h, which was the same velocity as the original materials.

The results for rear impacts at the vehicle centreline indicate an average AIS3+ reduction at impact velocities between 10 and 40km/h of 18%, 13%, 16%, 17% and 16% and 18% for 6016-T4, 6061-T6, 6111-T4, 5754-O, 5182-O and AZ31B, respectively, as shown in Figure F-7. Due to the reductions in serious upper neck

injury risk, it is estimated that the modified materials might produce average medical cost savings of between \$191 and \$270 [231].

4.6.2.2 Upper neck injury and injury risk level during primary impacts after vehicle modifications at 42cm offset from the vehicle's centreline

For frontal impacts, N_{ij} of the original auto rickshaw design exceeded the upper neck injury threshold $N_{ij}=1$ at 25km/h, shown in Figure 3-44. This suggests N_{ij} significantly reduced for all modified materials, see Figure 3-44. Aluminium 6061-T6, 6111-T4 and 5182-O produced N_{ij} values that exceeded the threshold at an impact velocity of 30km/h, whereas aluminium 5754-O produced an N_{ij} that exceeded the threshold at 35km/h. Following the trend of previous results, the aluminium 6061-T4 and magnesium AZ31B materials produced the lowest N_{ij} and did not exceed the threshold $N_{ij}=1$ at all impact velocities between 10 and 40km/h. Therefore, pedestrian upper neck safety was improved for all modified designs and resulted in the upper neck injury threshold being exceeded at impact velocities 5km/h, 10km/h and 15km/h greater than the original materials. For both aluminium 6016-T4 and magnesium AZ31B, the threshold would be exceeded at an impact velocity over 15km/h higher than the original materials.

Moreover, the results indicate an average AIS3+ reduction at impact velocities between 10 and 40km/h of 12%, 6, 7%, 9%, 8% and 12% for 6016-T4, 6061-T6, 6111-T4, 5754-O, 5182-O and AZ31B respectively, see Figure F-8. Due to the reductions observed to serious upper neck injury, these results estimate that the modified materials may produce an average medical cost saving of between \$88 and \$187 [231].

For rear impacts, the N_{km} of the original auto rickshaw design exceeded the upper neck injury threshold $N_{km}=1$ at 15km/h, shown in Figure 3-45. In addition, the figure shows the N_{km} values for all modified materials also exceeded the threshold at 15km/h and only exhibited minor improvements compared to that of the original design.

Furthermore, the results indicate an average AIS3+ reduction at impact velocities between 10 and 40km/h of 6%, 4%, 6%, 6% and 7% and 4% for 6016-T4, 6061-T6, 6111-T4, 5754-O, 5182-O and AZ31B respectively, see Figure F-9. Due to the reductions observed to serious upper neck injury, it is estimated that the modified materials may produce an average medical cost saving of between \$60 and \$98 [231].

4.6.3 Chest injury and injury risk level during primary impacts after vehicle modifications

4.6.3.1 Chest injury and injury risk level during primary impacts after vehicle modifications at the vehicle's centreline

For frontal impacts, the CTI of the original auto rickshaw design exceeded the chest injury threshold CTI=1 at 35km/h and greater, shown in Figure 3-46. This suggests CTI was considerably reduced for all modified materials and did not exceed the chest injury threshold at impact velocities between 10km/h and 40km/h, see Figure 3-46. However, aluminium 6061-T4 and magnesium AZ31B produced the lowest injury risks. The results indicate an average AIS3+ reduction at impact velocities between 10 and 40km/h of 20%, 19%, and 15% for 6016-T4, 6061-T6 and 6111-T4, respectively and 20% for 5754-O, 5182-O and AZ31B, see Figure F-10.

4.6.3.2 Chest injury and injury risk level during primary impacts after vehicle modifications at 42cm offset from the vehicle's centreline

For frontal impacts, the CTI of the original auto rickshaw model exceeded the chest injury threshold CTI=1 at 40km/h, shown in Figure 3-47. The CTI marginally reduced for all modified materials exceeding the chest injury threshold at 40km/h, see Figure 3-47. However, in most tests, aluminium 6061-T4 and magnesium AZ31B produced the lowest injury risk, as shown in Figure F-11. Thus, indicating an average AIS3+ reduction at impact velocities between 10 and 40km/h of 12%, 10% and 11% for 6016-T4, 6061-T6 and 6111-T4 respectively and 12% for aluminium 5754-O, 5182-O and AZ31B, as shown in Figure F-11.

For the safety of an adult male pedestrian and cost-effectiveness, therefore, it appears that of those materials tested, the optimal vehicle materials are the 6016-T4 and AZ31B windscreen frames, along with the PC windscreen. Mitigating potential road traffic injuries is paramount, for not only improving public health but also reducing the high cost burden for developing countries. The increased additional cost of implementing these suggested materials must be weighed up against the potential financial and societal costs saved by mitigating injury severity.

For the windscreen of the auto rickshaw, LS-DYNA estimated a mass of 8.13 kg for the original glass design, at an estimated cost of approximately \$14 [223]. The

estimated mass for the PC windscreen is just 3.74 kg and an estimated cost of approximately \$12 [223]. For the auto rickshaw windscreen frame, LS-DYNA estimated a mass of 7kg for the original mild steel design, which would cost approximately \$7[173]. For the aluminium 6016-T4 windscreen frame, LS-DYNA estimated its mass to be 3.64 kg at an estimated cost of \$8 [294]. For the magnesium AZ31B windscreen frame, LS-DYNA estimated its mass to be 1.589kg at an estimated cost of approximately \$9 [207]. Subsequently, it is clear that both the aluminium 6016-T4 windscreen frame and the PC windscreen has the potential to provide the greatest reduction in medical expenses, associated with head and upper neck injuries, whilst also showing potential to actually reduce material costs for the components. Regardless of the country in question, it is clear that if the severity of an injury was to be reduced, then this could save significantly in medical costs alone. When accrued, these cost savings could have a hugely beneficial impact on developing countries. Therefore, aluminium 6016-T4 and PC provides the best material combination between all modified vehicle designs tested for pedestrian head and neck injury risk reduction and safety improvement, since they show exceptional ability to absorb impact energy during pedestrian impacts. Thus, the materials have a considerable influence on head acceleration and head movement of the pedestrian. These findings are in close agreement with Binyamin et al (2018) [215], who commented that the aluminium structure has a greater ability to absorb energy during pedestrian-bonnet impacts whilst decreasing head acceleration. In addition, the findings are consistent with Masoumi et al (2011), who concluded that the aluminium bonnet leads to better improvement in HIC, compared to steel [216]. Moreover, this modification would assist in reducing the weight of the vehicle, allowing the auto rickshaw to reduce from an estimated mass of 373 kg, to a mass of 363 kg, including the driver's mass, which would also influence fuel consumption and associated pollution. However, many other factors have to be taken into consideration before these engineering modifications can be considered, such as the manufacturability of the chosen materials and occupant safety.

4.7 Limitations

This research study has identified limitations, which might lead to further research as follows:

- There is a lack of real-world primary and secondary impact accident data relevant to pedestrian-auto rickshaw impacts in developing countries; and no experimental data for pedestrian-auto rickshaw impact tests. It was, therefore, difficult to validate the computational simulations.
- This study has been focused on linear acceleration to assess the head injury risk for both adult and child pedestrian. Rotational acceleration, which is a contributory cause of head injury was not investigated.
- There is no valid supported injury criterion that specifically considers neck injuries sustained during side impacts, thus, no N_{ij} could be calculated for the side impacts in this study. One proposed solution to this issue is the multi-axial neck injury criteria (MANIC), which also includes the effects of side acceleration on the neck. In addition, no lower neck injuries were calculated, since the current 50th percentile adult and 6YO-child Hybrid III dummies did not support the lower neck injury calculation.
- Currently, the Hybrid III 6YO-Child dummy, which was used in this study, does not support the Combined Thoracic Index (CTI) calculation for chest injuries sustained during frontal impacts. Therefore, no CTI was calculated for the child pedestrian in this study.
- This study investigated head, neck and chest injuries during primary and secondary impacts. However, other injuries do occur, such as upper and lower extremities, lower neck injury and abdominal injuries, which require consideration to establish a complete understanding of combined injury risk.
- Two pedestrian dummies (50th adult and 6YO-child) were used to investigate the influence of pedestrian size on the kinematic response, injury metrics and injury risk during primary impacts. While, only the adult pedestrian was used to investigate the full secondary phase kinematics. Due to time constraints, other available pedestrian dummy sizes, such as the 95th adult and 5th female, were not investigated. In addition, the pedestrian is modelled as stationary

(pedestrian velocity=0). This might effect the kinematic response, including head impact locations and head impact angles and injury metrics.

- It must be acknowledged that simply changing the material composition of the vehicle in a binary manner will not optimally alleviate pedestrian injuries. Further material and geometric configurations require optimisation to produce an optimal solution, with respect to injury mitigation and medical cost saving.

5. CONCLUSIONS

5.1 Research conclusions

The aim of this research was to establish a computational model of an auto rickshaw to assess the safety of pedestrians in urban areas in developing countries through a series of auto rickshaw-pedestrian impact simulations. This study produced an improved understanding of pedestrian kinematics during auto rickshaw-pedestrian impacts, prior to head, neck and chest impacts against both the vehicle components and subsequently, the ground. In addition, several aluminium and magnesium alloys were investigated in an attempt to determine potential replacements for steel, for the purpose of impact mitigation of the windscreen frame and polycarbonate as a possible replacement for the glass windscreen. Key findings are summarised as follows:-

5.1.1 Primary impacts for the 50th percentile adult and 6YO-child pedestrians

- Varying pedestrian size, impact position, impact velocity and vehicle contact region had significant effects on the kinematics, head contact location, head contact time and angles.
- Varying pedestrian size, impact position, impact velocity and vehicle contact region had a considerable influence on HIC values and head injury risk. In addition, impacts at the vehicle offset produced greater head injury risk than centreline. The lowest risk impact scenario for the adult was the side offset, which produced no head contact at impact velocities between 5km/h and 48km/h. Moreover, adults were subject to a relatively high risk of head impact injury at velocities of 20 km/h or greater during primary impacts, whilst, a 6YO-child was subjected to a significant head injury risk at 10km/h and greater.
- There was a robust correlation between HIC values and impact velocity for both adult and child during primary impacts.
- Variation in pedestrian size, impact position, impact velocity and vehicle contact region had a noticeable influence on upper neck load cases and in addition, impact velocity and size had a significant influence on upper neck injury, N_{ij} , values and injury risk for both the adult and child during frontal

impacts. There was, however, no significant influence of the vehicle contact region on N_{ij} observed for both adult and child. Upper neck injury values were observed to exceed the threshold ($N_{ij}=1$) at 25km/h for the adult and 15km/h for child.

- Varying impact velocity and vehicle contact region had a significant influence on upper neck injury values, N_{km} , and injury risk for the adult during rear impacts. In addition, impacts to the rear at a vehicle offset produced higher upper neck injury values N_{km} and injury risk than centreline, and exceed the threshold at impact velocities of 10 km/h or greater. Moreover, there was a robust correlation between upper neck injury criteria and impact velocity for both adult and child during primary impacts.
- Varying impact velocity and vehicle contact region had a significant influence on adult chest injury and injury risk and chest injury values (CTI) were observed to exceed the injury threshold, (CTI=1) at 35km/h at the vehicle centreline and 40km/h at the vehicle offset. In addition, there was a robust correlation between CTI values and impact velocity for the adult during primary impacts.

5.1.2 Secondary impacts for the 50th percentile adult pedestrian

For many years, the automotive industry has been trying to favourably influence the primary vehicular impacts with pedestrians by adapting the vehicle's frontal shape design. Furthermore, vehicle speed management has been established as a means of reducing injury severity during primary impacts. Secondary impacts with the ground do, however, inevitably occur and require further study. The following conclusions are drawn from this study:

- Variations in impact position, impact velocity and vehicle contact regions had a significant influence on the body contact region and landing patterns with the ground.
- Variations in impact position, impact velocity and vehicle contact regions had a significant influence on throw distance. There is a robust correlation between the throw distance and vehicle impact velocity. However, impacts at the vehicle centreline were associated with significant, predominantly linear projections and offset impacts with rotation.

- During the simulation of a real-accident scenario, the pedestrian response showed the greatest agreement with the CCTV recording at 25 km/h during both the primary and secondary phases. The approach can, therefore, be very useful for predicting the likely impact velocity during a road accident and further, for reconstructing the kinematics of road accident scenarios; accurately analysing accidents and their associated impact environment and improve safety in urban areas.
- Varying impact velocity, impact position and vehicle contact region had a significant influence on head-ground impact direction, contact orders and head injury risk. The variation in head-ground impact direction dictated head injury (HIC values) threshold selection.
- There was no robust relationship established between HIC and impact velocity during secondary impacts. In most cases HIC values and head injury risk were greater than those produced during primary impacts. Moreover, even relatively low primary impact velocities, for example 10km/h, at the safest impact scenario (side offset) could change to a fatal and injurious impact scenario during the secondary phase, producing a 100% risk of fatal head injury.
- Variations in impact velocity, impact position and vehicle contact region had a significant influence on head-torso movement, upper neck loads and upper neck injury risk. No robust correlation was established during the secondary impacts between upper neck injury criteria, N_{ij} and N_{km} and impact velocity. Upper neck injury risks, produced from the ground contacts, were, however, significantly greater than those produced during primary impacts, even at the low impact velocity of 10km/h and could cause fatal upper neck injury risk. Therefore, upper neck injury risk, produced during secondary impacts has some sensitivity.
- Varying impact velocity, impact position and vehicle contact region did have a significant influence on chest-ground impact direction. Although there was no robust correlation established between CTI and impact velocity during secondary impacts. Moreover, CTI and chest injury risk during secondary impacts were lower than those produced during the primary impacts.

In conclusion, even at relatively low impact velocities, the original auto-rickshaw design cannot be considered to be ‘pedestrian-friendly’ for use in urban areas, due to its frontal geometry, which exposes the pedestrian to significant risks of both injurious vehicle-pedestrian and pedestrian-ground related interactions.

5.1.3 Auto rickshaw engineering modifications for adult pedestrian safety enhancement

Response kinematics identified different alternative materials for the auto rickshaw windscreen and windscreen frame, which can produce injury risk mitigation.

- Aluminium 6016-T4 and magnesium AZ31B were established to be the best windscreen frame metals, of the materials investigated, for mitigating potential pedestrian injuries, showing excellent reductions in HIC, upper neck injury (N_{ij}) and chest injury (CTI) during frontal impacts. Combining both material changes to the windscreen and windscreen frame structures resulted in significantly lower injury criteria at the majority of impact positions, although offset head injury and rear impact neck injury risks remained high, AIS 4+ and AIS 3+, respectively.
- After taking into consideration economic factors, the 6016-T4 windscreen frame and polycarbonate windscreen combination was identified as the most suitable vehicle design, whilst demonstrating the potential to keep costs relatively similar to the current design.
- The results further demonstrate that the proposed auto rickshaw design may reduce the severity of certain injuries and subsequently decrease associated medical costs in low- and middle-income countries. The engineering modification would also reduce the vehicle mass, which would also influence fuel consumption and associated pollution.

To decrease the number of pedestrian-vehicle road accidents in developing countries, many factors require consideration, such as road infrastructures, pedestrian-vehicle separation and vehicle speed management.

This study demonstrates the potential contribution of vehicle technical engineering solutions in significantly reducing the level of injury risk, such as retro fitting injury mitigation technologies to those auto rickshaw contact regions, which are the subject

of the greatest risk of producing pedestrian injury. Moreover, the study demonstrates a need to avoid or reduce adult pedestrian's secondary phase kinematics by modifying the vehicle's frontal geometry for improving pedestrian safety.

5.2 Future work

Considering the extensive review of the existing research limitations and results the motivations for future research are suggested as follow:

- A collection of pedestrian-auto rickshaw real-world accident epidemiological data for subsequent computational model development, validation and analysis.
- An investigation of associated head injury risk as a result of impact related rotational accelerations.
- Further research of side upper neck and lower neck injury risk.
- Further research of chest injury risk for 6YO-child pedestrian.
- Further research of upper and lower extremities and abdomen.
- Further investigation of the influence of pedestrian size and pedestrian speed during an impact to assess the kinematic response, injury patterns and injury risk during primary and secondary impacts.
- Computational and/or experimental research is required to investigate the influence of changing the front-end geometry of the auto rickshaw on pedestrian injury patterns and injury risk during primary and secondary interactions.
- A more in-depth analysis of additional manufacturing costs is required.

6. REFERENCES

- [1] Peden, M., Scurfield, R., Sleet, D., Mohan, D., Hyder, A. A., Jarawan, E., and Mathers, C. (2004). "World report on road traffic injury prevention". *World Health Organization (W.H.O)*, Geneva-Switzerland.
- [2] World Health Organization (W.H.O). (2015). "Global status report on road safety-Time for action", Geneva-Switzerland.
- [3] Gwilliam, K. (2003). "Urban transport in developing countries". *Transport Review journal*, vol. 23, no. 2, pp. 197–216.
- [4] Hoque, M., McDonald, M., and Hall, R. D. (2001). "Road safety improvements in developing countries: priority issues and options". *Proceedings of the 20th Australian Road Research Board (ARRB) Conference*, pp. 1–15.
- [5] Al-Ghamdi, A. S. (2002). "Pedestrian-vehicle crashes and analytical techniques for stratified contingency tables". *Journal of Accident Analysis and Prevention*, vol. 34, no. 2, pp. 205–214.
- [6] Odero, W., Garner, P., and Zwi, A. (1997). "Road traffic injuries in developing countries: a comprehensive review of epidemiological studies". *Journal of Tropical Medicine and International Health*, no. 5, pp. 445–460.
- [7] Jacobs, G. and Thomas, A. (2002). "Africa road safety review: final report". *Department of Transportation/ Federal Highway Administration*, U.S.A.
- [8] Sarkar, S., Tay, R. and Hunt, J. D. (2011). "Logistic regression model of risk of fatality in vehicle-pedestrian crashes on national highways in Bangladesh". *Transport Research Record Journal of Transportation Research Board*, vol. 2264, no. 2264, pp. 128–137.
- [9] World Health Organization (W.H.O). (2007). "Youth and road safety", Geneva-Switzerland.
- [10] Rivara, F. P. (1990). "Injuries in the United States: current status of the problem, potential interventions, and future research needs". *The Journal of American Medical Association*, vol. 144, no. 985, pp. 25–29.
- [11] Hyder, A. A., Labinjo, M. and Muzaffar, S. S. F. (2006). "A new challenge to child and adolescent survival in urban Africa: An increasing burden of road traffic injuries". *Journal of Traffic Injury Prevention*, vol. 7, no. 4, pp. 381–388.
- [12] World Bank (W.B). (2002). "road safety". [Online]. Available: World Bank, World bank group. [Accessed: 09-Sep-2016].
- [13] International Road Transport Union (ITRU). (2009). "Middle east trade & road transport survey 2009", İstanbul-Turkey.
- [14] Ossenbruggen, P. J., Pendharkar, J. and Ivan, J. (2001). "Roadway safety in rural and small urbanized areas". *Journal of Accident Analysis and Prevention*, vol. 33, no. 4, pp. 485–498.
- [15] Herrstedt, L. (1997). "Planning and safety of bicycles in urban areas". *Proceedings of the International Conference Traffic Safety on Two Continents, paper number: VTI konferens 9A part 3*, pp. 41–56.

- [16] Ansari, S., Akhdar, F., Mandoorah, M. and Moutaery, K. (2000). "Causes and effects of road traffic accidents in Saudi Arabia". *Journal of Public Health*, vol. 114, no. 1, pp. 37–39.
- [17] Ofosu, J. B., Abouammoh, A. M. and Bener, A. (1998). "A study of road traffic accidents in Saudi Arabia". *Journal of Accident Analysis and Prevention*, vol. 20, no. 2, pp. 95–101.
- [18] Zajac, S. S., and Ivan, J. N. (2003). "Factors influencing injury severity of motor vehicle-crossing pedestrian crashes in rural Connecticut". *Journal of Accident Analysis and Prevention*, vol. 35, no. 3, pp. 369–379.
- [19] Miles-Doan, R. (1996). "Alcohol use among pedestrians and the odds of surviving an injury: Evidence from Florida law enforcement data". *Journal of Accident Analysis and Prevention*, vol. 28, no. 1, pp. 23–31.
- [20] Öström, M. and Eriksson, A. (2001). "Pedestrian fatalities and alcohol". *Journal of Accident Analysis and Prevention*, vol. 33, no. 2, pp. 173–180.
- [21] Flórez Valero, C. F. and Patiño Puerta, C. (2014). "Identification of the main risk factors for vulnerable non-motorized users in the city of Manizales and its relationship with the quality of road infrastructure". *Journal of Procedia - Social and Behavioral Sciences*, vol. 162, no. Panam, pp. 359–367.
- [22] Elvik, R. (1997). "Effects of accidents of automatic speed enforcement in Norway". *Journal of the Transportation Research Board*, vol. 1595, no. 1, pp. 1–19.
- [23] Broughton, J. and Baughan, C. (2002). "The effectiveness of antilock braking systems in reducing accidents in Great Britain". *Journal of Accident Analysis and Prevention*, vol. 34, no. 3, pp. 347–355.
- [24] Lloyd, L., Cuerden, R., Wallbank, C. and Seidl, M. (2015). "Predicting the impact of vehicle safety developments in emerging markets following the industrialised countries' experience". *Proceedings of the 24th International Technical Conference on the Enhanced Safety of Vehicles (ESV)*, Technical Paper, 15-0239, pp. 1–9.
- [25] The International Council on Clean Transportation (ICCT). (2016). "European vehicle market statistics; pocketbook 2016/17".
- [26] National Highway Traffic Safety Administration (NHTSA). (2002). "Fatality analysis reporting system (FARS)". [Online]. Available: <http://www-fars.nhtsa.dot.gov/QueryTool/querysection/selectyear.aspx>. [Accessed: 20-Jun-2017].
- [27] Gavrilă, D. M., Marchal, P. and Meinecke, M. M. (2003). "Vulnerable road user scenario analysis". *SAVE-U Project Deliverable*.
- [28] Japan Automobile Research Institute (JARI). (1997). "Technical note NO.27 possible steps for the automobile in changing environment: reviews and previews on consumer needs and performances". Japan, 1997.
- [29] Lukic, S. M., Mulhall, P., Choi, G., Naviwala, M., Nimmagadda, S. and Emadi, A. (2007). "Usage pattern development for three-wheel auto rickshaw taxis in India". *Proceedings of the IEEE Vehicle Power and Propulsion Conference (VPPC)*, pp. 610–616.

- [30] Somasundaraswaran, A. K., Kumari, T. and Siriwardana, D. (2006). “Three-wheeler drivers view in small cities in Sri Lanka”. *Third Acad. Sess. University of Ruhuna*. Sri Lanka, pp. 11–13.
- [31] Dharmaratne, S. D. and Stevenson, M. (2006). “Public road transport crashes in a low income country”. *Journal of Injury Prevention*, vol. 12, no. 6, pp. 417–420.
- [32] Mukherjee, S., Mohan, D. and Gawade, T. R. (2007). “Three-wheeled scooter taxi: A safety analysis”. *Sadhana - Academy Proceedings in Engineering Sciences*, vol. 32, no. 4, pp. 459–478.
- [33] Replogle, M. (1993). “Bicycle and cycle rickshaws in Asian cities”. *Proceedings of the 6th Conference on Urban Transport in Developing Countries*, no. 1372, PP.76–84
- [34] Mani, A., Pai, M. and Aggarwal, R. (2012). “Sustainable urban transport policy in India-role of the auto-rickshaw sector”. *World Resources Institute*, Mumbai-INDIA.
- [35] Mohan, D. (2009). “Road Accidents in India”. *IATSS RESEARCH*, Vol.33 No.1, pp. 75–79.
- [36] Mutya, K. V. and Rudra, S. (2015). “Road safety mechanism to prevent overtaking accidents”. *International Journal of Engineering Trends & Technology (IJETT)*, vol. 28, no. 5, pp. 219–222.
- [37] Champion, H. R., Copes, W. S., Buyer, D., Flanagan, M. E., Bain, L. and Sacco, W. J. (1989). “Major trauma in geriatric patients”. *Journal of American Public Health Association (APHA)*, vol. 79, no. 9, pp. 1278–1282.
- [38] Rane, N. (2010). “Design of the exterior for a three passenger auto rickshaw”. Case study about passenger auto rickshaw manufacturers and models in India.
- [39] Mohan, D., Kajzer, J., Bawa-Bhalla, K. S. and Chawla, A. (1997). “Impact modelling studies for a three-wheeled scooter taxi”. *Accident Analysis and Prevention*, vol. 29, no. 2, pp. 161–170.
- [40] Chawla, A., Mukherjee, S., Mohan, D., SINGH, J. and RIZVI, N. (2003). “Crash simulations of three wheeled scooter taxi (Tst)”. *Proceedings of the 18th International Technical Conference on the Enhanced Safety of Vehicles (ESV)*, pp. 1–14.
- [41] Lane, P. L., McClafferty, K. J. and Nowak, E. S. (1994). “Pedestrians in real world collisions”. *Journal of Trauma*, vol. 36, no. 2, pp. 231–236.
- [42] Ashton, S.J. (1982). “Vehicle design and pedestrian injuries”. In: Chapman, A.J., Wade, F.M., Foot, H.C. (Eds.), *Pedestrian Accidents*. Wiley, London.
- [43] Ashton, S. J. (1979). “Some factors influencing the injuries sustained by child pedestrians struck by the fronts of cars”. *Society of Automotive Engineers (SAE) International*, vol. 791016, pp. 351–380.
- [44] States, J. D. (1969). “The abbreviated and the comprehensive research injury scales”. *Proceedings of the 13th Stapp car crash conference*, paper number: 690810, pp. 2625–2634.
- [45] Horst, H.M., Obeid, F.N., Sorensen, U.J. and Bivins, B.A. (1986). “Factors influencing survival of elderly trauma patients”. *Critical Care Medicine*, vol. 14, pp. 681–684.

- [46] DeMaria, E. J., Kenney, P. R., Merriam, M. A., Casanova, L. A. and Gann, D. S. (1987). "Survival after trauma in geriatric patients". *Annals of Surgery*, vol. 206, no. 6, pp. 738–743.
- [47] Champion, H.R., Sacco, W.J. and Copes. W. S. (1995). "Injury severity scoring again". *Journal of Trauma*, vol. 40, pp. 78–82.
- [48] Horan, M. A. (2003). "Injury in elderly people". Churchill, Livingstone, Edinburgh: Brockelhurst's Textbook of Geriatric Medicine and Gerontology.
- [49] Hyde, A. S. and Hyde, C. B. (1992). "Crash injuries: how and why they happen: A primer for anyone who cares about people in cars". Florida: HYDE ASSOCIATES, INC.
- [50] The Association for the Advancement of Automotive Medicine (AAAM). (2016). "Abbreviated injury scale (AIS)". [Online]. Available: <https://www.aaam.org/abbreviated-injury-scale-ais/>. [Accessed: 07-Oct-2016].
- [51] Barnes, J. and Hassan, A. (2009). "Comparison of injury severity between AIS 2005 and AIS 1990 in a large injury database". *Association of Advancement in Automotive Medicine (AMMM)*.
- [52] Linn, S. (1995). "The injury severity score-Importance and uses". *Annals of Epidemiology*, vol. 5, no. 6, pp. 440–446.
- [53] Bhalla, K., Montazemi, P., Crandall, J. and Yang, J. (2002). "Vehicle impact velocity prediction from pedestrian throw distance: Trade-offs between throw formulae, crash simulators, and detailed multi-body modeling". *Proceedings of the International Research Council on Biomechanics of Injury (IRCOBI) Conference*, pp. 263–276.
- [54] Otte, D. and Pohlemann, T. (2001). "Analysis and load assessment of secondary impact to adult pedestrians after car collisions on roads". *Proceedings of the International Research Council on Biomechanics of Injury (IRCOBI) Conference*, pp. 143–157.
- [55] Simms, C. K. and Wood, D. P. (2006). "Effects of pre-impact pedestrian position and motion on kinematics and injuries from vehicle and ground contact". *International Journal Crashworthiness*, vol. 11, no. 4, pp. 345–355.
- [56] Richardson, S., Josevski, N., Sandvik, A., Pok, T., Orton, T. L., Winter, B. and Wang, X. (2015). "Pedestrian throw distance impact speed contour plots using PC-crash". *Society of Automotive Engineers (SAE)*, Technical Paper, 2015-01-1418.
- [57] Yao, J., Yang, J. and Otte, D. (2007). "Head injuries in child pedestrian accidents-in-depth case analysis and reconstructions". *Journal of Traffic Injury Prevention*, vol. 8, no. 1, pp. 94–100.
- [58] Chidester, A. B. and Isenberg, R. A. (2001). "Final Report - The pedestrian crash data study". *Proceedings of the 17th International Conference on the Enhanced Safety of Vehicles (ESV)*, Technical Paper, 248.
- [59] Klinich, K. and Schneider, L. (2003). "Biomechanics of pedestrian injuries related to lower extremity injury assessment tools: A review of the literature and analysis of pedestrian crash database". *Alliance for Automobile Manufacturers (AAM)*, Michigan-USA.

- [60] Louis Martin, J. and Lardy, A. and Laumon, B. (2011). “Pedestrian injury patterns according to car and casualty characteristics in France”. *Proceedings of the 55th Annals of Advances in Automotive Medicine (AAAM) Annual Conference*, vol. 55, pp. 137–146.
- [61] Mizuno, Y. and Ishikawa, H. (2005). “Summary of IHRA pedestrian safety WG activities – proposed test methods to evaluate pedestrian protection afforded by passenger cars”. *Proceedings of the 19th International Technical Conference on the Enhanced Safety of Vehicles (ESV)*, pp. 1–17.
- [62] Zhao, H., Yin, Z., Chen, R., Chen, H., Song, C., Yang, G. and Wang, Z. (2010). “Investigation of 184 passenger car-pedestrian accidents”. *International Journal of Crashworthiness*, vol. 15, no. 3, pp. 313–320.
- [63] Alkabli, N. A. (2005). “Tri-wheeler induced accident in Khartoum state”. *University of Khartoum. Medical and Health Studies Board*.
- [64] Schmucker, U., Dandona, R., Kumar, G. A. and Dandona, L. (2011). “Crashes involving motorised rickshaws in urban India: Characteristics and injury patterns”. *Journal of Injury*, vol. 42, no. 1, pp. 104–111.
- [65] De Silva, M., Nellihala, L. P. and Fernando, D. (2001). “Pattern of accidents and injuries involving three-wheelers”. *Ceylon Medical Journal*, vol. 46, no. 1, pp. 15–16.
- [66] Ashton, S. J. (1975). “The cause and nature of head injuries sustained by pedestrians”. *Proceedings of the International Research Council on Biomechanics of Injury (IRCOBI) Conference*, Birmingham, United Kingdom.
- [67] Roudsari, B. S., Mock, C. N. and Kaufman, R. (2005). “An evaluation of the association between vehicle type and the source and severity of pedestrian injuries”. *Journal of Traffic Injury Prevention*, vol. 6, no. 2, pp. 185–19.
- [68] Kendall, R., Meissner, M. and Crandall, J. (2006). “The causes of head injury in vehicle pedestrian impacts: Comparing the relative danger of vehicle and road surface”. *Society of Automotive Engineers (SAE)*, Technical Paper, 2006-01-0462.
- [69] Yang, J., Yao, J. and Otte, D. (2005). “Correlation of different impact conditions to the injury severity of pedestrians in real world accidents”. *Proceedings of the 19th International Technical Conference on the Enhanced Safety of Vehicle (ESV)*, Technical Paper, 2005-0352.
- [70] Crocetta, G., Piantini, S., Pierini, M. and Simms, C. (2015). “The influence of vehicle front-end design on pedestrian ground impact”. *Journal of Accident Analysis and Prevention*, vol. 79, pp. 56–69.
- [71] Tamura, A. and Duma, S. (2011). “A study on the potential risk of traumatic brain injury due to ground impact in a vehicle-pedestrian collision using full-scale finite element models”. *International Journal of Vehicle Safety*, vol. 5, no. 2, pp. 117–136.
- [72] Hamacher, M., Eckstein, L. and Paas, R. (2012). “Vehicle related influence of post-car impact pedestrian kinematics on secondary impact”. *Proceedings of the International Research Council on Biomechanics of Injury (IRCOBI) Conference*, pp. 717–729.

- [73] Hiatt, J. L., Gartner, L. P. (2010). "Textbook-of-head-and-neck-anatomy". Fourth edition. Philadelphia: Lippincott Williams & Wilkins, a Wolters Kluwer business.
- [74] Assefa, N. and Yosief, T. (2003). "Human Anatomy and Physiology". Ethiopia Public Health Training Initiative (Ephti).
- [75] Bilo, R. A. C., Robben, S. G. F. and Van Rijn, R. R. (2010). "Forensic aspects of paediatric fractures: Differentiating accidental trauma from child abuse". *Proceedings of the Forensic Aspects of Pediatric Fractures: Differentiating Accidental Trauma from Child Abuse*, Berlin: Springer, pp. 1–209.
- [76] Toganel, G. and Soica, A. (2007). "Aspects Regarding the Impact Speed, Ais and Hic Relationship for Car-Pedestrian Traffic Accidents". *Annals of the Oradea University: Fascicle of Management and Technological Engineering*, vol. VI, no. Xvi, pp. 270–277.
- [77] Gray, H. (2000). "Gray's Anatomy", New York-USA.
- [78] Genneralli, T. A. (1985). "The state of the art of head injury biomechanics – a review". *Proceedings of the 29th Annual American Association for Automotive Medicine (AAAM) Conference*.
- [79] UChicago Medicine, "Skull fractures". [Online]. Available: www.uchospitals.edu. [Accessed: 05-May-2018].
- [80] Mclean, A. J. and Anderson, R. W. G. (1997). "Biomechanics of closed Head Injury". *Response of the Head to Impact*. First edition, P. Reilly and R. Bullock, Eds. London.: Chapman & Hall, pp. 25-37.
- [81] Association for the Advancement of Automotive Medicine (AAAM). (2005). "The Abbreviated Injury Scale (AIS) 2005 Revision AAAM". Des Plaines Illinois.
- [82] Prasad, P. and Mertz, H. J. (1985). "The Position of the United States Delegation to the ISO Working Group 6 on the Use of HIC in the Automotive Environment". *Society of Automotive Engineers (SAE)*, Technical Paper, 851246.
- [83] Mertz, H.J., Prasad, P., and Nusholtz, G. (1996). "Head injury risk assessments based on 15 ms HIC and peak head acceleration criteria". *Proceedings of the AGARD Meeting on Impact Head Injury: Responses, Mechanisms, Tolerance, Treatment and Countermeasures*, AGARD-CP-597, Ch. 11. Canada Comm. Group, Inc., Canada
- [84] Hertz, E. (1993). "A note on the head injury criterion (HIC) as a predictor of the risk of skull fracture". *Proceedings of the Association for the Advancement of Automotive Medicine Annual Conference*, vol. 37, pp. 303–312
- [85] The Trauma Audit & Research Network (TARN). (2015). "Injury Scoring & Assigning an ISS". Mancheste.
- [86] Howard, D. (1956). "Manage head, neck, and face injuries". United State Marine Corps Field Medical Training Battalion. Camp Lejeune, NC 28542-0042: FMST 408.
- [87] Mertz, H. J. and Patrick, L. M. (1971). "Strength and response of the human neck". *Society of Automotive Engineers (SAE)*, Technical Paper, 710855.
- [88] King, A. I. (2018). "The biomechanics of impact Injury: biomechanical response, mechanisms of injury, human tolerance and simulation". Gewerbestrasse-Switzerland: Springer.

- [89] Lilian, G. and Tamara, H. (2010). “Anatomy of the head and neck”. *The State Medical and Pharmaceutical University “Nicolae Testemitanu” Department of Human Anatomy*. Chisinau.
- [90] Di Giuseppe, A., Commons, G. and Scalise, A. (2013). “Cosmetic surgery: Art and techniques”. *Proceedings of the Cosmetic Surgery: Art and Techniques*, pp. 1–1192.
- [91] Panjabi, M. M., Cholewicki, J., Nibu, K., Grauer, J. N., Babat, L. B., Dvorak, J. and Bär, H. F. (1998). “Biomechanics of whiplash injury”. *Journal of Orthopaedics*, vol. 27, no. 5, pp. 813–819.
- [92] Ning, L. (2014). “Finite Element Modeling and Simulation of occupant response in Highway Crashes”. *The University of North Carolina*.
- [93] Eppinger, R., Sun, E., Bandak, F., Haffner, M., Khaewpong, N., Maltese, M., Kuppa, S., Nguyen, T., Takhounts, E., Tannous, R., Zhang, A. and Saul, R. (1999). “Development of improved injury criteria for the assessment of advanced automotive restraint systems-II”. *National Highway Traffic Safety Administration (NHTSA): National Transportation Biomechanics Research Center (NTBRC)*, USA.
- [94] Parr, J. C., Miller, M. E., Bridges, N. R., Buhman, J. R., Perry, C. E. and Wright, N. L. (2012). “Evaluation of the Nij neck injury criteria with human response data for use in future research on helmet mounted display mass properties”. *Proceedings of the Human Factors and Ergonomics Society Annual Meeting*, vol. 56, no. 1, pp. 2070–2074.
- [95] Muser, M. H. and Niederer, P. (2000). “A new neck injury criterion candidate for rear-end collisions taking into account shear forces and bending moments”. *Proceedings of the 17th International Technical Conference on the Enhanced Safety of Vehicle (ESV)*, pp. 1–9.
- [96] Mertz, H. J., Prasad, P. and Irwin, A. L. (1997). “Injury risk curves for children and adults in Frontal and Rear Collisions”. *Proceedings of the 41st Stapp Car Crash Conference*, pp. 13–30.
- [97] Berthet, F., Vezin, P., Kellendonk, G., Hynd, D. and Verriest, J. P. (2006). “Review of the thorax injury criteria”. *Integrated Project on Advanced Protection Systems: APROSYS*, Project no-FP6-PLT-506503.
- [98] Schneider, L. W. (1989). “Design requirements and specifications: Thorax-abdomen development Task. Interim Report: Trauma assessment device development program”. *Department of transportation: National Highway Traffic Safety Administration (NHTSA)*, U.S.A.
- [99] Holcombe, S. A. (2016). “The development of population-wide descriptions of human rib and rib cage geometry”. *Biomedical Engineering, University of Michigan*.
- [100] Javouhey, E., Céline Guérin, A., Chiron, M. (2006). “Incidence and risk factors of severe traumatic brain injury resulting from road accidents: A population-based study”. *Journal of Accident Analysis and Prevention*, vol. 38, no. 2, pp. 225–233.
- [101] Gray, H. (1918). “Anatomy of the human body”. *Annals of surgery*, Vol. 68(5), p.564.
- [102] Collants, M. (1990). “Evaluation of the importance of the using Head Injury Criteria (HIC) to estimate the likelihood of head impact injury as a result of a fall onto playground surface materials”. *US Consumer Product Safety Commission*.

- [103] Lissner H. R., Lebow M. and Evans F.G. (1960). "Experimental studies on the relations between acceleration and intracranial pressure changes in man". *Surgery, Gynecology and Obstetrics*, Vol 111, PP 329-338.
- [104] Gadd, C. M. (1966). "Use of a weighted impulse criterion for estimating injury hazard". *Proceedings of the 10th Stapp Car Crash Conference, Society of Automotive Engineers (SAE)*, New York, pp. 164-174.
- [105] Pritz, H. B., Weis, E. B. and Herridge, J. T. (1975). "Body-vehicle interaction: experimental study, Volume I". *National Highway Traffic Safety Administration (NHTSA)*, Washington, D.C.-USA.
- [106] Versace, J. (1971). "A Review of the Severity Index". *Proceedings of the 15th Stapp Car Crash Conference*, pp. 309-334.
- [107] Mellander, H. (1986). "HIC- the head injury criterion- practical significance for the automotive industry". *Acta Neurochirurgica*, vol. 36, pp.198-220.
- [108] Mertz, H. J., Irwin, A. L. and Prasad, P. (2003). "Biomechanical and scaling bases for frontal and side impact injury assessment reference values". *Stapp Car Crash Journal*, vol. 47, pp. 155-88.
- [109] Hodgson, V. R. and Thomas, L. M. (1972). "Effect of long-duration impact on head". *Proceedings of the 16th Stapp Car Crash Conference*, no. 720956, pp. 335-338.
- [110] Hodgson, V. R. and Thomas, L. M. (1977). "Breaking strength of the human skull vs. impact surface curvature". *Wayne State University, Dept. of Neurosurgery*, Detroit, Michigan., USA.
- [111] Got, C. Patel, A., Fayon, A., Tarrière, C. and Walfisch, G. (1978). "Results of experimental head impacts on cadavers: The various data obtained and their relations to some measured physical parameters". *Proceedings of the 22nd Stapp Car Crash Conference*, p. 780887.
- [112] Ono, K., Kikuchi, A., and Nakamura, M. (1980). "Human head tolerance to sagittal impact reliable estimation deduced from experimental head injury using subhuman primates and human cadaver skulls human head tolerance to sagittal impact reliable estimation deduced from experimental head injury using Subh". *Proceedings of the 24th Stapp Car Crash Conference*, pp. 103-160.
- [113] Mertz, H. J., Prasad, P. and Nusholtz, G. (1996). "Head injury risk assessment for forehead impacts". *Society of Automotive Engineers (SAE)*, pp. 1-23, 1996.
- [114] Yoganandan, M., Pintar, F. A. and Zhang, J. (2006). Gennarelli, "Biomechanical aspects of blunt and penetrating head injuries". *Proceedings of the IUTAM Symposium on Impact Biomechanics: From Fundamental Insights to Applications*, vol. 124, pp. 173-184.
- [115] Kikuchi, A., Ono, K. and Nakamura, N. (1982). "Human head tolerance to lateral impact deduced from experimental head injuries using primates". *Proceedings of the Enhanced Safety Vehicle Conference (ESV)*, pp. 251-261.
- [116] McIntosh, A. S., Svensson, N. I., Kallieris, D., Mattern, R., Krabbel, G. and Ikels, K. (1996). "Head impact tolerance in side impacts". *Proceedings of the International Technical Conference on the Enhanced Safety of Vehicles (ESV)*, pp. 1273-1280.

- [117] McIntosh, A. S., Svensson, N. I., Kallieris, D., Mattern, R., Krabbel, G. and Ikels, K. (1996). "Head impact tolerance in side impacts". *Proceedings of the International Technical Conference on the Enhanced Safety of Vehicles (ESV)*, pp. 1273–1280.
- [118] Mertz, H. J. (2002). "Injury risk assessments based on dummy responses". Nauham and Springer, pp.89-102.
- [119] Kleinberger, M., Sun, E., Eppinger, R. and Saul, R. (2000). "Supplement: Development of improved injury criteria for the assessment of advanced automotive restraint systems- II". *National Highway Traffic Safety Administration (NHSTA): National Transportation Biomechanics Research Center (NTBRC)*, U.S.A.
- [120] Kenedi, R. M. (1971). "Strength of Biological Materials". *Journal of Anatomy*, vol. 108, no. Pt 3, p. 582.
- [121] Sances, A., Weber, R.C., Larson, S.J., Cusick, J.S., Myklebust, J.B. and Walsh, P.R. (1981). "Bioengineering analysis of head and spine injuries". *Journal of Critical Reviews in Bioengineering*, vol. 5, no. 2, pp.79-122.
- [122] Mertz, H.J., Hodgson, V.R., Thomas, L. M. and Nyquist, G.W. (1978). "An Assessment of Compressive Neck Loads Under Injury-Producing Conditions". *Journal of Physician Sport. Medicine*, vol. 6, no. 11, pp. 95–106.
- [123] Nyquist, G. W., Begman, P. C., King, A. I. and Mertz, H. J. (1980). "Correlation of field injuries and GM hybrid III dummy responses for Lap-shoulder Belt Restraint". *Journal of biomechanical engineering*, vol. 102, no. 2, pp. 103–109, 1980.
- [124] Prasad, P. and Daniel, R. P. (1984). "A biomechanical analysis of head, neck, and torso injuries to child surrogates due to sudden torso acceleration". *Society of Automotive Engineers (SAE)*, Technical Paper, 841656.
- [125] Yoganandan, N., Walsh, P. R. and Pintar, F. A. (1996). "Human head-neck biomechanics under axial tension". *Journal of Medical Engineering and Physics*, vol. 18, no. 4, pp. 289–294.
- [126] Shea, M., Wittenberg, R. H., Edwards, W. T., White, A. A. and Hayes, W. C. (1992). "In vitro hyperextension injuries in the human cadaveric cervical spine". *Journal of Orthopaedic Research*, vol. 10, no. 6, pp. 911–916, 1992.
- [127] Kleinberger, M., Sun, E., Eppinger, R. and Saul, R. (1998). "Development of improved injury criteria for the assessment of advanced automotive restraint systems". *National Highway Traffic Safety Administration (NHSTA): National Transportation Biomechanics Research Center (NTBRC)*, U.S.A.
- [128] Yang, K. H., Begeman, P. C., Muser, M., Niederer, P. and Walz, F. (1997). "On the role of cervical facet joints in rear end impact neck injury mechanisms". *Society of Automotive Engineers (SAE)*, pp. 127–129.
- [129] Deng, B., Luan, F., Begeman, P. C., Yang, K.H., and King, A. I. and Tashman, S. (2000). "Testing shear hypothesis of whiplash injury using experimental and analytical approaches". *Frontiers in Whiplash Trauma*, Amsterdam, The Netherlands: IOS Press.
- [130] Muser, M. H., Walz, F. H. and Zellmer, H. (2000). "Biomechanical significance of the rebound phase in low speed rear end impacts". *Proceedings of the International Research Council on Biomechanics of Injury (IRCOBI) Conference on the Biomechanics of Impact*, pp. 393–410.

- [131] Parr, J. C., Miller, M. E., Colombi, J. M., Schubert Kabban, C. M. and Pellettiere, J. A. (2015). "Development of a side-impact (Gy) neck injury criterion for use in aircraft and vehicle safety evaluation". *IIE Transactions on Occupational Ergonomics and Human Factors*, vol. 0, pp. 1–14.
- [132] Morris, A., Welsh, R., Frampton, R., Charlton, J. and Fildes, B. (2002). "An overview of requirements for the crash protection of older drivers". *Annual Proceedings of the Association for the Advancement of Automotive Medicine*, vol. 46, pp. 141–156.
- [133] Frampton, R. J., Mackay, G. M. (1994). "The characteristics of fatal collisions for belted occupants". *Society of Automotive Engineers (SAE)*, China, Procs FISITA Congress, Beijing, Paper 945167.
- [134] Eiband, M. (1959). "Human tolerance to rapidly applied accelerations: a summary of the literature". *National Aeronautics and Space Administration (NASA)*, Lewis Research Centre, Cleveland, U.S.A, Ohio.
- [135] Kent, R., Patrie, J. and Benson, N. (2003). "The Hybrid III dummy as a discriminator of injurious and non-injurious restraint loading". *Proceedings of the in Annual Association for the Advancement of Automotive Medicine*, vol. 47, pp. 51–75.
- [136] Neathery, R. F., Kroell, C. K. and Mertz, H. J. (1975). "Prediction of thoracic injury from dummy responses". *Society of Automotive Engineers (SAE)*, vol. 84, no. 4, pp. 3178–3187.
- [137] Lau, I., Viano, D. (1986). "The viscous criterion - Bases and applications of an injury severity index for soft tissues". *Stapp Car Crash Journal*, vol. 30, pp. 123–142.
- [138] Viano, D., Lau, I., Asbury, C., King, A. I. and Begeman, P. (1989). "Biomechanics of the human chest, abdomen, and pelvis in lateral impact". *Journal of Accident Analysis and Prevention*, vol. 21, no. 6, pp. 553–574.
- [139] Schmitt, K.-U., Niederer, P.F., Muser, M.H. and Walz, F. (2004). "Trauma biomechanics: introduction to accidental injury". Fourth edition, Berlin; New York : Springer.
- [140] Kuppa, S. M., Kuppan, S. M. and Eppinger, R. H. (1998). "Development of an improved thoracic injury criterion". *Proceedings of the 42nd Stapp Car Crash Conference*.
- [141] Backaitis, S. H. and Laurent, A. (1986). "Chest deflection characteristics of volunteers and Hybrid III dummies". *Proceedings of the 13th Stapp Car Crash Conference*, pp 157-166.
- [142] Cesari, D. and Bouquet, R. (1990). "Behavior of human surrogates under belt loading". *Proceedings of the 34th Stapp Car Crash Conference*, pp 73-82.
- [143] Yu, M. (2010). "Finite element analysis of passenger multiple belt restraint configurations". *Wake Forest University*, North Carolina- USA.
- [144] McLean, A. (1972). "Car shape and pedestrian injury". *Proceedings of the National Road Safety Symposium, Canberra: Department of Shipping and Transport*, pp. 179–192.
- [145] Tanno, K., Kohno, M., Ohashi, N., Ono, K., Aita, K., Oikawa, H., Myo-Thaik-Oo, Honda, K. and Misawa, S. (2000). "Patterns and mechanisms of pedestrian injuries

- induced by vehicles with flat-front shape”. *Journal of Legal Medicine*, vol. 2, no. 2, pp. 68–74.
- [146] Roudsari, B. S., Mock, C. N., Kaufman, R., Grossman, D., Henary, B. Y. and Crandall, J. (2004). “Pedestrian crashes: Higher injury severity and mortality rate for light truck vehicles compared with passenger vehicles” *Journal of Injury Prevention*, vol. 10, no. 3, pp. 154–158.
- [147] Yang, J. (1997). “Injury biomechanics in car-pedestrian collisions: development, validation and application of human-body mathematical models”. Chalmers University of Technology, Sweden.
- [148] Zhang, G., Qin, Q., Chen, Z., Bai, Z. and Cao, L. (2018). “A Study of the effect of the front-end Styling of sport utility vehicles on pedestrian head injuries”. *Applied Bionics and Biomechanics*.
- [149] Henary, B. Y., Crandall, J., Bhalla, K., Mock, C. N. and Roudsari, B. S. (2003). “Child and adult pedestrian impact: the influence of vehicle type on injury severity,” *Proceedings of the Annual Association for the Advancement of Automotive Medicine*, vol. 47, no. January, pp. 105–26.
- [150] Ballesteros, M. F., Dischinger, P. C. and Langenberg, P. (2004). “Pedestrian injuries and vehicle type in Maryland, 1995-1999”. *Journal of Accident Analysis and Prevention*, vol. 36, no. 1, pp. 73–81.
- [151] Peng, Y., Deck, C., Yang, J. and Willinger, R. (2012). “Effects of pedestrian gait, vehicle-front geometry and impact velocity on kinematics of adult and child pedestrian head”. *International Journal of Crashworthiness*, vol. 17, no. 5, pp. 553–561.
- [152] Otte, D. (1999). “Severity and mechanism of head Impacts in car to pedestrian”. *Proceedings of the International Research Council on Biomechanics of Injury (IRCOBI) Conference on the Biomechanics of Impact*, pp. 329–341.
- [153] Maki, T., Kajzer, J., Mizuno, K. and Sekine, Y. (2003). “Comparative analysis of vehicle-bicyclist and vehicle-pedestrian accidents in Japan,” *Journal of Accident Analysis and Prevention*, vol. 35, no. 6, pp. 927–940.
- [154] Ashton, S. J. (1980). “Preliminary assessment of the potential for pedestrian injury reduction through vehicle design”. *Proceedings of the 24th Stapp car crash conference*, paper number, 801315.
- [155] Simms, C. K., Wood, D. P. and Walsh, D. G. (2004). “Confidence limits for impact speed estimation from pedestrian projection distance”. *International Journal of Crashworthiness*, vol. 9, no. 2, pp. 219–228.
- [156] Simms, C. K., Ormond, T. and Wood, D. P. (2011). “The influence of vehicle shape on pedestrian ground contact mechanisms”. *Proceedings of the International Research Council on Biomechanics of Injury (IRCOBI) Conference on the Biomechanics of Impact*, pp. 282–286.
- [157] Rosén, E., Källhammer, J. E., Eriksson, D., Nentwich, M., Fredriksson, R. and Smith, K. (2010). “Pedestrian injury mitigation by autonomous braking”. *Journal of Accident Analysis and Prevention*, vol. 42, no. 6, pp. 1949–1957.
- [158] Fredriksson, R., Rosén, E., and Kullgren, A. (2010). “Priorities of pedestrian protection - A real-life study of severe injuries and car sources,” *Journal of Accident Analysis and Prevention*, vol. 42, no. 6, pp. 1672–1681.

- [159] Peng, Y., Deck, C., Yang, J., Otte, D. and Willinger, R. (2013). “A study of adult pedestrian head impact conditions and injury risks in passenger car collisions based on Real-World accident data,” *Journal of Traffic Injury and Prevention*, vol. 14, no. 6, pp. 639–646.
- [160] Peng, Y., Deck, C., Yang, J., Otte, D. and Willinger, R. (2012). “A study of kinematics of adult pedestrian and head impact conditions in case of passenger car collisions based on real world accident data,” *Proceedings of the IRCOBI Conference Proceedings - International Research Council on the Biomechanics of Injury*, pp. 766–778.
- [161] Liu, X. and Yang, J. (2003). “Effects of vehicle impact velocity and front-end structure on dynamic responses of child pedestrians,” *Journal of Traffic Injury and Prevention*, vol. 4, no. 4, pp. 337–344.
- [162] Han, Y., Yang, J., Nishimoto, K., Mizuno, K., Matsui, Y., Nakane, D., Wanami, S. and Hitosugi, M. (2012). “Finite element analysis of kinematic behaviour and injuries to pedestrians in vehicle collisions,” *International Journal of Crashworthiness*, vol. 17, no. 2, pp. 141–152.
- [163] Peng, Y., Chen, Y., Yang, J., Otte, D. and Willinger, R. (2012). “A study of pedestrian and bicyclist exposure to head injury in passenger car collisions based on accident data and simulations,” *Journal of Safety Science*, vol. 50, no. 9, pp. 1749–1759.
- [164] Han, Y., Yang, J., Mizuno, K. and Matsui, Y. (2012). “Effects of Vehicle Impact Velocity, Vehicle Front-End Shapes on Pedestrian Injury Risk”. *Journal of Traffic Injury and Prevention*, vol. 13, no. 5, pp. 507–518.
- [165] Khorasani-Zavareh, D., Bigdeli, M., Saadat, S. and Mohammadi, R. (2015). “Kinetic energy management in road traffic injury prevention: a call for action”. *Journal of injury & Violence*, vol. 7, no. 1, pp. 36–37.
- [166] Watanabe, R., Katsuhara, T., Miyazaki, H., Kitagawa, Y. and Yasuki, T. (2012). “Research of the relationship of pedestrian injury to collision speed, car-type, impact location and pedestrian sizes using human FE model (THUMS Version 4)”. *Journal of Stapp Car Crash*, vol. 56, pp. 269–321.
- [167] Hyeok Park, J., Yun, S., Kim, H. and Moon, S. (2016). “Assessment of chest injury in unconstraint frontal collision between human-mobile robot using CTI and VC index : Preliminary results by MADYMO simulation”. *Proceedings of the 16th International Conference on Control, Automation and Systems (ICCAS 2016)*, pp. 1164–1166.
- [168] Rosén, E., Stigson, H. and Sander, U. (2011). “Literature review of pedestrian fatality risk as a function of car impact speed”. *Journal of Accident Analysis and Prevention*, vol. 43, no. 1, pp. 25–33.
- [169] Yang, J. (2005). “Review of injury biomechanics in car-pedestrian collisions,” *International Journal of Vehicle Safety*, vol. 1, no. 1/2/3, p. 100.
- [170] Morrison, D. S., Coetzer, R., Choonara, I., Gorman, D., Douglas, M., Noble, P. and Patton, G. (2001). “Reducing speed limit to 20 mph in urban areas: Child deaths and injuries would be decreased”. *The British Medical Journal (BMJ)*, vol. 322, no. 7277, p. 1160.
- [171] Department for Transport. (2004). “Speed: Know your limits”. London-UK.

- [172] EEVC/CEVE. (1974). “European Experimental Vehicles Committee : The future for car safety in Europe”. *Proceedings of the Fifth International Technical Conference on the Enhanced Safety of Vehicles (ESV)*, pp. 1–75.
- [173] United Nations (UN). (1998). “Agreement Concerning The Establishing of Global Technical Regulations for Wheeled Vehicles, Equipment and Parts which can be Fitted and/or be Used on Wheeled Vehicles”. Geneva-Switzerland.
- [174] McNally, D. S. and Rosenberg, N. M. (2013). “MADYMO simulation of children in cycle accidents: A novel approach in risk assessment”. *Accident Analysis and Prevention*, vol. 59, pp. 469–478.
- [175] Liu, W., Su, S., Qiu, J., Zhang, Y. and Yin, Z. (2016). “Exploration of pedestrian head injuries-collision parameter relationships through a combination of retrospective analysis and finite element method”. *International Journal of Environmental Research and Public Health*, vol. 13, no. 12, pp. 1–15.
- [176] Shi, L., Han, Y., Huang, H., Li, Q., Wang, W. and Mizuno, K. (2018). “Analysis of pedestrian-to-ground impact injury risk in vehicle-to-pedestrian collisions based on rotation angles”. *Journal of Safety Research*, vol. 64, pp. 37–47.
- [177] Elliott, J. R., Simms, C. K. and Wood, D. P. (2012). “Pedestrian head translation, rotation and impact velocity : The influence of vehicle speed, pedestrian speed and pedestrian gait”. *Accident Analysis and Prevention*, vol. 45, pp. 342–353.
- [178] Carcinoid, R., Liver, M., Nodes, L., Metastases, B. and Responded, T. (2010). “Pedestrian head impact dynamics: Comparison of dummy and PMHS in small sedan and large SUV impacts”. *Proceedings of the 21st International Technical Conference on the Enhanced Safety of Vehicles Conference (ESV)*, pp. 2349–2351.
- [179] Liu, X. J., Yang, J. K. and Lövsund, P. (2002). “A study of influences of vehicle speed and front structure on pedestrian impact responses using mathematical models”. *Journal of Traffic Injury Prevention*, vol. 3, no. 1, pp. 31–42.
- [180] Watanabe, R., Miyazaki, H., Kitagawa, Y. and Yasuki, T. (2011). “Research of collision speed dependency of pedestrian head and chest injuries using human FE Model (THUMS VERSION 4)”. *Proceedings of the Conference on the Enhanced Safety of Vehicles Conference (ESV)*, Paper Number, 11-0043.
- [181] Simms, C. K. and Wood, D. P. (2006). “Pedestrian risk from cars and sport utility vehicles – a comparative analytical study”. *The Institution of Mechanical Engineers (IMechE)*, vol. 220, pp. 1085–1100.
- [182] Gupta, V. and Yang, K. H. (2013). “Effect of vehicle front end profiles leading to pedestrian secondary head impact to ground”. *Stapp Car Crash Journal*, vol. 57, pp. 139–155.
- [183] Fugger, T., Randles, B., Wobrock, J., and Eubanks, J. (2002). “Pedestrian throw kinematics in forward projection collisions”. *Society of Automotive Engineers (SAE)*, paper number, 01–0019.
- [184] Otte, D. (2004). “Use of throw distances of pedestrians and bicyclists as part of a scientific accident reconstruction method”. *Proceedings of the World Congress and Exhibition*, SAE paper, pp. 2004-01-1216.
- [185] Carollo, F. and Virzi ’mariotti, G. (2016). “Injury and throwing distance in teenage cyclist-vehicle crash”. *WSEAS TRANSACTIONS on POWER SYSTEMS*, vol. 11, pp. 171–182.

- [186] Wood, D. P., Simms, C. K. and Walsh, D. G. (2005). “Vehicle – pedestrian collisions : validated models for pedestrian impact and projection”. *The Institution of Mechanical Engineers (IMechE)*, vol. 219, no. D, pp. 183–195.
- [187] Okamoto, Y., Sugimoto, T., Enomoto, K., and Kikuchi, J. (2017). “Pedestrian head impact conditions depending on the vehicle front shape and its construction-Full model simulation”. *Traffic Injury Prevention*, vol. 4, pp. 74–82.
- [188] Huelke, D. F. (1998). “An Overview of anatomical considerations of infants and children in the adult world of automobile safety designs”. *Proceedings of the 42nd Annual Proceedings Association for the Advancement of Automotive Medicine*, pp. 267–280.
- [189] Brun-Cassan, F., Page, M., Pincemaille, Y., Kallieris, D. and Tarriere, C. (1993). “Comparative study of restrained child dummies and cadavers in experimental crashes”. *Proceedings of the 37th Stapp Car Crash Conference*, pp. 243–260.
- [190] Eubanks, P. F., and Hill, J. (1994). “Pedestrian accident reconstruction and litigation”. Second edition. Arizona, USA: Lawyers & Judges Publishing Company.
- [191] Toor, A., Araszewski, A., Johal, M., Overgaard, R. and Happer, R. (2002). “Revision and validation of vehicle/pedestrian collision analysis method”. *Proceedings of the Society of Automotive Engineers (SAE) World Congress and 255 Exposition*, Paper number, 01-0550.
- [192] Venkatason, K., Sivaguru, S., Abdullah, K. A., Idres, M. M., Shah, Q. H. and Wong, S. V. (2014). “The head injury mitigation of an adult and child pedestrian in a frontal vehicle impact using response surface methodology”. *Journal of Applied Mechanics and Materials*, vol. 575, pp. 952–955.
- [193] Wiart, J., Hadjem, A., Wong, M. F. and Bloch, I. (2008). “Analysis of RF exposure in the head tissues of children and adults”. *Physics and Medicine and Biology*, vol. 53, no. 13, pp. 3681–3695.
- [194] Ito, K., Tokuyama, M., Miyazaki, H., Hayashi, S., Kitagawa, Y. and Yasuki, T. (2017). “Development of child Finite Element (FE) models and vehicle-to-pedestrian collision simulations”. *Proceedings of the 25th Conference on the Enhanced Safety of Vehicles Conference (ESV)*, pp. 1–17.
- [195] Teng, T.-L. and Nguyen, T.-H. (2010). “Assessment of the pedestrian friendliness of a vehicle using subsystem impact tests”. *International Journal of Automotive Technology*, vol. 11, no. 1, pp. 67–73.
- [196] Barbani, D., Baldanzini, N. and Pierini, M. (2014). “Development and validation of an FE model for motorcycle-car crash test simulations”. *International Journal of Crashworthiness*, vol. 19, no. 3, pp. 244–263.
- [197] Lapner, P. C., Nguyen, D. and Letts, M. (2003). “Analysis of a school bus collision: mechanism of injury in the unrestrained child”. *Canadian Journal of Surgery*, vol. 46, no. 4, pp. 269–272.
- [198] McGeehan, J., Annest, J. L., Vajani, M., Bull, M. J., Agran, P. E. and Smith, G. A. (2006). “School bus – Related injuries among children and teenagers in the United States, 2001-2003”. *Journal of Pediatrics*, vol. 118, no. 5, pp. 1978–1984.
- [199] Elias, J. C., Sullivan, L. K. and Mccray, L. B. (2001). “Large School Bus Safety Restraint Evaluation”. *Proceedings of the 17th Conference on the Enhanced Safety of Vehicles Conference (ESV)*, Paper no: 345.

- [200] Simms, C. K. and Wood, D. P. (2005). “Pedestrian Impact: The Effect of Pedestrian Motion on Head Contact Forces with Vehicle and Ground”. *Proceedings of the International Research Council on Biomechanics of Injury (IRCOBI) Conference on the Biomechanics of Impact*, pp. 451–454.
- [201] Watson, J. W. (2010). “Investigation of Cyclist and Pedestrian Impacts with Motor Vehicles using Experimentation and Simulation”. *School of Applied Science, Cranfield University*.
- [202] Niewöhner, W., Roth, F., Gwehenberger, J., Gruber, C., Kühn, M., Sferco, R., Pastor, C.-H., Nagel, U. and Stanzel, M. (2011). “Proposal for a Test Procedure of Assistance Systems regarding Preventive Pedestrian Protection,” *Proceedings of the 22nd Conference on the Enhanced Safety of Vehicles Conference (ESV)*, Paper no: 11-0393.
- [203] Yao, J. F., Yang, J. K. and Fredriksson, R. (2006). “Reconstruction of head-to-hood impact in an automobile-to-child-pedestrian collision”. *International Journal of Crashworthiness*, vol. 11, no. 4, pp. 387–395.
- [204] Jakobsson, L., Lundell, B., Norin, H., Isaksson-Hellman, I. (2000). “WHIPS – Volvo’s Whiplash Protection Study”. *Traffic Safety and Auto Engineering Stream. Accident Analysis and Prevention Vol. 32, No. 2*, pp. 307-319
- [205] Muser, M., Walz, F.H., Zellmer, H. (2000). “Biomechanical Significance of the Rebound Phase in Low Speed Rear End Impacts”. *Proc. of the IRCOBI Conference, Montpellier, France*
- [206] Linder, A., Avery, M., Krafft, M., Kullgren, A., Svensson, M, Y. (2001). “ACCELERATION PULSES AND CRASH SEVERITY IN LOW VELOCITY REAR IMPACTS – REAL WORLD DATA AND BARRIER TESTS”. *ESV. Paper no. 216-O*.
- [207] Hiliard, H. E. (2014). “Metal Prices in the United States through 1988 - Platinum Group Metals”. [Online]. Available: <http://minerals.usgs.gov/minerals/pubs/commodity/platinum/550798.pdf>. [Accessed: 10-Dec-2018].
- [208] Mallick, P. K. (2010). “Materials, design and manufacturing for lightweight vehicles”. Cambridge: Woodhead Publishing Limited.
- [209] Luo, A. A. (2002). “Magnesium: Current and potential automotive applications”. *JOM*, vol. 54, no. 2, pp. 42–48.
- [210] Danielsson, O., González Cocaña, A., Ekström, K., Bayani Khaknejad, M., Klomp, M. and Dekker, R. (2016). “Influence of body stiffness on vehicle dynamics characteristics”. *Department of Applied Mechanics Division of Vehicle Engineering and Autonomous Systems, Chalmers University of Technology*.
- [211] Thomas, W. and Altan, T. (2013). “Aluminum sheet forming for automotive applications, Part I Material properties and design guidelines”. *Stamping Journal*, pp. 12–13.
- [212] Bhargawa, A. (2015). “Synthesis and microscopic study of poly carbonate and poly methyl methacrylate blends”. *International Journal of Innovative Research in Science and Engineering*, vol. 1, no. 7, pp. 11–17.

- [213] Snow, D. (2017). "Polycarbonate: Special Windshields for Race Cars,". [Online]. Available: <https://info.glass.com/polycarbonate-race-car-windshield/>. [Accessed: 18-Apr-2018].
- [214] Nikolaevich, S. A., Valerievich, A. A., Igorevich, G. A., Alexandrovich, S. A. and Alexandrovich, S. M. (2014). "Advanced materials of automobile bodies in volume production". *European Transport*, issue, 56, pp. 1-27.
- [215] Binyamin, Sarjito, and Bill Haq, A. H. (2018). "Investigation of Aluminum alloy for lightweight outer hood panel of local compact SUV using finite element modeling". *Proceedings of the American Institute of Physics (AIP) Conference*, paper no, 030038.
- [216] Masoumi, A., Shojaeefard, M. H. and Najibi, A. (2011). "Comparison of steel, Aluminum and composite bonnet in terms of pedestrian head impact," *Journal of Safety Science*, vol. 49, no. 10, pp. 1371–1380.
- [217] Demirci, E. and Yildiz, A. R. (2016). "Lightweight design of vehicle energy Absorbers using steel, Aluminum and Magnesium alloys". *Proceedings of the 2nd International Conference on Engineering and Natural Science (ICENS)*, pp. 1–6.
- [218] Carter, J. T. and Krajewski, P. E. (2008). "The hot blow forming of AZ31 Mg sheet: Formability assessment and application development". *JOM*, vol. 60, no. 11, pp. 77–81.
- [219] Blawert, C., Hort, N. and Kainer, K. U. (2004). "Automotive applications of magnesium and Its alloys". *Transactions of the Indian Institute of Metals Indian*, vol. 57, no. 4, pp. 397–408.
- [220] Savic, V., Pawlicki, M., Krajewski, P., Voss, M., Hector, L. and Snaveley, K. (2014). "Passive pedestrian protection approach for vehicle hoods". *Society of Automotive Engineers (SAE)*, technical paper-4271.
- [221] Ledbetter, S. R., Walker, A. R., Keiller, A. P. (2006). "Structural use of glass". *Journal of architectural engineering Archit*, vol. 12, no. 3, pp. 53–56.
- [222] Reinholdt, E. (2015). "Materials Workshop: Polycarbonate – a Low-Cost Alternative to Glass". [Online]. Available: <https://www.houzz.com/ideabooks/43870464/list/materials-workshop-polycarbonate-a-low-cost-alternative-to-glass>. [Accessed: 26-Apr-2018].
- [223] Ashby, M. (2012). "Materials and the environment: Eco-informed material choice". Second Edition, Boston: Butterworth-Heinemann/Elsevier.
- [224] Independent Chemical Information Service (ICIS). (2018). "UTLOOK 18 ': Europe PMMA concerns mount on shortage, robust demand". [Online]. Available: <https://www.icis.com/explore/resources/news/2018/01/02/10178947/outlook-18-europe-pmma-concerns-mount-on-shortage-robust-demand/>. [Accessed: 31-Oct-2018].
- [225] Prest, A.R. and Turvey. (1965). "Cost-Benefit Analysis: A Survey". *The Economic Journal*, vol. 75, no. 300, pp. 683-735.
- [226] Mashreky, S. R., Rahman, A., Khan, T. F., Faruque, M., Svanstro, L. and Rahman, F. (2010). "Hospital burden of road traffic injury : Major concern in primary and secondary level hospitals in Bangladesh". *Journal of Public Health*, vol. 124, pp. 185–189.

- [227] Riewpaiboon, A., Piyauthakit, P. and Chaikledkaew, U. (2009). “Economic burden of road traffic injuries a micro-costing approach”. *Southeast Asian Journal Tropical Medicine and Public Health*, vol. 39, pp. 1139-1149.
- [228] TM Hoang, H., Pham, T. L., TN Vo, T., Nguyen, P. K., Doran, C. M. and Hill, P. S. (2008). “Cost Effectiveness and Resource: The costs of traumatic brain injury due to motorcycle accidents in Hanoi, Vietnam”. *Journal of Public Health*, vol. 7, pp. 1–7.
- [229] Sugiyanto, G. and Santi, M. Y. (2017). “Road traffic accident cost using human capital method (Case study in Purbalingga, Central Java, Indonesia)”. *Journal of Technology*, vol. 79, no. 2, pp. 107–116.
- [230] Wesson, H. K. H., Boikhutso, N., Bachani, A. M., Hofman, K. J. and Hyder, A. A. (2014). “The cost of injury and trauma care in low- and middle-income countries: a review of economic evidence”. *Journal of Health Policy Plan*, vol. 29, no. 6, pp. 795–808.
- [231] Nguyen, H., Ivers, R. Q., Jan, S., Martiniuk, A. L. C., Li, Q. and Pham, C. (2013). “The economic burden of road traffic injuries: Evidence from a provincial general hospital in Vietnam”. *Journal of Injury Prevention*, vol. 19, no. 2, pp. 79–84.
- [232] Nachimuthu, K. and Partheeban, P. (2013). “Economic analysis of road accident cost for Chennai city, India”. *Journal of Pollution Research*, vol. 32, no. 4, p. 893–898CSI
- [233] Hardy, R., Watson, J. and Howard, M. (2000). “Developments in the simulation of real world car to pedestrian accidents using a pedestrian humanoid finite element model”. *International Journal of Crashworthiness*, vol. 5, no. 1, pp. 103–118.
- [234] Yang, J. K. and Lövsund, P. (1997). “Development and validation of a human-body mathematical model for simulation of car-pedestrian collisions”. *Proceedings of the International Research Council on Biomechanics of Injury (IRCOBI) Conference on the Biomechanics of Impact*, Sweeden, Hannover, pp. 133-149.
- [235] Serre, T., Masson, C., Perrin, C., Chalandon, S., Llari, M., Py, M., Cavallero, C. and Cesari, D. (2007). “Real accidents involving vulnerable road users: In-depth investigation, numerical simulation and experimental reconstitution with PMHS”. *International Journal of Crashworthiness*, vol. 12, no. 3, pp. 227–234.
- [236] Hallquist, J. (1976). “Preliminary user’s manuals for DYNA 3D and DYNAP: (nonlinear dynamic analysis of solids in three dimensions)”. *California University, Livermore, Lawrence Livermore Lab, California-USA*.
- [237] Livermore Software Technology Corporation. (2007). “LS-DYNA keyword user’s manual, vol. I”. *Livermore Software Technology Corporation (LSTC), California- USA*.
- [238] Ray, M. H. and Ray, M. H. (1997). “The use of finite element analysis in roadside hardware design: The use of finite element analysis in roadside hardware design”. *International Journal of Crashworthiness*, vol. 2, no. 4, pp. 333–348.
- [239] Yadav, V. (2006). “Finite element modeling and side impact study of a low-floor mass transit bus”. *Mechanical Engineering, Wichita State University*.
- [240] Nahum, A. and Melvin, J. (2002). “Accidental Injury, biomechanics and prevention”. Springer + Business Media, INC, New York.

- [241] Jaśkiewicz, M., Jurecki, R., Witaszek, K. and Więckowski, D. (2013). “Overview and analysis of dummies used for crash tests”. *Scientific Journals of the Maritime University of Szczecin*, vol. 35, no. 107, pp. 22–31.
- [242] Eppinger, R. (2010). “Child Crash Test Dummies”. *National Transportation Biomechanics Research Center (NTBRC)*, USA.
- [243] Zhou, H., Rasico, J., Zhu, F. and Kant, R. (2007). “Hybrid III 50th Percentile Male”. *First Technology Innovative Solution, Dummy Models, LS-Dyna more*, GmbH Stuttgart.
- [244] Livemore Software Technology Corporation (LSTC), “LSTC Dummy Models.” [Online]. Available: <http://www.lstc.com/products/models/dummies>. [Accessed: 05-Apr-2016].
- [245] Henn, H. W. (1998). “Crash tests and the head injury criterion”. *Teaching Mathematics and its Applications*, vol. 17, no. 4, pp. 162–170.
- [246] Howard, M., Thomas, A., Koch, W., Watson, J. and Hardy, R. (2000). “Validation and Application of a Finite Element Pedestrian Humanoid Model for use in Pedestrian Accident Simulations”. *Proceedings of the International Research Council on Biomechanics of Injury (IRCOBI) Conference on the Biomechanics of Impact*, Montpellier (France), pp. 101-119.
- [247] Ishikawa, H., Kajzer, J. and Schroeder, G. (1993). “Computer simulation of impact response of the human body in car-pedestrian accidents”. *Proceedings of the 37th Stapp Car Crash Conference*, vol. 1, paper no, 933129.
- [248] Iwamoto, M., Kisanuki, Y., Watanabe, I., Furusu, K. and Miki, K. (2002). “Development of a Finite Element Model of the Total Human Model for Safety (Thums) and Application to Injury Reconstruction”. *Proceedings of the International Research Council on Biomechanics of Injury (IRCOBI) Conference on the Biomechanics of Impact*.
- [249] Ruan, J., El-Jawahri, R., Chai, L., Barbat, S. and Prasad, P. (2003). “Prediction and analysis of human thoracic impact responses and injuries in cadaver impacts using a full human body finite element model”. *Stapp Car Crash Journal*, vol. 47, no, pp. 299–321.
- [250] Mertz, H. J. (1985). “Biofidelity of the Hybrid III Head”. *Society of Automotive Engineers (SAE)*, vol. 49, Section. 5, pp. 97–105.
- [251] Mertz, H. J. (1985). “Definition and Development of A Crash Dummy Head”. *Journal of Athletic Training*, vol. 83, Section. 4, paper no, pp. 3836-3851.
- [252] Barth, J. T., Freeman, J. R., Broshek, D. K. and Varney, R. N. (2001). “Acceleration-deceleration sport-related concussion: The gravity of it all”. *Journal of Athletic Training*, vol. 36, no. 3, pp. 253–256.
- [253] Singh, P. K., Das, A., Sivaprasad, S., Biswas, P., Verma, R. K. and Chakrabarti, D. (2017). “Energy absorption behaviour of different grades of steel sheets using a strain rate dependent constitutive model” *Journal of Thin-Walled Structures.*, vol. 111, pp. 9–18, 2017.
- [254] Caliskan, A. G. (2000). “Crashworthiness of composite materials & structures for vehicle applications”. *Society of Automotive Engineers (SAE)*, paper no, 01-3536.

- [255] Dean, J., Dunleavy, C. S., Brown, P. M. and Clyne, T. W. (2009). “Energy absorption during projectile perforation of thin steel plates and the kinetic energy of ejected fragments”. *International Journal Impact Engineering*, vol. 36, no. 10–11, pp. 1250–1258.
- [256] Samaka, H., Manap, A., Tarlochan, F., Azman, R. F. R. and Ibrahim, N. (2016). “Finite element modelling of car hood panel for pedestrian protection during impact”. *International Journal of Integrated Engineering*, vol. 8, no. 1, pp. 11–14.
- [257] Karanam, V. M. and Ghosal, A. (2013). “Studies on the wobble mode stability of a three-wheeled vehicle”. *Institution of Mechanical Engineerings (IMechE)*, vol. 227, no. 8, pp. 1200–1209.
- [258] Bajaj. (2017). “three-wheeled-vehicles”. [Online]. Available: <http://lovson.com/lovson/three-wheeled-vehicles.html>. [Accessed: 31-Oct-2017].
- [259] Rust, W. and Schweizerhof, K. (2003). “Finite element limit load analysis of thin-walled structures by ANSYS (implicit), LS-DYNA (explicit) and in combination”. *Journal of Thin-Walled Structures*, vol. 41, no. 2–3, pp. 227–244.
- [260] Livermore Software Technology Corporation (LSTC). (2014). “LS - DYNA ® Analysis for structural mechanics” USA.
- [261] Knupp, P. M. (2007). “Remarks on Mesh Quality”. *Proceedings of the 45th American Institute of Aeronautics and Astronautics (AIAA), Aerospace Sciences Meeting and Exhibit*, Reno, France.
- [262] Krutilek, D. and Raida, Z. (2015). “Optimal meshing for high-frequency analysis of realistic structure”. *Proceedings of the Conference on Microwave Techniques (COMITE)*, pp. 1–4.
- [263] Lee, G. (2008). “Introduction to meshing”. *Proceedings of the Practical Finite additional material*, pp. 1–21.
- [264] Lee, G. (2008). “Element quality and checks”. *Proceedings of the Practical Finite Element Analysis*, Altair University, pp. 211–233.
- [265] ANSYS. (2011). “ANSYS meshing user ’s guide” U.S.A.
- [266] Wood, L. A., Bekkedahl, N. and Roth, F. L. (1942). “Measurement of densities of synthetic rubbers”. *National Bureau of Standards*, vol. 29, pp. 391–396.
- [267] LS-DYNA Examples. “Yaris dynamic shock absorber loading.” [Online]. Available: [http://www.dynaexamples.com/implicit/Yaris Dynamic Shock Absorber Loading](http://www.dynaexamples.com/implicit/Yaris%20Dynamic%20Shock%20Absorber%20Loading). [Accessed: 13-Apr-2017].
- [268] Hldimann, M, Luible, A. and Overened, M. (2008). “Structural use of glass”. *ETH Zürich and International Association for Bridge and Structural Engineering (AIBSE)*, Zürich-Zwitzerland.
- [269] Fors, C. (2014). “Mechanical properties of interlayers in laminated glass Experimental and Numerical Evaluation”. *Construction Sciences Department*, Lund University.
- [270] Srikanth, K. M. and Prakash, R. V. (2009). “Assessing the structural crashworthiness of a three-wheeler passenger vehicle”. *Proceedings of the 2nd International Conference on Research into Design*, pp. 152–159.

- [271] Ron Blair, G., Reynolds, J. I., Weierstall, M. D. (2008). “Automotive cushioning through the ages: A review”. *The Molded Polyurethane Foam Industry Panel*.
- [272] Clawson, J. K. (2013). “Structure nad defects in high-performance aramid fibers”. *Aerospace Engineering, University of Illinois at Urbana-Champaign*.
- [273] ANSYS, “Constraints and initial conditions.” [Online]. Available: https://www.sharcnet.ca/Software/Fluent14/help/ans_lsd/Hlp_L_load2.html. [Accessed: 22-Dec-2018].
- [274] Livermore Software Technology Corporation (LSTC). (1994). “Ls-dyna3d keyword examples manual”, USA.
- [275] Eggleston, T., Mindle, W. and Benson, D. (2002). “FEA information Inc. news & technical information”. *Livermore Software Technology Corp (LSTC), U.S.A.*
- [276] Boagey, R. and Bastien, C. (2014). “Meet the crash test dummies who risk limb so you don’t have to”. *Automotive World, est. 1992*. [Online]. Available: <https://www.automotiveworld.com/articles/meet-crash-test-dummies-risk-limb-dont/>. [Accessed: 03-Jun-2017].
- [277] Mohan, P., Marzougui, D., Van De Velde, R. and Kan, C. (2007). “Development of detailed Finite Element dummy models”. *Proceedings of the 6th LS-DYNA Anwenderforum*, pp. 13–22.
- [278] Mohan, p., Marzougui, D., Kan, S. (2009). “Development and validation of Hybrid III crash test dummy”. *Society of Automotive Engineers (SAE)*. Paper No, 01-0473.
- [279] LS-DYNA SUPPORT, “Contact modeling in LS-DYNA” [Online]. Available: <http://www.dynasupport.com/tutorial/ls-dyna-users-guide/contact-modeling-in-ls-dyna>. [Accessed: 01-Oct-2016].
- [280] Suman, M.L.J. (2012). “Contacts in LS-Dyna session”. *Ramaiah School of Advanced Studies, Bengaluru*.
- [281] LS-DYNA. (2016). “What is the difference between *CONTACT_AUTOMATIC_SINGLE_SURFACE and *CONTACT_AUTOMATIC_GENERAL?”. [Online]. Available: <http://www.dynasupport.com/faq/contact/what-is-the-difference-between-contact-automatic>. [Accessed: 02-Apr-2017].
- [281] Bunketorp, O., Al dman, B., Jonson, R., Romanus, B., Roos, B., Thorngren, L. (1980). “Experimenal studies on leg injuries in car-pedestrian accidents”. *Proceedings of the International Research Council on Biomechanics of Injury (IRCOBI) Conference on the Biomechanics of Impact*, pp. 180–193.
- [283] Guha, S., Bhalsod, D. and Krebs, J. (2008). “LSTC Hybrid III Dummies positioning and post-processing”. *Livermore Software Technology Corp (LSTC), Michigan-U.S.A.*
- [284] Mahadevaiah, C. M. U. and Burger, M. (2013). “LSTC Hybrid III 6 year-old Finite Element model documentation”. *Livermore Software Technology Corp (LSTC), Michigan-U.S.A.*
- [285] National Highway Traffic Safety Administration (NHTSA). (1997). “Actions to reduce the adverse effects of air bags FMVSS No. 208”. *Injury Risk Curves and*

- Protection* *References* *Values.* [Online]. Available:
<https://one.nhtsa.gov/cars/rules/rulings/80g/80gii.html#ii1>. [Accessed: 15-May-2018].
- [286] Svensson, M. (2005). “Neck injuries in car collisions - Injury mechanisms”. *Proceedings of the Injury in Low Velocity Collision Conference*, pp. 1–11.
- [287] Goldsmith, W. and Ommaya, A. (1984). “Head and neck injury criteria and tolerance levels”. In Chapon BA, (ed) *Biomechanics of Impact Trauma, International Center for Transportation Studies*. New York, Elsevier Science Publisher, pp 149–190.
- [288] Lukaszewicz, D. H.-J. A. (2013). “Automotive composite structures for crashworthiness”. *Advanced composite materials for automotive applications: structural integrity and crashworthiness*. Elmarakbi, Ed., pp. 99–148.
- [289] Chen, Y., Liu, G., Zhang, Z. and Hou, S. (2017). “Integrated design technique for materials and structures of vehicle body under crash safety considerations”. *Structural and Multidisciplinary Optimization*, vol. 56, no. 2, pp. 455–472.
- [290] Abedrabbo, N., Pourboghra, F. and Carsley, J. (2007). “Forming of AA5182-O and AA5754-O at elevated temperatures using coupled thermo-mechanical finite element models”. *International Journal of Plasticity*, vol. 23, no. 5, pp. 841–875.
- [291] Hazra, S., Williams, D., Roy, R., Aylmore, R. and Smith, A. (2011). “Effect of material and process variability on the formability of aluminium alloys”. *Journal of Materials Processing Technology*, vol. 211, no. 9, pp. 1516–1526.
- [292] Borrisutthekul, R., Miyashita, Y. and Mutoh, Y. (2005). “Dissimilar material laser welding between magnesium alloy AZ31B and aluminum alloy A5052-O”. *Science and Technology of Advanced Materials*, vol. 6, no. 2, pp. 199–204.
- [293] Shah, Q. H. (2009). “Impact resistance of a rectangular polycarbonate armor plate subjected to single and multiple impacts”. *International Journal of Impact Engineering*, vol. 36, no. 9, pp. 1128–1135.
- [294] General Statistical Office (GSO). (2010). “Result of the Vietnam’s household living standards survey 2010”. [Online]. Available: http://www.gso.gov.vn/default_en.aspx?tabid=515&ItemID=12426. [Accessed: 10-Nov-2018].
- [295] Vijith KK. “Indian man killed in an accident by an auto-rickshaw” 2016. [Online]. Available: <http://www.youtube.com/watch?v=gytzL9yysCM>. [Accessed: 02-Dec-2018].

7. APPENDICES

Appendix A.

This section including the results for an adult pedestrian impacted by the auto rickshaw during primary impacts.

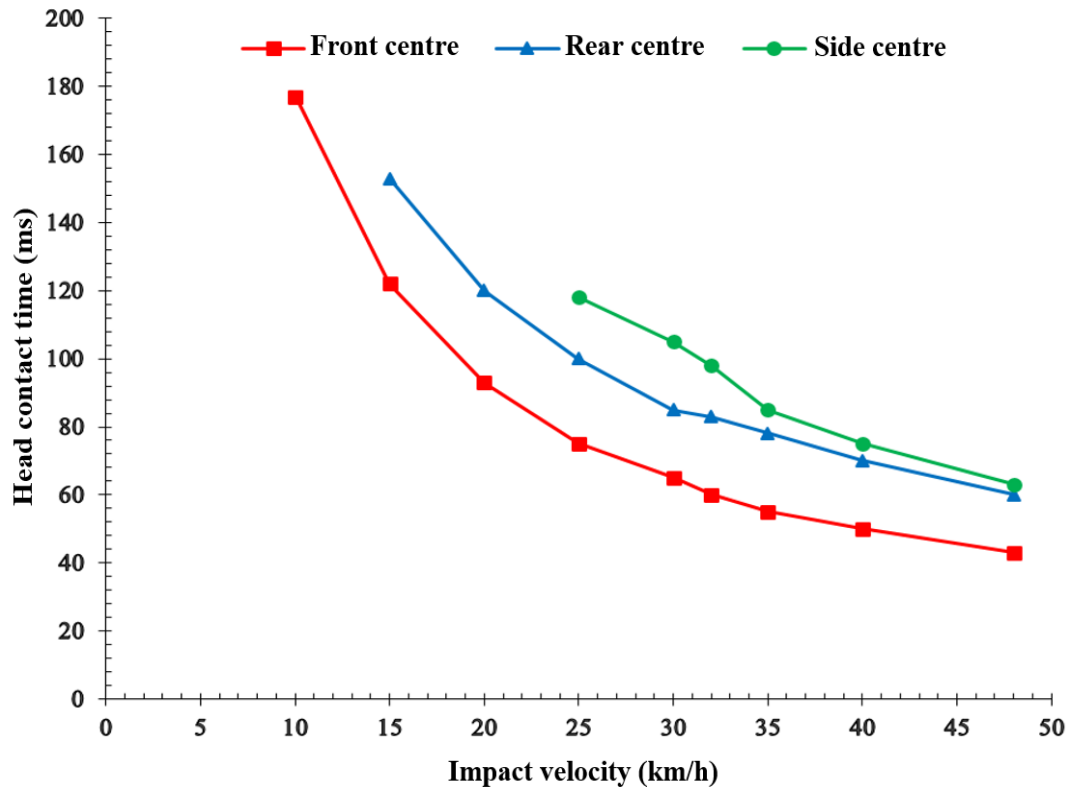


Figure A- 1. Head contact time for adult pedestrian at front, rear and side impact positions at the vehicle’s centreline

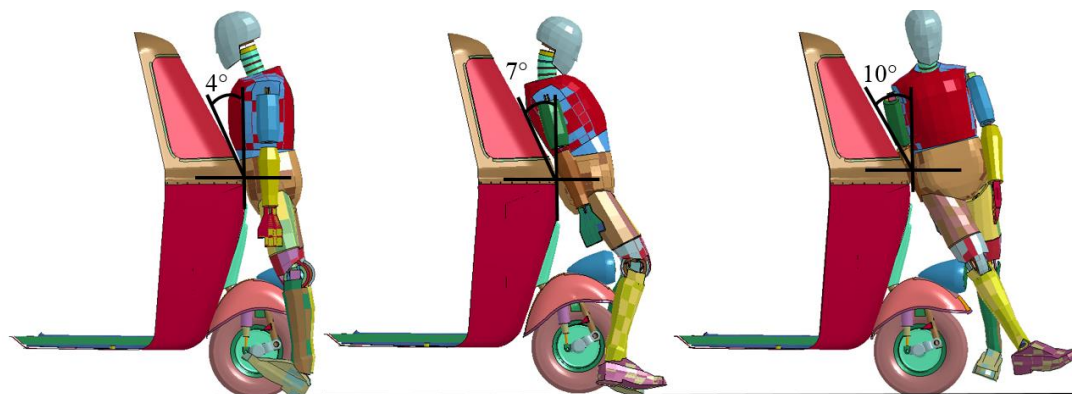


Figure A-2. Effective angles of rotation for the adult pedestrian about the frontal edge of the auto rickshaw sheet plate in the front, rear and side impact at the vehicle’s centreline

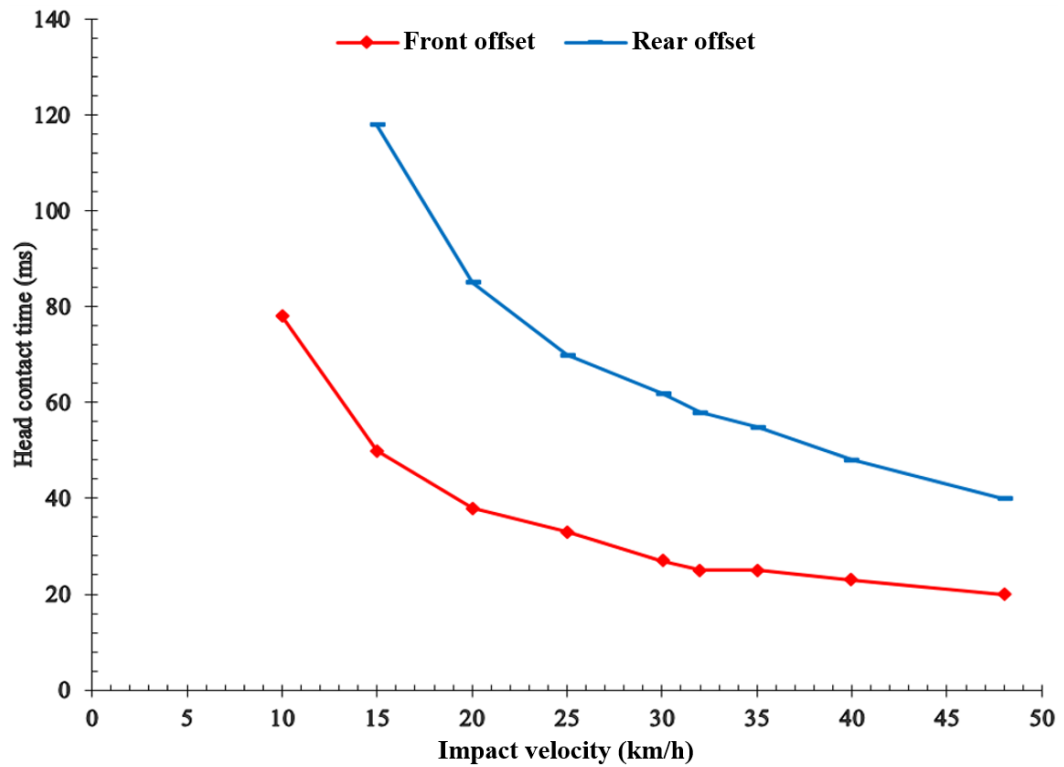


Figure A- 3. Head contact time for adult pedestrian at front and rear impact positions at 42cm offset from the vehicle's centreline

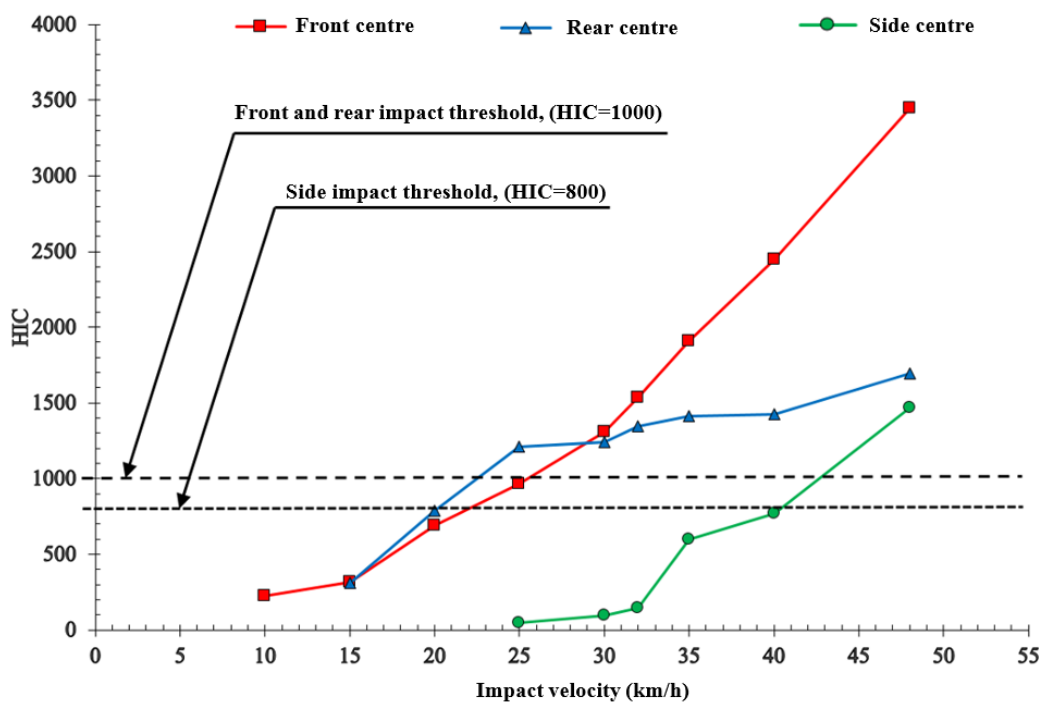


Figure A-4. HIC values for adult pedestrian at the vehicle's centreline at front, rear and side standing orientations.

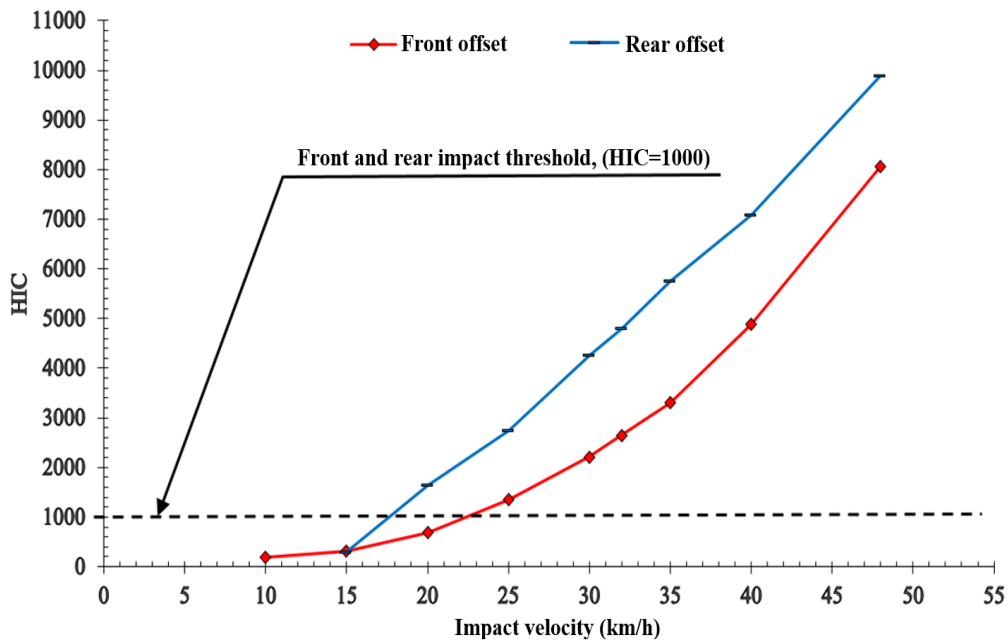


Figure A-5. HIC values for adult pedestrian at 42cm offset from the vehicle's centreline at front, rear and side standing orientations.

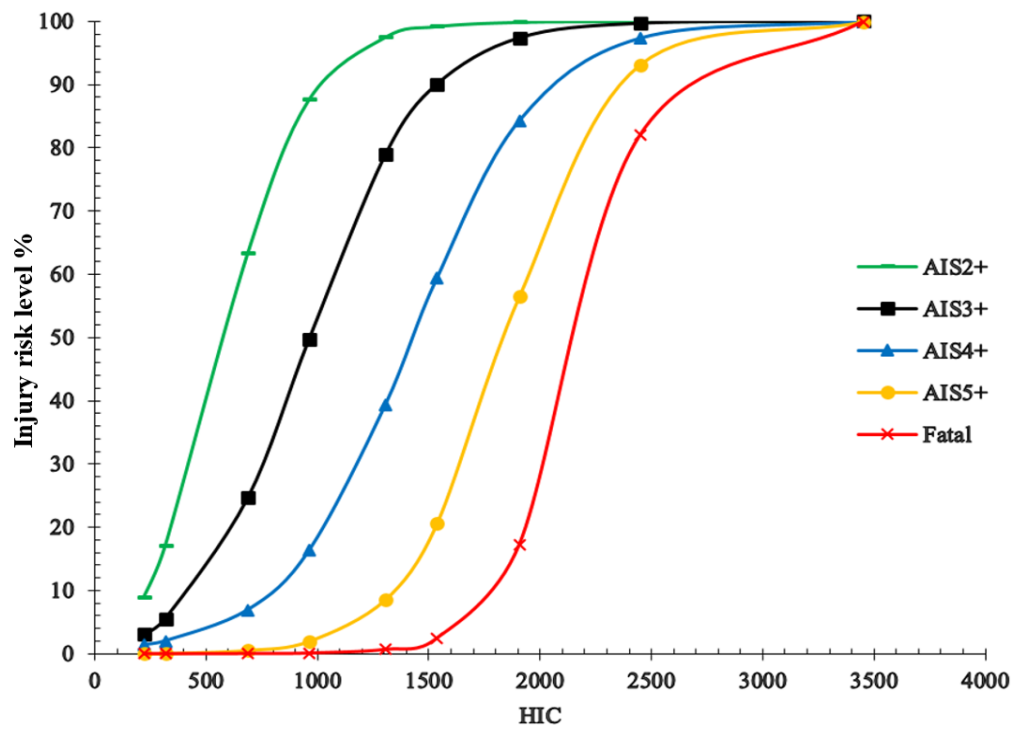


Figure A- 6. HIC values and injury risk level for adult pedestrian in front impact position at the vehicle's centreline

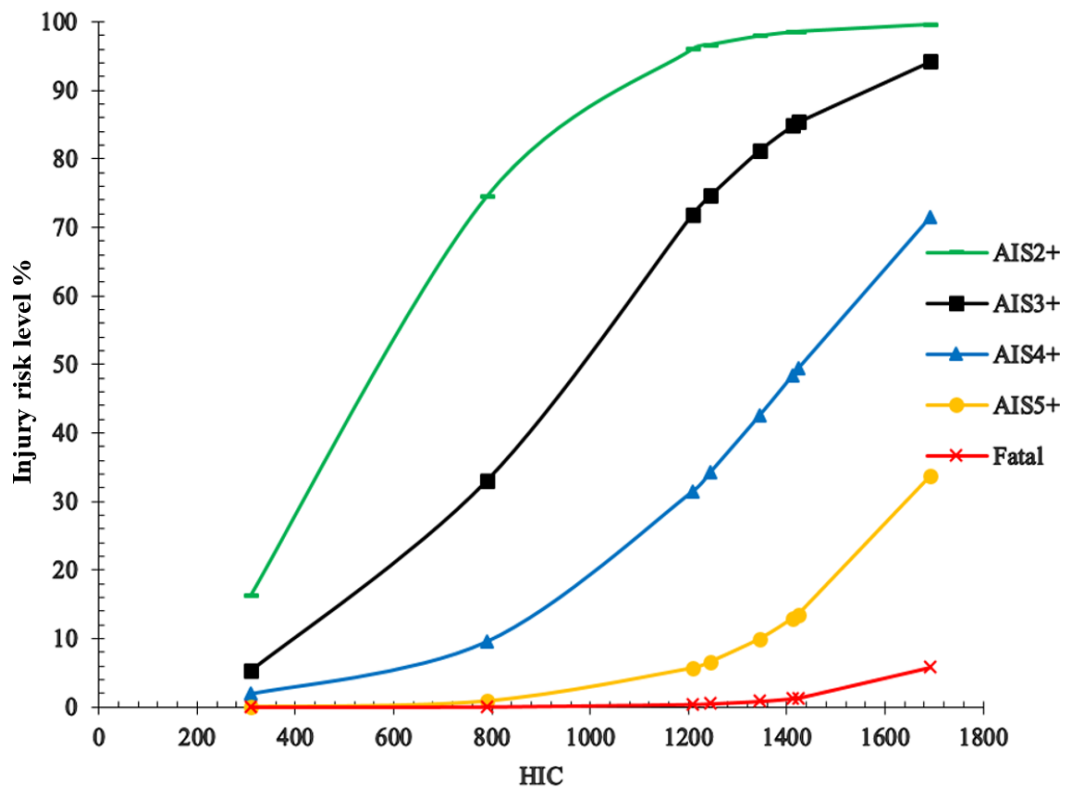


Figure A- 7. HIC values and injury risk level for adult pedestrian in rear impact position at the vehicle’s centreline

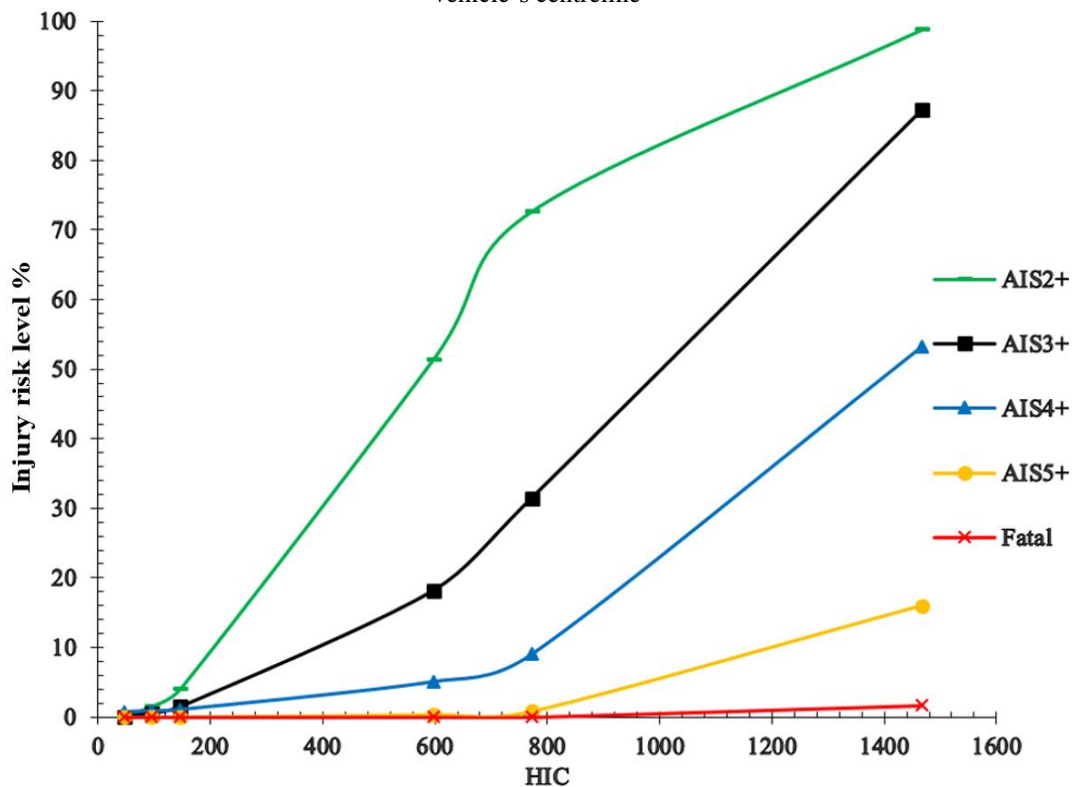


Figure A- 8. HIC values and injury risk level for adult pedestrian in side impact position at the vehicle’s centreline

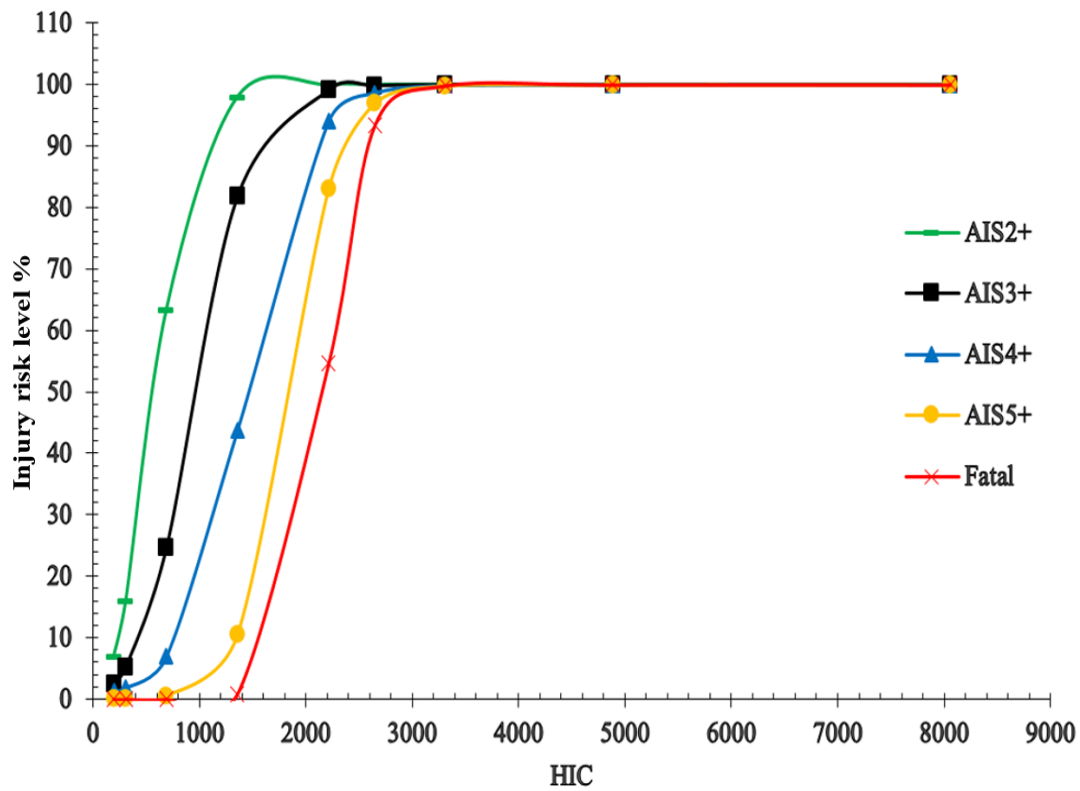


Figure A- 9. HIC values and injury risk level for adult pedestrian in front impact position at 42cm offset from the vehicle’s centreline

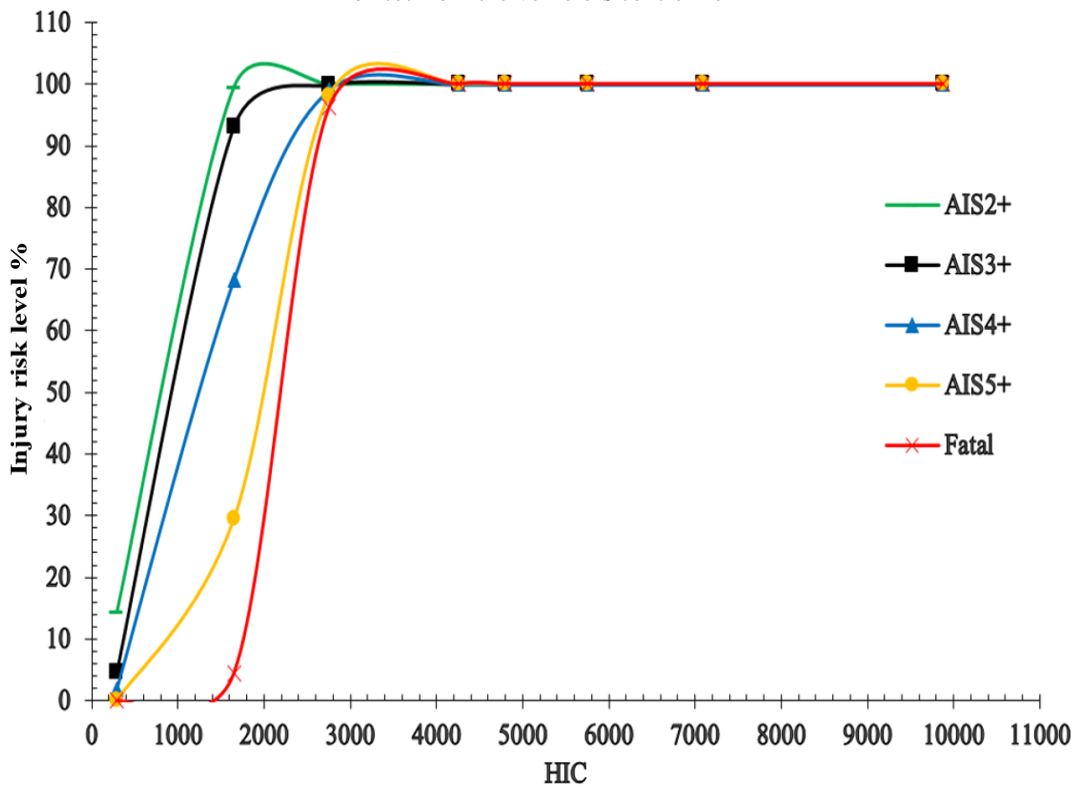


Figure A- 10. HIC values and injury risk level for adult pedestrian in rear impact position at 42cm offset from the vehicle’s centreline

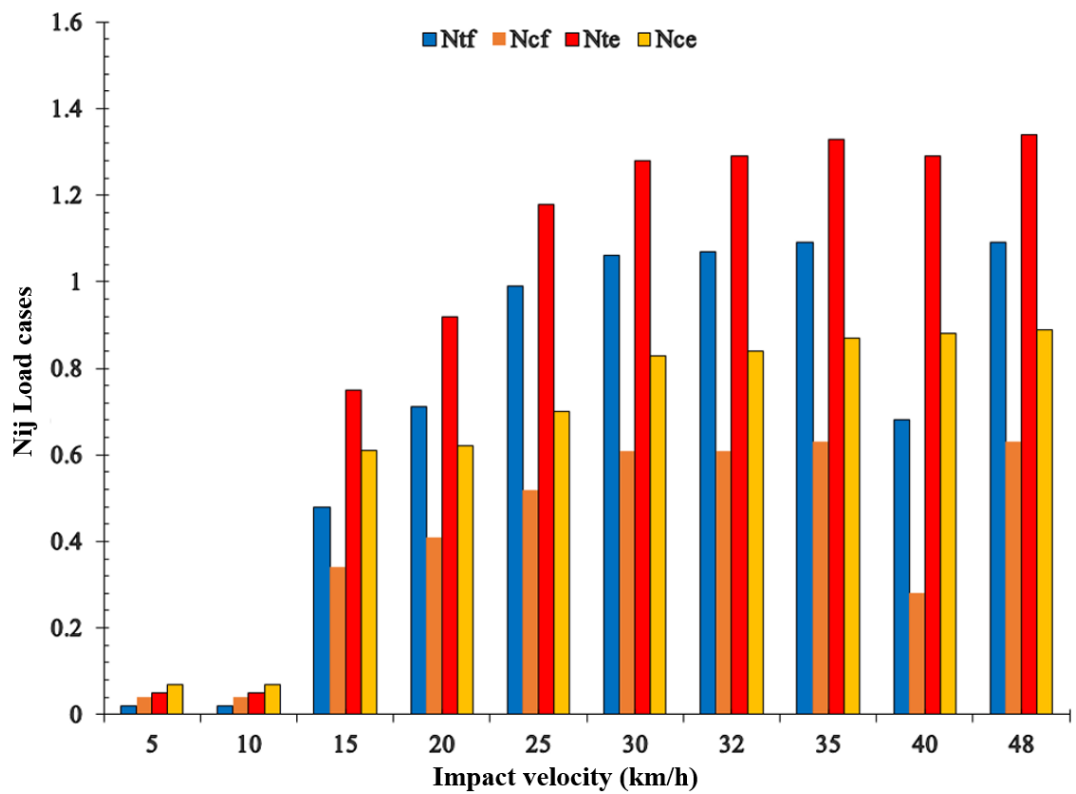


Figure A- 11. Upper neck load conditions for adult pedestrian impacts at the vehicle's centreline (front position)

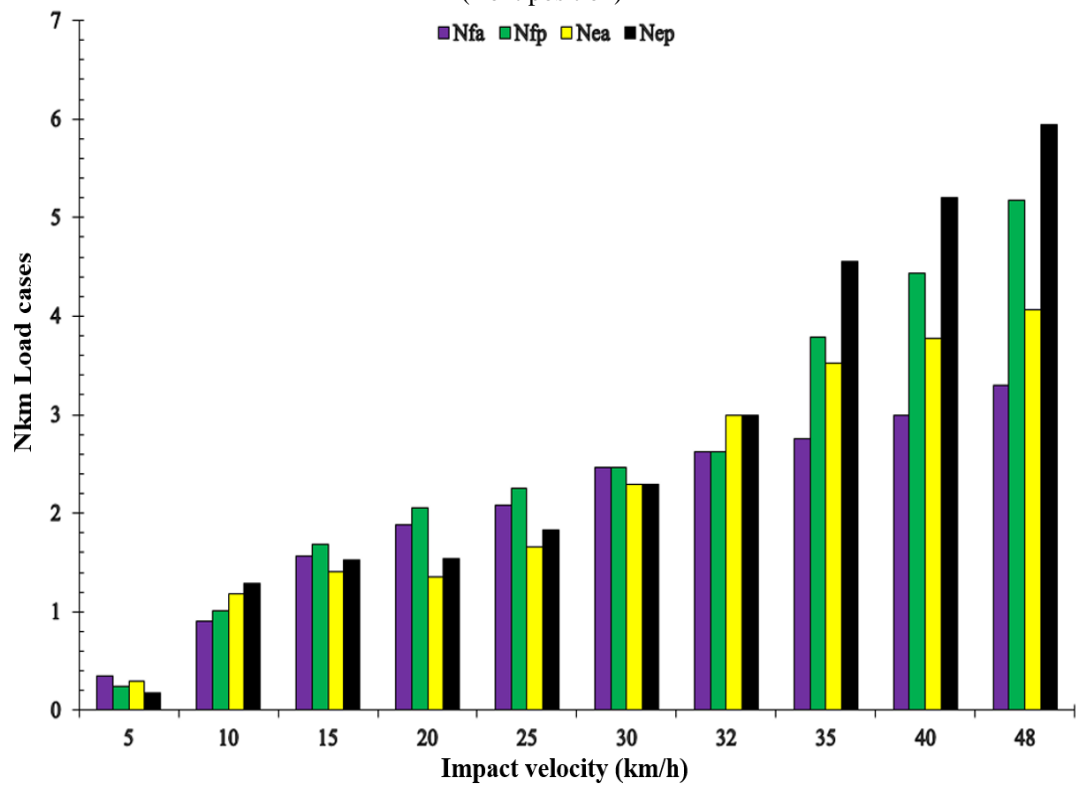


Figure A- 12. Upper neck load conditions for adult pedestrian impacts at the vehicle's centreline (rear position)

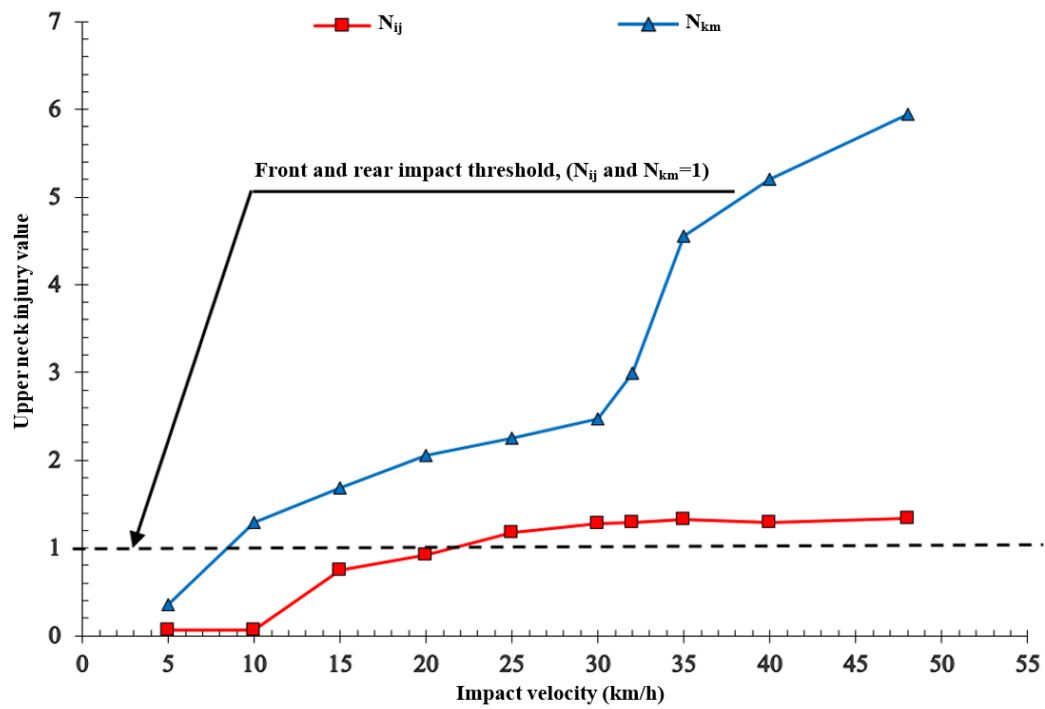


Figure A- 13. Upper neck injury values for adult pedestrian impacts at vehicle’s centreline (front and rear position).

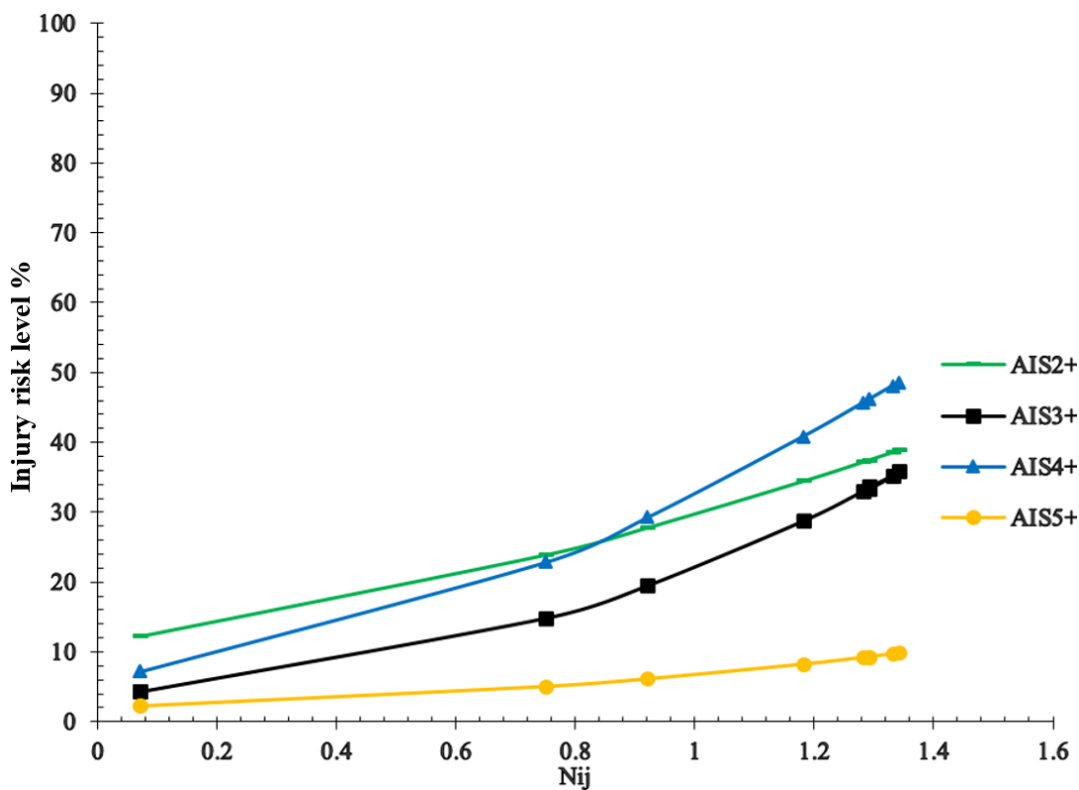


Figure A- 14. N_{ij} values and injury risk level for adult pedestrian in front impact position at the vehicle’s centreline

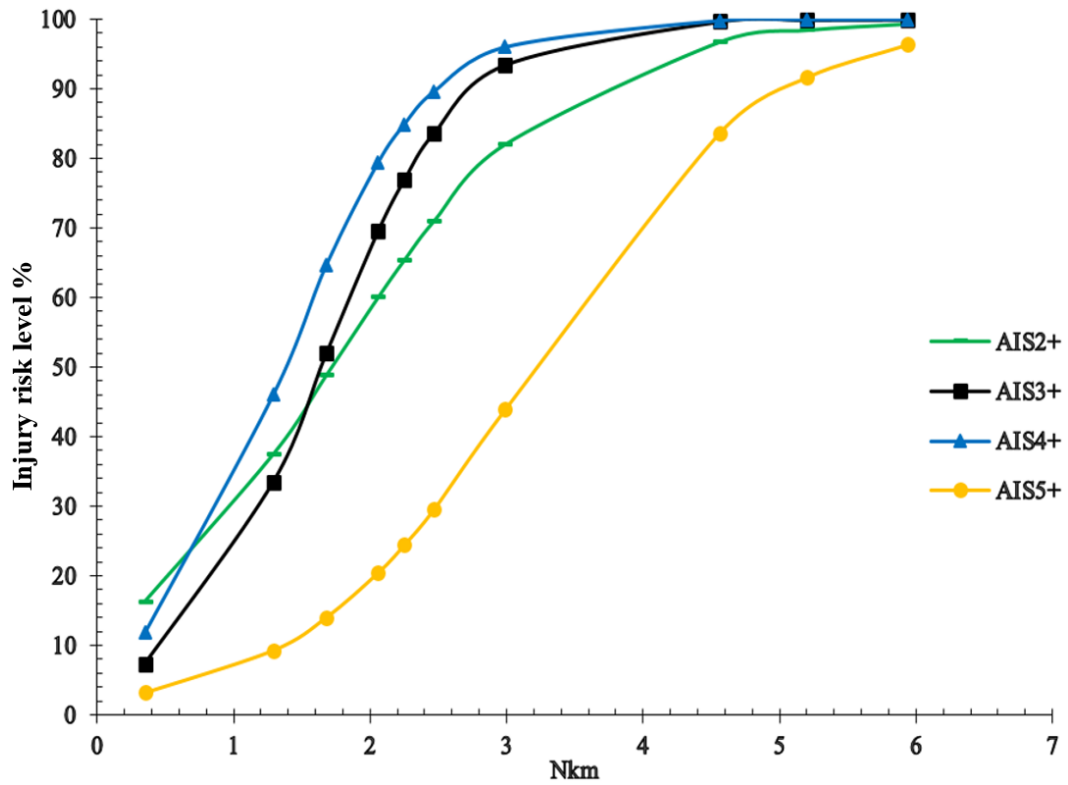


Figure A- 15. N_{km} values and injury risk level for adult pedestrian in rear impact position at the vehicle's centreline

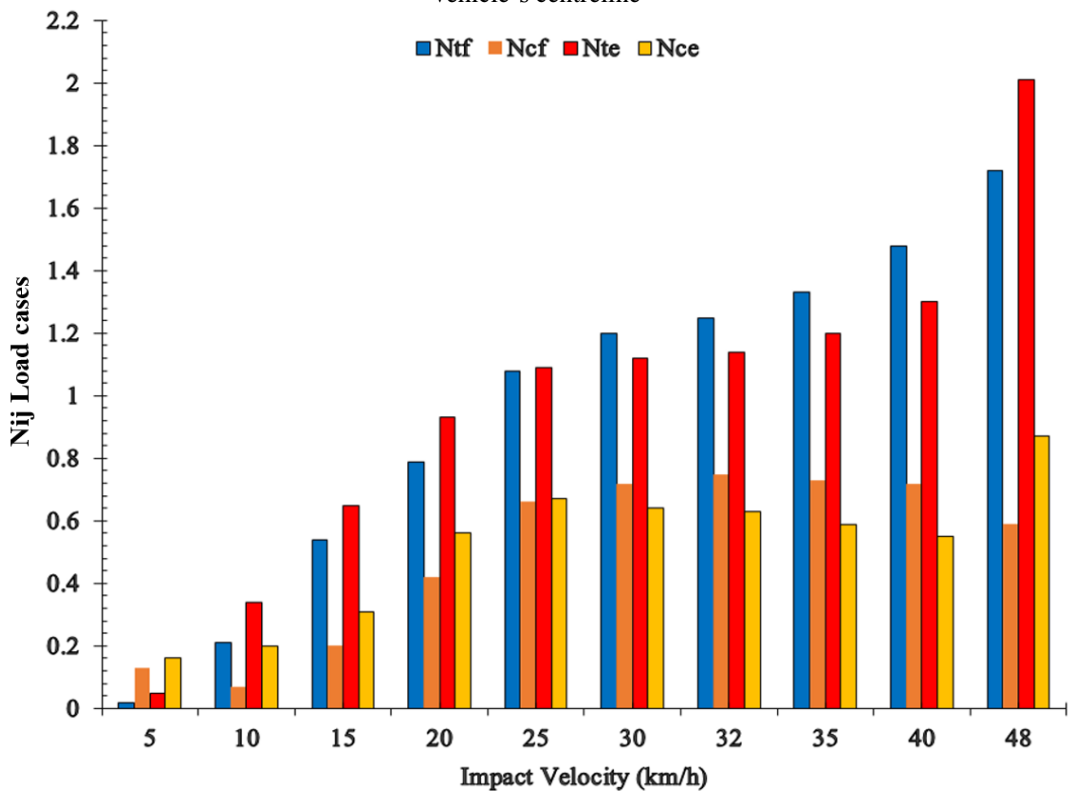


Figure A- 16. Upper neck load conditions for adult pedestrian impacts at 42cm offset from the vehicle's centreline (front position)

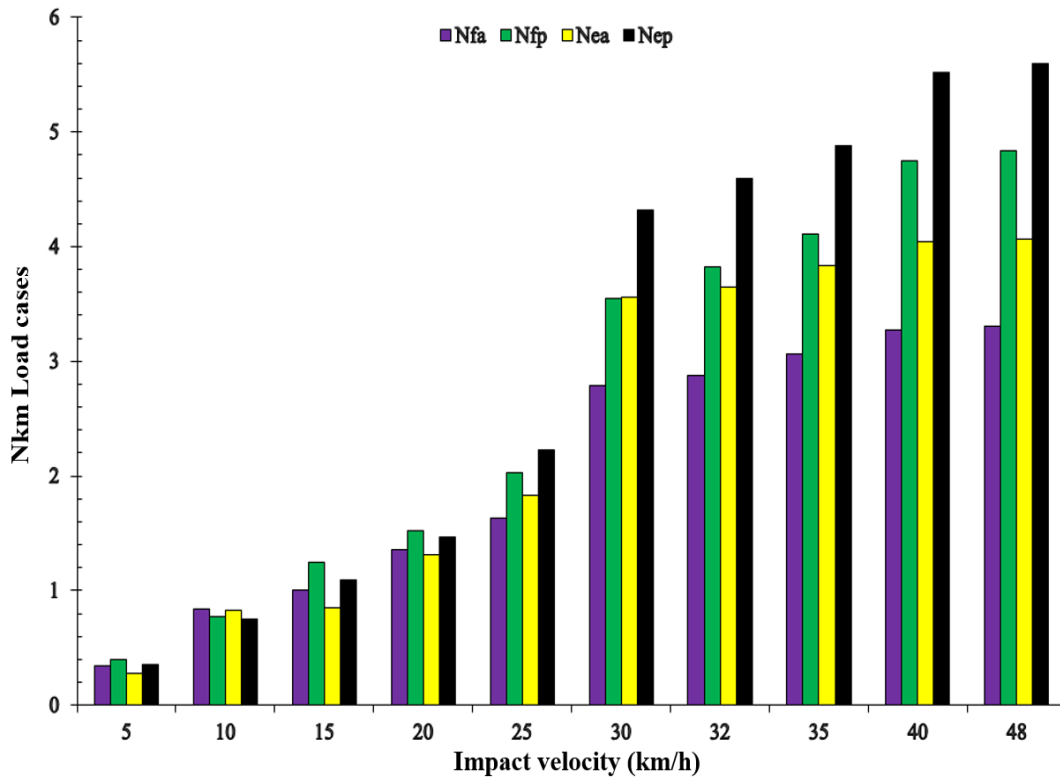


Figure A- 17. Upper neck load conditions for adult pedestrian impacts at 42cm offset from the vehicle’s centreline (rear position)

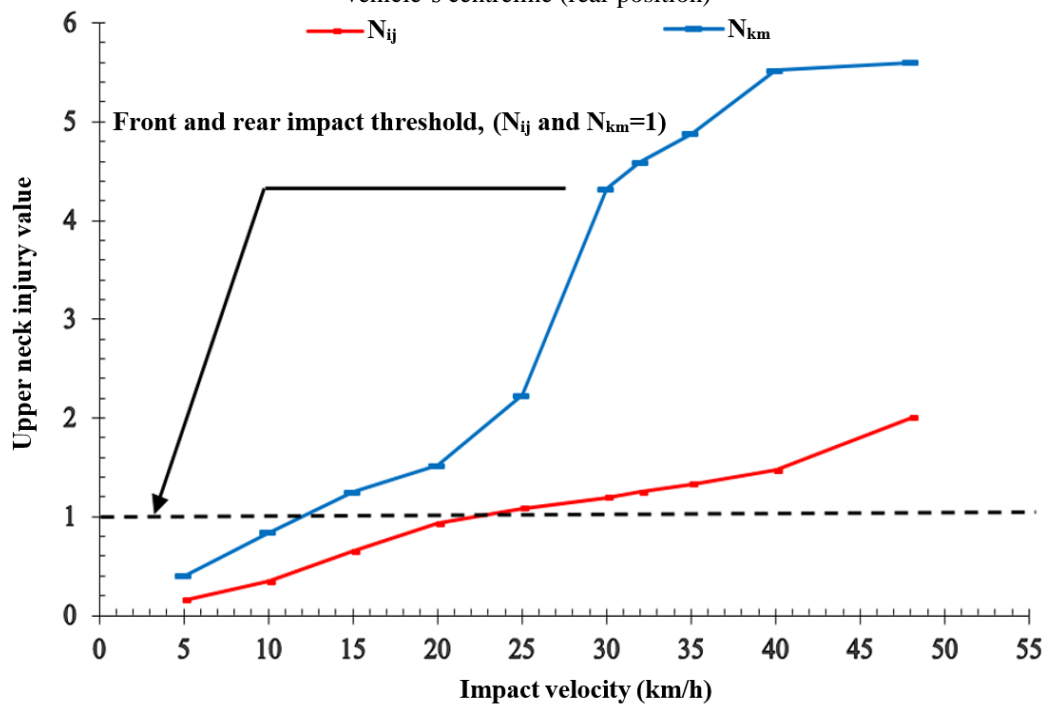


Figure A- 18. Upper neck injury values for adult pedestrian impacts at 42cm offset from the vehicle’s centreline (front and rear position).

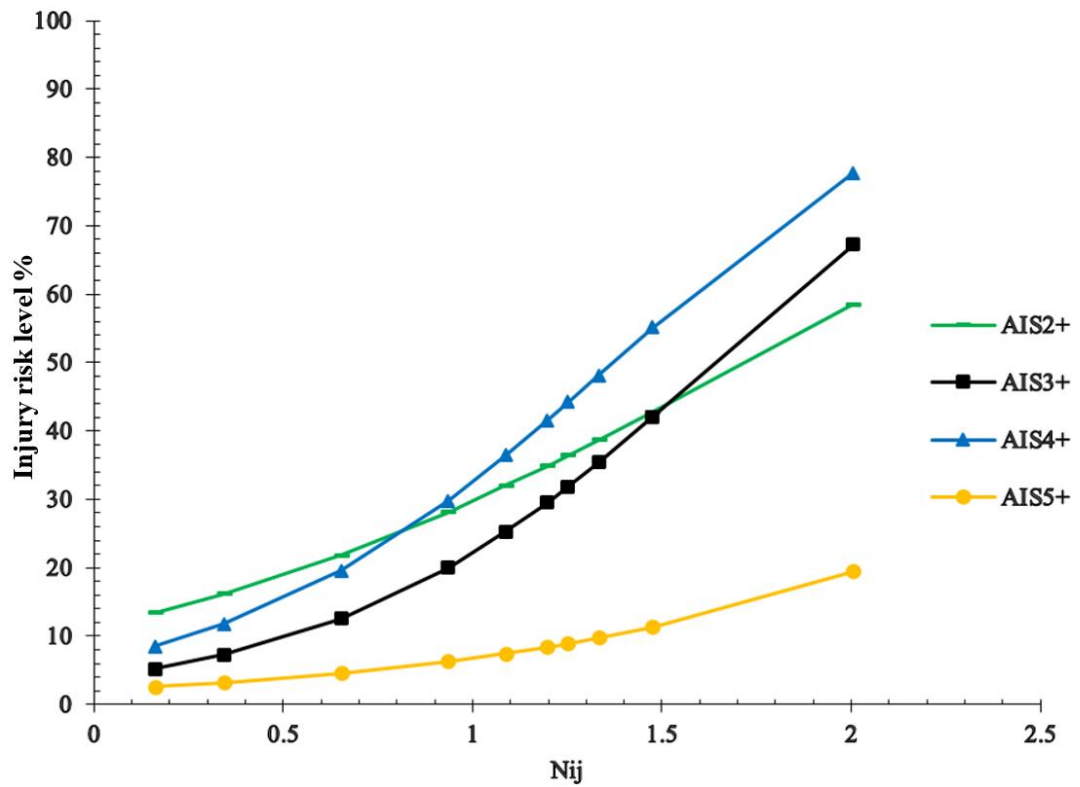


Figure A- 19. N_{ij} values and injury risk level for adult pedestrian in front impact position at 42cm offset from the vehicle's centreline

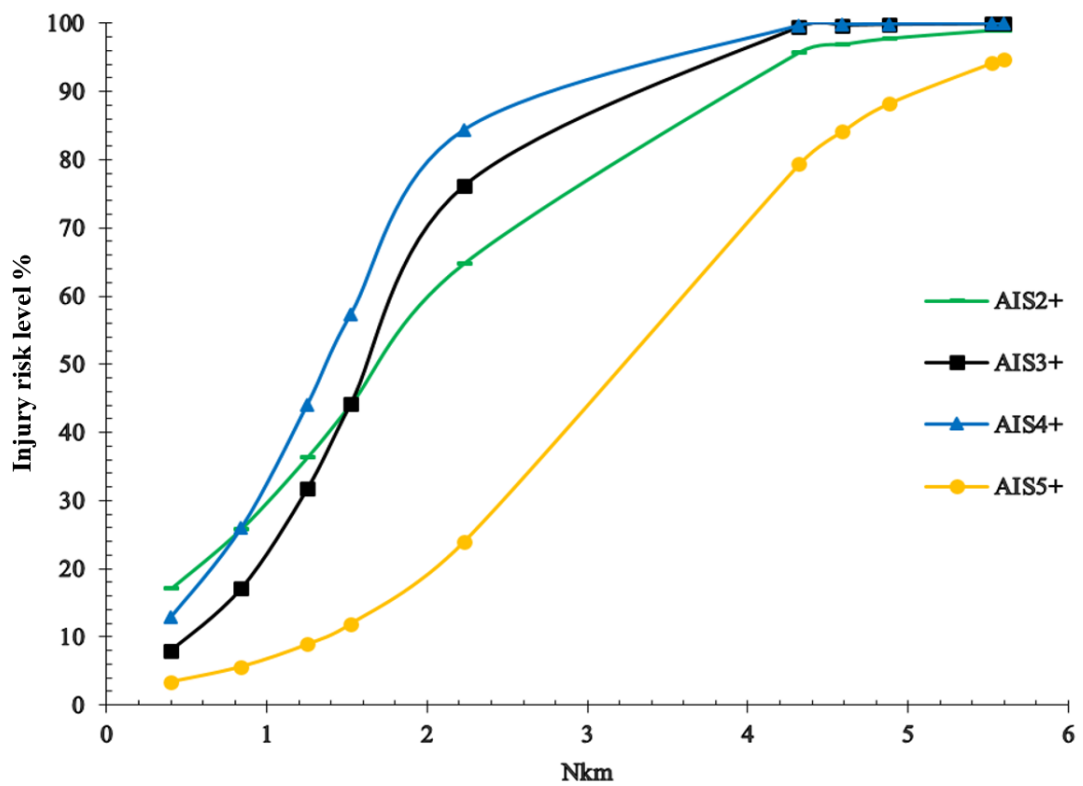


Figure A- 20. N_{km} values and injury risk level for adult pedestrian in rear impact position at 42cm offset from the vehicle's centreline

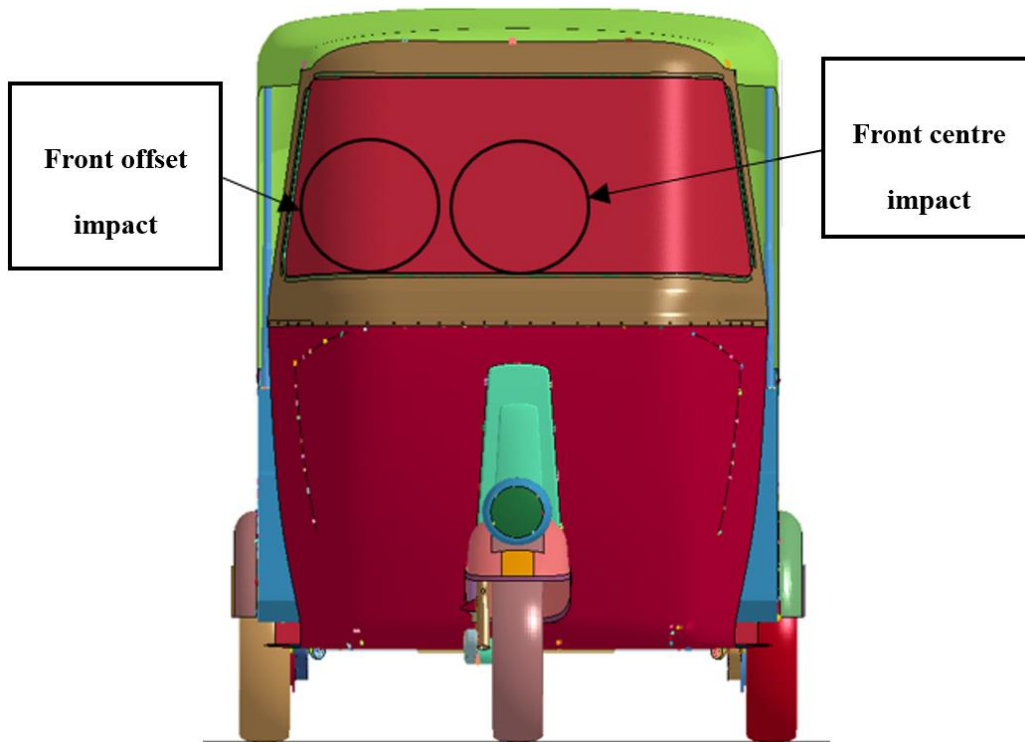


Figure A- 21. Chest Contact Locations for adult pedestrian of the Auto Rickshaw

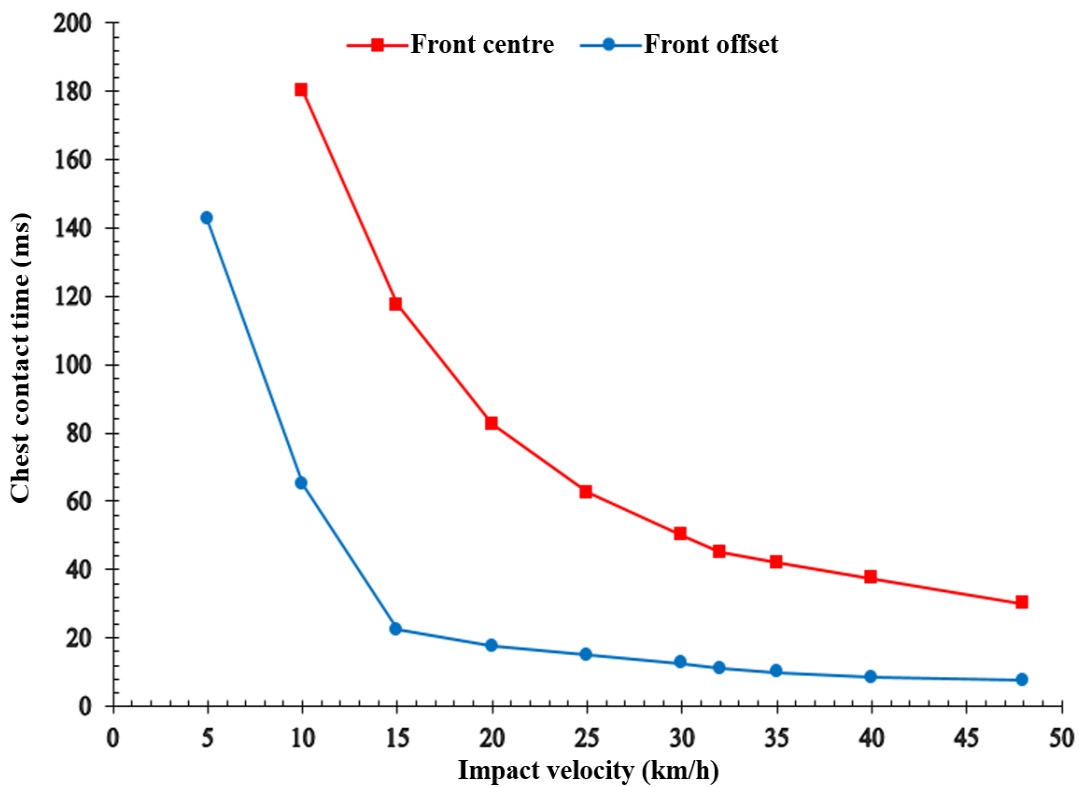


Figure A- 22. Chest Contact Time for Frontal adult pedestrian impacts at different vehicle contact region (centreline and offset)

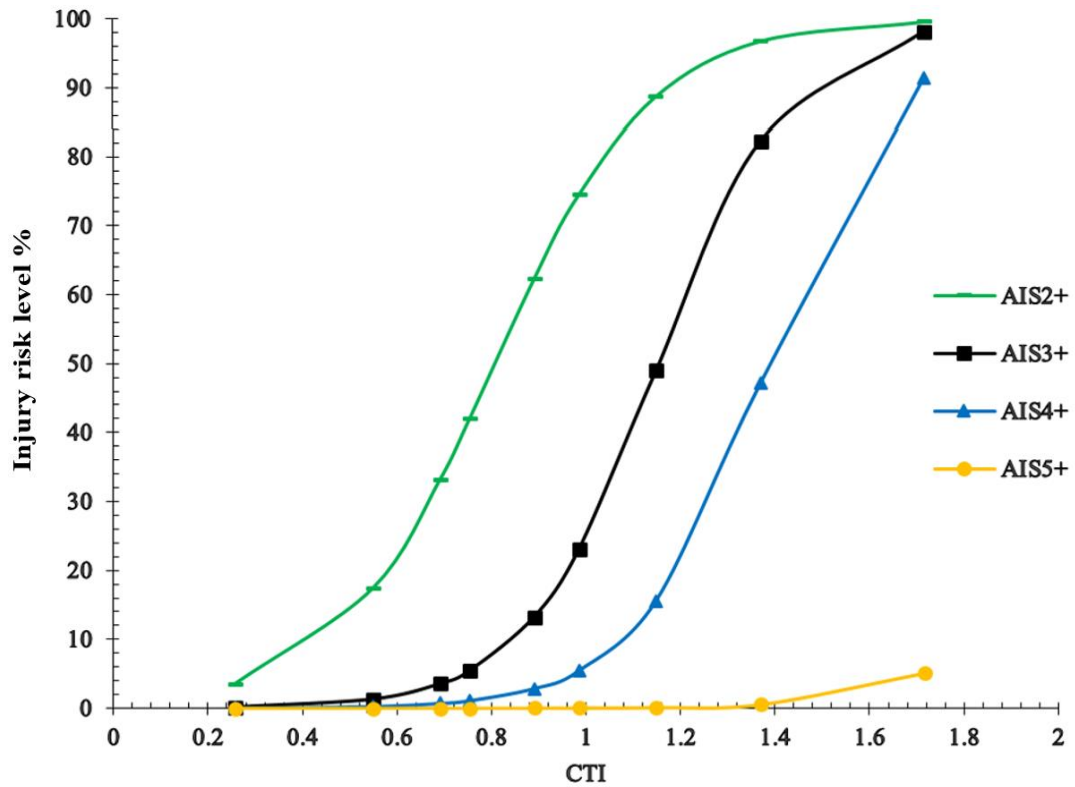


Figure A- 23. CTI values and injury risk level for adult pedestrian in front impact position at the vehicle's centreline

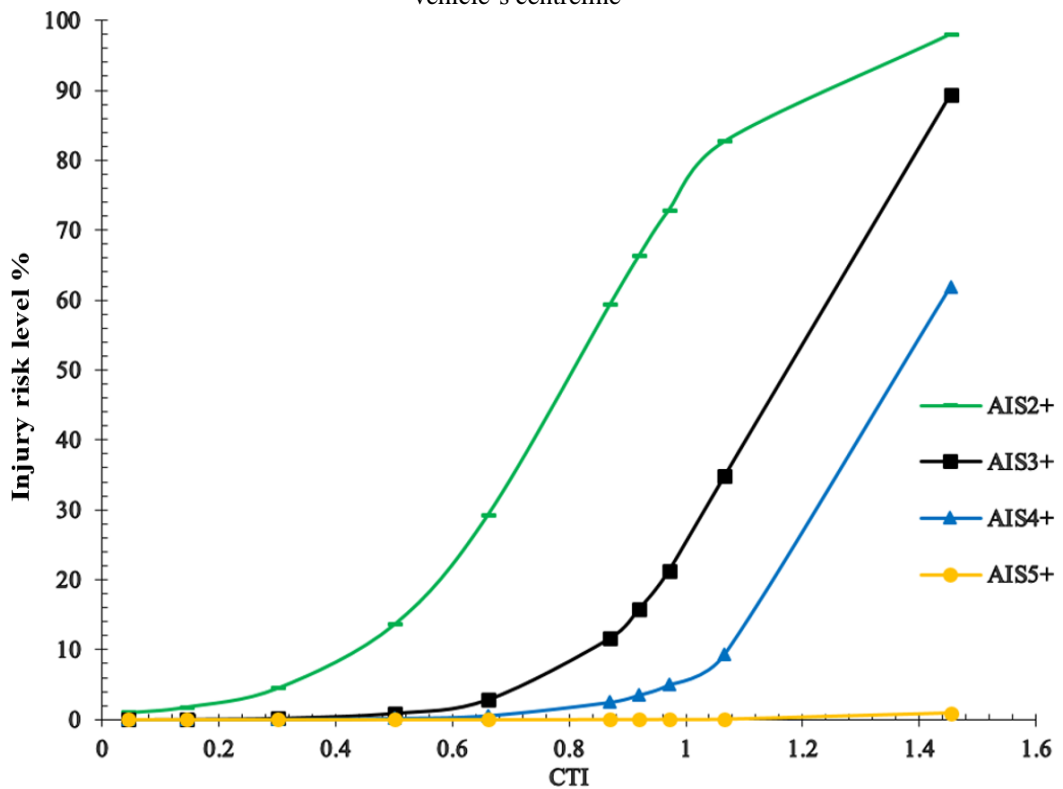


Figure A- 24. CTI values and injury risk level for adult pedestrian in front impact position at 42cm offset from the vehicle's centreline

Appendix B.

This section including the results for a 6YO-child pedestrian impacted by the auto rickshaw during primary impacts.

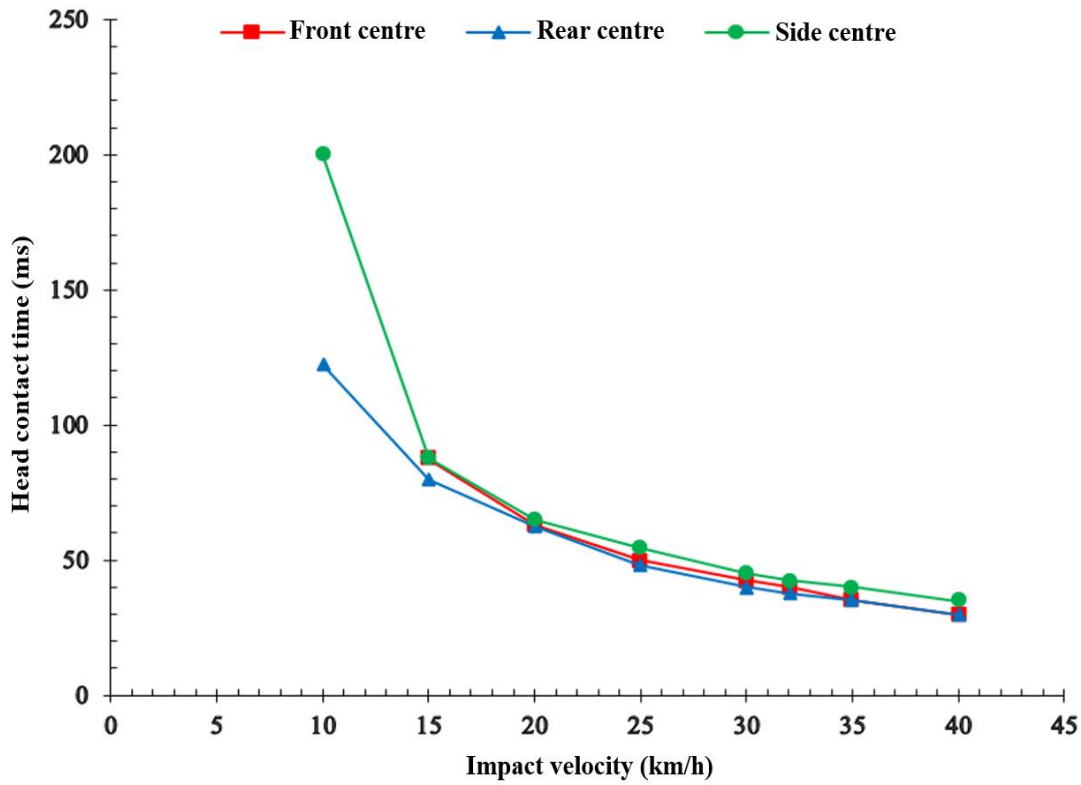


Figure B- 1. Head contact time for 6YO-child at the vehicle's centreline in different impact positions

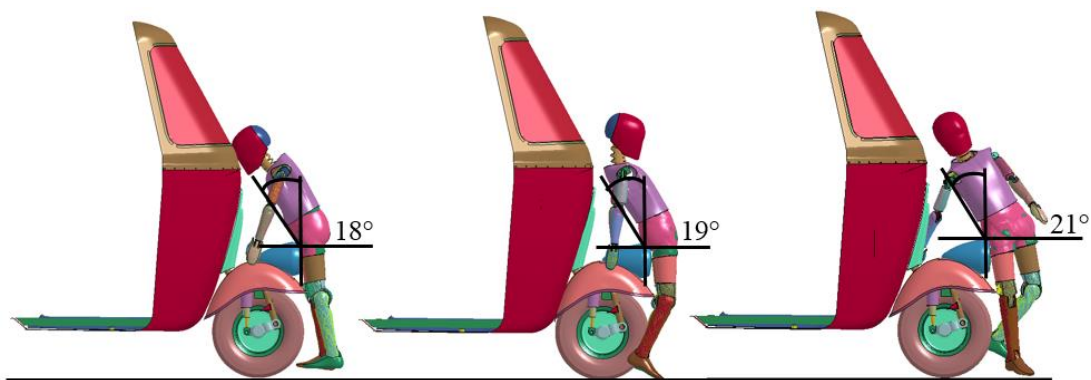


Figure B-2. Effective angles of rotation for the 6YO-child pedestrian about the headlamp of the auto rickshaw in the front, rear and side impact at the vehicle's centreline

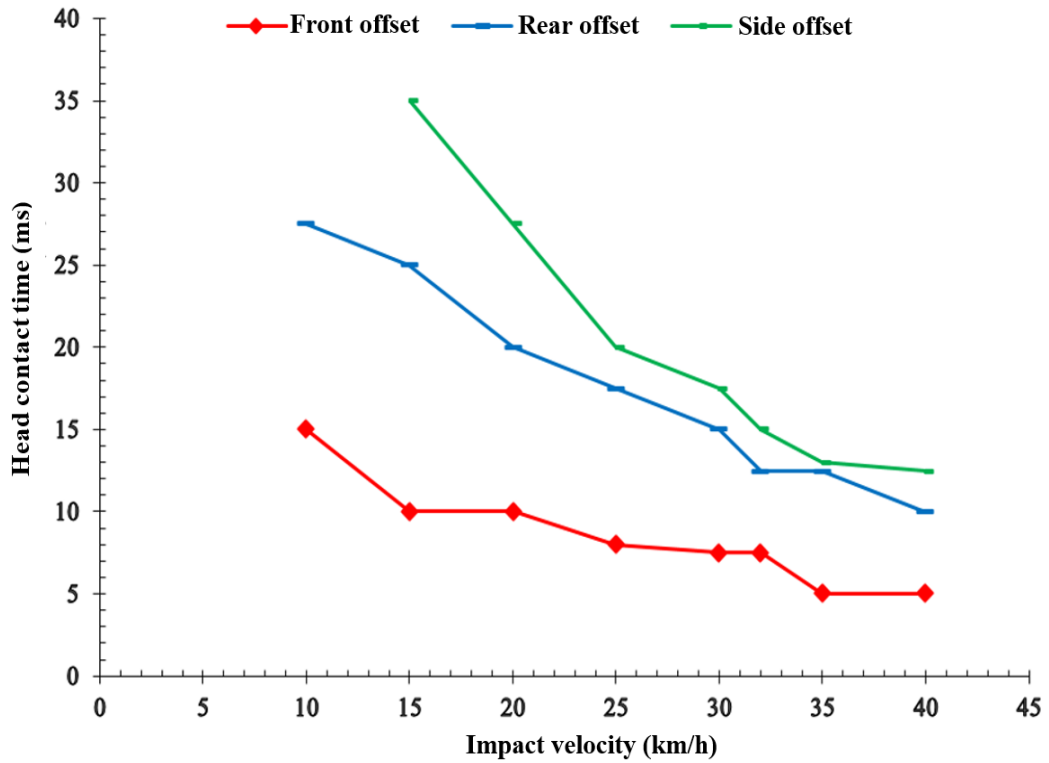


Figure B- 3. Head contact time for 6YO-child at 42cm offset from the vehicle’s centreline in different impact positions

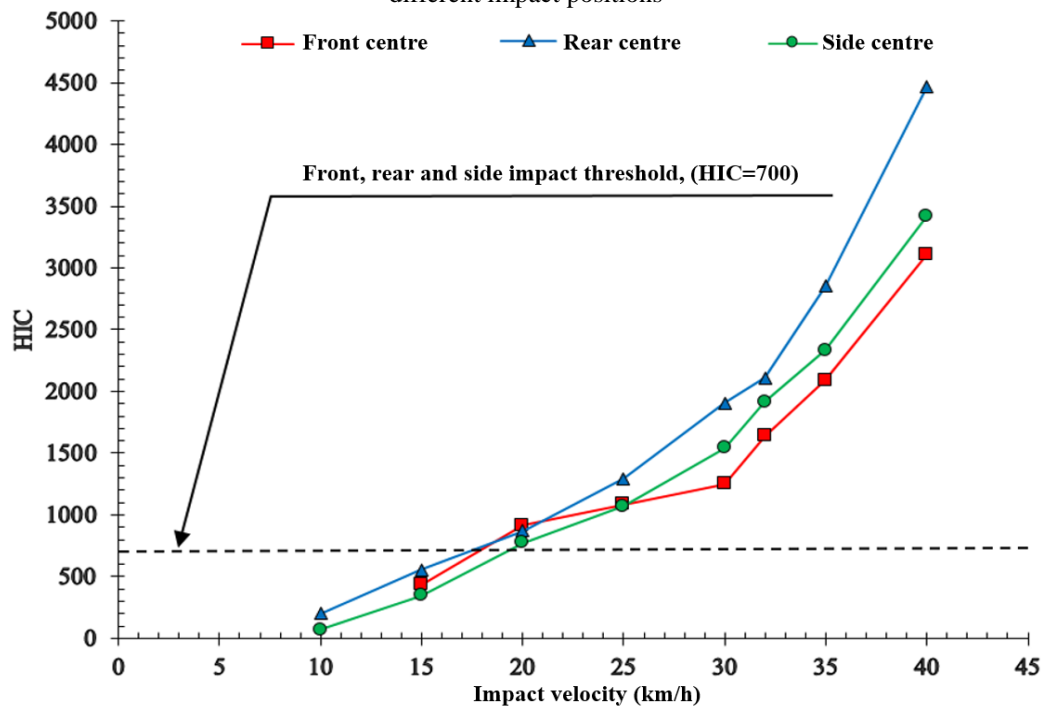


Figure B-4. HIC values for 6YO-child pedestrian at the vehicle’s centreline at front, rear and side standing orientations.

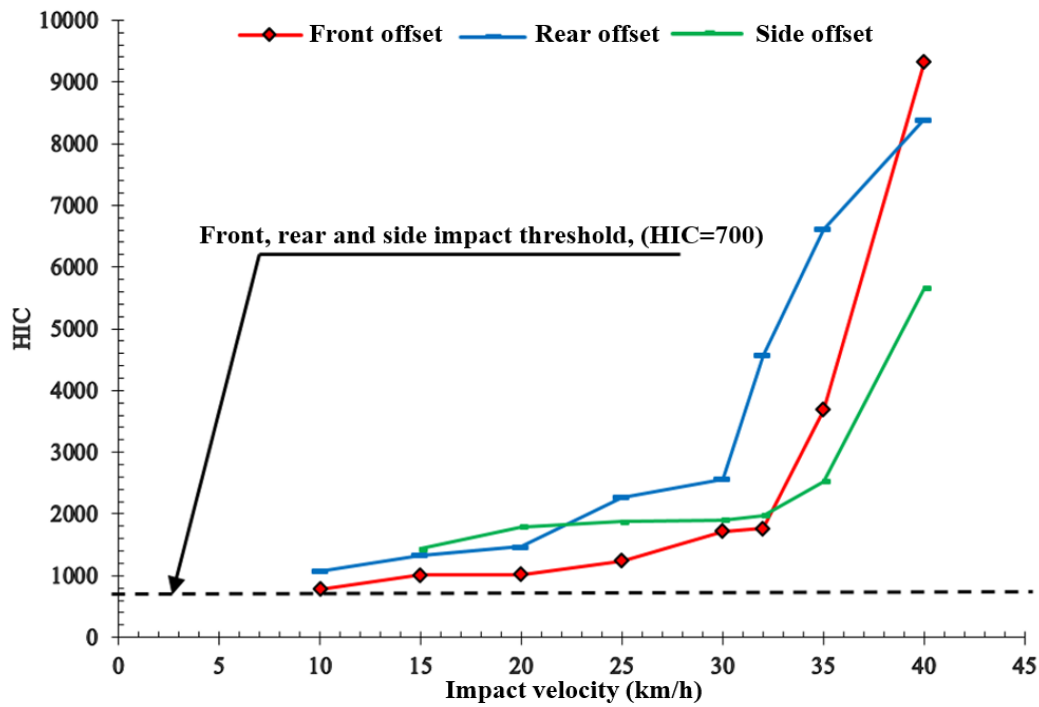


Figure B-5. HIC values for 6YO-child pedestrian at 42cm offset from the vehicle's centreline at front, rear and side standing orientations.

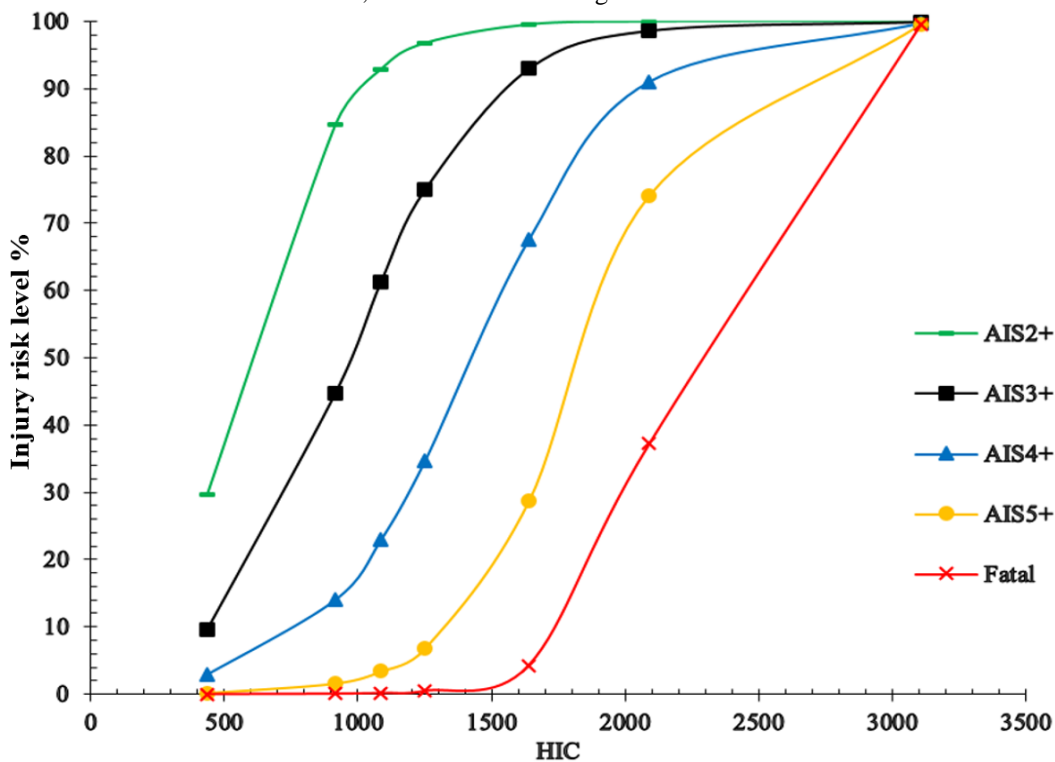


Figure B- 6. HIC values and injury risk level for 6YO-Child Pedestrian in front impact position at the vehicle's centreline

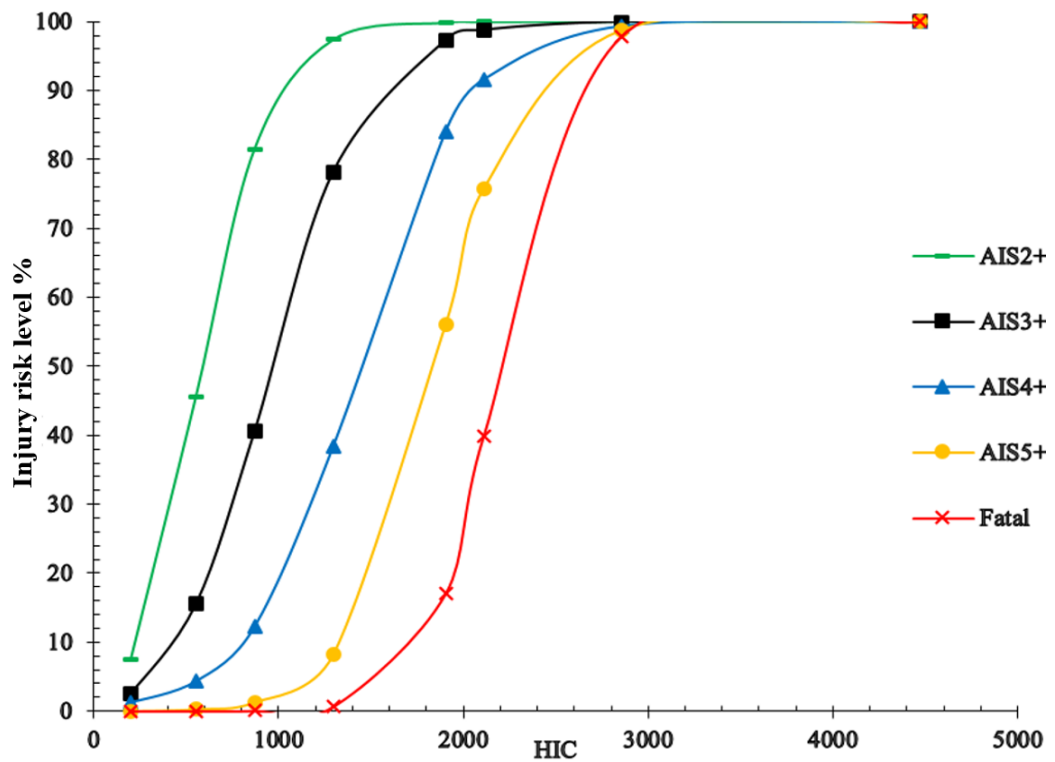


Figure B- 7. HIC values and injury risk level for 6YO-Child Pedestrian in rear impact position at the vehicle's centreline

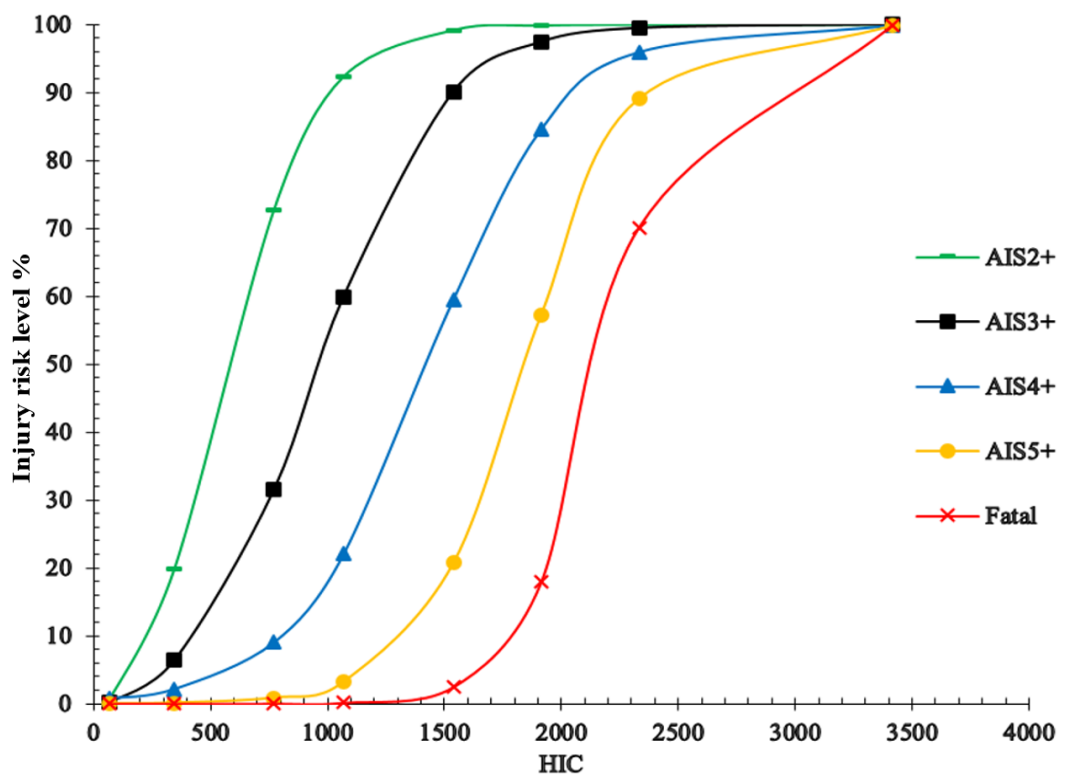


Figure B- 8. HIC values and injury risk level for 6YO-Child Pedestrian in side impact position at the vehicle's centreline

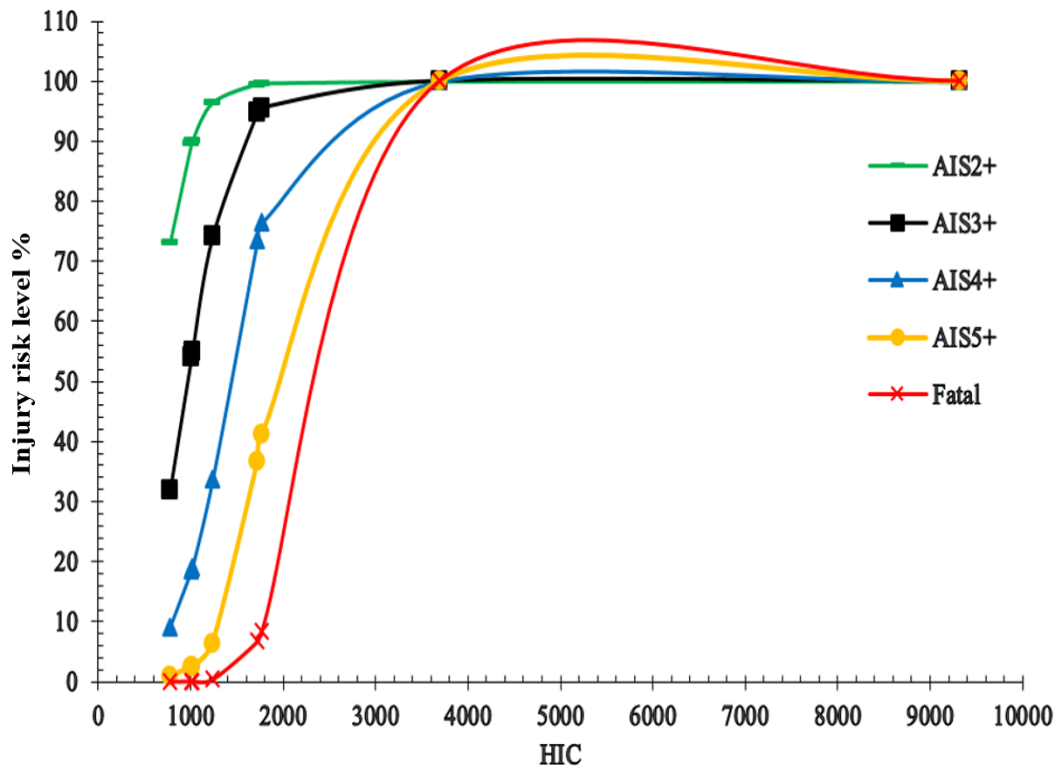


Figure B- 9. HIC values and injury risk level for 6YO-Child Pedestrian in front impact position at 42cm offset from the vehicle's centreline

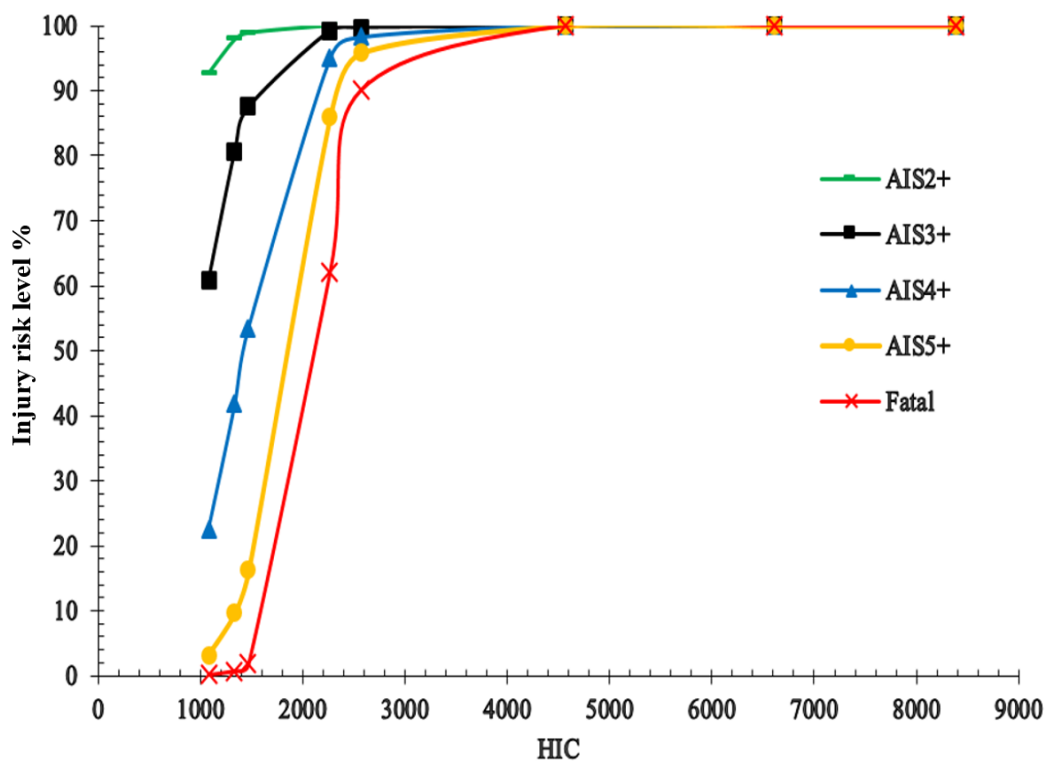


Figure B- 10. HIC values and injury risk level for 6YO-Child Pedestrian in rear impact position at 42cm offset from the vehicle's centreline

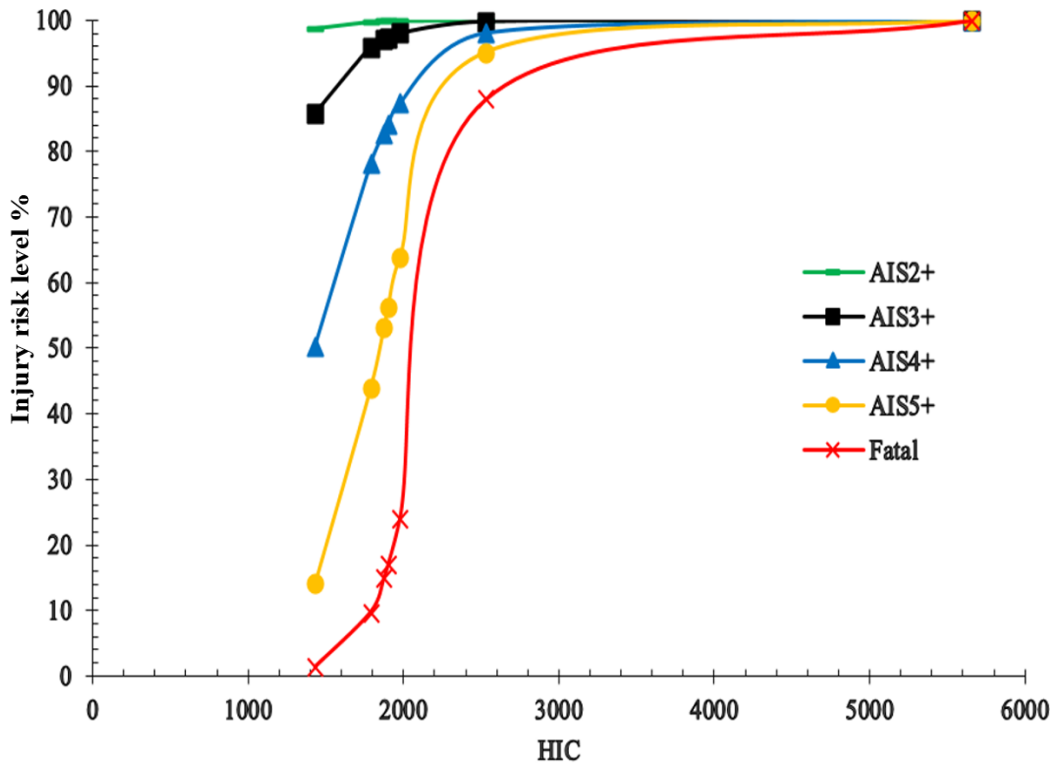


Figure B- 11. HIC values and injury risk level for 6YO-Child Pedestrian in side impact position at 42cm offset from the vehicle's centreline

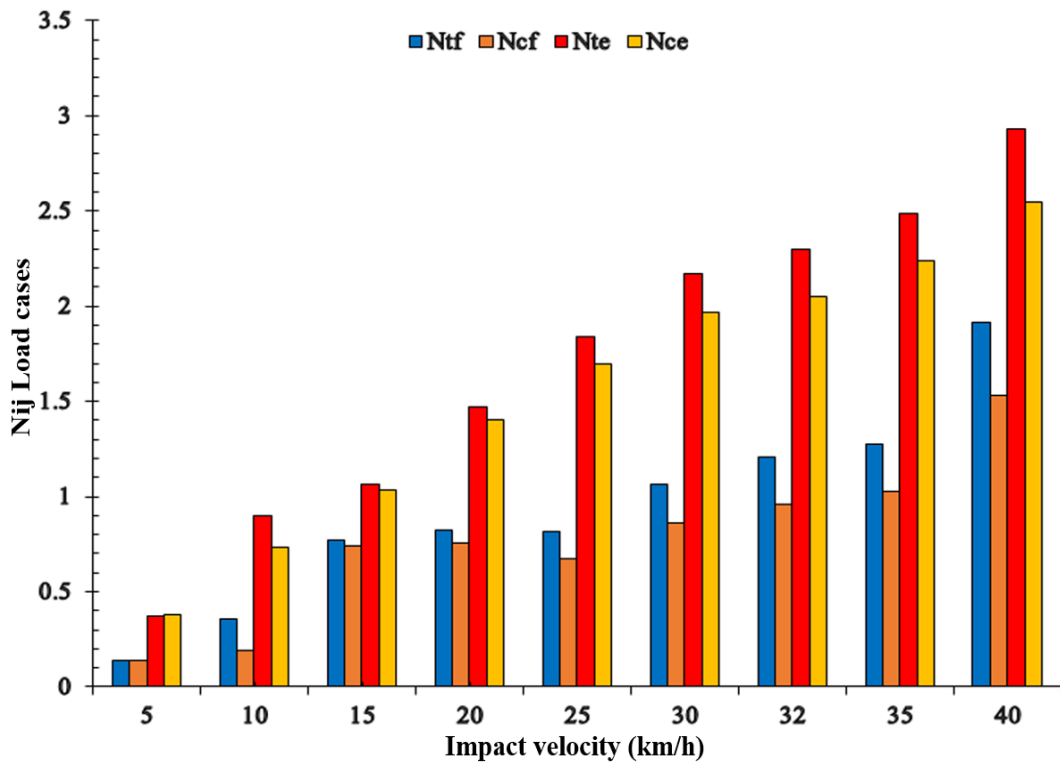


Figure B- 12. Upper neck load conditions for 6YO-Child Pedestrian impacts at the vehicle's centreline (front position)

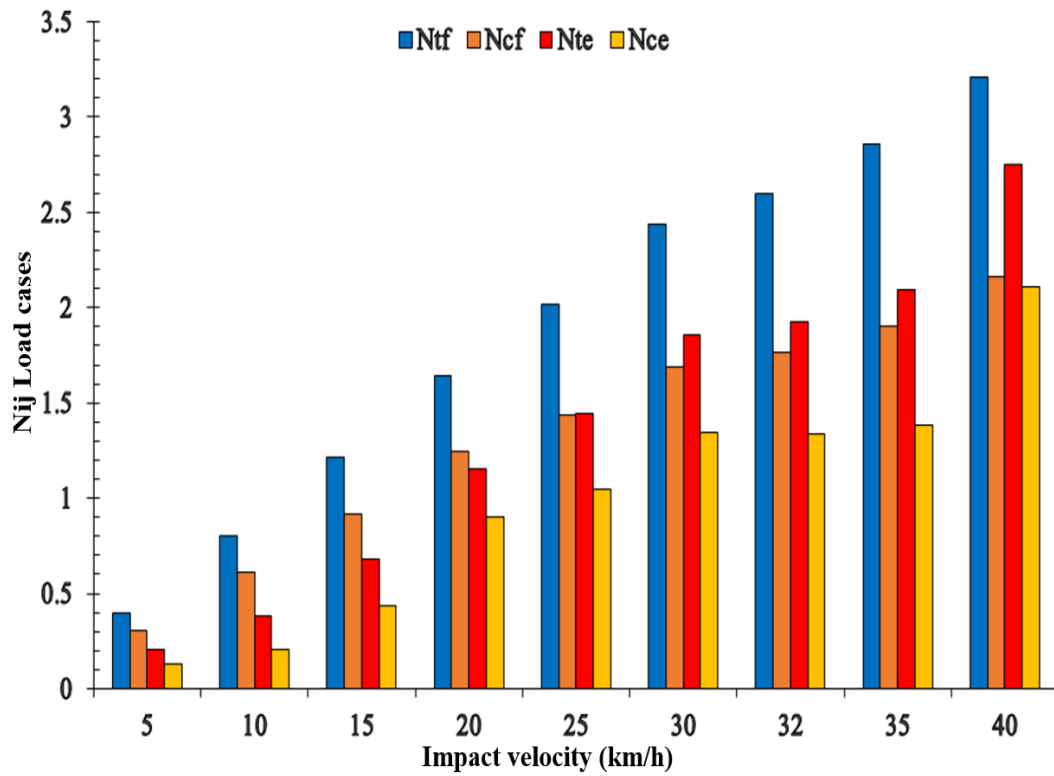


Figure B- 13. Upper neck load conditions for 6YO-Child Pedestrian impacts at 42cm offset from the vehicle’s centreline (front position)

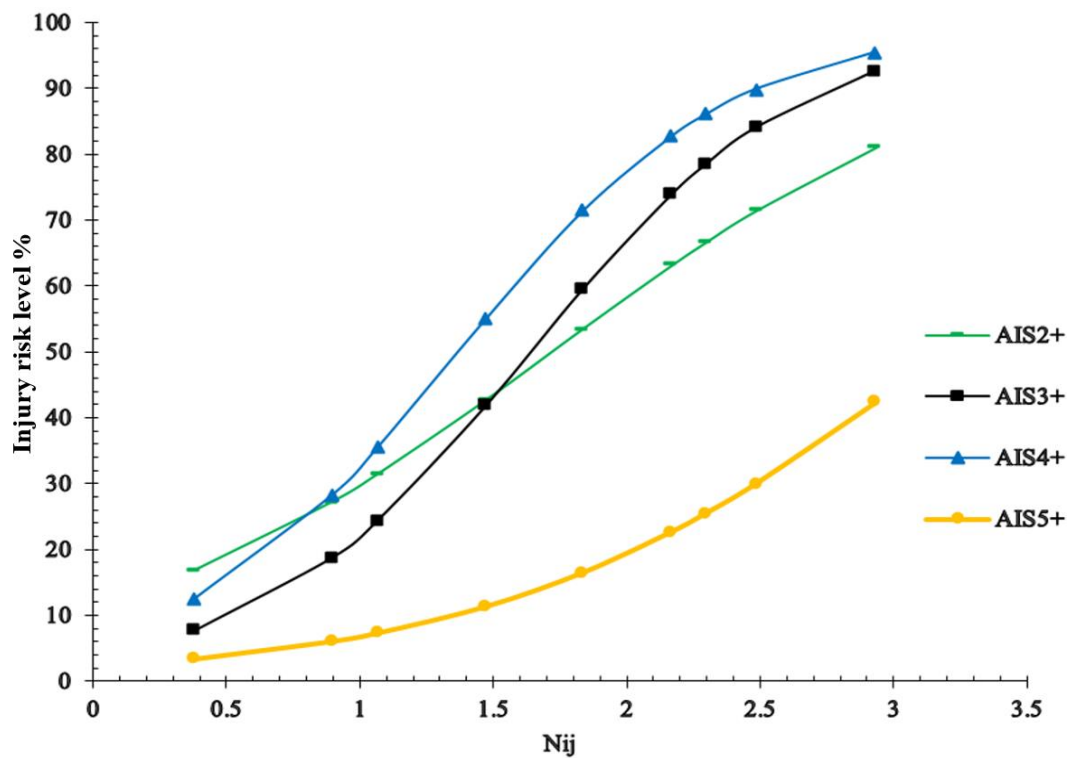


Figure B- 14. N_{ij} values and injury risk level for 6YO-Child Pedestrian in front impact position at the vehicle’s centreline

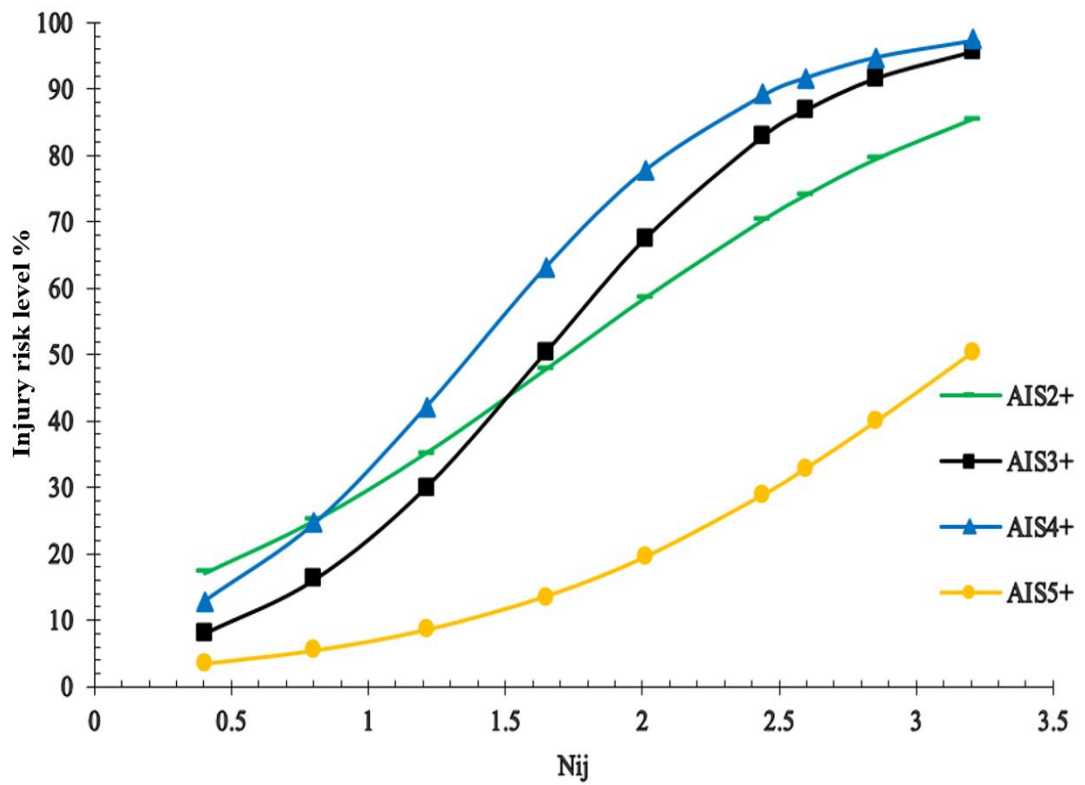


Figure B- 15. N_{ij} values and injury risk level for 6YO-Child Pedestrian in front impact position at 42cm offset from the vehicle's centreline

Appendix C.

This section including the compression results for adult and 6YO-child pedestrians impacted by the auto rickshaw during primary impacts.

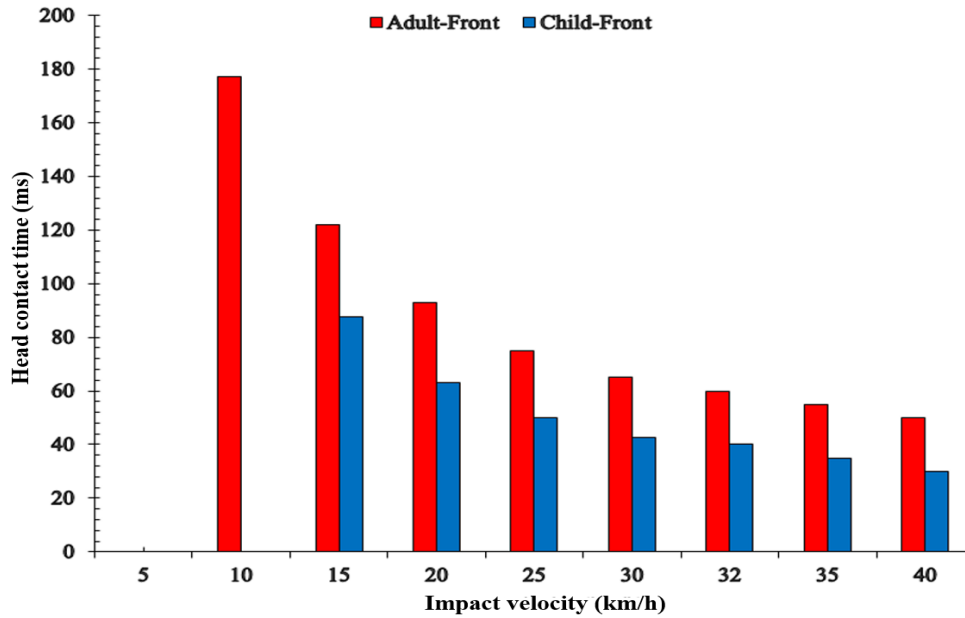


Figure C- 1. Head contact time for adult and child pedestrians in front impact at the vehicle's centreline

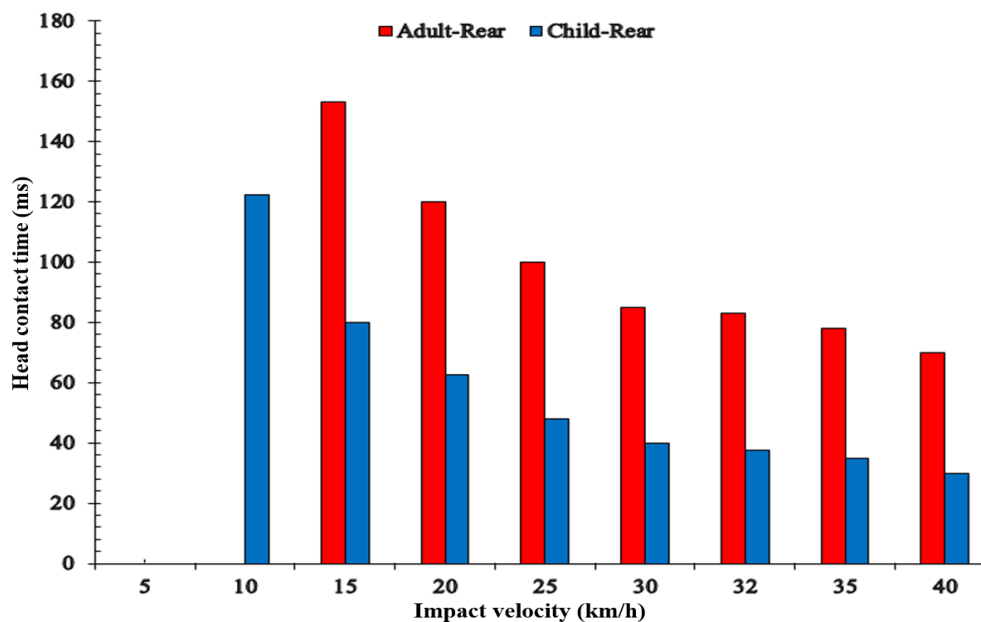


Figure C- 2. Head contact time for adult and child pedestrians in rear impact at the vehicle's centreline

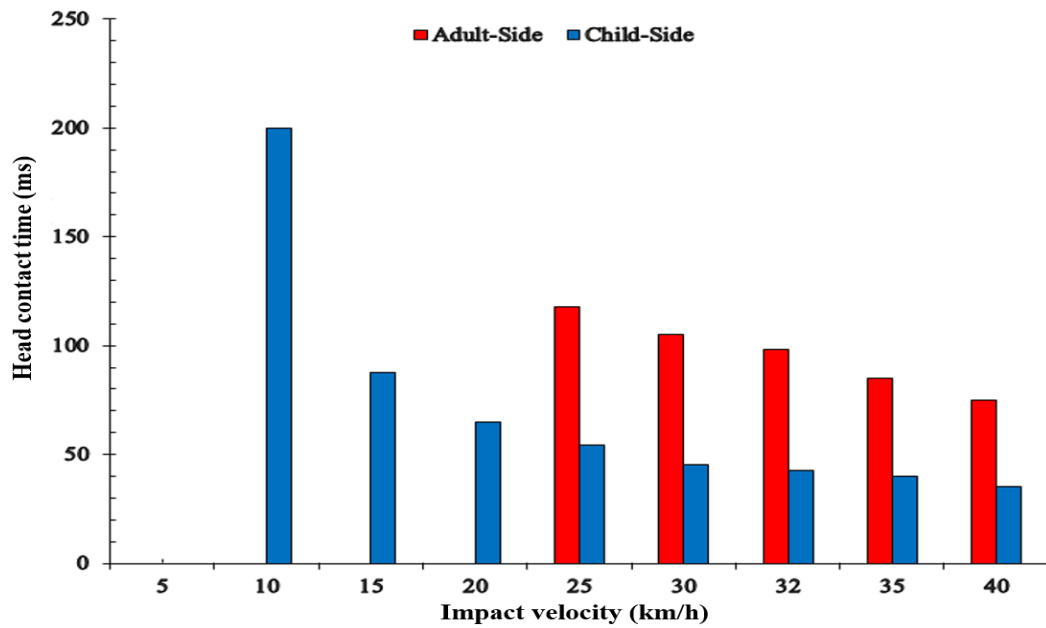


Figure C- 3. Head contact time for adult and child pedestrians in side impact at the vehicle’s centreline

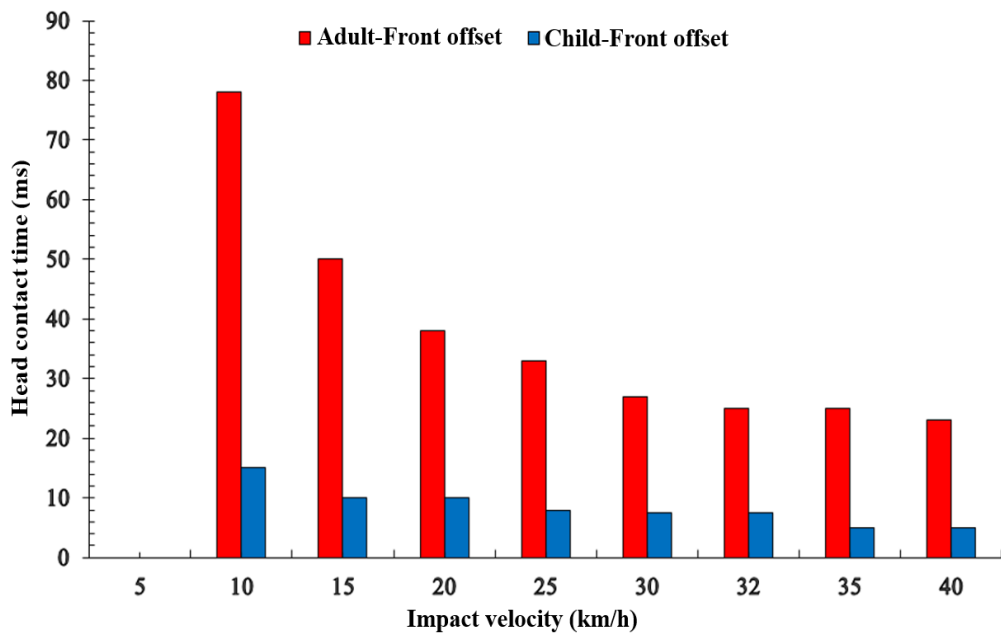


Figure C- 4. Head contact time for adult and child pedestrians in front impact at 42cm offset from the vehicle’s centreline

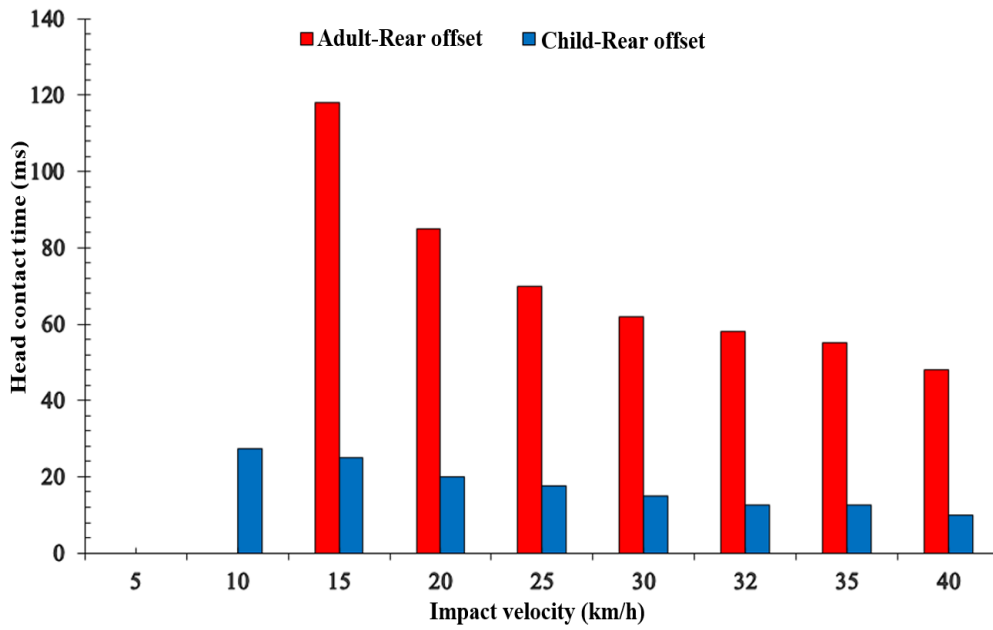


Figure C- 5. Head contact time for adult and child pedestrians in rear impact at 42cm offset from the vehicle’s centreline

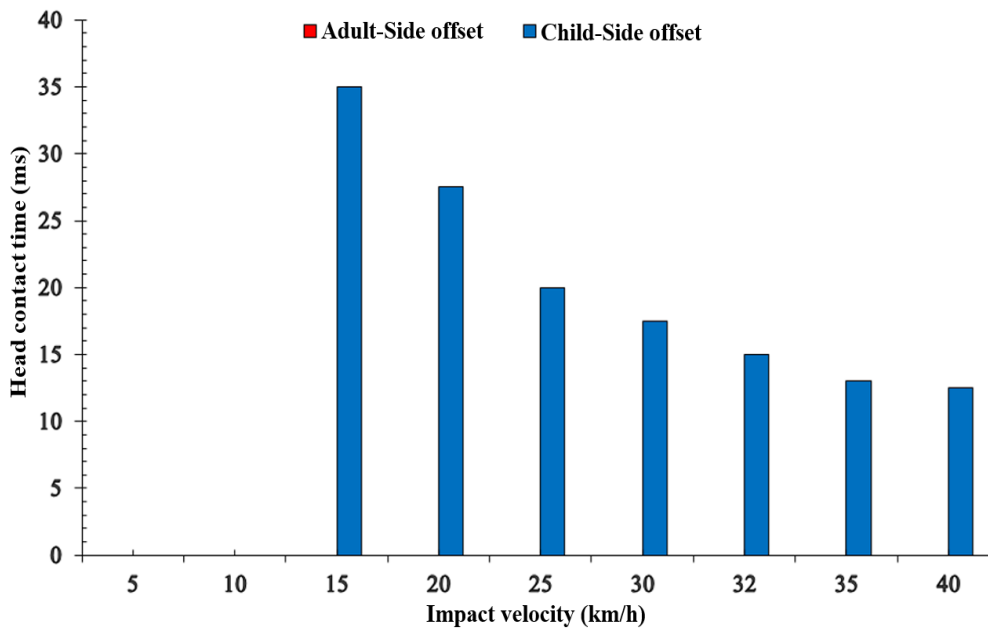


Figure C- 6. Head contact time for adult and child pedestrians in side impact at 42cm offset from the vehicle’s centreline

Table C- 1. Head injury risk for adult and child pedestrians in frontal impacts at the vehicle's centreline

HIC		Moderate (AIS2+) %		Serious (AIS3+) %		Severe (AIS4+) %		Critical (AIS5+) %		Fatal (AIS6+) %	
Adult	Child	Adult	Child	Adult	Child	Adult	Child	Adult	Child	Adult	Child
-	-	-	-	-	-	-	-	-	-	-	-
222	-	9	-	3	-	2	-	0	-	0	-
318	443.3	17	30	6	10	2	3	0	0.16	0	0
689	913.8	63	85	25	45	7	14	1	2	1	0.07
964	1085	88	93	50	61	17	23	2	3	2	0.2
1307	1251	98	97	88	75	40	35	9	7	2	0.5
1538	1639	100	100	90	93	59	68	21	29	2	4
1908	2091	100	100	97	99	84	91	56	74	17	37
2449	3108	100	100	100	100	100	100	100	100	100	100

Table C- 2. Head injury risk for adult and child pedestrians in rear impacts at the vehicle's centreline

HIC		Moderate (AIS2+) %		Serious (AIS3+) %		Severe (AIS4+) %		Critical (AIS5+) %		Fatal (AIS6+) %	
Adult	Child	Adult	Child	Adult	Child	Adult	Child	Adult	Child	Adult	Child
-	-	-	-	-	-	-	-	-	-	-	-
-	201	-	7.5	-	3	-	2	-	0.04	-	0
309	554.2	16	46	5	3	2	5	0.08	0.30	0	0.01
789	870.7	74	82	33	16	10	12	1	1.32	0.03	0.05
1208	1295	96	97	72	41	32	38	6	8.	0.38	1
1244	1905	97	100	75	78	34	84	7	56	0.5	17
1344	2111	98	100	81	97	43	92	10	76	1	40
1412	2854	99	100	85	100	48	100	13	100	1.21	98
1423	4470	99	100	85	100	50	100	14	100	2	100

Table C- 3. Head injury risk for adult and child pedestrians in side impacts at the vehicle's centreline

HIC		Moderate (AIS2+) %		Serious (AIS3+) %		Severe (AIS4+) %		Critical (AIS5+) %		Fatal (AIS6+) %	
Adult	Child	Adult	Child	Adult	Child	Adult	Child	Adult	Child	Adult	Child
-	-	-	-	-	-	-	-	-	-	-	-
-	70	-	0.62	-	0.24	-	0.83	-	0	-	0
-	345.5	-	20	-	6.39	-	2	-	0.10	-	0
-	772.4	-	73	-	31.53	-	9	-	0.84	-	0.03
47	1070	0.15	92	0.06	60	0.77	22	0	3.18	0	0.17
95	1540	2	100	0.58	90	0.91	60	0.01	20.70	0	2.49
147	1915	4	100	1.47	97.42	1.09	85	0.02	57.22	0	17.88
597	2332	52	100	18	100	5	96	0.37	89.08	0.01	70.06
772	3418	73	100	31.49	100	9.03	100	0.84	100	0.03	100

Table C- 4. Head injury risk for adult and child pedestrians in frontal impacts at 42cm offset from the vehicle's centreline

HIC		Moderate (AIS2+) %		Serious (AIS3+) %		Severe (AIS4+) %		Critical (AIS5+) %		Fatal (AIS6+) %	
Adult	Child	Adult	Child	Adult	Child	Adult	Child	Adult	Child	Adult	Child
-	-	-	-	-	-	-	-	-	-	-	-
195	777.4	7	73.25	2.43	31.97	1.29	9.18	0.03	0.86	0	0.03
307	1009	16	89.89	5.20	54.12	1.90	18.57	0.08	2.44	0	0.12
690	1018	63.48	90.30	24.60	55	6.93	19	0.58	2.54	0.02	0.12
1359	1238	98	96.54	82	74.15	44	33.75	11	6.47	1	0.45
2215	1722	100	100	99	100	94	73.58	83	36.62	54.60	6.74
2650	1766	100	100	100	100	98.64	76.47	97	41.17	93.44	8.51
3311	3688	100	100	100	100	100	100	100	100	100	100
4884	9323	100	100	100	100	100	100	100	100	100	100

Table C- 5. Head injury risk for adult and child pedestrians in rear impacts at 42cm offset from the vehicle's centreline

HIC		Moderate (AIS2+) %		Serious (AIS3+) %		Severe (AIS4+) %		Critical (AIS5+) %		Fatal (AIS6+) %	
Adult	Child	Adult	Child	Adult	Child	Adult	Child	Adult	Child	Adult	Child
-	-	-	-	-	-	-	-	-	-	-	-
-	1080	-	93	-	61	-	23	-	3	-	0.18
289	1335	14	98	5	81	2	42	0.07	10	0	0.78
1648	1470	100	99	93	87	69	53	30	16	5	1.68
2752	2270	100	100	100	99	100	95	98	86	96	62
4259	2569	100	100	100	100	100	98	100	96	100	90
4794	4569	100	100	100	100	100	100	100	100	100	100
5751	6618	100	100	100	100	100	100	100	100	100	100
7092	8388	100	100	100	100	100	100	100	100	100	100

Table C- 6. Head injury risk for adult and child pedestrians in side impacts at 42cm offset from the vehicle's centreline

HIC		Moderate (AIS2+) %		Serious (AIS3+) %		Severe (AIS4+) %		Critical (AIS5+) %		Fatal (AIS6+) %	
Adult	Child	Adult	Child	Adult	Child	Adult	Child	Adult	Child	Adult	Child
-	-	-	-	-	-	-	-	-	-	-	-
-	-	-	-	-	-	-	-	-	-	-	-
-	1433	-	98.65	-	85.83	-	50.25	-	14	-	1.36
-	1792	-	100	-	95.95	-	78.07	-	43.93	-	9.74
-	1876	-	100	-	97	-	82.70	-	53	-	14.84
-	1906	-	100	-	97.33	-	84.16	-	56.26	-	17.14
-	1978	-	100	-	97.95	-	87.24	-	63.75	-	23.77
-	2532	-	100	-	100	-	97.95	-	95	-	87.94
-	6565	-	100	-	100	-	100	-	100	-	100

Table C- 7. Upper Neck injury risk for adult and child pedestrians in frontal impacts at the vehicle's centreline

N_{ij}		Moderate (AIS2+) %		Serious (AIS3+) %		Severe (AIS4+) %		Critical (AIS5+) %	
Adult	Child	Adult	Child	Adult	Child	Adult	Child	Adult	Child
0.07	0.38	12.25	16.79	4.34	7.73	7.22	12.48	2.34	3.35
0.07	0.9	12.25	27.26	4.34	18.85	7.22	28.31	2.34	6.04
0.75	1.07	23.93	31.45	14.88	24.48	22.85	35.50	5.12	7.29
0.92	1.47	27.82	42.69	19.54	41.88	29.26	54.99	6.20	11.33
1.18	1.84	34.47	53.53	28.76	59.63	40.80	71.44	8.27	16.50
1.28	2.17	37	63.16	33.	74.00	46	82.79	9	22.73
1.29	2.30	37.49	66.57	33.62	78.46	46.11	86.03	9.33	25.46
1.33	2.49	38.62	71.42	35.17	84.11	48.07	89.94	9.74	30.00
1.29	2.93	37.49	81.04	33.32	92.76	46.11	95.58	9.33	42.30

Table C- 8. Upper Neck injury risk for adult and child pedestrians in frontal impacts at 42cm offset from the vehicle's centreline

N_{ij}		Moderate (AIS2+) %		Serious (AIS3+) %		Severe (AIS4+) %		Critical (AIS5+) %	
Adult	Child	Adult	Child	Adult	Child	Adult	Child	Adult	Child
0.16	0.40	13.45	17	5.16	8	8.49	13	2.60	4
0.34	0.80	16.21	25	7.24	16	11.74	25	3.21	5
0.65	1.21	21.85	35	12.54	30	19.61	42	4.58	9
0.93	1.65	28.16	48	20	50	29.82	63	6.30	14
1.09	2.01	32	58	25	68	36	78	7	20
1.20	2.44	34.91	70	29.55	83	41.58	90	8.43	29
1.25	2.60	36.40	74	31.82	87	44.20	92	8.94	33
1.33	2.86	38.67	80	35.37	92	48.15	95	9.76	40
1.48	3.21	42.78	86	42	96	55.14	98	11.37	51

Appendix D.

This section including the results for the adult pedestrian during secondary impacts.

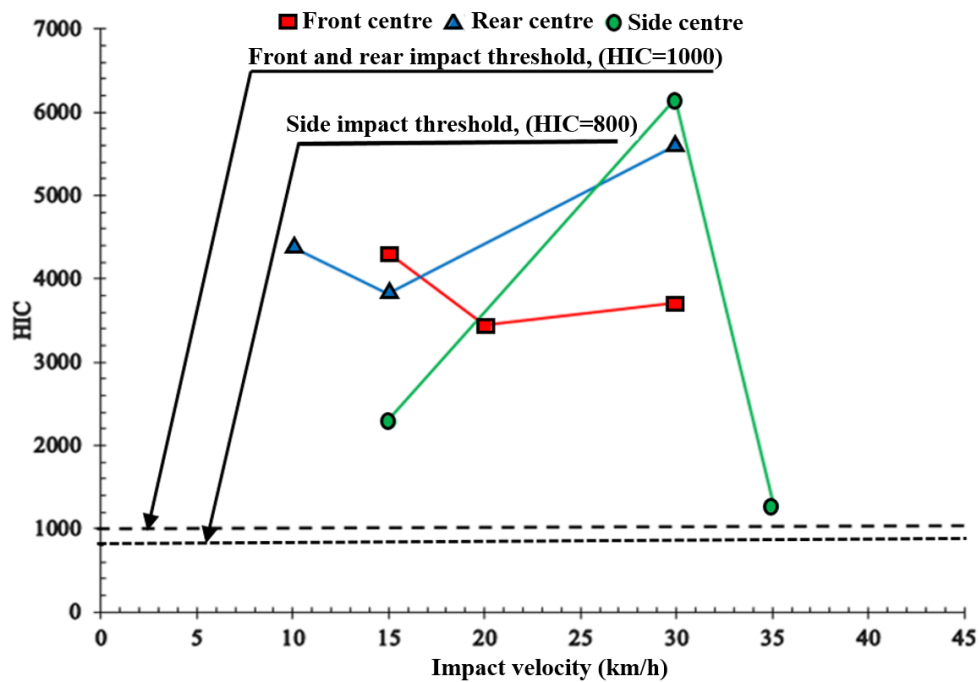


Figure D- 1. HIC values for adult pedestrian at the vehicle's centreline at front, rear and side standing orientations in secondary impacts

Table D- 1. Head injury risk against HIC values for adult pedestrians at the vehicle's centreline in front, rear and side impacts

Impact Position	HIC	(AIS2+)%	(AIS3+)%	(AIS4+)%	(AIS5+)%	Fatal %
Front	4277	100	100	100	100	100
	3426	100	100	100	100	100
	3696	100	100	100	100	100
Rear	4382	100	100	100	100	100
	3839	100	100	100	100	100
	5617	100	100	100	100	100
Side	2274	100	100	95	86	63
	6126	100	100	100	100	100
	1260	96.88	75.74	35.49	7.09	0.51

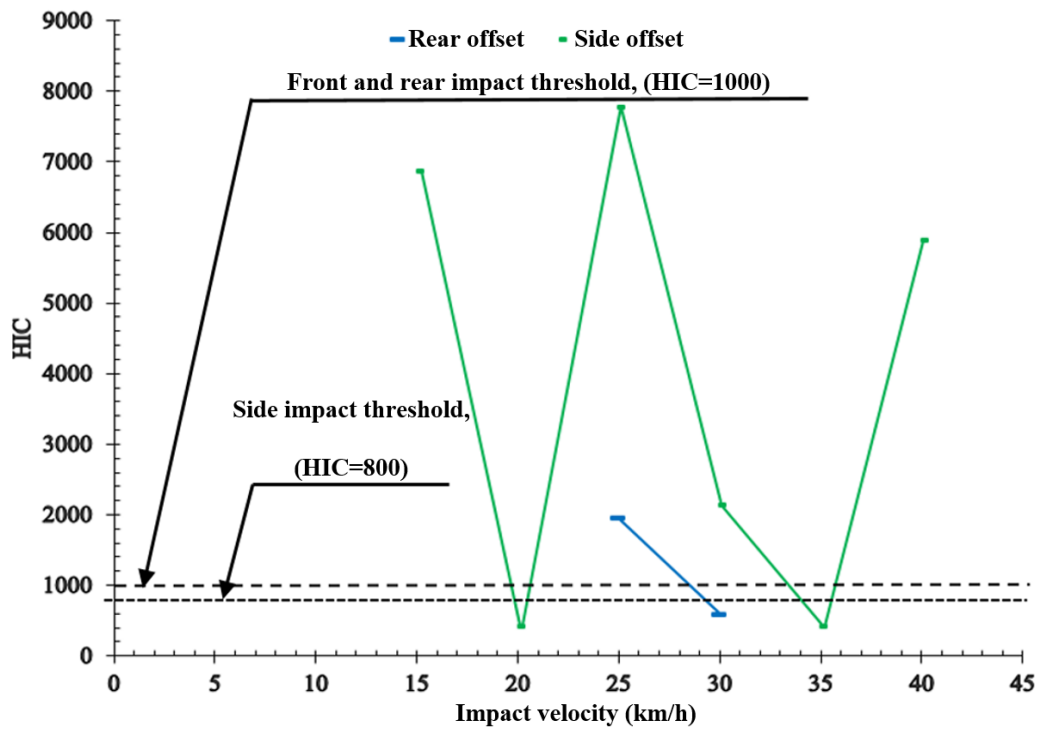


Figure D- 2. HIC values for adult pedestrian at 42cm offset from the vehicle’s centreline at front, rear and side standing orientations in secondary impacts

Table D- 2. Head injury risk against HIC values for adult pedestrians at 42cm offset from the vehicle’s centreline in front, rear and side impacts

Impact Position	HIC	(AIS2+)%	(AIS3+)%	(AIS4+)%	(AIS5+)%	Fatal %
Rear	-	-	-	-	-	-
	1957	100	98	86	61	22
	580	49.16	17.12	4.81	0.34	0.01
Side	6861	100	100	100	100	100
	419	28.02	9.04	2.79	0.15	0
	7780	100	100	100	100	100
	2130	100	98.83	92.10	77.27	42.57
	418	27.90	9.00	2.78	0.15	0
	5894	100	100	100	100	100

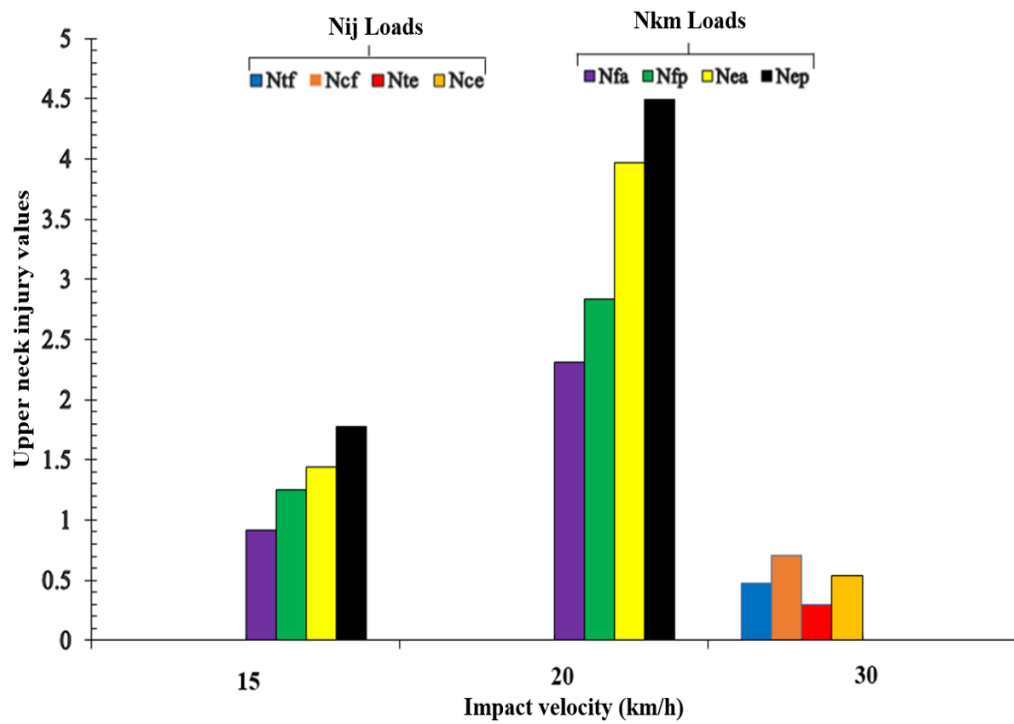


Figure D- 3. Upper neck load conditions of the secondary collisions for adult pedestrian impacted at the vehicle’s centreline in frontal impact position

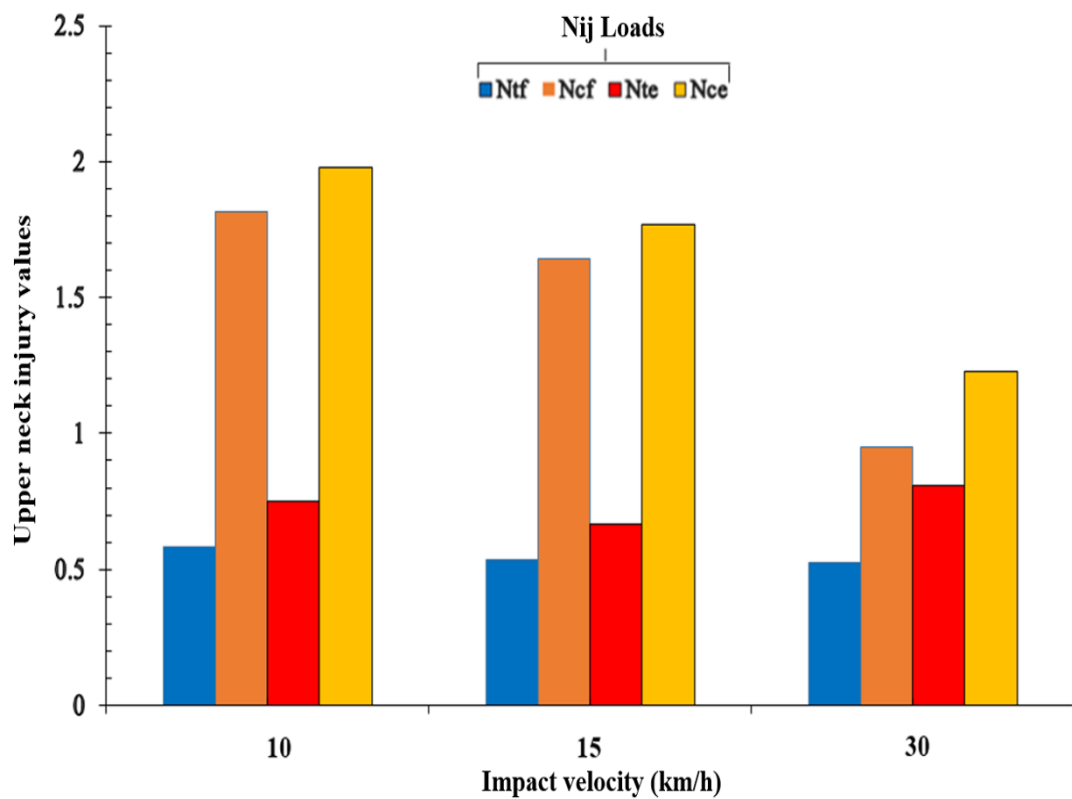


Figure D- 4. Upper neck load conditions of the secondary collisions for adult pedestrian impacted at the vehicle’s centreline in the rear impact position

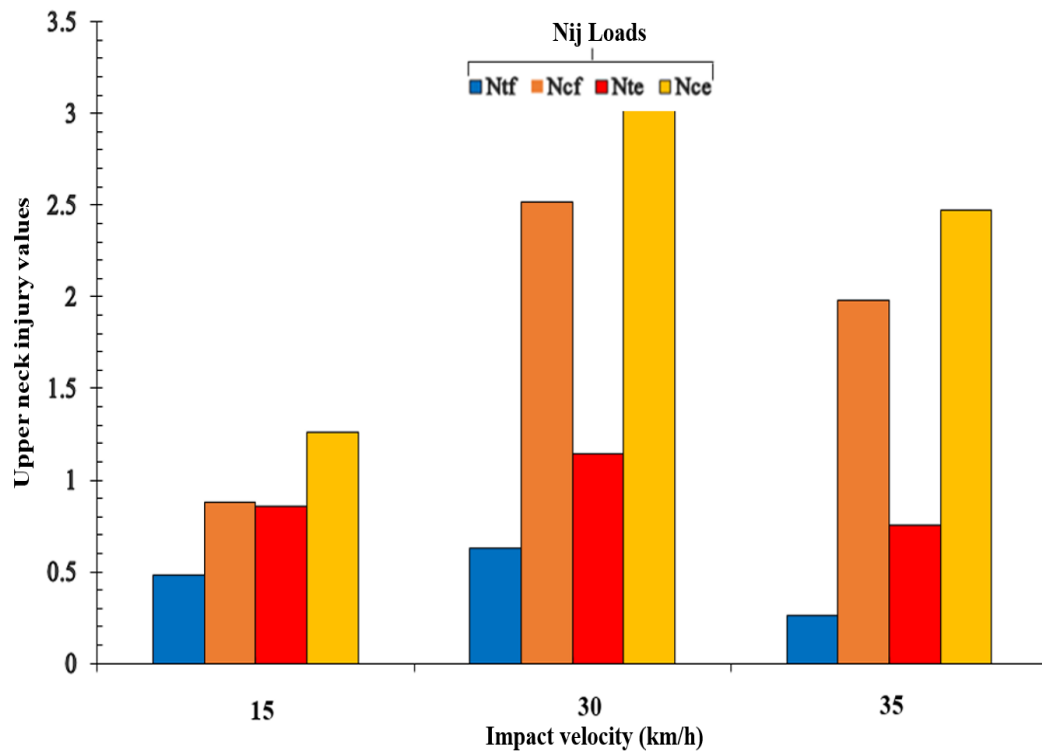


Figure D- 5. Upper neck load conditions of the secondary collisions for adult pedestrian impacted at the vehicle’s centreline in the side impact position

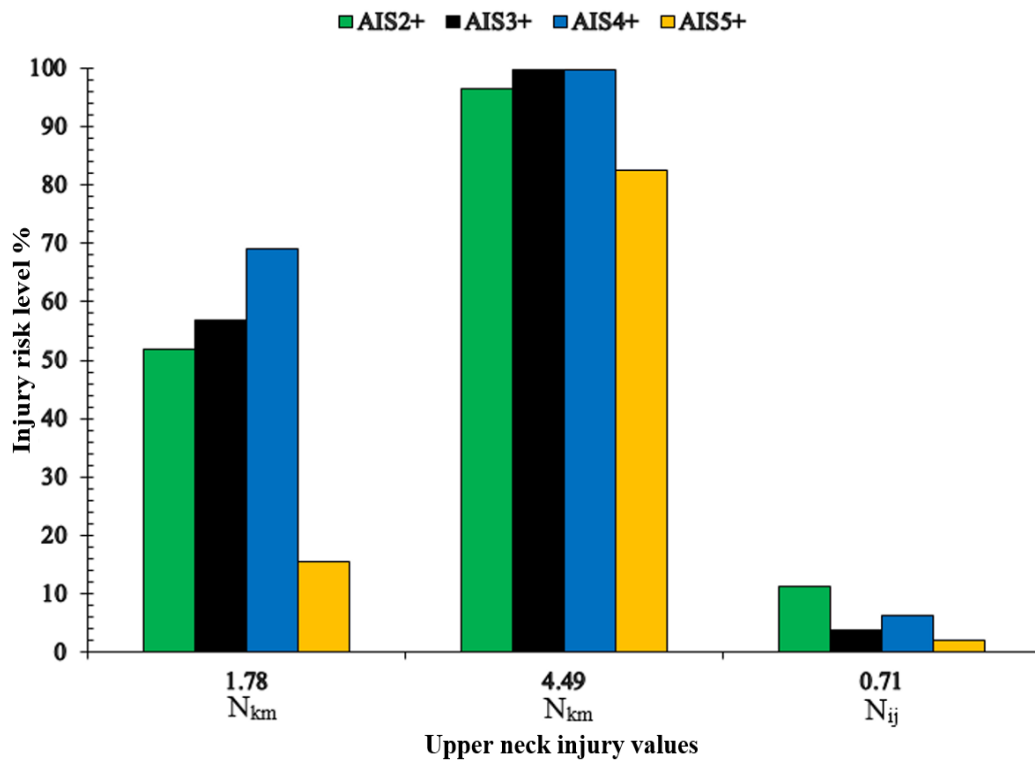


Figure D- 6. Upper neck injury risk against upper neck injury values in secondary impacts for adult pedestrian at the vehicle’s centreline in frontal impact position

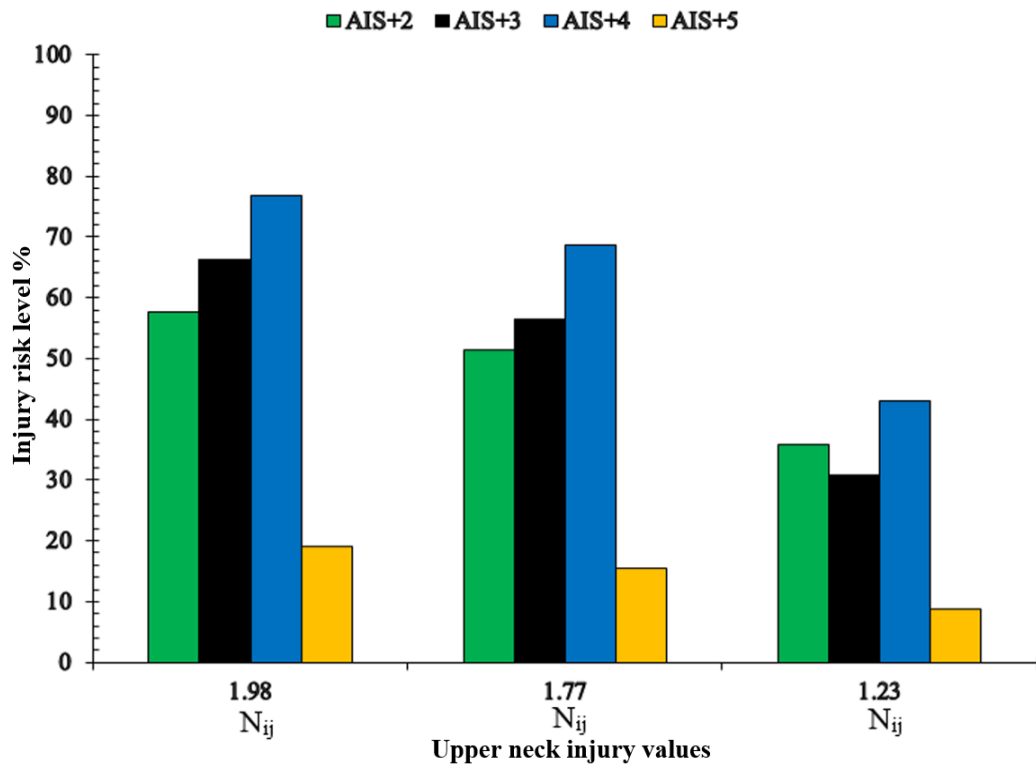


Figure D- 7. Upper neck injury risk against upper neck injury values in secondary impacts for adult pedestrian at the vehicle’s centreline in the rear impact position

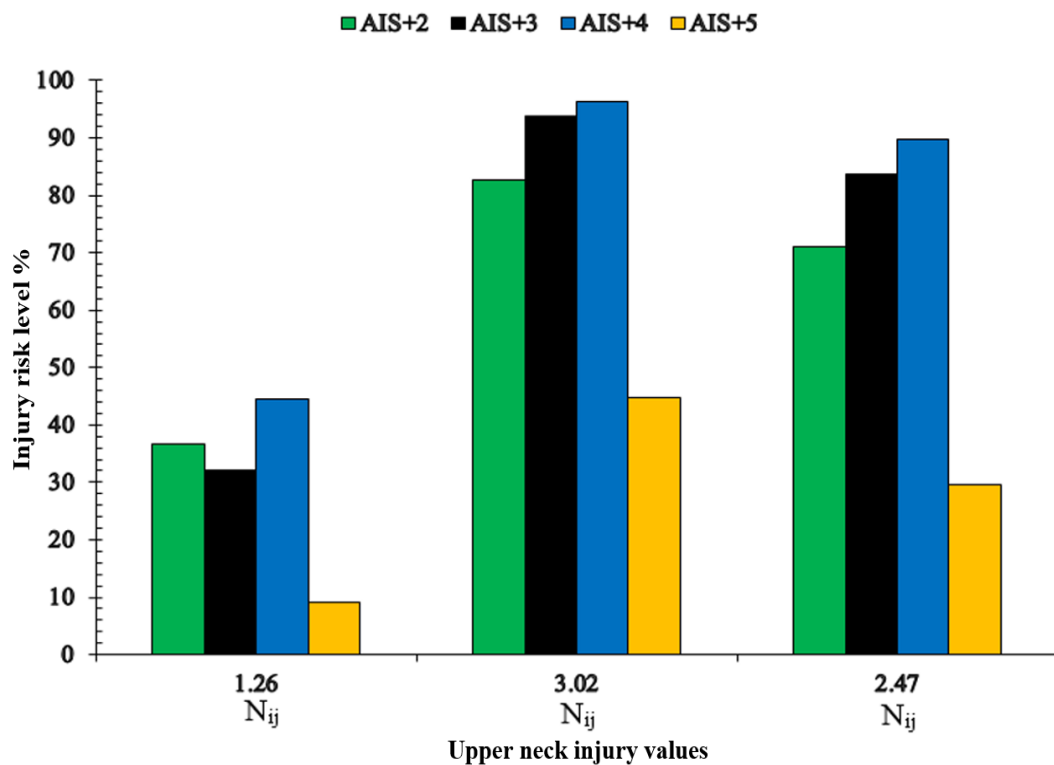


Figure D- 8. Upper neck injury risk against upper neck injury values in secondary impacts for adult pedestrian at the vehicle’s centreline in side impact position

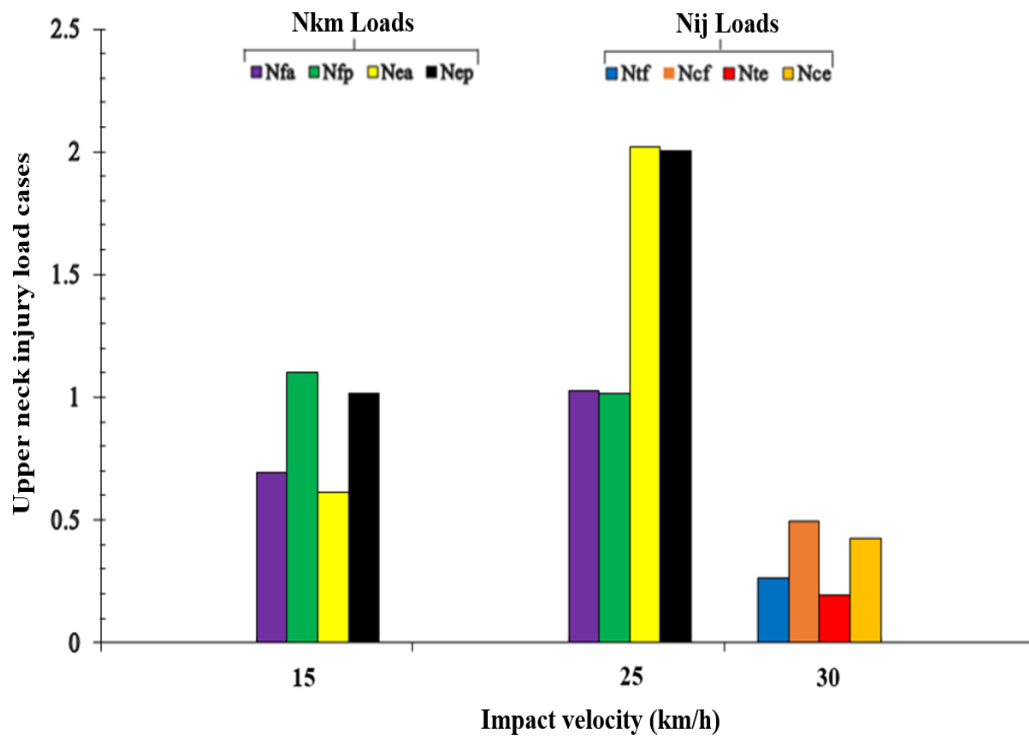


Figure D- 9. Upper neck load conditions of the secondary collisions or adult pedestrian impacted at 42cm offset from the vehicle’s centreline in the rear impact position

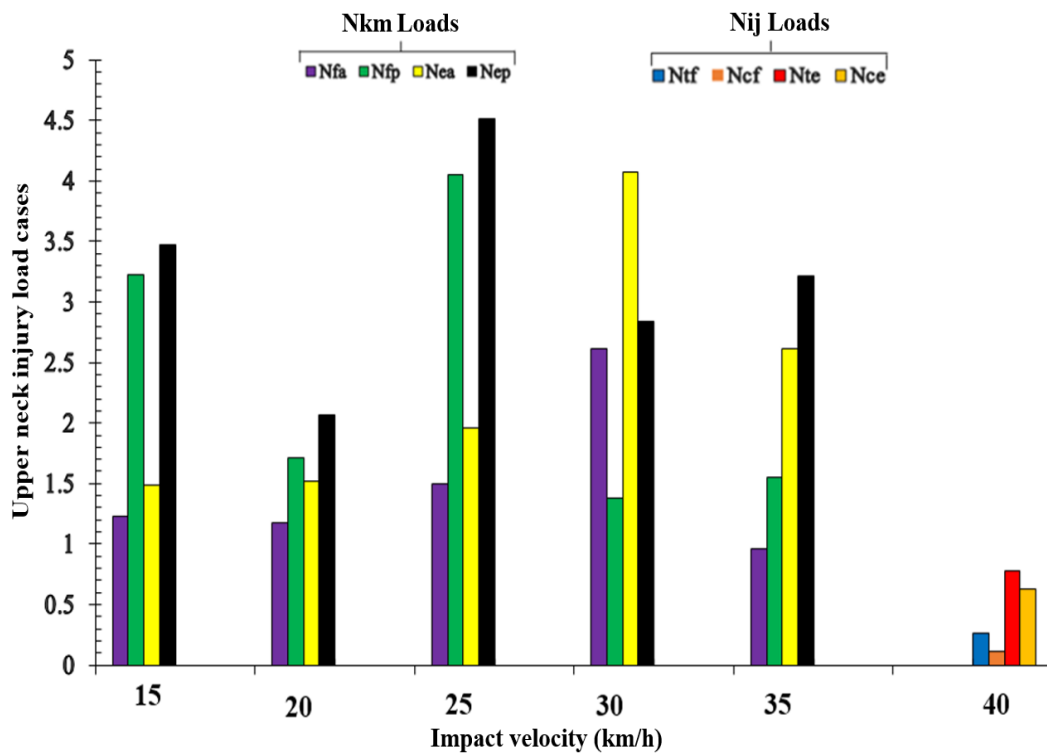


Figure D- 2. Upper neck load conditions of the secondary collisions for adult pedestrian impacted at 42cm offset from the vehicle’s centreline in the side impact position

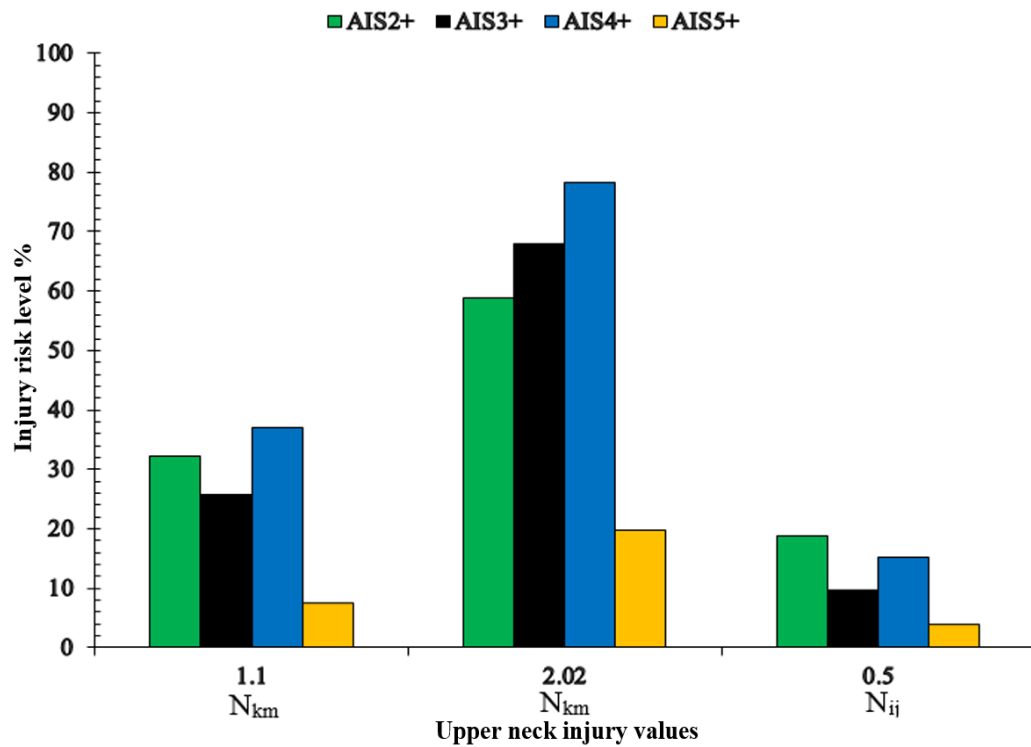


Figure D- 3. Upper neck injury risk against upper neck injury values for adult pedestrian impacts at 42cm offset from the vehicle's centreline in the rear impact position

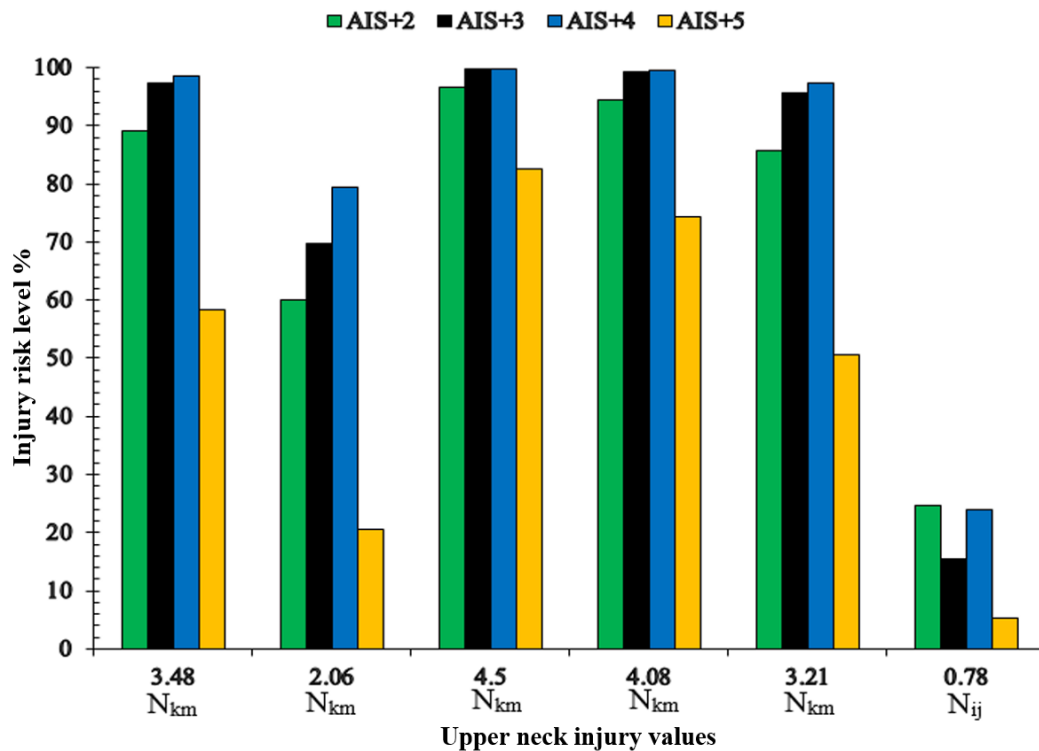


Figure D- 4. Upper neck injury risk against upper neck injury values for adult pedestrian impacts at 42cm offset from the vehicle's centreline in the side impact position

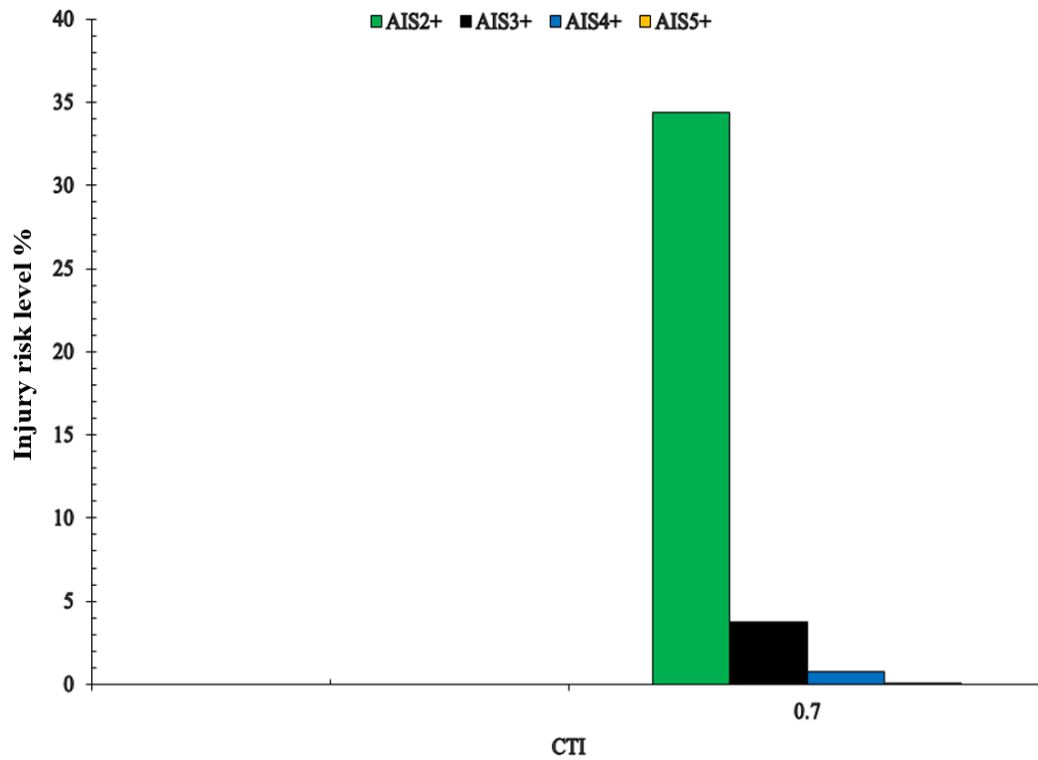


Figure D- 5. Chest injury risk against (CTI) values for adult pedestrian impacts at the vehicle's centreline in the front impact position

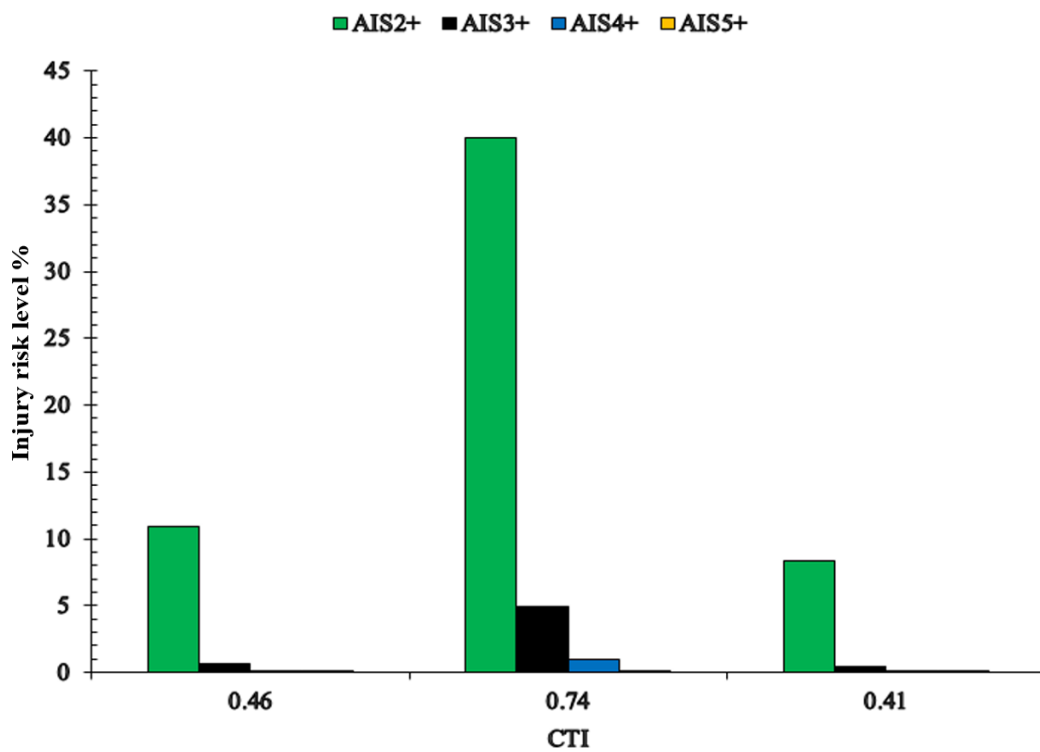


Figure D- 6. Chest injury risk against (CTI) values for adult pedestrian impacts at the vehicle's centreline in the rear impact position

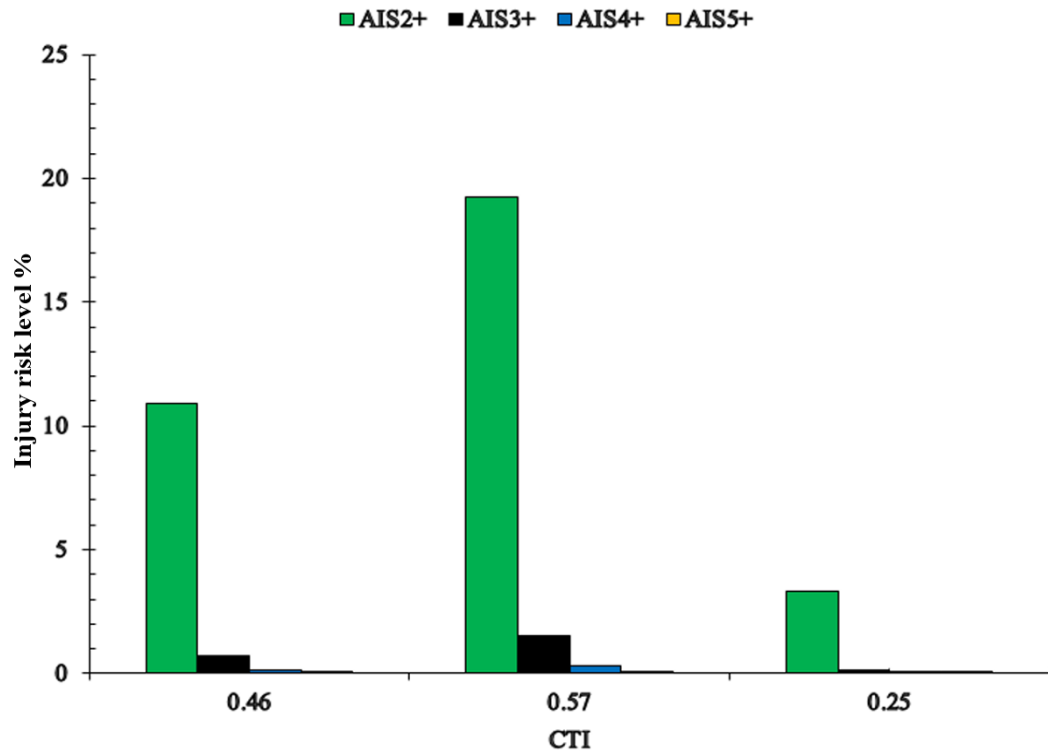


Figure D- 7. Chest injury risk against (CTI) values for adult pedestrian impacts at the vehicle's centreline in the side impact position

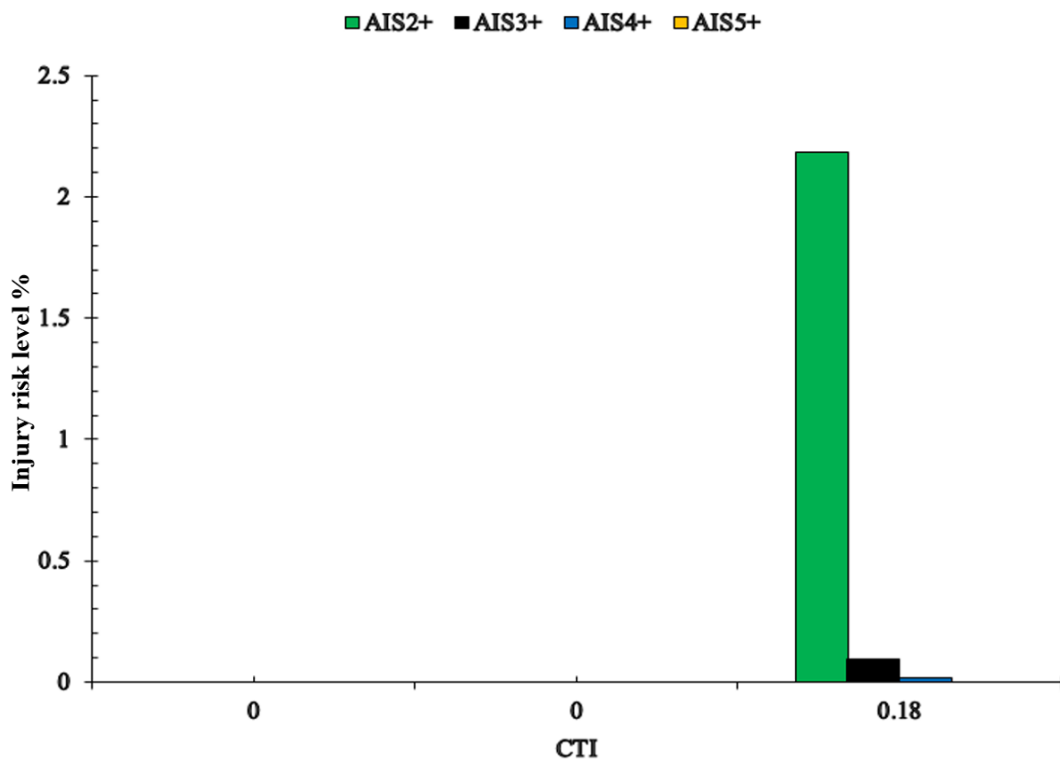


Figure D- 8. Chest injury risk against (CTI) values for adult pedestrian impacts at 42cm offset from the vehicle's centreline in the rear impact position

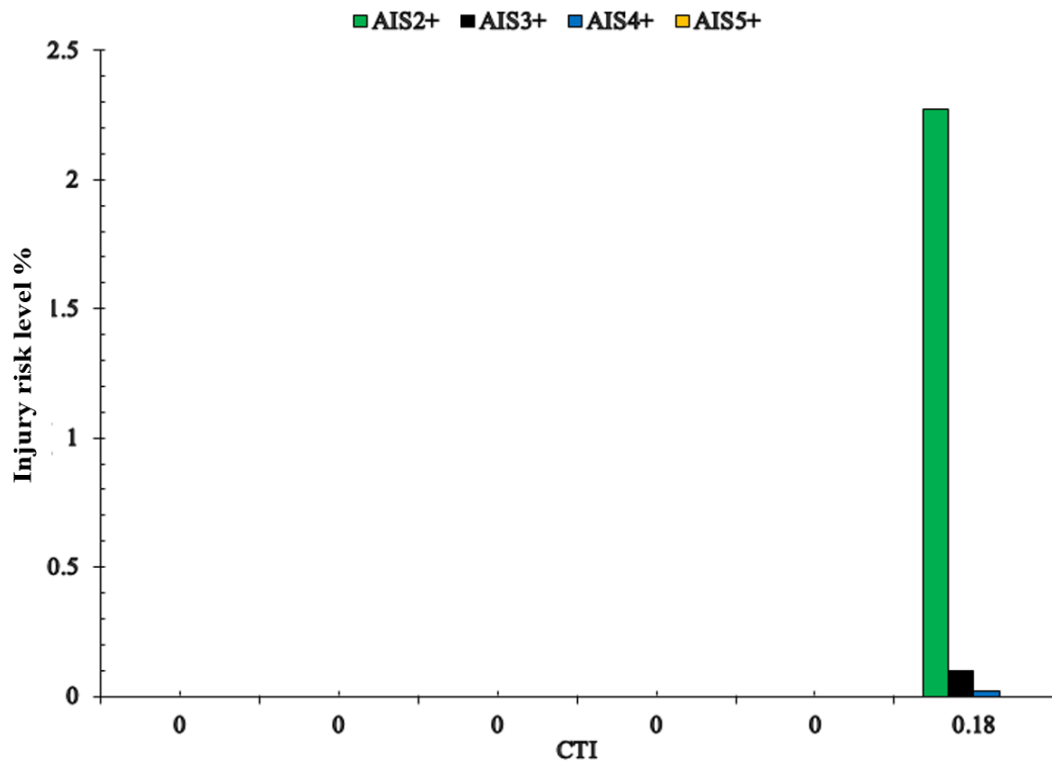


Figure D- 9. Chest injury risk against (CTI) values for adult pedestrian impacts at 42cm offset from the vehicle's centreline in the side impact position

Appendix E.

This section including the compression results for the adult pedestrian during primary and secondary impacts.

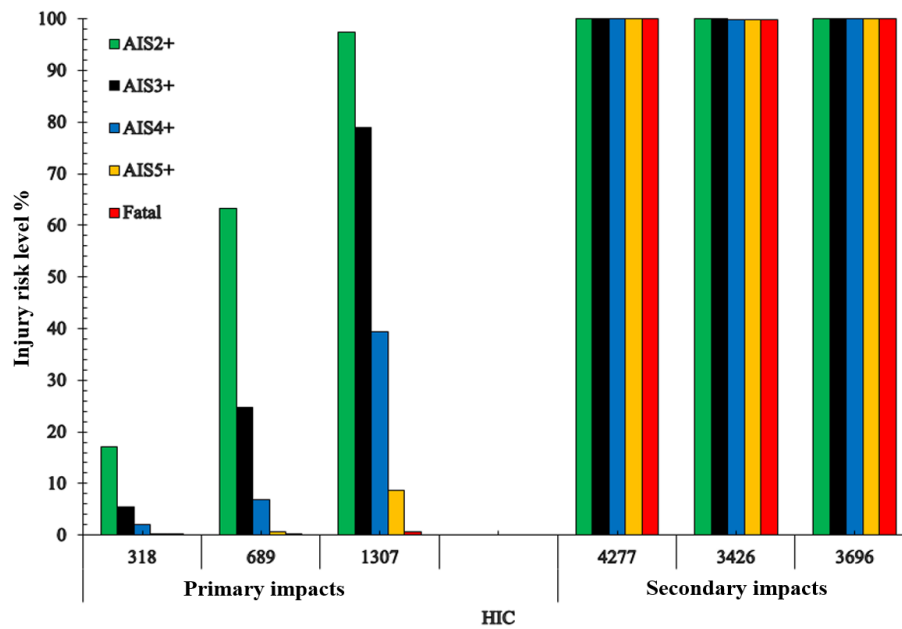


Figure E- 1. Head injury risk against HIC value for adult pedestrian in front impact at the vehicle's centreline in the primary and secondary impacts

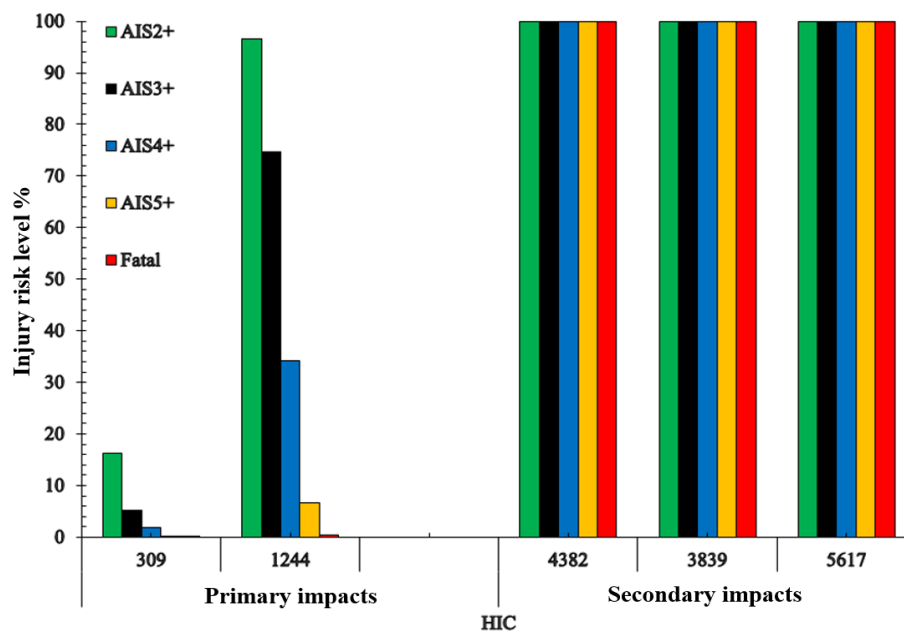


Figure E- 2. Head injury risk against HIC value for adult pedestrian in rear impact at the vehicle's centreline in the primary and secondary impacts

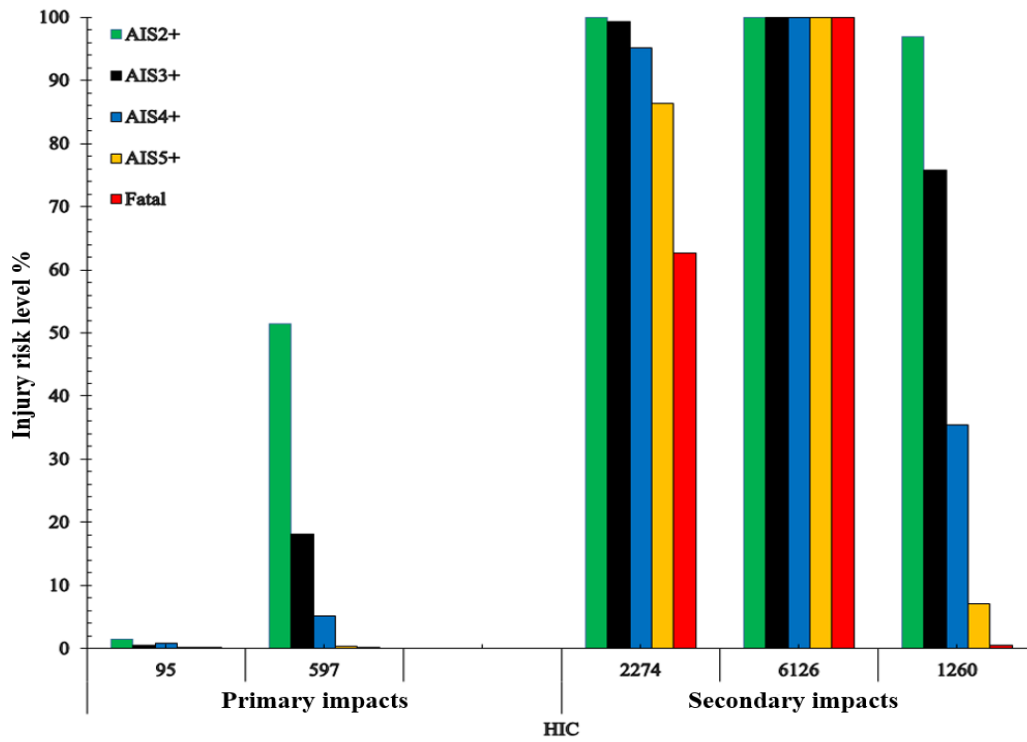


Figure E- 3. Head injury risk against HIC value for adult pedestrian in side impact at the vehicle's centreline in the primary and secondary impacts

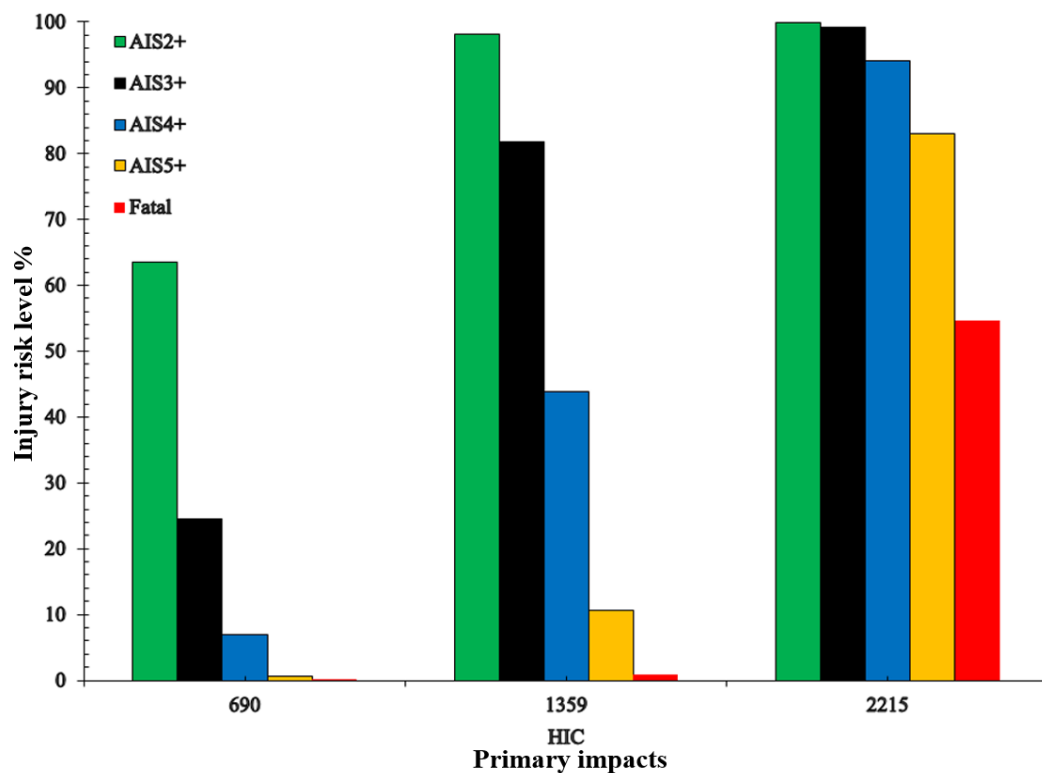


Figure E- 4. Head injury risk against HIC value for adult pedestrian in front impact at 42cm offset from the vehicle's centreline in the primary and secondary impacts

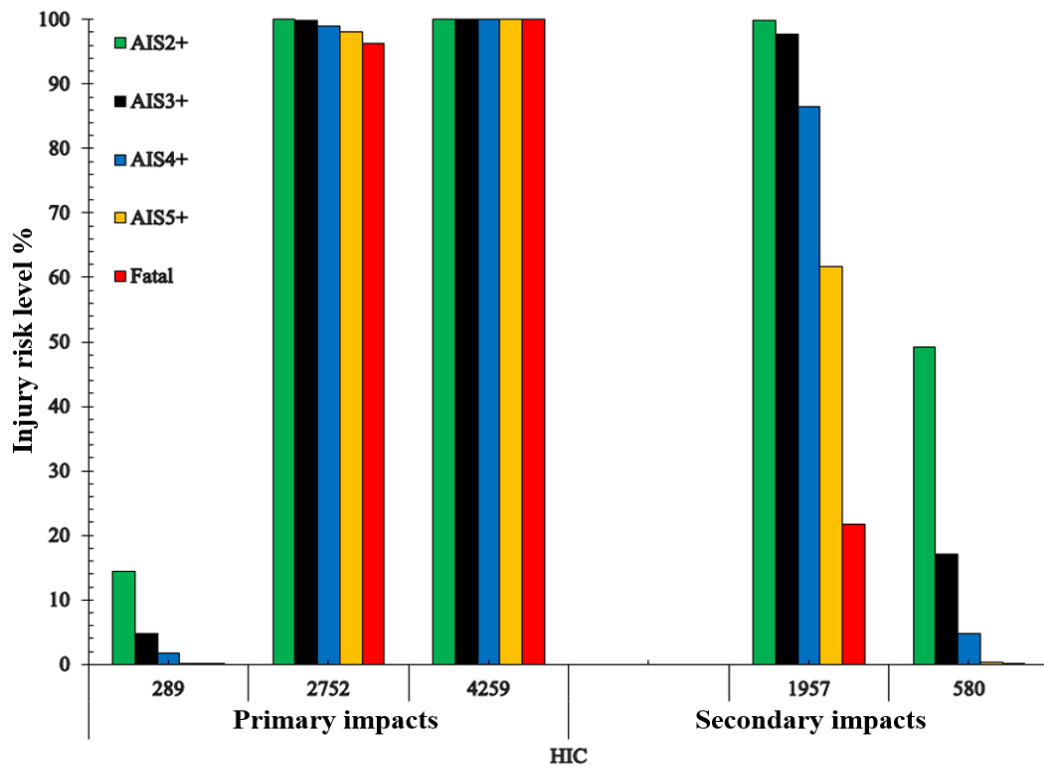


Figure E- 5. Head injury risk against HIC value for adult pedestrian in rear impact at 42cm offset from the vehicle’s centreline in the primary and secondary impacts

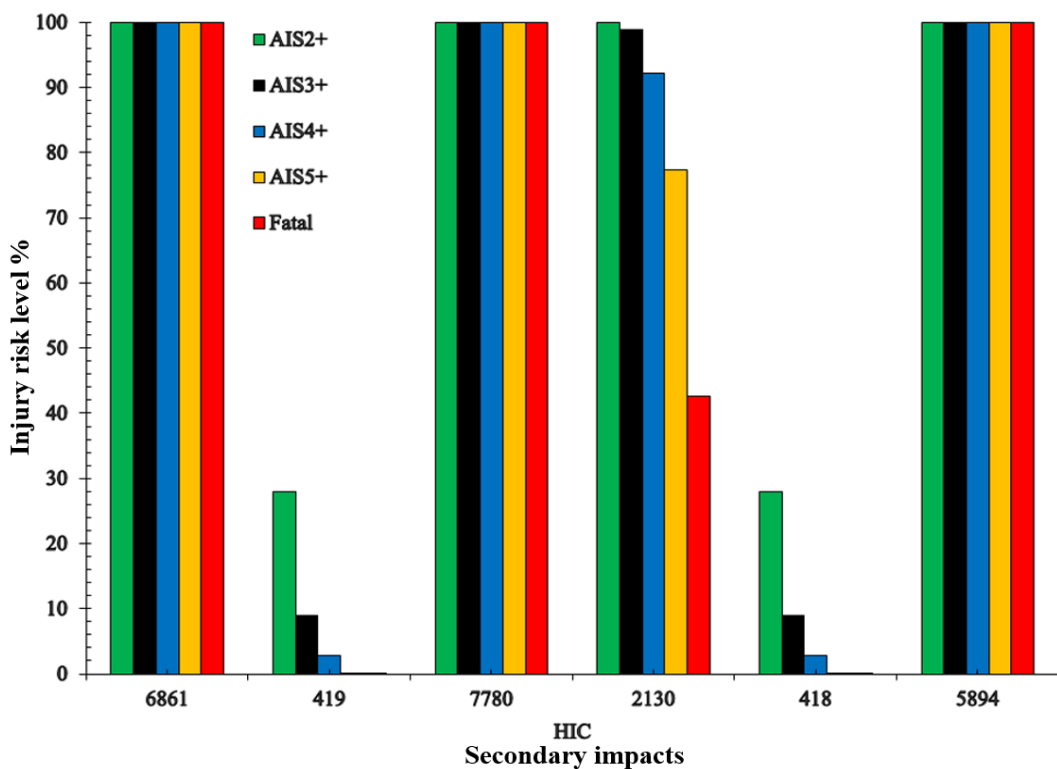


Figure E- 6. Head injury risk against HIC value for adult pedestrian in side impact at 42cm offset from the vehicle’s centreline in the primary and secondary impacts

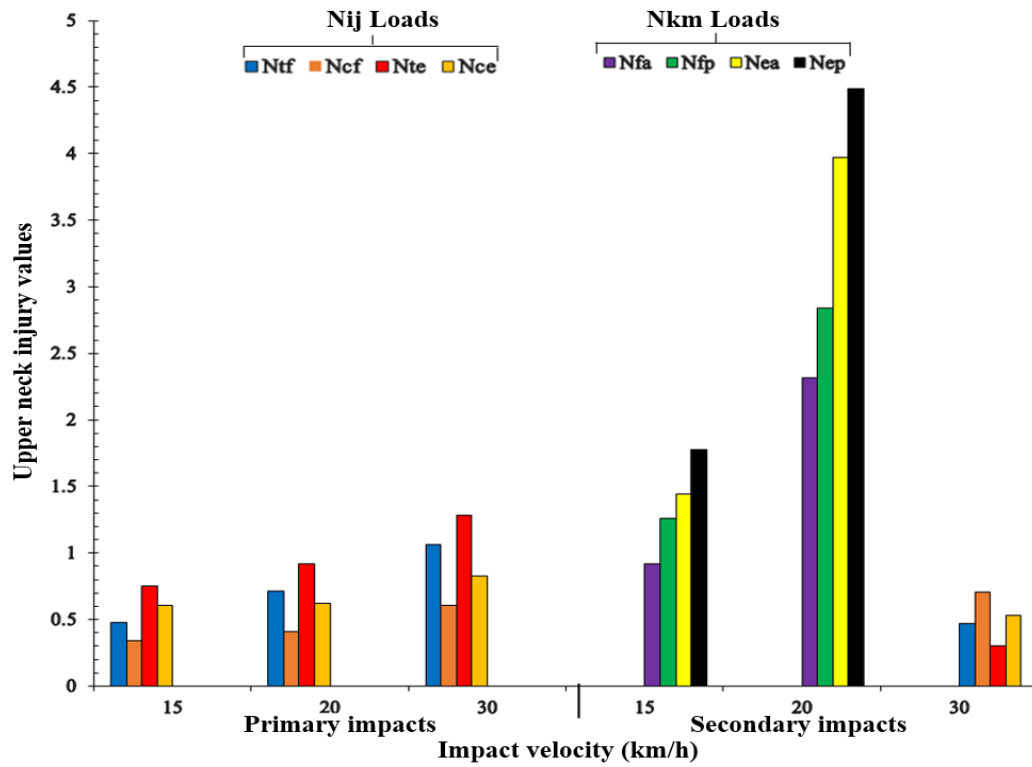


Figure E- 7. Upper neck load conditions for adult pedestrian in front impact at the vehicle’s centreline in primary and secondary collisions

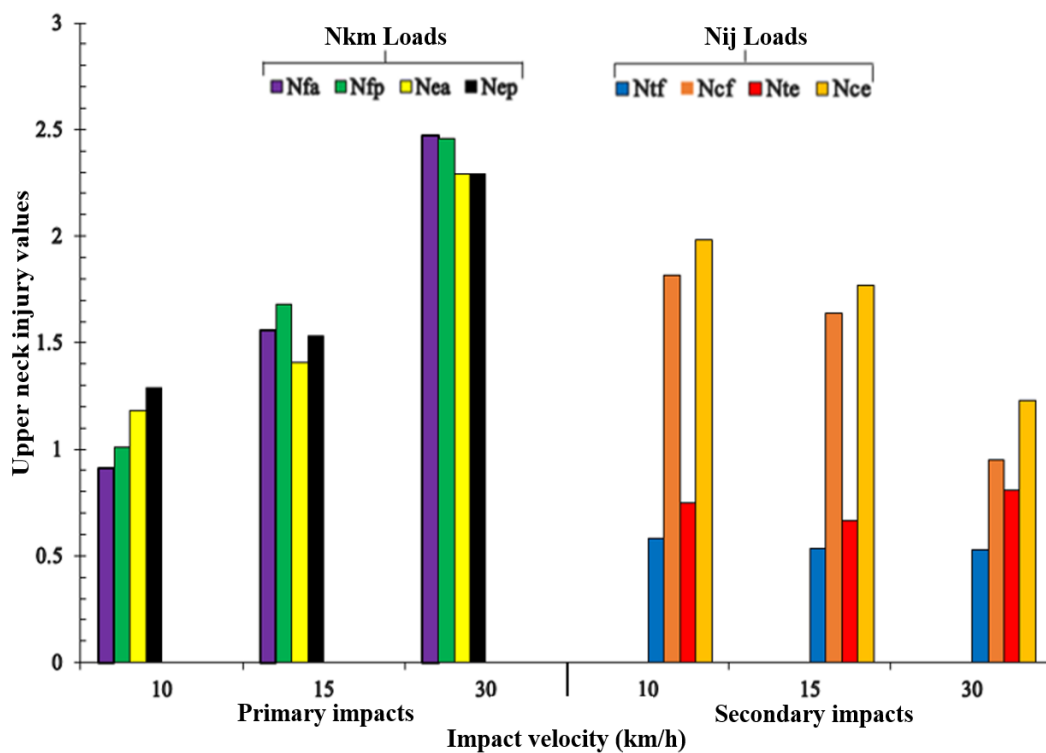


Figure E- 8. Upper neck load conditions for adult pedestrian in rear impact at the vehicle’s centreline in primary and secondary collisions

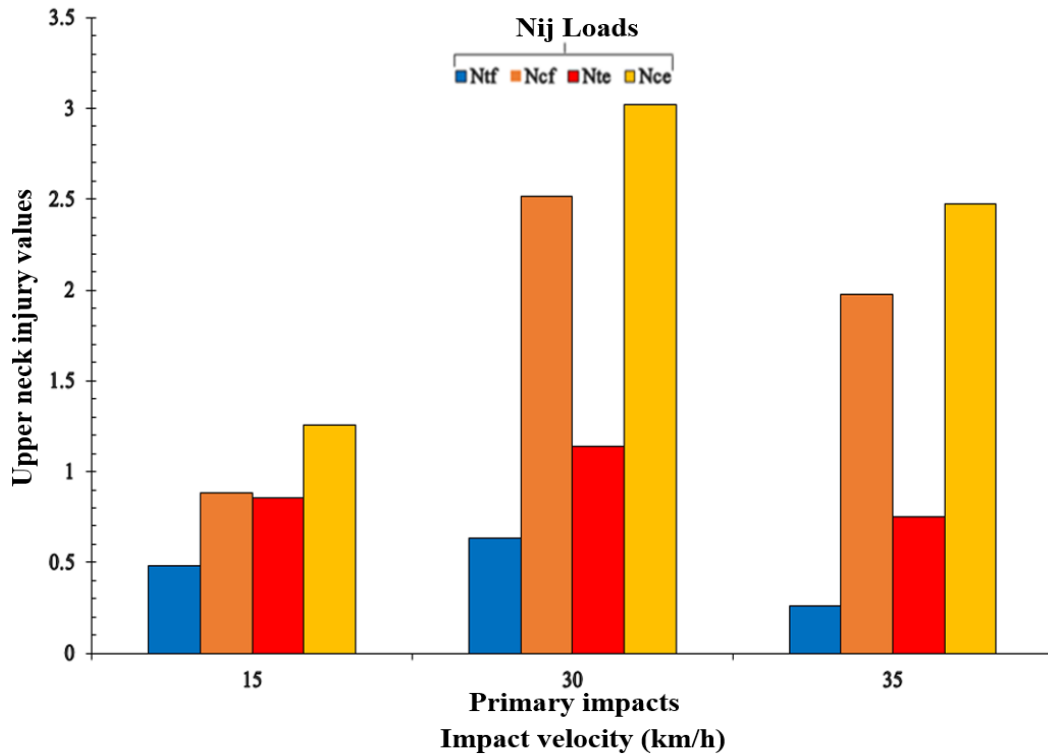


Figure E- 9. Upper neck load conditions for adult pedestrian in side impact at the vehicle’s centreline in primary and secondary collisions

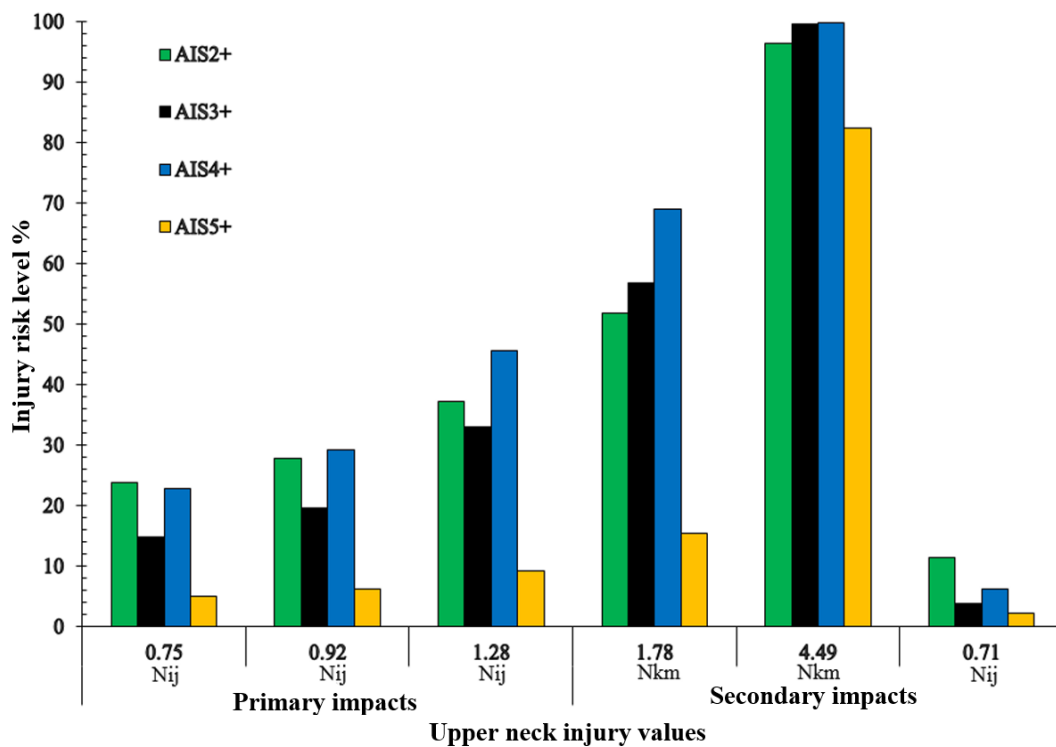


Figure E- 10. Upper neck injury risk against Nij and Nkm values in the primary and secondary collisions in front impact at the vehicle’s centreline

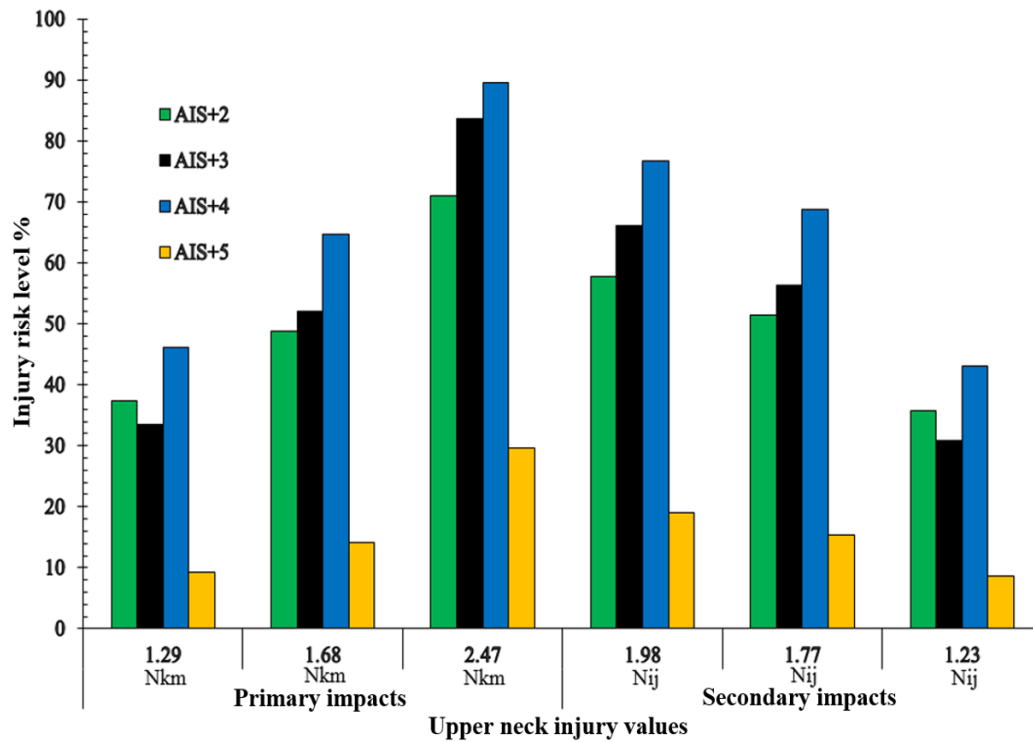


Figure E- 11. Upper neck injury risk against Nij and Nkm values in the primary and secondary collisions in rear impact at the vehicle's centreline

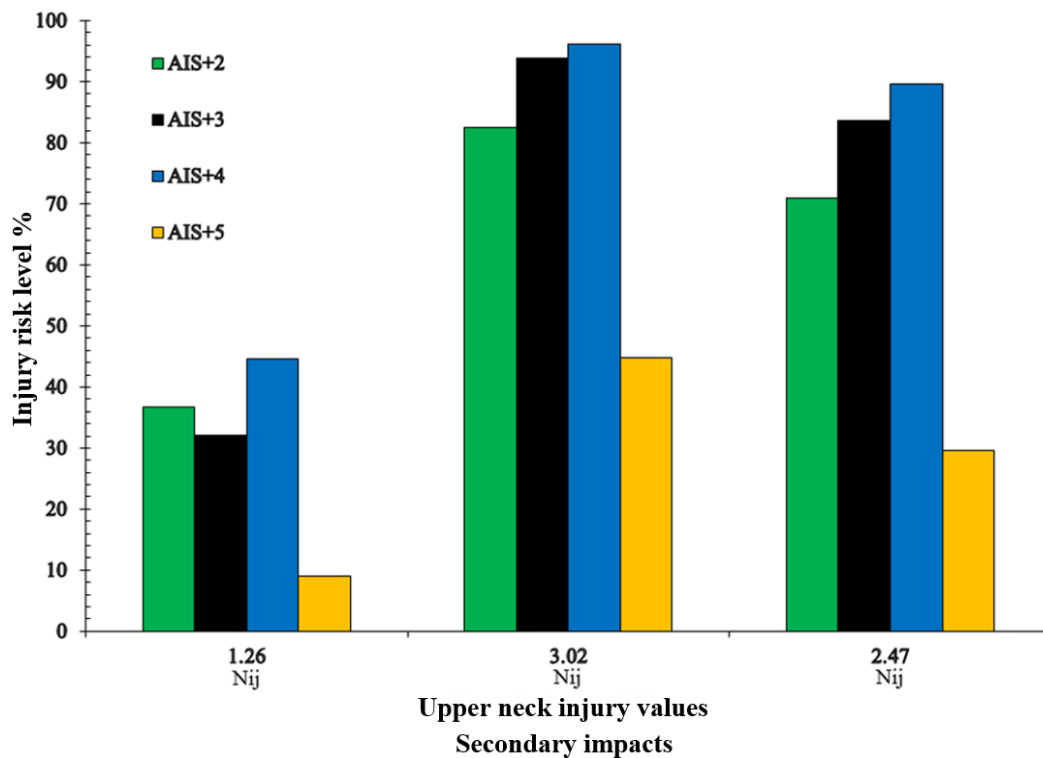


Figure E- 12. Upper neck injury risk against Nij and Nkm values in the primary and secondary collisions in side impact at the vehicle's centreline

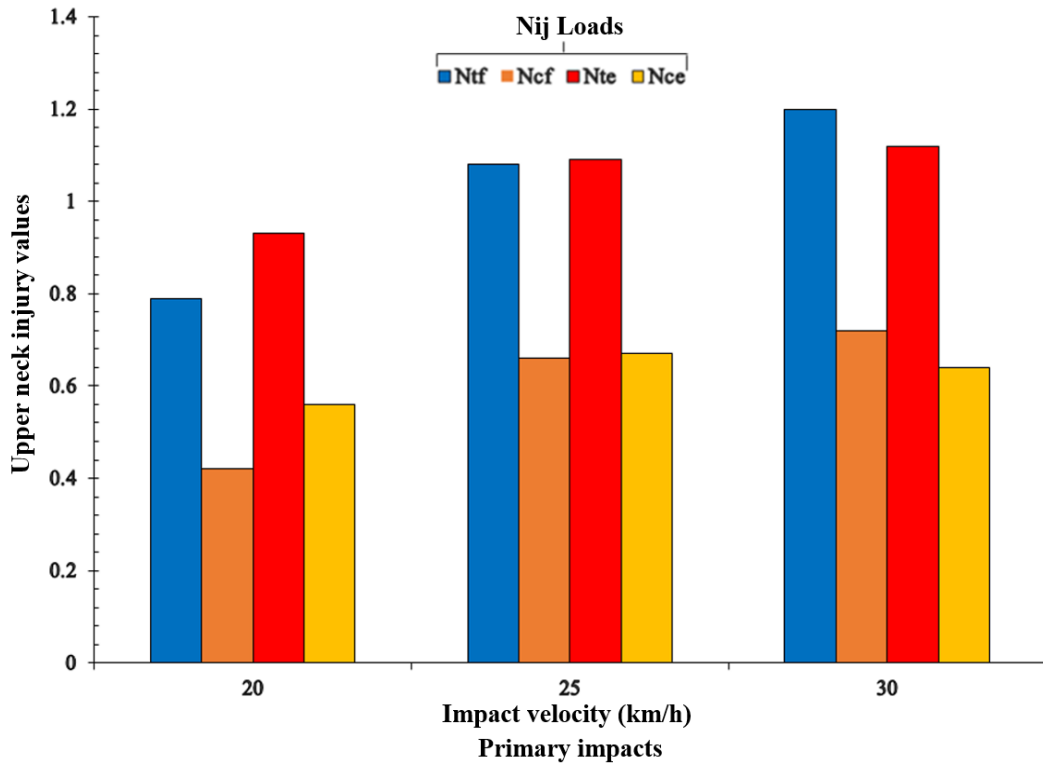


Figure E- 13. Upper neck load conditions for adult pedestrian in front impact at 42cm offset from the vehicle’s centreline in primary and secondary collisions

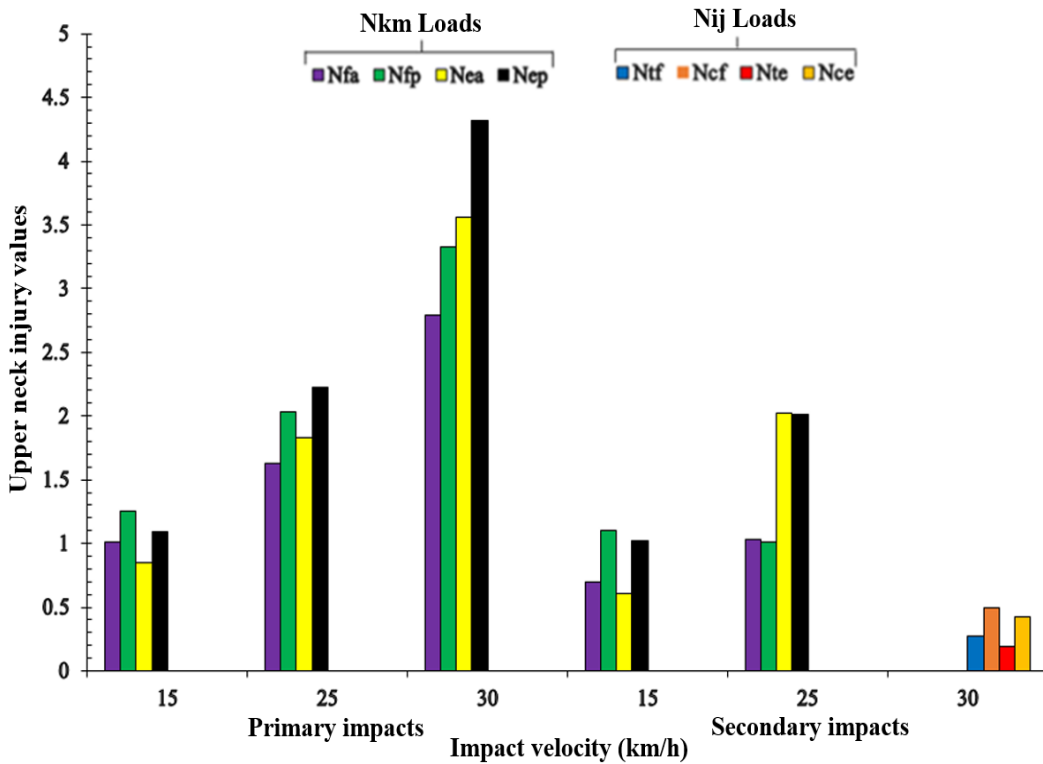


Figure E- 14. Upper neck load conditions for adult pedestrian in rear impact at 42cm offset from the vehicle’s centreline in primary and secondary collisions

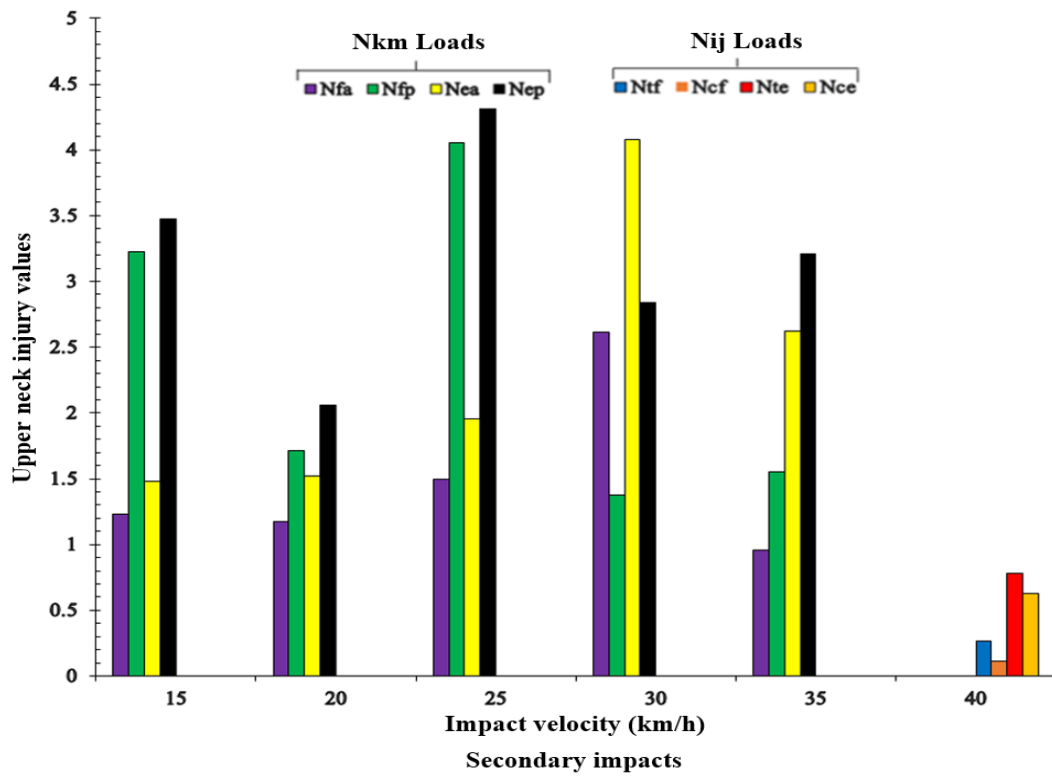


Figure E- 15. Upper neck load conditions for adult pedestrian in side impact at 42cm offset from the vehicle’s centreline in primary and secondary collisions

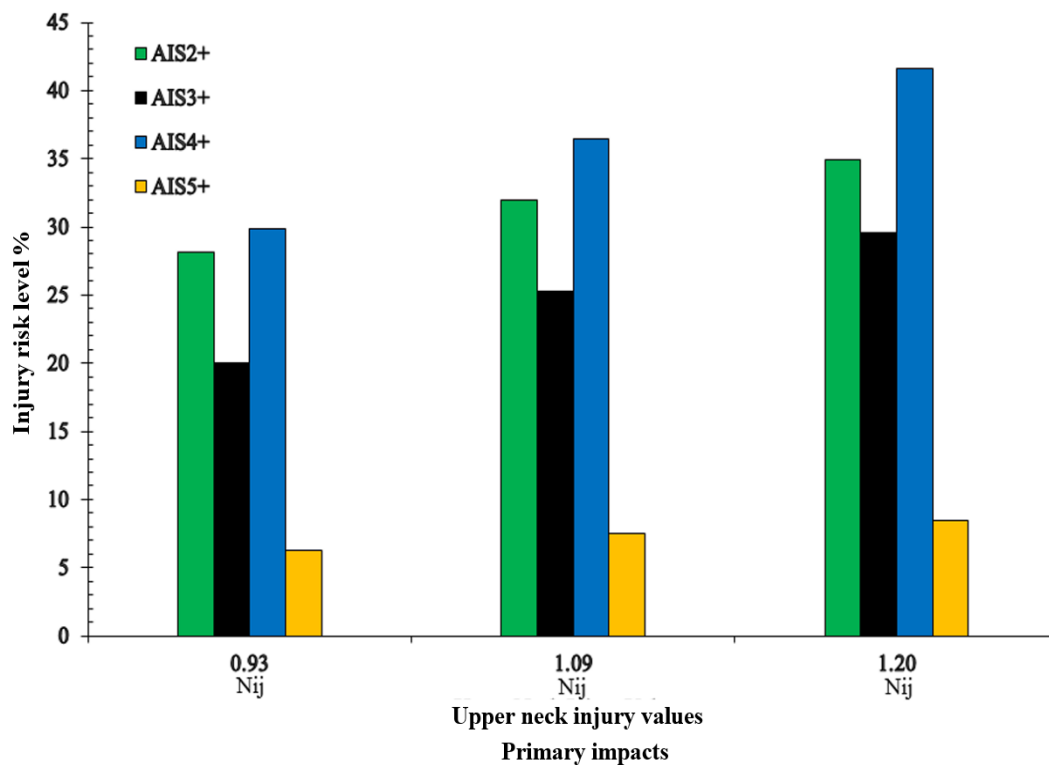


Figure E- 16. Upper neck injury risk against Nij and Nkm values in in front impact at 42cm offset from the vehicle’s centreline in primary and secondary impacts

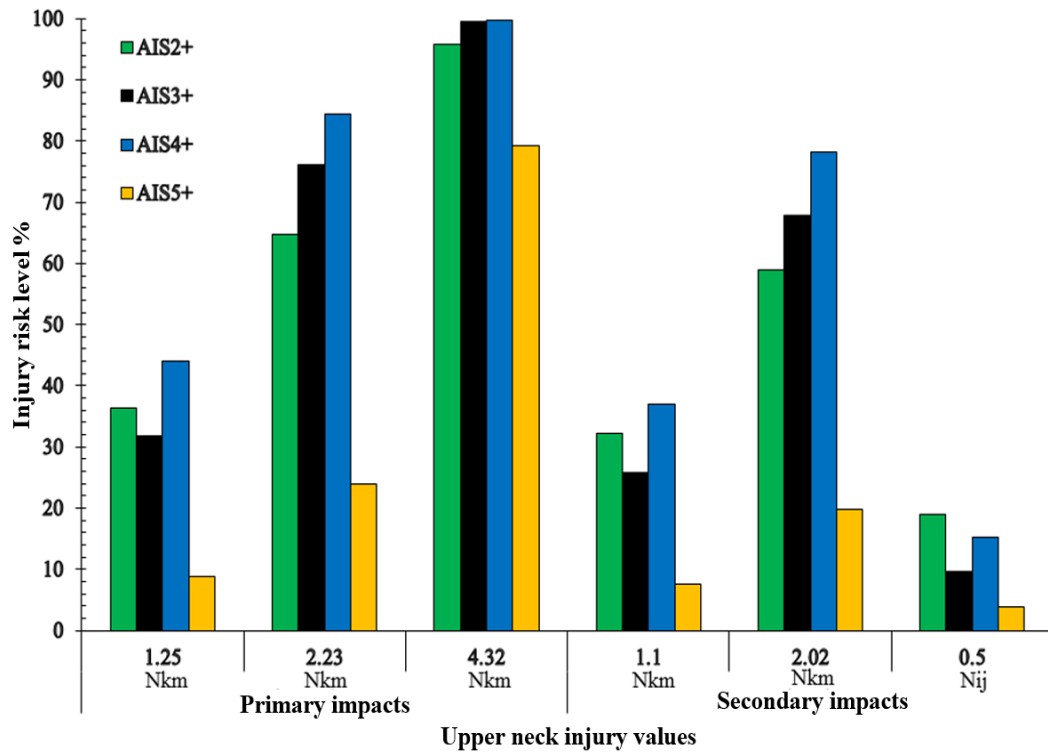


Figure E- 17. Upper neck injury risk against Nij and Nkm values in in rear impact at 42cm offset from the vehicle’s centreline in primary and secondary impacts

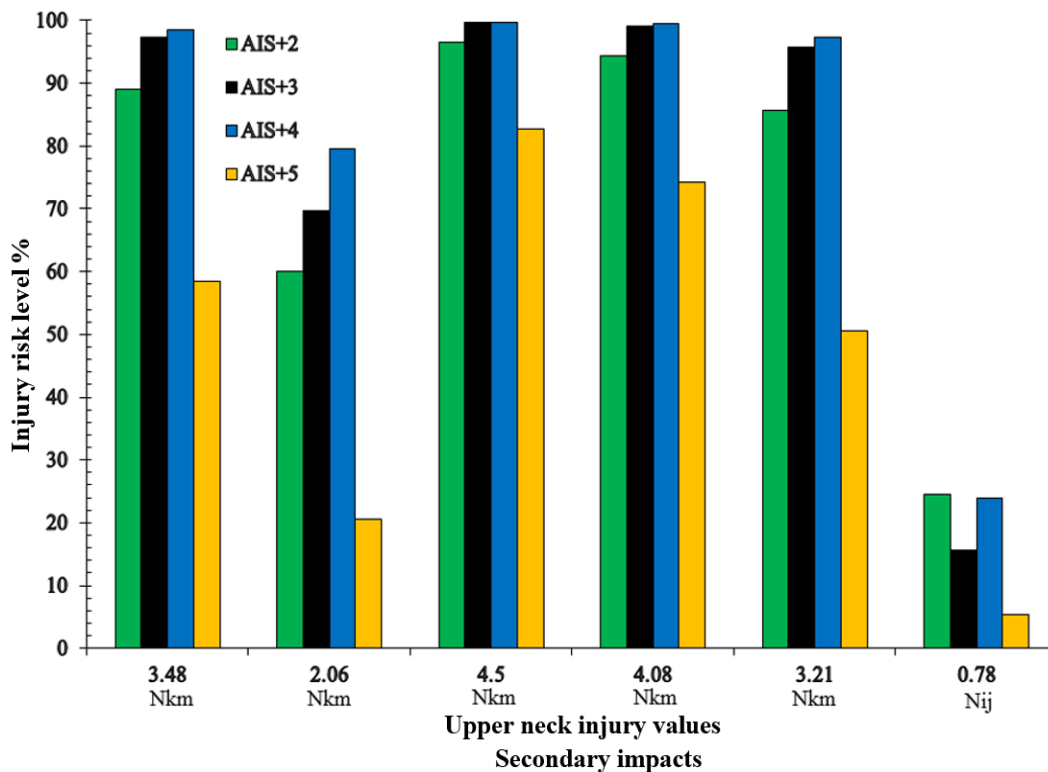


Figure E- 18. Upper neck injury risk against Nij and Nkm values in in side impact at 42cm offset from the vehicle’s centreline in primary and secondary impacts

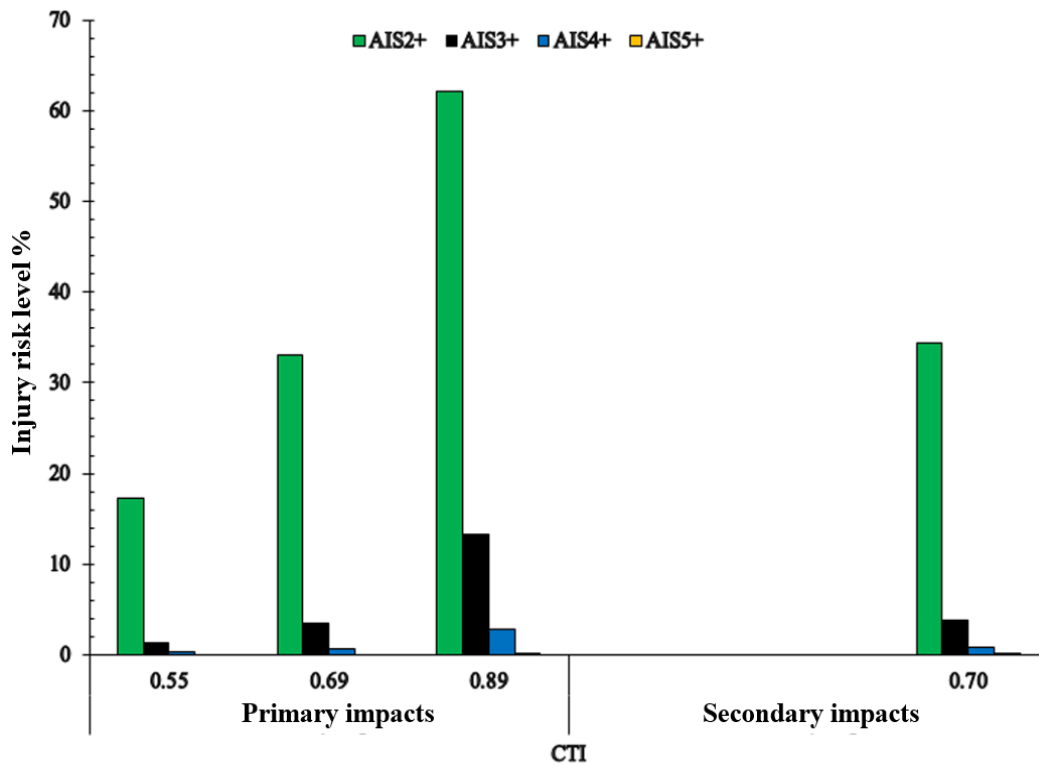


Figure E- 19. Chest injury risk against CTI values in front impact at the vehicle’s centreline in primary and secondary impacts

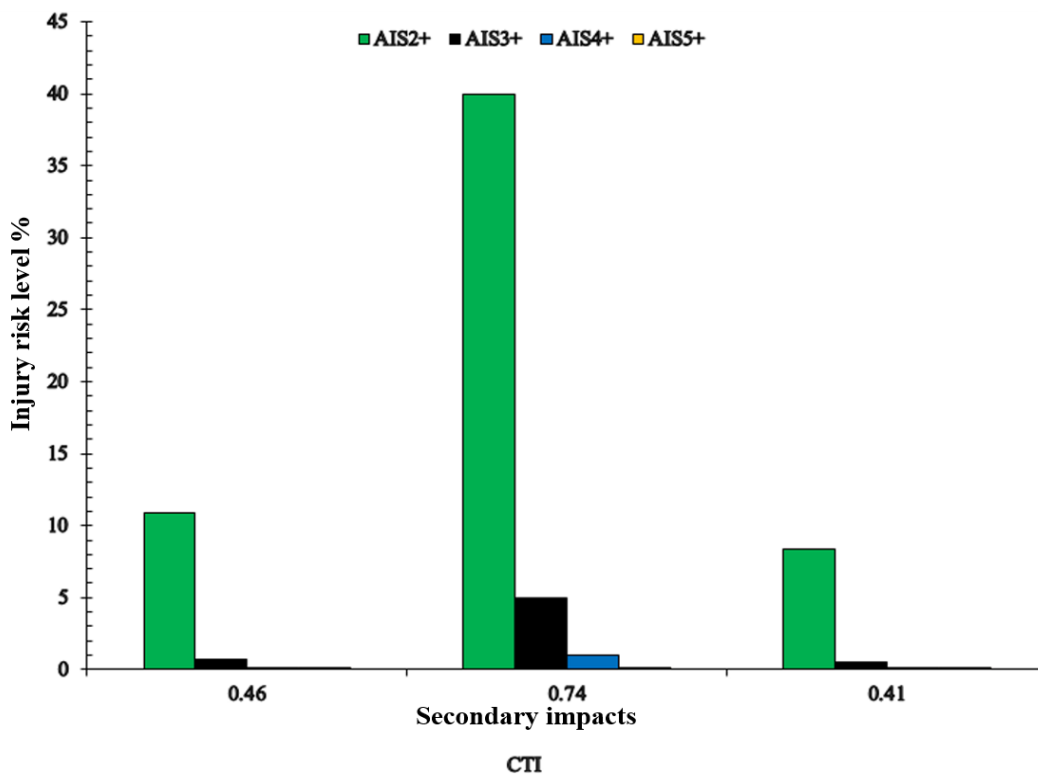


Figure E- 20. Chest injury risk against CTI values in rear impact at the vehicle’s centreline in primary and secondary impacts

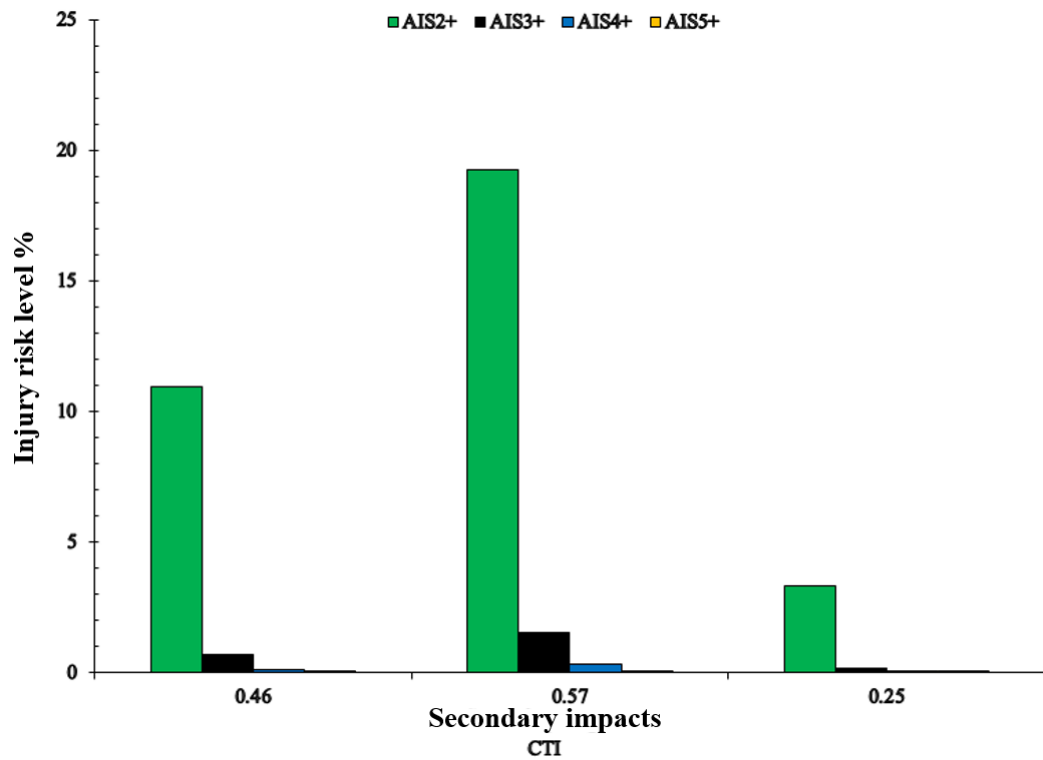


Figure E- 21. Chest injury risk against CTI values in side impact at the vehicle’s centreline in primary and secondary impacts

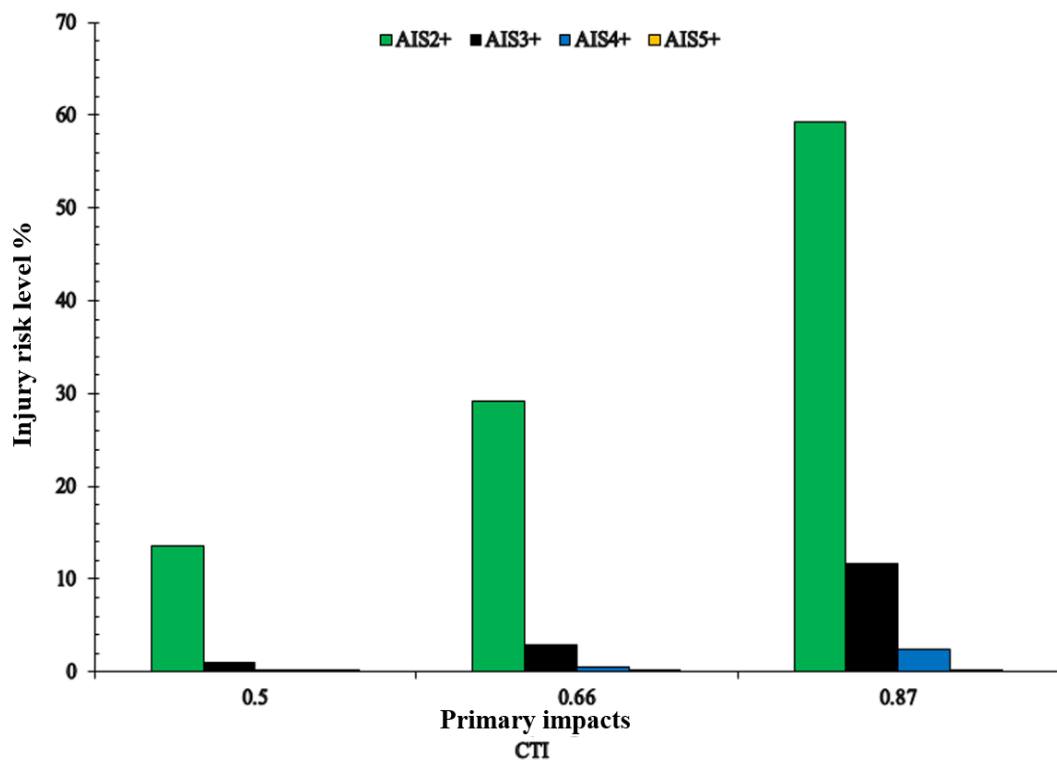


Figure E- 22. Chest injury risk against CTI values in front impact at 42cm offset from the vehicle’s centreline in primary and secondary impacts

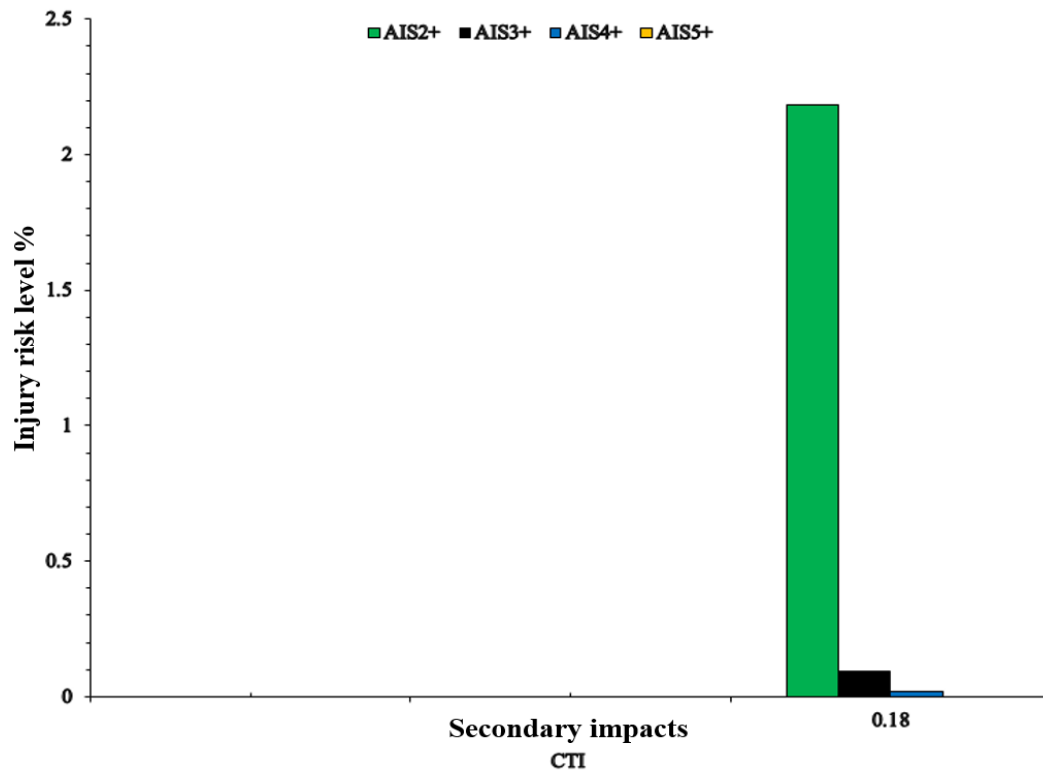


Figure E- 23. Chest injury risk against CTI values in rear impact at 42cm offset from the vehicle's centreline in primary and secondary impacts

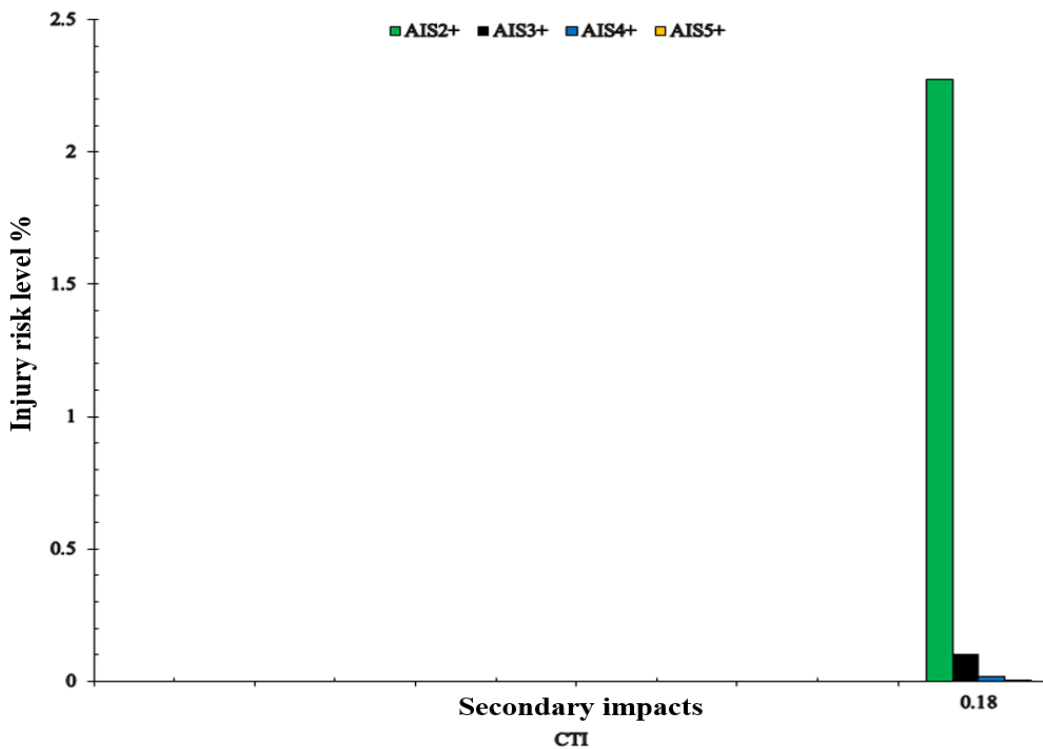


Figure E- 24. Chest injury risk against CTI values in side impact at 42cm offset from the vehicle's centreline in primary and secondary impacts

Appendix F.

This section including the results for the modified auto rickshaw-adult pedestrian impacts.

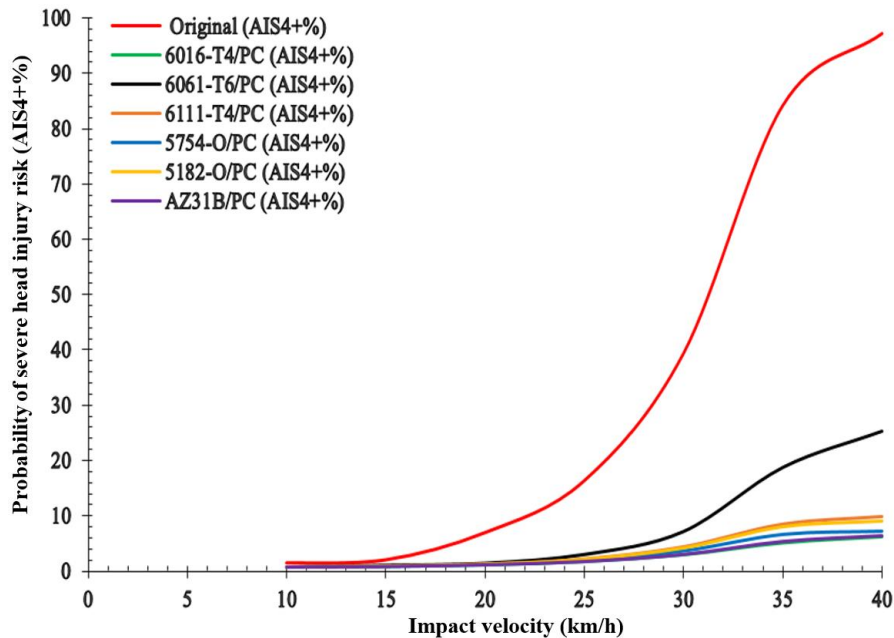


Figure F- 1. Impact Velocity against Probability of Severe Head Injury Risk (AIS4+) for Adult Pedestrian in frontal impact at the vehicle's centreline

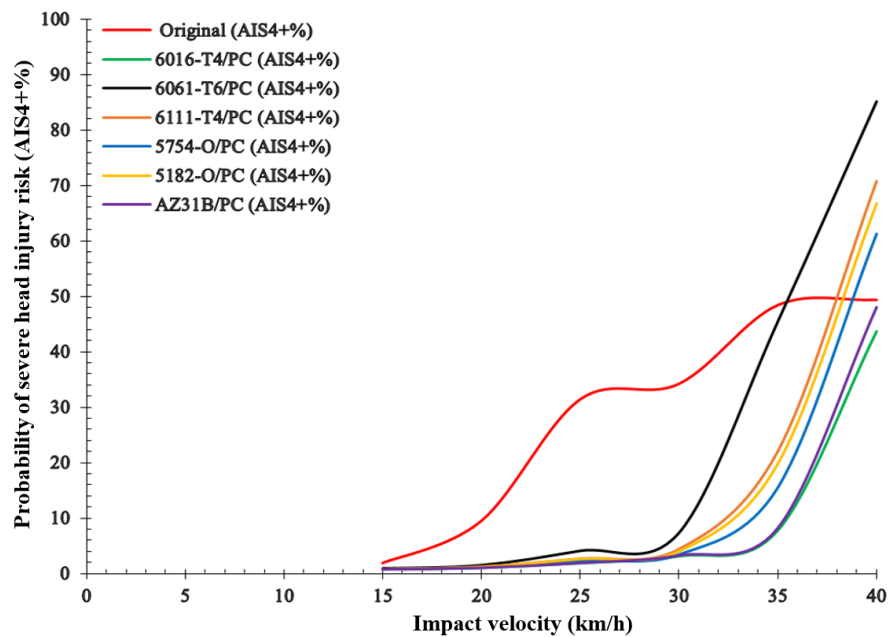


Figure F- 2. Impact Velocity against Probability of Severe Head Injury Risk (AIS4+) for Adult Pedestrian in rear impact at the vehicle's centreline

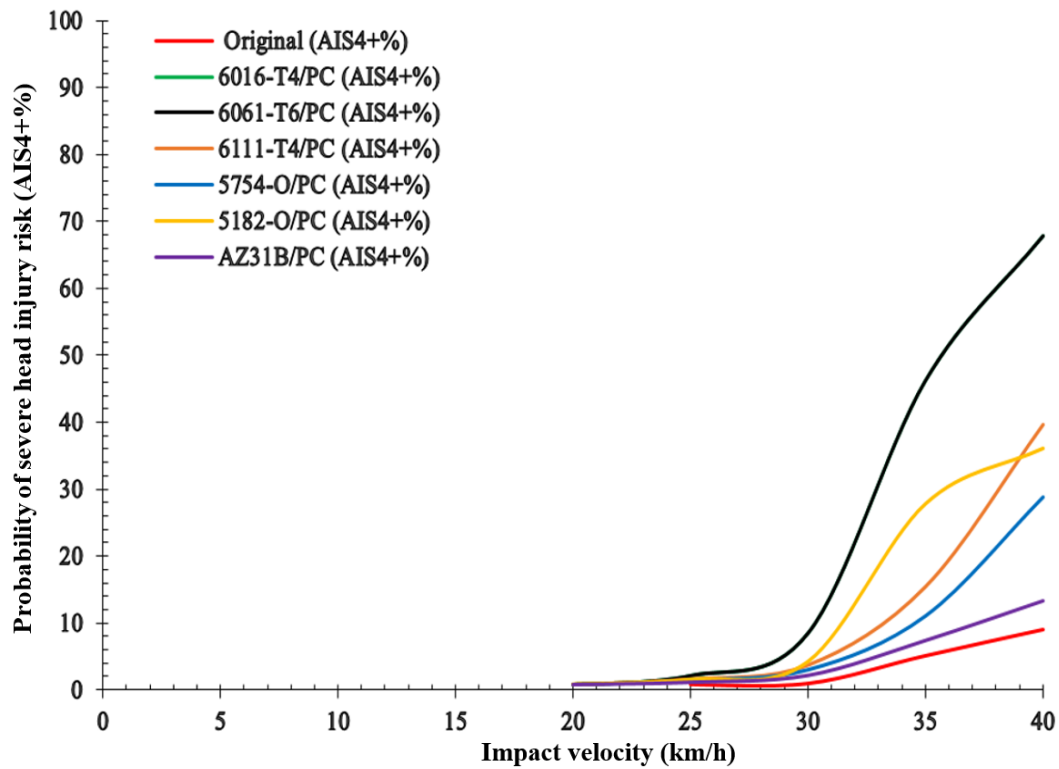


Figure F- 3. Impact Velocity against Probability of Severe Head Injury Risk (AIS4+) for Adult Pedestrian in side impact at the vehicle’s centreline

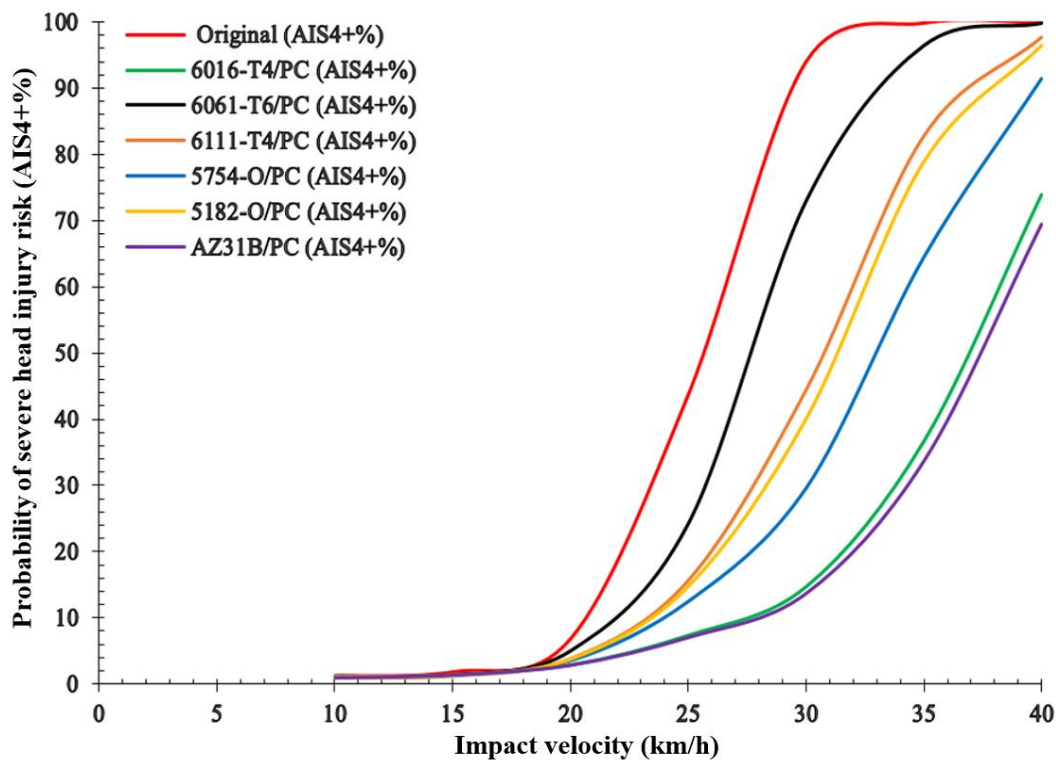


Figure F- 4. Impact Velocity against Probability of Severe Head Injury Risk (AIS4+) for Adult Pedestrian in front impact at 42cm offset from the vehicle’s centreline

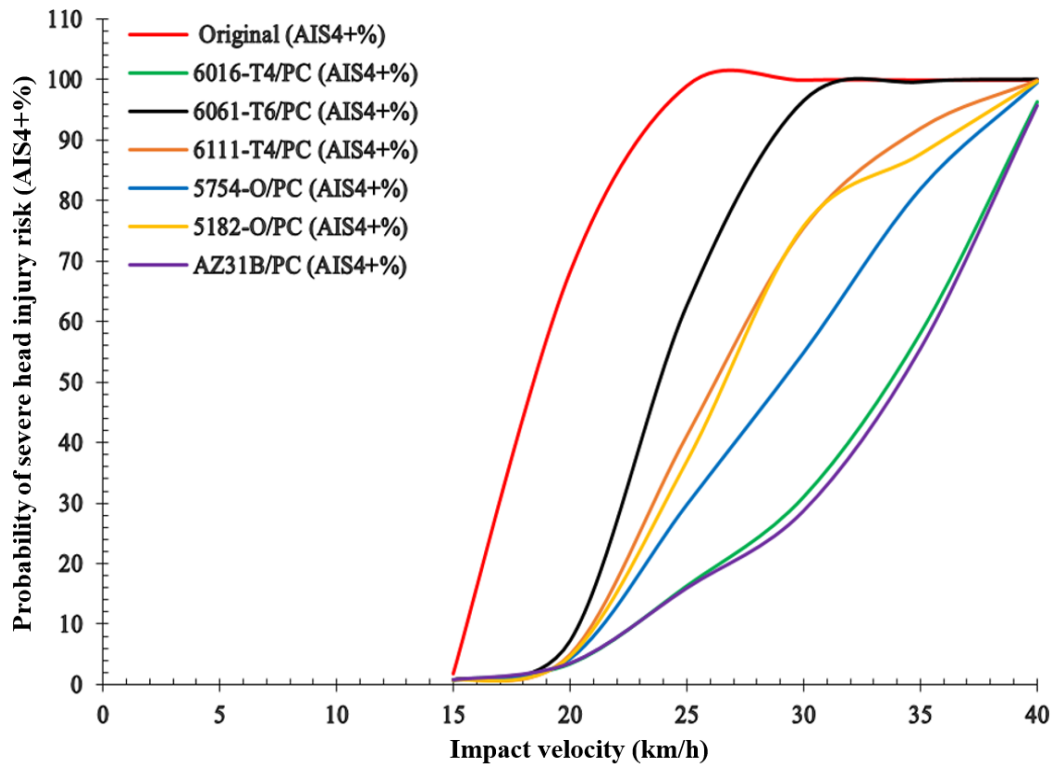


Figure F- 5. Impact Velocity against Probability of Severe Head Injury Risk (AIS4+) for Adult Pedestrian in rear impact at 42cm offset from the vehicle's centreline

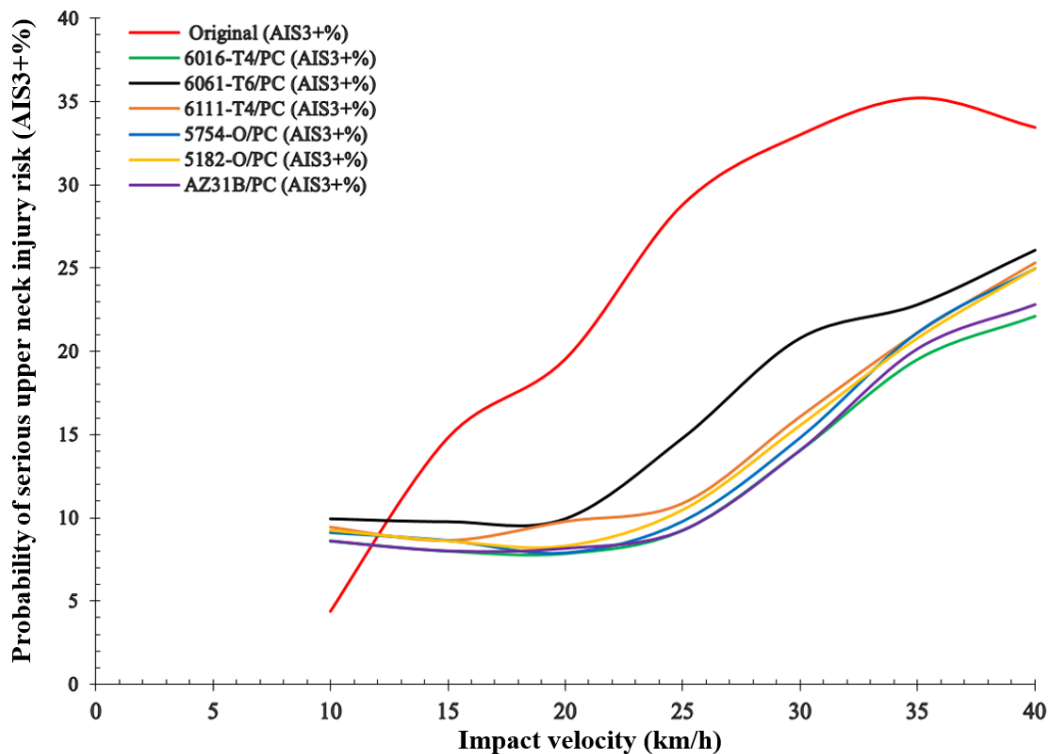


Figure F- 6. Impact Velocity against Probability of Serious Upper neck Injury Risk (AIS3+) for Adult Pedestrian in front impact at the vehicle's centreline

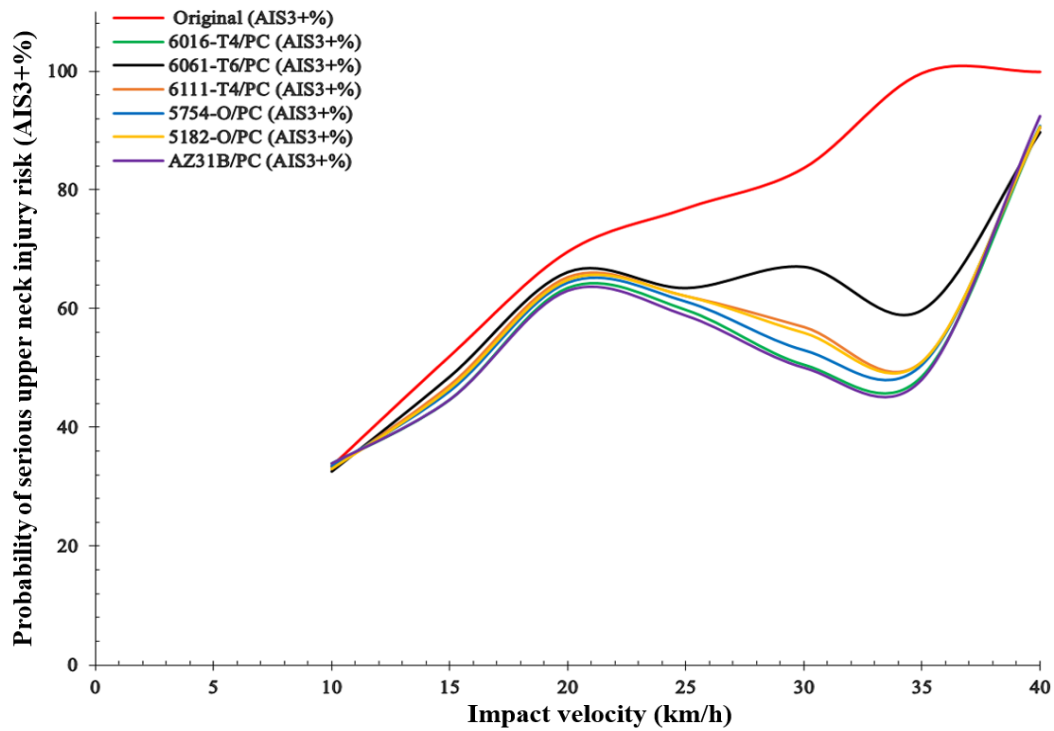


Figure F- 7. Impact Velocity against Probability of Serious Upper neck Injury Risk (AIS3+) for Adult Pedestrian in rear impact at the vehicle's centreline

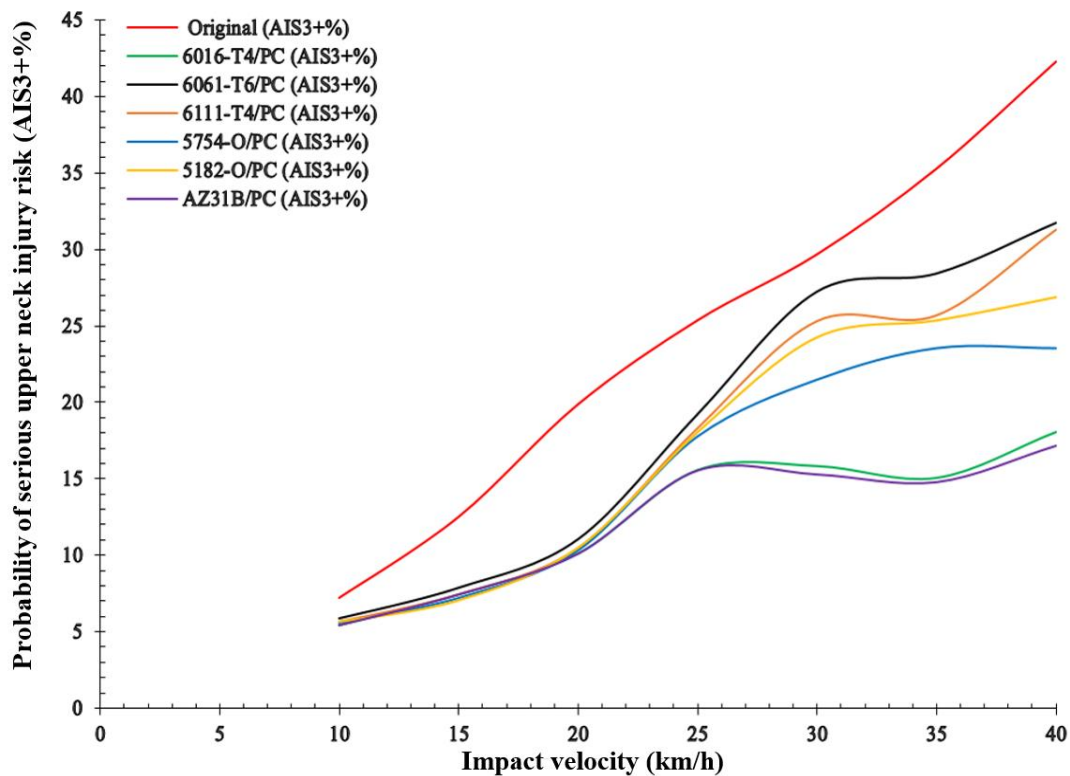


Figure F- 8. Impact Velocity against Probability of Serious Upper neck Injury Risk (AIS3+) for Adult Pedestrian in front impact at 42cm offset from the vehicle's centreline

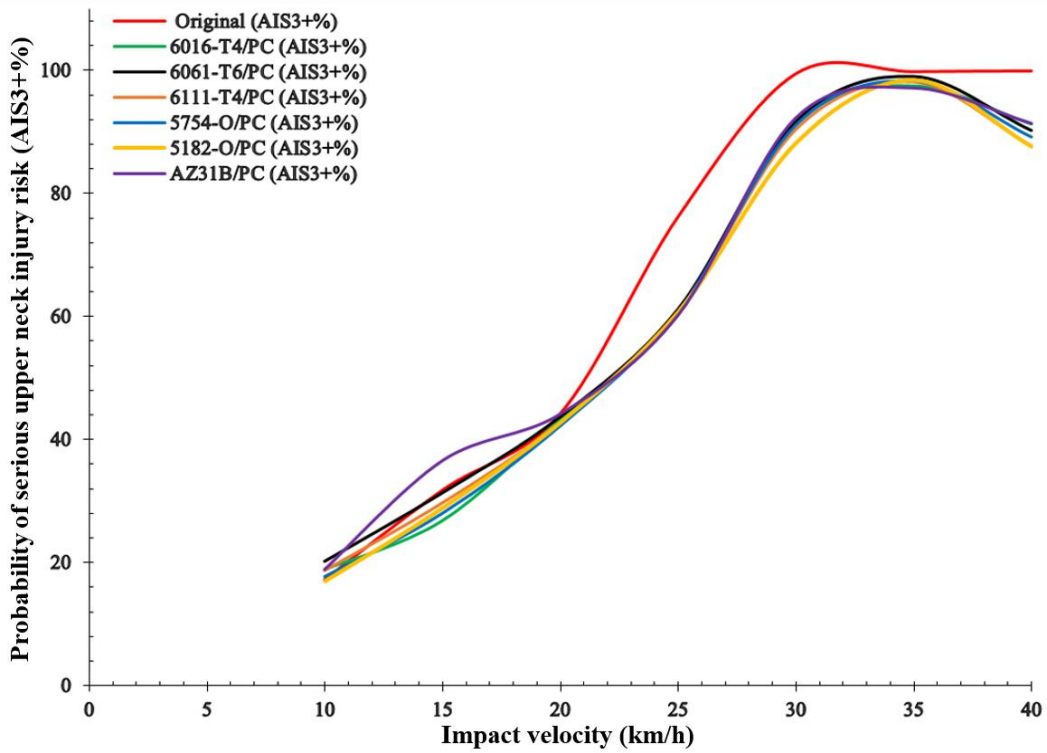


Figure F- 9. Impact Velocity against Probability of Serious Upper neck Injury Risk (AIS3+) for Adult Pedestrian in rear impact at 42cm offset from the vehicle’s centreline

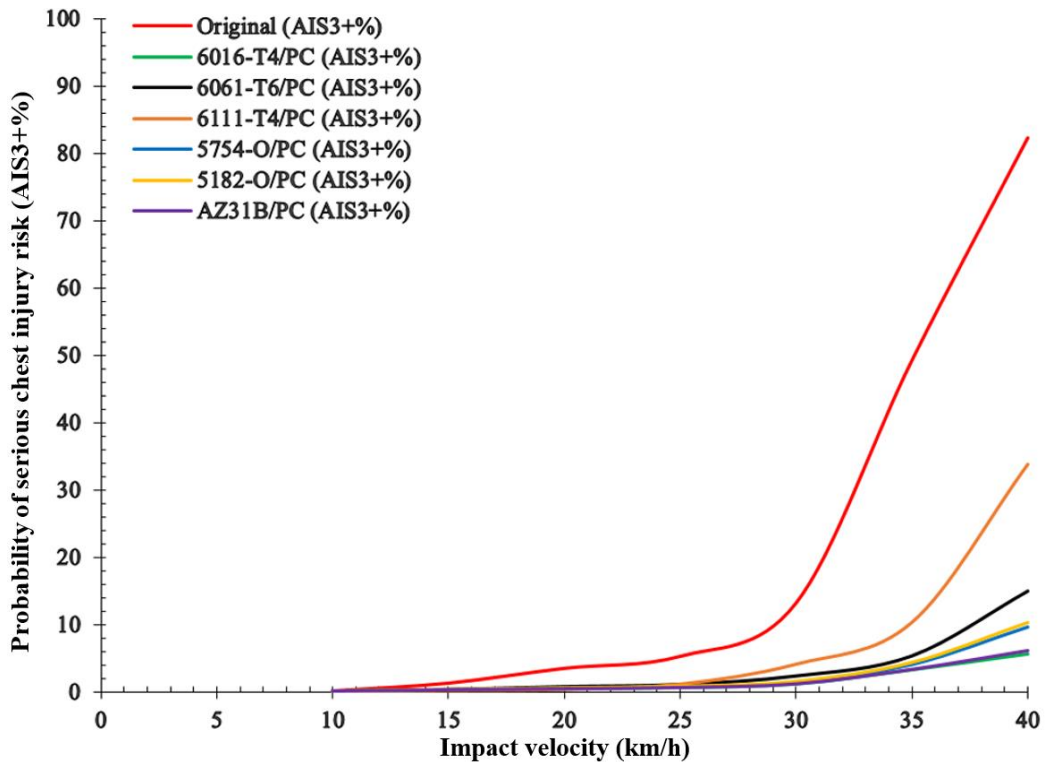


Figure F- 10. Impact Velocity against Probability of Serious Chest Injury Risk (AIS3+) for Adult Pedestrian in front impact at the vehicle’s centreline

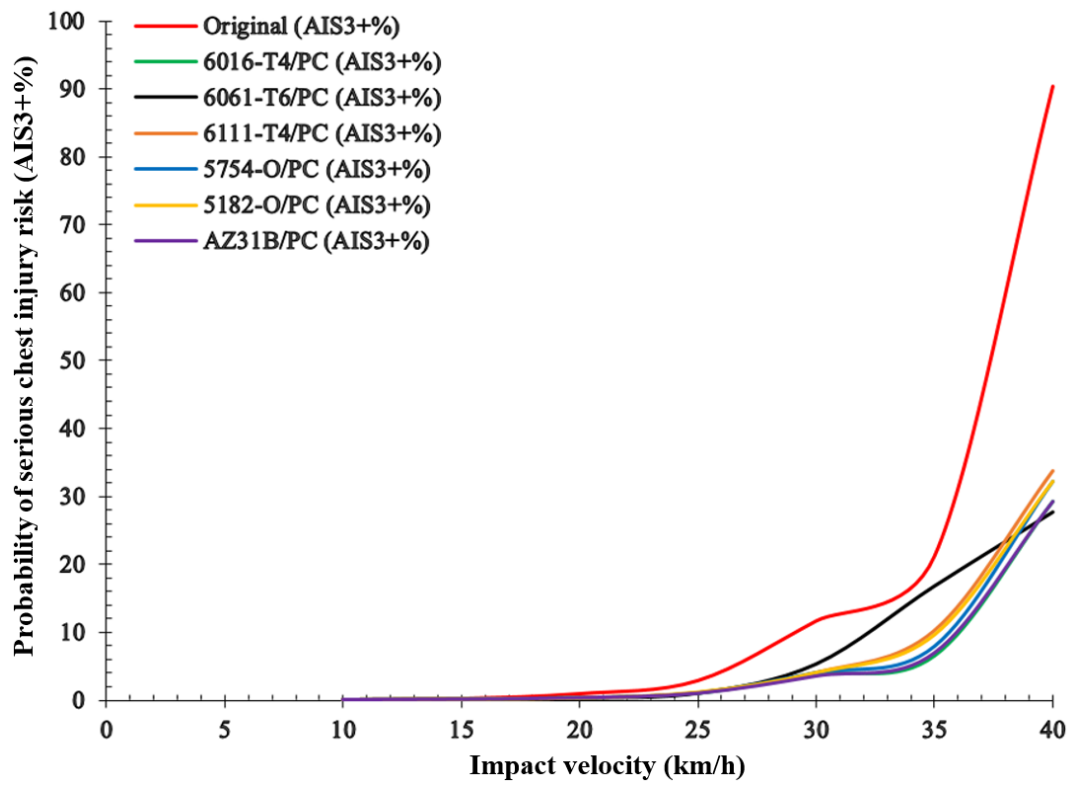


Figure F- 11. Impact Velocity against Probability of Serious Chest Injury Risk (AIS3+) for Adult Pedestrian in front impact at 42cm offset from the vehicle's centreline